

Université du Québec  
INRS-Eau, Terre & Environnement

**ORIGINE ET ÉVOLUTION GÉOCHIMIQUE DES  
EAUX SOUTERRAINES DU SYSTÈME AQUIFÈRE  
DES BASSES-LAURENTIDES DANS LES ROCHES  
SÉDIMENTAIRES PALÉOZOÏQUES DES BASSES-TERRES  
DU SAINT-LAURENT, QUÉBEC, CANADA**

Par  
**VINCENT CLOUTIER**

Thèse présentée pour l'obtention du grade  
de Philosophiae doctor (Ph.D.) en Sciences de la Terre

Jury d'évaluation

Examinateur externe	<b>Dr Stephen E. Grasby</b> Commission géologique du Canada Calgary (Alberta), T2L 2A7
Examinateur externe	<b>Dr Ken W.F. Howard</b> Department of physical and environmental sciences University of Toronto at Scarborough (Ontario), M1C 1A4
Examinateur interne et président du jury	<b>Dr Alfonso Rivera</b> Commission géologique du Canada Québec (Québec), G1S 2L2
Codirectrice de recherche	<b>Dr Martine M. Savard</b> Commission géologique du Canada Québec (Québec), G1S 2L2
Codirecteur de recherche	<b>Dr René Therrien</b> Département de géologie et de génie géologique Université Laval, Sainte-Foy (Québec), G1K 7P4
Directeur de recherche	<b>Dr René Lefebvre</b> Institut national de la recherche scientifique, INRS-Eau, Terre & Environnement, Sainte-Foy (Québec), G1V 4C7

Thèse soutenue le 28 mai 2004

© droits réservés de Vincent Cloutier, 2004



## **RÉSUMÉ**

Le projet «caractérisation hydrogéologique régionale du système aquifère fracturé du sud-ouest du Québec» a été initié par la Commission géologique du Canada (CGC). Cette thèse de doctorat est une étude détaillée de l'hydrogéochimie des eaux souterraines de ce système aquifère de roches sédimentaires paléozoïques, et a été réalisée dans le cadre de ce projet de la CGC. Les objectifs principaux de ce doctorat étaient d'évaluer la qualité régionale des eaux souterraines, de déterminer l'influence des contextes hydrogéologiques et géologiques sur la géochimie des eaux souterraines, d'identifier l'origine des eaux souterraines, de reconnaître les processus contrôlant la chimie des eaux souterraines et son évolution dans l'espace et le temps, ainsi que de développer un modèle intégré de l'évolution géochimique des eaux souterraines des Basses-Laurentides.

Des échantillons d'eau souterraine ont été prélevés à 153 sites répartis sur l'ensemble de la région d'étude de 1500 km<sup>2</sup>, caractérisant toutes les unités géologiques et les contextes hydrogéologiques jusqu'à une profondeur de 140 m. L'eau souterraine a été analysée pour les constituants inorganiques majeurs, mineurs et traces, les isotopes stables δ<sup>2</sup>H, δ<sup>18</sup>O et δ<sup>13</sup>C du carbone inorganique dissous (CID), et certains échantillons ont été analysés pour <sup>87</sup>Sr/<sup>86</sup>Sr, <sup>3</sup>H et <sup>14</sup>C du CID. L'analyse isotopique des précipitations et l'analyse chimique de l'eau interstitielle des argiles marines complètent la connaissance des sources susceptibles d'influencer la géochimie des eaux souterraines.

Les données hydrogéochimiques ont été analysées en utilisant une combinaison de méthodes géochimiques classiques et statistiques, dont l'utilisation de diagrammes géochimiques, la classification en types d'eau, la modélisation géochimique, la classification automatique hiérarchique (CAH), et l'analyse en composantes principales (ACP). La distribution régionale des types d'eau a montré le contrôle des conditions hydrogéologiques sur la chimie des éléments majeurs des eaux souterraines. Les zones de recharge sont caractérisées par une eau souterraine moderne enrichie en tritium de type Ca-Mg-HCO<sub>3</sub>, et les zones confinées par des eaux souterraines submodernes de types Na-HCO<sub>3</sub> et Na-Cl. L'analyse CAH a permis de reconnaître le contrôle des formations

géologiques sur les éléments mineurs et traces. Deux sources d'eau souterraine sont identifiées dans le système aquifère, l'eau météorique moderne et l'eau Pléistocène de la Mer de Champlain. L'eau souterraine est aussi affectée par les processus géochimiques au cours de son écoulement. La dissolution de minéraux carbonatés domine dans les zones de recharge produisant l'eau souterraine de type Ca-Mg-HCO<sub>3</sub>. Dans le système aquifère en conditions confinées, l'échange ionique Ca<sup>2+</sup>-Na<sup>+</sup> est responsable pour l'évolution de l'eau au type Na-HCO<sub>3</sub>, alors que le mélange avec l'eau de la Mer de Champlain et la diffusion d'ions des argiles marines sont responsables pour la présence d'eau de type Na-Cl. L'invasion marine qui a résulté en la Mer de Champlain est la cause de la salinisation du système aquifère caractérisé. Les traceurs conservateurs Cl<sup>-</sup> et Br<sup>-</sup>, ainsi que δ<sup>18</sup>O, ont permis de déterminer que l'eau originale de la Mer de Champlain, dans la région d'étude, était un mélange d'environ 34% d'eau de mer et de 66% d'eau douce. La géochimie actuelle de l'eau souterraine a permis de déterminer que le système aquifère est à différentes étapes du processus de désalinisation, de l'eau marine ancienne étant encore présente dans les parties stagnantes, alors que dans les secteurs à plus forte circulation, celle-ci a été complètement remplacée par une eau souterraine moderne.

L'intégration de l'hydrogéochimie, incluant l'origine, l'évolution et les processus, avec les contextes géologiques et hydrogéologiques a permis de diviser le territoire en quatre régions géochimiques, procurant un portrait global de la dynamique du système aquifère. Les facteurs suivants sont reconnus comme influençant l'évolution de l'eau souterraine observée dans chacune des régions géochimiques : 1) les caractéristiques géologiques, incluant le type de roche sédimentaire et la composition minéralogique du till ; 2) les caractéristiques hydrogéologiques, dont le niveau de confinement et le gradient hydraulique ; et 3) l'histoire géologique, dont la dernière glaciation et la Mer de Champlain. Avec son approche intégrée, cette étude hydrogéochimique apporte une contribution à la caractérisation et la compréhension de systèmes d'écoulement complexes, ainsi qu'à l'évolution à long terme de systèmes hydrogéologiques.



Vincent Cloutier



René Lefebvre

## **ABSTRACT**

The project on the «regional hydrogeological characterization of the fractured aquifer system in south-western Quebec» was initiated by the Geological Survey of Canada (GSC). This Ph.D. thesis is a comprehensive hydrogeochemical study of groundwater of this Paleozoic sedimentary rock aquifer system carried out as part of this GSC project. The main objectives of this thesis were to evaluate regional groundwater quality, determine the influence of hydrogeological and geological contexts on groundwater geochemistry, identify groundwater origin, recognize processes controlling groundwater geochemistry and its evolution in space and time, as well as develop an integrated model of the geochemical evolution of groundwater within the Basses-Laurentides aquifer system.

Groundwater samples were collected at 153 sites distributed over the whole 1500 km<sup>2</sup> study area, characterizing all geological units and hydrogeological contexts to a maximum depth of 140 m. Groundwater was analyzed for major, minor and trace inorganic constituents, stable isotopes  $\delta^2\text{H}$ ,  $\delta^{18}\text{O}$  and  $\delta^{13}\text{C}$  of dissolved inorganic carbon (DIC), and some samples were analyzed for  $^{87}\text{Sr}/^{86}\text{Sr}$ ,  $^3\text{H}$  and  $^{14}\text{C}$  of DIC. The isotopic analysis of precipitation and the chemical analysis of marine clay pore water complete the dataset on end-members that could influence groundwater geochemistry.

The hydrogeochemical data were analyzed by combining conventional geochemical and statistical methods: geochemical diagrams, water types classification, geochemical modeling, hierarchical cluster analysis (HCA) and principal components analysis (PCA). The regional distribution of groundwater types showed that the hydrogeological conditions exert a dominant control on the major ions chemistry of the groundwater. Preferential recharge areas are characterized by modern tritiated groundwater of Ca-Mg-HCO<sub>3</sub> type, and confined conditions by submodern groundwater of Na-HCO<sub>3</sub> and Na-Cl types. The HCA allowed the recognition of the importance of the geological formations on minor and trace elements. Two groundwater end-members are identified in the aquifer system, modern meteoric water and Pleistocene Champlain Sea water. Geochemical

processes along the flow system also affect groundwater. Dissolution of carbonates dominates in the preferential recharge areas resulting in Ca-Mg-HCO<sub>3</sub> groundwater type. In the aquifer system under confined conditions, Ca<sup>2+</sup>-Na<sup>+</sup> ion exchange is the cause of groundwater evolution to Na-HCO<sub>3</sub> type. In the deeper areas, groundwater mixing with Pleistocene Champlain Sea water as well as solutes diffusion from the marine clay aquitard are the causes of the occurrence of Na-Cl groundwater. Salinization of the aquifer system resulted from the marine invasion that created the Quaternary Champlain Sea. Conservative tracers Cl<sup>-</sup> and Br<sup>-</sup>, as well as δ<sup>18</sup>O, showed that the original Champlain Sea water, in the study area, was a mixture of about 34% seawater and 66% freshwater. The current geochemistry of the groundwater indicates that the aquifer system is at different stages of desalinization, ranging from the original Champlain Sea water still present in hydraulically stagnant areas of the aquifer to fully flushed conditions in the more active parts of the aquifer system, especially in preferential recharge zones.

The integration of hydrogeochemistry, including the origin, the evolution and the geochemical processes, within the geological and hydrogeological contexts allowed the division of the region into four main geochemical areas, providing a global picture of the aquifer system dynamics. The following factors were recognized as influencing the evolution of groundwater identified in all geochemical areas: 1) geological characteristics including sedimentary rock type and till mineralogy; 2) hydrogeological characteristics related to the level of confinement and the hydraulic gradient; and 3) geological history linked to the latest glaciation as well as Champlain Sea invasion. With its integrated approach, this hydrogeochemical study contributes to the characterization and understanding of complex groundwater flow systems, as well as an example of the long-term evolution of hydrogeological systems.

## **REMERCIEMENTS**

Au terme de ce doctorat, je tiens à remercier sincèrement René Lefebvre, directeur de recherche, pour sa grande disponibilité, le caractère positif et constructif de nos réunions de travail, ses conseils judicieux et pour avoir partagé avec moi sa vision intégrée de l'hydrogéologie. Je tiens aussi à remercier Martine Savard, co-directrice de recherche, ainsi que René Therrien, co-directeur de recherche, pour leur intérêt et leur appui au projet ainsi que pour avoir orienté et clarifié plusieurs parties des travaux. De plus, je suis reconnaissant envers Martine Savard pour sa gestion du projet de cartographie hydrogéologique de la Commission géologique du Canada (CGC). Je désire également remercier les autres membres du jury, Alfonso Rivera, Stephen Grasby et Ken Howard, pour avoir accepté d'évaluer cette thèse. Leur évaluation et commentaires constructifs ont contribué à améliorer la thèse ainsi que les articles qui seront soumis à des revues scientifiques.

Les travaux de ce projet de doctorat ont été réalisés avec le support de la CGC, d'INRS-Eau, Terre & Environnement (INRS-ETE), de l'Université Laval, d'Environnement Canada, et du Ministère de l'Environnement du Québec. Le projet de la CGC a aussi été supporté financièrement par Développement Économique Canada, les Municipalités régionales de comté d'Argenteuil, Mirabel, Deux-Montagnes et Thérèse-de-Blainville, le Conseil Régional de Développement-Laurentides, et l'Association des Professionnels de Développement Économique des Laurentides. Une partie des travaux de forage a été supportée par le Ministère des Transports du Québec. Les données utilisées dans la thèse et contenues dans le disque compact (Appendice G) sont des données publiques de la CGC. Ces données ont été obtenues dans le cadre de ce projet. Je suis reconnaissant envers le Conseil de recherche en sciences naturelles et en génie du Canada, le Fonds québécois de la recherche sur la nature et les technologies et l'INRS-ETE pour m'avoir accordé un financement sous forme de bourses d'études supérieures.

Je remercie sincèrement Édith Bourque pour sa collaboration précieuse dans plusieurs aspects de ce projet, dont les travaux d'échantillonnage. Je remercie également Miroslav

Nastev pour sa collaboration dans les travaux de terrain. Je tiens à saluer et à remercier l'ensemble des chercheurs(es) et étudiants(es), qui sont passés ou restés au chalet du parc d'Oka, le camp de base du projet pour les deux étés de terrain et qui ont contribué de différentes façons à ces travaux : Andrée Bolduc, Marc Étienne, Nathalie Fagnan, Pierre Gélinas, Frédéric Girard, Andréanne Hamel, Gilbert Karanta, Patricia Lapcevic, Jean-Michel Lemieux, Richard Martel, Yves Michaud, Kent Novakowski, Daniel Paradis, Michel Parent, Martin Ross et Osman Salad Hersi. Je désire souligner la contribution importante de plusieurs étudiants(es) qui nous ont assistés dans l'échantillonnage de l'eau souterraine. Il s'agit d'Alexandre Boutin, Martin Fleury, Pascal Lussier-Duquette, Valérie Maltais, Valérie Murat, et Tommy Thériault. Je remercie particulièrement John Voralek pour son aide précieuse sur le terrain, Chatelaïne Beaudry qui a dirigé une équipe d'échantillonnage multi-niveaux ainsi que Constance Beaubien qui a réalisé les travaux d'extraction de l'eau interstitielle des argiles.

Je tiens à souligner l'importance de la contribution du Ministère de l'Environnement du Québec pour les analyses chimiques, et je tiens à remercier Danielle Thomassin du Centre d'expertise en analyse environnementale du Québec pour la collaboration dans les analyses. Je remercie sincèrement Marc Luzincourt du Delta-Lab de la CGC pour les analyses des isotopes stables et pour m'avoir montré les techniques me permettant de faire une partie des analyses  $\delta^2\text{H}$  et  $\delta^{18}\text{O}$ . Merci également à Bill Davis du laboratoire Geochron de la CGC pour les analyses  $^{87}\text{Sr}/^{86}\text{Sr}$ . Mes remerciements vont aussi à Luce Dubé, Suzanne Dussault, Josée Posadzki, Normand Tassé de même qu'aux étudiants(es), personnel et chercheurs(es) de la CGC et d'INRS-ETE.

Enfin, je suis reconnaissant envers les résidants des Basses-Laurentides qui nous ont donné accès à leur propriété pour échantillonner leur puits, nous permettant ainsi d'obtenir une partie importante des données de base de cette étude.

Je dédie cette thèse de doctorat à mes parents pour leur encouragement au cours de mes études, à mon cher fils Félix ainsi qu'à mon épouse Somthawil qui m'a appuyé et encouragé tout au long de ce projet.

## **TABLE DES MATIÈRES**

RÉSUMÉ .....	iii
ABSTRACT.....	v
REMERCIEMENTS.....	vii
TABLE DES MATIÈRES .....	ix
LISTE DES TABLEAUX.....	xiv
LISTE DES FIGURES .....	xvi
PREMIÈRE PARTIE: INTRODUCTION.....	1
<b>CHAPITRE 1: INTRODUCTION .....</b>	<b>3</b>
1.1    INTRODUCTION .....	3
1.1.1    Contexte des travaux du doctorat .....	3
1.1.2    Structure de la thèse .....	4
1.1.3    Problématique et mise en contexte du projet de recherche .....	6
1.1.3.1    Écoulement de l'eau souterraine à l'échelle régionale .....	6
1.1.3.2    Évolution chimique de l'eau souterraine à l'échelle régionale .....	6
1.1.3.3    Isotopes et traceurs environnementaux .....	9
1.1.3.4    Hydraulique et transport de masse en milieu fracturé.....	10
1.1.3.5    Les modèles géochimiques.....	12
1.1.3.6    L'hydrogéochimie régionale, une approche intégrée.....	15
1.1.4    Objectifs du projet de recherche.....	17
1.2    DESCRIPTION DE LA RÉGION D'ÉTUDE .....	19
1.2.1    Contexte géologique.....	20
1.2.2    Contexte hydrogéologique .....	20
1.3    MÉTHODOLOGIE .....	22
1.3.1    Intégration du projet de recherche dans le projet de cartographie hydrogéologique .....	22
1.3.2    Échantillonnage de l'eau souterraine .....	24
1.3.2.1    Méthodes d'échantillonnage de l'eau souterraine .....	24
1.3.2.2    Travaux d'échantillonnage .....	25
1.3.2.3    Système d'échantillonnage multi-niveaux et protocole suivi.....	29
1.3.3    Caractérisation isotopique $\delta^2\text{H}$ et $\delta^{18}\text{O}$ des précipitations .....	32
1.3.4    Caractérisation de l'eau d'infiltration dans la zone non saturée .....	33
1.3.5    Extraction de l'eau interstitielle des argiles .....	34
1.3.6    Travaux de laboratoire .....	34

1.3.6.1	Analyses chimiques et microbiologiques .....	34
1.3.6.2	Analyses isotopiques .....	35
1.4	CONTRIBUTION DE L'AUTEUR .....	36
1.4.1	Autres contributions .....	38
	DEUXIÈME PARTIE: RAPPORT ET ARTICLES .....	41
	<b>CHAPITRE 2: CARACTÉRISATION HYDROGÉOCHIMIQUE ET QUALITÉ DE L'EAU SOUTERRAINE.....</b>	<b>43</b>
RÉSUMÉ.....		44
2.1	INTRODUCTION .....	45
2.2	PROCÉDURES.....	45
2.3	ÉVALUATION DE LA QUALITÉ DE L'EAU SOUTERRAINE .....	46
2.3.1	Variabilité régionale de la qualité de l'eau souterraine et représentation graphique.....	50
2.3.2	Concentrations chimiques et critères de qualité .....	51
2.4	TYPES D'EAU.....	54
2.5	SECTEURS DE QUALITÉ RELATIVE DE L'EAU SOUTERRAINE .....	55
2.5.1	Classification par secteur.....	55
2.5.2	Description des secteurs de qualité relative de l'eau.....	59
2.6	CONCLUSIONS – IMPLICATION POUR LA CONSOMMATION DE L'EAU SOUTERRAINE .....	62
	<b>CHAPITRE 3: HYDROGEOCHEMISTRY AND GROUNDWATER ORIGIN OF THE BASSES-LAURENTIDES SEDIMENTARY ROCK AQUIFER SYSTEM, ST. LAWRENCE LOWLANDS, QUÉBEC, CANADA.....</b>	<b>65</b>
RÉSUMÉ.....		66
ABSTRACT .....		67
3.1	INTRODUCTION .....	68
3.2	CONTEXT OF THE STUDY AREA.....	70
3.2.1	Geological setting and history .....	72
3.2.1.1	Paleozoic and Cretaceous geology .....	72
3.2.1.2	Quaternary geology .....	74
3.2.2	Hydrogeological setting.....	74
3.3	METHODS .....	79
3.3.1	Groundwater sampling .....	80
3.3.2	Precipitation sampling .....	81
3.4	RESULTS AND INTERPRETATION OF THE REGIONAL GROUNDWATER HYDROGEOCHEMICAL CHARACTERIZATION .....	82
3.4.1	Hydrogeochemical dataset.....	82
3.4.2	Precipitation and groundwater isotopic signatures .....	84
3.4.2.1	$\delta^{18}\text{O}$ and $\delta^2\text{H}$ values.....	84
3.4.2.2	Carbon-13 on DIC .....	88
3.4.2.3	Strontium isotopes .....	89
3.4.2.4	Tritium and radiocarbon dating .....	93

3.4.3	Major and minor ions groundwater geochemistry .....	96
3.4.4	Groundwater types .....	102
3.4.5	Groundwater groups based on major ions.....	104
3.5	DISCUSSION.....	109
3.5.1	Geological and hydrogeological contexts .....	109
3.5.2	Isotopic data main conclusions .....	110
3.5.3	Groundwater groups and end-members .....	112
3.5.4	Groundwater origin and evolution .....	113
3.5.5	Water quality and anthropogenic effects.....	116
3.6	SUMMARY AND CONCLUSIONS.....	117
	ACKNOWLEDGEMENTS.....	119
	APPENDIX.....	120
	ELECTRONIC SUPPLEMENTARY MATERIAL (ESM) .....	123
	<b>CHAPITRE 4: GEOCHEMICAL PROCESSES IN THE BASSES-LAURENTIDES SEDIMENTARY ROCK AQUIFER SYSTEM, ST. LAWRENCE LOWLANDS, QUÉBEC, CANADA .....</b>	<b>127</b>
	RÉSUMÉ .....	128
	ABSTRACT.....	129
4.1	INTRODUCTION .....	130
4.2	CONTEXT, GEOLOGY AND HYDROGEOLOGY .....	131
4.3	METHODS OF INVESTIGATION .....	136
4.4	REGIONAL HYDROGEOCHEMICAL CONTEXT .....	137
4.5	INTERPRETATION OF MAIN GEOCHEMICAL PROCESSES AND GROUNDWATER EVOLUTION .....	141
4.5.1	Dissolution of carbonates .....	142
4.5.2	Ion exchange .....	146
4.5.3	Groundwater mixing and salinity origin .....	151
4.6	DISCUSSION.....	160
4.6.1	Groundwater groups within the groundwater flow conceptual model..	160
4.6.2	Specific geochemical evolution paths.....	164
4.6.3	General geochemical evolution paths.....	167
4.7	SUMMARY AND CONCLUSIONS .....	168
	ACKNOWLEDGEMENTS .....	170
	<b>CHAPITRE 5: MULTIVARIATE STATISTICAL ANALYSIS OF GEOCHEMICAL DATA AS INDICATIVE OF THE HYDROGEOCHEMICAL EVOLUTION OF GROUNDWATER OF THE BASSES-LAURENTIDES SEDIMENTARY ROCK AQUIFER SYSTEM, ST. LAWRENCE LOWLANDS, QUÉBEC, CANADA .....</b>	<b>171</b>
	RÉSUMÉ .....	172
	ABSTRACT.....	173
5.1	INTRODUCTION .....	174
5.2	CONTEXT OF THE STUDY AREA .....	176
5.2.1	Geology and hydrogeology .....	176
5.2.2	Hydrogeochemistry .....	179

5.3	METHODOLOGY .....	182
5.3.1	Hydrogeochemical dataset.....	182
5.3.2	Data preparation for the multivariate statistical analysis.....	182
5.3.3	Hierarchical cluster analysis (HCA).....	186
5.3.4	Principal components analysis (PCA) .....	187
5.4	MULTIVARIATE STATISTICAL ANALYSIS .....	189
5.4.1	Hierarchical cluster analysis (HCA).....	189
5.4.2	Principal components analysis (PCA) .....	192
5.5	GEOCHEMICAL INTERPRETATION .....	196
5.5.1	Groundwater groups and clusters .....	196
5.5.2	Hydrogeological context.....	198
5.5.3	Areal distribution and zoning .....	201
5.5.4	Hydrogeochemical evolution.....	206
5.6	CONCLUSION.....	213
5.6.1	Approach and methodology.....	213
5.6.2	Interpretation of groundwater evolution.....	213
5.6.3	Complementarity of interpretation methods.....	217
5.6.4	Long-term system evolution.....	219
	ACKNOWLEDGEMENTS .....	220
	APPENDIX .....	221
	<b>CHAPITRE 6: CONCLUSIONS .....</b>	<b>225</b>
6.1	CONCLUSIONS GÉNÉRALES .....	225
6.2	CONTRIBUTIONS SCIENTIFIQUES ET APPORTS À L'AVANCEMENT DES CONNAISSANCES .....	233
6.3	QUESTIONS EN SUSPENS, TRAVAUX FUTURS ET PERSPECTIVES....	237
	LISTE DES RÉFÉRENCES .....	241
	<b>TROISIÈME PARTIE: APPENDICES.....</b>	<b>263</b>
	<b>APPENDICE A: RÉSULTATS DES ANALYSES GÉOCHIMIQUES ET ISOTOPIQUES DES EAUX SOUTERRAINES.....</b>	<b>265</b>
A1	Échantillonnage régional .....	266
A2	Échantillonnage avec le système multi-niveaux .....	286
	<b>APPENDICE B: LA CARACTÉRISATION ISOTOPIQUE DES PRÉCIPITATIONS .....</b>	<b>299</b>
B1	Information sur les stations.....	300
B2	Résultats des eaux de pluie .....	301
B3	Résultats de la neige.....	303
B4	Résultats des eaux d'infiltration.....	305
	<b>APPENDICE C: CARTES SUPPLÉMENTAIRES.....</b>	<b>307</b>
C1	Chapitre 3.....	308

C2	Chapitre 5.....	321
<b>APPENDICE D: GÉOCHIMIE DE L'EAU INTERSTITIELLE DES ARGILES MARINES.....</b>		<b>323</b>
D1	Introduction.....	324
D2	Méthodologie d'extraction de l'eau interstitielle des argiles.....	326
D3	Tableau des données géochimiques et isotopiques.....	329
<b>APPENDICE E: LA MODÉLISATION GÉOCHIMIQUE DE L'EAU SOUTERRAINE .....</b>		<b>333</b>
<b>APPENDICE F: COMPTES RENDUS DE CONFÉRENCES .....</b>		<b>343</b>
<b>APPENDICE G: DISQUE COMPACT DES DONNÉES HYDROGÉOCHIMIQUES .....</b>		<b>361</b>
<b>APPENDICE H: CARTES DU CHAPITRE 2.....</b>		<b>365</b>

## **LISTE DES TABLEAUX**

Tableau 1.1. Isotopes, traceurs environnementaux et leurs applications .....	10
Tableau 1.2. Modèles géochimiques.....	13
Tableau 1.3. Caractérisation, travaux et données produites dans le cadre du projet de «caractérisation hydrogéologique régionale du système aquifère fracturé du sud-ouest du Québec» de la CGC .....	23
Tableau 1.4. Paramètres physico-chimiques analysés sur le terrain.....	25
Tableau 1.5. Paramètres pour lesquels les échantillons d'eau souterraine ont été prélevés .....	26
Tableau 1.6. Méthode d'échantillonnage et provenance des échantillons d'eau souterraine prélevés en 1999 et 2000 .....	27
Tableau 1.7. Caractéristiques des puits au roc échantillonnés avec le système multi-niveaux .....	28
Tableau 1.8. Étapes et protocole suivi pour l'échantillonnage avec le système multi-niveaux.....	30
Tableau 2.1. Critères de qualité d'eau pour les paramètres microbiologiques mesurés et dépassements / échantillonnage de l'eau souterraine du Projet AFSOQ, 1999-2000 .....	47
Tableau 2.2. Critères de qualité de l'eau pour les paramètres physico-chimiques analysés en laboratoire et calculés. Le nombre de dépassements observés pour les échantillons de l'étude régionale (1999-2000) sont indiqués entre parenthèses .....	48
Tableau 2.3. Critères de qualité de l'eau pour les paramètres physico-chimiques mesurés au site d'échantillonnage et dépassements / échantillonnage de l'eau souterraine.....	50
Tableau 2.4. Statistiques physico-chimiques des différents types d'unités hydrogéologiques.....	53
Tableau 2.5. Synthèse hydrogéochimique de chaque secteur (groupe de sites d'échantillonnage possédant des conditions hydrogéologiques et des compositions chimiques de l'eau souterraine similaire <sup>a)</sup> ).....	56
Table 3.1. Lithology, mineralogy and fracture filling of the Cambrian-Ordovician sedimentary rocks .....	73
Table 3.2. Characteristics and hydraulic properties of the main hydrostratigraphic units.....	77
Table 3.3. Summary of the complete hydrogeochemical characterization program .....	79
Table 3.4. Descriptive statistics of selected measured and calculated parameters (concentrations in mg/L unless noted) .....	83
Table 3.5. Examples of determination of dominant, and mixed groundwater types .....	104
Table 3.6. Characteristics of groundwater types and groups .....	106
Table 3.7. List of parameters analyzed, field sampling protocol, and method of analysis.....	121
Table 4.1. Lithology, mineralogy and fracture filling of the Cambrian-Ordovician sedimentary rocks .....	133
Table 4.2. Groundwater groups and types determined by Cloutier et al. (in prep c).....	138
Table 4.3. Comparison of Cl <sup>-</sup> and Br <sup>-</sup> (mmol/L) between the groundwater S77 and seawater ...	156

Table 4.4. Relationship between groundwater groups, hydrogeological contexts and geochemical processes in the Basses-Laurentides sedimentary rock aquifer system .....	162
Table 5.1. Descriptive statistics for the 144 groundwater samples (concentrations in mg/L).....	185
Table 5.2. Geochemical and physical characteristics of each cluster (median concentrations in mg/L).....	191
Table 5.3. Principal component loadings and explained variance for the five components with Varimax normalized rotation .....	194
Table 5.4. Confinement Index for the cluster ellipses shown on Figure 5.12b .....	200
Table 5.5. Main geochemical areas, geological and hydrogeological contexts related to identified groundwater clusters. The main geochemical processes inferred responsible for the evolution of groundwater geochemistry are also indicated.....	209
Table 5.6. Relative advantages (+) and disadvantages (-) of conventional and multivariate methods for the classification, representation and interpretation of regional hydrogeochemical data.....	218

## LISTE DES FIGURES

Figure 1.1. Réactions et processus géochimiques contrôlant la composition de l'eau souterraine dans un système aquifère régionale (adaptée de Hounslow, 1995).....	7
Figure 1.2. Localisation de la région d'étude. ....	19
Figure 1.3. Système d'échantillonnage multi-niveaux mobile. ....	31
Figure 3.1. Location and geology of the Basses-Laurentides sedimentary rock aquifer system (geological map modified from Rocher et al., in press). ....	71
Figure 3.2. <b>a</b> Simplified hydrogeological conditions (modified from Hamel et al., 2001), and <b>b</b> cross-section A-A' illustrating the groundwater flow conceptual model and the main hydrostratigraphic units. ....	75
Figure 3.3. Potentiometric surface of the rock aquifer in the study area, with the location of the groundwater sampling sites, the stable isotopes monitoring stations, and clay cores (potentiometric surface map modified from Paradis, in press b). ....	78
Figure 3.4. <b>a</b> Local meteoric water line of the study area, the Basses-Laurentides Meteoric Water Line (BLMWL) based on rain $\delta^2\text{H}$ and $\delta^{18}\text{O}$ , and <b>b</b> $\delta^2\text{H}$ and $\delta^{18}\text{O}$ for groundwater of the Basses-Laurentides sedimentary rock aquifer system (N: Number of samples). ....	85
Figure 3.5. <b>a</b> Histograms of $\delta^{18}\text{O}$ values for the groundwater samples, <b>b</b> regional distribution map of $\delta^{18}\text{O}$ values for the rock, mixed, and sediments under clay samples, <b>c</b> histograms of $\delta^{13}\text{C}_{\text{DIC}}$ values for the groundwater samples, and <b>d</b> regional distribution map of $\delta^{13}\text{C}_{\text{DIC}}$ values for the rock, mixed, and sediments under clay samples (N: Number of samples; for Figures 3.5b and 3.5d, see Figure 3.9a for legend of geological units).....	88
Figure 3.6. <b>a</b> Diagram of $^{87}\text{Sr}/^{86}\text{Sr}$ ratios versus Sr (St. Jos : St. Joseph), <b>b</b> location map of the sampling sites for which strontium isotopes were analyzed (see Figure 3.9a for legend of geological units), and <b>c</b> vertical distribution of $^{87}\text{Sr}/^{86}\text{Sr}$ ratios and Sr concentrations at well SAP, Ste. Anne-des-Plaines. ....	90
Figure 3.7. <b>a</b> Qualitative interpretation of $^3\text{H}$ data, and location of cross-sections (hydrogeological conditions map modified from Hamel et al., 2001), <b>b</b> $^3\text{H}$ and $^{14}\text{C}$ of DIC along the 3 cross-sections, and <b>c</b> vertical distribution of $^3\text{H}$ and $^{14}\text{C}$ results at well SAP, Ste. Anne-des-Plaines.....	94
Figure 3.8. Piper diagrams illustrating the major ions chemistry of <b>a</b> the Basses-Laurentides sedimentary rock aquifer system proportional to TDS, <b>b</b> the recharge water, <b>c</b> the rock, mixed, and sediments under clay samples labeled with the hydrogeological conditions, and <b>d</b> the rock, mixed, and sediments under clay samples labeled with the geological units (N: Number of samples). ....	97
Figure 3.9. <b>a</b> Legend for Fig. 3.9b to 3.9f (Grenvile, St. Phil. : St-Philippe, Lach. : Lachute) (geological map modified from Rocher et al., in press), <b>b</b> box plots of the Basses-Laurentides aquifer system for the hydrogeological conditions of pH and Eh, <b>c</b> box plots of the Basses-Laurentides aquifer system for the hydrogeological conditions and regional distribution maps for the rock, mixed, and sediments under clay samples of $\text{Ca}^{2+}$ , <b>d</b> $\text{Na}^+$ , <b>e</b> $\text{F}^-$ , and <b>f</b> DOC (N: Number of samples; Surf. Sed. : Surface sediments and springs, Unconf.: Unconfined and semi-confined, Conf.: Confined). ....	99

Figure 3.10. Regional distribution map of groundwater types and groups, and their relation to the hydrogeological conditions (N: Number of samples; St. Phil. : St. Philippe) (hydrogeological conditions map modified from Hamel et al., 2001; groundwater relative quality zones from Cloutier and Bourque, in press). ....	105
Figure 3.11. Schoeller diagram for the clay pore water sample C85-14, and the groundwater sample S77. ....	108
Figure 3.12. Conceptual model of groundwater origin and relationships between groundwater end-members. ....	114
Figure 4.1. Location of the study area. ....	130
Figure 4.2. Geology of the Basses-Laurentides sedimentary rock aquifer system (modified from Rocher et al., in press). ....	131
Figure 4.3. Cross-section A-A' illustrating the groundwater flow conceptual model and the main hydrostratigraphic units (elevation in m above mean sea level; see Fig. 4.2 and 4.4 for location of cross-section A-A') (based on Cloutier et al., in prep c). ....	135
Figure 4.4. Regional distribution map of groundwater groups and their relation to the hydrogeological conditions (N: Number of samples; St. Phil. : St. Philippe) (hydrogeological conditions map modified from Hamel et al., 2001; groundwater relative quality zones from Cloutier and Bourque, in press). ....	139
Figure 4.5. Piper diagram illustrating the major ions chemistry of each groundwater group of the Basses-Laurentides sedimentary rock aquifer system (N: Number of samples). ....	141
Figure 4.6. Diagrams of (a) $\text{Ca}^{2+}$ (mmol/L) versus $\text{HCO}_3^-$ (mmol/L) and (b) Mg/Ca versus pH for the groundwater groups (precipitation calculated by averaging monthly data of stations Hemmingford, St. Simon, St. Hippolyte, and Montébello from the Department of the Environment, Québec, 1994-1996). ....	143
Figure 4.7. Diagrams of (a) log $\text{pCO}_2$ versus calcite saturation index, and (b) dolomite saturation index versus calcite saturation index for the groundwater groups. ....	145
Figure 4.8. Box plots of $\log(\text{Ca}+\text{Mg})/\text{Na}^2$ for the groundwater groups and seawater (N: Number of samples). ....	147
Figure 4.9. Diagrams of (a) pH versus $\text{Na}^+$ (mmol/L), (b) $\text{Ca}^{2+}$ (mmol/L) versus $\text{Na}^+$ (mmol/L), and (c) $\text{Na}^+$ (mmol/L) versus $\text{Cl}^-$ (mmol/L) for the groundwater groups. ....	151
Figure 4.10. Diagram of $\text{Cl}^-$ (mg/L) versus calculated TDS (mg/L) for the groundwater groups and seawater (fresh, brackish and saline water classification based on TDS from Freeze and Cherry, 1979). ....	152
Figure 4.11. Diagram of $\text{Cl}/\text{Br}$ (ratio of mmol/L) versus $\text{Cl}^-$ (mmol/L) for the groundwater groups and possible end-member samples. ....	155
Figure 4.12. Model for the origin of salinity using diagrams of $\text{Br}^-$ (mmol/L) versus $\text{Cl}^-$ (mmol/L) for (a) step 1, seawater dilution, and (b) step 2, groundwater mixing. ....	157
Figure 4.13. Model for the origin of salinity using diagrams of $\delta^{18}\text{O}$ versus salinity based on the work of Hillaire-Marcel (1988). ....	159
Figure 4.14. Groundwater flow conceptual model with the relative position of the groundwater groups within the Basses-Laurentides sedimentary rock aquifer system (see Table 4.4 for details). ....	161

Figure 4.15. Specific geochemical evolution paths for groundwater in different locations of the Basses-Laurentides sedimentary rock aquifer system (see Table 4.4 for details).....	165
Figure 4.16. Piper diagram illustrating the general geochemical processes involved in the evolution of groundwater of the Basses-Laurentides sedimentary rock aquifer system (see the Piper diagram of Figure 4.5 for all groundwater samples).....	167
Figure 5.1. Location of the Basses-Laurentides sedimentary rock aquifer system.....	174
Figure 5.2. Context of the study area: (a) geology (geological map modified from Rocher et al., in press), (b) hydrogeological conditions (Grenv.: Grenville, St. Phil.: St. Philippe, Lach.: Lachute) (hydrogeological conditions map modified from Hamel et al., 2001), (c) potentiometric surface (potentiometric surface map modified from Paradis, in press b), and (d) cross-section A-A' illustrating the groundwater flow conceptual model and the main hydrostratigraphic units (Elev. : elevation in m above mean sea level) (modified from Cloutier et al., in prep c).....	177
Figure 5.3. Piper diagram of groundwater of the Basses-Laurentides labeled with the groundwater groups (N: Number of samples) (modified from Cloutier et al., in prep a). ....	181
Figure 5.4. Methodological flow chart, from groundwater sampling to data analysis (N: Number of samples, D.L.: detection limit).....	183
Figure 5.5. Dendrogram for the groundwater samples, showing the division into 7 clusters and the median Stiff diagram of each cluster (N: Number of samples, GW: Groundwater, conc.: concentrations). .....	190
Figure 5.6. Dendrogram for the 14 chemical parameters. ....	192
Figure 5.7. Scree plot (plot of eigenvalues) of the PCA.....	193
Figure 5.8. Bar plots of principal component loadings with Varimax normalized rotation for (a) component 1, (b) component 2, (c) component 3, (d) component 4, and (e) component 5. .	195
Figure 5.9. Plot of loadings for the first two components with Varimax normalized rotation....	196
Figure 5.10. Piper diagram of the groundwater clusters with the groundwater group envelopes of Figure 5.3 (N: Number of samples).....	197
Figure 5.11. Relationship between groundwater clusters and groups (N: Number of samples, Bold values : highest values).....	198
Figure 5.12. Plot of principal component scores for the first two components labeled with (a) the hydrogeological conditions, with the definition of the Confinement Index, and (b) the groundwater clusters, with ellipses at a coefficient of 0.5 for each cluster (N: Number of samples).....	199
Figure 5.13. Regional distribution of principal component scores for (a) component 1 with the recharge zones (principal recharge zones to the rock aquifer modified from Paradis, in press c), (b) component 2, (c) component 4, and (d) component 5 with the geology (geological map modified from Rocher et al., in press) (see Fig. 5.2b for locations name). .....	203
Figure 5.14. Zoning of groundwater quality: Regional distribution of groundwater clusters, and their relation to the groundwater relative quality zones and to the hydrogeological conditions (N: Number of samples; Areas with exceptional clusters are circled with dashed lines) (hydrogeological conditions map modified from Hamel et al., 2001; groundwater relative quality zones from Cloutier and Bourque, in press).....	205

Figure 5.15. Evolution of groundwater geochemistry: (a) Range plot of the Confinement Index for the cluster ellipses related to the main geochemical areas (N: Number of samples), and (b) plot showing the relationship between the clusters and the groundwater groups evolution within the main geochemical areas (see Fig. 5.3 for definition of groundwater groups).....208

Figure 5.16. Hydrogeochemical evolution of groundwater of the Central Crests and Valleys area into the plane of principal components 1 and 2 (cluster ellipses from Fig. 5.12b). .....212



## **PREMIÈRE PARTIE**

### **INTRODUCTION**



# **Chapitre 1**

## **INTRODUCTION**

### **1.1 INTRODUCTION**

#### **1.1.1 Contexte des travaux du doctorat**

Cette thèse de doctorat a été réalisée dans le cadre d'un projet de cartographie hydrogéologique régionale de la Commission géologique du Canada (CGC). Les travaux de ce projet de la CGC, intitulé «caractérisation hydrogéologique régionale du système aquifère fracturé du sud-ouest du Québec», ont été exécutés en étroite collaboration avec l'INRS-Eau, Terre & Environnement (INRS-ETE) et l'Université Laval, et avec le support d'Environnement Canada, du Ministère de l'Environnement du Québec, de l'Université Queen's, du Service géologique des États-Unis (*U.S. Geological Survey*), et du Ministère des Transports du Québec (Savard et al., *in press*).

Un des objectifs généraux de ce projet de la CGC est d'acquérir une meilleure connaissance des eaux souterraines et du potentiel aquifère dans la région, afin de supporter la gestion et la protection de la ressource en eaux souterraines. Un second objectif important de l'étude est de développer une méthodologie permettant de caractériser, à l'échelle régionale, un système aquifère en milieux fracturés (Savard et al., *in press*). Il y a donc plusieurs volets à ce projet, ce doctorat s'inscrivant dans le volet sur la caractérisation hydrogéochimique des eaux souterraines.

Ce doctorat s'intègre donc dans un projet multidisciplinaire. Ces travaux ont ainsi bénéficié des résultats des autres parties du projet de la CGC, dont la caractérisation

hydrogéologique du système aquifère, des sédiments quaternaires et de la recharge des nappes. Cette approche intégrée a permis de développer un modèle conceptuel régional du système aquifère, menant à une compréhension exhaustive de l'écoulement de l'eau souterraine dans le système aquifère des Basses-Laurentides.

### 1.1.2 Structure de la thèse

Cette thèse par articles comporte trois parties distinctes. La première partie, le Chapitre 1, est l'**Introduction** de la thèse. Celle-ci inclus la problématique et les objectifs du projet de recherche, une description sommaire de la région d'étude, la méthodologie utilisée tant pour les travaux de terrain que ceux de laboratoire, ainsi que la contribution de l'auteur par rapport à l'ensemble des travaux ainsi qu'aux interprétations scientifiques présentées dans la deuxième partie de la thèse.

La deuxième partie comprend un chapitre de rapport et trois articles scientifiques :

Le Chapitre 2 est un chapitre de rapport intitulé **Caractérisation hydrogéochimique et qualité de l'eau souterraine**, par Vincent Cloutier, Édith Bourque, René Lefebvre, Martine M. Savard, et Richard Martel. Ce chapitre est extrait du rapport final suivant : Caractérisation hydrogéologique régionale du système aquifère fracturé du sud-ouest du Québec, Partie 1, Hydrogéologie régionale du système aquifère fracturé du sud-ouest du Québec (Édité par Martine M. Savard, Miroslav Nastev, René Lefebvre, Daniel Paradis, et Richard Martel), remis au Conseil Régional de développement des Laurentides, et aux Municipalités régionales de comté d'Argenteuil, Deux-Montagnes, Mirabel et Thérèse-de-Blainville en mai 2002. Ce chapitre introduit le programme de caractérisation géochimique des eaux souterraines, présente les résultats avec comme objectif l'évaluation de la qualité de l'eau souterraine, ainsi qu'une division de la région d'étude en secteurs de qualité relative de l'eau souterraine.

Le Chapitre 3 est un article intitulé **Hydrogeochemistry and groundwater origin of the Basses-Laurentides sedimentary rock aquifer system, St. Lawrence Lowlands**,

**Québec, Canada**, par Vincent Cloutier, René Lefebvre, Martine M. Savard, Édith Bourque, et René Therrien (soumis à la revue *Hydrogeology Journal* en novembre 2003). Cet article présente les résultats de la caractérisation hydrogéochimique régionale et la relation entre les types d'eau et le contexte géologique et hydrogéologique, avec comme objectif d'identifier l'origine des eaux souterraines dans le système aquifère des Basses-Laurentides.

Le Chapitre 4 est un article à soumettre à la revue *Applied Geochemistry*, et intitulé : **Geochemical processes in the Basses-Laurentides sedimentary rock aquifer system, St. Lawrence Lowlands, Québec, Canada**, par Vincent Cloutier, René Lefebvre, Martine M. Savard, et René Therrien. Cet article identifie les processus géochimiques principaux, ainsi que les évènements géologiques quaternaires, qui influencent l'évolution et la géochimie des eaux souterraines dans le système aquifère des Basses-Laurentides.

Le Chapitre 5 est un article à soumettre à la revue *Journal of Hydrology*, et intitulé : **Multivariate statistical analysis of geochemical data as indicative of the hydrogeochemical evolution of groundwater of the Basses-Laurentides sedimentary rock aquifer system, St. Lawrence Lowlands, Québec, Canada**, par Vincent Cloutier, René Lefebvre, René Therrien, et Martine M. Savard. L'article présente les interprétations de méthodes d'analyse statistique multivariable. L'intégration de l'analyse statistique avec l'ensemble de hydrogéochimie permet de diviser le territoire en quatre régions géochimiques, procurant un portrait global de l'évolution du système aquifère.

Le Chapitre 6, **Conclusions**, vient compléter la deuxième partie. Celles-ci inclus des conclusions générales portant sur les différents thèmes discutés dans le rapport et les articles scientifiques, une synthèse des contributions scientifiques de ces travaux et leurs apports à l'avancement des connaissances, ainsi qu'une revue des questions en suspens, travaux futurs, et des perspectives qu'offrent ces travaux de doctorat par rapport au domaine de recherche. Ce chapitre est suivi de la **Liste des références** qui présente les notices bibliographiques citées dans l'ensemble de la thèse.

Enfin, la troisième partie regroupe les **Appendices**. Ceux-ci présentent les données géochimiques et isotopiques des eaux souterraines, des précipitations et de l'eau interstitielle des argiles, des cartes supplémentaires au Chapitre 3 et au Chapitre 5, la méthodologie d'extraction de l'eau interstitielle des argiles, un exemple de fichier de la modélisation géochimique, deux comptes rendus de conférences, les données sous forme de fichiers numériques dans un disque compact, ainsi que les cartes du Chapitre 2.

### **1.1.3 Problématique et mise en contexte du projet de recherche**

#### *1.1.3.1 Écoulement de l'eau souterraine à l'échelle régionale*

Un système d'écoulement régional est composé de zones de recharge, de zones de transition et de zones d'émergence. Dans un système régional, la distribution des zones de recharge est souvent contrôlée par la topographie. Tóth (1963) a subdivisé les systèmes d'écoulement régional en trois sous-systèmes : les systèmes d'écoulement local, intermédiaire et régional. Les simulations de Freeze et Witherspoon (1967) ont montré les effets de la topographie et de la géologie sur l'écoulement régional de l'eau souterraine en régime permanent.

Ces travaux ont démontré l'importance des contrôles géologiques sur l'écoulement de l'eau souterraine à l'échelle régionale. L'hétérogénéité du milieu peut avoir un effet important sur un système d'écoulement régional. Les variations stratigraphiques et structurales influencent les propriétés hydrogéologiques du milieu (par exemple la conductivité hydraulique) et, conséquemment, l'écoulement de l'eau souterraine. Ceci démontre l'importance de la caractérisation géologique et hydrogéologique dans l'étude de systèmes d'écoulement régionaux.

#### *1.1.3.2 Evolution chimique de l'eau souterraine à l'échelle régionale*

L'écoulement de l'eau souterraine, des zones de recharge aux zones d'émergence, entraîne des modifications dans la composition chimique de l'eau. Chebotarev (1955) a

observé que l'eau souterraine évolue avec la distance dans un système d'écoulement. Il a décrit cette évolution par une séquence où les espèces anioniques dominantes changent avec l'écoulement. Cette évolution chimique est causée par les processus géochimiques et les réactions se produisant dans le système aquifère régional, tel l'interaction avec les minéraux des roches ou avec des gaz. La composition finale dépend de la lithologie de l'aquifère et du temps de résidence de l'eau souterraine. D'autres paramètres ont aussi une incidence importante sur l'évolution de l'eau souterraine : les caractéristiques structurales du milieu, la température et la pression, la vitesse d'écoulement, la surface de roc en contact avec l'eau et la composition chimique de l'eau. La Figure 1.1 présente une synthèse des réactions et des processus géochimiques susceptibles d'être importants dans un système d'écoulement régional de l'eau souterraine.

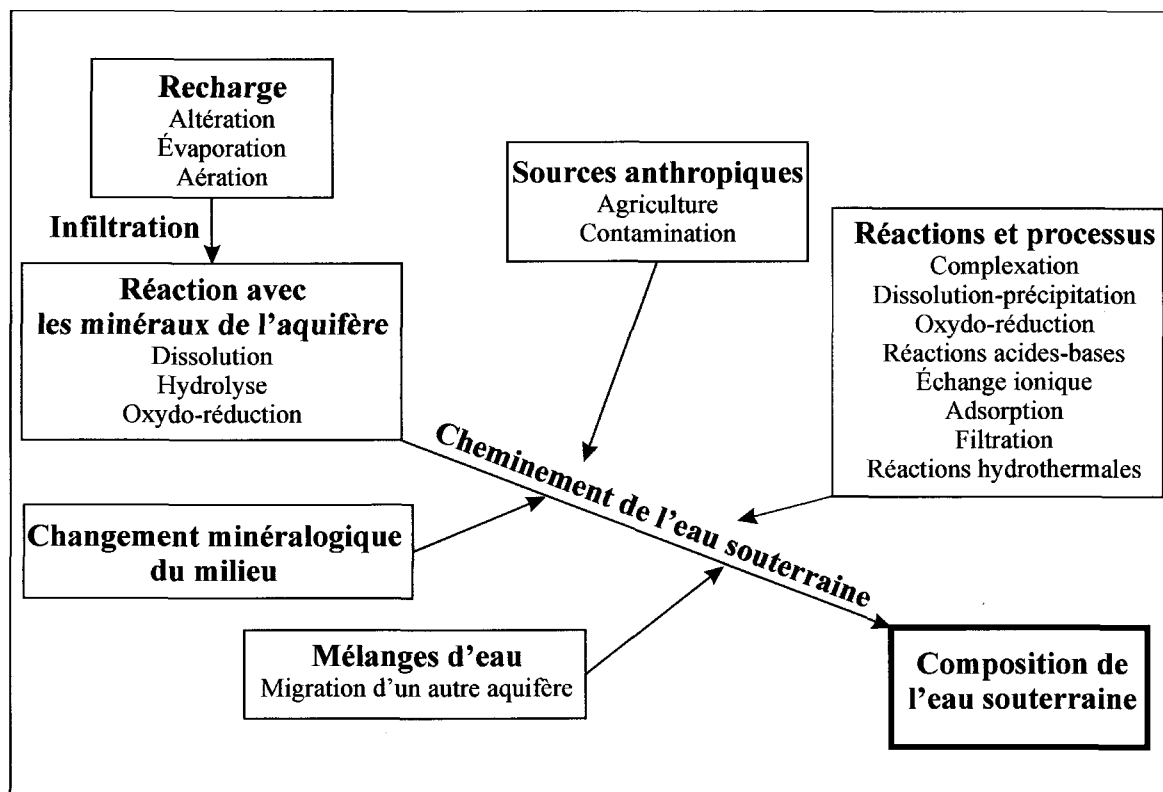


Figure 1.1. Réactions et processus géochimiques contrôlant la composition de l'eau souterraine dans un système aquifère régional (adaptée de Hounslow, 1995).

Plusieurs études ont identifié des processus et des réactions géochimiques permettant d'expliquer l'évolution de l'eau souterraine. Celles-ci sont basées sur les principes

d'équilibre chimique. Back et Hanshaw (1970) ont montré que la composition et la concentration des espèces dissoutes dans l'eau souterraine étaient reliées à la lithologie. Hanshaw et Back (1979) ont démontré que la composition des eaux souterraines de l'aquifère calcaire Floridien était influencée par les réactions impliquant le dioxyde de carbone, la calcite, l'aragonite, la dolomite et le gypse. Champ et al. (1979) ont observé une diminution du potentiel d'oxydo-réduction des zones de recharge vers les zones d'émergence dans un aquifère confiné. D'autres travaux importants ont été réalisés par Langmuir (1971) sur les aquifères carbonatés de l'est des États-Unis, Plummer et al. (1976a) sur les processus chimiques et physiques contrôlant la chimie des eaux souterraines dans l'aquifère carbonaté des Bermudes, Thorstenson et al. (1979) sur l'évolution géochimique des eaux souterraines dans l'aquifère Fox Hill du Dakota, Schwartz et al. (1981) sur le contrôle du système d'écoulement sur la géochimie de l'aquifère régional Milk River, et Edmunds et al. (1982) sur la géochimie des eaux souterraines d'un aquifère de grès en Angleterre.

Des cas hypothétiques ont aussi été étudiés pour illustrer les processus d'évolution de l'eau souterraine. Palmer et Cherry (1984) ont synthétisé les processus déterminant dans l'évolution de l'eau circulant à travers une séquence de roches sédimentaires. Hem (1985) présente plusieurs exemples sur les sources et les réactions chimiques des espèces dissoutes importantes dans les systèmes naturels. Back et al. (1993) présentent un cas similaire à la plaine côtière atlantique afin de démontrer le type de réactions pouvant se produire dans un système aquifère régional. Enfin, Stuyfzand (1999) décrit plusieurs séquences d'évolution de l'eau souterraine causées par l'écoulement.

Ces études utilisent la chimie inorganique pour aider à la compréhension de systèmes d'écoulement à l'échelle régionale. Bien que ces études reconnaissent l'effet du système d'écoulement sur l'évolution chimique de l'eau, la majorité de celles-ci sont de nature qualitative en ce qui concerne la relation entre l'écoulement et la géochimie. Enfin, l'utilisation combinée de la géochimie inorganique et isotopique fera évoluer de façon significative l'hydrogéochimie régionale.

### *1.1.3.3 Isotopes et traceurs environnementaux*

L'étude des isotopes de l'eau, des éléments dissous et des solides informe sur la qualité de l'eau, son évolution géochimique, les processus de recharge, l'interaction eau/roche, l'origine de la salinité, et les processus de contamination (Clark et Fritz, 1997). Les isotopes stables  $\delta^2\text{H}$  et  $\delta^{18}\text{O}$  sont largement utilisés pour déterminer, entre autre, l'origine des eaux et leur dynamique. Les isotopes radioactifs  ${}^3\text{H}$  et  ${}^{14}\text{C}$  sont utilisés dans la datation de l'eau souterraine, une information importante dans une étude hydrogéologique régionale. Le Tableau 1.1 présente une série d'isotopes stables, d'isotopes radioactifs et de traceurs utilisés en hydrogéologie. Les applications les plus communes, ainsi que des références d'utilisation, sont présentées pour chaque traceur. L'utilisation d'une combinaison d'isotopes est souvent l'approche utilisée pour comprendre et caractériser un système hydrogéologique. La section suivante présente des exemples d'études utilisant cette approche.

Hitchon et Friedman (1969) ont démontré, à l'aide de la géochimie et des isotopes  $\delta^2\text{H}$  et  $\delta^{18}\text{O}$ , que les mélanges d'eaux, l'interaction eau/roche, et l'ultrafiltration à travers des shales ont produit la composition chimique des eaux de formation dans le bassin sédimentaire de l'ouest canadien. Plummer et Back (1980) ont appliqué une approche d'équilibre de masse dans l'interprétation de l'évolution chimique des aquifères carbonatés Floridien et Madison. Avec ces exemples de terrain, ils ont montré que le couplage de l'équilibre de masse chimique avec les données isotopiques donne un meilleur contrôle sur l'identification des réactions et des vitesses d'écoulement dans un système naturel. Les travaux sur l'aquifère Milk River en Alberta, sont des exemples d'utilisation combinée de la géochimie et des isotopes afin de déterminer l'origine et l'âge de l'eau souterraine (Hendry et Schwartz, 1988; Drimmie et al., 1991). Matray et al. (1994) ont identifié l'origine d'eau de formation d'un aquifère carbonaté du Bassin de Paris par la géochimie et les isotopes  $\delta^2\text{H}$  et  $\delta^{18}\text{O}$ . Le Gal La Salle et al. (1996) ont utilisé la géochimie et les isotopes  $\delta^2\text{H}$ ,  $\delta^{18}\text{O}$ ,  $\delta^{13}\text{C}$  et  ${}^{14}\text{C}$  dans l'étude d'un aquifère du Bassin Aquitaine en France. Ils ont établi un lien entre les variations hydrogéochimiques et la lithologie et ont identifié des processus de dissolution, de dilution et de mélange.

Tableau 1.1. Isotopes, traceurs environnementaux et leurs applications

Traceurs	Applications
<b>Isotopes Stables</b>	
$\delta^2\text{H}$ et $\delta^{18}\text{O}$	<ul style="list-style-type: none"> <li>- Source, origine, temps de résidence et processus d'évolution des eaux souterraines (Long et al., 1988; Banner et al., 1989; Desaulniers et Cherry, 1989; Matray et al., 1994)</li> <li>- Mélanges d'eaux souterraines (Weaver et al., 1995)</li> <li>- Caractérisation de la recharge (Ayalon et al., 1998; Rosen et al., 1999; Cane et Clark, 1998; Landon et al., 2000; Lee et al., 1999; Abbott et al., 2000)</li> <li>- Diffusion dans les argiles (Desaulniers et al., 1981; Hiscock et al., 1996)</li> </ul>
$\delta^{13}\text{C}_{\text{CID}}$	<ul style="list-style-type: none"> <li>- Source du carbone inorganique dissous (Cane et Clark, 1998)</li> <li>- Correction des concentrations en <math>^{14}\text{C}</math> (Parkhurst et al., 1996)</li> </ul>
$\delta^{15}\text{N}$	<ul style="list-style-type: none"> <li>- Identification des sources de contamination au nitrate (Aravena et al., 1993; Kendall et McDonnell, 1998)</li> <li>- Étude de la dénitrification (Aravena et Robertson, 1998; Feast et al., 1998)</li> </ul>
$\delta^{37}\text{Cl}$	<ul style="list-style-type: none"> <li>- Traceur de la source de salinité (Kaufmann, 1993; Cloutier, 1994; Egginkamp, 1994)</li> </ul>
$^{87}\text{Sr}/^{86}\text{Sr}$	<ul style="list-style-type: none"> <li>- Interaction eau/roche, évolution (Starinsky et al., 1983; Frape et al., 1984; McNutt et al., 1987; Banner et Hanson, 1990; McNutt et al., 1990; Woods et al., 2000)</li> <li>- Origine du strontium dans le système (Singh et al., 1998; Jørgensen et al., 1999)</li> <li>- Traceur de l'écoulement (Johnson et al., 2000)</li> </ul>
<b>Isotopes Radioactifs</b>	
$^{3}\text{H}$ (tritium)	<ul style="list-style-type: none"> <li>- Datation de l'eau de 0 à 50 ans (<math>t_{1/2} = 12.43</math> ans) (Fritz et al., 1991)</li> <li>- Caractérisation de la recharge (Robertson et Cherry, 1989)</li> </ul>
$^{3}\text{H}-^{3}\text{He}$	<ul style="list-style-type: none"> <li>- Datation de l'eau de 0 à 50 ans (Solomon et al., 1992; Shapiro et al., 1999)</li> <li>- Traceur, milieu fracturé (Szabo et al., 1996; Aeschbach-Hertig et al., 1998)</li> </ul>
$^{14}\text{C}$	<ul style="list-style-type: none"> <li>- Datation de l'eau de 1000 à 40 000 ans (<math>t_{1/2} = 5715</math> ans) (Back et al., 1983; Plummer et al., 1990; Drimmie et al., 1991; Le Gal La Salle et al., 1996; Clark, et al., 1998)</li> <li>- Calage de modèles, taux de réaction et vitesse d'écoulement (Parkhurst et al., 1996)</li> </ul>
$^{36}\text{Cl}$	<ul style="list-style-type: none"> <li>- Datation de l'eau de 6000 à 1 200 000 (<math>t_{1/2} = 3 000 000</math> ans) (Phillips et al., 1986)</li> </ul>
<b>Autres Traceurs</b>	
CFC	<ul style="list-style-type: none"> <li>- Datation de l'eau et caractérisation de la recharge (Szabo et al., 1996; Plummer et al., 2000)</li> </ul>
Gaz nobles	<ul style="list-style-type: none"> <li>- Datation d'eau très vieille (Osenbrück et al., 1998)</li> <li>- Calage de modèles (Castro et al., 1998)</li> </ul>
Radon	<ul style="list-style-type: none"> <li>- Traceur, milieu fracturé (Cook et al., 1999)</li> </ul>

#### 1.1.3.4 Hydraulique et transport de masse en milieu fracturé

L'écoulement de l'eau souterraine en milieu fracturé s'effectue préférentiellement dans les discontinuités du milieu, tel les joints, fissures, fractures et plans de stratification. Le développement d'approches pour caractériser, représenter et modéliser l'écoulement en milieu fracturé est venue de plusieurs besoins, dont la recherche pour l'entreposage de

déchets radioactifs (Neretnieks, 1993; Bodvarsson et al., 1999), le transport de contaminant en milieu fracturé (Schmelling et Ross, 1989; Kueper et McWhorter, 1992), et la reconnaissance du rôle de la fracturation dans les argiles (Ruland et al., 1991; Harrison et al., 1992).

Deux approches pour simuler l'écoulement et le transport de masse en milieu fracturé supposent que l'écoulement est possible dans toutes les discontinuités. La première est de considérer le milieu fracturé comme un milieu poreux équivalent (MPE). Le milieu est alors représenté comme un milieu poreux continu. Des études de transport de contaminant ont représenté le milieu fracturé comme un MPE (Pankow et al., 1986; Berkowitz et al., 1988; Pohll et al., 1999). C'est aussi l'approche généralement utilisée dans les études régionales. La seconde approche représente le milieu fracturé comme un milieu à double porosité (McLaren et al., 2000). Cette approche permet de représenter globalement à la fois les fractures et la matrice. Dans le cas où le milieu est peu perméable, l'écoulement se fait principalement dans les fractures. La troisième approche, la fracturation discrète, représente chaque fracture individuellement (Therrien et Sudicky, 1996). Elle permet une représentation de l'écoulement et du transport de masse en milieux complexes, où toutes les discontinuités ne participent pas à l'écoulement.

Le transport de masse en milieu fracturé se fait par advection, dispersion et diffusion. Plusieurs études montrent que la diffusion peut avoir un rôle important sur la distribution de contaminants (Feenstra et al., 1984; Novakowski et Lapcevic, 1994; Parker et al., 1997). Ainsi, la diffusion pourrait être importante dans l'étude d'un système naturel. Un autre processus important est l'interaction entre l'eau et la roche lorsque l'eau souterraine circule dans le milieu fracturé. Cette interaction résulte en des échanges chimiques et isotopiques, des réactions entre l'eau et la matrice rocheuse (dissolution et précipitation) modifiant ainsi la géochimie de l'eau et la matrice. La compréhension des réactions chimiques (équilibre et cinétique) se produisant dans le système naturel est importante à la caractérisation de l'évolution de l'eau. Des modèles géochimiques ont été développés pour identifier et quantifier ces réactions.

Plusieurs méthodes hydrogéologiques, géophysiques, et des essais de traceurs ont été développés pour caractériser l'écoulement et le transport en milieu fracturé (Novakowski et Lapcevic, 1994; Cohen et al., 1996; Himmelsbach et al., 1998; Schulze-Makush et al., 1999; Dahan et al., 2000; Karasaki et al., 2000; Mayo et Koontz, 2000; Morin et al., 2000; Paillet et Reese, 2000). La modélisation de ces essais permet de déterminer des paramètres comme l'ouverture des fractures, la porosité de la matrice et la dispersion. Cook et al. (1996) ont caractérisé l'écoulement dans le roc fracturé avec les traceurs environnementaux CFC,  $^3\text{H}$  et  $^3\text{He}$ , et avec le radon (Cook et al., 1999). Schreiber et al. (1999) ont utilisé les faciès hydrochimiques pour caractériser l'écoulement dans un shale fracturé. Zanini et al. (2000) ont effectué des tests hydrauliques et un échantillonnage hydrogéochimique multi-niveaux avec obturateurs pour caractériser un système d'écoulement en milieu fracturé.

#### *1.1.3.5 Les modèles géochimiques*

Le développement de la modélisation (modèles d'écoulement et modèles géochimiques) a apporté à l'hydrogéologue de nouveaux outils d'interprétation et de compréhension des systèmes hydrogéologiques naturels. L'utilisation combinée de ces modèles permet de quantifier les liens entre l'évolution chimique des eaux souterraines et l'écoulement.

Parkhurst et Plummer (1993) identifient quatre objectifs d'utilisation de modèles géochimiques dans un système d'écoulement régional : 1) déterminer les réactions géochimiques dominantes; 2) quantifier dans quelle mesure ces réactions se produisent; 3) prédire le comportement de contaminants inorganiques; et 4) estimer les directions et les vitesses d'écoulement de l'eau souterraine. Le Tableau 1.2 présente les différents types de modèles géochimiques et des références d'application pour chaque modèle : les modèles de spéciation, d'équilibre de masse, de transfert de masse et de transport réactif de masse.

Tableau 1.2. Modèles géochimiques

Modèle	Description sommaire et références d'application
<b>Modèle de Spéciation</b>	
	<ul style="list-style-type: none"> <li>- Calculer les propriétés thermodynamiques de l'eau, incluant la molalité et l'activité des espèces dissoutes (ions libres, molécules neutres, complexes) ainsi que l'indice de saturation des minéraux.</li> <li>- Les données d'entrée sont le pH, le pe et les espèces chimiques en solution.</li> <li>- L'indice de saturation donne une information thermodynamique concernant quels minéraux peuvent ou ne peuvent pas précipiter ou se dissoudre, permettant de contraindre la série de réactions géochimiques possibles dans un système d'écoulement régional.</li> </ul>
WATSPEC (Wigley, 1977)	<ul style="list-style-type: none"> <li>- Calcule les espèces dissoutes en solution et leurs activités.</li> <li>- Calcule l'indice de saturation de l'eau par rapport à différents minéraux.</li> </ul>
<b>Modèle d'Équilibre de Masse</b>	
	<ul style="list-style-type: none"> <li>- Calculer le transfert de masse entre les phases liquides et solides le long de l'écoulement, des zones de recharge aux zones d'émergence, déterminant ainsi la nature et l'étendue des réactions chimiques dans le système d'écoulement.</li> <li>- Identifier les minéraux qui réagissent, et déterminer la quantité qui se dissout ou précipite.</li> </ul>
NETPATH (Plummer et al., 1994)	<ul style="list-style-type: none"> <li>- Interprète les réactions géochimiques d'équilibre de masse entre la composition initiale et finale le long d'une ligne d'écoulement.</li> <li>- Utilise les données géochimiques et isotopiques.</li> <li>- Processus considérés : dissolution, précipitation, échange ionique, oxydation/réduction, dégradation de composés organiques, réactions incongruentes, échanges gazeux, mélanges, évaporation, dilution, fractionnement et échange isotopique.</li> <li>- Corrections dans la détermination de l'âge de l'eau souterraine avec le <math>^{14}\text{C}</math> (tient compte des réactions géochimiques qui peuvent produire des pertes ou gains de carbone, ainsi que des effets de fractionnement).</li> <li>- Applications : Siegel et Anderholm, 1994; Plummer et al., 1994; Glynn et Brown, 1996; Parkhurst et al., 1996; Parkhurst, 1997; Kauffman et al., 1998; Katz et al., 1998</li> </ul>
<b>Modèle de Transfert de Masse</b>	
	<ul style="list-style-type: none"> <li>- Calculer l'équilibre chimique statique pour un système eau/solide.</li> <li>- Ces calculs prennent en considération l'échange ionique, la sorption d'ions, la dissolution et la précipitation de minéraux ainsi que les réactions de la phase gazeuse.</li> </ul>
PHREEQUE (Parkhurst et al., 1980)	<ul style="list-style-type: none"> <li>- Programme de calcul d'équilibres chimiques.</li> <li>- Calcule le pH, potentiel oxydo-réduction et le transfert de masse en fonction de la réaction.</li> <li>- Simule les effets des interactions eau/roche et les mélanges d'eau.</li> <li>- Applications : Plummer et al., 1983; Parkhurst et al., 1980; Back et al., 1983; Parkhurst et al., 1996; Toran et Saunders, 1999</li> </ul>
PHRQPITZ (Plummer et al., 1988)	<ul style="list-style-type: none"> <li>- Calcul d'équilibres chimiques avec des solutions très concentrées.</li> <li>- Incorpore le modèle d'interaction ionique de Pitzer pour le calcul des coefficients d'activités ioniques.</li> <li>- Applications : Siegel et Anderholm, 1994; Weaver et al., 1995; Xue et al., 2000</li> </ul>
MINTEQA2/PRODEFA2 (Allison et al., 1991)	<ul style="list-style-type: none"> <li>- Programme de calcul d'équilibres chimiques, même type que PHREEQUE.</li> <li>- Applications : Tellam, 1996</li> </ul>
EQ3/6 (Wolery, 1992)	<ul style="list-style-type: none"> <li>- Modèle de spéciation et de transfert de masse.</li> <li>- Applications : Xu et al., 1998</li> </ul>

Tableau 1.2. (suite)

Modèle	Description sommaire et références d'application
<b>Modèle de Transport Réactif de Masse</b>	
PHREEQM (Appelo et Postma, 1993)	<ul style="list-style-type: none"> <li>- Liens, plus ou moins complexes, entre les modèles de transfert de masse et les modèles d'écoulement de l'eau souterraine.</li> <li>- Ce sont des modèles dynamiques.</li> <li>- Un des buts de ces modèles est de prédire l'évolution chimique lors de l'écoulement de l'eau souterraine.</li> </ul>
PHREEQC (Parkhurst et Appelo, 1999)	<ul style="list-style-type: none"> <li>- PHREEQUE est le sous modèle d'équilibre géochimique</li> <li>- Transport de masse 1D (modèle <i>mixing cell</i>)</li> <li>- Advection simulée en déplaçant le contenu d'une cellule à la suivante</li> <li>- Considère la dispersion et la diffusion (mélange une fraction du contenu d'une cellule avec la cellule précédente ou suivante)</li> <li>- Applications : Appelo et Postma, 1993; Appelo, 1994; Glynn et Brown, 1996</li> </ul>
3DHYDROGEOCHEM (Yeh et Cheng, 1999)	<ul style="list-style-type: none"> <li>- Calcul de spéciation et d'indice de saturation.</li> <li>- Transport hydrogéochemique 1D par advection pour les réactions irréversibles, le mélange de solutions, l'équilibre minéral/gaz, les réactions de complexation de surface, et les réactions d'échanges ioniques.</li> <li>- Considère la cinétique des réactions chimiques.</li> <li>- Capacité de modélisation inverse.</li> <li>- Applications : Parkhurst, 1995; Glynn et Brown, 1996; Parkhurst, 1997; Van Breakelen et al., 1998; Stigter et al., 1998; Appelo et al., 1999; Postma et Appelo, 2000</li> </ul>
TOUGH2 (Pruess et al., 1999)	<ul style="list-style-type: none"> <li>- Modèle numérique d'éléments finis en 3 dimensions.</li> <li>- Simule le transport chimique, en tenant compte de la température et de l'effet de densité.</li> <li>- Représentation d'un milieu hétérogène, anisotrope, saturé/non saturée.</li> <li>- Conditions d'écoulement en régimes permanent ou transitoire.</li> <li>- Modèle fortement couplé (écoulement, transport chimique et transfert de chaleur) en régime permanent.</li> <li>- Modèle faiblement couplé en régime transitoire.</li> <li>- Utilise un modèle d'équilibre chimique.</li> <li>- Réactions chimiques : formation de complexes, adsorption, échange ionique, précipitation/dissolution, oxydation/réduction et acide/base.</li> <li>- Applications : Cheng et Yeh, 1998; Keating et Bahr, 1998; Yeh et Cheng, 1999</li> </ul>
FRAC3DVS (Ghogomu et Therrien, 2000)	<ul style="list-style-type: none"> <li>- Modèle numérique d'écoulement multicomposante et multiphasé non-isotherme.</li> <li>- Version TOUGHREACT pour le transport réactif.</li> <li>- Simulation en 1, 2 ,ou 3 dimensions pour un milieu poreux ou fracturé.</li> <li>- Applications : White et al., 1998; Xu et al., 1998; Pruess et al., 1999; Doughty, 1999</li> </ul>
-	
-	

Le développement et l'application de modèles de transport réactif est un domaine actif de recherche. Lichtner (1996) et Steefel et MacQuarrie (1996) présentent les bases théoriques, les approches et les méthodes numériques utilisées dans la modélisation du transport réactif. L'application de ces modèles porte sur des cas théoriques comme la dissolution de la pyrite (White et al., 1998), les processus de dédolomitisation (Ayora et al., 1998), et sur l'étude de systèmes fracturés (Steefel et Lichtner, 1998; Lichtner, 1999). Il y a aussi dans la littérature des applications sur des sites spécifiques, comme la formation de gisements (Xu et al., 1998; Bäverman et al., 1999), l'étude du drainage minier acide (Gerke, 1998; Bain et al., 2000), et l'étude pour l'entreposage de déchets radioactifs (Viswanathan et al., 1998). Ces modèles ont maintenant des capacités importantes, mais leur utilisation dans un système d'écoulement naturel est encore limitée.

Un défi de ce domaine de recherche est maintenant d'intégrer et d'adapter ces modèles dans l'étude de systèmes d'écoulement naturel. Une application géologique est présentée par Glynn et Brown (1996). Ils ont utilisé une approche de modélisation inverse dans le but d'identifier les réactions se produisant dans le drainage minier acide, pour ensuite effectuer des simulations de transport réactif. Van Breakelen et al. (1998) ont utilisé le modèle de transport réactif PHREEQC pour simuler les changements de la qualité de l'eau suite à un système de recharge naturel. Leur étude est assez unique dans l'utilisation des données de terrain pour la simulation du transport réactif. Enfin, Keating et Bahr (1998) ont utilisé le transport réactif pour contraindre un modèle régional d'écoulement de l'eau souterraine.

#### *1.1.3.6 L'hydrogéochimie régionale, une approche intégrée*

Depuis quelques années, la reconnaissance de la contamination diffuse (Back et al., 1993), le besoin de mieux gérer la ressource (Fagnan et al., 1999; Savard et al., 2000), l'augmentation des besoins en eau des villes (Özler, 1999; Guvanasen et al., 2000), et des problèmes d'intrusions d'eaux salines (Zubari, 1999), ont, entre autre chose, souligné l'importance des études hydrogéologiques régionales. Un autre fait marquant est la

meilleure définition du rôle déjà connu des eaux souterraines dans les processus géologiques, tel la formation de gisements (Garven et al., 1999), la diagenèse minérale (Machel, 1999), et la salinisation des sols (Salama et al., 1999; Valenza et al., 2000). Ingebritsen et Sanford (1998) ont publié un livre, et Tóth (1999), une publication synthèse sur le sujet. Les études régionales bénéficient des contributions et des concepts développés dans les travaux à l'échelle locale, par exemple, pour le transport en milieu fracturé. Il est important de poursuivre la recherche sur l'application de ces travaux aux études régionales et aux systèmes aquifères complexes.

Les études hydrogéochimiques intégrées de systèmes d'écoulement régional sont relativement peu nombreuses. Ces études utilisent, à différents degrés, la géologie, l'hydraulique, la géochimie inorganique et isotopique, et la modélisation dans l'étude et la compréhension de systèmes aquifères complexes. Le programme RASA (*Regional Aquifer-System Analysis*) du Service géologique des États-Unis (*U.S. Geological Survey*) a permis la réalisation de plusieurs études intégrées de systèmes aquifères majeurs des États-Unis (Henderson, 1985; Knobel et Phillips, 1988; Eberts et George, 2000). Panno et al. (1994) ont utilisé les ions majeurs et la géochimie isotopique pour développer un modèle conceptuel de l'écoulement dans un aquifère régional rocheux de l'Illinois. Vuillemenot et Guerin (1995) ont utilisé des données géologiques, tectoniques, hydrogéologiques, chimiques et thermométriques afin de caractériser un aquifère carbonaté (Bassin de Lodève, France). Enfin, l'évaluation de la qualité de l'eau souterraine du *Central Oklahoma Aquifer* par Parkhurst et al. (1996) est un excellent exemple d'approche intégrée.

#### 1.1.4 Objectifs du projet de recherche

Ces travaux de doctorat reposent sur une approche intégrée pour étudier l'hydrogéochimie des eaux souterraines du système aquifère des Basses-Laurentides. Les objectifs principaux de ce projet de recherche étaient les suivants :

- 1) Évaluer la qualité régionale des eaux souterraines du système aquifère des Basses-Laurentides.
- 2) Déterminer l'influence des contextes hydrogéologiques et géologiques sur la géochimie des eaux souterraines.
- 3) Identifier l'origine des eaux souterraines du système aquifère des Basses-Laurentides.
- 4) Évaluer différentes méthodes pour classifier et analyser les données hydrogéochimiques, incluant des méthodes classiques dont le regroupement en types d'eau dominants et mixtes, ainsi que des méthodes moins couramment utilisées dont l'analyse statistique multivariable.
- 5) Identifier et comprendre les processus géochimiques principaux contrôlant la géochimie des eaux souterraines et son évolution dans l'espace et le temps.
- 6) Présenter un modèle conceptuel intégré de l'évolution hydrogéochimique des eaux souterraines du système aquifère de roches sédimentaires des Basses-Laurentides.

Le projet avait aussi pour objectif le développement d'une méthodologie de caractérisation hydrogéochimique régionale pour un système aquifère de roc fracturé. La méthodologie développée utilise les approches suivantes :

- 1) échantillonnage de l'eau souterraine, régionale et verticale, des zones de recharge aux zones d'émergence;
- 2) caractérisation géochimique de l'ensemble des lithologies, dans les différents contextes géologiques et hydrogéologiques;
- 3) utilisation combinée de la géochimie inorganique et isotopique;
- 4) caractérisation isotopique des précipitations locales.

Des techniques spécifiques ont dû être développées afin d'acquérir les données scientifiques nécessaires pour répondre aux objectifs précédents. Ce projet avait donc aussi pour objectifs (1) de développer un système d'échantillonnage multi-niveaux dans le roc fracturé, et (2) de développer un système de collecte de précipitations pour les isotopes stables de l'eau et d'implanter un réseau de stations dans la région d'étude.

Pour arriver à la compréhension d'un système aquifère complexe comme celui des Basses-Laurentides, ce doctorat avait également pour objectif d'intégrer les interprétations scientifiques de l'hydrogéochimie aux autres volets du projet de cartographie hydrogéologique régionale. Les objectifs étaient que l'hydrogéochimie contribue au développement du modèle conceptuel de l'écoulement de l'eau souterraine, à la compréhension de la dynamique du système aquifère, de la distribution de la recharge et de la vulnérabilité du système aquifère.

## 1.2 DESCRIPTION DE LA RÉGION D'ÉTUDE

La région d'étude, présentée à la Figure 1.2, est située sur la rive nord du fleuve Saint-Laurent, au nord-ouest de Montréal. Le territoire étudié, d'une superficie d'environ 1500 km<sup>2</sup>, appartient à la région géographique des Basses-Laurentides, ainsi qu'à la région physiographique des Basses-Terres du Saint-Laurent. Les Basses-Terres du Saint-Laurent ont une topographie de plaine, marquée par la présence des collines montérégienennes reliées aux intrusions crétacées. Il y a deux intrusions crétacées dans les Basses-Laurentides, les collines d'Oka et de Saint-André. La région d'étude est limitée au nord par les Laurentides, de la province géologique du Grenville du Bouclier Canadien. La rivière des Outaouais, le lac des Deux Montagnes et la rivière des Milles Îles sont des limites d'eau de surface au sud-ouest, au sud, et au sud-est respectivement. À l'est, la limite du territoire se retrouve dans le bassin de la rivière Mascouche (voir la Fig. 3.1; Chapitre 3).

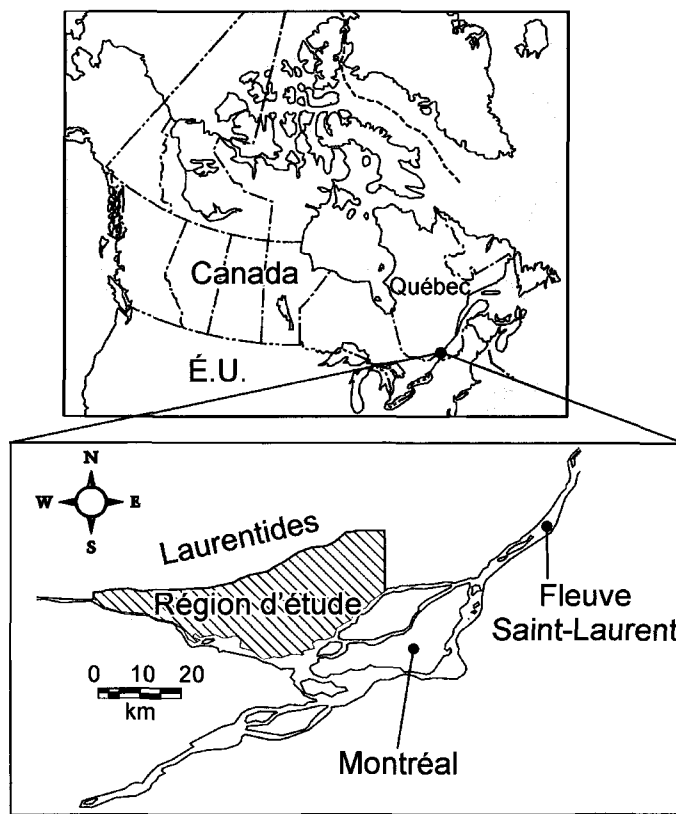


Figure 1.2. Locatisation de la région d'étude.

### 1.2.1 Contexte géologique

Le système aquifère des Basses-Laurentides fait partie de la province géologique de la plate-forme du Saint-Laurent. Les roches de cette plate-forme appartiennent à des formations sédimentaires autochtones d'âges Cambrien et Ordovicien, et sont disposées à peu près horizontalement. Ces roches, formées de grès, dolomies, calcaires et shales, reposent en discordance sur les roches ignées et métamorphiques précambriniennes de la province géologique du Grenville. La géologie de la plate-forme du Saint-Laurent est décrite dans les rapports géologiques de Clark (1972) et de Globensky (1987). Le Chapitre 3 de cette thèse présente la carte géologique (Fig. 3.1), ainsi qu'une description détaillée de la géologie du Paléozoïque et du Crétacé pour la région d'étude (Section 3.2.1.1).

Les formations sédimentaires affleurent rarement dans la région d'étude, car celles-ci sont généralement recouvertes par des sédiments du Quaternaire. Ceux-ci sont principalement des sédiments glaciaires (till), des sédiments fluvioglaciaires (sable et gravier), et des sédiments marins (argile de la Mer de Champlain) (Bolduc et Ross, 2001). Le till est présent en surface, recouvrant les formations sédimentaires dans les secteurs à topographie élevée. Le till, ainsi que des sédiments fluvioglaciaires, sont aussi présents sous les sédiments marins de la Mer de Champlain. Les sédiments de la Mer de Champlain peuvent atteindre une épaisseur de plus de 80 m dans les vallées enfouies de la région. Le Chapitre 3 de cette thèse présente une description de la géologie du Quaternaire, incluant les dépôts reliés à la Mer de Champlain pour la région d'étude (Section 3.2.1.2).

### 1.2.2 Contexte hydrogéologique

La Figure 3.2a (Chapitre 3) est la carte de conditions hydrogéologiques modifiée de Hamel et al. (2001). La région d'étude est divisée en secteurs où le système aquifère est en conditions non-confinées ou semi-confinées, et en secteurs où le système aquifère est en conditions confinées. Les secteurs en conditions non-confinées ou semi-confinées sont

généralement à topographie élevée, avec présence d'affleurements rocheux ou de sédiments perméables. Ces conditions caractérisent les zones préférentielles de recharge du système aquifère. Les secteurs en conditions confinées sont les régions caractérisées par la présence d'accumulations importantes de sédiments marins quaternaires de faible perméabilité, les argiles de la Mer de Champlain. Tel que mentionné précédemment, celles-ci coïncident avec les principales vallées enfouies de la région.

Les unités hydrogéologiques présentes dans la région d'étude incluent les sédiments perméables en surface (till) dans les secteurs non confinés, l'aquitard (argile de la Mer de Champlain) qui confine le système aquifère, les sédiments perméables (sable et gravier) sous les argiles de la Mer de Champlain dans les vallées enfouies, ainsi que le système aquifère de roches sédimentaires. Le système aquifère a été divisé en deux unités distinctes sur la base de leurs propriétés hydrogéologiques et géologiques : une unité de roche très fracturée et une unité de roche fracturée. L'unité de roche très fracturée caractérise les premiers mètres des roches sédimentaires. Il est possible de retrouver une unité mixte lorsque l'unité de roche très fracturée est en contact avec l'unité de sédiments perméables sous les argiles. La carte piézométrique de la Figure 3.3 (Chapitre 3) montre que l'écoulement régional de l'eau souterraine se fait principalement du nord au sud.

La Section 3.2.2 (Chapitre 3) de la thèse présente une description détaillée de la répartition des conditions hydrogéologiques, du modèle conceptuel de l'écoulement de l'eau souterraine (Fig. 3.2b), ainsi que les caractéristiques des différentes unités hydrogéologiques dans la région d'étude.

## 1.3 MÉTHODOLOGIE

La caractérisation hydrogéochimique régionale d'un système aquifère implique la détermination de la nature géochimique et isotopique de l'eau souterraine le long du système d'écoulement, ainsi que des différentes sources qui peuvent influencer la composition des eaux souterraines. Ces sources vont des précipitations (pluie et neige) dans les zones de recharge, à l'eau interstitielle des argiles marines dans les vallées enfouies. Cette approche a été suivie dans la planification des travaux de terrain et des analyses en laboratoire. Le Tableau 3.3 (Chapitre 3) résume l'ensemble du programme de caractérisation hydrogéochimique.

### 1.3.1 Intégration du projet de recherche dans le projet de cartographie hydrogéologique

L'approche intégrée de ces travaux de doctorat est due au caractère multidisciplinaire du projet de «caractérisation hydrogéologique régionale du système aquifère fracturé du sud-ouest du Québec» de la CGC. Cette étude hydrogéochimique a ainsi bénéficié, à différents degrés, des travaux et des résultats obtenus dans les autres volets du projet de cartographie hydrogéologique régionale, dont la caractérisation géologique des unités rocheuses et des sédiments du Quaternaire, la caractérisation hydrogéologique et l'étude de la recharge. Le Tableau 1.3 résume les données produites par ces différents travaux, et l'utilité de ces données spécifiquement pour ce projet de recherche.

Tableau 1.3. Caractérisation, travaux et données produites dans le cadre du projet de «caractérisation hydrogéologique régionale du système aquifère fracturé du sud-ouest du Québec» de la CGC

Caractérisation et références	Travaux	Utilité spécifique pour ce projet de recherche
<b>Géologie du roc</b> (Rocher et al., sous presse)	- Cartographie géologique - Stratigraphie des forages au roc	- Lithologie des sites échantillonnés - Lithologie des échantillons multi-niveaux
<b>Étude de la fracturation</b> (Lemieux, 2002)	- Étude des carrières - Étude des carottes de forages	- Information sur la représentation des fractures dans le système aquifère
<b>Géologie du Quaternaire</b> (Bolduc et Ross, 2001; Ross et al., 2003)	- Cartographie du Quaternaire - Modèle 3D des formations quaternaires - Stratigraphie des forages	- Définition des contextes hydrogéologiques - Évaluation de la vulnérabilité - Information stratigraphique pour les sites échantillonnés - Échantillons d'argile marine
<b>Hydrogéologie</b> (Fagnan et al., 2001; Karanta et al., 2001; Nastev et al., 2001)	- Relevés piézométriques - Essais de pompage locaux - Essais de perméabilité <i>Slug test</i> - Essais à pression constante (essais Lugeon)	- Choix des sites d'échantillonnage - Information sur le comportement hydrogéologique du roc fracturé - Propriétés hydrauliques des unités - Données de transmissivité par rapport à la profondeur
<b>Étude de la recharge</b> (Hamel et al., 2001)	- Essais d'infiltration - Estimation de la recharge	- Propriétés hydrogéologiques du till - Distribution de la recharge
<b>Géophysique</b> (Ross et al., 2001; Etienne, 2002)	- Profil sismique à haute résolution - Diagraphie sur les puits au roc	- Définition des vallées enfouies se trouvant dans les sections
<b>Hydrogéochimie</b> (Bourque et al., 2001; Cloutier et al., 2001)	- Échantillonnage régional - Échantillonnage avec le système multi-niveaux <sup>a</sup> - Échantillonnage des précipitations (pluie et neige) <sup>a</sup> - Échantillonnage des eaux d'infiltration <sup>a</sup>	- Information géochimique régionale - Information géochimique verticale - Caractérisation isotopique de la recharge

<sup>a</sup> Travaux sous la responsabilité de l'auteur.

### 1.3.2 Échantillonnage de l'eau souterraine

L'objectif de l'échantillonnage est de caractériser l'hydrogéochimie de l'eau souterraine selon ses divers cheminements possibles. Tel que mentionné précédemment, l'approche utilisée consiste à échantillonner l'eau souterraine des zones de recharge présumées, suivant les lignes d'écoulement jusqu'aux zones d'émergence, tout en caractérisant l'hydrogéochimie de l'ensemble des lithologies, dans les différents contextes géologiques et hydrogéologiques.

#### 1.3.2.1 Méthodes d'échantillonnage de l'eau souterraine

Pour réaliser les objectifs de l'échantillonnage, deux méthodes ont été adoptées. La première est l'échantillonnage régional, une méthode conventionnelle qui consiste à pomper l'eau de toute la section ouverte à l'écoulement. Cette méthode a permis d'assurer la couverture régionale par l'échantillonnage de puits municipaux, de puits privés et de puits d'observation. L'échantillonnage régional était sous la responsabilité d'Édith Bourque. La planification de l'échantillonnage, le choix des sites, ainsi que les travaux d'échantillonnage ont été réalisés en étroite collaboration avec l'auteur. La seconde méthode, l'échantillonnage avec le système multi-niveaux, était sous la responsabilité de l'auteur. Celle-ci consiste à échantillonner plusieurs niveaux de puits ouverts au roc, afin d'étudier les variations de qualité d'eau en fonction de la profondeur. La combinaison des deux méthodes d'échantillonnage donne ainsi une troisième dimension à la caractérisation hydrogéochimique du système aquifère.

Le choix des sites d'échantillonnage a été fait de façon à assurer une caractérisation des principales unités hydrogéologiques et des sources d'approvisionnement existantes. Les puits échantillonnés avec le système multi-niveaux sont des puits au roc existants ou des puits forés dans le cadre du projet de «caractérisation hydrogéologique régionale du système aquifère fracturé du sud-ouest du Québec» de la CGC. Pour ces nouveaux puits, le choix des sites a été fait en collaboration avec l'ensemble de l'équipe de recherche, afin

que chaque forage puisse répondre à plusieurs objectifs du projet, dont la caractérisation du roc et du Quaternaire, de l'hydrogéologie et des propriétés géophysiques.

### *1.3.2.2 Travaux d'échantillonnage*

L'échantillonnage régional s'est effectué en trois périodes : mars 1999, juillet à octobre 1999 et juin à août 2000. L'échantillonnage avec le système multi-niveaux a été réalisé de juin à août 2000. Les paramètres physico-chimiques qui évoluent après l'échantillonnage ont été analysés sur le terrain, et sont présentés au Tableau 1.4. Les puits étaient purgés jusqu'à ce que les mesures des paramètres physico-chimiques soient stables avant de procéder à l'échantillonnage. Le Tableau 1.5 montre l'ensemble des paramètres pour lesquels les échantillons d'eau souterraine ont été prélevés, ainsi que les protocoles d'échantillonnage. L'Appendice du Chapitre 3 donne plus de détails sur les protocoles d'échantillonnage. L'analyse complète est nécessaire afin de vérifier le respect des critères de qualité d'eau de Santé Canada (2001). L'analyse des espèces dissoutes et des isotopes est importante pour l'interprétation des processus géochimiques, et nécessaire pour la modélisation géochimique. Des duplicata ont été prélevés pour environ 7% des échantillons.

Tableau 1.4. Paramètres physico-chimiques analysés sur le terrain

Paramètre (unité)	Méthode d'analyse	Précision	Critère de stabilité <sup>a</sup>
Température (°C)	Thermomètre en verre	± 0,1	± 0,2
pH	Sonde YSI modèle 63 et multiparamètres	± 0,1	± 0,2
Conductivité électrique ( $\mu\text{S}/\text{cm}$ )	Sonde YSI modèle 63 et multiparamètres	± 2 %	± 4 %
Oxygène dissous (mg/L) <sup>b</sup>	Sonde YSI modèle 95 et multiparamètres	± 0,2 mg/L	± 0,4 mg/L
Potentiel d'oxydo-réduction (mV)	Sonde redox ORP d'Hanna (HI 98201)	± 10 mV	± 20 mV

<sup>a</sup> Observé durant la purge, échantillonnage avec le système multi-niveaux.

<sup>b</sup> Pour l'échantillonnage avec le système multi-niveaux, les lectures d'oxygène dissous ont été effectuées avec une cellule fermée.

Tableau 1.5. Paramètres pour lesquels les échantillons d'eau souterraine ont été prélevés

Paramètres	Bouteille <sup>a</sup>	Préservation	Filtration (0,45 µm)
Ag, Al, As, <b>B</b> , <b>Ba</b> , Ca, Cd, Cr, Cu, Fe, K, Li, Mg, Mn, Na, Ni, Pb, Se, Si, Sr, U, Zn	125 ml, P	Acide nitrique	oui
<b>Cl</b> , F, SO <sub>4</sub> , Alcalinité totale, Couleur	500 ml, P	non	non
Nutrients : NO <sub>3</sub> , NH <sub>4</sub> , PO <sub>4</sub>	125 ml, P	Acide sulfurique	oui
CN	125 ml, P	NaOH	non
Br, I	125 ml, P	non	non
<b>CID, COD</b>	125 ml, P	non	non
Sulfures	250 ml, P	Acétate de zinc + NaOH	non
Hg	250 ml, P	Acide chromique	oui
Coliformes totaux et fécaux	250 ml, P	non	non
δ <sup>2</sup> H et δ <sup>18</sup> O	60 ml, P	non	non
δ <sup>13</sup> C <sub>CID</sub>	250 ml, V	Chlorure de mercure	oui
<sup>87</sup> Sr/ <sup>86</sup> Sr <sup>b</sup>	1 L, P	non	non
<sup>3</sup> H <sup>b</sup>	1 L, P	non	non
<sup>14</sup> C <sup>b</sup>	1 L, P	non	non

Pour l'échantillonnage avec le système multi-niveaux, seuls les paramètres en caractères gras ont été analysés.

<sup>a</sup> P = Bouteille en plastique, V = Bouteille en verre

<sup>b</sup> Analyses effectuées sur quelques sites d'échantillonnage sélectionnés.

Les travaux d'échantillonnage régional ont permis de prélever de l'eau souterraine à 153 sites, jusqu'à une profondeur d'environ 140 m. Les sites échantillonnés proviennent de l'ensemble des unités hydrostratigraphiques perméables. Le Tableau 1.6 indique la provenance et le nombre d'échantillons prélevés lors de la caractérisation régionale et avec le système multi-niveaux. Les caractéristiques des puits échantillonnés avec le système multi-niveaux sont résumées au Tableau 1.7. La Carte 2.1 (Appendice H) montre la distribution, l'identification, ainsi que la provenance, des sites échantillonnés en 1999 et 2000. Les sites échantillonnés avec le système multi-niveaux y sont aussi indiqués. Les 7 échantillons rejetés (voir Tableau 1.6) ne sont pas présentés sur la Carte 2.1 (Appendice H), mais ceux-ci le sont dans les tableaux de données de l'Appendice A.

L'échantillonnage a été fait dans les différentes formations sédimentaires du Paléozoïque, et les roches du Grenville dans les collines d'Oka. La Carte 2.15 (Appendice H) montre la relation entre les sites échantillonnés et la géologie, alors que la carte 2.16 (Appendice H) montre la relation entre les sites échantillonnés et le contexte hydrogéologique, et la Figure 3.3 (Chapitre 3) montre la relation entre les sites échantillonnés et la direction de l'écoulement de l'eau souterraine. Enfin, l'Appendice A présente l'ensemble des données hydrogéochimiques, ainsi que les caractéristiques de chaque site d'échantillonnage, pour l'échantillonnage régional et multi-niveaux.

Tableau 1.6. Méthode d'échantillonnage et provenance des échantillons d'eau souterraine prélevés en 1999 et 2000

Méthode d'échantillonnage	Provenance des échantillons	Nombre d'échantillons
<b>Caractérisation régionale</b>	Roc Sédiments de surface Sédiments sous l'argile Mixte <sup>a</sup> Source captée Échantillons rejetés <sup>b</sup>	115 7 13 9 2 7
	Total	153
<b>Système multi-niveaux</b>	17 puits au roc (voir Tableau 1.7)	72 niveaux

<sup>a</sup> L'unité mixte est composée de l'unité de roche très fracturée en contact avec l'unité de sédiments perméables sous l'argile.

<sup>b</sup> Les échantillons rejetés ont une erreur d'équilibre cations/anions supérieure à 10%.

Tableau 1.7. Caractéristiques des puits au roc échantillonnés avec le système multi-niveaux

Site <sup>a</sup>	Nom du puits	Année forée, technique <sup>b</sup> et diamètre	Formation géologique	Longueur tubée (m)	Profondeur totale (m)	Intervalle ouvert au roc (m)	N
S77	Fromagerie	1995, 2, 6"	Covey Hill	63,2	141,5	78,3	5
SAP	Montée-Barette	1999, 1, 3"	Beauharnois	23,0	99,7	76,7	3
S84	Montée-Lavigne	2000, 2, 6"	Cairnside	10,5	81,1	70,6	5
S124	P-9	1984, 2, 6"	Chazy	16,5	56,7	40,2	4
S117	PE-2	1988, 2, 8"	Beauharnois Grenville	30,3	85,1	54,8	4
S127	R-3	1973, 2, 6"	Beauharnois	21,5	89,6	68,1	4
S26	R-13	1973, 2, 6"	Chazy	21,5	89,4	67,9	5
S125	R-14	1973, 2, 6"	Beauharnois	5,6	48,3	42,7	4
S126	R-15	1973, 2, 6"	Grenville	6,7	89	82,3	4
S129	R2-70	1970, 2, 8"	Thérèsa	9	45,5	36,5	3
S130	Rivière du Nord	1999, 1, 3"	Thérèsa	47,8	117,1	69,3	6
S140	Sintra	2000, 2, 6"	Chazy	1,2	61,9	60,7	2
S46	Saint-Benoît	2000, 2, 6"	Covey Hill	30,5	104,6	74,1	5
S85	Saint-Hermas	2000, 1, 3"	Cairnside	48	91,6	43,6	3
S123	Saint-Janvier	2000, 2, 8"	Beauharnois	16	73,2	57,2	5
S55	Saint-Louis	2000, 1, 3"	Trenton	11,0	91,7	80,7	4
S144	Saint-Vincent	1999, 2, 6"	Covey Hill	21	110,7	89,7	6

N : Nombre de niveaux échantillonnés par puits.

Les puits complétés en 1999 et 2000 ont été forés dans le cadre du projet de «caractérisation hydrogéologique régionale du système aquifère fracturé du sud-ouest du Québec» de la CGC.

<sup>a</sup> Identification du site correspondant à celle utilisée sur la Carte 2.1 (Appendice H), ainsi que dans les tableaux de données de l'Appendice A.

<sup>b</sup> 1 = Forage à diamant avec carottage, 2 = Forage à marteau fond de trou.

### 1.3.2.3 Système d'échantillonnage multi-niveaux et protocole suivi

Un système aquifère de roc fracturé est un milieu complexe à caractériser. Un puits ouvert au roc sur plusieurs dizaines de mètres peut intercepter différentes formations géologiques et différents réseaux de fractures. Dans cette situation, le même puits est alimenté par des eaux souterraines pouvant avoir des compositions géochimiques et des origines différentes. L'échantillonnage d'un tel puits donne un échantillon avec une composition géochimique intégrée de l'intervalle ouvert au roc. Dans ce projet de recherche, des efforts particuliers ont été faits pour obtenir des échantillons ponctuels représentatifs de la formation. Premièrement, les puits échantillonnés lors de la caractérisation régionale sont des puits dont la stratigraphie et l'intervalle ouvert au roc sont connus. Deuxièmement, une méthode d'échantillonnage avec un système multi-niveaux a été développée.

L'utilisation de l'échantillonnage avec un système multi-niveaux n'est pas très courante dans les études régionales. Ce type d'échantillonnage est plus souvent utilisé dans les études locales, particulièrement pour l'investigation de sites contaminés dans le roc fracturé. Dans de tels cas, des puits sont instrumentés avec des systèmes multi-niveaux permanents de type *Waterloo Multilevel System* ou *Westbay System* (McKay, et al., 1994; Jones et al., 1999; Lapcevic et al., 2000). Ces installations ne répondaient pas au besoin de cette étude régionale. Premièrement, les puits instrumentés avec de tels systèmes sont coûteux. Deuxièmement, avec ce système, le puits est instrumenté directement après le forage. Ceci n'aurait pas permis d'effectuer l'ensemble des tests hydrauliques et géophysiques requis par l'ensemble du projet. Il y a aussi des problèmes de contamination par l'eau de forage associés avec ce type d'installation.

Un système d'échantillonnage multi-niveaux mobile a été développé avec la collaboration de Miroslav Nastev de la Commission géologique du Canada et de Patricia Lapcevic et John Voralek d'Environnement Canada. Cette technique permet d'obtenir des profils verticaux dans un forage ouvert au roc. Le principe général, qui n'est pas nouveau, est d'isoler les niveaux à échantillonner à la profondeur voulue à l'aide d'obturateurs.

Lapcevic et al. (2000) ont utilisé un tel système pour l'échantillonnage de deux forages d'un diamètre de 7,62 cm (3") et d'une profondeur maximum de 55 m. Le système utilisé dans cette étude a dû être adapté pour l'échantillonnage de puits de diamètres de 15,25 cm (6") et 20,32 cm (8"), et d'une profondeur de plus de 100 m. La Figure 1.3 illustre le système d'échantillonnage multi-niveaux mobile, et le Tableau 1.8 résume les étapes et le protocole suivis pour l'échantillonnage.

Tableau 1.8. Étapes et protocole suivi pour l'échantillonnage avec le système multi-niveaux

Étape		Travaux et protocole
1	<b>Essai Lugeon</b> Responsabilité : - 1999 : F. Girard - 2000 : N. Fagnan	<ul style="list-style-type: none"> <li>- Profil de transmissivité du puits (Nastev et al., 2001)</li> <li>- Ce profil est utilisé pour localiser les zones perméables, et permet d'identifier les niveaux qui seront échantillonnés</li> </ul>
2	<b>Échantillonnage régional</b> Responsabilité : É. Bourque	<ul style="list-style-type: none"> <li>- Purge du puits (minimum de 5 volumes de puits <sup>a</sup>)</li> <li>- Type de pompe : Redi-Flo4</li> <li>- Contrôle des paramètres physico-chimiques lors de la purge</li> <li>- Échantillonnage</li> </ul>
3	<b>Échantillonnage avec le système multi-niveaux</b> Responsabilité : V. Cloutier	<ul style="list-style-type: none"> <li>- Installation de la crêpine entre les deux obturateurs</li> <li>- Ajout des longueurs de tuyau 2" pour descendre au premier niveau</li> <li>- Positionnement de la crêpine à la profondeur voulue</li> <li>- Gonflement des obturateurs avec l'azote à la pression nécessaire</li> <li>- Installation de la pompe dans les tuyaux 2"</li> <li>- Type de pompe : Redi-Flo2 et WaTerra HydroLift</li> <li>- Purge de la zone :           <ul style="list-style-type: none"> <li>- 3 à 5 volumes de puits <sup>b</sup></li> <li>- Débits de 4 à 10 litres/minutes selon la transmissivité de la zone</li> </ul> </li> <li>- Contrôle des paramètres physico-chimiques (critère de stabilité, voir Tableau 1.4)</li> <li>- Échantillonnage du niveau</li> <li>- Dégonflement des obturateurs et retrait de la pompe</li> <li>- Ajout des longueurs de tuyau 2" pour descendre au niveau suivant</li> </ul>

<sup>a</sup> Échantillonnage régional : 1 volume de puits = colonne d'eau avant pompage

<sup>b</sup> Échantillonnage avec le système multi-niveaux :

1 volume de puits = colonne d'eau entre les obturateurs + colonne d'eau dans le tuyau 2"

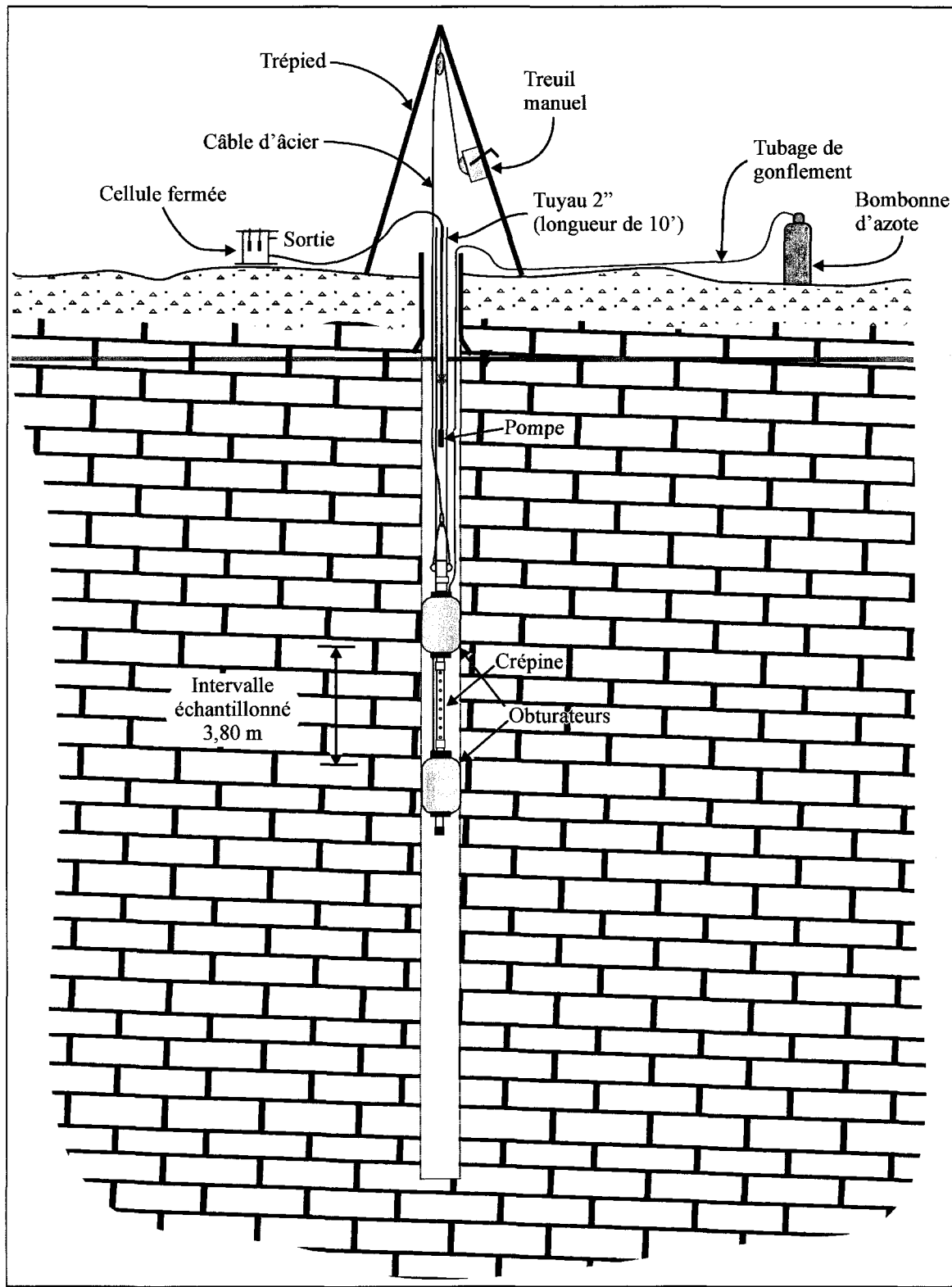


Figure 1.3. Système d'échantillonnage multi-niveaux mobile.

Le but de l'échantillonnage géochimique étant d'obtenir un échantillon représentatif de la formation géologique, la purge de la zone est une étape très importante. Une approche souvent utilisée pour la purge d'un puits est de pomper un certain nombre de volumes de puits (Gibs et al., 2000). La seconde approche est le contrôle des paramètres physico-chimiques. Dans ce projet, les deux approches ont été combinées afin d'assurer le meilleur échantillonnage pour le niveau. Dans le but de vérifier la qualité de la purge, des niveaux ont été échantillonnés en deux temps. Par exemple, un premier échantillon était pris après 5 volumes de puits, et un second après 10 volumes. La comparaison des analyses permet d'évaluer la technique de purge.

### **1.3.3 Caractérisation isotopique $\delta^2\text{H}$ et $\delta^{18}\text{O}$ des précipitations**

La caractérisation des rapports isotopiques  $\delta^2\text{H}$  et  $\delta^{18}\text{O}$  des précipitations (pluie et neige) est importante en hydrogéologie, particulièrement pour caractériser la recharge (voir Tableau 1.1). Dans l'étude d'un système régional, ces rapports permettent de discriminer entre les différentes sources potentielles d'eaux souterraines, notamment l'eau de mer, les eaux de fontes glaciaires, les eaux de formation et de précipitation.

Craig (1961) a défini la relation entre  $\delta^2\text{H}$  et  $\delta^{18}\text{O}$  pour les précipitations. Celle-ci s'exprime par la droite des eaux météoriques globale (DEMG):  $\delta^2\text{H} = 8\delta^{18}\text{O} + 10$ . Elle représente une moyenne globale de plusieurs droites locales. La droite des eaux météoriques locale pour une région dévie de la DEMG. Les facteurs qui contrôlent la composition isotopique des précipitations sont : l'effet de l'altitude, l'effet de la latitude, l'effet continental, les variations saisonnières, le mélange de masses d'air, l'effet de la quantité de précipitation et l'effet de la température (Rozanski et al., 1993; Clark et Fritz, 1997).

L'objectif de cette caractérisation était donc d'établir la Droite des Eaux Météoriques des Basses-Laurentides (*Basses-Laurentides Meteoric Water Line* dans le Chapitre 3) dans le but de caractériser la recharge et d'interpréter les résultats des eaux souterraines. Pour

répondre à cet objectif, un collecteur de pluie a été conçu en collaboration avec Miroslav Nastev. Le collecteur s'apparente à un pluviomètre en verre, avec un robinet à la base pour échantillonner l'eau de pluie. De l'huile de silicone (*Dow Corning 200 ® Fluid, 350 CST.*) a été utilisée afin de prévenir l'évaporation de l'eau. Un test sur l'huile de silicone a démontré qu'il n'y avait pas d'échange isotopique entre l'échantillon d'eau et l'huile.

Un réseau de dix stations a été établi de façon à évaluer la variation spatiale et saisonnière de la composition isotopique des précipitations dans la région d'étude. La Figure 3.3 (Chapitre 3) montre la distribution des stations. Le protocole d'échantillonnage des pluies a été adapté du protocole de prélèvement du *Global Network for Isotopes in Precipitation* (GNIP, 1996) et du *Canadian Network for Isotopes in Precipitation* (Environnement Canada, 1998). Les échantillons composites mensuels des pluies étaient collectés dans des bouteilles HDPE à la fin de chaque mois, de août à octobre 1999, et de mai à octobre 2000.

Des échantillons de neige ont aussi été prélevés à chacune des dix stations, ou à proximité, en mars 2000 et 2001. Un carottier a été utilisé pour échantillonner l'épaisseur complète de la neige. Quatre stations ont été échantillonnées par rapport à la profondeur afin d'évaluer les variations isotopiques à l'intérieur du dépôt de neige. Dans tous les cas, la neige a été mise dans une bouteille HDPE de 1 litre, laissée à fondre à la température de la pièce, transvidée dans des bouteilles HDPE de 60 ml et conservée au réfrigérateur. Le protocole suivi est similaire à celui d'autres études (Gibson et Prowse, 1999). L'ensemble des données isotopiques  $\delta^2\text{H}$  et  $\delta^{18}\text{O}$  des précipitations est présenté dans les tableaux de l'Appendice B.

### **1.3.4 Caractérisation de l'eau d'infiltration dans la zone non saturée**

Trois lysimètres à succion ont été installés afin de déterminer les rapports isotopiques  $\delta^2\text{H}$  et  $\delta^{18}\text{O}$  des eaux d'infiltration dans des secteurs de recharge (voir la Fig. 3.3; Chapitre 3). Les lysimètres ont été échantillonnés en même temps que les collecteurs de pluie. Rosen et al. (1999) et Landon et al. (2000) ont utilisé, entre autre méthode, les rapports

isotopiques  $\delta^2\text{H}$  et  $\delta^{18}\text{O}$  d'eau de pluie et d'eaux d'infiltration échantillonnées avec des lysimètres dans le but de caractériser la recharge. L'ensemble des données isotopiques  $\delta^2\text{H}$  et  $\delta^{18}\text{O}$  des eaux d'infiltration est présenté dans les tableaux de l'Appendice B.

### 1.3.5 Extraction de l'eau interstitielle des argiles

Des échantillons d'argiles marines ont été prélevés en 1999 et 2000 lors de travaux de forage lors de l'installation de puits au roc et pour l'étude Quaternaire (voir la Fig. 3.3; Chapitre 3). L'eau interstitielle des argiles a été extraite à cinq sites dans le but d'améliorer la compréhension de l'origine de la salinité de l'eau souterraine dans les vallées enfouies. Les travaux d'extraction ont été réalisés par Constance Beaubien au département de géologie et génie géologique de l'Université Laval. La planification des travaux d'extraction, ainsi que le choix des échantillons, ont été faits par l'auteur. Les échantillons d'eau interstitielle ont été analysés pour les éléments majeurs,  $\text{Br}^-$ ,  $\text{Sr}^{2+}$ , et les valeurs  $\delta^2\text{H}$  et  $\delta^{18}\text{O}$ . L'ensemble des données géochimiques et isotopiques des eaux interstitielles est présenté sous forme de tableaux à l'Appendice D.

### 1.3.6 Travaux de laboratoire

#### 1.3.6.1 Analyses chimiques et microbiologiques

Les analyses chimiques et microbiologiques des échantillons d'eau souterraine ont été effectuées au Centre d'expertise en analyse environnementale du Québec, laboratoire du Ministère de l'Environnement du Québec. Les échantillons d'eau interstitielle des argiles marines ont aussi été analysés au Centre d'expertise en analyse environnementale du Québec. Le Tableau 3.7 (Chapitre 3) présente les méthodes utilisées par le laboratoire pour l'analyse des différents paramètres. Les Appendices A et D présentent sous forme de tableaux les données chimiques pour l'ensemble des échantillons d'eau souterraine et d'eau interstitielle respectivement.

### 1.3.6.2 Analyses isotopiques

Les analyses de  $\delta^2\text{H}$  et  $\delta^{18}\text{O}$  des échantillons d'eau souterraine et de précipitation prélevés en 1999 ont été effectuées par l'auteur au trimestre hiver 2000 au Delta-Lab de la Commission géologique du Canada à Québec. Marc Luzincourt (Delta-Lab) a formé l'auteur aux techniques d'extraction et d'analyse sur spectromètres de masse. Les échantillons d'eau souterraine et de précipitation prélevés en 2000 ont été analysés en partie au Delta-Lab, et en partie au *G.G. Hatch Isotope Laboratories* de l'Université d'Ottawa. Enfin, les échantillons d'eau interstitielle et les échantillons de neige prélevés en 2001 ont été analysés au Delta-Lab. Les analyses  $\delta^{13}\text{C}_{\text{CID}}$  des échantillons d'eau souterraine ont été effectuées par Marc Luzincourt au Delta-Lab.

Des échantillons prélevés lors de la caractérisation régionale, ainsi que certains prélevés avec le système multi-niveaux, ont été analysés pour  $^{87}\text{Sr}/^{86}\text{Sr}$ , ainsi que pour la datation de l'eau souterraine. Vingt-cinq échantillons ont été analysés pour  $^{87}\text{Sr}/^{86}\text{Sr}$  au laboratoire Geochron de la Commission géologique du Canada. Deux techniques de datation ont été utilisées dans ce projet de recherche : le tritium,  $^3\text{H}$ , pour identifier les eaux souterraines modernes, et le radiocarbone,  $^{14}\text{C}$ , pour dater les eaux souterraines anciennes (Tableau 1.1). Le choix des échantillons à soumettre pour ces analyses a été réalisé par l'auteur. Ce choix a reposé sur les connaissances de l'hydrogéochimie du système aquifère acquises par l'interprétation des résultats des isotopes stables et de la chimie inorganique, tout en tenant compte du contexte hydrogéologique et géologique. Quatorze échantillons ont été analysés pour le  $^3\text{H}$  enrichi au *Environmental Isotope Laboratory* de l'Université de Waterloo. Douze de ces quatorze échantillons ont été analysés pour le  $^{14}\text{C}$  du carbone inorganique dissous au *IsoTrace Laboratory* de l'Université de Toronto.

L'Appendice du Chapitre 3 donne plus de détails sur les protocoles d'échantillonnage pour  $\delta^2\text{H}$ ,  $\delta^{18}\text{O}$ ,  $\delta^{13}\text{C}_{\text{CID}}$ ,  $^{87}\text{Sr}/^{86}\text{Sr}$ ,  $^3\text{H}$  et  $^{14}\text{C}$ , ainsi que les différentes techniques d'analyses isotopiques et leurs précisions. Les Appendices A, B et D présentent sous forme de tableaux les données isotopiques pour l'ensemble des échantillons d'eau souterraine, de précipitation, et d'eau interstitielle, respectivement.

#### **1.4 CONTRIBUTION DE L'AUTEUR**

Cette section est une synthèse de la contribution de l'auteur par rapport à l'ensemble des travaux et interprétations scientifiques présentés dans la deuxième partie de la thèse. Pour son doctorat, l'auteur a eu l'opportunité de s'intégrer à une équipe multidisciplinaire au commencement du projet de cartographie hydrogéologique régionale, participant ainsi aux différentes étapes du projet, soit la planification et l'exécution des travaux de terrain, l'interprétation des données, et la diffusion des résultats dans des rapports techniques, publications scientifiques et communications.

L'auteur a participé activement à la planification des travaux de caractérisation hydrogéochimique qui ont permis de récolter les données présentées et interprétées dans cette thèse. Cette planification a été réalisée en étroite collaboration avec Édith Bourque, qui était responsable du volet hydrogéochimique du projet pour la Commission géologique du Canada, René Lefebvre, directeur de recherche, Martine M. Savard, codirectrice de recherche, René Therrien, co-directeur de recherche, et Miroslav Nastev. Plusieurs personnes ont également contribué, par leurs suggestions et commentaires, à la planification de ces travaux, dont Nathalie Fagnan, Pierre Gélinas, Patricia Lapcevic, Richard Martel, Yves Michaud, Kent Novakowski, et John Voralek.

Les travaux de terrain ont été exécutés en 1999 et 2000. L'échantillonnage régional était sous la responsabilité d'Édith Bourque. L'auteur a participé à l'échantillonnage régional en 1999. Tant pour l'année 1999 que 2000, la planification de l'échantillonnage régional, le choix des sites, ainsi que les travaux d'échantillonnage ont été réalisés en étroite collaboration avec l'auteur. En 2000, l'auteur était responsable des travaux d'échantillonnage avec le système multi-niveaux. L'auteur a aussi supervisé les travaux d'une deuxième équipe effectuant de l'échantillonnage avec le système multi-niveaux. Cette deuxième équipe était dirigée par Chatelaïne Beaudry. Plusieurs personnes ont assisté Édith Bourque et l'auteur dans l'échantillonnage de l'eau souterraine, dont Alexandre Boutin, Martin Fleury, Pascal Lussier-Duquette, Valérie Maltais, Valérie Murat, et Tommy Thériault. L'auteur a mis en place le réseau de dix stations pour la

caractérisation isotopique des précipitations dans la région d'étude, et était responsable de l'échantillonnage mensuel. Enfin, l'auteur a participé à des travaux de forage, à la description d'échantillons de roc, à l'installation de puits d'observation, ainsi qu'à des essais hydrauliques.

Les échantillons d'argiles marines ont été prélevés en 1999 et 2000 lors de travaux de forage pour l'installation de puits au roc, ainsi que pour l'étude Quaternaire dans le cadre des travaux de doctorat de Martin Ross. Les travaux d'extraction de l'eau interstitielle des argiles ont été réalisés par Constance Beaubien au département de géologie et génie géologique de l'Université Laval. La planification des travaux d'extraction, ainsi que le choix des échantillons, ont été faits par l'auteur.

Les analyses chimiques des échantillons d'eau souterraine et de l'eau interstitielle ont été effectuées au Centre d'expertise en analyse environnementale du Québec, laboratoire du Ministère de l'Environnement du Québec. L'auteur a réalisé une partie des analyses des isotopes stables de l'eau,  $\delta^2\text{H}$  et  $\delta^{18}\text{O}$ , au Delta-Lab de la Commission géologique du Canada à Québec sous la supervision de Marc Luzincourt. Le choix des échantillons à analyser pour  $^{87}\text{Sr}/^{86}\text{Sr}$ ,  $^3\text{H}$  enrichi, et  $^{14}\text{C}$  du carbone inorganique dissous a été réalisé par l'auteur.

Le contenu scientifique du rapport (Chapitre 2) et des trois articles (chapitres 3 à 5) résulte essentiellement des travaux de représentation, d'analyse et d'interprétation des données hydrogéochimiques par l'auteur de la thèse. Ces travaux ont été réalisés en étroite collaboration avec René Lefebvre, directeur de recherche et co-auteur sur le rapport et les trois articles. Cette collaboration a permis, entre autre chose, d'orienter l'auteur dans le développement des interprétations scientifiques, d'améliorer la clarté des représentations graphiques, ainsi que de mieux définir les objectifs et la structure de chacun des articles.

La autres co-auteurs du Chapitre 2 (Édith Bourque, Martine M. Savard et Richard Martel), du Chapitre 3 (Martine M. Savard, Édith Bourque, et René Therrien), du

Chapitre 4 (René Therrien, et Martine M. Savard) ainsi que du Chapitre 5 (Martine M. Savard et René Therrien) ont contribué dans leur champ d'expertise à clarifier et à améliorer le contenu scientifique et la présentation de chacun des articles. Concernant le rapport scientifique (Chapitre 2), Édith Bourque avait réalisé les premières versions des cartes 2.1 à 2.14 (Appendice H). Celles-ci ont été finalisées par l'auteur dans l'élaboration de l'Atlas hydrogéologique. La division de la région d'étude en secteurs de qualité relative de l'eau souterraine est le résultat des travaux de l'auteur. La carte de Qualité de l'eau souterraine (Carte 2.17 en pochette) a bénéficié des commentaires et suggestions de René Lefebvre et de Miroslav Nastev.

#### **1.4.1 Autres contributions**

Dans le cadre du projet de «caractérisation hydrogéologique régionale du système aquifère fracturé du sud-ouest du Québec» de la CGC, l'auteur a participé de façon significative au volet hydrogéochemique des produits scientifiques remis aux partenaires financiers du projet de recherche, incluant la participation à l'écriture de rapports scientifiques, ainsi qu'à la réalisation de cartes pour un Atlas hydrogéologique. Parmi les autres contributions, mentionnons la participation à la table technique lors de la conférence de presse pour divulguer les réalisations scientifiques aux partenaires du projet en octobre 2002.

Au cours de ce projet de doctorat, l'auteur a contribué à des communications, des affiches, ainsi qu'à différents produits scientifiques de la Commission géologique du Canada. Puisque ces contributions ne font pas partie intégrante de la thèse, nous en fournissons la liste car elles sont importantes dans l'évolution de ce projet de recherche :

- Bourque, É., Cloutier, V., Lefebvre, R., Savard, M.M., Nastev, M., Martel, R., 2001. Résultats initiaux de la caractérisation hydrogéochimique des aquifères fracturés du sud-ouest du Québec. Commission géologique du Canada, Recherches en cours 2001-D8, 9 p., <http://www.nrcan.gc.ca/gsc/bookstore>.
- Bourque, É., Cloutier, V., Lefebvre, R., Savard, M.M., Martel, R., 2002. Caractérisation de la qualité de l'eau souterraine. Dans : Guide méthodologique pour la caractérisation hydrogéologique régionale des systèmes aquifères en roches sédimentaires fracturées. Édité par Savard, M.M., Lefebvre, R., Martel, R., Ouellet, M., Rousseau, N., Ministère de l'Environnement du Québec, chapitre 5, 23 p., en édition.
- Cloutier, V., Bourque, É., Lefebvre, R., Savard, M.M., Nastev, M., Martel, R., 2000. Regional hydrogeochemical characterization of groundwater in fractured aquifers of the St-Lawrence Lowlands. Proceedings, First Joint IAH-CNC and CGS, Groundwater Specialty Conference, October 2000, Montréal, Canada, 3-10. (Appendice F)
- Cloutier, V., 28 août 2000. Échantillonnage hydrogéochimique multi-niveaux. Excursion hydrogéologique, Projet d'hydrogéologie régionale des aquifères fracturés du sud-ouest du Québec.
- Cloutier, V., Lefebvre, R., Savard, M., Therrien, R., 2001. Hydrochimie régionale des aquifères fracturés du sud-ouest du Québec. Journée des Sciences de la Terre, Édition 2001, Université Laval, 19 mars 2001.
- Cloutier, V., Bourque, É., Lefebvre, R., Savard, M.M., Nastev, M., Martel, R., Therrien, R., 2001. Regional groundwater hydrogeochemistry of fractured rock aquifers in south-western Quebec. Proceedings, 2nd Joint IAH-CNC and CGS, Groundwater Specialty Conference, 54th Canadian Geotechnical Conference, Sept. 16-19, 2001, Calgary, Canada, 1068-1076. (Appendice F)
- Cloutier, V., Bourque, É., Lefebvre, R., Savard, M.M., Martel, R., 2002. 3. Caractérisation hydrogéochimique et qualité de l'eau souterraine. Dans Savard et al., éd., Hydrogéologie régionale du système aquifère fracturé du sud-ouest du Québec. Rapport final, Commission Géologique du Canada, 15 mai 2002, 12-19. (Chapitre 2)
- Cloutier, V., Lefebvre, R., Savard, M.M., Therrien, R., 2002. Analyse statistique multivariable de l'hydrogéochimie régionale des aquifères fracturés du sud-ouest du Québec. Journée des Sciences de la Terre, Édition 2002, Université Laval, 11 mars.
- Cloutier, V., Lefebvre, R., Savard, M., Therrien, 2004. Groundwater origin and geochemical processes in the Basses-Laurentides sedimentary rock aquifer system, St. Lawrence Lowlands, Quebec, Canada. Proceedings, 5<sup>th</sup> Joint IAH-CNC and CGS Groundwater Specialty Conference, 57<sup>th</sup> Canadian Geotechnical Conference, September 2004, Quebec City, Canada, 8 p.

Nastev, M., Bourque, É., Cloutier, V., Paradis, D., Ross, M., 2002. Étude détaillée d'un site sélectionné : Cas du secteur de St-Benoît, Mirabel. Dans : Partie IV, Études locales de secteurs choisis du système aquifère fracturé du sud-ouest du Québec, rapport final. Édité par Savard, M.M., Lefebvre, R., Nastev, M., p. 13-28, 79-88.

Savard, M.M., Nastev, M., Lefebvre, R., Martel, R., Fagnan, N., Bourque, É., Cloutier, V., Lauzière, K., Gélinas, P., Kirkwood, D., Lapcevic, P., Karanta, G., Hamel, A., Bolduc, A., Ross, M., Parent, M., Lemieux, J.-M., Boisvert, E., Salad Hersi, O., Lavoie, D., Girard, F., Novakowski, K., Therrien, R., Etienne, M., Fortier, R., 2000. Regional Hydrogeology of fractured rock aquifers of southwestern Quebec (St.Lawrence Lowlands). Proceedings, First Joint IAH-CNC and CGS, Groundwater Specialty Conference, October 2000, Montréal, Canada, 247-254.

Savard, M., Nastev, M., Martel, R., Lefebvre, R., Bourque, É., Fagnan, N., Cloutier, V., Girard, F., Hamel, A., Lauzière, K., Lemieux, J.-M., Ross, M., Lapcevic, P., Gélinas, P., Kirkwood, D., Karanta, G., Étienne, M., Parent, M., Therrien, R., Novakovski, K., Fortier, R., 2000. Cartographie hydrogéologique régionale des aquifères fracturés en roches sédimentaires du sud-ouest du Québec, (Basses-Terres du Saint-Laurent). Rapport d'étape du Projet AFSOQ pour l'année 1999-2000, présenté à l'APDEL, DEC, CRDL et les MRC d'Argenteuil, Deux-Montagnes, Mirabel, et Thérèse-de-Blainville, 10 avril 2000, 10 p.

Savard, M.M., Lefebvre, R., Nastev, M., Paradis, D., Cloutier, V., Martel, R., 2002. 6. Conclusions générales et recommandations. Dans Savard et al., éd., Hydrogéologie régionale du système aquifère fracturé du sud-ouest du Québec. Rapport final, Commission Géologique du Canada, 15 mai 2002, 26-32.

Savard, M.M., Nastev, M., Paradis, D., Lefebvre, R., Martel, R., Cloutier, V., Murat, V., Bourque, É., Ross, M., Lauzière, K., Parent, M., Hamel, A., Lemieux, J.-M., Therrien, R., Kirkwood, D., Gélinas, P., in press. Regional hydrogeological characterization of the fractured aquifer system in south-western Quebec: Part I-Regional hydrogeology of the aquifer system. Geological Survey of Canada, Bulletin.

## **DEUXIÈME PARTIE**

### **RAPPORT ET ARTICLES**



## **Chapitre 2**

# **CARACTÉRISATION HYDROGÉOCHIMIQUE ET QUALITÉ DE L'EAU SOUTERRAINE**

Vincent Cloutier<sup>1</sup>, Édith Bourque<sup>2,3</sup>, René Lefebvre<sup>1</sup>,  
Martine M. Savard<sup>2</sup>, Richard Martel<sup>1</sup>

<sup>1</sup>Institut national de la recherche scientifique, INRS-Eau, Terre & Environnement, C.P. 7500, Sainte-Foy (Québec), G1V 4C7, Canada

<sup>2</sup>Commission géologique du Canada, Ressources naturelles Canada, 880, chemin Sainte-Foy, bureau 840, Québec (Québec), G1S 2L2, Canada

<sup>3</sup>Maintenant au Bureau d'audiences publiques sur l'environnement, 575, rue Saint-Amable, bureau 2.10, Québec (Québec), G1R 6A6, Canada

## RÉSUMÉ

À l'échelle régionale, l'eau souterraine du territoire à l'état naturel est de qualité variable et très peu contaminée par les activités humaines. Un échantillonnage systématique de l'eau souterraine a été fait dans 151 puits et 2 sources de la région pour couvrir aussi représentativement que possible la région d'étude en fonction des sources d'approvisionnement et des unités hydrogéologiques. En terme de qualité des eaux souterraines, le territoire d'étude a été subdivisé en 7 secteurs classés sur une échelle de qualité relative, selon les propriétés hydrogéochimiques, les conditions hydrogéologiques et la vulnérabilité à la contamination. Les secteurs où l'eau souterraine est de meilleure qualité sont ceux de Saint-Hermas, de Rivière du Nord et de Lachute/Saint-Janvier, de Sainte-Monique/Saint-Eustache et de Saint-Vincent. Les secteurs des collines d'Oka et de Grenville/Chatham ont une qualité moyenne, alors que les secteurs de Sainte-Anne-des-Plaines et de Sainte-Thérèse, et de Saint-Benoît/Saint-Joseph ont une qualité inférieure. Le bilan des dépassements des critères de qualité reliés à la santé nous indique une eau souterraine de bonne qualité sur la majorité du territoire (cartes 2.2 à 2.13; les cartes du Chapitre 2 sont dans l'Appendice H). En effet, un seul dépassement directement relié à l'activité humaine, soit pour les nitrates, a été identifié dans la zone de recharge de Lachute/Saint-Janvier. De plus, deux dépassements des critères de qualité reliés à la santé sont notés pour le baryum, et dix pour les fluorures (principalement dans le secteur Grenville/Chatham et de Sainte-Anne-des-Plaines). Plusieurs dépassements des critères esthétiques sont observés à partir des échantillons d'eau, mais ils sont généralement reliés à des processus naturels. Seuls les quelques dépassements en chlorures et en sodium dans les secteurs à nappe libre à proximité des routes 15 et 117 peuvent être attribués à l'activité humaine (sels déglaçants). Enfin, bien que ne faisant pas l'objet de recommandations ou de normes, la dureté est relativement élevée sur l'ensemble de la région. La majorité de ces problèmes esthétiques de qualité de l'eau souterraine, ainsi que la dureté, peuvent être corrigés par des méthodes de traitement simples.

## 2.1 INTRODUCTION

C'est en analysant les constituants chimiques présents dans l'eau que l'on peut évaluer la qualité de l'eau souterraine. Les concentrations des différents éléments présents dans l'eau sont souvent variables d'un secteur à l'autre pour une région donnée. Cette variabilité peut être reliée à des facteurs d'ordre: 1) géologique (échanges eau-roche), 2) hydrogéochimique (temps de résidence de l'eau souterraine dans l'aquifère, niveau de confinement de la zone aquifère), 3) mélanges d'eaux d'origines différentes, et 4) anthropique (activités polluantes comme l'installation de fosses septiques, l'aménagement de lieux d'enfouissement sanitaires, l'épandage de sels déglaçants, d'engrais ou de pesticides, les fuites de réservoirs d'hydrocarbures). La variabilité hydrogéochimique est étudiée afin d'évaluer le potentiel de la ressource et d'identifier des problématiques de qualité d'eau qui pourraient nécessiter des mesures particulières de gestion et de protection.

Les objectifs de la caractérisation de la qualité de l'eau souterraine sont de :

- vérifier si la qualité de l'eau est appropriée pour différents usages;
- évaluer la variabilité hydrogéochimique régionale;
- identifier les facteurs responsables de la variabilité;
- établir un portrait régional de la qualité de l'eau.

## 2.2 PROCÉDURES

Afin d'évaluer la qualité de l'eau souterraine, trois campagnes d'échantillonnage de l'eau ont été effectuées au printemps et à l'été 1999, puis à l'été 2000. Au total, 151 puits de particuliers, municipaux, et d'observation, et 2 sources captées ont été échantillonnés. Des cartes géologiques des formations superficielles, du socle rocheux, des épaisseurs de dépôts meubles, des sous-bassins et des zones de recharge et d'émergence ont guidé le choix des sites où il a été jugé nécessaire de prélever des échantillons d'eau afin de bien caractériser le système d'écoulement. Différents paramètres inorganiques et

microbiologiques ont été mesurés pour tous les échantillons. Le contrôle de la qualité de l'échantillonnage et des analyses consiste à l'analyse de duplicita (environ 7% des échantillons dans la présente étude), et au calcul de l'équilibre chimique (électro-neutralité de la solution). Un équilibre chimique de +/- 5% est considéré acceptable (Freeze et Cherry, 1979). Dans cette étude, 134 échantillons ont un équilibre chimique inférieur à 5%, 12 échantillons entre 5 et 8%, et 7 échantillons supérieur à 10%. Les échantillons pour lesquels l'équilibre cations/anions représentent une erreur inférieure à 8% (146 résultats, dont 144 puits et 2 sources captées) sont retenus pour l'évaluation de la qualité de l'eau souterraine. Les puits échantillonnés exploitent des formations rocheuses (115), des formations de dépôts meubles (20, dont les sédiments de surface (7) et sédiments sous l'argile (13)), et parfois même les deux à la fois (mixte) (9). La Carte 2.1 (Appendice H) présente la distribution des sites d'échantillonnage, la provenance des échantillons d'eau souterraine, leur localisation par rapport aux routes et villes importantes, ainsi que les numéros d'identification des sites.

### **2.3 ÉVALUATION DE LA QUALITÉ DE L'EAU SOUTERRAINE**

Afin d'évaluer la qualité de l'eau souterraine, les concentrations naturelles des éléments chimiques contenus dans l'eau sont comparées à des critères de qualité de l'eau établis pour différents usages. Les usages pour lesquels la qualité de l'eau souterraine est évaluée sont : 1) l'approvisionnement en eau potable, 2) l'abreuvement d'animaux et 3) l'irrigation. Les critères proposés sont ceux du Gouvernement du Québec (2001), de Santé Canada (2001) et du Conseil canadien des ministres de l'environnement, CCME (1999). Les critères du CCME, contrairement aux critères du gouvernement du Québec, n'ont pas force de loi, à moins qu'il n'en ait été décidé autrement par les autorités provinciales, territoriales ou fédérales appropriées.

Les tableaux 2.1 à 2.3 présentent des bilans des dépassements des critères de qualité d'eau. On peut voir que les dépassements des critères reliés à la santé sont peu nombreux. En effet, quelques dépassements des critères reliés à la santé sont observés dans le cas des coliformes totaux (12/80), des fluorures (10/142 échantillons), du baryum (2/146

échantillons) et des nitrates (1/144 échantillons). Des dépassements de critères esthétiques ont aussi été identifiés pour les paramètres tels le fer (47/143 échantillons), les sulfures (28/142 échantillons), le manganèse (48/146 échantillons), le sodium (25/146 échantillons), les chlorures (21/146 échantillons), le pH (11/146 échantillons), les sulfates (2/144 échantillons) et les concentrations en matière dissoute totale (MDT) (43/146 échantillons).

Tableau 2.1. Critères de qualité d'eau pour les paramètres microbiologiques mesurés et dépassements / échantillonnage de l'eau souterraine du Projet AFSOQ, 1999-2000

Paramètres microbiologiques	Critères de qualité d'eau (nombre de dépassements du critère)				Nombre total de résultats d'analyses	
	Norme <sup>a</sup>	Recommandations pour la qualité de l'eau potable au Canada <sup>b</sup>	Recommandations canadiennes pour la qualité de l'environnement <sup>c</sup>			
	Eau potable CM	Eau potable CMA	Irrigation	Abreuvement des animaux d'élevage		
Coliformes totaux	10/100 mL (12)	10/100 mL (12)	1000/100 mL (0)	aucune	80	
Coliformes fécaux ou Escherichia coli	0/100 mL (0)	0/100 mL (0)	100/100 mL (0)	aucune	80	

CM: concentration maximale, CMA: concentration maximale acceptable

<sup>a</sup> Gouvernement du Québec (2001)

<sup>b</sup> Santé Canada (2001)

<sup>c</sup> CCME (1999).

Tableau 2.2. Critères de qualité de l'eau pour les paramètres physico-chimiques analysés en laboratoire et calculés. Le nombre de dépassements observés pour les échantillons de l'étude régionale (1999-2000) sont indiqués entre parenthèses

Paramètres analysés en laboratoire  (unité = mg/L lorsque non spécifiée)	Critères de qualité d'eau (nombre de dépassements du critère <sup>a</sup> )					Nombre total de résultats d'analyses	
	Norme <sup>b</sup>	Recommandations pour la qualité de l'eau potable au Canada <sup>c</sup>		Recommandations canadiennes pour la qualité de l'environnement <sup>d</sup>			
	Eau potable, CM	Eau potable, CMA/CMAP	Eau potable, OE	Irrigation	Abreuvement des animaux d'élevage		
Alcalinité totale (mg/L CaCO <sub>3</sub> )						142	
Ammoniac (en N)						144	
Arsenic	0,025 (0)	CMAP 0,025 (0)		0,1 (0)	0,025 (0)	132	
Baryum	1 (2)	1 (2)				146	
Bore	5 (0)	CMAP 5,0 (0)		0,5-6,0 (9)	5,0 (0)	145	
Bromure						144	
Cadmium	0,005 (0)	0,005 (0)		0,0051 (0)	0,08 (0)	133	
Calcium					1000 (0)	146	
Carbone organique dissous						143	
Chlorure			≤ 250 (21)	100-700 (36)		146	
Chrome	0,05 (0)	0,05 (0)				146	
Cyanure	0,2 (0)	0,2 (0)				111	
Fer			≤ 0,3 (47)	5,0 (2)		143	
Fluorure	1,5 (10)	1,5 (10)		1,0 (9)	1,0-2,0 (6)	142	
Magnésium						146	
Manganèse			≤ 0,05 (48)	0,2 (18)		146	
Mercure	0,001 (0)	0,001 (0)			0,003 (0)	127	
Nitrate + nitrite (en N)	10 (1)	10,0 (1)			22 (0)	144	
Phosphore total (en P)						141	
Plomb	0,01 (0)	0,01 (0)		0,2 (0)	0,1 (0)	132	
Potassium						146	
Selenium	0,01 (0)	0,01 (0)		0,02-0,05 (0)	0,05 (0)	122	
Silice (en SiO <sub>2</sub> )						146	
Sodium			≤ 200 (25)			146	
Strontium						145	
Sulfate			≤ 500 (2)		1000 (1)	144	
Sulfure (en S)			≤ 0,05 (28)			142	
Uranium	0,02 (0)	0,1 (0)		0,01 (4)	0,2 (0)	115	

Tableau 2.2. (suite)

Paramètres calculés	Critères de qualité d'eau (nombre de dépassements du critère <sup>a</sup> )				Nombre total de résultats d'analyses
	Norme <sup>b</sup>	Recommandations pour la qualité de l'eau potable au Canada <sup>c</sup>	Recommandations canadiennes pour la qualité de l'environnement <sup>d</sup>	Irrigation	
Eau potable, CM	Eau potable, CMA/CMAP	Eau potable, OE			
Dureté totale <sup>e</sup> (mg/L CaCO <sub>3</sub> )					146
Bicarbonates, HCO <sub>3</sub> <sup>-</sup> (mg/L) (à partir de l'alcalinité totale) <sup>f</sup>					146
MDT (mg/L) (matières dissoutes totales) <sup>g</sup>		≤ 500 (43)	500-3500 (43)	3000 (2)	146
TAS (sans unité) (Taux d'adsorption du sodium) <sup>h</sup>					146

CM: concentration maximale, CMA: concentration maximale acceptable,  
CMAP: concentration maximale acceptable provisoire, OE: objectif esthétique

<sup>a</sup> Lorsque le critère est un intervalle, le nombre de dépassements est calculé à partir de la limite inférieure de l'intervalle et constitue donc un nombre de dépassements maximal

<sup>b</sup> Gouvernement du Québec (2001)

<sup>c</sup> Santé Canada (2001)

<sup>d</sup> CCME (1999)

<sup>e</sup> Les concentrations en Ca<sup>2+</sup> et Mg<sup>2+</sup> permettent de calculer la dureté totale. La dureté est un paramètre ne faisant pas l'objet de recommandations. On considère qu'une eau dont le degré de dureté se situe entre 80 et 100 mg/L est jugée acceptable, que lorsqu'elle est supérieure à 200 mg/L, elle est de qualité médiocre mais peut être tolérée par les consommateurs, et que lorsqu'elle est supérieure à 500 mg/L, elle est inacceptable pour la plupart des usages domestiques (Santé Canada, 2001)

<sup>f</sup> La concentration en HCO<sub>3</sub><sup>-</sup> = 1.219 \* alcalinité totale en CaCO<sub>3</sub> composée par des HCO<sub>3</sub><sup>-</sup>

<sup>g</sup> La concentration en MDT est calculée à partir de la somme des concentrations des ions et du SiO<sub>2</sub> (Hounslow, 1995) et n'est qu'une approximation des MDT mesurées en laboratoire (résidus d'évaporation à une température donnée), l'objectif de 500 mg/L doit donc n'être considéré qu'à titre indicatif

<sup>h</sup> Le TAS est calculé à partir des concentrations en Na<sup>+</sup>, Ca<sup>2+</sup> et Mg<sup>2+</sup> (voir la Carte 2.14; Appendice H).

Tableau 2.3. Critères de qualité de l'eau pour les paramètres physico-chimiques mesurés au site d'échantillonnage et dépassements / échantillonnage de l'eau souterraine

Paramètres mesurés au site d'échantillonnage	Critères de qualité d'eau (nombre de dépassements du critère)					Nombre total de résultats d'analyses	
	Norme <sup>a</sup>	Recommandations pour la qualité de l'eau potable au Canada <sup>b</sup>		Recommandations canadiennes pour la qualité de l'environnement <sup>c</sup>			
		Eau potable, CM	Eau potable, CMA/CMAP	Eau potable, OE	Irrigation	Abreuvement des animaux d'élevage	
Température (°C)				≤15°C			129
pH (sans unité)	6,5-8,5 (11)			6,5-8,5 (11)			146
Conductivité électrique spécifique à 25 °C (mS/cm)							146
Potentiel d'oxydo-réduction Eh (mV)							123
Oxygène dissous (mg/L)							129

CM: concentration maximale, CMA : concentration maximale acceptable,

CMAP: concentration maximale acceptable provisoire, OE: objectif esthétique

mS/cm: millSiemens/cm, mV: millivolt

<sup>a</sup> Gouvernement du Québec (2001)

<sup>b</sup> Santé Canada (2001)

<sup>c</sup> CCME (1999).

### 2.3.1 Variabilité régionale de la qualité de l'eau souterraine et représentation graphique

La représentation graphique et cartographique des résultats d'analyses physico-chimiques aide à la compréhension des caractéristiques hydrogéochimiques qui ont une variabilité spatiale. Tous les résultats obtenus au cours du projet de recherche sont présentés dans la base de données (Appendice A sous forme de tableaux, et Appendice G sous forme de fichiers numériques dans le disque compact en pochette de la thèse).

### 2.3.2 Concentrations chimiques et critères de qualité

Les cartes 2.2 à 2.13 (Appendice H) présentent la distribution des paramètres géochimiques. Des points, de grosseur proportionnelle à la concentration d'un élément chimique présent dans l'eau, à l'emplacement des sites d'échantillonnage, permettent de visualiser la variabilité de la présence d'un paramètre. Les sites d'échantillonnage dépassant les critères de qualité (normes et objectifs esthétiques) sont représentés avec une couleur différente. La carte géologique des unités rocheuses est utilisée comme carte de fond. On peut distinguer des tendances particulières pour certains secteurs pour la majorité des paramètres.

Des facteurs géologiques semblent être déterminants pour les paramètres suivants: le pH (Carte 2.2), les sulfates (Carte 2.3), le manganèse (Carte 2.4), le fer (Carte 2.5), le baryum (Carte 2.6), les sulfures (Carte 2.7), la dureté totale élevée (Carte 2.8), et les fluorures (Carte 2.9). Les valeurs élevées et les dépassements en fluorures, baryum, sulfures et pH sont concentrés dans la partie est, soit la région de Sainte-Anne-des-Plaines. Ces valeurs sont associées aux dolomies et calcaires de la Formation de Carillon, ainsi qu'aux calcaires et argilites des groupes de Chazy, Black River et Trenton. Des valeurs élevées en fluorures se retrouvent également dans la partie ouest, la région de Chatham (dolomies et calcaires de la Formation de Carillon et calcaires du Groupe de Chazy), et les collines d'Oka. Les valeurs élevées en fer et en manganèse sont distribuées sur l'ensemble de la région. Les sources pourraient être les minéraux présents dans les sédiments de surface ou dans les fractures des roches sédimentaires. Les valeurs élevées en dureté totale sont aussi distribuées sur l'ensemble de la région. Les sources des valeurs élevées sont les minéraux carbonatés présents dans les sédiments de surface, et les roches sédimentaires (dolomies, calcaires).

Le niveau de confinement de l'aquifère à l'endroit de l'échantillonnage, certains facteurs hydrogéologiques et la présence d'eau saline expliqueraient plutôt la distribution des concentrations du sodium (Carte 2.10), des chlorures (Carte 2.11) et de la matière dissoute totale (MDT; Carte 2.12) (voir aussi Cloutier et al., 2001). Les faibles valeurs de

dureté totale (Carte 2.8) pourraient quant à elles être expliquées par des échanges eau-roche. Les valeurs élevées en nitrates (Carte 2.13) se retrouvent dans les zones en conditions de nappe libre. Ce paramètre permet de détecter une contamination possible par les activités agricoles (utilisation de fertilisants) ou par des installations septiques.

Des calculs statistiques (moyenne, médiane, minimum, maximum et écart type) sont effectués pour les échantillons d'eau provenant de différents types d'unités hydrogéologiques (sédiments de surface, sédiments enfouis sous l'argile, et formations rocheuses), afin de distinguer les particularités hydrogéochimiques de chacun des types d'unités (Tableau 2.4). La variabilité de la qualité de l'eau relative aux différents paramètres peut ainsi être évaluée.

Le taux d'adsorption du sodium (TAS) exprime l'activité relative des ions de sodium dans les réactions d'échange avec les ions calcium et magnésium adsorbés des sols argileux, causant des dommages à la structure du sol. Le TAS sert donc à déterminer si l'eau est appropriée aux fins d'irrigation agricole. Une carte des valeurs de TAS (Carte 2.14) permet d'identifier les secteurs où le TAS est élevé et où l'irrigation agricole peut être problématique. La carte des conditions hydrogéologiques adaptée de Hamel et al. (2001) est utilisée comme carte de fond. La valeur de TAS pour laquelle l'eau est moins appropriée à l'irrigation est fonction des types de sol et de culture.

Tableau 2.4. Statistiques physico-chimiques des différents types d'unités hydrogéologiques

Paramètres (unité = mg/L lorsque non spécifiée)	Sédiments de surface (7 sites)							Sédiments sous l'argile (13 sites)							Formations rocheuses et mixtes (124 sites)											
	Nombre de résultats résultats			Moyenne		Minimum		Nombre de résultats résultats			Moyenne		Maximum		Nombre de résultats résultats			Moyenne		Maximum		Nombre de résultats résultats				
	Nombre de résultats résultats			Moyenne		Maximum		Nombre de résultats résultats			Moyenne		Maximum		Nombre de résultats résultats			Moyenne		Maximum		Nombre de résultats résultats				
Conductivité spécifique (mS/cm)	7	0,573	0,65	0,279	0,803	0,197	13	0,811	0,678	0,34	1,952	0,457	124	1,144	0,688	0,265	18,53	1,837								
Potentiel d'oxydo-réduction, Eh (mV)	5	+ 47	+ 46	- 30	+ 94	48	11	- 46	- 50	- 150	+ 159	82	105	- 15	+ 12	- 223	+ 196	1,04								
Oxygène dissous	5	2,95	1,96	0,26	8,95	3,45	12	2,83	1,97	0,85	8,46	2,18	110	2,94	2,1	0,12	11,48	2,59								
pH (sans unité)	7	7,48	7,50	7,14	8	0,28	13	8	8,01	6,3	9,26	7,6	124	7,59	6,4	8,35	0,46									
Température (°C)	5	11,1	10,5	8,2	16,3	3,1	12	9,1	8,8	10,5	0,8	110	9,5	9,1	7,6	16,9	1,6									
Alcalinité totale (mg/L CaCO <sub>3</sub> )	7	271	310	96	430	117	13	260	250	140	500	97	120	267	260	33	810	99								
Ag	4	0,0003	0,0003	0,0003	0,0003	0	12	0,0003	0,0002	0,0003	0,0003	0	114	0,0003	0,0003	0,0003	0,0001	0,0003	0,0002	0,0002	0,0002	0,0002	0,0002			
Al	7	0,011	0,007	0,007	0,007	0,007	0,02	0,006	0,012	0,01	0,007	0,013	0,009	122	0,024	0,028	0,007	0,7	0,68							
As	4	0,001	0,001	0,001	0,001	0	12	0,001	0,001	0,001	0,002	0,004	114	0,001	0,001	0,001	0,005	0,004								
B	7	0,006	0,002	0,002	0,02	0,007	13	0,15	0,1	0,02	0,37	0,17	123	0,159	0,14	0,002	1,40	0,22								
Ba	7	0,07	0,06	0,01	0,22	0,07	13	0,15	0,14	0,008	0,32	0,08	124	0,198	0,14	0,001	1,1	0,2								
Br	6	0,014	0,01	0,008	0,026	0,007	13	0,41	0,15	0,01	1,5	0,5	123	0,364	0,04	0,002	23	2,89								
Ca	7	69,1	81	95	24,9	13	31,7	32	1,2	61	19,8	124	59,4	44,5	0,2	790	83,8									
Cd	4	0,0012	0,0013	0,0006	0,0018	0,0005	13	0,0008	0,0006	0,0003	0,0014	0,0004	114	0,0012	0,0012	0,0003	0,005	0,001								
Cl	7	12,6	6,1	0,6	49	16,9	13	11,0	35	2,5	430	137	124	19,2	37	0,1	6500	639								
CN	2	0,003	0,003	0,003	0,003	0	11	0,004	0,003	0,003	0,008	0,008	124	0,004	0,003	0,003	0,03	0,003								
Cu	7	0,0017	0,002	0,0009	0,0003	0,0008	13	0,001	0,001	0,001	0,001	0,001	124	0,002	0,002	0,001	0,03	0,003								
Carbone inorganique dissous	7	68	76	23	110	30	12	63	58	33	110	22	110	65	62	0	180	24								
Carbone organique dissous	7	1,6	1,5	0,3	4	1,2	13	1,5	0,8	0,2	7,4	2,1	121	2,6	1,3	0,2	16,2	3								
Durité totale (mg/L CaCO <sub>3</sub> )	7	296	344	122	423	109	13	162	172	9	280	84	124	270	221	0,7	3575	343								
F	7	0,15	0,12	0,04	0,34	0,1	12	0,38	0,34	0,13	0,83	0,19	121	0,59	0,35	0,05	3,2	0,63								
Fe	7	0,5197	0,34	0,007	1,4	0,32	12	0,14	0,097	0,002	0,37	0,16	122	0,527	0,13	0,001	15	1,57								
HCO <sub>3</sub> (calculé)	7	330	378	117	524	143	13	317	305	171	610	119	124	322	305	40	987	121								
Hg	2	0,0001	0,0001	0,0001	0,0001	0	12	0,0001	0,0001	0,0001	0,0001	0	111	0,0001	0,0001	0,0001	0,0003	0,0003								
I	4	0,1	0,1	0,1	0,10	0	12	0,1	0,1	0,1	0,3	0,06	114	0,1	0,1	0,1	0,6	0,06								
K	7	4,02	3,7	0,76	13	4,2	13	6,7	5,7	2,7	16,5	4,4	124	8,1	6	1,3	34	6,7								
Li	5	0,004	0,004	0,001	0,009	0,003	11	0,01	0,001	0,001	0,02	0,006	112	0,017	0,017	0,01	0,04	0,04								
MDT (calculées)	7	361	392	218	455	193	13	407	326	191	944	223	124	647	369	138	1,108	1,136	1,121							
Mg	7	30,1	26	10,9	47	12,8	13	20,2	23	1,4	31	9,7	124	29,6	26	0,04	390	35,5								
Mn	7	0,1485	0,13	0,0003	0,44	0,1678	13	0,16	0,05	0,0003	0,93	0,28	124	0,0703	0,017	0,0003	0,64	0,126								
N total	7	0,7	0,2	0,1	3,7	1,3	13	0,39	0,31	0,10	1,25	0,32	120	0,79	0,35	0,03	11,7	1,58								
Na	7	10	7	3	26	8	13	11,9	73	12,6	400	120	124	147	48	6	3,100	3,34								
NH <sub>4</sub> (en N)	7	0,04	0,02	0,02	0,11	0,03	13	0,3	0,22	0,02	1,25	0,34	122	0,35	0,1	0,02	7	0,74								
NO <sub>3</sub> (en N)	7	0,0029	0,002	0,0008	0,007	0,0023	13	0,001	0,001	0,001	0,006	0,001	122	0,002	0,001	0,001	0,02	0,003								
P total dissous (en P)	7	0,37	0,22	0,02	0,01	1,38	13	0,07	0,02	0,02	0,6	0,16	122	0,37	0,02	0,02	11,7	1,45								
Pb	4	0,004	0,004	0,004	0,004	0	12	0,004	0,004	0,004	0,004	0	114	0,004	0,004	0,004	0,04	0,003								
PO <sub>4</sub> (en P)	7	0,02	0,01	0,01	0,04	0,01	13	0,11	0,04	0,01	0,4	0,13	122	0,18	0,18	0,02	2,1	0,43								
HS (en S)	7	0,03	0,02	0,02	0,05	0,01	12	0,05	0,03	0,02	0,2	0,05	121	0,16	0,16	0,02	4,7	0,62								
Se	4	0,001	0,001	0,001	0,001	0	11	0,001	0,001	0,001	0,001	0	105	0,001	0,001	0,001	0,001	0,001								
SiO <sub>2</sub>	7	13,2	11,9	9,3	20	3,6	13	13	11,5	9,3	18,1	3	124	12,9	12,2	5,5	24	3,7								
SO <sub>4</sub>	7	41	49	15	75	21	13	17,5	16	0,5	43	11,8	122	61,8	33,5	0,5	1200	1284								
St	7	0,18	0,14	0,06	0,42	0,12	12	0,52	0,33	0,09	1,7	0,49	124	1,948	0,5	0,05	29	4,46								
TAS (calculé)	7	0,25	0,21	0,09	0,6	0,18	13	6,79	2,08	0,33	33,82	9,86	124	5,36	1,29	0,05	80,1	10,32								
U	2	0,005	0,005	0,005	0,005	0,005	11	0,006	0,005	0,005	0,001	0,001	100	0,006	0,005	0,005	0,01	0,002								
Zn	7	0,015	0,005	0,005	0,078	0,028	13	0,022	0,005	0,005	0,096	0,03	124	0,034	0,03	0,005	0,005	1,2	0,117							

## 2.4 TYPES D'EAU

Il est fort utile de classifier par type les eaux souterraines sur la base de leur composition chimique. Une façon de visualiser la variation régionale des types d'eau est de représenter la composition chimique (ions majeurs) de l'eau à l'aide de diagrammes radiaux placés aux sites d'échantillonnage et d'utiliser la carte géologique du socle rocheux comme fond de carte (Carte 2.15; Appendice H). Les diagrammes radiaux permettent de visualiser la distribution des différents types d'eau, grâce à l'orientation des apex du polygone, selon le principe d'une rose des vents.

La grosseur des cercles composant les diagrammes radiaux est proportionnelle à la racine carrée des concentrations en MDT. Ceci permet de distinguer la minéralisation des eaux et de les comparer, même lorsque les concentrations en MDT sont très variables. Les types d'eau différents sont identifiés à l'aide de couleurs distinctes.

Les types d'eau se distinguent par les constituants chimiques dominant:  $\text{Ca}^{2+}$ ,  $\text{Mg}^{2+}$ ,  $\text{Na}^+$ ,  $\text{K}^+$ ,  $\text{Cl}^-$ ,  $\text{SO}_4^{2-}$  et  $\text{HCO}_3^-$  (milliéquivalents, %). On parle par exemple d'eau 'chlorurée sodique' ou 'bicarbonatée calcique' pour des eaux dont les chlorures et le sodium et les bicarbonates et le calcium sont les ions majeurs, respectivement. Les types d'eau fournissent des informations générales, des indices quant à la compréhension du contexte hydrogéologique et du système d'écoulement de l'eau souterraine.

Afin de visualiser la variabilité régionale de la composition chimique de l'eau, les types d'eau simplifiés (cation et anion dominant) sont présentés à l'aide de symboles différents sur la Carte 2.16 (Appendice H). La carte des conditions hydrogéologiques est utilisée comme fond de carte. Le type d'eau le plus important est Ca-HCO<sub>3</sub> (67 échantillons). Ces sites d'échantillonnage sont concentrés dans les zones en conditions de nappe libre (zones préférentielles de recharge). Le type d'eau Mg-HCO<sub>3</sub> (8 échantillons) est aussi associé aux zones préférentielles de recharge. Le second type d'eau en importance est Na-HCO<sub>3</sub> (41 échantillons). Ce type d'eau caractérise les zones en conditions de nappe captive, particulièrement la région de Sainte-Anne-des-Plaines. Ce type d'eau pourrait être le

résultat de processus géochimiques (échange ionique, précipitation de minéraux). Le troisième type d'eau en importance est Na-Cl (26 échantillons). Ce type d'eau caractérise les vallées en conditions captives, particulièrement la région de Saint-Benoît. La source de cette salinité est le mélange, en différentes proportions, d'eau souterraine nouvellement rechargée avec de l'eau de la Mer de Champlain. On retrouve aussi quelques sites avec un type d'eau Na-Cl dans des zones en conditions de nappe libre. Pour ces sites, une contamination anthropique, comme l'utilisation de sels déglaçants, peut être la cause des concentrations élevées en sodium et chlorures.

## **2.5 SECTEURS DE QUALITÉ RELATIVE DE L'EAU SOUTERRAINE**

### **2.5.1 Classification par secteur**

La région étudiée est divisée en 7 secteurs selon une échelle de qualité relative de l'eau souterraine: le secteur 1 (Saint-Hermas), le secteur 2 (Rivière du Nord), le secteur 3 (sous-secteurs 3a, Lachute/Saint-Janvier; 3b, Sainte-Monique/Saint-Eustache; et 3c, Saint-Vincent), le secteur 4 (Collines d'Oka), le secteur 5 (Grenville/Chatham), le secteur 6 (sous secteur 6a, Sainte-Anne-des-Plaines; et 6b, Sainte-Thérèse), et le secteur 7 (Saint-Benoît/Saint-Joseph). La distribution des secteurs est présentée à la Carte 2.16 (Appendice H). La carte des conditions hydrogéologiques est utilisée comme fond de carte et les sites d'échantillonnage sont représentés par leur type d'eau respectif (voir section 2.4). Le Tableau 2.5 présente une synthèse hydrogéochimique pour chacun des secteurs: le type d'eau dominant, le pourcentage de puits échantillonnés dépassant les recommandations pour la qualité de l'eau potable au Canada (Santé Canada, 2001), les conditions hydrogéologiques, ainsi que les contrôles et processus hydrogéochimiques importants. La Carte 2.17 à l'échelle du 1/100 000, *Qualité de l'eau souterraine, Aquifère fracturé du sud-ouest du Québec* (Appendice H; en pochette), intègre l'ensemble de ces informations, incluant la classification par secteur, la synthèse hydrogéochimique, les types d'eau ainsi que les caractéristiques des sites d'échantillonnage, en utilisant la représentation des sites d'échantillonnage par diagrammes radiaux.

Tableau 2.5. Synthèse hydrogéochimique de chaque secteur (groupe de sites d'échantillonnage possédant des conditions hydrogéologiques et des compositions chimiques de l'eau souterraine similaire<sup>a</sup>)

N°	Secteurs et sous-secteurs	Nombre de puits de puits de sous-secteurs	Type d'eau Dominant <sup>b</sup>	Pourcentage des puits échantillonnés dépassant les recommandations pour la qualité de l'eau potable au Canada <sup>c</sup>								Durée totale <sup>g</sup>	
				Critère de qualité <sup>d</sup>				Objectifs esthétiques <sup>d</sup>					
				Ba	F	NO <sub>3</sub> (en N)	Fe	Mn	Na	Cl	SO <sub>4</sub>		
1	Saint-Hermès	16	Mixte-HCO <sub>3</sub> <sup>h</sup>			6%	63%	13%	13%		6%	13%	
2	Rivière-du-Nord	18	Na-HCO <sub>3</sub>	6%		22%	6%	17%	17%		28%	17%	
3	Lachute/Saint-Janvier (3a) Sainte-Monique/St-Eustache (3b) Saint-Vincent (3c)	62 <sup>i</sup>	Ca-Mg-HCO <sub>3</sub>	2%	2%	38%	38%	4%	7%	7%	7%	2%	
4	Collines d'Oka	6	Na-HCO <sub>3</sub>	17%		17%	17%					17%	
5	Grenville/Chatham	12	Ca-HCO <sub>3</sub>	33%		25%				17%	8%	25%	
6	Sainte-Anne-des-Plaines (6a) Sainte-Thérèse (6b)	17	Na-HCO <sub>3</sub>	6%	24%		24%	12%	41%	18%	71%	29%	
7	Saint-Benoît/Saint-Joseph	15	Na-Cl				47%	53%	73%	60%	27%	13%	

Meilleure qualité relative de l'eau souterraine

<sup>a</sup> Cette synthèse fournit des informations sur la qualité générale de l'eau souterraine que l'on peut s'attendre à retrouver dans un secteur donné, et ne doit être utilisée qu'à titre indicatif de la qualité d'eau d'un secteur. En effet, les zones de transition entre les secteurs, la complexité des conditions hydrogéologiques, la variété des unités géologiques et des effets locaux (contamination anthropique et profondeur des puits) font qu'il est toujours possible de rencontrer des exceptions dans chacun des secteurs.

<sup>b</sup> Le type d'eau dominant est déterminé à partir des médianes des cations et anions majeurs pour chaque secteur (concentrations en méq/L). Les éléments majeurs ayant une valeur de 20% (méq/L) du total des cations et anions définissent le type d'eau (Unesco, 1975).

Tableau 2.5 (suite)

N°	Secteurs et sous-secteurs	Conditions hydrogéologiques	Contrôles et processus hydrogéochimiques
			Autres commentaires
<b>1</b>	<b>Saint-Hermès</b>	<ul style="list-style-type: none"> <li>• 94% des puits échantillonnés en conditions de nappe captive;</li> <li>• Conditions de nappe libre à proximité de la colline Saint-André.</li> </ul>	<ul style="list-style-type: none"> <li>• 44% des puits échantillonnés sont artésiens (puits coulants);</li> <li>• 63% des puits exploitent l'interface depuis sous argile/roc fracturé;</li> <li>• Problèmes de salinité possibles dans le centre de la vallée.</li> </ul>
<b>2</b>	<b>Rivière-du-Nord</b>	<ul style="list-style-type: none"> <li>• 71% des puits échantillonnés en conditions de nappe captive;</li> <li>• Conditions de nappe libre non continues le long de la vallée.</li> </ul>	<ul style="list-style-type: none"> <li>• Problèmes de salinité possibles;</li> <li>• Possibilité de contamination anthropique.</li> </ul>
<b>3</b>	<b>Lachute/Saint-Jeanvier (3a)</b> <b>Sainte-Monique/Saint-Eustache (3b)</b> <b>Saint-Vincent (3c)</b>	<ul style="list-style-type: none"> <li>• 60% des puits échantillonnés en conditions de nappe libre;</li> <li>• Conditions de nappe captives locales et non continues;</li> <li>• Zones de recharge régionale et locale.</li> </ul>	<ul style="list-style-type: none"> <li>• Possibilité de contamination anthropique : <ul style="list-style-type: none"> <li>⇒ Sels déglaçanis (Na, Cl)</li> <li>⇒ Fertilisants chimiques ou organiques (<math>\text{NO}_3</math>)</li> </ul> </li> </ul>
<b>4</b>	<b>Collines d'Oka</b>	<ul style="list-style-type: none"> <li>• 60% des puits échantillonnés en conditions de nappe libre;</li> <li>• Conditions de nappe captives locales et non continues;</li> <li>• Zone de recharge.</li> </ul>	<ul style="list-style-type: none"> <li>• 83% des puits échantillonnés sont installés dans les roches du Grenville;</li> <li>• Problématique environnementale d'exposition au radon résidentiel ;</li> <li>• Possibilité de contamination anthropique.</li> </ul>
<b>5</b>	<b>Grenville/Chatham</b>	<ul style="list-style-type: none"> <li>• 73% des puits échantillonnés en conditions de nappe libre;</li> <li>• Conditions de nappe captives locales et non continues;</li> <li>• Zone de recharge.</li> </ul>	<ul style="list-style-type: none"> <li>• Influence géologique sur la qualité de l'eau souterraine : <ul style="list-style-type: none"> <li>⇒ Formation de Carillon, groupe de Chazy</li> <li>⇒ Concentrations élevées en F, Sr</li> </ul> </li> <li>• Possibilité de contamination anthropique.</li> </ul>
<b>6</b>	<b>Sainte-Anne-des-Plaines (6a)</b> <b>Sainte-Thérèse (6b)</b>	<ul style="list-style-type: none"> <li>• 100% des puits échantillonnés en conditions de nappe captive;</li> <li>• Conditions de nappe libre locales et non continues (Blainville);</li> <li>• Qualité de l'eau souterraine diminue avec la profondeur dans le roc (Sainte-Anne-des-Plaines).</li> </ul>	<ul style="list-style-type: none"> <li>• Influence géologique sur la qualité de l'eau souterraine : <ul style="list-style-type: none"> <li>⇒ Formation de Carillon, groupes de Chazy, Black River et Trenton</li> <li>⇒ Concentrations élevées en F, Ba, HS, Sr, PO<sub>4</sub></li> </ul> </li> <li>• Le sous-secteur Blainville a peu de puits de particuliers.</li> </ul>
<b>7</b>	<b>Saint-Benoît/Saint-Joseph</b>	<ul style="list-style-type: none"> <li>• 100% des puits échantillonnés en conditions de nappe captive.</li> </ul>	<ul style="list-style-type: none"> <li>• Problèmes de salinité importants (Mélange, en différentes proportions, d'eau souterraine nouvellement rechargeée, avec de l'eau de la Mer de Champlain).</li> </ul>

<sup>c</sup> Santé Canada (2001)  
<sup>d</sup> Unités en mg/L lorsque non spécifiées  
<sup>e</sup> Sans unité

f Matières dissoutes totales calculées en mg/L

<sup>g</sup> La dureté totale est la somme des concentrations de  $\text{Ca}^{2+}$  et  $\text{Mg}^{2+}$  exprimées en mg/L de  $\text{CaCO}_3$ . La dureté est un paramètre ne faisant pas l'objet de recommandations. On considère qu'une eau dont le degré de dureté se situe entre 80 et 100 mg/L est jugée acceptable, que lorsqu'elle est supérieur à 200 mg/L, elle est de qualité médiocre mais peut être tolérée par les consommateurs, et que lorsqu'elle est supérieure à 500 mg/L, elle est inacceptable pour la plupart des usages domestiques (Santé Canada, 2001).

<sup>h</sup> Un type d'eau est mixte lorsqu'il n'y a pas de cations dominants. Les valeurs (méq/L en %) des cations majeurs ( $\text{Ca}^{2+}$ ,  $\text{Mg}^{2+}$ ,  $\text{Na}^+$ ) sont du même ordre.

<sup>i</sup> 7 des 62 puits sont des puits installés à des sites ayant des niveaux d'échantillonnage multiples. Ces 7 puits ne sont pas utilisés pour les calculs de pourcentages de ce secteur.

<sup>j</sup> Référence sur l'exposition au radon résidentiel à Oka (Savard et al., 1998).

Les étapes suivies pour définir les secteurs de qualité relative de l'eau souterraine sont résumées ci-dessous.

En première étape, une méthode d'analyse par classification automatique hiérarchique (analyse *cluster*, méthode hiérarchique) est utilisée pour classifier les sites d'échantillonnage (Davis, 1986). Cette classification est réalisée pour les échantillons d'eau souterraine et 14 paramètres chimiques ( $\text{Ca}^{2+}$ ,  $\text{Mg}^{2+}$ ,  $\text{Na}^+$ ,  $\text{K}^+$ ,  $\text{HCO}_3^-$ ,  $\text{Cl}^-$ ,  $\text{SO}_4^{2-}$ ,  $\text{Fe}^{2+}$ ,  $\text{Mn}^{2+}$ ,  $\text{Br}^-$ ,  $\text{Sr}^{2+}$ ,  $\text{F}^-$ ,  $\text{Ba}^{2+}$ , HS $^-$ ). Cette méthode de classification groupe les échantillons selon un critère de similarité. Les résultats de cette analyse permettent de diviser les sites d'échantillonnage en 7 groupes ayant des caractéristiques géochimiques distinctes. Géographiquement, la distribution de ces groupes suit les contextes hydrogéologiques. Les résultats de l'analyse par classification automatique hiérarchique, combinés aux informations tirées des cartes de distribution des paramètres géochimiques (cartes 2.2 à 2.13), de la carte des diagrammes radiaux et des types d'eau (cartes 2.15 et 2.16), de la carte d'épaisseur des sédiments (Paradis, in press a) et de la carte des contextes hydrogéologiques (Hamel et al., 2001), sont utilisés pour établir la carte des secteurs de qualité relative de l'eau souterraine (Carte 2.16; Carte 2.17 *Qualité de l'eau souterraine* à l'échelle du 1/100 000).

Les secteurs sont classés selon une échelle de qualité relative de l'eau souterraine, de 1 (meilleure qualité) à 7 (qualité inférieure). Les caractéristiques hydrogéochimiques de chacun des 7 secteurs, présentées au Tableau 2.5, montrent qu'il y a des différences hydrogéochimiques importantes entre chaque secteur. Ce tableau fournit des informations sur la qualité générale de l'eau souterraine que l'on peut s'attendre à retrouver dans un secteur donné. Il doit être utilisé à titre indicatif de la qualité d'eau d'un secteur. En effet, les zones de transition entre les secteurs, la complexité des conditions hydrogéologiques, la variété des unités géologiques et des effets locaux (contamination anthropique et profondeur des puits) font qu'il est toujours possible de rencontrer des exceptions dans chacun des secteurs. L'évaluation de la qualité de l'eau souterraine d'un site doit toujours être accompagnée de l'évaluation des conditions hydrogéologiques de ce site, de la vulnérabilité, et des contrôles géochimiques possibles. Les caractéristiques

hydrogéochimiques importantes de chacun des secteurs sont résumées dans les paragraphes suivants.

### **2.5.2 Description des secteurs de qualité relative de l'eau**

Le secteur 1 (Saint-Hermas), dont le type d'eau dominant est Na-Ca-Mg-HCO<sub>3</sub> (mixte-HCO<sub>3</sub>), possède la meilleure qualité relative de l'eau souterraine de la région. Aucun des puits échantillonnés n'a de dépassements de critères de qualité pour l'eau potable. Par contre, ce secteur montre des dépassements d'objectifs esthétiques fréquents de manganèse pour 63% des sites d'échantillonnage; les pourcentages de dépassements sont calculés en fonction du nombre de puits échantillonnés dans le secteur. Trente-huit pour cent (38%) des échantillons ont une dureté totale supérieure à 200 mg/L, et 6% supérieure à 500 mg/L. Localement, des problèmes de salinité sont observés, causant des dépassements d'objectifs esthétiques pour le sodium (13%) et le chlorure (13%). Les sites d'échantillonnage ayant des dépassements pour ce secteur, et les secteurs suivants, peuvent être visualisés sur les cartes de distribution des paramètres géochimiques (cartes 2.2 à 2.13). Le secteur de Saint-Hermas, dominée par des conditions de nappe captive, a une vulnérabilité faible et présente une bonne protection pour la qualité des eaux souterraines. Enfin, le secteur de Saint-Hermas est dominée par une unité géologique peu réactive (les grès de la Formation de Cairnside), limitant ainsi les processus d'interaction eau-roche pouvant dégrader la qualité de l'eau souterraine.

Le secteur 2 (Rivière du Nord), de type d'eau dominant Na-HCO<sub>3</sub>, peut présenter des problèmes de dépassements en fluorures, principalement dans la partie ouest de la vallée. Ce secteur est caractérisé par des dépassements d'objectifs esthétiques moyennement fréquents de fer (22%) et de sulfures (28%). Localement, des problèmes de salinité sont observés, causant des dépassements d'objectifs esthétiques pour le sodium et les chlorures. Cette vallée, bien que dominée par des conditions de nappe captive, présente des conditions de nappe libre locales et non continues. La vulnérabilité de l'eau souterraine pour ce secteur varie selon les conditions hydrogéologiques.

Le secteur 3 est le plus étendu des secteurs, il a été divisé en trois sous-secteurs: les axes de Lachute/Saint-Janvier (3a), de Sainte-Monique/Saint-Eustache (3b) et de Saint-Vincent (3c). Le type d'eau dominant, Ca-Mg-HCO<sub>3</sub>, est représentatif d'une eau souterraine d'une zone de recharge. Cette information est confirmée par des conditions dominantes de nappe libre. Ce secteur est donc vulnérable à la contamination anthropique, telle que l'utilisation de sels déglaçants et de fertilisants chimiques et organiques. Les cas de contamination anthropique sont reliés à l'utilisation du territoire. Près de 40% des puits échantillonnés montrent des dépassements d'objectifs esthétiques pour le fer et le manganèse, alors que 76% des échantillons ont une dureté totale supérieure à 200 mg/L, et 9% supérieure à 500 mg/L.

Le secteur 4 (collines d'Oka), dont la majorité des puits échantillonnés sont installés dans les roches du Grenville, est de type d'eau dominant Na-HCO<sub>3</sub>. La densité de puits échantillonnés dans ce secteur est moins importante car le projet porte sur les aquifères sédimentaires rocheux fracturés. Un seul puits montre un dépassement en fluorures. Les collines d'Oka sont dominées par des conditions de nappe libre, avec présence locale de nappes captives. Ce secteur est donc vulnérable à la contamination anthropique. Une problématique environnementale importante pour le secteur des collines d'Oka est l'exposition domiciliaire au radon (Savard et al., 1998). Le radon est généré par la désintégration de l'uranium 238 présent dans les roches de l'intrusion alcaline d'âge Crétacé. Aucun des puits échantillonnés dans le cadre du projet régional n'est localisé dans l'intrusion. Les échantillons d'eau souterraine de 5 puits localisés dans les roches du socle grenvillien qui entourent l'intrusion ont des concentrations en uranium inférieures à la limite de détection (<0.005 mg/L). Aucune analyse du gaz radon n'a été effectuée dans l'eau souterraine du secteur dans le cadre de ce projet.

Le secteur 5 (Grenville/Chatham), localisé à l'extrême ouest de la région étudiée, est caractérisé par le type d'eau dominant Ca-HCO<sub>3</sub>. Ce secteur, dominé par des conditions de nappe libre, constitue une zone de recharge. Le problème de qualité le plus important pour ce secteur est relié aux concentrations élevées en fluorures. En effet, 33% des puits échantillonnés ont des dépassements du critère de qualité pour les fluorures. Les unités

géologiques (dolomie et calcaires de la Formation de Carillon et calcaires du Groupe de Chazy) semblent influencer la géochimie des eaux souterraines. Des dépassements d'objectifs esthétiques moyennement fréquents pour le fer (25%) et les sulfates (17%) sont dénombrés. Quarante-deux pour-cent (42%) des échantillons ont une dureté totale supérieure à 200 mg/L, et 17% supérieure à 500 mg/L. Des conditions de nappe libre dominent ce secteur, le rendant vulnérable à la contamination anthropique.

Le secteur 6, localisé à l'extrême est de la région étudiée, est divisé en deux sous-secteurs: Sainte-Anne-des-Plaines (6a), et Sainte-Thérèse (6b). Le secteur 6 est dominé par le type d'eau Na-HCO<sub>3</sub>. Des dépassements des critères de qualité pour les fluorures (24%) et le baryum (6%) y sont notés. On y compte aussi un bon nombre de dépassements d'objectifs esthétiques, 71% pour les sulfures, 47% pour les MDT, 41% pour le sodium, 29% pour le pH, et 24% pour le fer. Vingt-neuf pour-cent (29%) des échantillons ont une dureté totale supérieure à 200 mg/L. Les dolomies et les calcaires de la Formation de Carillon, ainsi que les calcaires et les argilites des groupes de Chazy, Black River et Trenton, ont une influence sur la qualité des eaux souterraines de ce secteur. Des processus d'échange ionique Ca<sup>2+</sup>-Na<sup>+</sup> sont probablement responsables des concentrations élevées en sodium et faibles en calcium. L'aquifère rocheux de la plaine argileuse du sous-secteur Sainte-Anne-des-Plaines (6a) est en conditions de nappe captive. La vulnérabilité de ce secteur est donc faible. Enfin, les résultats de deux puits échantillonnés à différentes profondeurs dans le cadre de ce projet, et des études effectuées pour la municipalité de Sainte-Anne-des-Plaines ont montré que la qualité des eaux souterraines de ce secteur diminue rapidement avec la profondeur (augmentation de la salinité et des concentrations en sulfures). Il est donc possible d'envisager que le pompage excessif d'un puits puisse causer une dégradation de la qualité d'eau par la venue d'eau de moins bonne qualité provenant de zones plus profondes. Le sous-secteur Sainte-Thérèse (6b) compte peu de puits de particuliers par comparaison avec les autres secteurs, il n'était donc pas un secteur prioritaire pour le projet de caractérisation. Ce sous-secteur ayant des similarités avec celui de Sainte-Anne-des-Plaines (conditions de nappe captive et même unités géologiques), il est possible d'estimer que la qualité de l'eau souterraine y soit similaire.

Enfin, le secteur 7 (Saint-Benoît/Saint-Joseph), dont le type d'eau dominant est Na-Cl, possède la moins bonne qualité relative d'eau souterraine de la région. Le problème de qualité le plus important pour ce secteur est la salinité. La valeur médiane de la conductivité spécifique des échantillons de ce secteur est de 1,4 mS/cm. Cette valeur, la plus élevée des 7 secteurs, s'explique par des concentrations élevées en sodium (73% de dépassements) et en chlorures (60% de dépassements). La source de cette salinité est le mélange, en différentes proportions, d'eau souterraine nouvellement rechargée, avec de l'eau de l'ancienne Mer de Champlain. Pour le puits le plus salin échantillonné, la conductivité spécifique de 18,5 mS/cm rend l'eau souterraine inapte à la consommation. Le secteur 7 présente d'autres dépassements d'objectifs esthétiques, dont les MDT (67%), le manganèse (53%), le fer (47%), le sulfure (27%). Vingt pour-cent (20%) des échantillons ont une dureté totale supérieure à 200 mg/L, et 7% supérieure à 500 mg/L. La distribution des secteurs ayant une eau souterraine à salinité plus élevée que la moyenne est difficile à prévoir. Il est donc possible d'envisager que le pompage excessif d'un puits puisse causer une dégradation de la qualité de l'eau par la venue d'eau plus salée provenant de zones adjacentes.

## **2.6 CONCLUSIONS – IMPLICATION POUR LA CONSOMMATION DE L'EAU SOUTERRAINE**

La qualité de l'eau souterraine peut être qualifiée de bonne sur l'ensemble des territoires groupés des quatre MRC impliquées puisqu'elle répond toujours, à l'exception de 12/146 échantillons, aux exigences des critères de qualité établis pour protéger la santé des consommateurs. Mais, lorsque l'on considère les objectifs esthétiques, la qualité de l'eau sur le territoire étudié est plutôt variable. En effet, 99/146 échantillons ne répondent pas aux objectifs esthétiques pour au moins l'un des paramètres suivants:  $\text{Fe}^{2+}$ ,  $\text{Mn}^{2+}$ ,  $\text{HS}^-$ ,  $\text{SO}_4^{2-}$ ,  $\text{Na}^+$ ,  $\text{Cl}^-$ , MDT et pH. De plus, 72/146 échantillons ont une dureté supérieure à 200 mg/L, et 9/146 échantillons ont une dureté supérieure à 500 mg/L. On considère que lorsque la dureté est supérieure à 200 mg/L, l'eau est de qualité médiocre mais peut être tolérée par les consommateurs, et que lorsqu'elle est supérieure à 500 mg/L, elle est inacceptable pour la plupart des usages domestiques. Toutefois, tous les dépassements de

critères esthétiques mentionnés ici sont remédiabes par divers traitements de l'eau disponibles commercialement.

Une problématique de salinité de l'eau a été identifiée dans le secteur de Saint-Benoît tout particulièrement, elle a fait l'objet d'une étude locale. Pour ce qui est des critères de qualité d'eau pour les paramètres microbiologiques, 12/80 échantillons ont des dépassements mesurés en coliformes totaux. Les causes de ces dépassements ne sont pas identifiées, mais elles pourraient être reliées aux situations locales, par exemple à la contamination à partir de fosses septiques.

Les représentations cartographiques de différents paramètres géochimiques (cartes 2.2 à 2.13; Appendice H) démontrent que la qualité naturelle des eaux souterraines varie en fonction des contextes géologiques et hydrogéologiques. Les résultats documentés dans ce rapport présentent un portrait régional de la qualité de l'eau nécessaire au suivi ultérieur de cette qualité et à la détection d'une éventuelle détérioration.



## **Chapitre 3**

# **HYDROGEOCHEMISTRY AND GROUNDWATER ORIGIN OF THE BASSES-LAURENTIDES SEDIMENTARY ROCK AQUIFER SYSTEM, ST. LAWRENCE LOWLANDS, QUÉBEC, CANADA**

Vincent Cloutier<sup>1</sup>, René Lefebvre<sup>1</sup>, Martine M. Savard<sup>2</sup>, Édith Bourque<sup>2,3</sup>, René Therrien<sup>4</sup>

<sup>1</sup>Institut national de la recherche scientifique, INRS-Eau, Terre & Environnement, C.P. 7500, Sainte-Foy (Québec), G1V 4C7, Canada

<sup>2</sup>Geological Survey of Canada, Natural Resources Canada, 880, chemin Sainte-Foy, Suite 840, Québec (Québec), G1S 2L2, Canada

<sup>3</sup>Maintenant au Bureau d'audiences publiques sur l'environnement, 575, rue Saint-Amable, Suite 2.10, Québec (Québec), G1R 6A6, Canada

<sup>4</sup>Département de géologie et de génie géologique, Université Laval, Sainte-Foy (Québec), G1K 7P4, Canada

## RÉSUMÉ

Une étude hydrogéochimique détaillée a été réalisée sur le système aquifère de roches sédimentaires paléozoïques des Basses-Laurentides, au Québec, sur une région d'étude de 1500 km<sup>2</sup>. Les objectifs étaient de déterminer l'influence des contextes hydrogéologiques et géologiques sur la géochimie de l'eau souterraine, d'identifier l'origine de l'eau souterraine, de reconnaître les processus contrôlant la chimie des eaux souterraines ainsi que son évolution dans l'espace et le temps. Des échantillons d'eau souterraine ont été prélevés à 153 sites, caractérisant l'ensemble des unités géologiques et hydrogéologiques jusqu'à une profondeur de 140 m. L'eau souterraine a été analysée pour les constituants inorganiques majeurs, mineurs et traces, les isotopes stables  $\delta^2\text{H}$ ,  $\delta^{18}\text{O}$  et  $\delta^{13}\text{C}$  du carbone inorganique dissous (CID), et certains échantillons ont été analysés pour  $^{87}\text{Sr}/^{86}\text{Sr}$ ,  $^3\text{H}$  et  $^{14}\text{C}$  du CID. Les précipitations ont été échantillonnées pour établir leur valeurs  $\delta^2\text{H}$  et  $\delta^{18}\text{O}$  et la droite locale des eaux météoriques. Les zones préférentielles de recharge sont caractérisées par une eau souterraine enrichie en  $^3\text{H}$  de type Ca-Mg-HCO<sub>3</sub>, et les zones confinées par des eaux souterraines submodernes de types Na-HCO<sub>3</sub> et Na-Cl. Deux sources d'eau souterraine sont identifiées dans le système aquifère, l'eau météorique moderne et l'eau Pléistocène de la Mer de Champlain. La région est caractérisée par des variations significatives de la géochimie et de la qualité des eaux souterraines, contrôlées par la dernière glaciation, l'invasion de la Mer de Champlain, la diversité lithologique des roches, et les systèmes d'écoulement locaux. Cette situation engendre donc une grande variété de types et d'origines d'eau souterraine à l'intérieur d'une région restreinte.

**ABSTRACT**

A comprehensive hydrogeochemical study was carried out in the Paleozoic Basses-Laurentides sedimentary rock aquifer system in Québec, over a 1500 km<sup>2</sup> study area. The objectives were to determine the influence of hydrogeological and geological contexts on groundwater geochemistry, identify groundwater origin, recognize processes controlling groundwater geochemistry and its evolution in space and time. Groundwater samples were collected at 153 sites, characterizing all geological and hydrogeological units to a maximum depth of 140 m. Groundwater was analyzed for major, minor and trace inorganic constituents, stable isotopes  $\delta^2\text{H}$ ,  $\delta^{18}\text{O}$ , and  $\delta^{13}\text{C}$  of dissolved inorganic carbon (DIC), and some samples were analyzed for  $^{87}\text{Sr}/^{86}\text{Sr}$ ,  $^3\text{H}$ , and  $^{14}\text{C}$  of DIC. Precipitation samples were analyzed for their  $\delta^2\text{H}$  and  $\delta^{18}\text{O}$  values to establish the local meteoric water line. Preferential recharge areas are characterized by tritiated Ca-Mg-HCO<sub>3</sub> groundwater, and confined conditions by submodern Na-HCO<sub>3</sub> and Na-Cl groundwater types. Two groundwater end-members are identified in the aquifer system, modern meteoric water and Pleistocene Champlain Sea water. The region displays significant variations of groundwater geochemistry and quality, controlled by the latest glaciation, Champlain Sea invasion, rock diversity, and local flow systems. This situation leads to varied water types and origins within a restricted area.

### 3.1 INTRODUCTION

Groundwaters of the Basses-Laurentides sedimentary rock aquifer system are a very important supply of freshwater for the region. With a population of about 250 000 inhabitants, approximately 23% depend on groundwater for their water supply. From this 23%, about 62% have their own wells and 38% are served by municipal well fields (MENV, 2000). Groundwater also plays an important role in a variety of sectors, as in agriculture for irrigation of crops and animal watering, groundwater-dependant industries (freshwater bottling, fish farming), rock quarries, or golf courses irrigation (Nastev et al., in press). All these activities use large quantities of groundwater, and some are also potential sources of contamination of the aquifer system.

In the new context of sustainable development, and with regard to different conflicts between groundwater users, a regional hydrogeological characterization project was initiated by the regional, provincial and federal governments. The general objective of this large project was to gain a better knowledge of the groundwater resources (quantity and quality) of the area to support their management and protection. A second objective of this study was to develop a methodology to characterize, at the regional scale, fractured sedimentary rock aquifers (Savard et al., in press). As part of this regional hydrogeological study, Nastev et al. (2001; in prep a) investigated the hydraulic properties and presented a numerical model of the groundwater flow for the regional aquifer, and Hamel et al. (2001) studied groundwater recharge in the sedimentary rock aquifer. Thus, the overall program covers both the hydrodynamics and hydrogeochemistry of the aquifer system.

The hydrogeochemical characterization reported here specifically aimed at assessing groundwater quality at the regional scale, determining groundwater origin, identifying the processes controlling groundwater geochemistry and understanding the geochemical evolution of groundwater in space and time. The project also has practical results, such as evaluating if there are inorganic constituents exceeding the guidelines for Canadian drinking water quality (Health Canada, 2003), and in that case, determining if their

origins result from natural or human-induced processes (Cloutier et al., *in press*). The geochemical data set establishes the natural geochemical background of the groundwater in the region. That database can be used to follow the evolution of the water quality due to human activities, identify areas vulnerable to contamination (Ross et al., 2003), elaborate management strategies for the resource and evaluate the impact of future development on the groundwater resource. The Basses-Laurentides region has a highly variable groundwater geochemistry that made it a very interesting scientific case study. As it will be shown, that variability is largely due to the hydrogeological context, the geology, and the Quaternary paleo-hydrogeology of the region.

The following approach was developed for the hydrogeochemical characterization: 1) regional groundwater sampling to a depth of about 140 m, from the recharge areas and along groundwater flow paths, 2) the geochemical characterization of all hydrogeological units, including the different rock formations, the till sediments and the clay aquitard, 3) the combined use of inorganic and isotopic geochemistry, and 4) the isotopic characterization of local precipitation. This paper presents results of the regional groundwater geochemical characterization and the relationship between groundwater types and geological as well as hydrogeological context. The complete geochemical dataset and the physical characteristics of the sampling sites are available in a table as Electronic Supplementary Material (ESM) on Springer's server (<http://link.springer.de>).

Regional hydrogeochemical studies have been shown to be valuable to study groundwater issues, amongst others, management of regional aquifers (Gosselin et al., 2001), groundwater evolution (Hendry and Schwartz, 1990; Hiscock et al., 1996), tracing groundwater flow (Panno et al., 1994; Clark et al., 1998; Stimson et al., 2001), and salinization of groundwater (Vengosh et al., 2002) and soils (Valenza et al., 2000). These integrated hydrogeochemical studies combine a variety of tools, including major and minor ions, isotope geochemistry, groundwater dating and hydrogeochemical modeling, with geological framework, physical hydrogeology, or geophysics, to understand fluid flow and mass transport in complex aquifer systems. By its comprehensive characterization program, the hydrogeochemical study of the Basses-Laurentides

sedimentary rock aquifer system presented here is an integrated study, as it uses the knowledge of the geological and hydrogeological characterization to support the geochemical interpretation. The extent of the characterization, in terms of area covered, number of wells sampled, and parameters analyzed, is also exceptional. Finally, the particular context of the study area, including a complex geological history, a variety of geological and hydrogeological context, result in a groundwater geochemistry influenced by ancient and present hydrogeological processes. This study thus sheds light both on ongoing geochemical processes as well as on the quaternary geological events that have influenced groundwater geochemistry in the area. This paper focuses on a complete description of the results of the geochemical characterization program and on identification of the origin of groundwater in the area. Other papers using results from this investigation focus respectively on the geochemical processes (Cloutier et al., in prep a; *Chapitre 4*) and on a multivariate statistical analysis of regional hydrogeochemistry data (Cloutier et al., in prep b; *Chapitre 5*).

### **3.2 CONTEXT OF THE STUDY AREA**

The study area, shown on Figure 3.1, is located on the North shore of the St. Lawrence River, northwest of Montréal. It covers approximately 1500 km<sup>2</sup>, in a geographical region named the Basses-Laurentides. The Basses-Laurentides belong to the physiographic region of the St. Lawrence Lowlands, a region having a generally flat topography, with the exception of the Monteregian Hills related to Cretaceous intrusions. There are two such intrusions in the Basses-Laurentides, the Oka Hills with a maximum elevation of about 250 m above mean sea level (masl), and the St. André Hills with an elevation of about 130 masl. The Laurentian Highlands, part of the Grenville Province of the Canadian Shield, border the study area to the North. The southwest, south, and southeast borders of the study area are surface water limits, namely the Outaouais River, the Deux Montagnes Lake, with an elevation of about 23 masl, and the Mille Îles River. To the East, the study area ends in the watershed of the Mascouche River. Many rivers and small streams drain the study area, the main ones being the du Nord River, Rouge River, du Chêne River, du Chicot River, and Mascouche River (Fig. 3.1).

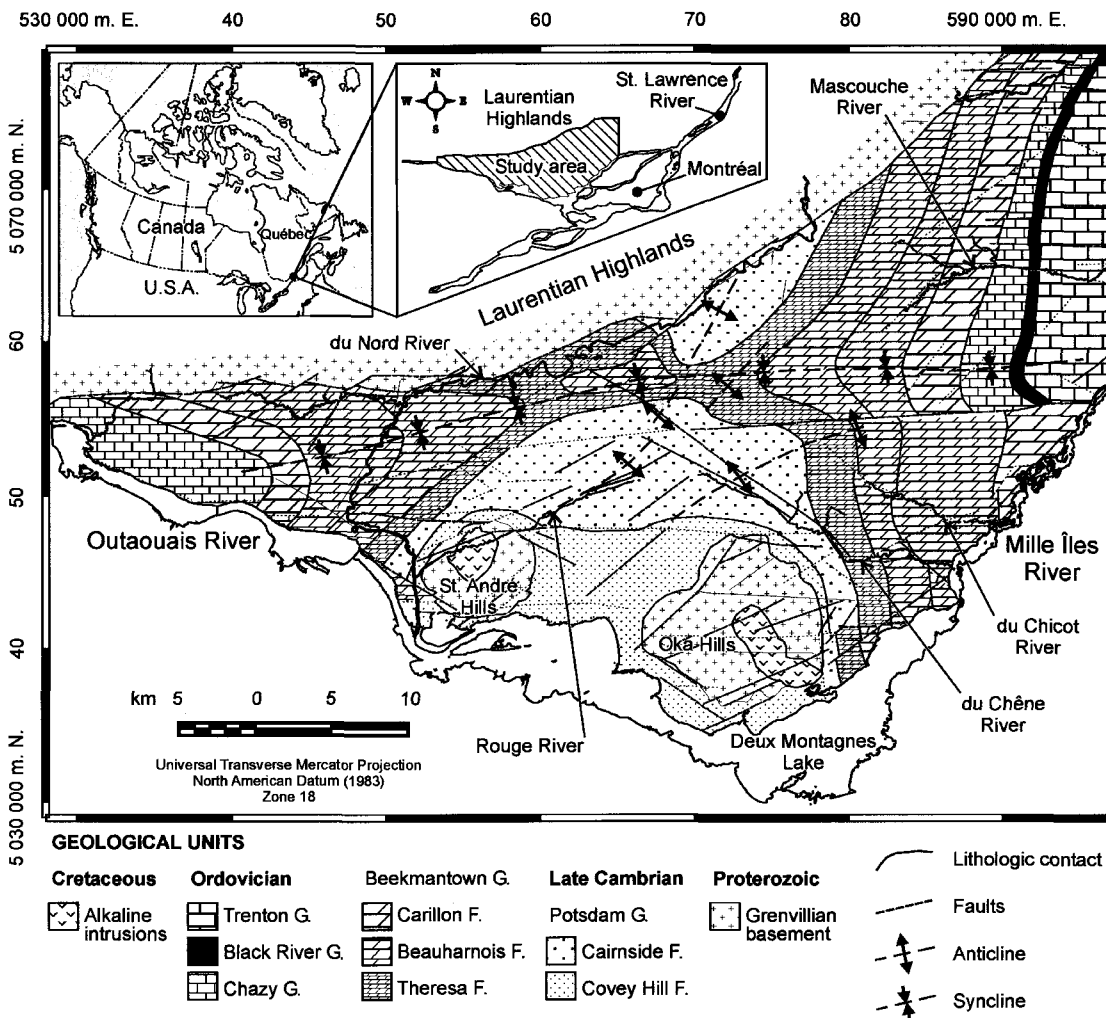


Figure 3.1. Location and geology of the Basses-Laurentides sedimentary rock aquifer system (geological map modified from Rocher et al., in press).

### 3.2.1 Geological setting and history

#### 3.2.1.1 *Paleozoic and Cretaceous geology*

The Basses-Laurentides aquifer system, which is the focus of this study, is part of the geological Province of the St. Lawrence Platform, which consists of nearly horizontal Cambrian-Ordovician autochthonous sedimentary formations lying in unconformity on crystalline basement of the Precambrian Grenville Province. In the study area, the sedimentary formations rarely crop out, as Quaternary sediments cover them. The geology of the St. Lawrence Platform is described in the geological reports of Clark (1972) and Globensky (1987). The geological map (Fig. 3.1), modified from Rocher et al. (in press), shows the distribution of the main geological units.

Details on lithology, mineralogy and fracture filling of the sedimentary formations are summarized in Table 3.1. The Cambrian siliciclastic rocks of the Potsdam Group are at the base of the sequence. The Potsdam Group is divided into two formations, the Covey Hill and the Cairnside (Globensky, 1987). The Covey Hill Formation is made of a reddish feldspathic sandstone, locally conglomeratic and poorly cemented. The Cairnside Formation is a well-cemented, pure, quartz arenite sandstone. Bernstein (1992), Salad Hersi and Lavoie (2001), and Salad Hersi et al. (2003) subdivide the Ordovician Beekmantown Group into three formations. The first two formations are the dolomitic sandstone and sandy dolostone of the Theresa, and the sandy to pure, massive, dolostone of the Beauharnois. The third formation is the Carillon, a pure dolostone with limestone near the top. The dissolution porosity of the dolostone units of the Beekmantown were cemented mostly by quartz and calcite (Chi et al., 2000). Following are the sandstone of the Lower Chazy, and the limestone and shale of the Upper Chazy Group, the dolostone, shale and limestone of the Black River Group and the limestone and shale of the Trenton Group (Globensky, 1987; Salad Hersi and Lavoie, 2001). Organic matter is found in the carbonates of the Cambrian-Ordovician sequence as zooclasts and solid bitumen (Héroux and Bertrand, 1991). Within the limits of the Montréal area, this sedimentary sequence is at least 1200 m thick (Clark, 1972).

Table 3.1. Lithology, mineralogy and fracture filling of the Cambrian-Ordovician sedimentary rocks

Geological units	Lithology, mineralogy, and fracture filling	Ref. <sup>a</sup>
Covey Hill F.	Feldspathic sandstone; 10-30% of fresh and weathered K-feldspar; traces of micas >0.03 mm (biotite, muscovite, chloritic matter, illite); <1% heavy minerals (zircon, apatite, tourmaline, sphene-rutile, leucoxene, pyrite, hematite); carbonates in fractures	1
Cairnside F.	Pure quartz sandstone (>95% SiO <sub>2</sub> ); overgrowth-cementation of quartz; <1-2% of alkali feldspar and microcline; traces of micas >0.03 mm rare; trace of heavy minerals (zircon, apatite, tourmaline, sphene-rutile, leucoxene, pyrite, hematite); carbonates in fractures	1
Theresa F.	Observed dolomite-quartz proportions highly variable; 1-2% of microcline and plagioclase; traces-5% of magnetite, zircon, pyrite, and hornblende; fossiliferous	2
Beauharnois F.	Mainly dolomite crystals; few quartz grains and clay minerals; magnetite and pyrite; cavities filled mainly by calcite, and a few by dolomite, gypsum and halite; fossiliferous	2
Carillon F.	Pure dolostone with limestone near its summit; calcite and dolomite nodules	3
Chazy G. Lower	61% of quartz; 35% of carbonate; 1% of microcline; 3% of hornblende, biotite and zircon	2
Upper	Limestone and shale; highly fossiliferous	2
Black River G.	Dolostone with small quantities of sandy, clayey, and calcareous materials; disseminated pyrite; limestone with thin shale beds; fossiliferous	2
Trenton G.	Clayey limestone; highly fossiliferous; shale beds	2

<sup>a</sup> References: 1: Lewis (1971), 2: Globensky (1987), 3: Salad Hersi and Lavoie (2001).

Precambrian rocks, such as quartzite, crystallized limestone, gneiss, and anorthosite, crop out north of the study area in the Grenville Province, and form a window through the Paleozoic sequence with the Cretaceous alkaline intrusions of Oka and St. André Hills. The Cretaceous intrusions are made of a variety of rocks, such as carbonatites, okaïte, lamprophyre, as well as metasomatic alteration of surrounding rocks. The Oka complex was exploited for pyrochlore, a niobium oxide, and for apatite, magnetite and calcite (Gold, 1972). Ultramafic sills, associated to the intrusions emplacement, are present in the Potsdam Group (Lewis, 1971). The main structural features are the normal faults systems to the North along the contact with the Grenville Province, the faults associated with the Cretaceous intrusions, and the northeast-southwest anticlines in the center of the study area, exposing the Ordovician units on both sides of the Cambrian sandstone. The fault

systems, the Cretaceous intrusions, and the erosion processes that followed the Paleozoic period contributed to shaping of the Basses-Laurentides.

### *3.2.1.2 Quaternary geology*

The last Quaternary glaciation covered the Paleozoic and Grenvillian units with Upper Wisconsinan sediments, such as glacial till, and glacio-fluvial sand and gravel (Bolduc and Ross, 2001). During deglaciation, the retreat of the Laurentide Ice Sheet of the St. Lawrence Valley, combined with the depression of the continent due to the glaciation, allowed marine invasion from the St. Lawrence Gulf. This marine invasion, which created the Champlain Sea, established its main basin at about 12 000 BP (Parent and Occhietti, 1988). The study area was submerged for about 2000 years by water of the Champlain Sea (Lévesque, 1982). This water was a mixture of continental waters, including meltwater from the Laurentide Ice Sheet and local precipitation, and salt water from the St. Lawrence Gulf (Hillaire-Marcel, 1988).

The Champlain Sea episode left marine sediments, mainly clayey-silts to silty-clays, that can reach a thickness of more than 80 m (Bolduc and Ross, 2001). The Champlain Sea clay is overlying till or glacio-fluvial sand and gravel units of variable thickness. The till is also found at the surface, above the rock sequence, in elevated topographic areas. The Champlain Sea reworked the upper part of this till unit. The till is highly variable in composition and texture depending of the underlying rock units (Ross and Bolduc, 2001); its composition relates mainly to the glacial erosion of Paleozoic sedimentary formations, such as sandstone, dolostone, and limestone, with some contribution of Precambrian rocks.

### **3.2.2 Hydrogeological setting**

Hamel et al. (2001) have presented a map of the hydrogeological conditions of the study area, Figure 3.2a. The map illustrates the regions of the study area with unconfined or semi-confined conditions, and with confined conditions. The following is a description of

how the area can be divided based on the hydrogeological contexts. This division of the study area is used to facilitate the presentation and discussion of the hydrogeochemical results.

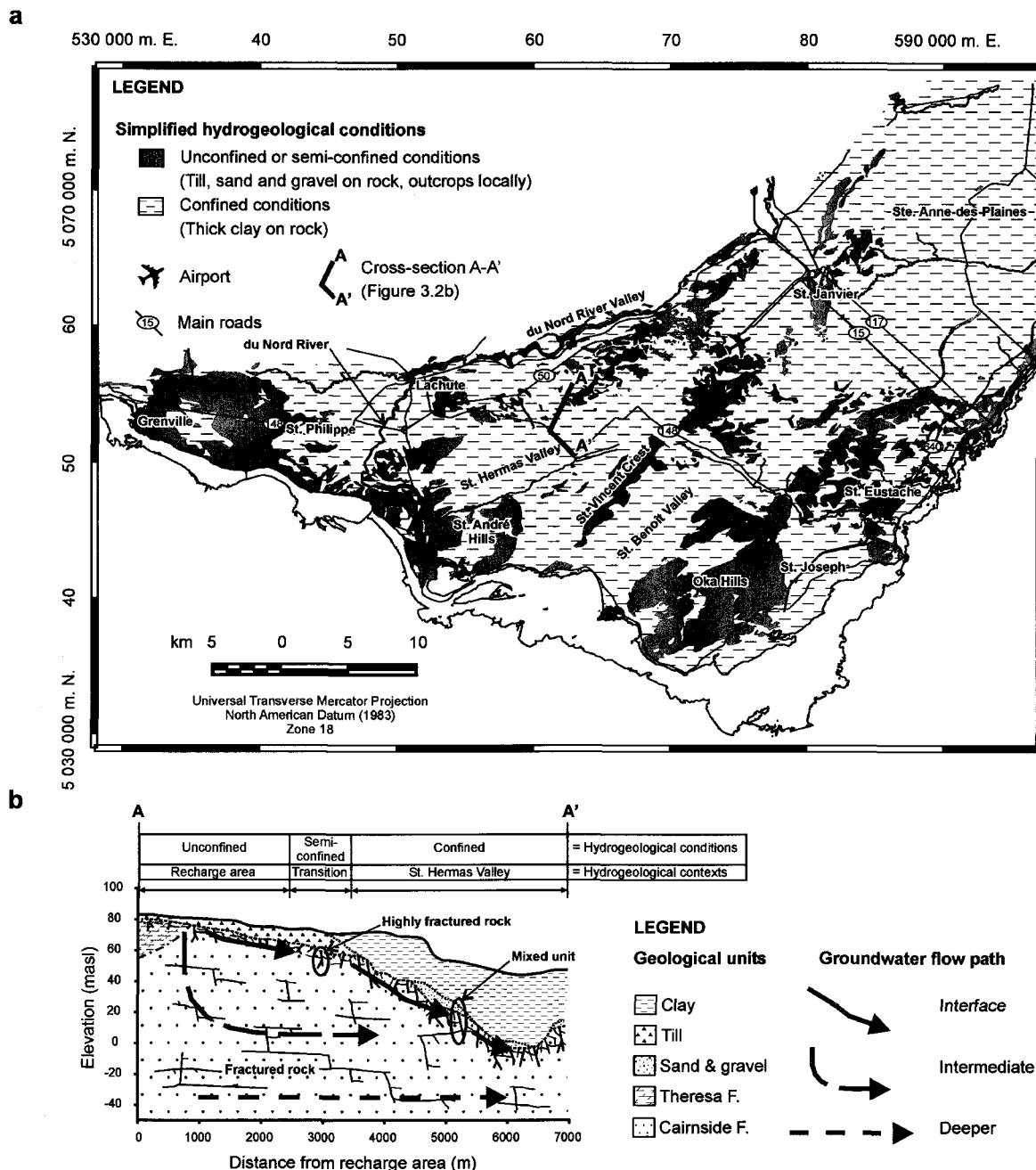


Figure 3.2. **a** Simplified hydrogeological conditions (modified from Hamel et al., 2001), and **b** cross-section A-A' illustrating the groundwater flow conceptual model and the main hydrostratigraphic units.

Unconfined or semi-confined conditions are generally found in areas of elevated topography, sometimes with rock outcrops or with thin to thick permeable surface sediments. These sediments are generally till, but can also be alluvial sand and gravel. This hydrogeological condition is very important, as it characterizes areas of preferential groundwater recharge. The main recharge for the Basses-Laurentides sedimentary rock aquifer system is along a southwest-northeast axis, from Lachute to St. Janvier (Fig. 3.2a). This axis has an elevation between 70 masl and more than 80 masl. The other recharge zones are the Oka and St. André Hills, the region from the airport to St. Eustache, and the region from Grenville to St. Philippe, West of du Nord River. The last zone is the St. Vincent Crest, northwest of Oka Hills. This southwest-northeast Crest, with an elevation of about 60 masl, is a local recharge zone for the rock aquifer system.

For the remainder of the region, the rock aquifer system is confined by thick low permeability Champlain Sea clays. These confined conditions prevail in three southwest-northeast trending buried valleys: 1) du Nord River Valley, bordering the Laurentian Highlands, 2) St. Hermas Valley, north of St. André Hills and St. Vincent Crest, and 3) St. Benoît Valley, between St. Vincent Crest and Oka Hills. Flowing artesian wells are found in these three buried valleys. The clay thickness can reach more than 90 m in St. Benoît Valley (Paradis, in press a). The surface elevation is about 60 masl in du Nord Valley, and 50 masl in St. Hermas and St. Benoît valleys. Bedrock depressions, filled with marine clay, are also found along the north-south segment of du Nord River, and at St. Joseph, east of Oka Hills. Finally, the clay reaches a thickness of more than 30 m in the eastern region of Ste. Anne-des-Plaines.

The transition from unconfined to confined conditions in the area, as well as the main hydrostratigraphic units adapted from Savard et al. (in press), are illustrated on the cross-section of the groundwater flow conceptual model (Fig. 3.2b). Precipitation recharges the aquifer mainly by infiltration through the till unit, in the unconfined area. At greater distance from the recharge zone, the clay aquitard unit confines the aquifer. Based on hydrogeological and geological properties, the aquifer system can be divided into two distinct units: the highly fractured and the fractured rocks. The highly fractured rock

consists of the first few meters of the sedimentary units that are more weathered, with fractures more connected and more effective, than the underlying rock. Simard (1977) also observed this highly fractured unit in a hydrogeological study of the same aquifer. A mixed unit, consisting of highly fractured rock in hydraulic connection with sand and gravel, is also observed in the buried valleys. These sand and gravel units can be fluvio-glacial sediments or washed-out till deposited above the sedimentary rocks, below the clay aquitard. In the buried valleys, some wells are screened in the sand and gravel unit only, and others through the mixed unit. Below the highly fractured rock is the fractured rock unit of the aquifer system. As the sedimentary rocks are well cemented by quartz or calcite, the primary porosity is very low. Thus, groundwater flows through secondary porosity, such as fractures, bedding planes, alteration zones, or dissolution cavities. The groundwater flow through the highly fractured rock is faster than in the deeper fractured rock unit, due to a higher hydraulic conductivity. As part of the same regional hydrogeological project, Nastev et al. (2001; in prep b) characterized the hydraulic properties of the rock formations to a depth of about 140 m, Nastev et al. (in prep a) developed a regional groundwater flow model, and Hamel et al. (2001) characterized the hydraulic properties of the till in the recharge areas. Table 3.2 summarizes the characteristics and the hydraulic properties of the main hydrostratigraphic units.

Table 3.2. Characteristics and hydraulic properties of the main hydrostratigraphic units

Hydrostratigraphic unit	Characteristics and type of hydraulic tests	$K_m^a$ (m/s)	Ref. <sup>b</sup>
Clay aquitard	Clayey-silt to silty-clay Champlain Sea sediments Field-determined in unweathered clay, Varennes, northeast of Montréal	$3.4 \times 10^{-10}$	1
Till	Sediments of variable thickness above bedrock Infiltrometers, slug and pumping tests	$3 \times 10^{-7}$	2
Highly fractured rock	Mixed unit (first few meters of sedimentary rock & sand and gravel) 6 multi-well pumping, 6 well productivity, and 13 slug tests	$7.8 \times 10^{-4}$	3
Fractured rock	Sedimentary (sandstone, dolostone, limestone), and Precambrian rocks 20 packer, 132 specific capacity, 23 single-well, and 12 multi-well pumping tests	$2.6 \times 10^{-5}$	4

<sup>a</sup> Geometric mean hydraulic conductivity

<sup>b</sup> References: 1: Desaulniers and Cherry (1989), 2: Hamel et al. (2001), 3: Nastev et al. (2001), 4: Nastev et al. (in prep b).

Figure 3.3 shows the potentiometric surface of the regional rock aquifer, with arrows showing the general direction of groundwater flow. The main groundwater flow paths are generally from North to South. The potentiometric surface follows the rock or surface topography, and is higher in the preferential groundwater recharge areas identified previously. The groundwater divides are observed in the main recharge areas, such as from Lachute to St. Janvier, and in the local groundwater flow system of the St. Vincent Crest.

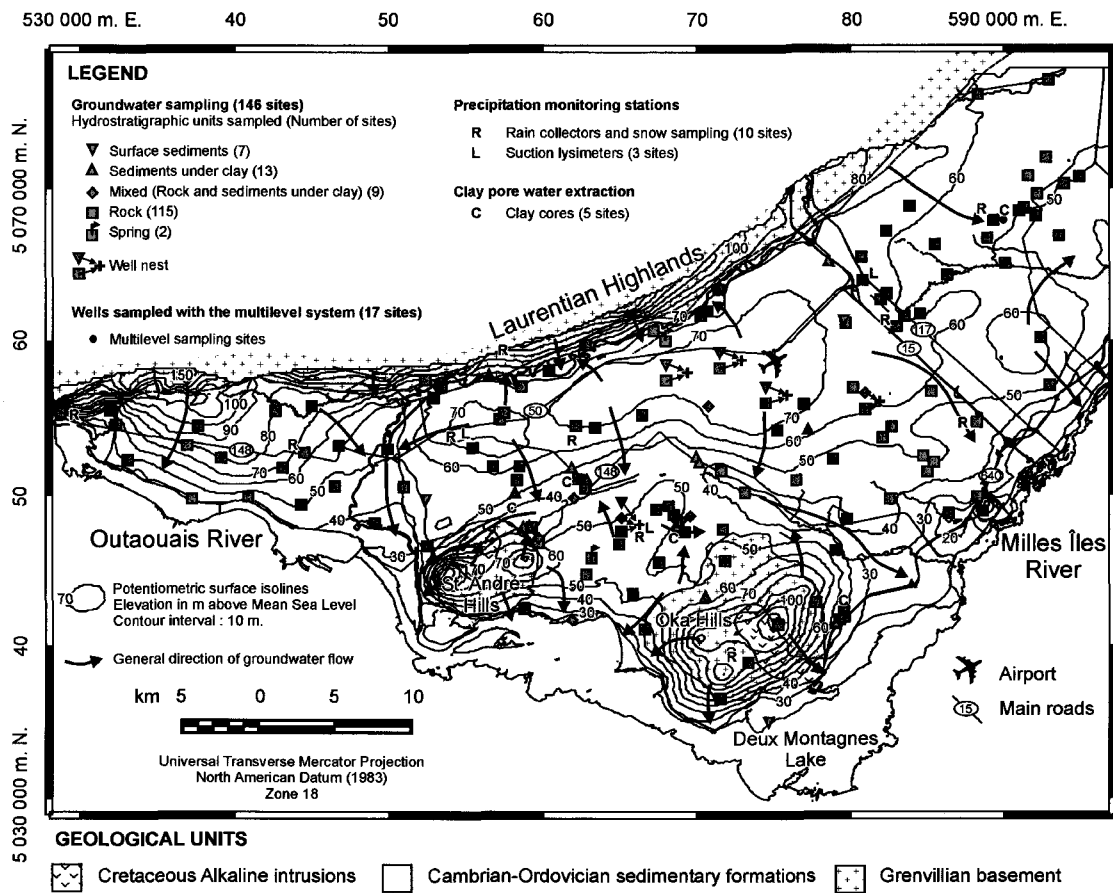


Figure 3.3. Potentiometric surface of the rock aquifer in the study area, with the location of the groundwater sampling sites, the stable isotopes monitoring stations, and clay cores (potentiometric surface map modified from Paradis, in press b).

The knowledge of the geological and hydrogeological setting provides key information on the possible groundwater end-members in the Basses-Laurentides sedimentary rock aquifer system. These end-members could include: 1) Cambrian-Ordovician formation waters, that are still present in the original sedimentary units or that have migrated from

these units, 2) Champlain Sea water, composed of a mixture of Pleistocene meteoric water and glacial meltwater from the Laurentide Ice Sheet, and seawater from the St. Lawrence Gulf, and 3) modern meteoric water, including rain and snow infiltration in the recharge areas.

### 3.3 METHODS

The approach used to study this fractured rock aquifer system was to determine the hydrogeochemistry of groundwater for all hydrogeologic units, starting from the groundwater recharge areas, and following the regional flow paths. The study also involves the hydrogeochemical recognition of all sources that could influence the composition of groundwater, such as rain and snow in recharge zones, and clay pore water in the buried valleys. The complete hydrogeochemical characterization program is summarized in Table 3.3. All sampling sites that were investigated during the characterization, including groundwater sampling sites, precipitation monitoring stations, and clay cores for pore water extraction, are indicated in Figure 3.3.

Table 3.3. Summary of the complete hydrogeochemical characterization program

Characterization	Number of sites	Sampled years	Acquired data
<b>Groundwater sampling</b>			
Regional characterization	153 sampling sites 146 sites retained	1999-2000	Major, minor, trace elements $\delta^2\text{H}$ , $\delta^{18}\text{O}$ , $\delta^{13}\text{C}_{\text{DIC}}$ , $^{87}\text{Sr}/^{86}\text{Sr}$ , $^3\text{H}$ , $^{14}\text{C}$ of DIC
Multilevel system <sup>a</sup>	17 wells (72 levels) 70 levels retained	2000	Major, minor, trace elements $\delta^2\text{H}$ , $\delta^{18}\text{O}$ , $\delta^{13}\text{C}_{\text{DIC}}$ , $^{87}\text{Sr}/^{86}\text{Sr}$ , $^3\text{H}$ , $^{14}\text{C}$ of DIC
<b>Precipitation sampling <sup>a</sup></b>			
Rain sampling	10 rain collectors	1999-2000	$\delta^2\text{H}$ and $\delta^{18}\text{O}$
Snow sampling	10 stations	2000-2001	$\delta^2\text{H}$ and $\delta^{18}\text{O}$
Infiltrated water sampling <sup>a</sup>	Lysimeters at three sites	2000	$\delta^2\text{H}$ and $\delta^{18}\text{O}$
Clay pore water extraction <sup>a</sup>	Profiles at five sites	2001	Major ions, Sr, Br, $\delta^2\text{H}$ , $\delta^{18}\text{O}$

<sup>a</sup> Details of methodology presented in *Chapitre 1*.

### 3.3.1 Groundwater sampling

The regional characterization of groundwater hydrogeochemistry, performed in 1999 and 2000, consisted of groundwater sampling of private, municipal and observation wells. The private wells in the area are generally 15.24 cm boreholes, with a steel casing over surface sediments, and open across all bedrock intervals without screen. Thus, pumping draws groundwater from the whole open interval in bedrock. The private wells sampled were wells with known construction details, such as casing depth and total depth, and known stratigraphy as much as possible. For the private and municipal wells, sampling was done using the in place pumps, while bypassing water treatment units if present. Observation wells belong mainly to two series of wells. The first series sampled are 15.24 cm boreholes installed by the Department of Natural Resources, Québec, in 1973, and sampled previously in 1973 and 1974 (Simard, 1978). The second series were installed for the project of the Geological Survey of Canada (Savard et al., *in press*) in 1999 and 2000. They consist of 7.62 cm and 15.24 cm open boreholes in sedimentary rocks, as well as PVC screened piezometers installed in the surface sediments or mixed units. Sampling of the observation wells was done using either submersible or inertial pumps. Sampling and analytical protocols are detailed in the Appendix.

Regional groundwater samples were collected at 153 sites, to a maximum depth of about 140 m. Thus, the hydrogeochemical study covers the upper portion of the aquifer system, which is used for industrial, agricultural, and drinking water supply. The sampled sites cover all permeable hydrostratigraphic units (Fig. 3.3): the surface sediments such as till, the sediments under clay deposits, the mixed unit consisting of highly fractured rock and sediments under clay deposits, and the fractured rock unit. The sampling sites are distributed over the whole region, characterizing the aquifer under unconfined and confined conditions, and for all geological formations. Figure 3.3 also shows the sampling sites relative to the general direction of groundwater flow. Most wells intercept only one geological formation, as the geological units are flat lying and the wells open interval is short relative to the formation thickness.

In 2000, 17 observation wells out of the 153 sites were sampled with a multilevel system (Fig. 3.3). This system uses discrete groundwater sampling of permeable zones isolated by packers in boreholes open to bedrock. The location of the levels sampled was based on transmissivity profiles established previously by constant-head injection tests (Nastev et al., 2001). A double packer system, with a screened interval of 3.80 m length, was used to isolate the intervals. The system can sample open boreholes of various diameters (7.62, 15.24, and 20.32 cm) to a depth of about 100 m, which allows the characterization of vertical trends in groundwater geochemistry. Between 2 and 6 levels were sampled per well for all 17 wells, for a total of 72 sampling levels. *Chapitre 1* provides details on the characterization methodology, including the sampling protocol, for sampling with the multilevel system. In this paper, only the multilevel samples analyzed for  $^{87}\text{Sr}/^{86}\text{Sr}$ ,  $^3\text{H}$ , and  $^{14}\text{C}$  of DIC are discussed.

### **3.3.2 Precipitation sampling**

A network of 10 monitoring stations was established to evaluate the spatial and seasonal variability of the isotopic composition of rain and snow (Fig. 3.3). Rain collectors, consisting of glass pluviometers with a tap at the bottom to sample rain water, were installed at each station. Silicone oil was used to prevent evaporation. Tests previously performed showed no isotopic exchange between water samples and silicone oil. Composite monthly rain samples were collected in HDPE bottles at the end of the months, from August to October in 1999 and from May to October in 2000. Samples were kept in a cold room until analysis. The sampling protocol was adapted from the Global Network for Isotopes in Precipitation (GNIP, 1996) and the Canadian Network for Isotopes in Precipitation (Environment Canada, 1998). Composite snow samples were collected at, or in the vicinity of each of the 10 stations in March 2000 and 2001. A core sampler was used to sample the snowpack. Snow was collected in 1L HDPE bottles, left to melt at room temperature, and kept in a cold room until analysis. Rain and snow samples were analyzed for  $\delta^2\text{H}$  and  $\delta^{18}\text{O}$  values. This characterization program allowed the establishment of a local meteoric water line for the Basses-Laurentides, the Basses-Laurentides Meteoric Water Line (BLMWL), and provided a good knowledge of the

isotopic signature of recharge water. *Chapitre 1* provides further details on the rain collectors, the silicone oil, and the sampling protocols for rain and snow.

### **3.4 RESULTS AND INTERPRETATION OF THE REGIONAL GROUNDWATER HYDROGEOCHEMICAL CHARACTERIZATION**

This section presents the results and interpretation of the regional groundwater hydrogeochemical characterization. In the discussion following this section, the main observations are integrated into a conceptual model for the origin and evolution of groundwater geochemistry in the study area.

#### **3.4.1 Hydrogeochemical dataset**

The complete geochemical dataset of the 146 samples having an electro-neutrality below 8% is available in Table ESM-1, on Springer's server (<http://link.springer.de>). The dataset includes *in situ* field measurements, dissolved inorganic constituents, isotopic data, and geochemical modeling results. The dataset also includes physical characteristics (easting, northing, elevation, depth of sampling interval), and hydrogeological characteristics (geological and hydrostratigraphic units, hydrogeological conditions) of the sampling sites. Groundwater samples were taken in order to cover the entire surface of the aquifer system (Fig. 3.3). As a synthesis of the geochemical dataset, Table 3.4 presents selected descriptive statistics for the 146 samples, including *in situ* field measurements, major, minor, and trace elements, as well as stable isotopes. For calculation of the descriptive statistics, the elements with concentrations lower than the detection limit were replaced by the value of the limit. Results of Table 3.4 give important information about the range of concentrations for 30 parameters, and the geochemical background that could be expected in the groundwater of the Basses-Laurentides sedimentary rock aquifer system.

Table 3.4. Descriptive statistics of selected measured and calculated parameters (concentrations in mg/L unless noted)

Parameters	N	Mean	Min.	Max.	St. dev.
pH	146	7.62	6.30	9.26	0.50
EC <sup>a</sup>	146	1077	265	18530	1706
DO <sup>b</sup>	129	2.99	0.12	11.48	2.60
Eh (mV)	123	+202	-6	+413	101
Ca	146	57.3	0.2	790	78
Mg	146	28.8	0.04	390	33
Na	146	135.7	1.6	3100	312
K	146	7.67	0.13	34	6.45
Cl	146	174	0.1	6500	591
SO <sub>4</sub>	144	56.2	0.5	1200	119
Tot. Alk. <sup>c</sup>	142	266	33	810	99
DIC	130	65	14.4	180	23
Fe	143	0.487	0.0007	15	1.456
Mn	146	0.0812	0.0003	0.93	0.1477
Br	144	0.78	0.002	23	2.69
Sr	145	1.72	0.005	29	4.15
F	142	0.54	0.04	3.2	0.6
Ba	146	0.19	0.001	1.1	0.19
HS (as S)	142	0.14	0.02	4.7	0.58
SiO <sub>2</sub>	146	12.9	5.5	24	3.6
B	145	0.15	0.002	1.4	0.21
NO <sub>3</sub> (as N)	144	0.40	0.02	11.7	1.49
NH <sub>4</sub> (as N)	144	0.33	0.02	7	0.69
PO <sub>4</sub> (as P)	144	0.16	0.01	2.1	0.40
DOC <sup>d</sup>	143	2.4	0.2	16.2	2.9
TDS <sup>e</sup>	146	610	138	11337	1025
HCO <sub>3</sub> <sup>f</sup>	146	310.1	40.0	922.0	113.3
δ <sup>2</sup> H (‰)	146	-76	-97	-56	5
δ <sup>18</sup> O (‰)	146	-11.3	-14.0	-8.5	0.6
δ <sup>13</sup> C <sub>DIC</sub> (‰)	105	-14.3	-20.2	-4.7	2.4

N: Number of samples, Min.: Minimum,

Max.: Maximum, St. dev.: Standard deviation

<sup>a</sup> Electrical conductivity corrected to 25 °C (µS/cm)

<sup>b</sup> Dissolved oxygen

<sup>c</sup> Total alkalinity as CaCO<sub>3</sub>

<sup>d</sup> Dissolved organic carbon

<sup>e</sup> Calculated total dissolved solids

<sup>f</sup> Geochemical calculations with PHREEQC 2.6

(Parkhurst and Appelo, 1999).

### 3.4.2 Precipitation and groundwater isotopic signatures

#### 3.4.2.1 $\delta^{18}\text{O}$ and $\delta^2\text{H}$ values

Through infiltration in the preferential groundwater recharge areas, precipitation is the main source of groundwater renewal to the Basses-Laurentides sedimentary rock aquifer system. Thus, the isotopic characterization of precipitation constitutes a prerequisite to help discriminate between the potential sources of groundwater in these aquifers, namely formation water, Champlain Sea water, and modern precipitation. The  $\delta^2\text{H}$  and  $\delta^{18}\text{O}$  values of precipitation samples are used to establish the local meteoric water line, the Basses-Laurentides Meteoric Water Line (BLMWL), presented in Figure 3.4a. The meteoric water line was established from 71 composite monthly rain samples collected in 1999 and 2000 at the 10 stations of the network (Fig. 3.3). The snow samples collected in 2000 and 2001 were not used to calculate the BLMWL as these were collected by coring the snowpack in March, during snow melt. Thus, the isotopic values of snow samples could be different than at the time of precipitation. The variation during snow melt could be due to sublimation and vapor exchange, and isotope exchange between snow and meltwater (Clark and Fritz, 1997). All precipitation isotopic data, as well as details on the monitoring stations, are presented in *Appendice B*.

Linear regression was performed on the rain data with the least-squares method, generally used to define local meteoric water line (Rozanski et al., 1993; Simpkins, 1995; Harvey, 2001). This regression gives the relation  $\delta^2\text{H}=7.588^{18}\text{O}+10.98$  for the BLMWL (Fig. 3.4a). The BLMWL falls slightly above the Global Meteoric Water Line,  $\delta^2\text{H}=8\delta^{18}\text{O}+10$  (Craig, 1961), having a lower slope and a slightly higher deuterium intercept. Local meteoric water lines are controlled by local climatic factors such as the origin of the vapor mass which affects the deuterium excess, as well as the secondary evaporation during rainfall and the seasonality of precipitation which affects the slope of the line (Clark and Fritz, 1997). Thus, the attitude of the BLMWL likely results from the combined effects of humidity at the site of ocean evaporation, and the mixing of three air masses in eastern Canada. The Tropical and Atlantic air streams dominate these air

masses during summer, and Arctic air masses during the winter months (Fritz et al., 1987).

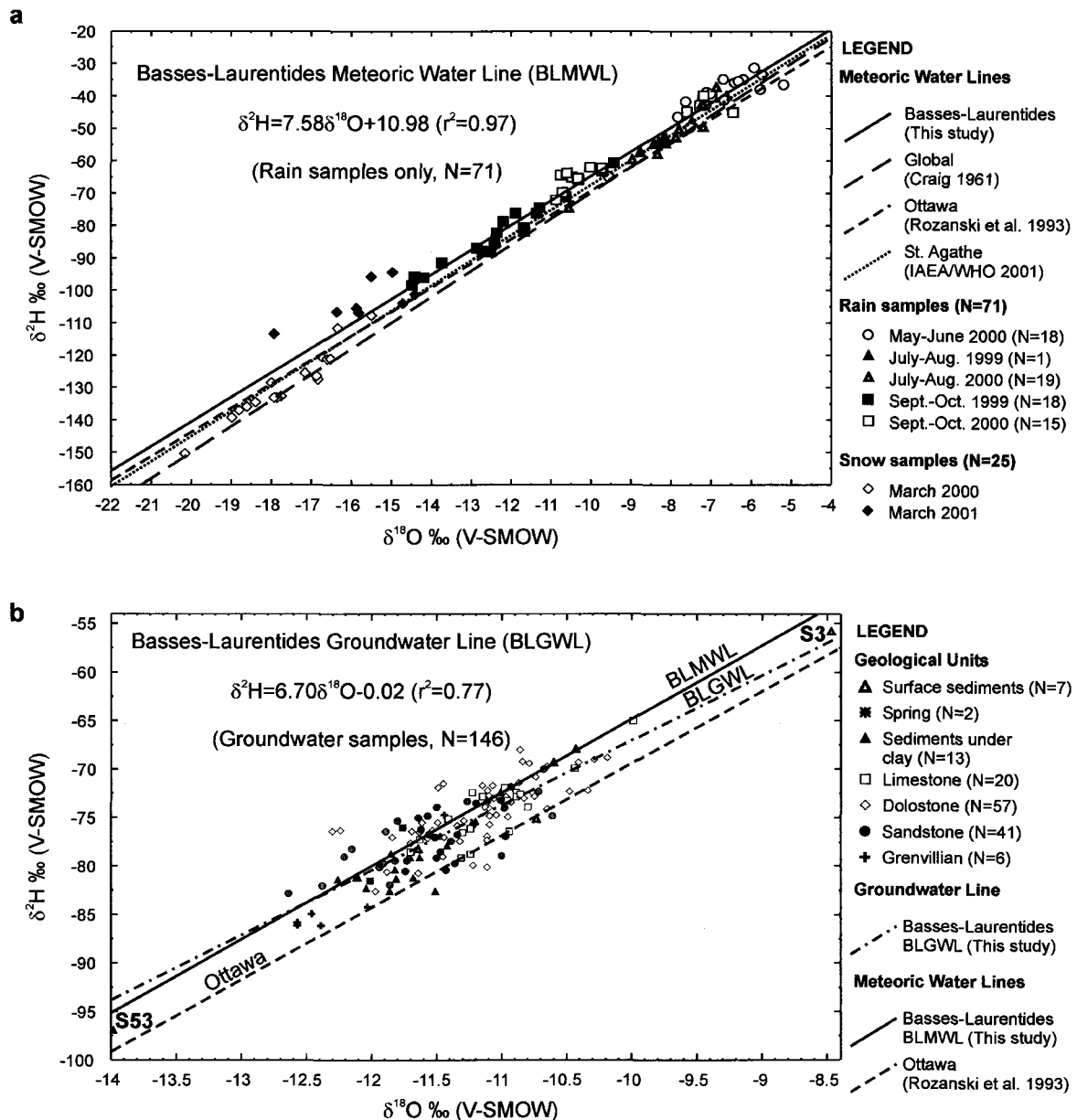


Figure 3.4. **a** Local meteoric water line of the study area, the Basses-Laurentides Meteoric Water Line (BLMWL) based on rain  $\delta^2\text{H}$  and  $\delta^{18}\text{O}$ , and **b**  $\delta^2\text{H}$  and  $\delta^{18}\text{O}$  for groundwater of the Basses-Laurentides sedimentary rock aquifer system (N: Number of samples).

The BLMWL can also be compared to the meteoric water lines of Ottawa and Ste. Agathe, in the vicinity of the study area. These two stations are part of the Global Network for Isotopes in Precipitation (GNIP) program of the International Atomic Energy

Agency (IAEA) and World Meteorological Organization (WMO). The Ottawa station, in operation since 1953, has an elevation of 114 m and is located about 120 km West of the study area, in the continuation of the St. Lawrence Lowlands. The meteoric water line for Ottawa is presented in Rozanski et al. (1993) as  $\delta^2\text{H}=7.44\delta^{18}\text{O}+5.01$  ( $r^2=0.973$ ). The Ste. Agathe station, in operation from 1975 to 1982, has an elevation of 395 m and is located about 50 km North of the study area, in the Laurentian Highlands. The meteoric water line for Ste. Agathe,  $\delta^2\text{H}=7.75\delta^{18}\text{O}+9.96$  ( $r^2=0.98$ ), was calculated by least-squares regression of the data ( $N=80$ ) retrieved from the GNIP database (IAEA/WMO, 2001). Even though the characterization of the Basses-Laurentides precipitation is for a short time period, the similarity with Ottawa and Ste. Agathe meteoric water lines confirms that the BLMWL is representative of the study area.

The  $\delta^{18}\text{O}$  in precipitation varies from  $-20.2\text{\textperthousand}$  for a snow sample collected in March 2000, to  $-5.2\text{\textperthousand}$  for a rain sample collected in June 2000. This important range is coherent with the strong seasonal variation in temperature, and its related isotopic fractionation combined with the strong Rayleigh distillation effects during winter (Clark and Fritz, 1997). The analysis of the climate record for the period of 1970-1998 showed that the coldest month, January, and the warmest month, July, have mean daily temperatures of  $-11.9\text{ }^\circ\text{C}$  and  $20.1\text{ }^\circ\text{C}$  respectively (Hamel et al., 2001). The meteoric input function for groundwater can be defined by the  $\delta^{18}\text{O}$  annual mean, weighted by the amount of precipitation for the Basses-Laurentides. This calculation needs at least one full year of monthly isotopic characterization of precipitation. As the meteoric water line of stations Ottawa and Ste. Agathe are not that different from the BLMWL, their  $\delta^{18}\text{O}$  weighted annual means provide an estimate of the meteoric input function for the Basses-Laurentides. The  $\delta^{18}\text{O}$  weighted annual means for Ottawa is  $-11.21\text{\textperthousand}$  and for Ste. Agathe is  $-12.55\text{\textperthousand}$  (IAEA, 2001).

Comparison of the  $\delta^2\text{H}$  and  $\delta^{18}\text{O}$  results of the groundwater samples to the BLMWL shows that the samples are distributed around the BLMWL, and indicates no significant isotopic modifications by water rock interaction (Fig. 3.4b). The meteoric water line for Ottawa (Rozanski et al., 1993) is at the lower limit of the groundwater samples, more or

less parallel to the BLMWL. Apparently there is no preferential grouping of samples in relation with geology (Fig. 3.4b). The Basses-Laurentides Groundwater Line (BLGWL),  $\delta^2\text{H}=6.70\delta^{18}\text{O}-0.02$ , was calculated by least-squares regression of the 146 groundwater samples. The BLGWL is not far from the BLMWL, but has a lower slope and lower deuterium intercept. The mean  $\delta^{18}\text{O}$  for all groundwater samples is  $-11.3\text{\textperthousand}$ , with a standard deviation of 0.6 (Table 3.4). With the exception of the two extreme values, S53 and S3, the  $\delta^{18}\text{O}$  values have a relatively small range of  $-12.6\text{\textperthousand}$  to  $-10.0\text{\textperthousand}$ , with about 83% of the samples between  $-12.0\text{\textperthousand}$  to  $-10.5\text{\textperthousand}$ .

Histograms of  $\delta^{18}\text{O}$  for the different hydrogeological conditions are presented in Figure 3.5a. With only 9 samples, the surface sediments and spring samples have  $\delta^{18}\text{O}$  values that fall in the range of  $\delta^{18}\text{O}$  obtained for the regional precipitations. The histogram of the groundwater in unconfined and semi-confined conditions has a normal distribution, with a mean  $\delta^{18}\text{O}$  of  $-11.4\text{\textperthousand}$  and a standard deviation of 0.5. An interesting observation is that no significant variations are found in  $\delta^{18}\text{O}$  between groundwater from unconfined and confined conditions. The normal distribution is relatively similar, and the mean  $\delta^{18}\text{O}$  of confined groundwater is  $-11.3\text{\textperthousand}$  with a standard deviation of 0.6. The regional distribution of  $\delta^{18}\text{O}$  for the rock, mixed, as well as sediments under clay units does not show a distinct regional  $\delta^{18}\text{O}$  pattern, but samples from the northeast region generally have higher values relative to the whole study area (Fig. 3.5b). On the other hand, samples from center-south of the study area, particularly the Oka Hills, have lower values.

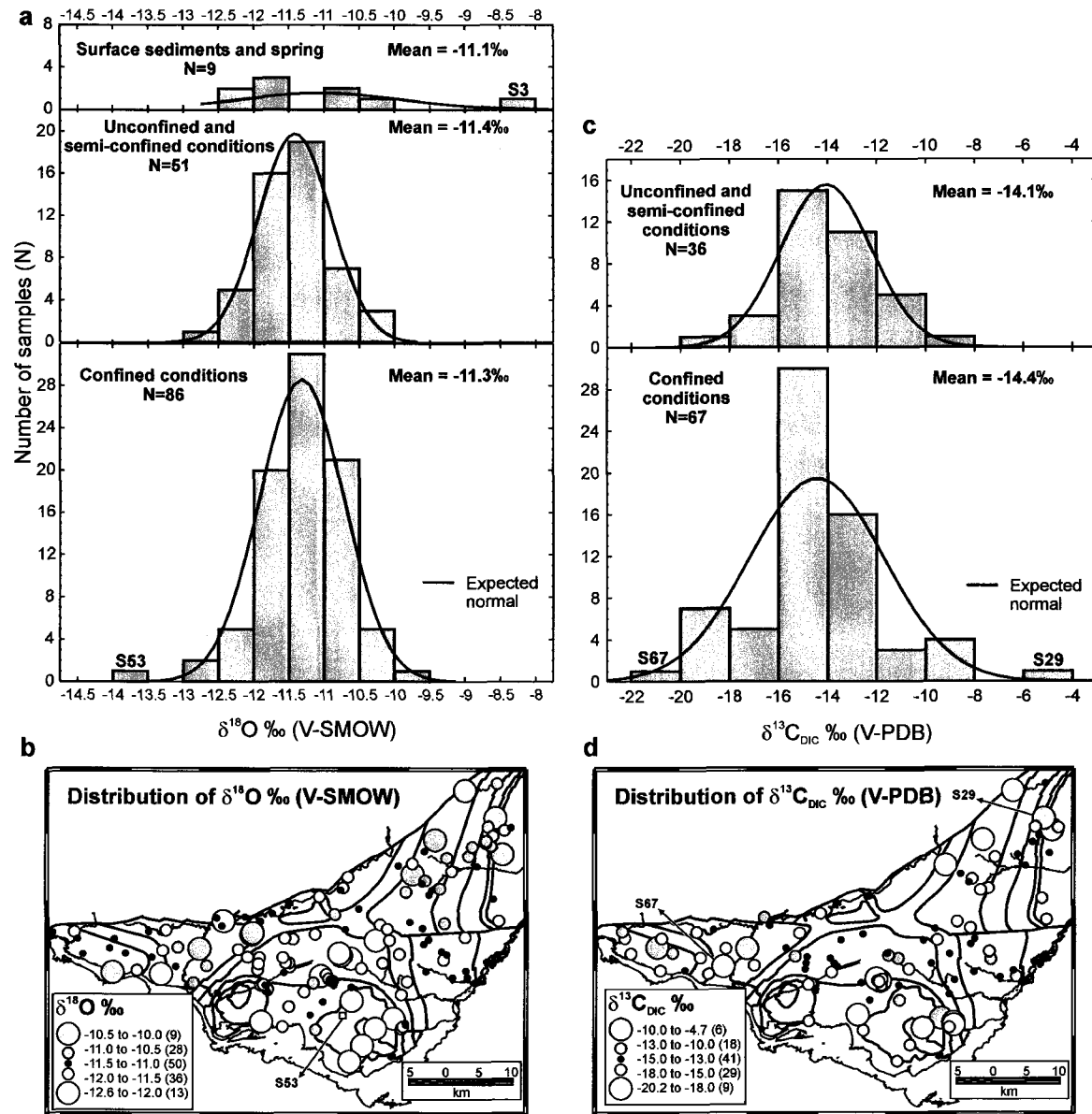


Figure 3.5. **a** Histograms of  $\delta^{18}\text{O}$  values for the groundwater samples, **b** regional distribution map of  $\delta^{18}\text{O}$  values for the rock, mixed, and sediments under clay samples, **c** histograms of  $\delta^{13}\text{C}_{\text{DIC}}$  values for the groundwater samples, and **d** regional distribution map of  $\delta^{13}\text{C}_{\text{DIC}}$  values for the rock, mixed, and sediments under clay samples (N: Number of samples; for Figures 3.5b and 3.5d, see Figure 3.9a for legend of geological units).

### 3.4.2.2 Carbon-13 on DIC

Stable carbon isotopes on DIC are useful as tracers of dissolved inorganic carbon sources and carbonate evolution in groundwaters (Chapelle and Knobel, 1985; Clark and Fritz, 1997; Cane and Clark, 1998). Study of  $\delta^{13}\text{C}_{\text{DIC}}$  is particularly relevant in the groundwater

of the Basses-Laurentides sedimentary rock aquifer system as it comprises carbonate formations, and the till in recharge areas is made in part of carbonate minerals.

$\delta^{13}\text{C}_{\text{DIC}}$  were analyzed for 105 out of the 146 groundwater samples. The  $\delta^{13}\text{C}_{\text{DIC}}$  values are highly variable, and range from  $-20.2\text{\textperthousand}$  to  $-4.7\text{\textperthousand}$ . The mean  $\delta^{13}\text{C}_{\text{DIC}}$  for the samples is  $-14.3\text{\textperthousand}$ , with a standard deviation of 2.4 (Table 3.4). Histograms of  $\delta^{13}\text{C}_{\text{DIC}}$  for the unconfined and semi-confined conditions, as well as confined conditions, are presented in Figure 3.5c. Surface sediments and spring samples are not included as  $\delta^{13}\text{C}_{\text{DIC}}$  was analyzed on 2 samples only. These groundwater samples are S146, a groundwater from the till at St. Vincent Crest, and S59, a spring along the du Nord River, with a  $\delta^{13}\text{C}_{\text{DIC}}$  of  $-15.0\text{\textperthousand}$  and  $-14.5\text{\textperthousand}$  respectively. The histogram of the groundwater in unconfined and semi-confined conditions has a more or less normal distribution, with a mean  $\delta^{13}\text{C}_{\text{DIC}}$  of  $-14.1\text{\textperthousand}$  and a standard deviation of 1.8. The histogram for confined conditions shows more spread, and is farther from the expected normal distribution, with a mean  $\delta^{13}\text{C}_{\text{DIC}}$  of  $-14.4\text{\textperthousand}$  and a standard deviation of 2.7. Including S146 and S59, about 70% of the samples have a  $\delta^{13}\text{C}_{\text{DIC}}$  between  $-16.0\text{\textperthousand}$  to  $-12.0\text{\textperthousand}$ . The regional distribution of  $\delta^{13}\text{C}_{\text{DIC}}$  for the rock, mixed, as well as sediments under clay units is highly variable (Fig. 3.5d). Enriched  $\delta^{13}\text{C}_{\text{DIC}}$  samples are found in the limestone formations, on the West and East side of the study area, as well as on Oka Hills. Depleted values are found in the confined aquifers in St. Benoît Valley, St. Joseph, and in the middle of St. Hermas Valley, as well as in some recharge areas.

### 3.4.2.3 Strontium isotopes

Strontium isotopes have been used as indicators of water-rock interaction (McNutt et al., 1987), and as tracers for groundwater flow (Johnson et al., 2000) and groundwater evolution (Woods et al., 2000). For this project, twenty-five samples were analyzed for  $^{87}\text{Sr}/^{86}\text{Sr}$ . Results are presented in Figure 3.6a, a diagram of  $^{87}\text{Sr}/^{86}\text{Sr}$  versus  $\text{Sr}^{2+}$ , and the location of the sampling sites on the regional map are shown on Figure 3.6b (see also Fig. C1.2; *Appendice C1*). Four samples from three wells were collected using the multilevel system and analyzed for  $^{87}\text{Sr}/^{86}\text{Sr}$ . These are labeled as S117-L4, S140-L2, SAP-L2, and

SAP-L3. The left part of the label represents the observation well ID, as S117, that was also sampled by conventional sampling. The right part is the level sampled, as L4, which represents the forth level sampled in well S117. Samples SAP-L2 and SAP-L3 were collected at well SAP, an observation well that does not appear in the geochemical dataset of the 146 samples because its conventional sample SAP was rejected due to analytical problems.

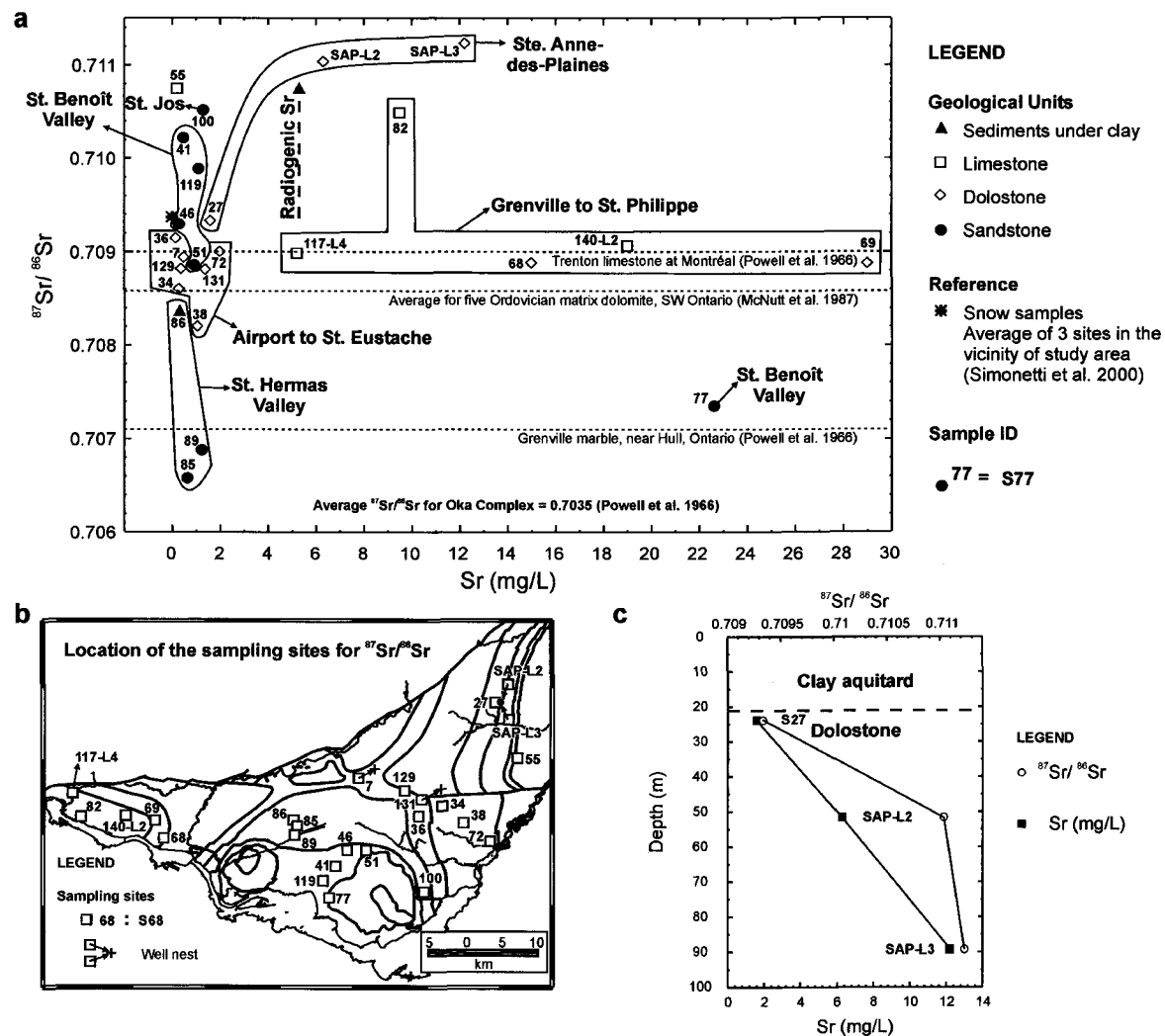


Figure 3.6. a Diagram of  $^{87}\text{Sr}/^{86}\text{Sr}$  ratios versus Sr (St. Jos : St. Joseph), b location map of the sampling sites for which strontium isotopes were analyzed (see Figure 3.9a for legend of geological units), and c vertical distribution of  $^{87}\text{Sr}/^{86}\text{Sr}$  ratios and Sr concentrations at well SAP, Ste. Anne-des-Plaines.

The  $^{87}\text{Sr}/^{86}\text{Sr}$  ratio ranges from 0.706580 (S85) to 0.711231 (SAP-L3), which corresponds to a large variation for a single study area. To facilitate the description of the results, samples are grouped according to their location and hydrogeological contexts (Fig. 3.6a). The first samples to be discussed are from the preferential recharge areas, from the airport to St. Eustache, and from Grenville to St. Philippe. Groundwaters in the dolostone, from the airport to St. Eustache, have a narrow range of  $^{87}\text{Sr}/^{86}\text{Sr}$ , between 0.708201 (S38) and 0.709147 (S36), and  $\text{Sr}^{2+}$  below 2 mg/L. Their values are in the range of the snow samples (Simonetti et al., 2000) and of the value of  $0.70858 \pm 0.00020$  reported by McNutt et al. (1987) for five Ordovician matrix dolomite of the Michigan Basin in southwestern Ontario (Fig. 3.6a). This suggests that  $\text{Sr}^{2+}$  is derived from the aerosols and the dolostone. Groundwaters in the dolostone and limestone of Grenville to St. Philippe, on the West side of the study area, have elevated  $\text{Sr}^{2+}$  concentrations. The two samples from the dolostone (S68 and S69) have a  $^{87}\text{Sr}/^{86}\text{Sr}$  in the same range as the ones from the airport to St. Eustache. With the exception of S82, groundwaters in the limestone (S117-L4 and S140-L2) have a  $^{87}\text{Sr}/^{86}\text{Sr}$  similar to a Trenton limestone reported by Powell et al. (1966), indicating that the  $\text{Sr}^{2+}$  in groundwater is mostly derived from Trenton limestone. Even though the source for radiogenic Sr of S82 is not determined, it could be due to water-rock interaction with Rb-bearing minerals, as clay minerals in shales of the Upper Chazy Group (Globensky, 1987; Table 3.1).

Samples from the confined areas are characterized by a much less uniform range of  $^{87}\text{Sr}/^{86}\text{Sr}$  values. Groundwaters in the confined sandstone units have the largest range of  $^{87}\text{Sr}/^{86}\text{Sr}$  values, varying from 0.706580 (S85) in St. Hermas Valley to 0.710516 (S100) at St. Joseph. With the exception of S77, groundwaters from St. Benoît Valley and St. Joseph (S100) show a trend toward increasing  $^{87}\text{Sr}/^{86}\text{Sr}$ . As the Covey Hill Formation is a feldspathic sandstone (Lewis, 1971; Table 3.1), the source of  $^{87}\text{Sr}$  would be the radiogenic K-feldspar. Sample S77, located close to the Oka Hills, has a lower  $^{87}\text{Sr}/^{86}\text{Sr}$  value of 0.70735, and a higher  $\text{Sr}^{2+}$  concentration than the other samples from sandstone. An explanation for this value could be the interaction with crystallized limestone from the Grenville around the Cretaceous alkaline intrusions. Powell et al. (1966) reported a  $^{87}\text{Sr}/^{86}\text{Sr}$  value from a Grenville marble in Ontario in the same range as S77 (Fig. 3.6a).

Samples from the St. Hermas Valley show a  $^{87}\text{Sr}/^{86}\text{Sr}$  decrease from 0.708368 (S86) on the edge of the valley, to low values of 0.706580 (S85) and 0.706881 (S89) in the center. One possible source for these low  $^{87}\text{Sr}/^{86}\text{Sr}$  values could be the interaction with rocks of the Cretaceous Oka intrusion. These rocks could be present as sills, associated with the intrusions emplacement, in the sandstone formations. Powell et al. (1966) reported an average value of 0.7035 for the Oka complex.

In Ste. Anne-des-Plaines, well SAP was sampled using the multilevel system. The vertical distribution of  $\text{Sr}^{2+}$  and  $^{87}\text{Sr}/^{86}\text{Sr}$  shows an increase with depth in the dolostone of the Carillon Formation (Fig. 3.6c). Located adjacent to well SAP, well S27 is screened at about the same level as multilevel sample SAP-L1.  $\text{Sr}^{2+}$  for S27 could be derived from the aerosols and the dolostone. The increase in  $\text{Sr}^{2+}$  concentration for SAP-L2 and SAP-L3 could be explained by greater water-rock interaction at depth, due to longer residence time. As shale beds were observed in the rock cores of well SAP, the source for radiogenic Sr could be the clay minerals of the shale. Finally, the enriched value for S55 could also be due to clay minerals in the shale beds of the Trenton Group (Globensky, 1987; Table 3.1).

#### *3.4.2.4 Tritium and radiocarbon dating*

To evaluate the mean residence time of groundwater and, by extension, the activity of the flow system, fourteen samples were analyzed for enriched  ${}^3\text{H}$ , and twelve for radiocarbon analysis of DIC. The samples were chosen to represent the different hydrogeological settings of the Basses-Laurentides sedimentary rock aquifer system. Figure 3.7a presents the distribution of the sampling sites, as well as the cross-sections of Figure 3.7b (see also Fig. C1.3; *Appendice C1*). Of the fourteen samples, seven were collected using the multilevel sampling system. The  ${}^3\text{H}$  data were corrected for the elapsed time between sampling and analysis, in order to determine the  ${}^3\text{H}$  concentrations at the time of sampling. These calculations were made using the  ${}^3\text{H}$  decay equation, and a tritium's half-life,  $t_{1/2}$  of 12.43 years (Clark and Fritz. 1997). Measured and corrected  ${}^3\text{H}$  data are presented in the Table ESM-1 dataset on Springer's web server.

The qualitative interpretation of the  ${}^3\text{H}$  data (Fig. 3.7a) is based on presence of tritium in groundwater, and allows the division in modern and submodern waters, i.e. recharged prior to 1952 (Clark and Fritz, 1997). A quantitative interpretation of  ${}^{14}\text{C}$  data will be presented in a subsequent paper. The qualitative interpretation of the mean residence time of groundwater is generally consistent with the hydrogeological conditions map of Hamel et al. (2001) (Fig. 3.7a). Modern tritiated water characterized groundwater in the preferential recharge areas, in unconfined or semi-confined conditions. On the other hand, submodern water characterized groundwater in the confined aquifers, such as the buried valleys. Two samples in confined conditions, S86 and SAP-L1, could have been affected by groundwater mixing, modifying their  ${}^3\text{H}$  and  ${}^{14}\text{C}$  values.

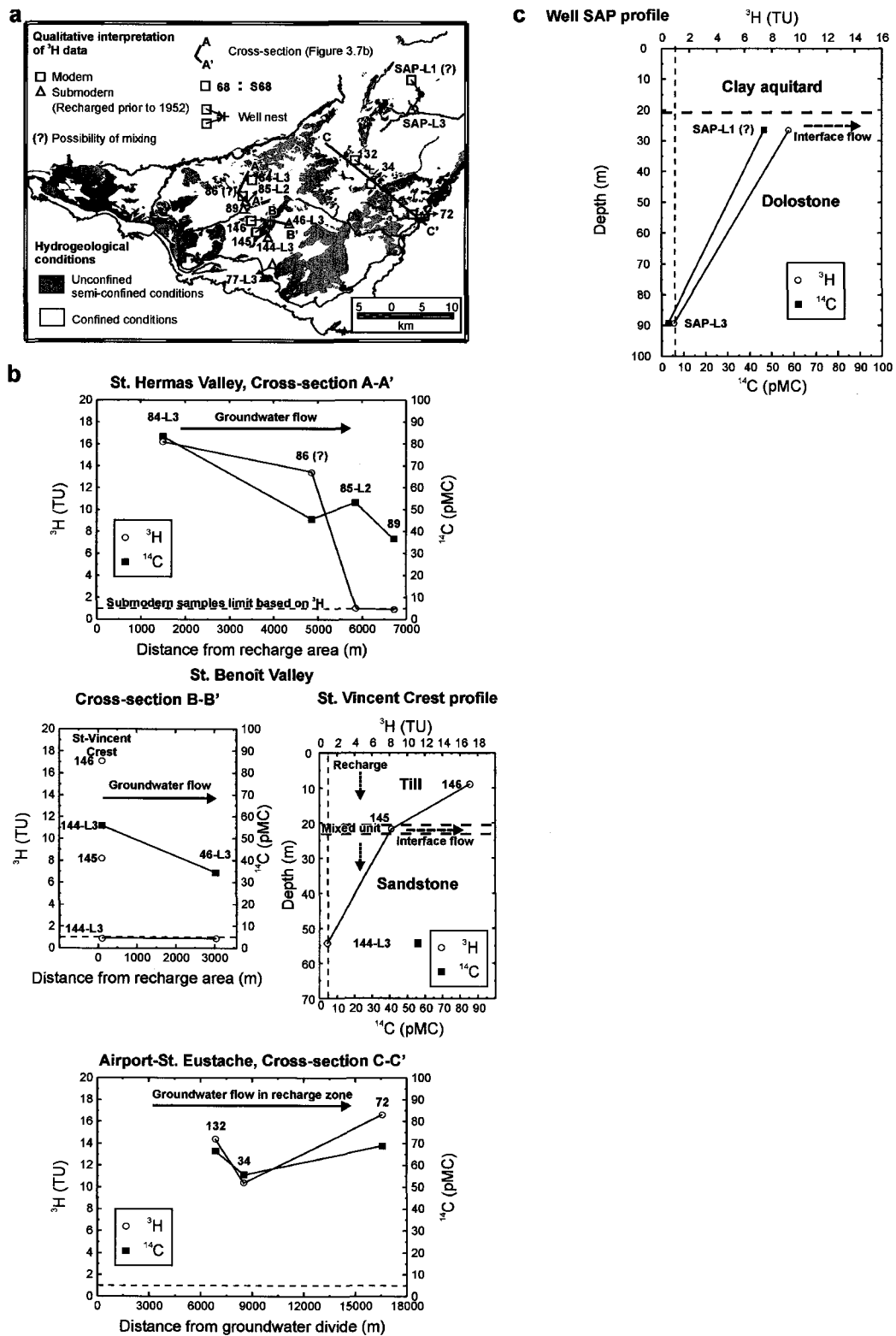


Figure 3.7. **a** Qualitative interpretation of  $^3\text{H}$  data, and location of cross-sections (hydrogeological conditions map modified from Hamel et al., 2001), **b**  $^3\text{H}$  and  $^{14}\text{C}$  of DIC along the 3 cross-sections, and **c** vertical distribution of  $^3\text{H}$  and  $^{14}\text{C}$  results at well SAP, Ste. Anne-des-Plaines.

Figure 3.7b shows  $^3\text{H}$  and  $^{14}\text{C}$  variations along three cross-sections. Four samples were analyzed in St. Hermas Valley cross-section A-A', from S84-L3 in the recharge area, to S89 in the confined aquifer downgradient. With a  $^3\text{H}$  value of 16.2 TU and a  $^{14}\text{C}$  of 83.5 pMC, S84-L3 is clearly a modern, recent recharge, groundwater. The first well downgradient in the valley, S86, with a  $^3\text{H}$  of 13.4 TU, has also a value that could indicate the presence of recent recharge groundwater. On the other hand, its much lower  $^{14}\text{C}$ , 45.7 pMC, could indicate older water. This apparent contradiction in age could result from mixing of old groundwater with modern water infiltrating along the well casing. The last two sites, S85-L2 and S89, having 1 and <0.9 TU respectively, associated with low  $^{14}\text{C}$ , are classified as submodern groundwater. Five samples were analyzed in the St. Benoît Valley. Four of these sites are on the cross-section B-B'. Sites S146, S145 and S144-L3 are part of a well nest located in the local recharge zone of St. Vincent Crest, and are illustrated in a profile (Fig. 3.7b). The first two samples, from the till and mixed unit, were analyzed for  $^3\text{H}$  only. Their values of 17.1 TU in the till, and 8.2 TU in the mixed unit, clearly show that groundwater recharges the aquifer through the till. The rock sample S144-L3 has no detectable  $^3\text{H}$ , indicating that the recent recharge likely flows preferentially in the upper, highly fractured rock unit. The sample downgradient in the valley, S46-L3, has no detectable  $^3\text{H}$ , and a  $^{14}\text{C}$  lower than S144-L3. The last sample from St. Benoît Valley, S77-L3, has no detectable  $^3\text{H}$ , and a very low  $^{14}\text{C}$  of 10.9 pMC. The next three sites are from the cross-section C-C', in the unconfined to semi-confined area from the airport to St. Eustache. S132, S34 and S72, have all  $^3\text{H}$  above 10 TU, indicative of modern groundwater, and their  $^{14}\text{C}$  vary from 55.7 to 68.8 pMC. Groundwater recharge thus probably occurs along the flow path in this area.

Finally, the profile of well SAP shows the results of two samples collected with the multilevel system (Fig. 3.7c). Sample SAP-L1, below the clay aquitard, has 9.2 TU and a  $^{14}\text{C}$  of 46.5 pMC. The deepest sample, SAP-L3, has no detectable  $^3\text{H}$ , and a very low  $^{14}\text{C}$  of 3.0 pMC. The presence of tritium below the aquitard suggests that groundwater flows preferentially in the highly fractured rock at the interface zone. The source for this modern water would be the recharge zone, located about 5 km northwest of well SAP (Karanta et al., 2001). It is possible that mixing in the well, prior to sampling, has

contributed to lower the tritium and  $^{14}\text{C}$  values of SAP-L1 by mixing modern groundwater with deeper, much older, groundwater.

### 3.4.3 Major and minor ions groundwater geochemistry

Figure 3.8 shows the composition of the groundwater samples on Piper diagrams (Piper, 1944). In Figure 3.8a, the 146 groundwater samples are represented with a symbol size proportional to TDS. Figure 3.8a illustrates that the Basses-Laurentides sedimentary rock aquifer system has a highly variable major ion chemistry. Actually, groundwater samples are distributed in the various zones of the diamond-shaped field, mainly the Ca-Mg-HCO<sub>3</sub>, Na-HCO<sub>3</sub>, and Na-Cl zones. Samples in the Na-Cl zone are characterized by higher TDS. Sample S77, a sample from St. Benoît Valley, has the highest TDS of all the wells sampled in the course of this project (calculated TDS = 11 337 mg/L). Figure 3.8b presents the seven groundwater samples from surface sediments, as well as the two spring samples that are believed to flow in surface sediments. All samples plot in the Ca-Mg-HCO<sub>3</sub> zone, characterizing the infiltrated water in the quaternary sediments, mainly till. Thus, this piper diagram shows the major ion composition of the recharge water to the Basses-Laurentides sedimentary rock aquifer system.

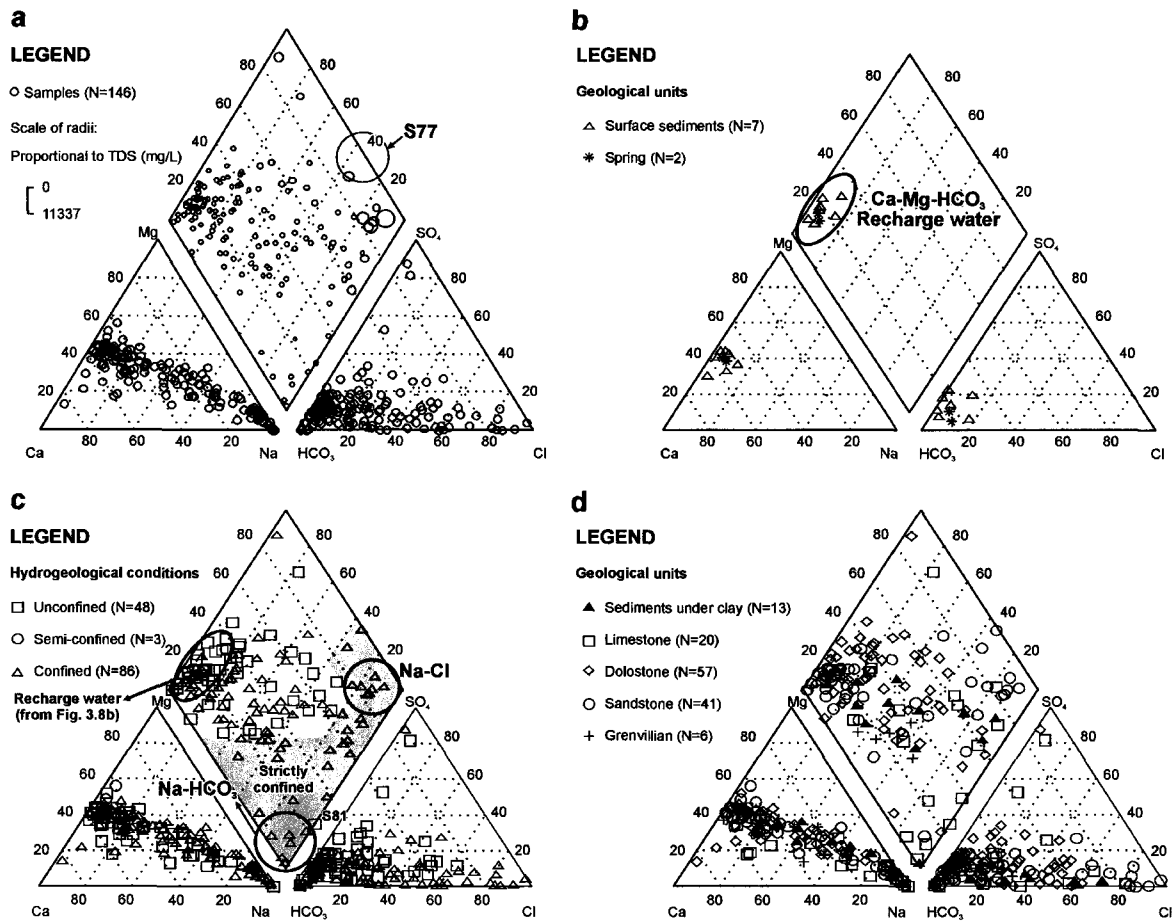


Figure 3.8. Piper diagrams illustrating the major ions chemistry of **a** the Basses-Laurentides sedimentary rock aquifer system proportional to TDS, **b** the recharge water, **c** the rock, mixed, and sediments under clay samples labeled with the hydrogeological conditions, and **d** the rock, mixed, and sediments under clay samples labeled with the geological units (N: Number of samples).

The remaining 137 groundwater samples are labeled according to their hydrogeological conditions, and geological units respectively (Fig. 3.8c and 3.8d). These samples come from the rock, mixed, and sediments under clay hydrostratigraphic units. Samples from sediments under the clay unit are included as they could be in hydraulic connection with the fractured rocks. As in Figure 3.8b, the unconfined and semi-confined sampling sites are concentrated mainly in the Ca-Mg-HCO<sub>3</sub> zone of the diamond-shaped field (Fig. 3.8c). Groundwater originates mainly from infiltration through the till in the preferential recharge areas. On the other hand, the confined samples are found in the Ca-Mg-HCO<sub>3</sub>, Na-HCO<sub>3</sub>, and Na-Cl zones. In the transition from Ca-Mg-HCO<sub>3</sub> to Na-HCO<sub>3</sub> and Na-Cl zones of the diamond-shaped field, the unconfined samples are becoming less abundant

relative to the confined samples. With the exception of sample S81, the Na-HCO<sub>3</sub> and Na-Cl zones are dominated exclusively by samples under confined conditions. No such grouping is observed when samples are divided by geological formations (Fig. 3.8d). In this last piper diagram, the limestone includes the Chazy, Black River, and Trenton groups, the dolostone the Theresa, Beauharnois, and Carillon formations, and the sandstone the Covey Hill and Cairnside formations. Thus, Piper diagrams indicate that the major ion chemistry is controlled more by the hydrogeological conditions, than by the geology of the aquifer. The large number of samples, and the highly variable hydrogeochemistry of the aquifer limit a detailed interpretation of these diagrams.

To facilitate the description and understanding of the regional groundwater hydrogeochemistry, geographical representations of some major and minor elements are used in Figure 3.9 (geographical representations of most major and minor elements are also presented in Fig. C1.1 of *Appendice C1*). The chemical parameters chosen show regional variations, and can be used to identify and understand the processes controlling groundwater geochemistry and the geochemical evolution of groundwater. Samples plotted in the geological maps are from the rock units, including the mixed unit, as well as the sediments under clay unit. Thus, the regional distribution maps do not include samples from the surface sediments. Each map has a box plot diagram of the parameter to present the statistical results of surface sediments, unconfined and confined conditions. The surface sediments include the two spring samples, and the unconfined include the semi-confined samples. Descriptive statistics of the samples, in relation to the hydrogeological conditions and the geological units, are presented in Table ESM-2 and ESM-3 on Springer's web server. The combination of descriptive statistics, box plots and dot maps will help characterize the relationships between the groundwater geochemistry and the hydrogeological and geological contexts.

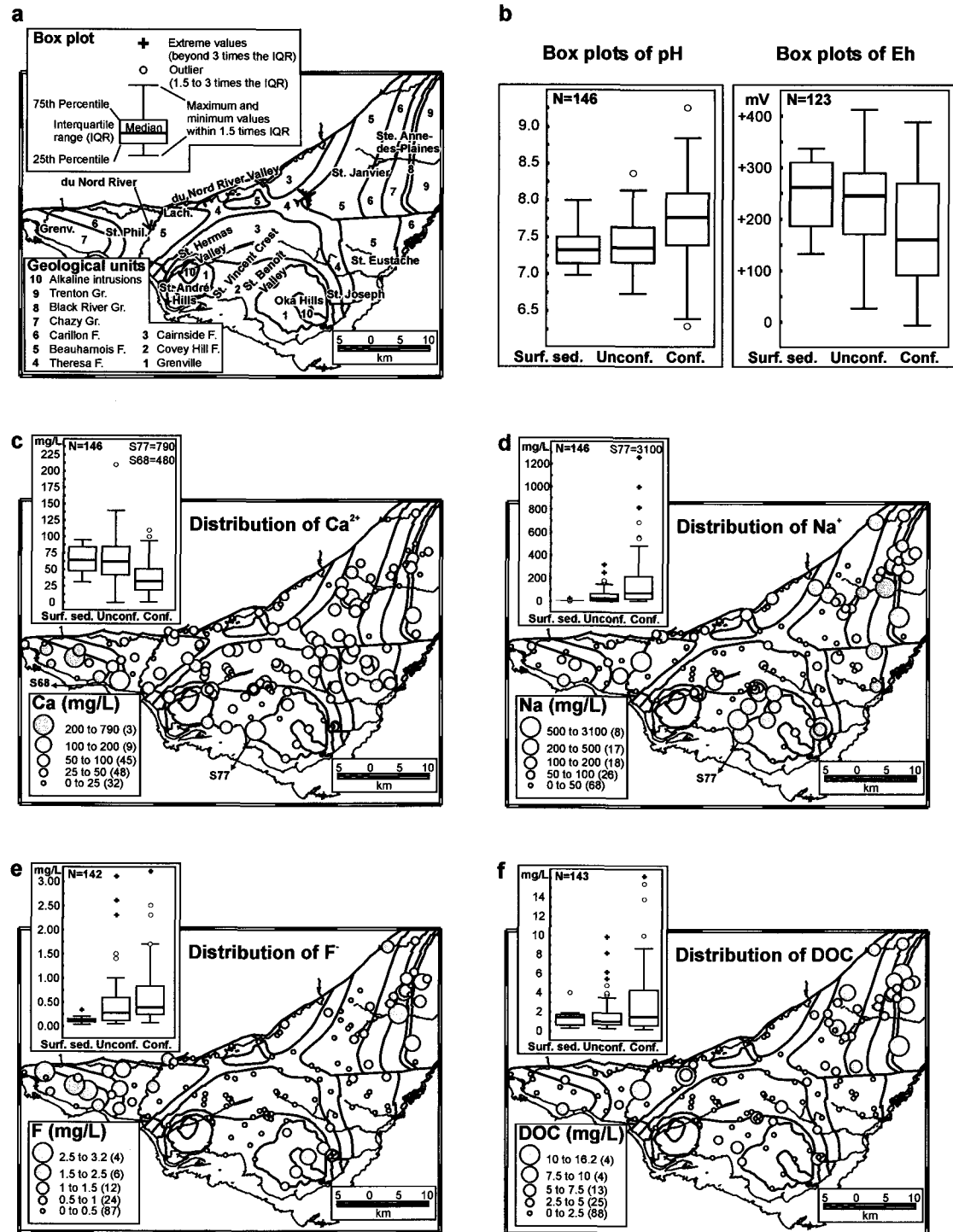


Figure 3.9. **a** Legend for Fig. 3.9b to 3.9f (Grenv. : Grenville, St. Phil. : St-Philippe, Lach. : Lachute) (geological map modified from Rocher et al., in press), **b** box plots of the Basses-Laurentides aquifer system for the hydrogeological conditions of pH and Eh, **c** box plots of the Basses-Laurentides aquifer system for the hydrogeological conditions and regional distribution maps for the rock, mixed, and sediments under clay samples of  $\text{Ca}^{2+}$ , **d**  $\text{Na}^+$ , **e** F, and **f** DOC (N: Number of samples; Surf. Sed. : Surface sediments and springs, Unconf.: Unconfined and semi-confined, Conf.: Confined).

Figure 3.9a presents the legend for Figures 3.9b to 3.9f. Box plots of field parameters show an increasing pH and a decreasing Eh from the surface sediments, to the unconfined, and confined samples (Fig. 3.9b). Values of pH greater than 8 are associated with the confined limestone of Ste. Anne-des-Plaines, and are found as well in St. Hermas and du Nord River valleys, and St. Joseph. Values of pH between 7 and 8, or lower than 7, characterize the preferential recharge areas. The distribution of Eh gives general information on the redox conditions of the aquifer system. The recharge areas are generally characterized by higher Eh values than confined areas. DO has a behavior similar to Eh, with DO values decreasing from the surface sediments, to the unconfined, and confined samples (Table ESM-2).

The distribution of  $\text{Ca}^{2+}$  (Fig. 3.9c) is similar to that of  $\text{Mg}^{2+}$ . In the box plots,  $\text{Ca}^{2+}$  concentrations are more or less similar in the surface sediments and unconfined samples. The concentrations decrease in the confined areas of Ste. Anne-des-Plaines and buried valleys. The decrease is more important for  $\text{Ca}^{2+}$  than  $\text{Mg}^{2+}$ , with a median concentration of 62 mg/L in the unconfined, to 32.5 mg/L in the confined samples (Table ESM-2). The dolostone unit has the highest median concentrations for both ions (Table ESM-3). The distribution of  $\text{Na}^+$  (Fig. 3.9d) has some similarities with that of  $\text{Cl}^-$ . Concentrations are higher in the buried valleys, particularly in St. Benoît Valley, and at St. Joseph. High values of both ions are also found in the unconfined area close to St. Janvier, along the main roads 15 and 117 (see Fig. 3.2a for roads location). On the other hand, the  $\text{Na}^+$  increase in the confined limestone of Ste. Anne-des-Plaines is not coupled to a  $\text{Cl}^-$  increase. Box plots show very low values of  $\text{Na}^+$  in the surface sediments. An important increase in concentration is observed from the unconfined to confined areas, characterized by elevated outliers and extreme values.  $\text{K}^+$  has a behavior similar to  $\text{Na}^+$  (Table ESM-2 and ESM-3). The distribution of  $\text{Br}^-$  is very similar to  $\text{Cl}^-$  and thus  $\text{Na}^+$ , with an increase from the unconfined to confined conditions (Table ESM-2). An important observation is that  $\text{Br}^-$  values, unlike  $\text{Cl}^-$  and  $\text{Na}^+$ , do not increase in the unconfined area of St. Janvier, along the main roads 15 and 117.

The values for  $\text{SO}_4^{2-}$  increase from the surface sediments to the unconfined samples, and decrease from the unconfined to confined conditions (Table ESM-2). This decrease is coupled to an increase in  $\text{HS}^-$ , mainly in the confined limestone of Ste. Anne-des-Plaines. The higher  $\text{HS}^-$  concentrations correlate with observations of  $\text{H}_2\text{S}$  smells during field sampling at Ste. Anne-des-Plaines. With a median concentration of 45 mg/L, the dolostone is characterized by higher  $\text{SO}_4^{2-}$  concentrations than the other geological units (Table ESM-3). This is clearly shown for the dolostone on the East side of the center anticline.  $\text{NO}_3^-$  is generally low in the Basses-Laurentides sedimentary rock aquifers, 125 samples out of 135 having a concentration lower than 1 mg/L. Samples with concentrations higher than 2.5 mg/L are from surface sediments, and unconfined areas. One sample is from a confined area close to a recharge zone. The distribution of major ions  $\text{Ca}^{2+}$ ,  $\text{Mg}^{2+}$ ,  $\text{Na}^+$ ,  $\text{Cl}^-$ , and  $\text{SO}_4^{2-}$ , and minor ions  $\text{HS}^-$ ,  $\text{Br}^-$ , and  $\text{NO}_3^-$ , is thus greatly influenced by the hydrogeological conditions.

The descriptive statistics of  $\text{Fe}^{2+}$  and  $\text{Mn}^{2+}$  show no major control of the hydrogeological conditions on these ions (Table ESM-2). The interquartile range is more or less similar for the surface sediments, the unconfined, and confined conditions. Extreme values are found in both the unconfined and confined samples. The regional distribution of  $\text{Fe}^{2+}$  shows higher concentrations in the sandstone, particularly the Covey Hill Formation, and the dolostone, particularly in the area of the airport and St. Janvier. These sites with higher  $\text{Fe}^{2+}$  form a southwest-northeast axis from St. Benoît Valley to St. Janvier. The distribution of  $\text{Mn}^{2+}$  follows that of  $\text{Fe}^{2+}$ , but in addition,  $\text{Mn}^{2+}$  has elevated concentrations in the Cairnside sandstone of the St. Hermas Valley. The distribution of  $\text{F}^-$  shows similar patterns for unconfined and confined conditions, with elevated numbers of outliers and extreme values for both hydrogeological conditions (Fig. 3.9e). Concentrations in the surface sediments are much lower.  $\text{F}^-$  dominates in the dolostone and limestone of the Carillon Formation, and in the limestone of the Chazy, Black River and Trenton groups. Thus, elevated concentrations are found in the eastern region of Ste. Anne-des-Plaines, and in the western region of Grenville to St. Philippe.  $\text{F}^-$  in higher concentrations is also present in the Precambrian rocks of Oka Hills (Fig. 3.9e).  $\text{Sr}^{2+}$  dominates in the dolostone and limestone of the Carillon Formation, and in the limestone

of the Chazy Group, particularly in the western region of Grenville to St. Philippe.  $\text{Ba}^{2+}$  is generally low in the aquifers, with 107 samples out of 137 having a concentration lower than 0.25 mg/L. Outliers and extreme values are found in unconfined and confined conditions, particularly in the dolostone of the Beauharnois and Carillon formations, and the limestone of the Chazy Group, in the eastern area of St. Janvier and Ste. Anne-des-Plaines. The distribution of minor ions, as  $\text{Fe}^{2+}$ ,  $\text{Mn}^{2+}$ ,  $\text{F}^-$ ,  $\text{Sr}^{2+}$  and  $\text{Ba}^{2+}$ , is thus highly influenced by the geological units.

The distribution of  $\text{B}^{3+}$  is highly variable, with higher concentrations being found in the confined areas (Table ESM-2). With a median value of 0.32 mg/L, the limestone unit has the highest median concentrations in  $\text{B}^{3+}$ , particularly in Ste. Anne-des-Plaines (Table ESM-3). The regional distribution of DOC (Fig. 3.9f) is not that different from the ones of  $\text{PO}_4^{2-}$  and  $\text{NH}_4^+$ . These three parameters have higher interquartile ranges, outliers and extreme values, in the confined conditions. Even though there is some local variability, the larger grouping of elevated concentrations is found in the confined limestone of Ste. Anne-des-Plaines. The limestone unit has the highest median value for all three parameters (Table ESM-3). The distribution of  $\text{B}^{3+}$ ,  $\text{PO}_4^{2-}$ ,  $\text{NH}_4^+$ , and DOC, could be influenced by both the hydrogeological conditions and geology.

### **3.4.4 Groundwater types**

The previous subsection described the regional groundwater hydrogeochemistry of the Basses-Laurentides sedimentary rock aquifer system within the geological and hydrogeological contexts. The next step is to determine groundwater origin, identify the main geochemical processes controlling groundwater chemistry, as well as identifying all water sources and phases involved in these processes. This knowledge will contribute to the understanding of the geochemical evolution of the groundwater, including the events that have had an impact on the groundwater quality of the region as well as those that still influence the groundwater geochemistry. To help understand groundwater origin in the study area, the approach chosen is to discuss the hydrogeochemical data by groups of

groundwater types. Groundwater type is an integrating classification, and thus, a practical way to group groundwater samples.

Various approaches have been taken to classify groundwater types (Piper, 1944; Back, 1961; Unesco, 1975; Hem, 1985) and they have been applied to regional studies (Back, 1966; Ophori and Tóth, 1989; Panno et al., 1994; Hiscock et al., 1996; Eberts and George, 2000; Adams et al., 2001; Gosselin et al., 2001). Major cations ( $\text{Ca}^{2+}$ ,  $\text{Mg}^{2+}$ ,  $\text{Na}^+$ ,  $\text{K}^+$ ) and anions ( $\text{HCO}_3^-$ ,  $\text{Cl}^-$ ,  $\text{SO}_4^{2-}$ ) are most often used to determine the groundwater type of a sample. The groundwater types are calculated by converting major ion concentrations from meq/L to percentages. In this project geochemical dataset (Table ESM-1), the cations and anions exceeding 10 meq% are listed in order of importance, and define the groundwater types. In the study area, this classification produces several groundwater types, making it very difficult to represent them on a map. To facilitate the geographic representation of water types, an approach of dominant, and mixed groundwater types is used for the study area. Table 3.5 presents two examples to illustrate how this classification is applied. The dominant groundwater type is defined by its dominant cation and anion. In this project, dominant groundwater types require that both dominant cation and anion exceed 20 meq%. This is the case for sample S84 that has a Ca-HCO<sub>3</sub> dominant groundwater type (Table 3.5). If all major cations, or major anions, of a sample fall below 20 meq%, the sample is defined as having a mixed groundwater type. To be classified as a mixed groundwater type, the ion concentration must fall within 10 and 20 meq%. Sample S13 is a mixed cations-HCO<sub>3</sub> groundwater type, meaning that  $\text{Ca}^{2+}$ ,  $\text{Mg}^{2+}$ , and  $\text{Na}^+$  all have meq% between 10 and 20% (Table 3.5). Even though  $\text{Ca}^{2+}$  has the highest meq% for the cations, this classification allows us to include the information that  $\text{Mg}^{2+}$  and  $\text{Na}^+$  are also important characteristics of sample S13. For this classification, mixed anions mean that  $\text{HCO}_3^-$ ,  $\text{Cl}^-$ , and  $\text{SO}_4^{2-}$  have all meq% between 10 and 20%, and an alkaline earth means that  $\text{Ca}^{2+}$  and  $\text{Mg}^{2+}$  have meq% between 10 and 20%.

Table 3.5. Examples of determination of dominant, and mixed groundwater types

Sample ID	Major ions	meq/L	meq%	Groundwater types
<b>Dominant groundwater type</b>				
→ Dominant cation and anion more than 20 meq%				
S84	Ca <sup>2+</sup>	3.393	<b>26.18</b>	
	Mg <sup>2+</sup>	2.797	21.58	
	Na <sup>+</sup>	0.109	0.84	
	K <sup>+</sup>	0.033	0.25	<b>Ca-HCO<sub>3</sub></b>
	HCO <sub>3</sub> <sup>-</sup>	5.871	<b>45.29</b>	
	Cl <sup>-</sup>	0.093	0.72	
	SO <sub>4</sub> <sup>2-</sup>	0.666	5.14	
<b>Mixed groundwater type</b>				
→ No single cation or anion more than 20 meq%				
→ Cation or anion between 10 and 20 meq%				
S13	Ca <sup>2+</sup>	2.096	<b>18.91</b>	
	Mg <sup>2+</sup>	1.892	<b>17.07</b>	
	Na <sup>+</sup>	1.522	<b>13.73</b>	
	K <sup>+</sup>	0.069	0.62	<b>Mixed cations-HCO<sub>3</sub></b>
	HCO <sub>3</sub> <sup>-</sup>	4.501	<b>40.60</b>	
	Cl <sup>-</sup>	0.818	7.38	
	SO <sub>4</sub> <sup>2-</sup>	0.187	1.69	

### 3.4.5 Groundwater groups based on major ions

Figure 3.10 shows the distribution map of the groundwater types for the 146 samples, and their relationships with the general hydrogeological conditions. As illustrated previously by the Piper diagrams (Fig. 3.8), the Basses-Laurentides aquifer system shows significant variations in groundwater geochemistry. The ten groundwater types are associated with four main groups. Table 3.6 summarizes the information regarding each group, including the percentage of samples in the study area, the hydrogeological conditions where these types of water are more likely to be found, the main and secondary geographical areas where they are found, as well as the median values for the major elements. To help visualize the geographical grouping of water types, the groundwater relative quality zones defined by Cloutier et al. (in press) are mapped (Fig. 3.10). These water quality zones were defined by combining the information from a hierarchical cluster analysis (Cloutier et al., in prep b), the hydrogeological conditions map (Hamel et al., 2001), the surficial formations thickness map (Paradis, in press a), as well as from the comparison of parameters to the guidelines for Canadian drinking water quality of Health Canada (2003)

(Cloutier et al., in press). The main features of Fig. 3.10 and Table 3.6 are that samples located in the unconfined or semi-confined areas, and within their proximity, are characterized by groundwater belonging to Group 1 (G1) and Group 4 (G4), particularly by the dominant groundwater types Ca-HCO<sub>3</sub>. Group 2 (G2) and Group 3 (G3) characterize the confined aquifers, dominated by the groundwater types Na-HCO<sub>3</sub> and Na-Cl respectively. Thus, the distribution map of groundwater types shows that the major ion chemistry of the groundwater is strongly related to the hydrogeological conditions.

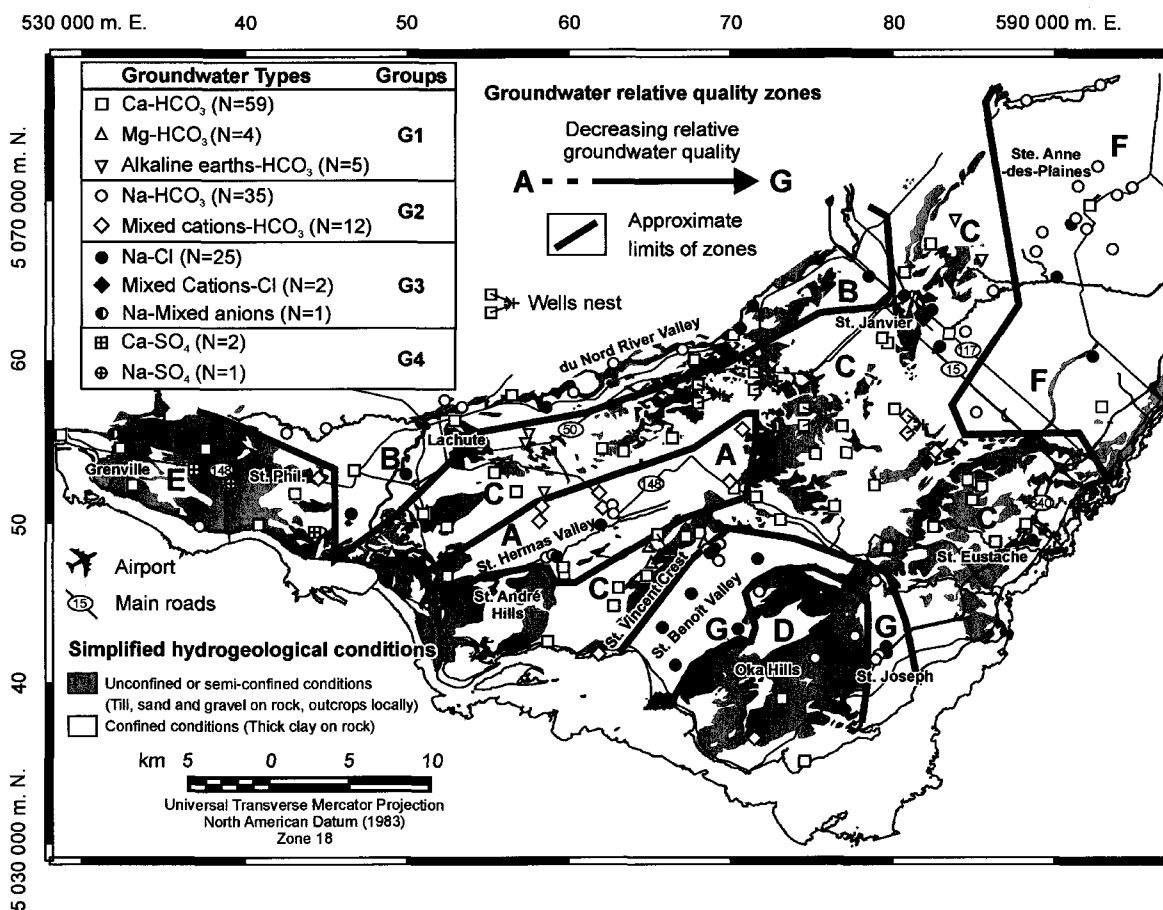


Figure 3.10. Regional distribution map of groundwater types and groups, and their relation to the hydrogeological conditions (N: Number of samples; St. Phil. : St. Philippe) (hydrogeological conditions map modified from Hamel et al., 2001; groundwater relative quality zones from Cloutier and Bourque, in press).

Table 3.6. Characteristics of groundwater types and groups

	Group 1 (G1)	Group 2 (G2)	Group 3 (G3)	Group 4 (G4)
Dominant Water Type (N)	Ca-HCO <sub>3</sub> (59) Mg-HCO <sub>3</sub> (4)	Na-HCO <sub>3</sub> (35)	Na-Cl (25)	Ca-SO <sub>4</sub> (2) Na-SO <sub>4</sub> (1)
Mixed Water Type (N)	Alkaline earth-HCO <sub>3</sub> (5)	Mixed cations-HCO <sub>3</sub> (12)	Mixed cations-Cl (2) Na-Mixed anions (1)	
%	47	32	19	2
Hydro. Conditions	Unconfined Semi-confined	Confined	Confined	Unconfined Semi-confined
Main Locations	Lachute to St. Janvier Airport to St. Eustache St. Vincent Crest Grenville to St. Philippe	Ste. Anne-des-Plaines St. Hermas Valley du Nord River Valley Oka Hills	St. Benoît Valley	Grenville to St. Philippe
Secondary Locations	Around St. André Hills du Nord River Valley Oka Hills	St. Benoît Valley St. Joseph	St. Joseph St. Hermas Valley du Nord River Valley Ste. Anne-des-Plaines St. Janvier (along main roads)	
Median concentration (mg/L)				
Ca <sup>2+</sup>	61	28	24.5	210
Mg <sup>2+</sup>	29	21	29	38
Na <sup>+</sup>	13.6	77	305	90
K <sup>+</sup>	3.7	7.8	15	5.3
HCO <sub>3</sub> <sup>-</sup>	291	297	332	181
Cl <sup>-</sup>	11.5	47	390	33
SO <sub>4</sub> <sup>2-</sup>	34	24	48.5	660

N: Number of samples, Hydro.: Hydrogeological.

The groundwater G1, representing 47% of the samples, is mainly found under unconfined and semi-confined conditions (Fig. 3.10 and Table 3.6). These samples are prevalent in the preferential groundwater recharge areas, namely from Lachute to St. Janvier, from the airport to St. Eustache, the St. Vincent Crest, as well as from Grenville to St. Philippe. The seven groundwater samples from the surface sediments, as well as the two springs, have a Ca-HCO<sub>3</sub> water type, and thus, belong to G1. As groundwater in the surface sediments is at the beginning of the flow system, its geochemistry is key to understand the geochemical processes occurring during groundwater recharge, the starting point of the evolution of groundwater in the area. Groundwater in preferential recharge areas has <sup>3</sup>H

present, and has  $\delta^2\text{H}$  and  $\delta^{18}\text{O}$  similar to modern precipitation. Thus, the origin of groundwater G1 is modern meteoric water.

The groundwater G2, representing 32% of the samples, characterizes areas mainly under confined conditions (Fig. 3.10 and Table 3.6). These samples are prevalent in the clay plain of Ste. Anne-des-Plaines, in the buried valleys of St. Hermas and du Nord River, as well as Oka Hills. Some geochemical characteristics of sites from these areas were illustrated previously, such as elevated  $\text{Na}^+$  (Fig. 3.9d), low  $\text{Ca}^{2+}$  concentrations (Fig. 3.9c), and elevated pH. Table 3.6 shows that, from G1 to G2, the median value of  $\text{Ca}^{2+}$  decreases and that of  $\text{Na}^+$  increases.  $\text{Cl}^-$  increases as well, but not as much as  $\text{Na}^+$ . The increase in  $\text{Na}^+$  and pH, combined with a decrease in  $\text{Ca}^{2+}$ , suggest that  $\text{Ca}^{2+}$ - $\text{Na}^+$  ion exchange, where  $\text{Ca}^{2+}_{\text{water}}$  exchanges with  $\text{Na}^+_{\text{mineral}}$ , could be responsible for the evolution of groundwater from  $\text{Ca}-\text{Mg}-\text{HCO}_3$  to  $\text{Na}-\text{HCO}_3$  water (Thorstenson et al., 1979; Chapelle and Knobel, 1983; Henderson, 1985). Table 3.6 also shows that the median value of  $\text{SO}_4^{2-}$  decreases from G1 to G2. This decrease is observed mainly in Ste. Anne-des-Plaines, where  $\text{HS}^-$  increases and low Eh suggest the occurrence of sulfate reduction. The qualitative interpretation of the tritium and radiocarbon dating data shows that the areas where G2 samples are found, with the exception of the interface sample SAP-L1 in Ste. Anne-des-Plaines, are characterized by submodern groundwater.

The groundwater G3, representing 19% of the samples, is prevalent under confined conditions (Fig. 3.10 and Table 3.6). These samples are characteristic of the buried valley of St. Benoît, but can be found sporadically in the buried valleys of St. Hermas and du Nord River, at St. Joseph, and Ste. Anne-des-Plaines as well. Some sites along the main roads 15 and 117, particularly around St. Janvier, have Na-Cl or mixed cations-Cl groundwater types even though they are located in, or close to, unconfined areas. Table 3.6 shows that, from G1 to G3, the median values of  $\text{Na}^+$  and  $\text{Cl}^-$  increase significantly. From the knowledge of the geological history of the area, the sources for  $\text{Na}^+$  and  $\text{Cl}^-$  could be Cambrian-Ordovician formation waters or Champlain Sea water.

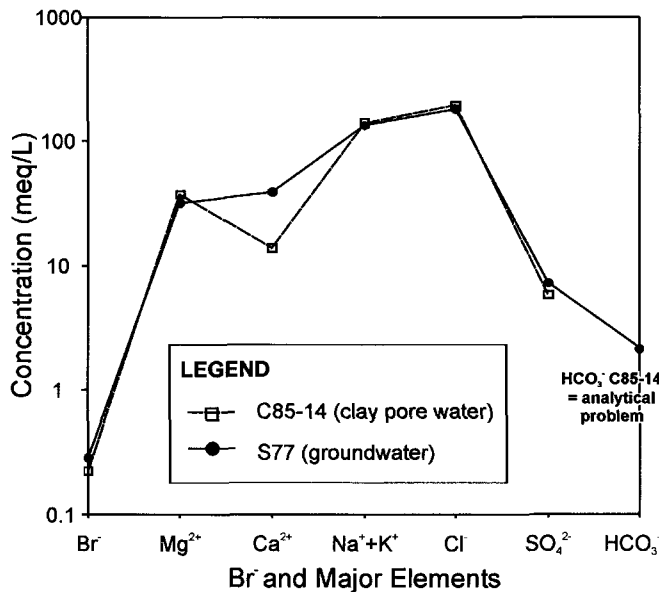


Figure 3.11. Schoeller diagram for the clay pore water sample C85-14, and the groundwater sample S77.

In order to understand the origin of the Na-Cl water, pore water was extracted from the clay aquitard at five sites and analyzed for major elements, as well as for Br<sup>-</sup>, Sr<sup>2+</sup>, δ<sup>2</sup>H and δ<sup>18</sup>O. Figure 3.11 presents a Schoeller diagram for sample S77, the most saline groundwater located in St. Benoît Valley, and for the clay pore water sample C85-14. The pore water is from site S85, in St. Hermas Valley (see Fig. 3.6b for site location). The clay thickness at this site is 46 m. Sample C85-14, from a depth of 14.1 m, has the highest Cl<sup>-</sup> concentration in this profile. With the exception of Ca<sup>2+</sup>, the Schoeller diagram shows similarities in elements concentration between the clay pore water and the groundwater S77. Most important, the Schoeller diagram shows that concentrations from the conservative elements Cl<sup>-</sup> and Br<sup>-</sup>, that can be used as tracers to identify the origin of groundwater salinity (Vengosh et al., 2002), are about similar. This similarity in Cl<sup>-</sup> and Br<sup>-</sup> suggests a unique and common origin for both samples. As the clay was deposited in the Champlain Sea, it is supposed that sample C85-14, the most saline sample at that site, represents the original Champlain Sea water for this area. As mentioned previously, Champlain Sea water was composed of a mixture of Pleistocene meteoric water and glacial meltwater from the Laurentide Ice Sheet, and seawater from the Gulf. Thus, the groundwater sample S77 is believed to belong to a stagnant part of the aquifer system, and is interpreted as the original Champlain Sea end-member for the study area.

Similarity between the two samples is also observed in their  $\delta^{18}\text{O}$ , the clay pore water having a  $\delta^{18}\text{O}$  of  $-10.9\text{\textperthousand}$ , and S77 of  $-11.0\text{\textperthousand}$ . The detailed model for the origin of groundwater salinity, based on the conservative elements and  $\delta^{18}\text{O}$ , is presented in a subsequent paper (Cloutier et al., in prep a).

The other samples from G3 would be the result of groundwater mixing between residual Champlain Sea water, and water infiltrating the aquifers following deglaciation. For the St. Janvier samples, the low  $\text{Br}^-$  concentrations indicate a different source. Located in a recharge area, and close to main roads, de-icing salts are the most plausible source of  $\text{Na}^+$  and  $\text{Cl}^-$  for these samples. The qualitative interpretation of the tritium and radiocarbon dating data shows that the areas where G3 samples are found, with the exception of the samples contaminated by de-icing salts, are characterized by submodern groundwater. Finally, groundwater G4, present in only 2% of the samples, is a minor group (Fig. 3.10 and Table 3.6). The G4 samples are present in the dolostone and limestone on the West side of the territory, in the recharge area of Grenville to St. Philippe. Their elevated  $\text{SO}_4^{2-}$  and  $\text{Ca}^{2+}$  concentrations relative to G1 result from local geochemical processes, and could be related to gypsum dissolution.

### **3.5 DISCUSSION**

This discussion integrates the main observations to develop a conceptual model for the origin and evolution of groundwater geochemistry in the study area.

#### **3.5.1 Geological and hydrogeological contexts**

The regional aquifer is mostly made up of Palaeozoic sedimentary rock formations, consisting of sandstone, dolostone and limestone. The surface of the rock formations has some topographic expression, with extended deep valleys and linear high areas. Quaternary sediments mostly cover the rock aquifer. Bedrock topographic highs are characterized by absence of sediment cover or a thin till or sand layer, thus leading to

unconfined or semi-confined conditions. Preferential groundwater recharge occurs in these areas. Deep bedrock surface valleys are buried under thick marine clay accumulations leading to confined conditions. Regional groundwater flow occurs in the fractured sedimentary rock aquifer, with preferential groundwater flow occurring in the upper part of the bedrock aquifer which is more fractured than the underlying rock. Locally, especially in buried valleys, sand and gravel accumulations can be in contact with the highly fractured rock, thus leading to a mixed granular/rock unit. Groundwater flows from rock topographic highs corresponding to preferential recharge areas, and this flow occurs preferentially from North to South.

### **3.5.2 Isotopic data main conclusions**

The mean  $\delta^{18}\text{O}$  for the recharged groundwater to the Basses-Laurentides sedimentary rock aquifer system is  $-11.4\text{\textperthousand}$  (Fig. 3.5a). This mean value is very similar to the  $\delta^{18}\text{O}$  weighted annual means for Ottawa precipitation ( $-11.21\text{\textperthousand}$ ; IAEA, 2001). Even though the precipitations show a large range of isotopic values through the year, the groundwater isotopic composition is smoothed out during the recharge processes, resulting in a relatively uniform isotopic composition. Thus the seasonal input, as the depleted spring meltwater, is not preserved in the groundwater of recharge areas in the Basses-Laurentides. This is in agreement with Fritz et al. (1987) who showed that the distribution of  $\delta^{18}\text{O}$  in shallow groundwater of eastern Canada closely reflects the average annual isotopic composition of local precipitation. It was also seen that the mean  $\delta^{18}\text{O}$  for the confined groundwater is  $-11.3\text{\textperthousand}$ , very similar to the recharged groundwater (Fig. 3.5a). This uniformity in  $\delta^{18}\text{O}$  between unconfined and confined conditions could indicate a single origin for the groundwater, namely precipitation, or well mixed groundwater sources in the confined aquifers. The discrimination between these possibilities is discussed in a subsequent paper which describes geochemical processes in greater details (Cloutier et al., in prep a).

About 70% of the groundwater samples have a  $\delta^{13}\text{C}_{\text{DIC}}$  between  $-16.0\text{\textperthousand}$  to  $-12.0\text{\textperthousand}$  (Fig. 3.5c), which indicates that dissolution of marine carbonates could be an important process in this sedimentary rock aquifer system. In the recharge area, the infiltrated water is in equilibrium with the soil  $\text{CO}_2$  which has, for natural vegetation in temperate regions ( $\text{C}_3$  vegetation), a  $\delta^{13}\text{C}$  of about  $-23\text{\textperthousand}$  V-PDB (Clark and Fritz, 1997). Dissolution of carbonate minerals in recharge areas adds  $\text{HCO}_3^-$  to the DIC of groundwater. As most marine carbonates have  $\delta^{13}\text{C}$  of  $-2$  to  $0\text{\textperthousand}$  V-PDB (Mazor, 1991), their dissolution, and the addition of enriched  $\text{HCO}_3^-$ , contribute to the enrichment of groundwater  $\delta^{13}\text{C}_{\text{DIC}}$  relative to  $\delta^{13}\text{C}$  of soil  $\text{CO}_2$ . In a study of groundwater recharge to Paleozoic carbonate aquifer located in the St. Lawrence Lowlands southwest of this present study, Cane and Clark (1998) calculated the  $\delta^{13}\text{C}_{\text{DIC}}$  of groundwater resulting from infiltration through  $\text{C}_3$  vegetation ( $\delta^{13}\text{C}_{\text{CO}_2} = -23\text{\textperthousand}$ ) following the dissolution of carbonate ( $\delta^{13}\text{C} = 0\text{\textperthousand}$ ). The final  $\delta^{13}\text{C}_{\text{DIC}}$  calculated is  $-14.0\text{\textperthousand}$  for open system, and  $-11.5\text{\textperthousand}$  for closed system conditions. Sample S146, a groundwater from the till at St. Vincent Crest recharge area, has  $\delta^{13}\text{C}_{\text{DIC}}$  of  $-15.0\text{\textperthousand}$ , very close to the calculated value of Cane and Clark (1998) for carbonate dissolution in an open system condition. Thus, the variation in  $\delta^{13}\text{C}_{\text{DIC}}$  of samples from depleted to enriched values would be caused by carbonate dissolution operating in open, to semi-open, and finally under closed conditions.

Strontium isotopes in the groundwater from the dolostone and limestone of the preferential recharge areas are consistent with water-rock interaction of carbonates along the flow system (Fig. 3.6a). Groundwater from the confined areas have a larger spread of  $^{87}\text{Sr}/^{86}\text{Sr}$  values. Samples from St. Benoît Valley, St. Joseph, and Ste. Anne-des-Plaines have a radiogenic source of Sr that could be related to the presence of K-feldspar in the sandstone, and clay minerals of shale beds in the confined dolostone and limestone. Lower  $^{87}\text{Sr}/^{86}\text{Sr}$  for sample S77 in St. Benoît Valley, and St. Hermas Valley, could be the result of water-rock interaction with crystallized limestone from the Grenville around Oka Hills, and from rocks of the Oka intrusion respectively. The uniformity in the  $^{87}\text{Sr}/^{86}\text{Sr}$  values from the dolostone and limestone of the recharge areas could suggest that the groundwater flow system in the preferential recharge areas is more continuous, thus more active, than the system of the buried valleys. The  $\text{Sr}^{2+}$  and  $^{87}\text{Sr}/^{86}\text{Sr}$  profiles at well SAP

suggest a longer residence time for the deeper samples and faster groundwater flow in the interface zone below the clay aquitard (Fig. 3.6c).

The qualitative interpretation of the tritium and radiocarbon dating data shows that the preferential recharge areas are characterized by modern, tritiated groundwater, and that the confined aquifers are characterized by submodern groundwater (Fig. 3.7a). The St. Hermas Valley cross-section A-A' shows an evolution from modern groundwater in the recharge area, to submodern groundwater in the buried valley (Fig. 3.7b). The St. Benoît Valley cross-section B-B' indicates that precipitation recharges the aquifer through the till, and that groundwater flows preferentially in the interface zone. In the fractured rock aquifer,  $^{14}\text{C}$  decreases from St. Vincent Crest to the buried valley downgradient. The C-C' cross-section shows that the region from the airport to St. Eustache is characterized by modern groundwater. Even though the main recharge area for cross-section C-C' is in the North part of the section, the hydrogeological conditions of the area allows infiltration of precipitation all along the section. Finally, the profile for wells SAP and St. Vincent Crest suggest that groundwater may flow preferentially in the highly fractured rock at the interface zone (Fig. 3.7c). This observation is consistent with the strontium data for the same well (Fig. 3.6c).

### 3.5.3 Groundwater groups and end-members

The Basses-Laurentides sedimentary rock aquifer system shows significant variations in groundwater geochemistry. Thus, groundwater types and groups were defined based on major ions concentrations. Previous work by Cloutier et al. (in press) led to the zoning of the study area in terms of relative groundwater quality. Within these zones, some groundwater types are dominant. These related groundwater types could be classified in 4 groups (G1 to G4). There is a spatial relationship between the groundwater groups and the hydrogeological contexts of the area. G1 (Ca-HCO<sub>3</sub> and Mg-HCO<sub>3</sub>) and G4 (Ca-SO<sub>4</sub> and Na-SO<sub>4</sub>) are found in preferential groundwater recharge areas, whereas G2 (Na-HCO<sub>3</sub>) and G3 (Na-Cl) are found under confined conditions.

Some samples among certain groundwater groups are interpreted to represent geochemical end-members having different origin within the groundwater flow system. Some samples of the Ca-HCO<sub>3</sub> and Mg-HCO<sub>3</sub> G1 groundwater represent infiltration of precipitation water in the preferential recharge areas. The samples representing this end-member were obtained in the till in preferential recharge zones. On the other hand, it was shown that the most concentrated G3 groundwater sample (S77) found under confined conditions at the center of a buried valley has a Na-Cl geochemistry very similar to the marine clay pore-water extracted in the middle of clay accumulations. Both of these are interpreted to represent Champlain Sea water that was a mixture of St. Lawrence Gulf seawater with Pleistocene meteoric water and glacial meltwater. The last end-member has not been characterized but its presence in the deepest part of the aquifer is inferred. This end-member would represent Cambrian-Ordovician formation waters in the Palaeozoic rocks under the lower limit of the active groundwater flow system.

### **3.5.4 Groundwater origin and evolution**

Figure 3.12 is a synthesis of the hydrogeochemical systems found in the study area. The purpose of this figure is to show the relationships between the geological history and geochemical evolution of groundwater with the various groundwater groups as well as their relative qualitative isotopic age. This synthesis illustrates the relationships among groundwater groups, the role of these groups within the geochemical system and the main geochemical processes that are believed to influence the evolution of groundwater geochemistry along flow paths originating at preferential groundwater recharge areas. These geochemical processes are not discussed in detail in the present paper but are the subject of a subsequent paper (Cloutier et al., in prep. a). The relationships among the groundwater groups and the overall groundwater geochemical evolution represented here constitute the conceptual hydrogeochemical model for the Basses-Laurentides. This provides a framework for explaining the observations made following the characterization of the groundwater flow system in the regional sedimentary rock aquifer.

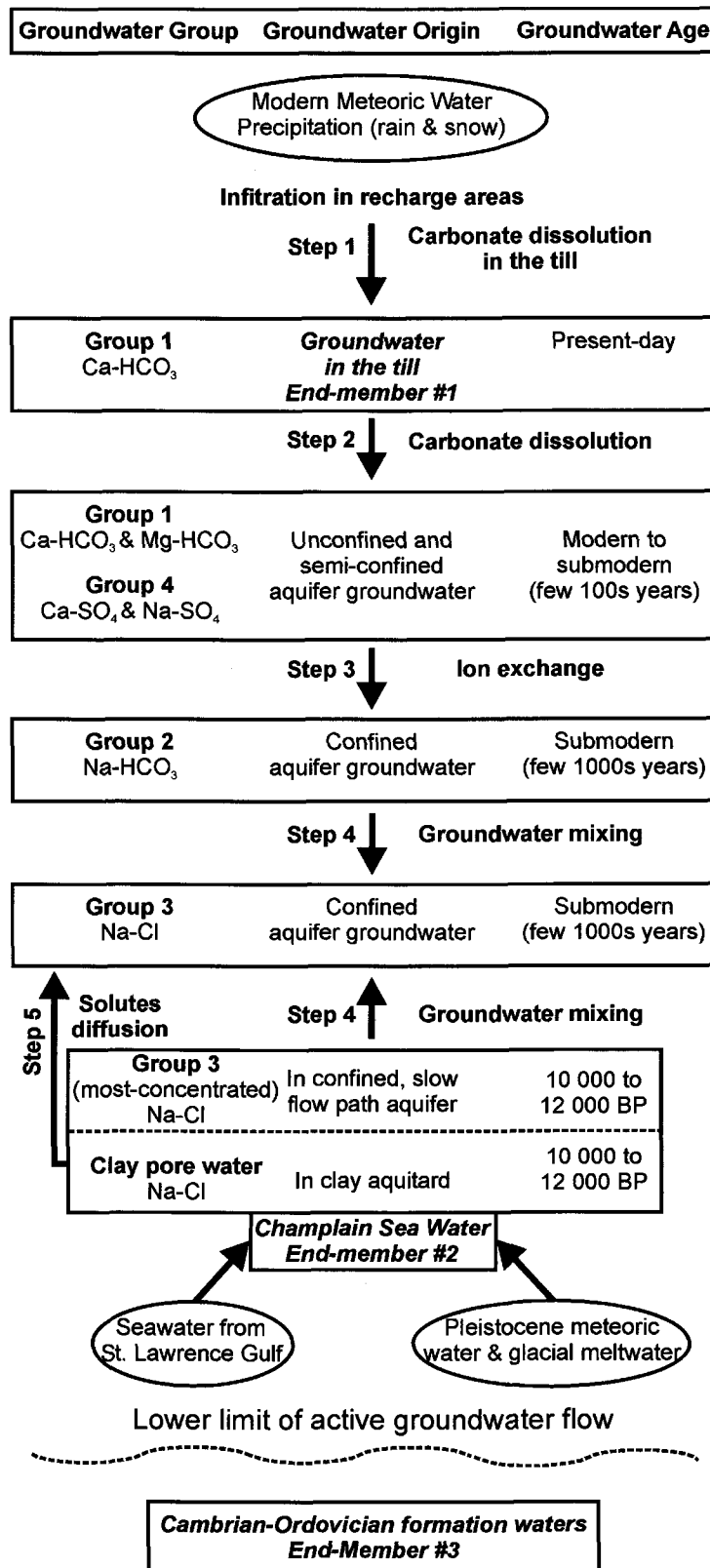


Figure 3.12. Conceptual model of groundwater origin and relationships between groundwater end-members.

Modern meteoric water, as rain and snow, infiltrates the Basses-Laurentides sedimentary rock aquifer system in the preferential recharge areas (Step 1). These recharge areas generally consist of elevated topographic regions covered by carbonate-rich till sediments. Groundwater in the till, the end-member #1, belongs to G1 and is characterized by dominant water types Ca-HCO<sub>3</sub>. δ<sup>18</sup>O and δ<sup>2</sup>H values of the groundwater from the surface sediments fall in the range of δ<sup>18</sup>O and δ<sup>2</sup>H obtained for the regional precipitation. Tritium data from the local recharge zone of St. Vincent Crest indicate the presence of modern meteoric water in the till. Also from St. Vincent Crest, δ<sup>13</sup>C<sub>DIC</sub> value in the till indicates carbonates dissolution, consistent with the characteristic Ca-Mg-HCO<sub>3</sub> of recharging water. From the surface sediments, groundwater flows in the fractured sedimentary rocks of the unconfined and semi-confined aquifer, in the preferential recharge areas (Step 2). This groundwater is dominated by G1 (Ca-HCO<sub>3</sub> and Mg-HCO<sub>3</sub>), with a few samples of G4 (Ca-SO<sub>4</sub> and Na- SO<sub>4</sub>) in the carbonates of the western part of the study area (Fig. 3.10). Their mean δ<sup>18</sup>O is very similar to the δ<sup>18</sup>O weighted annual means for Ottawa precipitation. The qualitative interpretation of the tritium data shows that these groundwaters are generally modern. With no tritium detected, the sample from the fractured rock aquifer at St. Vincent Crest is classified as submodern, even though it belongs to G1. Thus, this sample is older than 1952, and could be a few 100s of years old. Strontium isotopes in the groundwater from the dolostone and limestone of G1 and G4 are consistent with water-rock interaction of carbonates along the flow system. Carbonate dissolution could occur in contact with carbonate formations or with carbonate minerals on fracture faces.

The groundwater flow, from the unconfined to confined aquifer, results in a groundwater evolution to G2 (Na-HCO<sub>3</sub>) and G3 (Na-Cl). This evolution is particularly noticeable in St. Hermas Valley, where modern meteoric Ca-Mg-HCO<sub>3</sub> water G1 in the recharge area evolves to mixed cations-HCO<sub>3</sub> and Na-HCO<sub>3</sub> water G2 (Step 3), to finally Na-Cl water G3 (Step 4) in the center of the valley (Fig. 3.10). Hydrogeochemical data suggest that Ca<sup>2+</sup><sub>water</sub>-Na<sup>+</sup><sub>mineral</sub> ion exchange could be responsible for the evolution of groundwater from G1 to G2. Supply of sodium is also available from overlying clay accumulations. Conservative tracers Cl<sup>-</sup> and Br<sup>-</sup> allow the identification of Champlain Sea water, the

Pleistocene end-member #2 for the study aquifer. The end-member is found at site S77 in St. Benoît Valley, as well as in the clay pore water. As both samples are interpreted as original Champlain Sea water for the study area, their groundwater age is estimated at 10 000 to 12 000 BP. Two possibilities could be invoked for the evolution to G3 water: First, is the mixing of water G2 with stagnant aquifer zones previously saturated with Champlain Sea water as S77 (Step 4), and second is the diffusion of solutes from low permeable units, as the clay aquitard (Step 5). With the exception of the interface sample in Ste. Anne-des-Plaines, and of a sample from St. Hermas Valley that is believed to be affected by mixing with meteoric water, the tritium data indicate submodern groundwater for G2 and G3 waters. As these groundwaters cannot be older than the Champlain Sea water end-member, their groundwater ages are interpreted as being a few 1000s years. The end-member #3 in the study area is the Cambrian-Ordovician formation waters, below the lower limit of active groundwater flow. Since this study covers only the upper portion of the Basses-Laurentides sedimentary rock aquifer system, this end-member was not sampled.

### **3.5.5 Water quality and anthropogenic effects**

Cloutier et al. (in press), and the analysis presented in the present article, showed that most concentrations exceeding the guidelines for Canadian drinking water quality (Health Canada, 2003) for maximum acceptable concentrations (MAC) and aesthetic objectives (AO) have natural origin. These origins are largely related to the hydrogeological contexts in the case of TDS, HS<sup>-</sup>, Na<sup>+</sup>, Cl<sup>-</sup>, and pH, and to the geological contexts for F<sup>-</sup>, Ba<sup>2+</sup>, Mn<sup>2+</sup>, Fe<sup>2+</sup> and SO<sub>4</sub><sup>2-</sup>. The effects of the hydrogeological contexts on the water quality are mainly for G2 (Na-HCO<sub>3</sub>) and G3 (Na-Cl) groundwater in the confined aquifers. On the other hand, the geological contexts can have an effect on the water quality for all groundwater groups, in unconfined or confined conditions.

Anthropogenic effects must be put forward for TDS, Na<sup>+</sup> and Cl<sup>-</sup> concentrations exceeding the AO in the unconfined area close to St. Janvier, and for NO<sub>3</sub><sup>-</sup> exceeding the MAC in the recharge area. The local presence of Na<sup>+</sup> and Cl<sup>-</sup> in a recharge zone along a

main highway, without the presence of  $\text{Br}^-$ , is interpreted to be the result of de-icing salts providing components to the recharging water. The presence of  $\text{NO}_3^-$ , attributed to agricultural activities as fertilizers, is local and has a relatively limited observed impact so far. The effects of de-icing salts and agriculture are on groundwater of G1 ( $\text{Ca}-\text{HCO}_3$  and  $\text{Mg}-\text{HCO}_3$ ) in the preferential recharge areas. Due to its relatively elevated samples with concentrations exceeding AO, the water quality of the Basses-Laurentides sedimentary rock aquifer system is variable, but not too affected by human activities (Cloutier et al., in press). Even though anthropogenic effects are limited so far, local detection of  $\text{NO}_3^-$  and de-icing salts indicates, as does tritium, that these aquifers are vulnerable to contamination in some areas. Being associated to preferential recharge areas, the distribution of  $\text{Ca}-\text{Mg}-\text{HCO}_3$  water G1 is a qualitative indication of the aquifer vulnerability, and thus a practical application of the geochemistry to the management of the resources.

### 3.6 SUMMARY AND CONCLUSIONS

This paper presented the results obtained from a regional and comprehensive hydrogeochemical study, allowing the assessment of groundwater quality, the determination of groundwater origin, and a first qualitative understanding of the main geochemical processes controlling groundwater geochemistry and its spatial evolution. The  $\delta^2\text{H}$  and  $\delta^{18}\text{O}$  of the groundwater samples are distributed around the local meteoric water line, the BLMWL. The mean  $\delta^{18}\text{O}$  for the recharged groundwater to the aquifer system is very similar to the  $\delta^{18}\text{O}$  weighted annual means for the region. Qualitative interpretation of  ${}^3\text{H}$  data shows that zones identified as preferential recharge areas have modern groundwater ages whereas zones under deep buried valleys have submodern ages. Isotopic data in profiles where discrete groundwater samples were obtained show evidence of preferential groundwater flow in the upper part of the bedrock aquifer.  $\delta^{13}\text{C}_{\text{DIC}}$  and  ${}^{87}\text{Sr}/{}^{86}\text{Sr}$  also indicate that water-rock interactions occur from recharge areas along groundwater flow paths. Piper diagrams, as well as the distribution map of groundwater types and the descriptive statistics, indicate that the major ion chemistry is

controlled mainly by the hydrogeological conditions. Groundwater groups G1 (Ca-HCO<sub>3</sub> and Mg-HCO<sub>3</sub>) and G4 (Ca-SO<sub>4</sub> and Na-SO<sub>4</sub>) are found in preferential groundwater recharge areas, whereas G2 (Na-HCO<sub>3</sub>) and G3 (Na-Cl) groundwater are found under confined conditions. On the other hand, the distribution of minor ions, such as Sr<sup>2+</sup> and F<sup>-</sup>, is controlled by the geological formations.

The study shows the importance of the geological history on the hydrogeochemistry of the aquifer system. The till mineralogy, related mainly to the glacial erosion of sedimentary formations, has a large influence on the geochemistry of the modern recharge groundwater end-member. The glacio-fluvial deposits, and the highly fractured and weathered upper bedrock, represent a highly permeable zone under the clay deposit. Some hydrogeochemical indications of faster interface flow were presented for this zone. The Pleistocene Champlain sea invasion led to salinization of the aquifer, and a Champlain Sea water end-member is still present in the aquifer. The clay deposits from the Champlain Sea episode act as a protection for the aquifer, but also as a long term source of Na<sup>+</sup> and Cl<sup>-</sup> to the underlying aquifer. The buried valleys and the Cretaceous intrusions, with their influence on the groundwater flow, could be the cause of stagnant zones of Champlain Sea water, as for site S77 in St. Benoît Valley. The complex geological history, including the latest glaciation and the Champlain Sea invasion, and the variety of geological and hydrogeological contexts, result in distinctive groundwater origin, and in groundwater geochemistry influenced by ancient and present hydrogeological and geochemical processes. The main geochemical processes involved are carbonate dissolution, Ca<sup>2+</sup>-Na<sup>+</sup> ion exchange, mixing with saline water, and diffusion from the Champlain Sea clay. The combined results of these ancient and present hydrogeological and geochemical processes confer to the Basses-Laurentides sedimentary rock aquifer system its present-day, highly variable, groundwater geochemistry. Most of the processes affecting this regional aquifer are discussed by Tóth (1999) in his representation of groundwater evolution of a regional, gravity-driven flow system. The original characteristics of the studied system, relative to Tóth's (1999) general conceptual model, are the presence of confined aquifer and stagnant zones of saline water of ancient geological event origin. The recognition of the origin of this saline water indicates that

one could expect to find remaining saline and brackish groundwater in aquifers of similar settings, as in other areas flooded by the Champlain Sea, in parts of the St. Lawrence, Ottawa, and modern Lake Champlain lowlands (Parent and Occhietti, 1988), or in areas flooded by other post-glacial seas, as the Laflamme and Goldthwait Sea in eastern Canada.

## ACKNOWLEDGEMENTS

The project was carried out by the Geological Survey of Canada (GSC contribution 2003192), in collaboration with INRS-Eau, Terre & Environnement (INRS-ETE), Université Laval and Environment Canada. Funding for the study came from the GSC, Economic Development Canada, Regional County Municipalities (RCM) of Argenteuil, Mirabel, Deux-Montagnes and Thérèse-de-Blainville, Department of the Environment of Québec, Conseil Régional de Développement-Laurentides, and Association des Professionnels de Développement Économique des Laurentides. Financial support for the first author was provided by the Natural Sciences and Engineering Research Council (NSERC) of Canada, Fonds québécois de la recherche sur la nature et les technologies, and INRS-ETE as postgraduate scholarships. We acknowledge the Department of the Environment of Québec for providing the analyses of inorganic constituents in groundwater. The drilling was partly supported by the Department of Transports of Québec. The authors thank Marc Luzincourt (Delta-Lab, GSC-Québec) for stable isotopes analyses, and Dr. Bill Davis (Geochron Laboratory, GSC-Ottawa) for  $^{87}\text{Sr}/^{86}\text{Sr}$  analyses. We also thank Dr. Christine Rivard (GSC-Québec) for her internal review. NSERC also supported R.L. and R.T. through operating grants. The work of all students involved in the project as field assistants, and the collaboration of the population of the RCM giving site access are greatly appreciated.

## APPENDIX

This appendix presents details on the sampling and analytical protocols.

### Field and laboratory analyses

*In situ* field measurements were made on water samples for the following parameters: temperature with a glass thermometer, pH and electrical conductivity (EC) with a YSI 63 meter, dissolved oxygen (DO) with a YSI 95 meter, and redox potential with a Hanna instruments ORP HI 98201 meter. The redox measurements ( $E_{\text{measured}}$  in mV) were corrected for the difference between the standard potential of the reference electrode being used at the solution temperature and the potential of the standard hydrogen electrode (Nordstrom and Wilde, 1998). The standard potential for a Ag-AgCl electrode with 3.5 M KCl filling solution (reference electrode for ORP HI 98201) at the sample temperature ( $E_{\text{reference}}$  in mV) were interpolated from data provided by Nordstrom and Wilde (1998). Thus the potential of the sample relative to the standard hydrogen electrode,  $E_h$ , is obtained by adding  $E_{\text{reference}}$  to  $E_{\text{measured}}$ . Private wells were purged until stabilization of field measurements before sampling. The observation wells and sampled levels were purged with an approach combining field measurement stabilization, and a minimum of 3 to 5 well bore volumes.

Samples for major, minor and trace constituents were collected in plastic bottles, kept in coolers, and shipped to the laboratory at the end of the sampling day. Duplicate samples, about 7% of the total, were also submitted to verify data quality and accuracy. The laboratory of the Department of the Environment of Québec (*Centre d'expertise en analyse environnementale du Québec*), performed the analyses using standard methods. Table 3.7 provides a the list of parameters analyzed, the field sampling protocol, and the method of analysis. Electro-neutrality was calculated to verify the analyses reliability. An electro-neutrality of  $\pm 5\%$  is acceptable (Freeze and Cherry, 1979). For the 153 regional groundwater samples, 134 samples have an electro-neutrality below 5%, 12 between 5 and 8%, and 7 above 10%. Samples with an electro-neutrality above 10% were rejected as

they were generally missing important ions. The 146 groundwater samples, with electro-neutrality below 8%, are retained for the geochemical interpretation of the major, minor, and trace elements data (Fig. 3.3). For the 72 multilevel samples, only two levels were rejected due to missing ions.

Table 3.7. List of parameters analyzed, field sampling protocol, and method of analysis

Parameters	Filtration (0.45 µm)	Preservation	Method of analysis
Ag <sup>a</sup> , Al, B, Ba, Ca, Cd <sup>a</sup> , Cr, Cu, Fe, K, Li, Mg, Mn, Na, Ni, Pb <sup>a</sup> , Si, Sr, U <sup>a</sup> , Zn	Yes	Nitric acid	ICP-AES <sup>b</sup>
As <sup>a</sup> , Se <sup>a</sup>	Yes	Nitric acid	HG-AAS <sup>c</sup>
Cl, total alkalinity	No		Conductivity method
F, SO <sub>4</sub> , DIC, DOC	No		Colorimetric method
NO <sub>3</sub> , NH <sub>4</sub> , PO <sub>4</sub>	Yes	Sulfuric acid	Colorimetric method
CN <sup>a</sup>	No	Sodium hydroxide	Colorimetric method
Br, I <sup>a</sup>	No		Ion chromatography
HS	No	Zinc acetate + Sodium hydroxide	Colorimetric method
Hg <sup>a</sup>	Yes	Chromic acid	Cold vapor-AAS

<sup>a</sup> Parameters that were not analyzed for the multilevel samples

<sup>b</sup> Inductively coupled plasma-atomic emission spectrometry

<sup>c</sup> Hydride generation-atomic absorption spectrophotometry.

Samples for δ<sup>2</sup>H and δ<sup>18</sup>O were collected in 60 ml HDPE bottles. The analyses were performed at the Delta-Lab of the Geological Survey of Canada-Québec Division and at the G.G. Hatch Isotope Laboratories of the University of Ottawa. H<sub>2</sub> gas was extracted from water samples using the zinc reduction method (Coleman et al., 1982). An IRM spectrometer (Micromass Prism III) (Delta-Lab) and an automated double collector VG 602E mass spectrometer (G.G. Hatch) were used to analyze the δ<sup>2</sup>H ratios. Oxygen of 1 ml water samples was equilibrated with commercial CO<sub>2</sub> at a controlled temperature using an automated system. δ<sup>18</sup>O<sub>water</sub> was subsequently analyzed on the equilibrated CO<sub>2</sub> with a VG-SIRA 12 IRMS. Isotopic results are reported with the standard δ notation as

per mil (‰) deviations relative to V-SMOW. Analytical precision is  $\pm 0.1\text{‰}$  for  $\delta^{18}\text{O}$  and  $\pm 1.5\text{‰}$  to  $\pm 2\text{‰}$  for  $\delta^2\text{H}$ . Snow samples collected in 2001, as well as the clay pore water, were analyzed for  $\delta^2\text{H}$  and  $\delta^{18}\text{O}$  at the Delta-Lab with a gas bench attached to an IRMS. The gas bench is an automated system performing equilibration of  $\text{H}_2\text{O}$  with  $\text{CO}_2$  and with  $\text{H}_2$  for the analysis of  $\delta^{18}\text{O}$  and  $\delta^2\text{H}$  respectively. Precisions obtained were  $\pm 0.1\text{‰}$  for  $\delta^{18}\text{O}$  and  $\pm 1\text{‰}$  for  $\delta^2\text{H}$ . Samples for  $\delta^{13}\text{C}_{\text{DIC}}$  were filtered, collected in 250 ml glass bottles, and preserved with  $\text{HgCl}_2$  to prevent modifications due to bacteriological reactions. Samples were analyzed by the Delta-Lab within a week following sampling. The  $\delta^{13}\text{C}_{\text{DIC}}$  extractions were made by vacuum line acid stripping using 100%  $\text{H}_3\text{PO}_4$ , converting all dissolved inorganic carbon to  $\text{CO}_2$ . A VG-SIRA 12 IRMS was used to analyze the extracted  $\text{CO}_2$ . Isotopic results are reported with the standard  $\delta$  notation as per mil (‰) deviations relative to NBS-19 (V-PDB), with an analytical precision of  $\pm 0.1\text{‰}$ .

Some regional and multilevel groundwater samples, collected in 1 L HDPE bottles, were analyzed for  $^{87}\text{Sr}/^{86}\text{Sr}$ , enriched  $^3\text{H}$  and  $^{14}\text{C}$  of DIC. Twenty-five samples were analyzed for  $^{87}\text{Sr}/^{86}\text{Sr}$  at the Geochron Laboratory of the Geological Survey of Canada in Ottawa by thermal ionization mass spectrometry. Average measurement of seven analyses of the standard NBS-987 run with the samples gave  $^{87}\text{Sr}/^{86}\text{Sr}$  of  $0.710253 \pm 0.000004$  ( $1\sigma$  error). Fourteen samples were analyzed for enriched  $^3\text{H}$  at the Environmental Isotope Laboratory of the University of Waterloo by liquid scintillation counting. The precision for enriched  $^3\text{H}$  is  $\pm 0.8$  TU. From these fourteen samples, twelve were analyzed for radiocarbon analysis of DIC.  $\text{CO}_2$  was extracted at the Environmental Isotope Laboratory of the University of Waterloo, and analyzed by AMS at the IsoTrace Laboratory of the University of Toronto. The average precision for  $^{14}\text{C}$  is  $\pm 0.5$  pMC.

**ELECTRONIC SUPPLEMENTARY MATERIAL (ESM)**

This section presents Table ESM-2 and Table ESM-3. These tables were submitted along with this manuscript, **Hydrogeochemistry and groundwater origin of the Basses-Laurentides sedimentary rock aquifer system, St. Lawrence Lowlands, Québec, Canada**, to be published as electronic materials. Table ESM-1, a large table of the original geochemical dataset, could not be inserted in the core of the thesis due to its size. Thus Table ESM-1 is included in the compact disc accompanying the thesis (*Appendice G*). All the data of Table ESM-1 are also included in the *Appendice A* of the thesis.

Table ESM-2. Descriptive statistics of the sampling sites in relation to hydrogeological conditions (concentrations in mg/L unless noted otherwise)

Parameters	Surface sediments and springs				Unconfined and semi-confined				Confined			
	N	Median	Lower Quartile	Upper Quartile	N	Median	Lower Quartile	Upper Quartile	N	Median	Lower Quartile	Upper Quartile
Top (m) <sup>a</sup>	7	4.9	2.8	8.8	49	8.2	6.1	13.1	77	27.7	18.3	40.9
Bot (m) <sup>b</sup>	7	7.0	4.6	9.1	49	38.1	24.4	73.2	83	37.5	27.5	79.3
pH	9	7.33	7.15	7.51	51	7.36	7.16	7.64	86	7.78	7.40	8.10
EC to 25 °C <sup>c</sup>	9	500	409	717	51	653	529	882	86	685	479	1155
DO	7	2.36	1.22	7.86	47	2.4	1.51	5.53	75	1.83	1.17	2.96
Eh (mV)	7	+261	+187	+310	44	+245	+171	+289	72	+160	+92	+269
Ca	9	64	48	84	51	62	42	85	86	32.5	19	51
Mg	9	26	23	36	51	31	22	39	86	23	14	30
Na	9	7.4	7	9.4	51	27	7.4	67	86	74.5	26	220
K	9	3.4	1.1	3.8	51	4.1	2.3	8.6	86	7.3	3.9	14
Cl	9	12	5	13	51	33	10	75	86	47.5	10	170
SO <sub>4</sub>	9	27	22	49	51	45	27	90	84	22	10.5	43.5
Fe	9	0.25	0.007	0.67	50	0.093	0.016	0.47	84	0.15	0.026	0.45
Mn	9	0.019	0.0005	0.15	51	0.012	0.003	0.059	86	0.024	0.005	0.096
Br	8	0.01	0.01	0.015	50	0.0225	0.01	0.06	86	0.1145	0.019	0.56
Sr	9	0.107	0.09	0.19	51	0.45	0.195	1.45	85	0.51	0.23	1.272
F	9	0.12	0.09	0.15	50	0.275	0.12	0.59	83	0.39	0.25	0.83
Ba	9	0.06	0.03	0.11	51	0.11	0.06	0.18	86	0.145	0.1	0.26
HS (as S)	9	0.02	0.02	0.03	51	0.02	0.02	0.04	82	0.03	0.02	0.07
SiO <sub>2</sub>	9	11.9	10.7	13	51	11.6	9.9	14.2	86	13	10.6	15
B	9	0.002	0.002	0.009	51	0.04	0.01	0.14	85	0.11	0.04	0.32
NO <sub>3</sub> (as N)	9	0.02	0.02	0.47	50	0.02	0.02	0.28	85	0.02	0.02	0.03
NH <sub>4</sub> (as N)	9	0.02	0.02	0.06	50	0.05	0.02	0.11	85	0.25	0.06	0.72
PO <sub>4</sub> (as P)	9	0.01	0.01	0.025	50	0.01	0.01	0.01	85	0.065	0.015	0.2
DOC	9	1.4	0.6	1.7	51	1	0.7	1.9	83	1.5	0.6	4.3
HCO <sub>3</sub> <sup>d</sup>	9	274.4	214.5	368.6	51	318.9	252.1	356.7	86	294.9	237.9	364.5

N: Number of samples

<sup>a</sup> Depth of top of sampling interval

<sup>b</sup> Depth of bottom of sampling interval

<sup>c</sup> EC in µS/cm

<sup>d</sup> Geochemical calculations with PHREEQC 2.6 (Parkhurst and Appelo, 1999).

Table ESM-3. Descriptive statistics of the sampling sites in relation to geological units (concentrations in mg/L unless noted otherwise)

Parameters	Sed. under clay		Limestone		Dolostone		Sandstone		Grenvillian	
	N	Median	N	Median	N	Median	N	Median	N	Median
pH	13	8.01	20	7.79	57	7.43	41	7.46	6	7.80
EC to 25 °C <sup>a</sup>	13	678	20	855	57	740	41	583	6	482
DO	12	1.97	18	1.57	51	2.01	35	2.48	6	2.83
Eh (mV)	11	+166	18	+141	48	+228	34	+261	5	+170
Ca	13	32	20	33.5	57	56	41	40	6	32.5
Mg	13	23	20	14.5	57	31	41	26	6	15.9
Na	13	73	20	125	57	44	41	28	6	61
K	13	5.7	20	9.2	57	7.4	41	4.3	6	3.4
Cl	13	35	20	37.5	57	42	41	29	6	17.5
SO <sub>4</sub>	13	16	20	23	55	45	41	25	6	22
Fe	12	0.097	20	0.024	55	0.16	41	0.15	6	0.0795
Mn	13	0.05	20	0.0055	57	0.017	41	0.049	6	0.0165
Br	13	0.15	20	0.12	57	0.04	40	0.03	6	0.025
Sr	12	0.33	20	1.395	57	0.45	41	0.331	6	1.12
F	12	0.34	20	1.15	54	0.345	41	0.25	6	1.2
Ba	13	0.14	20	0.13	57	0.15	41	0.13	6	0.08
HS (as S)	12	0.025	20	0.04	57	0.02	38	0.02	6	0.02
SiO <sub>2</sub>	13	11.5	20	12.7	57	11.7	41	12.2	6	13.7
B	13	0.1	20	0.32	57	0.08	40	0.04	6	0.045
NO <sub>3</sub> (as N)	13	0.02	20	0.02	57	0.02	39	0.02	6	0.02
NH <sub>4</sub> (as N)	13	0.22	20	0.585	57	0.11	39	0.05	6	0.03
PO <sub>4</sub> (as P)	13	0.04	20	0.06	57	0.01	39	0.03	6	0.01
DOC	13	0.8	19	4.9	57	1.7	39	0.8	6	0.55
HCO <sub>3</sub> <sup>b</sup>	13	294.7	20	356.7	57	319.3	41	275.3	6	243.0

Sed. under clay: Sediments under clay, N: Number of samples

<sup>a</sup> EC in µS/cm

<sup>b</sup> Geochemical calculations with PHREEQC 2.6 (Parkhurst and Appelo, 1999).



## **Chapitre 4**

# **GEOCHEMICAL PROCESSES IN THE BASSES-LAURENTIDES SEDIMENTARY ROCK AQUIFER SYSTEM, ST. LAWRENCE LOWLANDS, QUÉBEC, CANADA**

Vincent Cloutier<sup>1</sup>, René Lefebvre<sup>1</sup>, Martine M. Savard<sup>2</sup>, René Therrien<sup>3</sup>

<sup>1</sup>Institut national de la recherche scientifique, INRS-Eau, Terre & Environnement, C.P. 7500, Sainte-Foy (Québec), G1V 4C7, Canada

<sup>2</sup>Geological Survey of Canada, Natural Resources Canada, 880, chemin Sainte-Foy, Suite 840, Québec (Québec), G1S 2L2, Canada

<sup>3</sup>Département de géologie et de génie géologique, Université Laval, Sainte-Foy (Québec), G1K 7P4, Canada

## RÉSUMÉ

L'hydrogéochimie des eaux souterraines du système aquifère de roches sédimentaires paléozoïques des Basses-Laurentides a été étudiée pour déterminer les processus principaux contrôlant la chimie des eaux souterraines et son évolution dans l'espace et le temps. Les constituants inorganiques majeurs et mineurs, ainsi que des paramètres isotopiques, ont été analysés pour 146 échantillons d'eau souterraine prélevés sur l'ensemble de la région d'étude de 1500 km<sup>2</sup>, caractérisant toutes les unités géologiques et les contextes hydrogéologiques jusqu'à une profondeur de 140 m. La dissolution de minéraux carbonatés domine dans les zones de recharge produisant une eau souterraine de type Ca-Mg-HCO<sub>3</sub>. Dans le système aquifère en conditions confinées, l'échange ionique Ca<sup>2+</sup>-Na<sup>+</sup> est responsable pour l'évolution de l'eau au type Na-HCO<sub>3</sub>, alors que le mélange avec l'eau de la Mer de Champlain et la diffusion d'ions des argiles marines sont responsables pour la présence d'eau de type Na-Cl. L'invasion marine qui a résulté en la Mer de Champlain est la cause de la salinisation du système aquifère caractérisé. Les traceurs conservateurs Cl<sup>-</sup> et Br<sup>-</sup> ont permis de déterminer que l'eau originale de la Mer de Champlain, dans la région d'étude, était un mélange d'environ 34% d'eau de mer et de 66% d'eau douce. La géochimie actuelle de l'eau souterraine a permis de déterminer que des portions du système aquifère sont à différentes étapes du processus de désalinisation, de l'eau marine ancienne étant encore présente dans les parties stagnantes, alors que dans les secteurs à plus forte circulation, celle-ci a été complètement remplacée par une eau souterraine moderne. Les processus géochimiques sont intégrés avec les contextes géologiques et hydrogéologiques afin de produire des modèles d'évolution géochimique spécifique et régional pour l'eau souterraine du système aquifère de roches sédimentaires des Basses-Laurentides.

**ABSTRACT**

Groundwater hydrogeochemistry of the Paleozoic Basses-Laurentides sedimentary rock aquifer system in Québec was studied to determine the main processes controlling the spatial and temporal evolution of groundwater geochemistry. Major and minor inorganic constituents, as well as isotopic indicators, were analyzed for 146 groundwater samples collected over a 1500 km<sup>2</sup> study area, from all geological and hydrogeological units to a maximum depth of 140 m. Dissolution of carbonates dominates in the preferential recharge areas resulting in Ca-Mg-HCO<sub>3</sub> groundwater. In the aquifer system under confined conditions, Ca<sup>2+</sup>-Na<sup>+</sup> ion exchange is the cause of groundwater evolution to Na-HCO<sub>3</sub> type. Groundwater mixing with Pleistocene Champlain Sea water and solutes diffusion from the marine clay aquitard are the causes of the occurrence of Na-Cl groundwater under confined conditions as well. The marine invasion that resulted in the Champlain Sea is the cause of the salinization of the aquifer system. Using conservative tracers Cl<sup>-</sup> and Br<sup>-</sup>, the original Champlain Sea water is shown to have been, in the study area, a mixture of about 34% seawater and 66% freshwater. The current geochemistry of the groundwater indicates that the aquifer system is at different stages of desalinization, ranging from the original Champlain Sea water still present in hydraulically stagnant areas of the aquifer to fully flushed conditions in the more active parts of the aquifer system, especially in recharge zones. The geochemical processes are integrated within the hydrogeological and geological contexts to produce area-specific as well as regional geochemical evolution paths models for groundwater of the Basses-Laurentides sedimentary rock aquifer system.

#### 4.1 INTRODUCTION

The study area, shown in Figure 4.1, is located on the North shore of the St. Lawrence River, northwest of Montréal. It covers approximately 1500 km<sup>2</sup> in the Basses-Laurentides geographical region. The hydrogeology and hydrogeochemistry of the Basses-Laurentides sedimentary rock aquifer system has been studied extensively. Nastev et al. (2001; in prep a) investigated the hydraulic properties of the rock aquifer and developed a numerical groundwater flow model for the region, Hamel et al. (2001) assessed groundwater recharge for the sedimentary rock aquifer and Ross et al. (2003) used a 3D geological model of the overlying Quaternary units to assess the vulnerability of the rock aquifer system. Cloutier et al. (in prep c) characterized the regional groundwater hydrogeochemistry and established the relationship between groundwater types and geological as well as hydrogeological setting, with the specific objective of identifying the origins of groundwater in the Basses-Laurentides aquifer system (*Chapitre 3*).

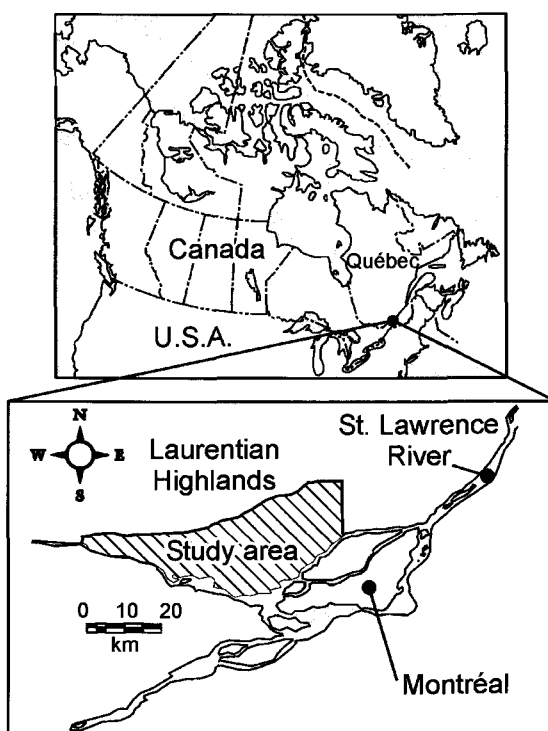


Figure 4.1. Location of the study area.

Following the work of Cloutier et al. (in prep c), this paper focuses on the identification of on-going geochemical processes as well as on the Quaternary geological events that have influenced groundwater geochemistry in this aquifer system. The evolution of groundwater is traced by locating the occurrence of the main geochemical processes with respect to their relative position in the groundwater system, from the recharge zones and along groundwater flow paths. The understanding of geochemical processes controlling current groundwater geochemistry and its evolution is required for the sound management and future development of groundwater resources in the region.

#### 4.2 CONTEXT, GEOLOGY AND HYDROGEOLOGY

The Basses-Laurentides belong to the St. Lawrence Lowlands, a physiographic region having a generally flat topography, with the exception of the Montréal Hills related to Cretaceous alkaline intrusions. The geological map of Figure 4.2 shows the two intrusions located in the Basses-Laurentides, the Oka and St. André Hills. The Laurentian Highlands, part of the Grenville Province of the Canadian Shield, border the study area to the North. The study area is bounded to the southwest, south, and southeast by the Outaouais River, the Deux Montagnes Lake, and the Mille Îles River, respectively. The watershed of the Mascouche River forms the eastern limit of the study area (Fig. 4.2).

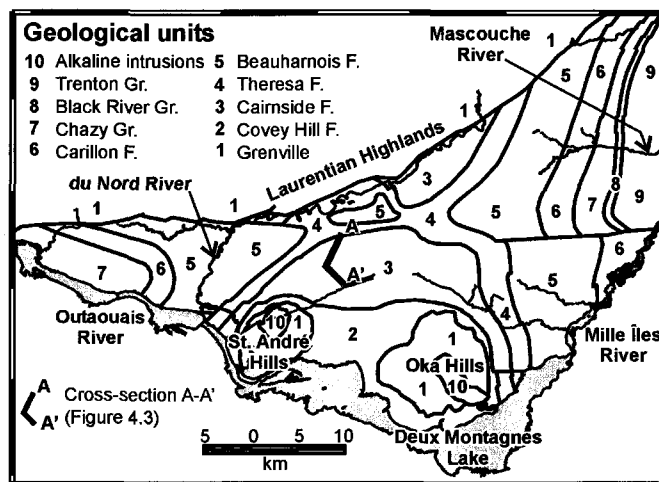


Figure 4.2. Geology of the Basses-Laurentides sedimentary rock aquifer system (modified from Rocher et al., in press).

The Basses-Laurentides aquifer system is part of the geological Province of the St. Lawrence Platform and consists of nearly horizontal Cambrian-Ordovician sedimentary formations lying in unconformity on the crystalline basement of the Precambrian Grenville Province (Fig. 4.2). In the study area, the sedimentary formations rarely outcrop, as Quaternary sediments cover them. Table 4.1 summarizes information on the lithology, mineralogy and fracture filling of the sedimentary formations. The Cambrian Potsdam Group, at the base of the sequence, is divided into two formations: the Covey Hill, a reddish feldspathic sandstone, locally conglomeratic and poorly cemented, and the Cairnside, a well-cemented, pure, quartz arenite sandstone (Globensky, 1987). Salad Hersi et al. (2003) subdivided the Ordovician Beekmantown Group into three formations: the dolomitic sandstone and sandy dolostone of the Theresa Formation, the sandy to pure, massive, dolostone of the Beauharnois Formation, and the pure dolostone with limestone near its summit of the Carillon Formation. The dissolution porosity of the dolostone units of the Beekmantown was cemented mostly by quartz and calcite (Chi et al., 2000). The Beekmantown Group is overlain by sandstone of the Lower Chazy, and limestone and shale of the Upper Chazy Group, dolostone, shale and limestone of the Black River Group and finally by limestone and shale of the Trenton Group (Globensky, 1987; Salad Hersi and Lavoie, 2001). Organic matter is found in the carbonates of the Cambrian-Ordovician sequence as zooclasts and solid bitumen (Héroux and Bertrand, 1991). Around Montréal, this Cambrian-Ordovician sedimentary sequence is at least 1200 m thick (Clark, 1972).

Precambrian rocks, such as quartzite, crystallized limestone, gneiss, and anorthosite, outcrop north of the study area in the Grenville Province, and also form a window through the Paleozoic sequence with the Cretaceous intrusions of Oka and St. André Hills. These alkaline intrusions are made of carbonatites, okaïte, lamprophyre, as well as metasomatic alteration of encasing rocks (Gold, 1972). Ultramafic sills, associated with the emplacement of the intrusions, are present in the Potsdam Group (Lewis, 1971).

Table 4.1. Lithology, mineralogy and fracture filling of the Cambrian-Ordovician sedimentary rocks

Geological units	Lithology, mineralogy, and fracture filling	Ref. <sup>a</sup>
Covey Hill F.	Feldspathic sandstone; 10-30% of fresh and weathered K-feldspar (microcline, orthoclase); traces of micas >0.03mm common (biotite, muscovite, chloritic matter, illite); <1% heavy mineral (zircon, apatite, tourmaline, sphene-rutile, leucoxene, pyrite, hematite); carbonates in fracture filling 80-99% of quartz ; 3-10% of plagioclase and microcline; 1-3% of zircon, magnetite, hornblende, biotite, apatite, and tourmaline	1 2
Cairnside F.	Essentially pure quartz sandstone (>95% SiO <sub>2</sub> ); overgrowth-cementation of quartz; <1-2% of alkali feldspar and microcline; traces of micas >0.03mm rare; trace of heavy minerals (zircon, apatite, tourmaline, sphene-rutile, leucoxene, pyrite, hematite); carbonates in fracture filling 91-99% of quartz; 1-3% of plagioclase and microcline; traces of magnetite, zircon, biotite, hornblende, sericite, epidote, and apatite; very few clayey matrices; trace fossils	1 2
Theresa F.	Observed dolomite-quartz proportions highly variable (35%-59%, 70%-27%, 50%-50%, 98%-2%, 85%-10%); 1-2% of microcline and plagioclase; traces-5% of magnetite, zircon, pyrite, and hornblende; fossiliferous	2
Beauharnois F.	Mainly dolomite crystals; few quartz grains and clay minerals; magnetite and pyrite; cavities filled mainly by calcite, and a few by dolomite, gypsum and halite; fossiliferous	2
Carillon F.	Pure dolostone with limestone near its summit; calcite and dolomite nodules	3
Chazy G. Lower	61% of quartz; 35% of carbonate; 1% of microcline; 3% of hornblende, biotite and zircon	2
Upper	Limestone and shale; highly fossiliferous	2
Black River G.	Dolostone with small quantities of sandy, clayey, and calcareous materials; disseminated pyrite; limestone with thin shale beds; fossiliferous	2
Trenton G.	Clayey limestone; highly fossiliferous; shale beds	2

<sup>a</sup> References: 1: Lewis (1971), 2: Globensky (1987), 3: Salad Hersi and Lavoie (2001).

The main structural features in the region are normal fault systems to the North along the contact with the Grenville Province, faults associated with the Cretaceous intrusions, and northeast-southwest anticlines in the center of the area, exposing the Ordovician units on both sides of the Cambrian sandstone (Fig. 4.2).

The last Quaternary glaciation covered the rock units with Upper Wisconsinan sediments, such as glacial till and glacio-fluvial sand and gravel (Bolduc and Ross, 2001). During deglaciation, the Laurentide Ice Sheet retreated from the St. Lawrence Valley. Combined with the depression of the continent due to the glaciation, the retreat of the Laurentide Ice Sheet lead to marine invasion from the St. Lawrence Gulf, which in turn created the Champlain Sea. The main basin of the Champlain Sea was established around 12 000 BP (Parent and Occhietti, 1988) and submerged the study area for about 2000 years (Lévesque, 1982). The Champlain Sea water was a mixture of continental waters, including meltwater from the Laurentide Ice Sheet and local precipitation, and salt water from the St. Lawrence Gulf (Hillaire-Marcel, 1988). The Champlain Sea episode led to the deposition of marine sediments, mainly clayey-silts to silty-clays that can reach a thickness of more than 80 m (Bolduc and Ross, 2001). The Champlain Sea clay is overlying till or glacio-fluvial sand and gravel units of variable thickness. The till is also found at ground surface, above the rock sequence, in elevated areas. The till is highly variable in composition and texture depending on the underlying rock units (Ross and Bolduc, 2001): Its composition relates mainly to glacial erosion of Paleozoic sedimentary formations, such as sandstone, dolostone, and limestone, and to a lesser extend to erosion of Precambrian rocks.

A cross-section of the conceptual groundwater flow model, showing the transition from unconfined to confined conditions, is illustrated in Figure 4.3. Also shown are the main hydrostratigraphic units adapted from Savard et al. (in press). The unconfined conditions, characterizing areas of preferential groundwater recharge, are generally areas of elevated topography, sometimes with rock outcrops or with thin to thick permeable surface sediments, generally till. Thus, precipitation recharges the aquifer mainly by infiltration through the till unit that has a  $K_m$  (geometric mean hydraulic conductivity) of  $3 \times 10^{-7}$  m/s (Hamel et al., 2001). Away from the recharge zone, the clay aquitard unit, consisting of thick low permeability Champlain Sea clays, confines the rock aquifer such as in buried valleys (Fig. 4.3).

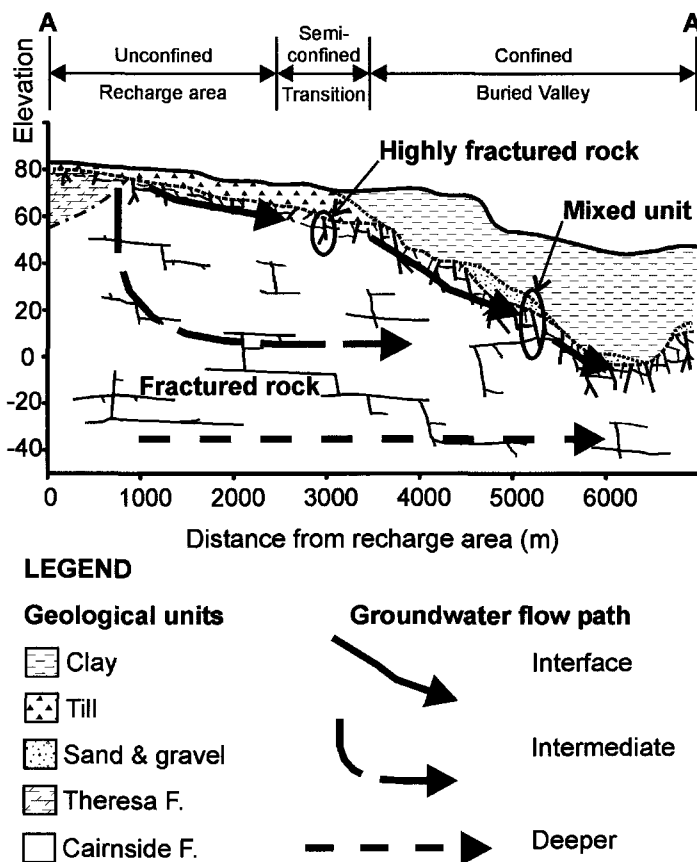


Figure 4.3. Cross-section A-A' illustrating the groundwater flow conceptual model and the main hydrostratigraphic units (elevation in m above mean sea level; see Fig. 4.2 and 4.4 for location of cross-section A-A') (based on Cloutier et al., in prep c).

Based on its hydrogeological and geological properties, the aquifer system can be divided into two distinct units: the highly fractured rock and the fractured rock. The highly fractured rock consists of the first few meters of the sedimentary units that are more weathered, with fractures more connected and more effective, than the underlying rock. Simard (1977) recognized this unit in an early hydrogeological study of the same aquifer. A mixed unit, consisting of highly fractured rock in hydraulic connection with sand and gravel, is also observed in the buried valleys and has a  $K_m$  of  $7.8 \times 10^{-4}$  m/s (Nastev et al., 2001). The lower unit of the aquifer system is the fractured rock. The sedimentary rock is well cemented by quartz or calcite and its primary porosity is very low. Thus, groundwater flows mainly through secondary porosity, such as fractures, bedding planes, alteration zones, or dissolution cavities. Hydraulic tests on the fractured rock unit provide a value of  $K_m$  of  $2.6 \times 10^{-5}$  m/s (Nastev et al., in prep b). The interface groundwater flow

through the highly fractured rock and mixed unit is faster than the intermediate and deeper groundwater flow in the fractured rock, due to their higher hydraulic conductivity. Evidence of preferential interface flow in the highly fractured rock has been obtained from isotopic data profiles of  $^3\text{H}$ ,  $^{14}\text{C}$  of dissolved inorganic carbon (DIC), and  $^{87}\text{Sr}/^{86}\text{Sr}$  where discrete groundwater samples were collected (Cloutier et al., in prep c). The general groundwater flow direction in the regional rock aquifer is from North to South (Paradis, in press b). The potentiometric surface follows the bedrock or surface topography and is higher in the preferential groundwater recharge areas.

#### **4.3 METHODS OF INVESTIGATION**

The approach used to study the Basses-Laurentides sedimentary rock aquifer system was to determine the hydrogeochemistry of groundwater for all hydrogeologic units, starting from the groundwater recharge areas along the regional flow direction. The study also characterized the hydrogeochemistry of all sources that could influence the composition of groundwater, such as rain and snow in recharge zones, and clay pore water in the buried valleys. The regional characterization of groundwater hydrogeochemistry, performed in 1999 and 2000, consisted of groundwater sampling of private, municipal and observation wells. *In situ* field measurements were made on water samples for temperature (T), pH, electrical conductivity (EC), dissolved oxygen (DO), and redox potential (Eh). Groundwater samples were analyzed for major, minor and trace inorganic constituents for a total of 36 parameters, stable isotopes  $\delta^2\text{H}$ ,  $\delta^{18}\text{O}$  and  $\delta^{13}\text{C}_{\text{DIC}}$ , and some samples were analyzed for  $^{87}\text{Sr}/^{86}\text{Sr}$ ,  $^3\text{H}$  and  $^{14}\text{C}$  of DIC.

Regional groundwater samples were collected at 153 sites, to a maximum depth of about 140 m. The sites sampled are equally distributed over the whole region and cover the following permeable hydrostratigraphic units: the surface sediments such as till, the sediments under clay deposits, the mixed unit consisting of highly fractured rock and sediments under clay deposits, and the fractured rock units. For the 153 groundwater samples, 134 samples have an electro-neutrality below 5%, 12 between 5 and 8%, and 7 above 10%. Samples with an electro-neutrality above 10% were rejected as their analyses

were generally missing major ions. The remaining 146 groundwater samples with electro-neutrality below 8% are retained for the interpretation of the main geochemical processes and groundwater evolution.

Figure 4.4 shows the distribution map of the 146 groundwater samples. The geochemical dataset for the 146 samples, including *in situ* field measurements, dissolved inorganic constituents, isotopic data, geochemical modeling results, physical and hydrogeological characteristics of the sampling sites, are available as an electronic file from Cloutier et al. (in prep c). The complete hydrogeochemical characterization program, including the sampling and analytical protocols, are described in *Chapitre 1* and Cloutier et al. (in prep c; *Chapitre 3*).

#### 4.4 REGIONAL HYDROGEOCHEMICAL CONTEXT

Cloutier et al. (in prep c) shows that the Basses-Laurentides sedimentary rock aquifer system has a highly variable groundwater geochemistry. The following description of the regional hydrogeochemical context uses the groundwater classification approach of dominant and mixed groundwater types presented by Cloutier et al. (in prep c). This approach, based on major ions concentrations, classifies the samples of the Basses-Laurentides into six dominant and four mixed groundwater types. As shown in Table 4.2, Cloutier et al. (in prep c) classified these ten groundwater types into four main groundwater groups, G1 to G4. Unconfined to semi-confined areas are characterized by groundwater of G1 (Ca-Mg-HCO<sub>3</sub>) and G4 (Ca-SO<sub>4</sub>, Na-SO<sub>4</sub>), and have modern tritiated groundwater. Submodern groundwater from G2 and G3 have dominant water types Na-HCO<sub>3</sub> and Na-Cl respectively and characterize the aquifer in confined conditions.

Table 4.2. Groundwater groups and types determined by Cloutier et al. (in prep c)

Groundwater group (N <sup>a</sup> )	Dominant water type (N <sup>a</sup> )	Mixed water type (N <sup>a</sup> )	Hydrogeological conditions	Groundwater origin <sup>b</sup>
Group 1 G1 (68)	Ca-HCO <sub>3</sub> (59) Mg-HCO <sub>3</sub> (4)	Alkaline earth-HCO <sub>3</sub> (5)	Unconfined Semi-confined	Modern meteoric water
Group 2 G2 (47)	Na-HCO <sub>3</sub> (35)	Mixed cations-HCO <sub>3</sub> (12)	Confined	Evolved G1 (submodern)
Group 3 G3 (28)	Na-Cl (25)	Mixed cations-Cl (2) Na-Mixed anions (1)	Confined	Mixing of G2 with Pleistocene Champlain Sea water (submodern) <sup>c</sup>
Group 4 G4 (3)	Ca-SO <sub>4</sub> (2) Na-SO <sub>4</sub> (1)		Unconfined Semi-confined	Modern meteoric water

<sup>a</sup> N: Number of samples.<sup>b</sup> The division in modern and submodern waters, i.e. recharged prior to 1952, is a qualitative interpretation of the <sup>3</sup>H data (Clark and Fritz, 1997).<sup>c</sup> Except the samples located in the recharge zone, principally at St. Janvier along the main roads 15 and 117, contaminated by de-icing road salts (see Fig. 4.4 for road locations).

Figure 4.4 shows the distribution map of the groundwater groups for the 146 samples, and their relationships with areas of unconfined, semi-confined and confined conditions. Main recharge for the Basses-Laurentides sedimentary rock aquifer system is along the southwest-northeast axis from Lachute to St. Janvier (Fig. 4.4). The other recharge zones are the Oka and St. André Hills, the region from the airport to St. Eustache and from Grenville to St. Philippe, and the southwest-northeast St. Vincent Crest. Elsewhere, thick low permeability Champlain Sea clays confine the aquifer system. Confining conditions prevail in three southwest-northeast trending buried valleys: 1) the du Nord River Valley, which borders the Laurentian Highlands, 2) the St. Hermas Valley, North of St. André Hills and the St. Vincent Crest, and 3) the St. Benoît Valley, between the St. Vincent Crest and Oka Hills, and where the clay thickness can reach more than 90 m (Paradis, in press a). Bedrock depressions filled with marine clay are also found along the north-south segment of du Nord River, and at St. Joseph, East of Oka Hills. The clay reaches a thickness of more than 30 m in the eastern part of the region, around Ste. Anne-des-Plaines.

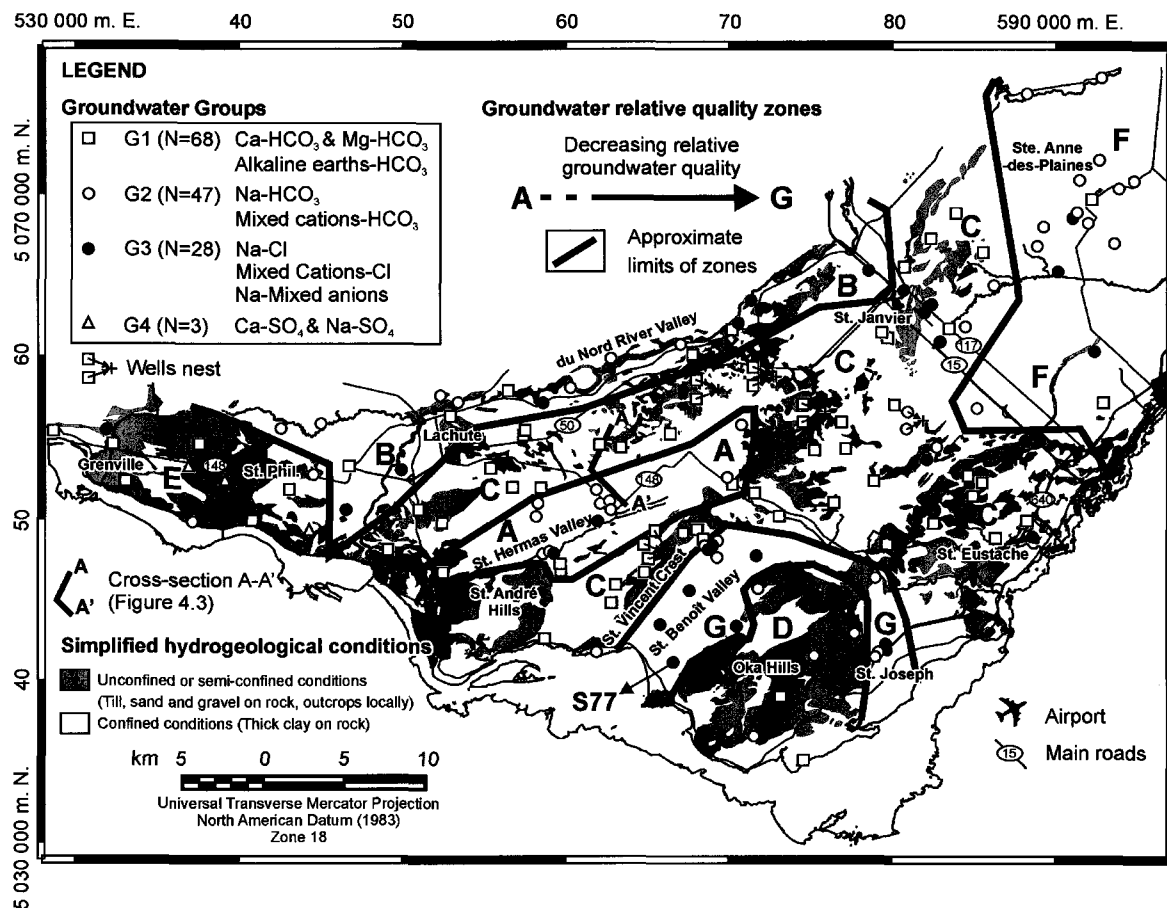


Figure 4.4. Regional distribution map of groundwater groups and their relation to the hydrogeological conditions (N: Number of samples; St. Phil. : St. Philippe) (hydrogeological conditions map modified from Hamel et al., 2001; groundwater relative quality zones from Cloutier and Bourque, in press).

To help visualize the geographical distribution of the groundwater groups, the groundwater relative quality zones defined by Cloutier et al. (in press) are presented on Figure 4.4. These water quality zones were defined by combining the information from a hierarchical cluster analysis (Cloutier et al., in prep b), the hydrogeological conditions map (Hamel et al., 2001), and the surficial formations thickness map (Paradis, in press a), and by comparing selected geochemical parameters to guidelines for Canadian drinking water quality of Health Canada (2003) (Cloutier et al., in press). Figure 4.4 shows that samples located in, or near, the unconfined or semi-confined areas are characterized by groundwater belonging to Group 1 (G1) and Group 4 (G4), particularly by the dominant groundwater types Ca-HCO<sub>3</sub> (water quality zones C and E). Group 2 (G2) and Group 3 (G3) characterize the aquifer in confined conditions, dominated by the groundwater types

Na-HCO<sub>3</sub> (water quality zones A, B and F) and Na-Cl (water quality zone G), respectively. Groundwater from G3 (Na-Cl) is also found locally in water quality zones A, B and F (Fig. 4.4). Qualitative interpretation of <sup>3</sup>H data shows that preferential recharge areas, characteristic of G1 (Ca-Mg-HCO<sub>3</sub>) and G4 (Ca-SO<sub>4</sub>, Na-SO<sub>4</sub>), have modern, tritiated groundwaters, and that the confined aquifer, characteristic of G2 (Na-HCO<sub>3</sub>) and G3 (Na-Cl), have submodern groundwaters. Groundwater G2 results from the evolution of G1, and groundwater G3 from the mixing of G2 with Pleistocene Champlain Sea water (Cloutier et al, in prep c; Table 4.2). Although they are located in, or close to, unconfined areas, some samples collected along the main highways 15 and 117, particularly around St. Janvier, have G3 groundwater (Fig. 4.4). It is assumed that groundwater for these samples is contaminated by de-icing road salts, which gives its Na-Cl characteristic (Cloutier et al., in prep c).

The distribution map of groundwater groups shows that the hydrogeological conditions exert an important control on hydrogeochemistry. Figure 4.5 shows the position of the groundwater samples, labeled according to their groundwater group, on a Piper diagram (Piper, 1944). Groundwater samples are distributed in the various zones of the diamond-shaped field, mainly the Ca-Mg-HCO<sub>3</sub>, Na-HCO<sub>3</sub>, and Na-Cl zones. Seven groundwater samples from surface sediments, mainly till, as well as two spring samples that are believed to flow in surface sediments, have a Ca-HCO<sub>3</sub> water type, and thus, belong to groundwater G1. These nine samples are labeled as G1<sub>Till</sub>, and represent a geochemical end-member for the aquifer system (Cloutier et al., in prep c) (Fig. 4.5). G1<sub>Till</sub> characterizes the infiltrated water in the quaternary sediments, and thus represents the major ions geochemistry of the recharge water to the Basses-Laurentides aquifer system. Cloutier et al. (in prep c) showed that higher total dissolved solids (TDS) values characterize samples of the Na-Cl groundwater G3. Sample S77, located in the buried valley of St. Benoît (Fig. 4.4), has the highest TDS of the wells sampled in the course of this project (calculated TDS = 11 337 mg/L). It is assumed that this sample represents Champlain Sea water, and is a second geochemical end-member to the aquifer system (Cloutier et al., in prep c) (Fig. 4.5).

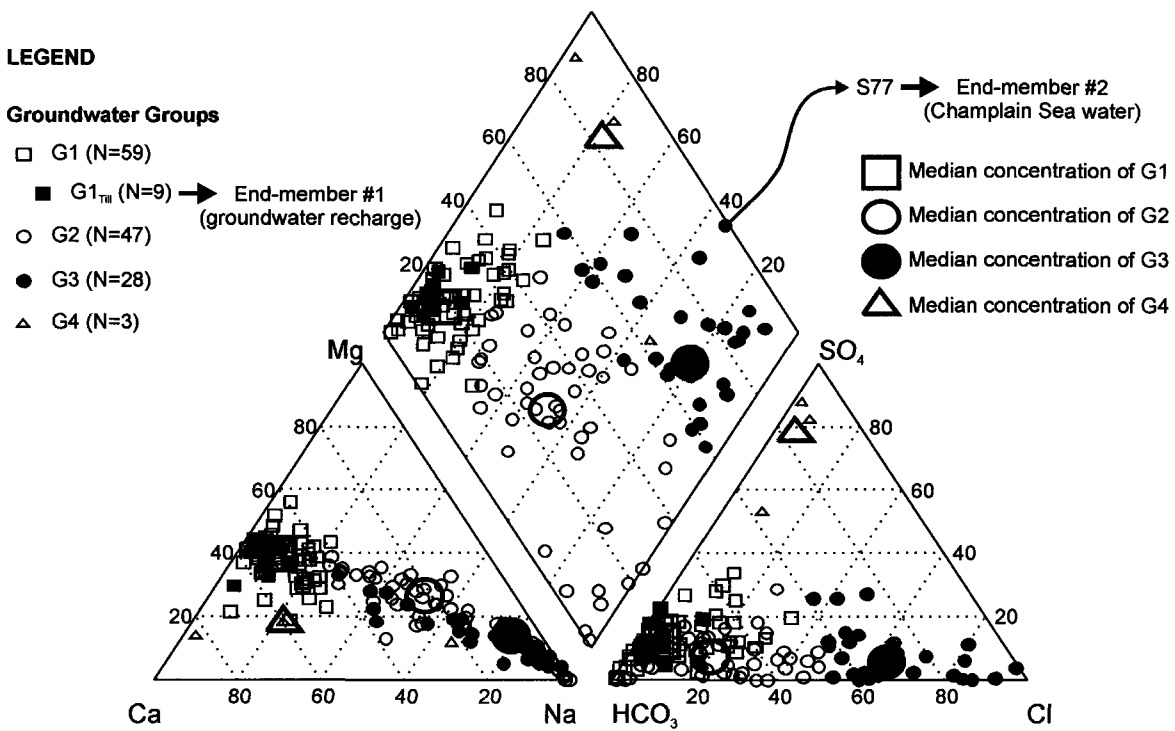


Figure 4.5. Piper diagram illustrating the major ions chemistry of each groundwater group of the Basses-Laurentides sedimentary rock aquifer system (N: Number of samples).

#### 4.5 INTERPRETATION OF MAIN GEOCHEMICAL PROCESSES AND GROUNDWATER EVOLUTION

This section includes the presentation and the interpretation of the main geochemical processes that are affecting the evolution of groundwater groups, starting from processes occurring in the recharge areas, such as carbonates dissolution, to processes occurring under confined conditions, such as ion exchange and groundwater mixing. Other geochemical processes, identified by Cloutier et al. (in prep c), will not be discussed in detail in this paper as they operate only locally. These include water-rock interaction causing elevated F<sup>-</sup> and Sr<sup>2+</sup> concentrations in the dolostone and limestone formations of the eastern area of Ste. Anne-des-Plaines and of the western area from Grenville to St. Philippe, elevated Fe<sup>2+</sup> and Mn<sup>2+</sup> concentrations locally in both confined and unconfined conditions, and sulfate reduction in the confined conditions of Ste. Anne-des-Plaines (Fig. 4.4).

#### 4.5.1 Dissolution of carbonates

The pH values, as well as  $\text{Ca}^{2+}$  and  $\text{Mg}^{2+}$  concentrations, are more or less similar for groundwater in surface sediments and for the unconfined sedimentary rock aquifer (Cloutier et al, in prep c). This similarity is an indication that in recharge areas, groundwater in the rock aquifer inherits its major ions mostly from geochemical processes occurring during infiltration through soil and permeable surface sediments. Therefore, sources of  $\text{Ca}^{2+}$  and  $\text{Mg}^{2+}$  must be present in surface sediments, which are mainly till in the area. The diagram of Figure 4.6a shows a linear relation ( $r^2=0.70$ ) of increasing concentration between  $\text{Ca}^{2+}$  and  $\text{HCO}_3^-$  for the samples of G1 (Ca-Mg-HCO<sub>3</sub>) and G1<sub>Till</sub> (Ca-HCO<sub>3</sub>), which could be explained by dissolution of calcite that can be written as  $\text{CaCO}_3 + \text{CO}_2 + \text{H}_2\text{O} \leftrightarrow \text{Ca}^{2+} + 2\text{HCO}_3^-$  (Appelo and Postma, 1993). The surface sediments and the spring samples, G1<sub>Till</sub>, were given a different symbol to evaluate their relative position compared to the other samples of G1. Groundwaters of G1<sub>Till</sub> plot in the same field as groundwaters from the rock aquifer belonging to G1, suggesting that similar processes affect them. Samples of G2 (Na-HCO<sub>3</sub>) and G3 (Na-Cl) show more spread. For  $\text{HCO}_3^-$  above 7 mmol/L,  $\text{Ca}^{2+}$  concentrations for both groups G2 and G3 decrease to values lower than 0.5 mmol/L (Fig. 4.6a). A clear trend of increasing Mg/Ca with increasing pH is observed, from precipitation to groundwaters of G1 and G4 in preferential recharge areas, to groundwaters of G2 and G3 in confined conditions (Fig. 4.6b). Again, groundwaters from the surface sediments and the springs, G1<sub>Till</sub>, plot in the same field as groundwaters from the rock aquifer belonging to G1. The majority of samples from G1 have a pH between 6.8 and 8, and a Mg/Ca ratio between 0.6 and 0.9. The values for the ratio Mg/Ca for G1 are close to the expected value of 0.8 for groundwater in equilibrium with calcite ( $\text{CaCO}_3$ ) and dolomite ( $\text{CaMg}(\text{CO}_3)_2$ ) (Appelo and Postma, 1993). Thus, the relationship between  $\text{Ca}^{2+}$  and  $\text{HCO}_3^-$  and that between Mg/Ca ratio and pH indicate dissolution of calcite during infiltration, as well as dissolution of dolomite that can be written as  $\text{CaMg}(\text{CO}_3)_2 \leftrightarrow \text{Ca}^{2+} + \text{Mg}^{2+} + 2\text{CO}_3^{2-}$  (Appelo and Postma, 1993). Occurrence of marine carbonate dissolution has been shown by Cloutier et al. (in prep c) from stable carbon isotopes on DIC in the till groundwater, and is consistent with the presence of calcite and dolomite in the till matrix as described

in previous works (Lévesque, 1982). Groundwaters of G2 and G3 dominate at elevated pH and at Mg/Ca above 1 (Fig. 4.6b), and other processes that contribute to their increase in pH, as well as Mg/Ca ratios, must affect these two groups.

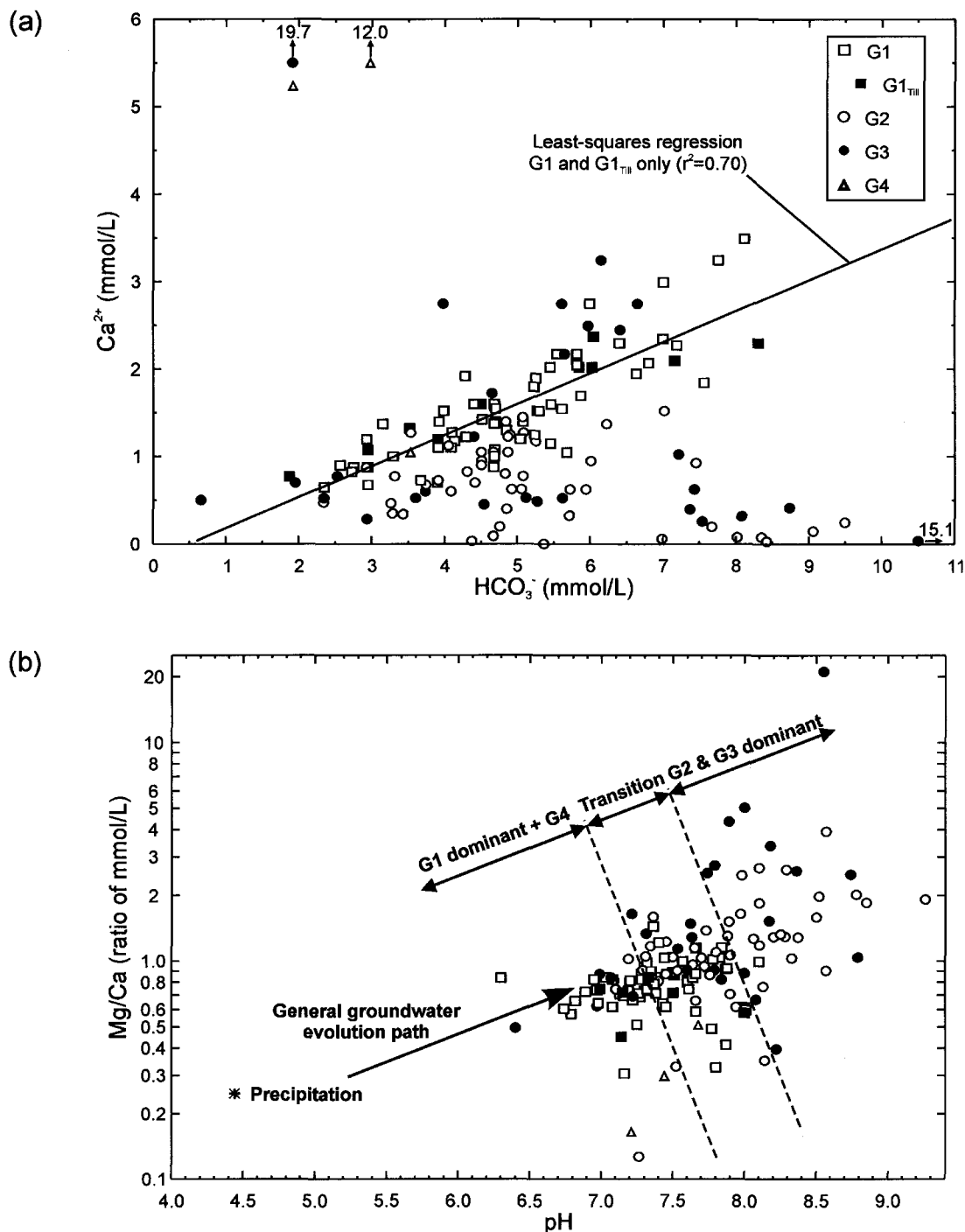


Figure 4.6. Diagrams of (a)  $\text{Ca}^{2+}$  (mmol/L) versus  $\text{HCO}_3^-$  (mmol/L) and (b) Mg/Ca versus pH for the groundwater groups (precipitation calculated by averaging monthly data of stations Hemmingford, St. Simon, St. Hippolyte, and Montébello from the Department of the Environment, Québec, 1994-1996).

Carbonates dissolution is caused partly by processes occurring in the surface soils. Respiration and decay of organic matter increase the CO<sub>2</sub> partial pressure (pCO<sub>2</sub>) in the soil gases relative to the atmosphere, which has a pCO<sub>2</sub> of 10<sup>-3.5</sup> atm (Drever, 1988). Appelo and Postma (1993) mention that pCO<sub>2</sub> values of 10<sup>-1.5</sup> to 10<sup>-2.5</sup> atm are commonly found in soils. This elevated pCO<sub>2</sub> for soil water has a major impact on the interaction with carbonate minerals present in surface sediments. Geochemical modeling was performed with PHREEQC 2.6 (Parkhurst and Appelo, 1999) to evaluate the likelihood of carbonate dissolution during infiltration through soil and surface sediments. The diagram shown in Figure 4.7a indicates that the majority of samples from G1 (Ca-Mg-HCO<sub>3</sub>), including the surface sediments and springs G1<sub>Till</sub>, and G4 (Ca-SO<sub>4</sub>, Na-SO<sub>4</sub>), have a pCO<sub>2</sub> of 10<sup>-1.5</sup> to 10<sup>-2.5</sup> atm, and a calcite saturation index undersaturated or near equilibrium, with an uncertainty of ±0.1 units (Langmuir, 1971). Samples from G2 (Na-HCO<sub>3</sub>) and G3 (Na-Cl), under confined conditions, are showing a trend of lower pCO<sub>2</sub>, with a calcite saturation index evolving from undersaturated to near equilibrium and supersaturated. The results from G1 and G4 indicate that samples in preferential groundwater recharge areas are dissolving calcite in an open system with respect to CO<sub>2</sub>. As calcite dissolution consumes H<sup>+</sup>, pH buffering must be observed in the infiltrated water. The pH of the precipitations is low, with a monthly average of 4.44 (Fig. 4.6b), but it is buffered to a median pH of 7.33 in surface sediments (Cloutier et al., in prep c). A linear relation exists between the dolomite and calcite saturation indexes (Fig. 4.7b). As for calcite, the majority of samples from G1, including G1<sub>Till</sub>, and G4, have a dolomite saturation index undersaturated or near equilibrium, with an uncertainty of ±0.5 units (Plummer et al., 1990). Samples from G2 and G3, under confined conditions, have a dolomite saturation index evolving from undersaturated to near equilibrium and supersaturated. Therefore, samples in preferential groundwater recharge areas have the potential to dissolve dolomite as well as calcite.

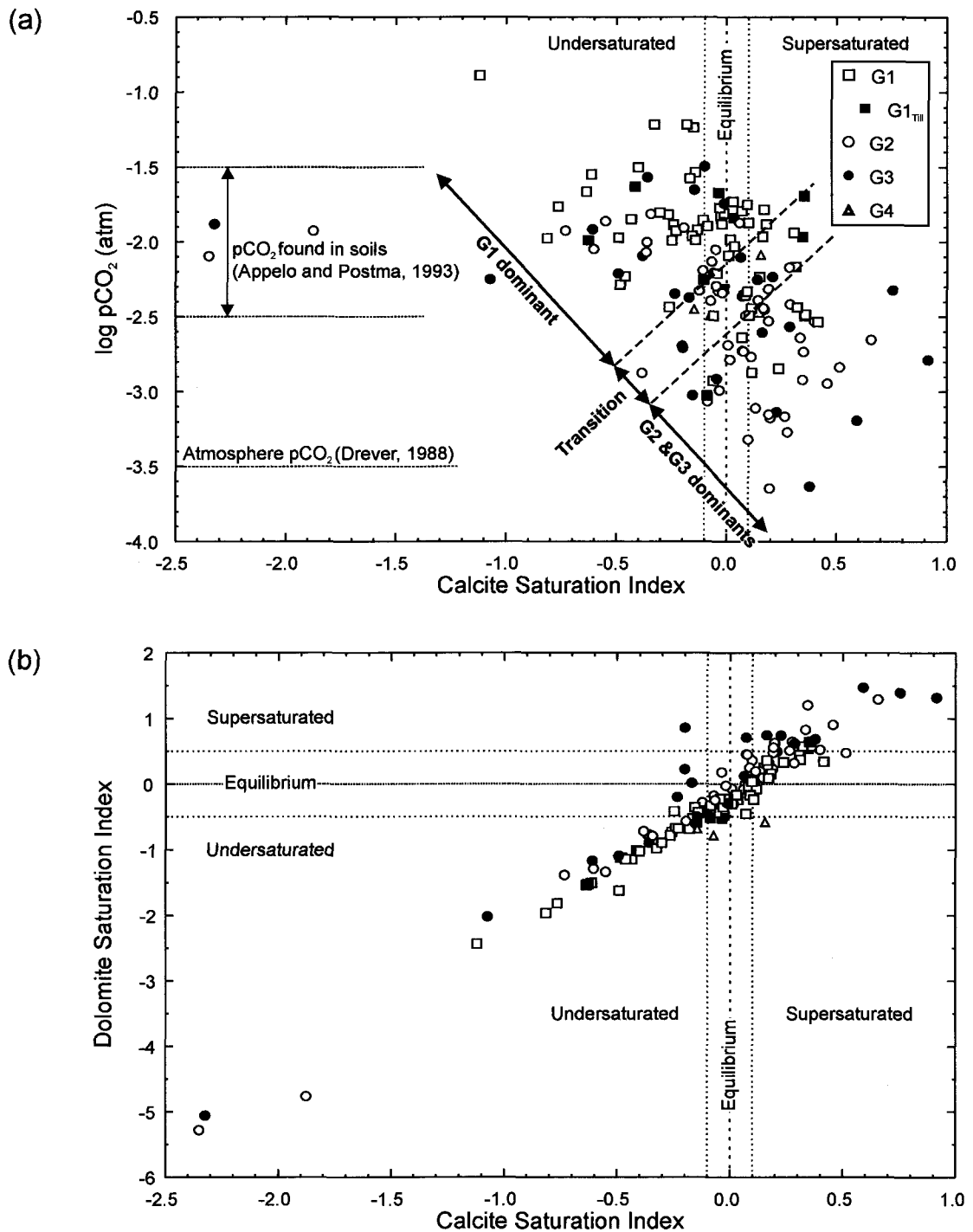


Figure 4.7. Diagrams of (a)  $\log p\text{CO}_2$  versus calcite saturation index, and (b) dolomite saturation index versus calcite saturation index for the groundwater groups.

The increase of  $\text{Ca}^{2+}$ ,  $\text{Mg}^{2+}$ , and  $\text{HCO}_3^-$  concentrations in surface sediments is the main characteristic of all groundwater samples from G1 (Ca-Mg-HCO<sub>3</sub>). The dissolution of carbonates, initiated in the surface sediments, is active in the sedimentary rock aquifer

system as well, and is mainly the result of water-rock interaction with the dolostone and limestone formations. Elevated  $\text{Ca}^{2+}$  and  $\text{Mg}^{2+}$  are found particularly in groundwater of the dolostone formations in the recharge area of St. Janvier, and from the airport to St. Eustache (Cloutier et al., in prep c). The dolostone unit has the highest median concentrations for both ions  $\text{Ca}^{2+}$  and  $\text{Mg}^{2+}$  (Cloutier et al., in prep c), indicating that some dissolution must be occurring along the flow system in the rock aquifer.  $\text{SO}_4^{2-}$  concentrations are also elevated in these dolostone units (Cloutier et al., in prep c), suggesting that gypsum ( $\text{CaSO}_4 \cdot 2\text{H}_2\text{O}$ ) could be dissolving as well. This is consistent with the availability of gypsum as filling mineral in the Beauharnois Formation (Globensky, 1987; Table 4.1), and with measurements showing that all samples are undersaturated with respect to gypsum (Cloutier et al., in prep c).

#### 4.5.2 Ion exchange

Henderson (1985) used the log ratio of the molalities of exchangeable divalent and monovalent cations,  $\log(\text{Ca}+\text{Mg})/\text{Na}^2$ , to demonstrate the progressive nature of ion exchange reactions in a sandstone aquifer in Montana. The progression from positive to negative  $\log(\text{Ca}+\text{Mg})/\text{Na}^2$  was used to identify recharge areas and groundwater flow direction in the aquifer (Henderson, 1985). Figure 4.8 illustrates box plots of  $\log(\text{Ca}+\text{Mg})/\text{Na}^2$  for the groundwater groups  $\text{G1}_{\text{Till}}$ , G1, G2 and G3 for the Basses-Laurentides sedimentary rock aquifer system. Similar to the results from Henderson (1985), the positive values are associated to the recharge areas characterized by  $\text{G1}_{\text{Till}}$  ( $\text{Ca}-\text{HCO}_3$ ) and G1 ( $\text{Ca}-\text{Mg}-\text{HCO}_3$ ), such as the unconfined to semi-confined region from Lachute to St. Janvier, from the airport to St. Eustache, from Grenville to St. Philippe, and the St. Vincent Crest (Fig. 4.4). Negative values are found in confined areas, where G2 ( $\text{Na}-\text{HCO}_3$ ) samples dominate, such as Ste. Anne-des-Plaines, St. Hermas and du Nord River valleys (Fig. 4.4). This distribution indicates that  $\text{Ca}^{2+}-\text{Na}^+$  ion exchange, where  $\text{Ca}^{2+}_{\text{water}}$  exchanges with  $\text{Na}^+_{\text{mineral}}$ , could be the main geochemical processes involved in the evolution of groundwater from  $\text{Ca}-\text{Mg}-\text{HCO}_3$  (G1) to  $\text{Na}-\text{HCO}_3$  (G2) water types (Fig. 4.8). The ion exchange reaction is written as  $\frac{1}{2}\text{Ca}^{2+} + \text{Na-X} \rightarrow \frac{1}{2}\text{Ca-X}_2 + \text{Na}^+$ , where X indicates the mineral exchanger (Appelo and Postma, 1993). Negative

values are also associated with samples of G3 (Na-Cl), as in the St. Benoît Valley, and in St. Janvier along the main roads (Fig. 4.4). Groundwaters from G3 have  $\text{Cl}^-$  as their major anion, unlike G2 that has  $\text{HCO}_3^-$ . The median value of the  $\log(\text{Ca}+\text{Mg})/\text{Na}^2$  for G3 groundwater is more negative than that for G2, and falls between the median value for G2 and that for seawater, which is about -3.5 (Fig. 4.8). Thus, other processes must also be invoked for the evolution of groundwater from Na-HCO<sub>3</sub> (G2) to Na-Cl (G3) water types.

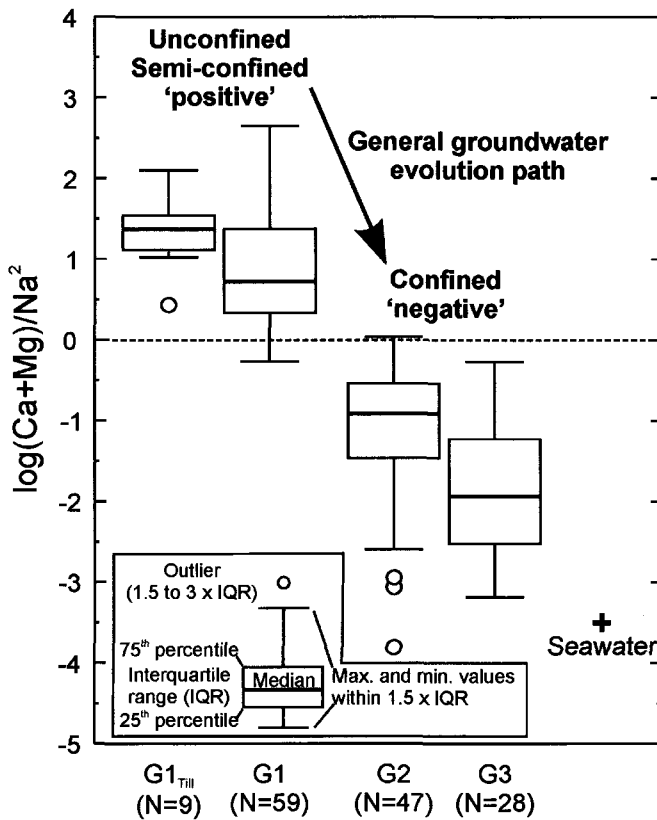


Figure 4.8. Box plots of  $\log(\text{Ca}+\text{Mg})/\text{Na}^2$  for the groundwater groups and seawater (N: Number of samples).

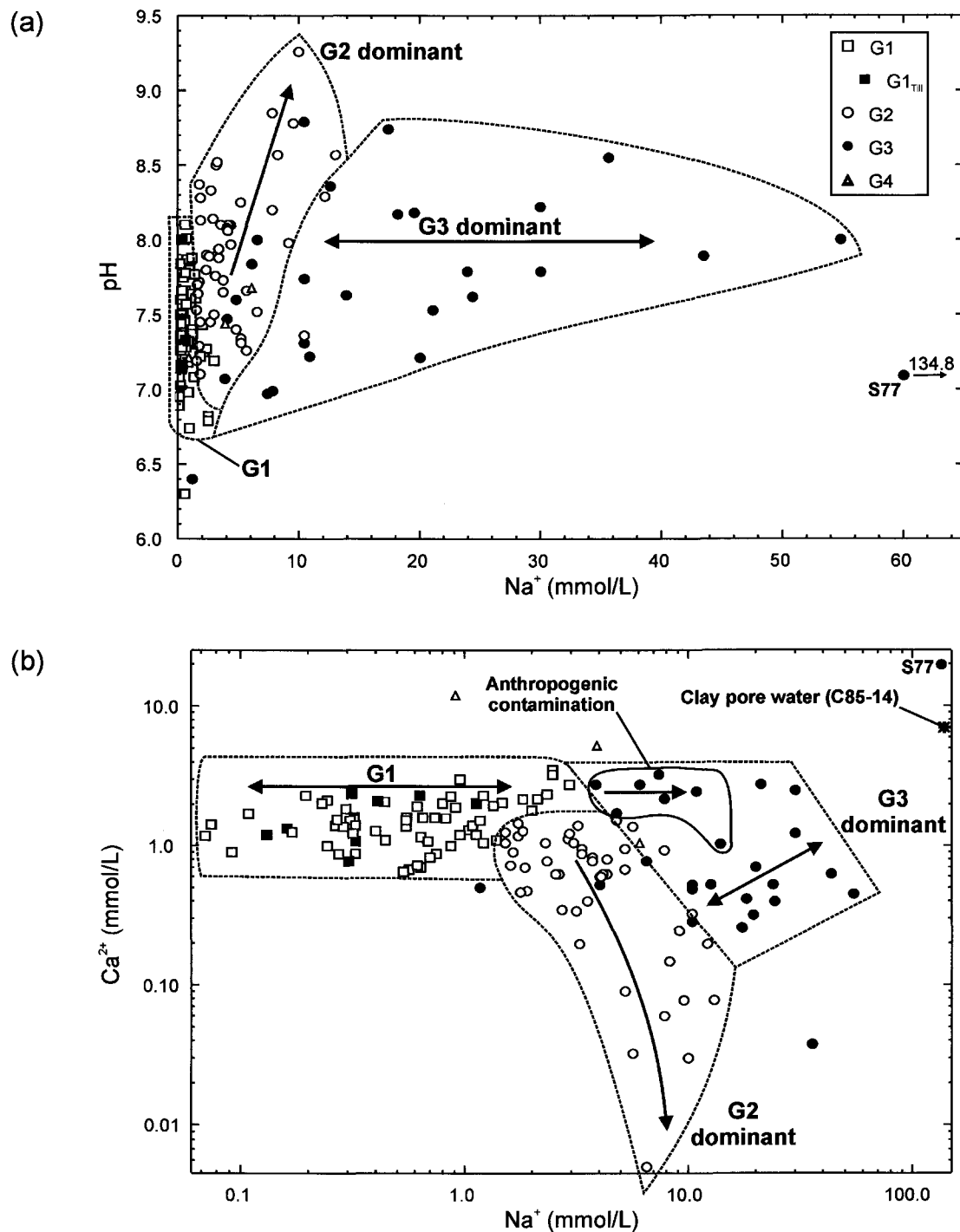
Conditions required in the aquifer system for ionic exchange to operate are a recharged groundwater with elevated  $\text{Ca}^{2+}$  concentrations, and the presence of minerals with both high cation exchange capacities (CEC) and  $\text{Na}^+$  on their exchange sites. The first condition was demonstrated in sub-section 4.5.1 on carbonate dissolution, which showed that recharged water dissolves carbonates in the till, and thus, increases its  $\text{Ca}^{2+}$  concentration. In Ste. Anne-des-Plaines, the limestone of the Chazy, Black River and Trenton groups, as well as the dolostone of the Beauharnois and Carillon formations

dominate the rock geology. The limestone has clay minerals, and shale beds, that could act as mineral exchangers (Globensky, 1987; Table 4.1). In addition, organic matter, identified in the carbonates by Héroux and Bertrand (1991), could also participate in the ion exchange reactions. Table 4.1 (Globensky, 1987) indicates that the dolostone have some clay minerals and iron oxides that could act as mineral exchangers, but it is unknown if they are abundant enough to account for the amount of  $\text{Ca}^{2+}$ - $\text{Na}^+$  exchange. This is also the case in St. Hermas Valley, where the pure quartz sandstone has some traces of micas, and iron oxides. When clay minerals and iron oxides are not present in sufficient quantity to account for ion exchange, other sources for the exchange must be found. A possible source in the sandstone of the Potsdam Group are the minerals of the ultramafic sills observed in the rock cores retrieved from a well in St-Hermas Valley, which are associated to the intrusions emplacement (Lewis, 1971). A second possible source is the ionic exchange with minerals in the till and in the clay aquitard unit above the highly fractured rock unit. This possibility could be the case in Ste. Anne-des-Plaines, where most of the wells have a relatively short opening in the highly fractured rock unit, just below the clay, as well as in St. Hermas Valley, where the majority of the wells are installed in the sediments under the clay unit, or in the mixed unit, in contact with the clay aquitard. Thus, as water flows in the confined aquifer,  $\text{Ca}^{2+}_{\text{water}}$  could exchange with  $\text{Na}^+_{\text{mineral}}$  of the confining aquitard, producing the  $\text{Na}-\text{HCO}_3$  water type of G2. As mentioned, the mineral exchangers must have  $\text{Na}^+$  adsorbed on their exchange sites for the exchange reaction to happen. This issue, related to the origin of salinity in the Basses-Laurentides sedimentary rock aquifer system, is discussed in sub-section 4.5.3 on groundwater mixing and salinity origin.

Figure 4.9a shows that groundwaters of G1 ( $\text{Ca}-\text{Mg}-\text{HCO}_3$ ) have low  $\text{Na}^+$  concentrations and pH values ranging from 6.3 to 8.1, characteristics of unconfined conditions. From the recharge areas, groundwater flows through the aquifer system in confined conditions, which is the case for the du Nord River, St. Hermas, and St. Benoît valleys, as well as for Ste. Anne-des-Plaines. Samples of G2 ( $\text{Na}-\text{HCO}_3$ ) and G3 ( $\text{Na}-\text{Cl}$ ), characteristic of these confined conditions, form separate fields of the diagram (Fig. 4.9a). Relative to G1, samples of G2 show increasing pH values with increasing  $\text{Na}^+$  concentrations, which is

consistent with ion exchange operating from G1 to G2 (Fig. 4.9 a). Groundwaters from G3 show a trend of increasing  $\text{Na}^+$  concentrations relative to G2 samples, indicating that a second  $\text{Na}^+$  source is involved in the evolution from G2 to G3 groundwaters. The increase in  $\text{Na}^+$  concentrations for groundwaters of G2 is coupled to a sharp decrease in  $\text{Ca}^{2+}$  concentrations, confirming the importance of  $\text{Ca}^{2+}$ - $\text{Na}^+$  ion exchange (Fig. 4.9b). As illustrated in Fig. 4.9a, samples from G3 are characterized by an increase in  $\text{Na}^+$  concentration compared to G2 (Fig. 4.9b). This  $\text{Na}^+$  concentration increase is towards the clay pore water sample C85-14, which is representative of the original Pleistocene Champlain Sea water for the Basses-Laurentides aquifer system (Cloutier et al., in prep c). The issue of Champlain Sea water as being the source of salinity for the evolution of samples from G2 to G3 is discussed in sub-section 4.5.3 on groundwater mixing and salinity origin. Seven samples of G3, located in recharge areas, are labeled as anthropogenic contamination (Fig. 4.9b). These are the samples identified in section 4.4 has being contaminated by de-icing road salts. Their position on the diagram indicates that their geochemistry results from the addition of  $\text{Na}^+$  to waters of G1.

The increase in  $\text{Na}^+$  concentration for groundwaters of G2 ( $\text{Na}-\text{HCO}_3$ ) is not really coupled to a  $\text{Cl}^-$  increase, which constitutes another argument in favor of  $\text{Ca}^{2+}$ - $\text{Na}^+$  ion exchange for the evolution of G2 (Fig. 4.9c). On the other hand, G3 ( $\text{Na}-\text{Cl}$ ) samples show a linear increase between  $\text{Na}^+$  and  $\text{Cl}^-$ . In addition, groundwaters from G3 plot near, or slightly above, the seawater dilution line. Groundwaters from G2 plot above the seawater dilution line, having a  $\text{Na}^+$  surplus relative to  $\text{Cl}^-$ . Figures 4.9a to 4.9c indicate that  $\text{Ca}^{2+}$ - $\text{Na}^+$  ion exchange is the main geochemical processes affecting groundwater belonging to G2. The distribution of G2 also indicates the possibility of mixing with groundwater of G3, increasing its  $\text{Cl}^-$  concentrations relative to  $\text{Na}^+$  (Fig. 4.9c). Groundwaters from G3, which are affected by mixing with G2, must originate from another process to explain their elevated  $\text{Na}^+$  as well as  $\text{Cl}^-$  concentrations. The trend of G3 groundwaters towards seawater suggests that groundwater mixing, with an end-member having a seawater component, is characteristic of G3 groundwaters evolution.



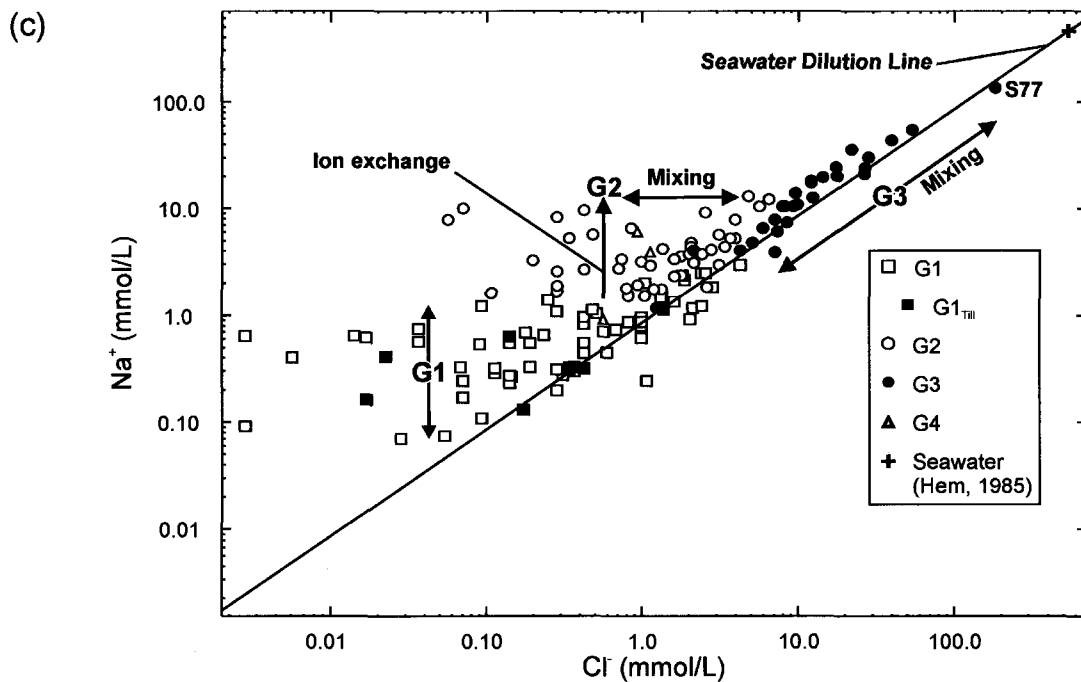


Figure 4.9. Diagrams of (a) pH versus  $\text{Na}^+$  (mmol/L), (b)  $\text{Ca}^{2+}$  (mmol/L) versus  $\text{Na}^+$  (mmol/L), and (c)  $\text{Na}^+$  (mmol/L) versus  $\text{Cl}^-$  (mmol/L) for the groundwater groups.

#### 4.5.3 Groundwater mixing and salinity origin

The occurrence of groundwater with elevated salinity in the Basses-Laurentides aquifer system was identified in previous studies (Simard, 1978; Soucy, 1998). For the municipalities of St. Benoît and Ste. Anne-des-Plaines, groundwater with elevated salinity is a problem for potable water provision. Thus, the knowledge of the distribution and origin of salinity is important for their planning and managing of the groundwater resource. Figure 4.10 shows that  $\text{Cl}^-$  concentrations increase linearly with calculated TDS, especially for samples of G3 (Na-Cl). Thus, the salinity increase is related mainly to an increase in  $\text{Cl}^-$ , as well as  $\text{Na}^+$ , recalling the linear relationship between  $\text{Na}^+$  and  $\text{Cl}^-$  for G3 groundwater (Fig. 4.9c). Two samples from G4, of Ca-SO<sub>4</sub> water type, have a TDS above 1000 mg/L due to elevated SO<sub>4</sub><sup>2-</sup> concentrations (Fig 4.10). Most of the samples of G3 can be categorized as brackish water defined by a TDS between 1000 and 10000 mg/L (Freeze and Cherry, 1979). These samples exceed therefore the Canadian drinking water quality guideline for  $\text{Cl}^-$  (aesthetic objective) of 250 mg/L (Health Canada, 2003). With a calculated TDS of 11337 mg/L, sample S77 from St. Benoît Valley is the only

sample in the saline water class. As for Figure 4.9c, there is a trend of G3 groundwaters towards seawater with sample S77, the most concentrated groundwater, located along this trend (Fig. 4.10).

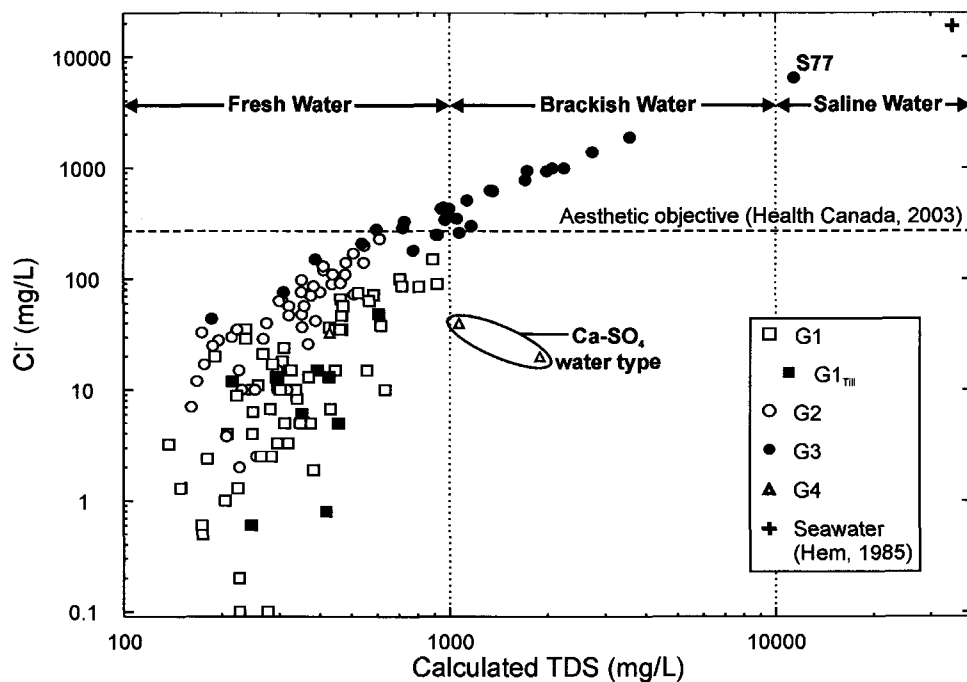


Figure 4.10. Diagram of  $\text{Cl}^-$  (mg/L) versus calculated TDS (mg/L) for the groundwater groups and seawater (fresh, brackish and saline water classification based on TDS from Freeze and Cherry, 1979).

Increasing salinity in groundwater may result from different processes, such as water-rock interaction along the flow path, dissolution of evaporite rocks, old or current seawater intrusion, mixing with formation water, solute diffusion from aquitard containing saline pore water, and anthropogenic contamination, such as de-icing road salts or agricultural input (Hem, 1985; Appelo and Postma, 1993; Richter and Kreitler, 1993). In the Basses-Laurentides sedimentary rock aquifer system, the increase in salinity is associated with an increase in  $\text{Na}^+$  and  $\text{Cl}^-$  (Fig. 4.9c and 4.10). In the geological context of the region, it is unlikely that water-rock interaction could produce the Na-Cl water type of G3. As there are no evaporite formations in the aquifer, and this is not a coastal aquifer, other sources must be examined to explain the origin of salinity. Contamination by de-icing road salts explains the salinity in the recharge areas, but not in the valleys where thick clay deposits protect the aquifer system. The geological background of the area gives a limited number

of possibilities for the presence of brackish to saline water in the upper portion of the sedimentary rock aquifer system.

Since the Cambrian-Ordovician sedimentary formations of the St. Lawrence Lowlands represent a complete cycle of marine transgression-regression (Globensky, 1987), it is expected that brine formation waters could still be present in those geological units. In fact, Globensky (1972) mentioned that salt water is found in the Trenton and Potsdam groups, generally in wells deeper than about 150 m, thus, below the studied portion of the aquifer system. The salt water is often associated with presence of oil and natural gas (Globensky, 1972). In more recent geological times, series of glaciations during the Quaternary may have affected the geochemistry of the groundwater, by flushing the upper portion of the aquifer system with glacial meltwater. The last major geological event to affect the study area is the marine invasion from the St. Lawrence Gulf during the last deglaciation. There is a linear relationship between  $\text{Cl}^-$  and  $\text{Na}^+$  for samples of G3 (Na-Cl), and these samples plot near the seawater dilution line (Fig. 4.9c). The relation between  $\text{Cl}^-$  and TDS is also suggesting a dilution of seawater to explain the salinity of samples of G3 (Fig. 4.10). As the Champlain Sea occupied the study area during late Pleistocene, a seawater component could be the source of salinity in the upper portion of the aquifer system. The Champlain Sea clays, deposited during the marine episode, could also contribute to the salinity of the aquifer system through solute diffusion of its saline pore water.

Cloutier et al. (in prep c) have shown that sample S77, the most saline of G3 (Na-Cl) groundwater samples found under confined condition in St. Benoît Valley (Fig. 4.4), has a geochemistry very similar to the pore water in marine clay (sample C85-14), with the exception of  $\text{Ca}^{2+}$ . The clay pore water was extracted by squeezing Champlain Sea clay samples from a clay core retrieved at a site in St. Hermas Valley, where the clay has a thickness of 46 m. Sample C85-14, from a depth of 14.1 m, has the highest  $\text{Cl}^-$  concentration in this profile (6900 mg/L). Similarities between the groundwater S77 and the clay pore water were observed for  $\text{Cl}^-$  and  $\text{Br}^-$ , two conservative ions that can be used as tracers to identify the origin of groundwater salinity (Richter and Kreitler, 1993;

Andreasen and Fleck, 1997; Vengosh et al., 2002), as well as in  $\delta^{18}\text{O}$  values ( $-10.9\text{\textperthousand}$  for the clay pore water C85-14 and  $-11.0\text{\textperthousand}$  for the groundwater S77).

Figure 4.11 shows the relationship between Cl/Br ratio and  $\text{Cl}^-$  for the groundwater groups, as well as for possible end-members, including the clay pore water sample C85-14, seawater, and brine samples. The brine samples have representative compositions of formation waters for the Cambrian and Trenton formations of southern Ontario presented by McNutt et al. (1987). Sample S77, the groundwater sample with the highest salinity (TDS expressed as salinity of 11.3 g/L), plots on the seawater Cl/Br line, suggesting that seawater is a component of this sample (Fig. 4.11). The other samples from G3 (Na-Cl), as well as some samples from G2 (Na-HCO<sub>3</sub>), plot on or near the seawater Cl/Br line. The clay pore water sample, C85-14, plots slightly above the seawater Cl/Br line, and has a similar  $\text{Cl}^-$  concentration as S77. The two brines compositions have a Cl/Br lower than seawater, showing enrichment in Br<sup>-</sup> relative to seawater. Two samples from the limestone in the eastern area of St. Anne-des-Plaines have a Cl/Br lower than seawater that could result from solute diffusion from the shale beds of the Chazy and Trenton groups (Globensky, 1987; Table 4.1). Radiogenic values of  $^{87}\text{Sr}/^{86}\text{Sr}$  between 0.711037 and 0.711231 in groundwater of St. Anne-des-Plaines are also suggesting an interaction with clay minerals of shale beds (Cloutier et al., in prep c). Figure 4.11 is also helpful in distinguishing the samples from G3 that are affected by anthropogenic contamination. The samples plot above the seawater Cl/Br line, indicating that the  $\text{Cl}^-$  increase is not coupled to a Br<sup>-</sup> increase. This group of groundwater includes the samples in the preferential recharge areas along main highways 15 and 117, as well as two samples in the recharge area between the airport and St. Eustache (Fig. 4.4). High Cl/Br ratio may be produced by dissolution of de-icing road salts or agricultural chemicals such as fertilizers (Davis et al., 2001). The trend in the samples from G1 characterizes groundwater in unconfined conditions affected by an increase in  $\text{Cl}^-$  concentrations, when Br<sup>-</sup> concentrations are still at low, background level (Fig. 4.11). Andreasen and Fleck (1997) used a similar trend to show the effect of  $\text{Cl}^-$  contamination from an anthropogenic source that does not contain Br<sup>-</sup>. In the Basses-Laurentides, the  $\text{Cl}^-$  concentrations for the G1 samples that are part of the trend are low, generally below 1 mmol/L. The sources of this

relatively slight contamination, when compared to samples from G3 affected by anthropogenic contamination, could be many and include de-icing road salts or fertilizers.

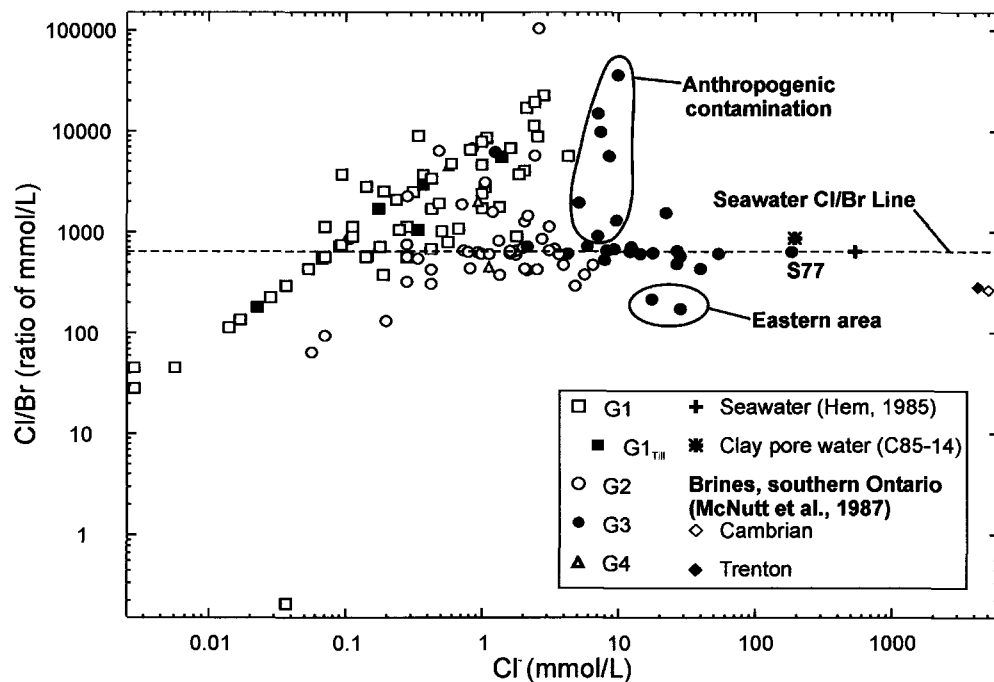


Figure 4.11. Diagram of  $\text{Cl}/\text{Br}$  (ratio of mmol/L) versus  $\text{Cl}^-$  (mmol/L) for the groundwater groups and possible end-member samples.

Because the clay was deposited in the Champlain Sea environment, Cloutier et al. (in prep c) assumed that the clay pore water sample C85-14, the most saline sample at that site, represents the original Pleistocene Champlain Sea water for the Basses-Laurentides aquifer system. As mentioned previously, the Champlain Sea did not have a typical seawater composition. It was diluted seawater resulting from the mixture between continental waters, including meltwater from the Laurentide Ice Sheet and local precipitation, and salt water from the St. Lawrence Gulf (Hillaire-Marcel, 1988). The similarity between the clay pore water and the groundwater S77, in their conservative ions ratio and concentrations, as well as in their  $\delta^{18}\text{O}$ , suggests that both samples have the same water origin. Thus, it could be assumed that the groundwater from S77 is close to the original saline end-member of the area. Conservative tracers  $\text{Cl}^-$  and  $\text{Br}^-$  can be used to determine the percentage of seawater present in the original Champlain Sea water. Table 4.3 compares concentrations of  $\text{Cl}^-$  and  $\text{Br}^-$ , in mmol/L, for groundwater S77 and

seawater. For that sample, the ratios to seawater for both conservative ions are 0.34. Thus, the original Champlain Sea water in the Basses-Laurentides was likely a mixture of about 34% "normal" seawater and 66% freshwater. In a study of Champlain Sea clay near Varennes, northeast of Montréal, Desaulniers and Cherry (1989) calculated a very similar mixture of 33% seawater and 67% freshwater at a depth of 27 m in the clay deposit.

Table 4.3. Comparison of  $\text{Cl}^-$  and  $\text{Br}^-$  (mmol/L) between the groundwater S77 and seawater

Ions	S77	Seawater <sup>a</sup>	S77/Seawater
$\text{Cl}^-$	183.34	535.92	0.34
$\text{Br}^-$	0.2878	0.8385	0.34

<sup>a</sup>Hem (1985).

Figure 4.12 uses  $\text{Br}^-$  and  $\text{Cl}^-$  diagrams to explain the model proposed for the origin of salinity in the area. Step 1 (Fig. 4.12a) presents the dilution line between a saline end-member, the seawater invading the study area during late Pleistocene, and a freshwater end-member, the glacial meltwater from the Laurentide Ice Sheet and Pleistocene meteoric water. This freshwater end-member is assumed to be free of  $\text{Cl}^-$  and  $\text{Br}^-$ . There is a perfect linear trend between seawater, groundwater sample S77, and the freshwater end-member (Fig. 4.12a). This supports that dilution is responsible for the salinity observed for groundwater S77, representing the composition of the original Champlain Sea water for the study area. Thus, sample S77 is assumed to represent the Pleistocene saline water end-member for the Basses-Laurentides aquifer system. Step 2 illustrates the mixing of the Pleistocene water source, S77, with modern meteoric water (Fig. 4.12b). In this diagram, the log scale is used for better visualization. The mixing line of Figure 4.12b has the same equation as the dilution line of Figure 4.12a, assuming a modern meteoric water free of  $\text{Cl}^-$  and  $\text{Br}^-$ . Most samples from G3 (Na-Cl) and G2 (Na-HCO<sub>3</sub>) plot along the mixing line, resulting from the mixing between recharged groundwater and Champlain Sea water. The contaminated samples identified in Figure 4.11 plot below the mixing line, confirming the different origin for their salinity (de-icing road salts).

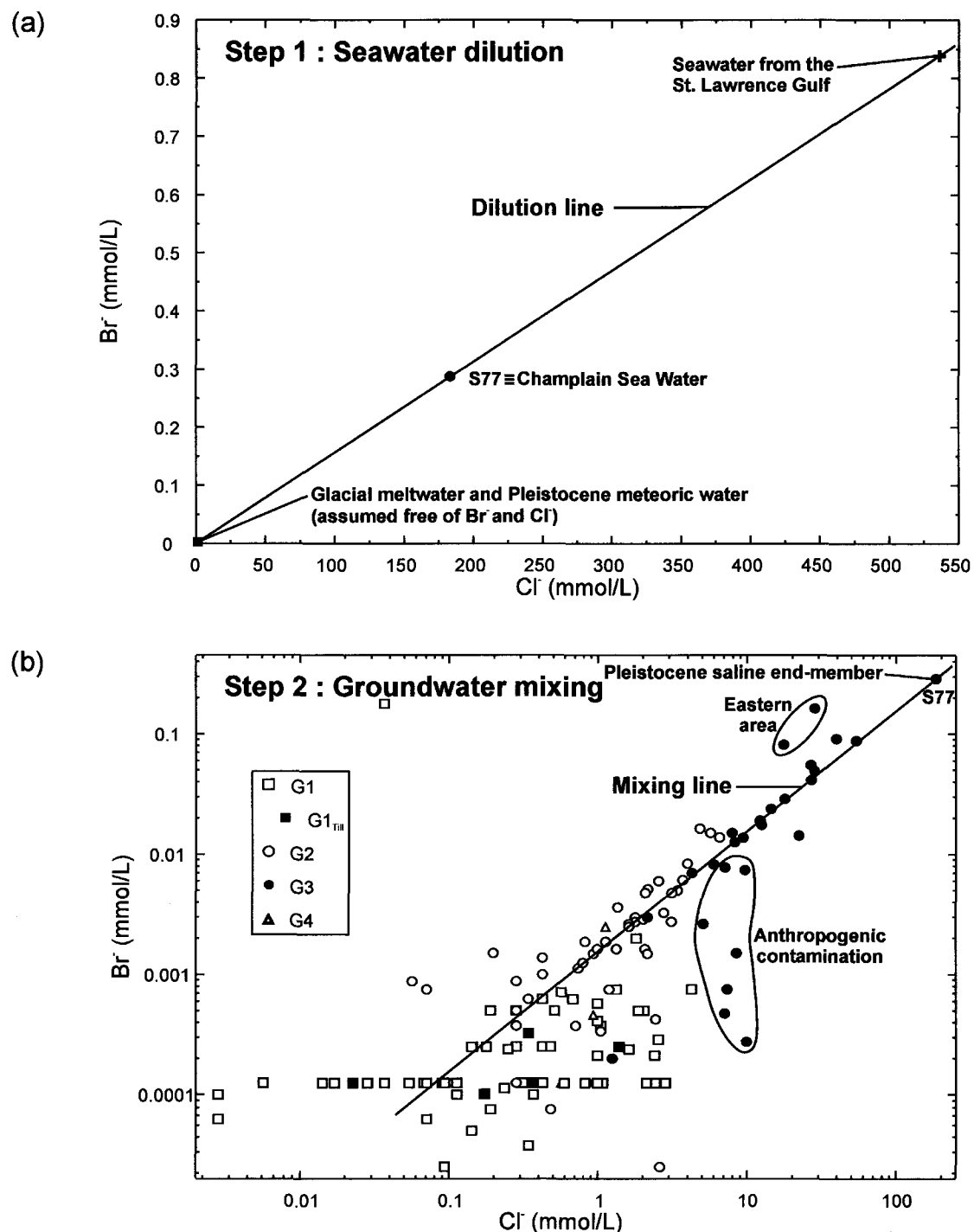


Figure 4.12. Model for the origin of salinity using diagrams of  $\text{Br}^-$  (mmol/L) versus  $\text{Cl}^-$  (mmol/L) for (a) step 1, seawater dilution, and (b) step 2, groundwater mixing.

The isotopic lines of evidence also supports the interpretation of groundwater salinity by mixing with Champlain Sea water. Figure 4.13 shows a diagram of  $\delta^{18}\text{O}$  and salinity. The two end-members of this mixing system are seawater from the St. Lawrence Gulf and the freshwater component defined as glacial meltwater from the Laurentide Ice Sheet and Pleistocene meteoric water. The ratios of the conservative tracers of Table 4.3 can be used to evaluate the  $\delta^{18}\text{O}$  and salinity of the Champlain Sea water in the study area. Thus, by mixing both end-members in a proportion of 34% seawater with 66% freshwater, a calculated original Champlain Sea water with a  $\delta^{18}\text{O}$  of  $-10.6\text{\textperthousand}$  and a salinity of 11.9 g/L is obtained. This is close to groundwater sample S77 that has a  $\delta^{18}\text{O}$  of  $-11.0\text{\textperthousand}$  and a salinity of 11.3 g/L. The dilution and mixing models shown in Figures 4.12 and 4.13 demonstrate that groundwater S77 has for origin the Champlain Sea water, and can be defined as the Pleistocene water end-member for the study area. The  $\delta^{18}\text{O}$  value of the Pleistocene water is not that different from the local modern meteoric water. As an example, the  $\delta^{18}\text{O}$  weighted annual means for the precipitation in Ottawa, located about 120 km West of the study area, is  $-11.21\text{\textperthousand}$  (IAEA, 2001). This similarity prevents the discrimination of Pleistocene water on the basis of  $\delta^{18}\text{O}$  only, and thus, is responsible for this uniformity in  $\delta^{18}\text{O}$  between unconfined and confined conditions identified by Cloutier et al. (in prep c). This situation is different from southwestern Ontario where Pleistocene water can be identified based on its depleted  $\delta^{18}\text{O}$  relative to modern meteoric water. There, the last glaciation was in a glacio-lacustrine environment, and  $\delta^{18}\text{O}$  values in the clay pore water, and in the aquifer below the clay, vary from  $-16.0\text{\textperthousand}$  to  $-17.5\text{\textperthousand}$  (Desaulniers et al., 1981; Husain et al., 1998). These values for southwestern Ontario Pleistocene water are in the range of the freshwater component  $\delta^{18}\text{O}$  value estimated by Hillaire-Marcel (1988), and used in Figure 4.13.

The groundwater mixing model demonstrates the importance of the Champlain Sea episode on the hydrogeochemical evolution of the groundwater of the Basses-Laurentides sedimentary rock aquifer system. The Champlain Sea water, defined as the mixture of seawater with Pleistocene glacial meltwater and precipitation, contributed to the salinization of the upper part of the aquifer system. This initial Champlain Sea water is preserved today in the clay, such as in the clay pore water sample C85-14, and locally in

the rock aquifer such as site S77 in the buried valley of St. Benoît. This salinization event is similar to a seawater intrusion problem, with the intruding saline water exchanging  $\text{Na}^+$ <sub>water</sub> with  $\text{Ca}^{2+}$ <sub>mineral</sub> present in the geological formations, and can be written as  $\text{Na}^+ + \frac{1}{2}\text{Ca-X}_2 \rightarrow \text{Na-X} + \frac{1}{2}\text{Ca}^{2+}$  (Appelo and Postma, 1993). The retreat of the Champlain Sea allowed the start of the desalinization processes, or the refreshening of the aquifer as described by Appelo and Postma (1993). Flushing of the aquifer system by fresh groundwater recharge leads to  $\text{Ca}^{2+}$ - $\text{Na}^+$  ion exchange and to the mixing of the recharged water with the Pleistocene saline water end-member. The number of flushing episodes and the presence of preferential flow paths and stagnant zones are largely responsible for the present-day geochemistry of groundwater in the rock aquifer system. Thus, the Basses-Laurentides aquifer system can be viewed as being at different stages of desalinization.

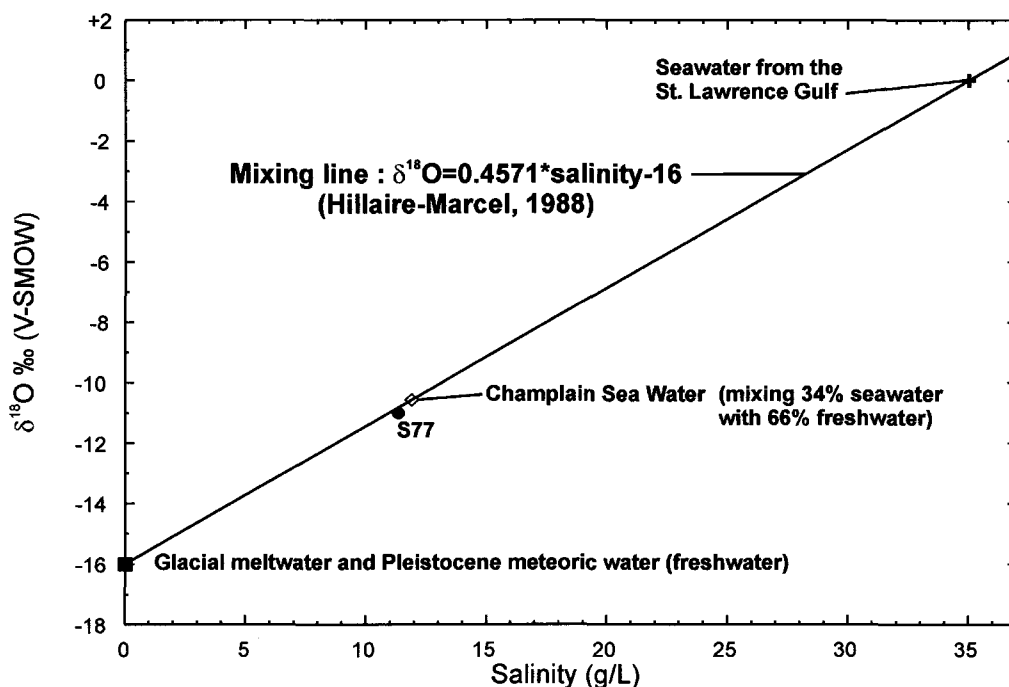


Figure 4.13. Model for the origin of salinity using diagrams of  $\delta^{18}\text{O}$  versus salinity based on the work of Hillaire-Marcel (1988).

The St. Benoît Valley, with most of its groundwater samples having a Na-Cl water types G3 and with sample S77, is in the least advanced stage of this desalinization process. This poorly flushed area could be considered a relatively stagnant part of the aquifer system.

Low groundwater flow can be related to the pattern of groundwater flow towards the valley that causes a singularity where little flow occurs at the valley center. The buried valley and the presence of the Oka Hills cause this flow pattern to the South. The other two buried valleys in the study area, St. Hermas and du Nord River, as well as the Ste. Anne-des-Plaines area, are in a more advanced stage of desalinization. A good part of the  $\text{Cl}^-$  has already been flushed, with  $\text{Na}^{2+}$  staying behind on exchange sites. Cationic exchange of  $\text{Ca}^{2+}_{\text{water}}$  with  $\text{Na}^+_{\text{mineral}}$  gives the  $\text{Na}-\text{HCO}_3$  groundwater type that dominates in these areas. The sites with Na-Cl groundwater types in these two valleys could be local, stagnant water, or solutes diffusing downward from the clay aquitard. In Ste. Anne-des-Plaines, it was shown that the salinity increase could be related to the solutes diffusion from shale beds, and thus be influenced by a formation water component preserved in the shale beds. Finally, the recharge areas, such as the zone from the airport to St. Eustache, are completely flushed of the Champlain Sea water component. It was demonstrated that the Na-Cl water types in these areas were the results of anthropogenic contamination.

## 4.6 DISCUSSION

### 4.6.1 Groundwater groups within the groundwater flow conceptual model

The main groundwater groups and water sources are represented in Figure 4.14 to show their relative position within the groundwater flow conceptual model introduced previously (Fig. 4.3). Table 4.4, a complement to Figures 4.14 and 4.15, presents the groups and water sources, the contexts in which they are found, the physical processes affecting them, the period of their origin, as well as the geochemical processes that contribute to their evolution to the resulting water types.

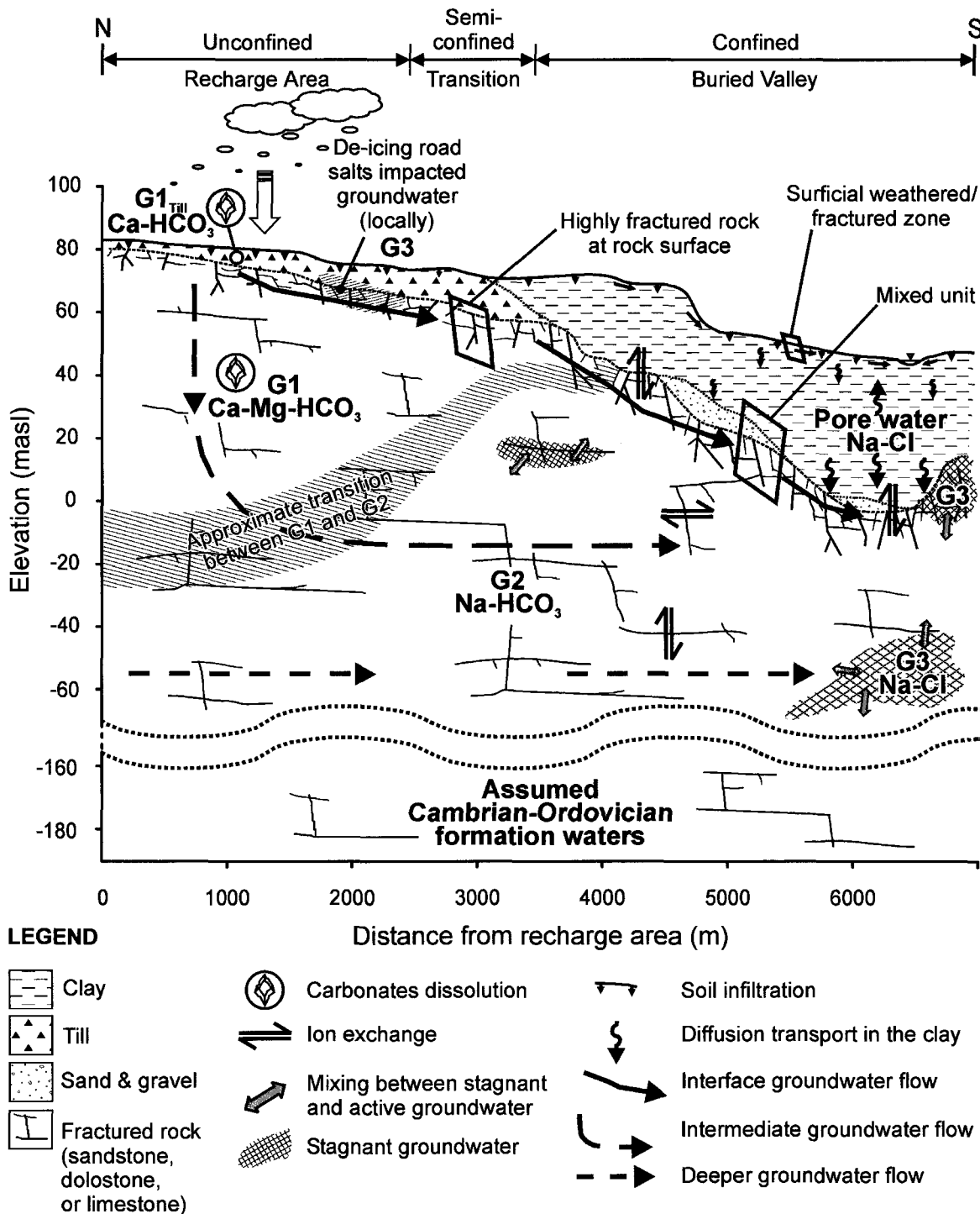


Figure 4.14. Groundwater flow conceptual model with the relative position of the groundwater groups within the Basses-Laurentides sedimentary rock aquifer system (see Table 4.4 for details).

Table 4.4. Relationship between groundwater groups, hydrogeological contexts and geochemical processes in the Basses-Laurentides sedimentary rock aquifer system

Groups Water sources	Hydrogeological contexts and physical processes	Period	Geochemical processes	Resulting water types
G1 <sub>TM</sub>	<b>Preferential recharge areas</b> - Recharge of precipitations (rain and snow) - Infiltration through soil and till	Present day	<b>Respiration &amp; decay of organic matter (soil zone)</b> - Increased pCO <sub>2</sub> - Till minerals/water interaction - Carbonates dissolution	Ca-HCO <sub>3</sub> Mg-HCO <sub>3</sub> Alkaline earth-HCO <sub>3</sub>
G1	<b>Preferential recharge areas and vicinity</b> - Unconfined and semi-confined conditions - Recharged groundwater in sedimentary rock aquifer	Modern submodern	<b>Water-rock interaction</b> - Carbonates dissolution	Ca-HCO <sub>3</sub> Mg-HCO <sub>3</sub> Alkaline earth-HCO <sub>3</sub>
G2	<b>Aquifer system under confined conditions</b> <i>Active interface groundwater flow</i> - Preferential groundwater flow, in contact with till or clay aquitard <i>Active intermediate and deeper groundwater flow in fractured rock</i>	Post-Champlain Sea (submodern)	<b>Ion exchange</b> - Rock/clay deposit interface and sedimentary rock - St. Hermas & du Nord River valleys, Ste. Anne-des-Plaines <b>Water-rock interaction</b> - Elevated Sr <sup>2+</sup> & F (Ste. Anne-des-Plaines) - Sulfate reduction (Ste. Anne-des-Plaines)	Na-HCO <sub>3</sub> Mixed cations-HCO <sub>3</sub>
G3	<b>Aquifer system under confined conditions</b> <i>Active interface groundwater flow</i> - Preferential groundwater flow, in contact with till or clay aquitard <i>Active intermediate and deeper groundwater flow in fractured rock</i>	Post-Champlain Sea (submodern)	<b>Groundwater mixing (mainly St. Benoit Valley)</b> - Champlain Sea water mixed with G2 water <b>Solutes diffusion</b> - Rock/clay deposit interface - From shale beds (Ste. Anne-des-Plaines) <b>Pleistocene Champlain Sea water</b> - As site S77 in St. Benoit Valley - Input of dissolved de-icing road salts - Mainly at St. Janvier (along main roads 15 & 117)	Na-Cl
Most concentrated Anthropogenic source	<b>Stagnant groundwater</b> <b>Locally in preferential recharge areas</b> - Contamination by de-icing road salts	About 12 000- 10 000 BP Present day		Na-Cl Na-Cl Mixed cations-Cl
G4	<b>Preferential recharge areas (Grenville to St. Philippe)</b> - Recharged groundwater in dolostone and limestone	Modern	<b>Water-rock interaction</b> - Dissolution of gypsum	CaSO <sub>4</sub> Na-SO <sub>4</sub>
Clay pore water	<b>Champlain Sea marine clays</b> <i>Surface weathered/fractured zone</i> <i>Unweathered clay</i> - Downward & upward diffusion	About 12 000- 10 000 BP	<b>Interaction with the aquifer system below</b> - Ionic exchange Ca <sup>2+</sup> -Na <sup>+</sup> - Solutes diffusion, as for Cl <sup>-</sup>	Na-Cl
Formation waters	<b>Deeper than 150 m in the rock aquifer system (Below the studied active groundwater flow system)</b>		Cambrian-Ordovician	Not sampled

Present-day precipitation infiltrates the soils and the permeable surface sediments, generally till, in the preferential groundwater recharge areas. The resulting sub-group, G1<sub>Till</sub>, has a Ca-HCO<sub>3</sub> water type. The geochemistry of G1<sub>Till</sub> is very important as it controls to a large extent that of G1 (Ca-Mg-HCO<sub>3</sub>). Groundwater G1 is the recharged groundwater in the sedimentary rock aquifer system, following its infiltration through the till. Samples that belong to this group are located in unconfined to semi-confined conditions of the preferential recharge areas. Locally, in the preferential recharge area of Grenville to St. Philippe, recharged groundwater has the geochemical characteristics of G4 (Ca-SO<sub>4</sub> and Na-SO<sub>4</sub>). From the recharge areas, groundwater flows through the active aquifer system under confined conditions, resulting in a geochemical evolution to G2 (Na-HCO<sub>3</sub>) and G3 (Na-Cl). This groundwater flow occurs as interface preferential groundwater flow in the highly fractured rock or mixed unit, as well as intermediate to deeper groundwater flow in the fractured sedimentary rock.

Active post-Champlain Sea groundwater flow is responsible for the on-going desalinization of the confined aquifer system. The approximate transition front from G1 (Ca-Mg-HCO<sub>3</sub>) to G2 (Na-HCO<sub>3</sub>) is more advanced in the interface zone due to faster groundwater flow (Fig. 4.14). Being confined by the clay aquitard, the geochemistry of G2 and G3 (Na-Cl) groundwaters is not affected by direct recharge but by the geochemical processes occurring along the flow path, from the recharge areas to the sampling site. Pleistocene Champlain Sea water is still present in the aquifer system either as the most concentrated stagnant groundwater, in poorly flushed zones of the aquifer system, such as site S77 in St. Benoît Valley, and as pore water of the Champlain Sea marine clay aquitard. Because of downward diffusion transport of solutes, the brackish to saline pore water of the aquitard has major impacts on the geochemistry of groundwater from the interface zone, increasing the groundwater salinity in more isolated sections of the aquifer system. Groundwater G3 is also observed locally in preferential recharge areas, and results from a contamination by de-icing road salts.

#### 4.6.2 Specific geochemical evolution paths

The specific geochemical evolution paths of Figure 4.15 are a complement to the physical model introduced above (Fig. 4.14) and indicates the inferred origin of groundwater geochemical peculiarities in different locations of the study area. Figure 4.15 presents the integrated hydrogeochemical and groundwater evolution model of the Basses-Laurentides aquifer system, showing the relationship between the groundwater groups, as well as their relationship with the hydrogeological contexts, the groundwater flow system, the geological formations, as well as the geographical areas where the geochemical processes are effective.

The starting point for the various geochemical evolution paths is the same, and consists of carbonates dissolution in the surface sediments following water infiltration in the soil zone. The linear relation between  $\text{Ca}^{2+}$  and  $\text{HCO}_3^-$ , the Mg/Ca ratios between 0.6 and 0.9, the pH increase relative to precipitation, as well as the undersaturated to near equilibrium calcite and dolomite saturation indexes, have been presented as evidence of carbonate dissolution operating in the surface sediments. Carbonate dissolution is responsible for the geochemical characteristics of G1<sub>Till</sub> ( $\text{Ca}-\text{HCO}_3$ ) and is consistent with both the  $\delta^{13}\text{C}_{\text{DIC}}$  of the till groundwater (Cloutier et al., in prep c) and the availability of calcite and dolomite in the till matrix. Groundwater infiltrates the unconfined to semi-confined sedimentary rock aquifer system in the various recharge areas, producing the G1 water type ( $\text{Ca}-\text{Mg}-\text{HCO}_3$ ). Water-rock interaction, as carbonate dissolution, is also active in the sedimentary rock particularly in the dolostone and limestone formations. Strontium isotopes in groundwater from these formations are also consistent with carbonate dissolution (Cloutier et al., in prep c). In the recharge area, from the airport to St. Eustache, the groundwater groups are relatively uniform and are dominated by G1. Some local peculiarities are observed, as water-rock interaction responsible for the elevated concentrations in  $\text{F}^-$  and  $\text{Sr}^{2+}$  in the dolostone and limestone of the western region, from Grenville to St. Philippe. In this same region, a few sites evolved to G4 ( $\text{Ca}-\text{SO}_4$  and  $\text{Na}-\text{SO}_4$ ) groundwater possibly due to gypsum dissolution. The input of de-icing road salts in the unconfined area of St. Janvier leads to the occurrence of G3 ( $\text{Na}-\text{Cl}$ ) groundwaters in

this recharge area. The  $\text{Cl}^-$  concentrations of these de-icing road salts impacted groundwater is not coupled to a  $\text{Br}^-$  increase as it is for the samples of G3 located in confined condition, thus confirming their different origin.

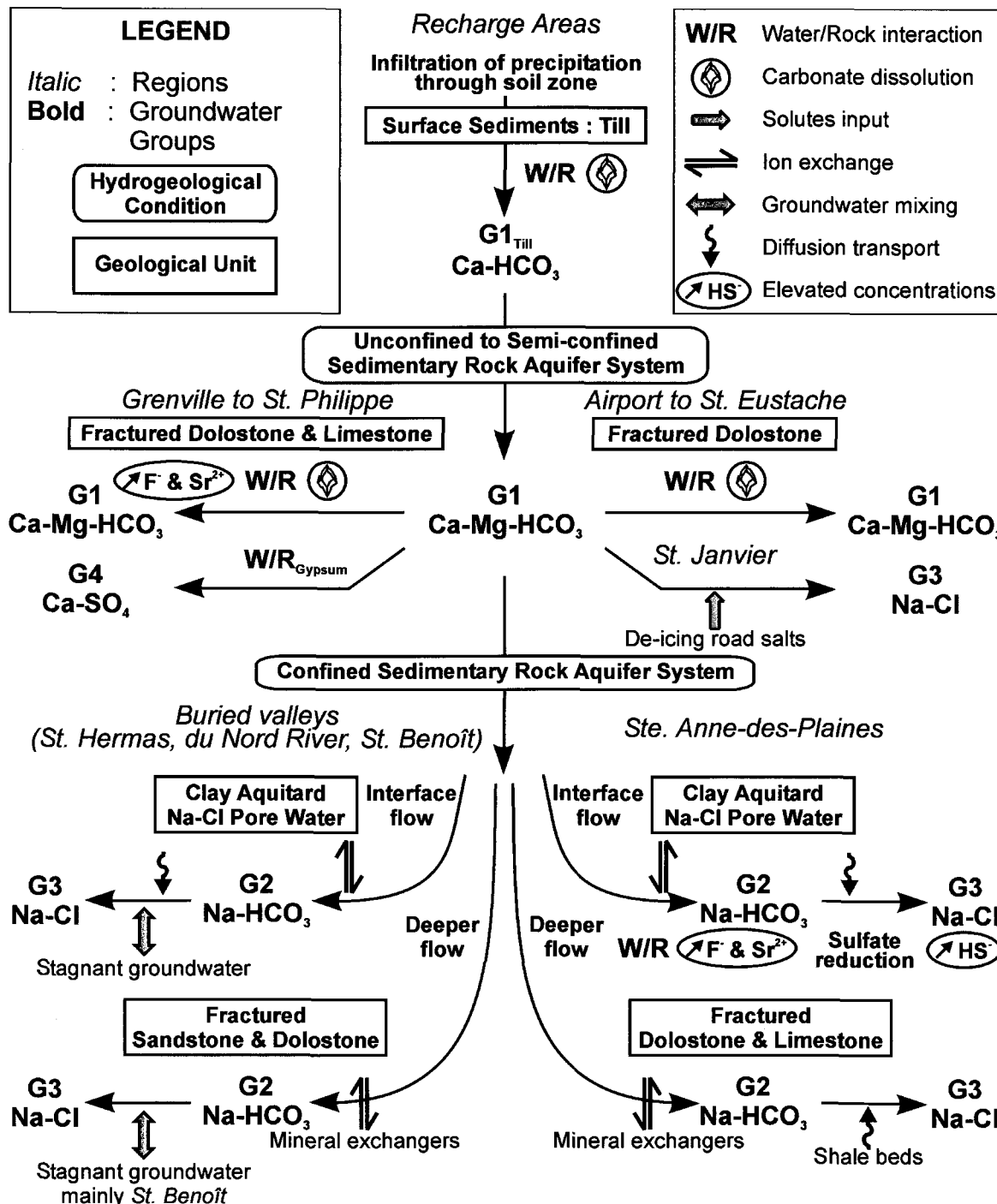


Figure 4.15. Specific geochemical evolution paths for groundwater in different locations of the Basses-Laurentides sedimentary rock aquifer system (see Table 4.4 for details).

From the recharge areas, groundwater flows through the confined sedimentary rock aquifer system, in the three buried valleys and Ste. Anne-des-Plaines. Because of the diversified geological and hydrogeological contexts of the Basses-Laurentides, the geochemical evolution paths and the resulting water types vary accordingly to the sedimentary formations, the depth of groundwater flow, as well as the geographical area. In buried valleys, interface flow occurs below the Champlain Sea clay aquitard that has a Na-Cl pore water geochemistry. The contact with the clays leads to  $\text{Ca}^{2+}_{\text{water}}-\text{Na}^+_{\text{mineral}}$  ion exchange that results in G2 (Na-HCO<sub>3</sub>) groundwater in the confined aquifer system. Evidence of  $\text{Ca}^{2+}-\text{Na}^+$  ion exchange occurring along the groundwater flow path includes negative  $\log(\text{Ca}+\text{Mg})/\text{Na}^2$ , an increasing trend between pH and Na<sup>+</sup> concentrations coupled to a decrease in Ca<sup>2+</sup> concentrations, as well as an increase in Na<sup>+</sup> concentrations not really coupled to a Cl<sup>-</sup> increase. Locally, in stagnant parts of the system, downward diffusion of Cl<sup>-</sup> and Na<sup>+</sup> from the aquitard could result in groundwater with G3 (Na-Cl) characteristics. These two processes,  $\text{Ca}^{2+}-\text{Na}^+$  ion exchange and solute diffusion, are also active for the interface flow of Ste. Anne-des-Plaines. The active intermediate and deeper groundwater flow in the sandstone and dolostone of the buried valleys is also impacted by ion exchange with mineral exchangers of the rock formations, resulting in G2 groundwaters. Locally, stagnant brackish to saline groundwater mixes with G2 groundwaters to produce areas of G3 groundwaters. The conservative tracers Cl<sup>-</sup> and Br<sup>-</sup>, as well as δ<sup>18</sup>O, confirmed that these brackish to saline groundwaters origin from the Champlain Sea water. This mixing is observed at a larger scale for the St. Benoît Valley, where the Pleistocene Champlain Sea water was sampled (site S77), but can be present sporadically in the St. Hermas and the du Nord River valleys as well. Groundwater flow in Ste. Anne-des-Plaines shows some peculiarities due to geochemical processes operating locally, such as sulfate reduction producing elevated HS<sup>-</sup> in the groundwater, water-rock interaction with the dolostone and the limestone conducting to elevated concentrations in F<sup>-</sup> and Sr<sup>2+</sup>, and solute diffusion from the shale beds that could produce G3 groundwaters.

#### 4.6.3 General geochemical evolution paths

Figure 4.15 synthesized the geochemical evolution paths assumed to explain the varied groundwater characteristics found in specific locations within the study area. Such local evolution paths are variations of more general paths affecting the entire area. The Piper diagram of Figure 4.16, built from the Piper diagram of the groundwater groups (Fig. 4.5), illustrates these general geochemical evolution paths of groundwater within the Basses-Laurentides aquifer system.

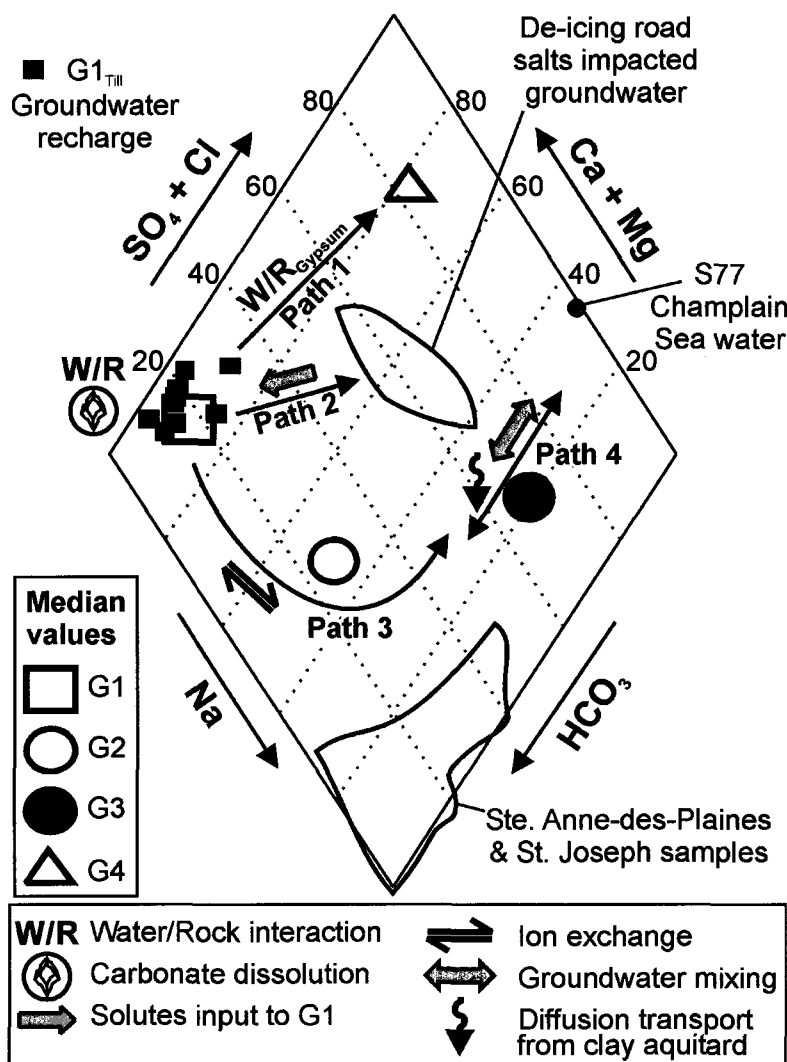


Figure 4.16. Piper diagram illustrating the general geochemical processes involved in the evolution of groundwater of the Basses-Laurentides sedimentary rock aquifer system (see the Piper diagram of Figure 4.5 for all groundwater samples).

The groundwater recharge end-member, G1<sub>Till</sub>, and the groundwater of G1 are in the Ca-Mg-HCO<sub>3</sub> zone of the diagram. From the recharge areas, the evolution of groundwater follows three possible paths. The first two paths, observed locally under unconfined conditions, are gypsum dissolution resulting in groundwater of G4 type in the SO<sub>4</sub> zone (path 1), and the input of de-icing road salts to groundwater of G1 resulting in some samples moving from the Ca-Mg-HCO<sub>3</sub> through the Na-Cl zone (path 2). The third path is the most widespread and occurs as groundwater flows through the confined aquifer system (path 3). This curved path represents the evolution due to Ca<sup>2+</sup>-Na<sup>+</sup> ion exchange of groundwater G1 to G2 in the Na-HCO<sub>3</sub> zone of the Piper diagram, a desalinization path in the context of the Basses-Laurentides aquifer system. The location of samples from the confined areas of Ste. Anne-des-Plaines and St. Joseph is indicated on the Piper diagram, as they are the most affected by ion exchange. Groundwater mixing with the Pleistocene Champlain Sea end-member, as well as solute diffusion from the Champlain Sea clay aquitard, causes the evolution of G2 groundwaters to G3 in the Na-Cl zone of the Piper diagram (path 4). Path 4 represents an average mixing trend based on the position of the groundwater samples of G2 and G3 in the Piper diagram (Fig. 4.5).

#### 4.7 SUMMARY AND CONCLUSIONS

This paper identified the main active geochemical processes as well as the Quaternary geological events that have influenced groundwater geochemistry in the Basses-Laurentides. The aquifer system of the Basses-Laurentides consists of Cambrian-Ordovician sedimentary formations (sandstone, dolostone, and limestone) lying on Precambrian crystalline basement. The last major geological event to affect the study area is the marine invasion from the St. Lawrence Gulf during the last deglaciation. The resulting Champlain Sea was a mixture of continental fresh water and seawater from the Gulf. Original Champlain Sea water is still found in stagnant parts of the aquifer system and in the pore water of thick marine clays left by the Champlain Sea episode. Unconfined conditions characterize areas of preferential groundwater recharge, where precipitation infiltrates soils and till. The marine clay aquitard confines the rock aquifer, for example in buried valleys. From the recharge areas, groundwater flows through the

highly fractured rock and mixed unit at the interface with the overlying clay aquitard, as well as intermediate to deep groundwater flow in the fractured sedimentary rock unit.

The interpretation of the main geochemical processes presented in this paper relies on the classification of groundwater groups determined by Cloutier et al. (in prep c). A spatial relationship exists between the groundwater groups and the hydrogeological contexts of the Basses-Laurentides. G1 (Ca-HCO<sub>3</sub> and Mg-HCO<sub>3</sub>) and G4 (Ca-SO<sub>4</sub> and Na-SO<sub>4</sub>) types are found in unconfined to semi-confined conditions of the preferential groundwater recharge areas, whereas G2 (Na-HCO<sub>3</sub>) and G3 (Na-Cl) are found under confined conditions as in the buried valleys. A sub-group of G1, G1<sub>Till</sub> (Ca-HCO<sub>3</sub>), represents the groundwater recharge end-member to the aquifer system. The most concentrated sample, site S77 in St. Benoît Valley, is the second end-member corresponding to the older Champlain Sea water component.

The main geochemical processes that are affecting the evolution of groundwater groups were presented with respect to their relative position in the groundwater system, starting from the recharge and along groundwater flow paths. Dissolution of carbonates, calcite and dolomite, dominates in the preferential recharge areas resulting in Ca-Mg-HCO<sub>3</sub> (G1) groundwater. Ca<sup>2+</sup>-Na<sup>+</sup> ion exchange, groundwater mixing with Pleistocene Champlain Sea water as well as solute diffusion from the marine clay aquitard are the main processes under the confined conditions resulting in a Na-HCO<sub>3</sub> (G2) and Na-Cl (G3) groundwater. The marine invasion that resulted in the Champlain Sea is the cause of the salinization of the aquifer system. Conservative tracers Cl<sup>-</sup> and Br<sup>-</sup>, supported by δ<sup>18</sup>O values, allowed an estimation of the percentage of seawater present in the original Champlain Sea water for the Basses-Laurentides, a mixture of about 34% seawater and 66% freshwater. The present geochemistry of the groundwater indicates that the aquifer system is at different stages of desalinization, from the older Champlain Sea water in stagnant parts to fully flushed sections of the aquifer system. A modern salinity source, de-icing road salts, was identified in recharge areas and could be distinguished by its Cl/Br ratio. The geochemical processes are integrated within the hydrogeological and geological contexts to produce specific and general geochemical evolution paths models for groundwater of

the Basses-Laurentides sedimentary rock aquifer system. The specific geochemical evolution paths explain local groundwater peculiarities, such as elevated F<sup>-</sup> and Sr<sup>2+</sup> concentrations and sulfate reduction.

The description of the regional groundwater hydrogeochemistry (Cloutier et al., in prep c), the identification of the main water sources, mineral phases, and geochemical processes, allowed the understanding of the hydrogeochemical evolution of the groundwater in the Basses-Laurentides sedimentary rock aquifer system. This understanding, within the geological and hydrogeological contexts of the Basses-Laurentides, is possible due to the extent of the characterization of the aquifer system, in term of area covered, number of wells sampled, and parameters analyzed.

## ACKNOWLEDGEMENTS

The project was carried out by the Geological Survey of Canada (GSC), in collaboration with INRS-Eau, Terre & Environnement (INRS-ETE), Université Laval and Environment Canada. Funding and support for the study came from the GSC, Economic Development Canada, Regional County Municipalities (RCM) of Argenteuil, Mirabel, Deux-Montagnes and Thérèse-de-Blainville, Department of the Environment of Québec, Conseil Régional de Développement-Laurentides, and Association des Professionnels de Développement Économique des Laurentides. Financial support for the first author was provided by the Natural Sciences and Engineering Research Council (NSERC) of Canada, Fonds québécois de la recherche sur la nature et les technologies, and INRS-ETE as postgraduate scholarships. We acknowledge the Department of the Environment of Québec for providing the analyses of inorganic constituents in groundwater. The drilling was partly supported by the Department of Transports of Québec. The authors thank Marc Luzincourt (Delta-Lab, GSC-Québec) for stable isotopes analyses. NSERC also supported R.L. and R.T. through operating grants. The work of all students involved in the project as field assistants, and the collaboration of the population of the RCM giving site access are greatly appreciated.

## **Chapitre 5**

# **MULTIVARIATE STATISTICAL ANALYSIS OF GEOCHEMICAL DATA AS INDICATIVE OF THE HYDROGEOCHEMICAL EVOLUTION OF GROUNDWATER OF THE BASSES-LAURENTIDES SEDIMENTARY ROCK AQUIFER SYSTEM, ST. LAWRENCE LOWLANDS, QUÉBEC, CANADA**

Vincent Cloutier<sup>1</sup>, René Lefebvre<sup>1</sup>, René Therrien<sup>2</sup>, Martine M. Savard<sup>3</sup>

<sup>1</sup>Institut national de la recherche scientifique, INRS-Eau, Terre & Environnement, C.P. 7500, Sainte-Foy (Québec), G1V 4C7, Canada

<sup>2</sup>Département de géologie et de génie géologique, Université Laval, Sainte-Foy (Québec), G1K 7P4, Canada

<sup>3</sup>Geological Survey of Canada, Natural Resources Canada, 880, chemin Sainte-Foy, Suite 840, Québec (Québec), G1S 2L2, Canada

## RÉSUMÉ

L'étude de l'hydrogéochimie des eaux souterraines du système aquifère de roches sédimentaires paléozoïques des Basses-Laurentides a généré une quantité importante de données géochimiques. Des échantillons d'eau souterraine ont été prélevés à 153 sites répartis sur la région d'étude de 1500 km<sup>2</sup> et ont été analysés pour 47 paramètres incluant les paramètres de terrain, les constituants inorganiques et des paramètres isotopiques. Le nombre important de données peut conduire à des difficultés lors de l'intégration, l'interprétation et la représentation des résultats. Deux méthodes d'analyse statistique multivariable, la classification automatique hiérarchique (CAH) et l'analyse en composantes principales (ACP), ont été appliquées à un sous-groupe de la base de données afin d'évaluer leurs capacités à classifier les échantillons, et à identifier les processus géochimiques contrôlant la géochimie des eaux souterraines. Ce sous-groupe est composé de 144 échantillons et de 14 paramètres (Ca<sup>2+</sup>, Mg<sup>2+</sup>, Na<sup>+</sup>, K<sup>+</sup>, HCO<sub>3</sub><sup>-</sup>, Cl<sup>-</sup>, SO<sub>4</sub><sup>2-</sup>, Fe<sup>2+</sup>, Mn<sup>2+</sup>, Br<sup>-</sup>, Sr<sup>2+</sup>, F<sup>-</sup>, Ba<sup>2+</sup>, HS<sup>-</sup>). La CAH a permis de diviser les échantillons en sept *clusters*, C1 à C7. Les *clusters* C1, C2 et C5 caractérisent le système aquifère en conditions confinées, alors que les *clusters* C3, C4, C6, et C7 sont majoritairement localisés dans les zones préférentielles de recharge. En plus de reconnaître l'importance des conditions hydrogéologiques sur la géochimie des eaux souterraines, la distribution régionale des *clusters* a permis de reconnaître l'influence des formations géologiques sur les concentrations en éléments mineurs et traces. Les cinq premières composantes de l'ACP comptent pour 78.3% de la variance totale des données. Les deux premières composantes, qui comptent pour 40.6% de la variance, sont reliées à la salinité et à la dureté. Les composantes 3 à 5 sont reliées à des effets locaux et géologiques. L'intégration de la CAH et de l'ACP, avec des méthodes de classification en types d'eau, ainsi qu'avec les contextes géologiques et hydrogéologiques a permis de diviser le territoire en quatre régions géochimiques, procurant un portrait global de la dynamique du système aquifère. Avec son approche intégrée, cette étude hydrogéochimique apporte une contribution à la caractérisation et la compréhension de systèmes d'écoulement complexes, ainsi qu'à l'évolution à long terme de systèmes hydrogéologiques.

**ABSTRACT**

The study of groundwater hydrogeochemistry of the Paleozoic Basses-Laurentides sedimentary rock aquifer system in Québec produced a large geochemical dataset. Groundwater samples were collected at 153 sites over a 1500 km<sup>2</sup> study area and analyzed for 47 parameters including *in situ* field measurements, inorganic constituents, and isotopic indicators. This large number of data can lead to difficulties in the integration, interpretation, and representation of the results. Two multivariate statistical methods, hierarchical cluster analysis (HCA) and principal components analysis (PCA), were applied to a subgroup of the dataset to evaluate their usefulness to classify the groundwater samples, and to identify geochemical processes controlling groundwater geochemistry. This subgroup consisted of 144 samples and 14 parameters (Ca<sup>2+</sup>, Mg<sup>2+</sup>, Na<sup>+</sup>, K<sup>+</sup>, HCO<sub>3</sub><sup>-</sup>, Cl<sup>-</sup>, SO<sub>4</sub><sup>2-</sup>, Fe<sup>2+</sup>, Mn<sup>2+</sup>, Br<sup>-</sup>, Sr<sup>2+</sup>, F<sup>-</sup>, Ba<sup>2+</sup>, HS<sup>-</sup>). Seven geochemically distinct clusters, C1 to C7, resulted from the HCA. Three clusters, C1, C2, and C5, characterize samples from the aquifer system under confined conditions. Samples that belong to the other four clusters, C3, C4, C6, and C7, are located mostly in preferential recharge areas. In addition to recognizing the importance of hydrogeological conditions on groundwater geochemistry, the distribution of clusters also identified the importance of the geological formations on minor and trace elements. The PCA was performed by extracting the principal components on the correlation matrix. The first five components of the PCA account for 78.3% of the total variance in the dataset. The first two components, accounting for 40.6% of the variance, are related to salinity and hardness. Components 3 to 5 are related to more local and geological effects. The integration of the HCA and the PCA, with conventional classification of groundwater as types and groups, as well as with the hydrogeological and geological contexts, allowed the division of the region into four main geochemical areas, providing a global picture of the aquifer system dynamics. With its integrated approach, this hydrogeochemical study brings a contribution to the characterization and understanding of complex groundwater flow systems, as well as an example of the long-term evolution of hydrogeological systems.

## 5.1 INTRODUCTION

The study area, shown on Figure 5.1, is located on the North shore of the St. Lawrence River, northwest of Montréal, in a geographical region named the Basses-Laurentides. Groundwater hydrogeochemistry of the Basses-Laurentides sedimentary rock aquifer system was studied extensively as part of a regional hydrogeological characterization project (Savard et al., *in press*). Cloutier et al. (*in prep c*) presented results of the regional groundwater hydrogeochemical characterization and the relationship between groundwater types and geological as well as hydrogeological contexts, with the specific objective of identifying the origin of groundwater in the Basses-Laurentides aquifer system (*Chapitre 3*). Cloutier et al. (*in prep a*) identified the on-going geochemical processes as well as the quaternary geological events that have influenced groundwater geochemistry in this aquifer system (*Chapitre 4*).

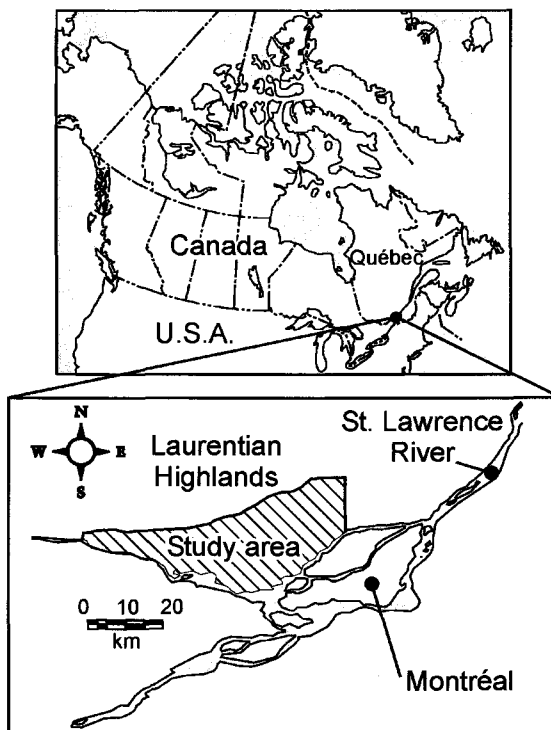


Figure 5.1. Location of the Basses-Laurentides sedimentary rock aquifer system.

The basic information for an hydrogeochemical study results from the geochemical analysis of groundwater samples. Each sampling site is thus characterized by a set of chemical, isotopic and physical parameters. Consequently, the hydrogeochemical characterization produces a large quantity of data that have to be integrated, interpreted, and represented graphically. Different maps and graphical representations can be used in the classification and interpretation of geochemical data, such as : dot map of chemical parameters, Piper diagram (Piper, 1944), Pie diagram, Stiff pattern diagram, Schoeller diagram, box plots and scatterplots of chemical parameters (Freeze and Cherry, 1979; Hem, 1985; Alley, 1993; Güler et al., 2002). Most of these maps and graphical representations, as well as a map of water types, were used in the hydrogeochemical study of the Basses-Laurentides aquifer system (Cloutier et al., in prep c; Cloutier et al., in prep a). The information resulting from these classical graphical methods, essential to hydrogeochemical studies, is generally more qualitative than quantitative and presents some limitations. The Piper and Pie diagrams use relative percentages of concentrations in meq/L instead of absolute concentrations, and are limited to major ions ( $\text{Ca}^{2+}$ ,  $\text{Mg}^{2+}$ ,  $\text{Na}^+$ ,  $\text{K}^+$ ,  $\text{HCO}_3^-$ ,  $\text{Cl}^-$ ,  $\text{SO}_4^{2-}$ ). On the other hand, samples can be represented proportionally to their TDS. The map of water types is a good classification method, but it is restricted to major ions. Finally, the number of samples that can be clearly represented using these maps and graphical methods is often limited, confirming the need for other classification methods of groundwater samples in regional hydrogeochemical studies.

The knowledge, the understanding and the particularities of the hydrogeochemistry of the Basses-Laurentides sedimentary rock aquifer system represent a great opportunity to evaluate the application of multivariate statistical analysis, a quantitative approach allowing to classify groundwater samples, to study correlations between the variables (all chemical, isotopic and physical parameters), and to evaluate the similarity between the observations (groundwater sampling sites). Multivariate statistical analysis was used in a number of hydrogeochemical studies (Steinhorst and Williams, 1985; Usunoff and Guzmán-Guzmán, 1989; Melloul and Collin, 1992; Schot and van der Wal, 1992; Ribeiro and Macedo, 1995; Güler et al., 2002). Among other things, as an aid to management and future development of the groundwater resources of the region, it will be evaluated if the

territory can be divided in areas with distinct groundwater quality. Moreover, two of these methods, hierarchical cluster analysis (HCA) and principal components analysis (PCA), will be tested for their applicability to the identification of the processes controlling the evolution of groundwater and the role of geological and hydrogeological contexts on this evolution.

## **5.2 CONTEXT OF THE STUDY AREA**

### **5.2.1 Geology and hydrogeology**

The Basses-Laurentides belong to the St. Lawrence Lowlands, a physiographic region having a generally flat topography, with the exception of the Monteregean Hills related to Cretaceous intrusions. The geological map of Figure 5.2a shows the two alkaline intrusions of Oka and St. André Hills. The Laurentian Highlands, part of the Grenville Province of the Canadian Shield, border the study area to the North. The southwest, south, and southeast borders are surface water limits, namely the Outaouais River, the Deux Montagnes Lake, and the Mille Îles River. To the East, the study area ends in the watershed of the Mascouche River (Fig. 5.2a).

The Basses-Laurentides aquifer system consists of nearly horizontal Cambrian-Ordovician sedimentary formations lying in unconformity on crystalline basement of the Precambrian Grenville Province (Fig. 5.2a). In the study area, the sedimentary formations rarely outcrop, as Quaternary sediments cover them. The Cambrian Potsdam Group, at the base of the sequence, is divided into two formations; the Covey Hill, a reddish feldspathic sandstone, locally conglomeratic and poorly cemented, and the Cairnside, a well-cemented, pure, quartz arenite sandstone (Globensky, 1987). Salad Hersi et al. (2003) subdivide the Ordovician Beekmantown Group into three formations; the dolomitic sandstone and sandy dolostone of the Theresa, the sandy to pure, massive, dolostone of the Beauharnois, and the pure dolostone with sommital limestone of the Carillon. Following are the sandstone of the Lower Chazy, and the limestone and shale of

the Upper Chazy Group, the dolostone, shale and limestone of the Black River Group and the limestone and shale of the Trenton Group (Globensky, 1987). More details on the lithology, mineralogy and fracture filling of the sedimentary formations are provided by Cloutier et al. (in prep a).

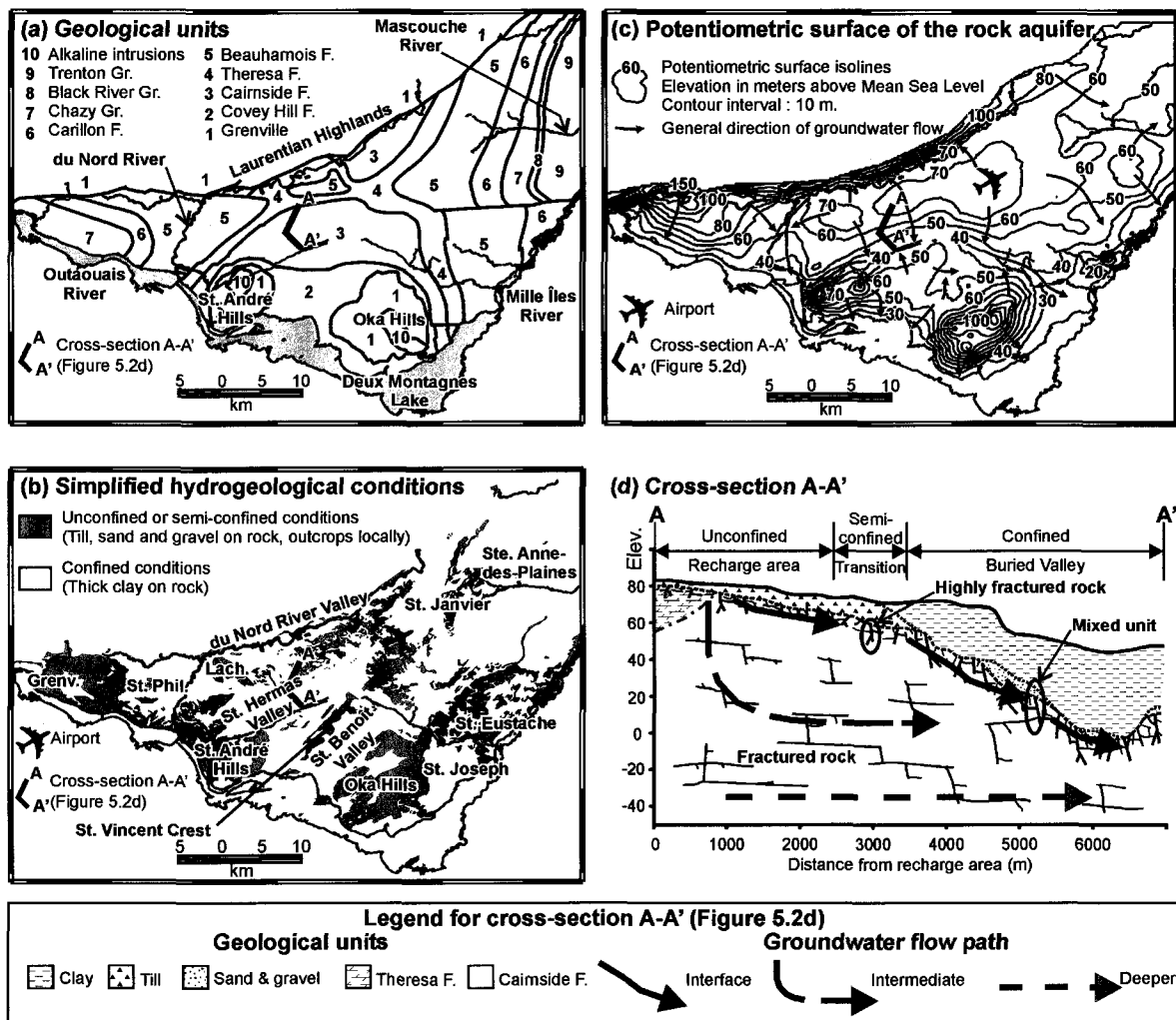


Figure 5.2. Context of the study area: (a) geology (geological map modified from Rocher et al., in press), (b) hydrogeological conditions (Grenv.: Grenville, St. Phil.: St. Philippe, Lach.: Lachute) (hydrogeological conditions map modified from Hamel et al., 2001), (c) potentiometric surface (potentiometric surface map modified from Paradis, in press b), and (d) cross-section A-A' illustrating the groundwater flow conceptual model and the main hydrostratigraphic units (Elev. : elevation in m above mean sea level) (modified from Cloutier et al., in prep c).

The last Quaternary glaciation covered the rock units with Upper Wisconsinan sediments, such as glacial till, and glacio-fluvial sand and gravel (Bolduc and Ross, 2001). During the deglaciation, the retreat of the Laurentide Ice Sheet of the St. Lawrence Valley,

combined with the depression of the continent due to the glaciation, allowed a marine invasion from the St. Lawrence Gulf which created the Champlain Sea. The Champlain Sea water was a mixture of continental waters, including meltwater from the Laurentide Ice Sheet and local precipitation, and salt water from the St. Lawrence Gulf (Hillaire-Marcel, 1988; Cloutier et al., in prep a). The Champlain Sea episode left marine sediments, mainly clayey-silts to silty-clays, that can reach a thickness of more than 80 m (Bolduc and Ross, 2001). The Champlain Sea clay is overlying till or glacio-fluvial sand and gravel units of variable thickness. The till is also found at ground surface, above the rock sequence, in elevated topography areas. The till is highly variable in composition and texture depending of the underlying rock units (Ross and Bolduc, 2001); its composition relates mainly to the glacial erosion of Paleozoic sedimentary formations, such as sandstone, dolostone, and limestone, with some influence of Precambrian rocks.

The map of the hydrogeological conditions illustrates the sectors of the territory with unconfined or semi-confined conditions as opposed to confined conditions (Fig. 5.2b). The main groundwater recharge for the Basses-Laurentides aquifer system is the southwest-northeast axis from Lachute to St. Janvier. The other recharge zones are the Oka and St. André Hills, the region from the airport to St. Eustache, from Grenville to St. Philippe, and the local recharge zone of southwest-northeast St. Vincent Crest. On the remaining territory, thick low permeability Champlain Sea clays confine the aquifer system. These conditions prevail in three southwest-northeast trending buried valleys: 1) du Nord River Valley, at the border with the Laurentian Highlands, 2) St. Hermas Valley, North of St. André Hills and St. Vincent Crest, and 3) St. Benoît Valley, between the St. Vincent Crest and Oka Hills. Bedrock depressions, filled with marine clay, are also found along the north-south segment of du Nord River, and at St. Joseph, East of Oka Hills. Finally, the clay reaches a thickness of more than 30 m in the eastern region of Ste. Anne-des-Plaines.

The main groundwater flow paths of the regional rock aquifer are generally from North to South (Fig. 5.2c). The potentiometric surface follows the bedrock or surface topography, and is higher in the preferential groundwater recharge areas. Cross-section A-A'

illustrates the groundwater flow conceptual model and presents the main hydrostratigraphic units adapted from Savard et al. (in press) (Fig. 5.2d). The unconfined conditions, that characterize areas of preferential groundwater recharge, are generally areas of elevated topography, sometimes with rock outcropping or with thin to thick permeable surface sediments, generally till. At distance from the recharge zone, the aquitard unit, consisting of thick low permeability Champlain Sea clays, confines the rock aquifer such as for buried valleys. Based on hydrogeological and geological properties, the aquifer system is divided into two distinct units: the highly fractured and the fractured rocks. The highly fractured rock consists of the first few meters of the sedimentary units that are more weathered, with fractures more connected and more effective, than the underlying rock. A mixed unit, consisting of highly fractured rock in hydraulic connection with sand and gravel, is also observed in the buried valleys and has a  $K_m$  (geometric mean hydraulic conductivity) of  $7.8 \times 10^{-4}$  m/s (Nastev et al., 2001). The lower unit of the aquifer system is the fractured rock that has a  $K_m$  of  $2.6 \times 10^{-5}$  m/s (Nastev et al., in prep b). The interface groundwater flow through the highly fractured rock and mixed unit is faster than the intermediate and deeper groundwater flow in the fractured rock, due to its higher hydraulic conductivity. Pieces of evidence of preferential interface flow in the highly fractured rock were obtained from isotopic data profiles of  $^3\text{H}$ ,  $^{14}\text{C}$  of dissolved inorganic carbon (DIC), and  $^{87}\text{Sr}/^{86}\text{Sr}$  where discrete groundwater samples were collected at different depths in open boreholes (Cloutier et al., in prep c).

### **5.2.2 Hydrogeochemistry**

Groundwater flow, from recharge to discharge zones, is subjected to geochemical processes that lead to the evolution of groundwater chemical composition. The groundwater geochemistry is thus controlled by numerous factors, such as : aquifer mineralogy, groundwater residence time, the hydrogeological context, mixing of groundwater of different origin, and anthropogenic contamination. Previous studies of the Basses-Laurentides aquifer system (Cloutier et al., in prep c; Cloutier et al., in prep a), demonstrated the importance of these factors on the present geochemistry of the groundwater.

The Basses-Laurentides sedimentary rock aquifer system has a highly variable groundwater geochemistry. An approach of dominant and mixed groundwater types, based on major ions concentrations, was used to classify the samples of the Basses-Laurentides into six dominant and four mixed groundwater types (Cloutier et al., in prep c). The distribution of groundwater types in the study area, as well as the descriptive statistics show that the hydrogeological conditions exert an important control on the geochemistry of the groundwater. The ten groundwater types were associated into four main groundwater groups, G1 to G4. The preferential recharge areas are characterized by groundwater of G1 (Ca-Mg-HCO<sub>3</sub>) and G4 (Ca-SO<sub>4</sub>, Na-SO<sub>4</sub>), and have modern tritiated groundwater. Submodern groundwater from G2 and G3 characterizes the aquifer under confined conditions, dominated by the groundwater types Na-HCO<sub>3</sub> (St. Hermas and du Nord River valleys, Ste. Anne-des-Plaines) and Na-Cl (St. Benoît Valley) respectively (see Fig. 5.2b for location of areas). Groundwater from G3 is also found locally in St. Hermas and du Nord River valleys, as well as Ste. Anne-des-Plaines. The distribution of minor ions, such as F<sup>-</sup> and Sr<sup>2+</sup>, is controlled instead by the geological units (Cloutier et al., in prep c).

Figure 5.3 is a Piper diagram of groundwater labeled with the groundwater groups. Groundwater samples are distributed in the various zones of the diamond-shaped field, mainly the Ca-Mg-HCO<sub>3</sub>, Na-HCO<sub>3</sub>, and Na-Cl zones. The seven groundwater samples from surface sediments, generally till, as well as two spring samples that are believed to flow in surface sediments, have a Ca-HCO<sub>3</sub> water type, and thus, belong to groundwater group G1. These nine samples are labeled as G1<sub>Till</sub>, as they were interpreted by Cloutier et al. (in prep c) to represent a geochemical groundwater end-member to the aquifer system (Fig. 5.3). G1<sub>Till</sub> thus represents the major ions geochemistry of the recharge water to the Basses-Laurentides aquifer system. Cloutier et al. (in prep c) showed that higher TDS values characterize samples of groundwater G3 (Na-Cl). Sample S77, located in the buried valley of St. Benoît, has the highest TDS of the wells sampled in the course of this project (calculated TDS = 11 337 mg/L). This sample was interpreted by Cloutier et al. (in prep c) to represent Champlain Sea water, a second geochemical end-member to the

aquifer system (Fig. 5.3). Thus, numerous geochemical processes are involved in this resultant present-day, highly variable groundwater geochemistry.

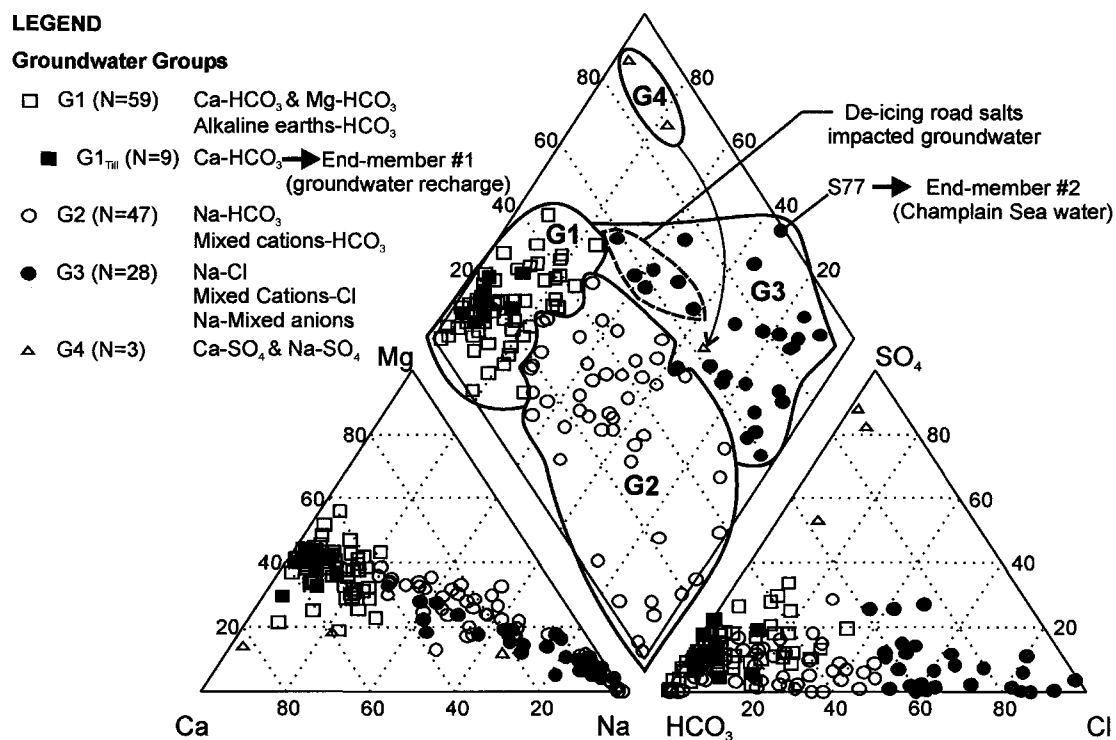


Figure 5.3. Piper diagram of groundwater of the Basses-Laurentides labeled with the groundwater groups (N: Number of samples) (modified from Cloutier et al., in prep a).

Cloutier et al. (in prep a) presented the geochemical processes that are effective for the evolution of groundwater groups, starting from the recharge zones and along groundwater flow paths. Dissolution of carbonates, calcite and dolomite, dominates in the preferential recharge areas resulting in Ca-Mg-HCO<sub>3</sub> (G1) groundwater. Ca<sup>2+</sup>-Na<sup>+</sup> ion exchange, groundwater mixing with Pleistocene Champlain Sea water as well as solutes diffusion from the marine clay aquitard are the main processes under the confined conditions resulting in Na-HCO<sub>3</sub> (G2) and Na-Cl (G3) groundwater, respectively. The marine invasion that resulted in the Champlain Sea is the cause of the salinization of the aquifer system (Cloutier et al., in prep a). A modern salinity source, de-icing road salts, was identified in a recharge area in the unconfined area of St. Janvier, leading to the occurrence of Na-Cl (G3) groundwater (Fig. 5.3) (Cloutier et al., in prep a).

## 5.3 METHODOLOGY

### 5.3.1 Hydrogeochemical dataset

The regional hydrogeochemical characterization of the Basses-Laurentides aquifer system, performed in 1999 and 2000, consisted of groundwater sampling of private, municipal and observation wells (Cloutier et al., in prep c). The first part of Figure 5.4 presents a summary of the sampling protocol and the methodology used for geochemical data collection. Groundwater samples were collected at 153 sites, to a maximum depth of about 140 m. The sampled sites, distributed over the whole region, cover all permeable hydrostratigraphic units: the surface sediments such as till, the sediments under clay deposits, the mixed unit consisting of highly fractured rock and sediments under clay deposits, and the fractured rock units. Of the 153 samples, 7 groundwater samples with an electro-neutrality above 10% were rejected as they were generally missing major ions. The sampling methodology is detailed in *Chapitre 1* and Cloutier et al. (in prep c). *In situ* field measurements were made on water samples for temperature (T), pH, electrical conductivity (EC), dissolved oxygen (DO), and redox potential (Eh). Groundwater samples were analyzed for major, minor and trace inorganic constituents for a total of 36 parameters, plus stable isotopes  $\delta^2\text{H}$ ,  $\delta^{18}\text{O}$  and  $\delta^{13}\text{C}_{\text{DIC}}$ , and some samples were also analyzed for  $^{87}\text{Sr}/^{86}\text{Sr}$ ,  $^3\text{H}$  and  $^{14}\text{C}$  of DIC. The complete hydrogeochemical dataset of the 146 sites is presented as a spreadsheet on Springer's server (Cloutier et al., in prep c).

### 5.3.2 Data preparation for the multivariate statistical analysis

As it was demonstrated, each sampling site is characterized by an elevated number of chemical and physical variables, making the regional hydrogeochemical study a multivariate problem. The multivariate statistical analysis is a quantitative and independent approach of groundwater classification allowing the definition of distinct groups of groundwater samples, and correlations between chemical parameters and groundwater samples. In this project, two multivariate methods are applied using

Statistica version 6.1 (StatSoft Inc., 2004), the hierarchical cluster analysis (HCA), and the principal components analysis (PCA).

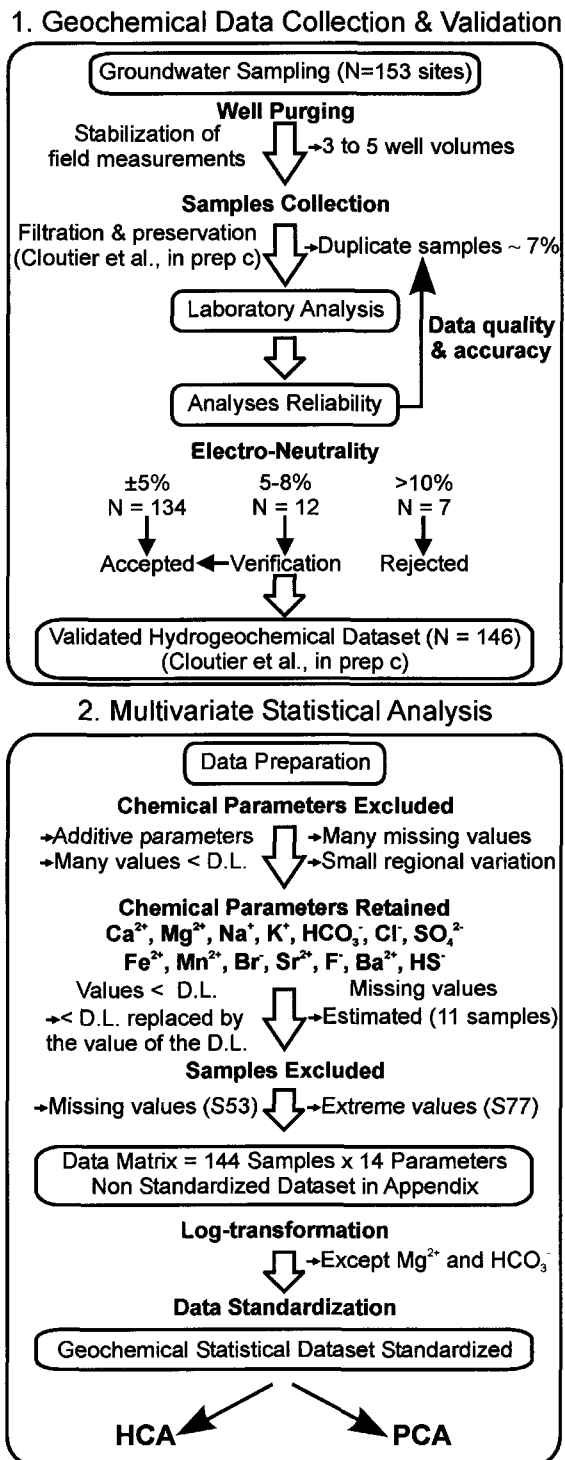


Figure 5.4. Methodological flow chart, from groundwater sampling to data analysis (N: Number of samples, D.L.: detection limit).

The second part of Figure 5.4 is a summary of the methodology used in the preparation of geochemical data for multivariate statistical analysis. The Appendix presents a subgroup of the hydrogeochemical dataset of Cloutier et al. (in prep c). This subgroup consists of the 146 groundwater samples and 14 parameters chosen to carry out the multivariate statistical analysis. These parameters include major constituents  $\text{Ca}^{2+}$ ,  $\text{Mg}^{2+}$ ,  $\text{Na}^+$ ,  $\text{K}^+$ ,  $\text{HCO}_3^-$ ,  $\text{Cl}^-$ , and  $\text{SO}_4^{2-}$ , as well as minor and trace constituents  $\text{Fe}^{2+}$ ,  $\text{Mn}^{2+}$ ,  $\text{Br}^-$ ,  $\text{Sr}^{2+}$ ,  $\text{F}^-$ ,  $\text{Ba}^{2+}$ , and  $\text{HS}^-$ . Thus, a certain number of parameters were excluded from the multivariate statistical analysis for the following reasons: parameters with additive characteristics such as EC and TDS, parameters with an elevated number of samples below the detection limit such as  $\text{NO}_3^-$ ,  $\text{PO}_4^{2-}$ ,  $\text{Al}^{3+}$  and most trace constituents, parameters missing or not analyzed for a large number of sampling site such as T, DO, Eh,  $\delta^{13}\text{C}_{\text{DIC}}$ ,  $^{87}\text{Sr}/^{86}\text{Sr}$ ,  $^3\text{H}$  and  $^{14}\text{C}$  of DIC, and parameters that show small regional variation such as  $\text{SiO}_2$ , pH,  $\delta^2\text{H}$  and  $\delta^{18}\text{O}$ .

For multivariate statistical analysis, the parameters with values of concentration lower than the detection limit, the censored data, have to be replaced. A number of methods exists to replace censored data (Alley, 1993; Güler et al., 2002). For this study, it was chosen to replace the censored data by the value of the detection limit. The indications of values lower than the detection limit were kept in the Appendix geochemical dataset to indicate which data were replaced for the analysis. Twelve sampling sites have missing values for one or two chemical parameters among the following:  $\text{SO}_4^{2-}$ ,  $\text{Fe}^{2+}$ ,  $\text{Br}^-$ ,  $\text{Sr}^{2+}$ ,  $\text{F}^-$ , or  $\text{HS}^-$ . In HCA, a missing value in a chemical parameter will automatically exclude the corresponding sample from the analysis. To avoid sample exclusion, an evaluation of the twelve sampling sites was done to see if the missing elements could be estimated by averaging values of nearby sampling sites. In the case of two samples with missing  $\text{SO}_4^{2-}$ , values were estimated from the electro-neutrality of the samples. Estimation of missing values was possible for 11 out of the 12 samples. All missing, and estimated values, are indicated in the Appendix geochemical dataset. Güler et al. (2002) discuss different statistical methods and geochemical relationships that can be used to estimate missing values. Site S53 was excluded from the multivariate statistical analysis as the estimation of missing values for  $\text{Fe}^{2+}$  and  $\text{F}^-$  could not be justified for this sample. A second site, S77, was also excluded from the analysis as its TDS is well above the other samples.

Thus the final dataset used for the multivariate statistical analysis is a data matrix of 144 sampling sites (observations) by 14 chemical parameters (variables). Table 5.1 compiles the descriptive statistics of the parameters for the 144 groundwater samples.

Table 5.1. Descriptive statistics for the 144 groundwater samples (concentrations in mg/L)

Parameters	Mean	Median	Minimum	Maximum	Standard deviation	Skewness
Ca <sup>2+</sup>	52.6	44.5	0.2	480	48.8	5.1
Mg <sup>2+</sup>	26.4	26	0.04	76	13.6	0.6
Na <sup>+</sup>	114.4	42	1.6	1260	191.0	3.3
K <sup>+</sup>	7.58	5.25	0.13	34	6.30	1.4
HCO <sub>3</sub> <sup>-</sup>	312.3	296.9	40.0	922.0	112.4	1.2
Cl <sup>-</sup>	129	35	0.1	1900	270	3.8
SO <sub>4</sub> <sup>2-</sup>	53.7	27.5	0.5	1200	116.6	7.8
Fe <sup>2+</sup>	0.4694	0.12	0.0007	15	1.4456	8.0
Mn <sup>2+</sup>	0.0783	0.0175	0.0003	0.93	0.1426	3.1
Br <sup>-</sup>	0.608	0.04	0.002	14.2	1.934	5.2
Sr <sup>2+</sup>	1.567	0.445	0.005	29	3.777	4.7
F <sup>-</sup>	0.54	0.32	0.04	3.2	0.60	2.3
Ba <sup>2+</sup>	0.187	0.13	0.001	1.1	0.192	2.5
HS <sup>-</sup>	0.14	0.02	0.02	4.7	0.57	6.6

Following the observation of the frequency distribution for each chemical parameter in mg/L, they were log-transformed except for Mg<sup>2+</sup> and HCO<sub>3</sub><sup>-</sup> that have a distribution close to the expected normal distribution. The other parameters are highly positively skewed (Table 5.1) and their frequency diagrams do not follow a normal distribution. Finally, standardization was applied to the twelve lognormal and two normal distributions to ensure that each variable is weighted equally. Standardization of the data ( $X_i$ ) results in new values ( $Z_i$ ) that have zero mean and are measured in units of standard deviation ( $s$ ). The standardized data are obtained by subtracting the mean of the distribution from each data and dividing by the standard deviation of the distribution,  $Z_i = (X_i - \text{mean})/s$  (Davis, 1986). Log-transformation of positively skewed chemical parameters, as well as data standardization, were done in other studies (Steinhorst and Williams, 1985; Schot and van der Wal, 1992; Güler et al., 2002).

### 5.3.3 Hierarchical cluster analysis (HCA)

The HCA is a data classification technique. There are different clustering techniques, but the hierarchical clustering is the one most widely applied in Earth sciences (Davis, 1986), and often used in the classification of hydrogeochemical data (Steinhorst and Williams, 1985; Schot and van der Wal, 1992; Ribeiro and Macedo, 1995; Güler et al., 2002).

In the Basses-Laurentides aquifer system, the standardized dataset of 144 sampling sites (observations) by 14 chemical parameters (variables) forms a 144 by 14 data matrix. Similarity measurements between every pair of sampling sites are computed and results in a symmetrical, 144 by 144, similarity matrix. For this project, the Euclidean distance was chosen as the distance measure, or similarity measurement, between sampling sites. The sampling sites with the larger similarity are first grouped. Next, groups of samples are joined with a linkage rule, and the steps are repeated until all observations have been classified. The levels of similarity at which observations are joined are used to construct the dendrogram (Davis, 1986). Visual observation of the dendrogram allows the grouping of samples into clusters. With this geochemical dataset, Ward's method was a more successful linkage rule than the other methods, such as the weighted pair-group average, to form clusters more or less homogenous and geochemically distinct from other clusters. Ward's method is distinct from other linkage rule because it uses an analysis of variance approach to evaluate the distances between clusters (StatSoft Inc., 2004). Other studies used Ward's method as linkage rule in their cluster analysis (Adar et al., 1992; Schot and van der Wal, 1992). The use of the Euclidean distance as a distance measure and Ward's method as a linkage rule was also found by Güler et al. (2002) to be the best combination in producing the most distinctive groups. Once the clusters are formed, the characteristics of each cluster are determined using descriptive statistics and graphical methods, and the relations between the clusters can be interpreted within the hydrogeological and geological contexts. Finally, the HCA can be performed on the variables instead of the observations, and this results for this study in a dendrogram of the 14 chemical parameters.

The Cluster Analysis module in the Multivariate Exploratory Techniques of Statistica version 6.1 was used to carry out the HCA. The Joining (tree clustering) is first selected as the clustering method. The second step is to select the 14 variables of the geochemical standardized dataset. This dataset is an input file of raw data, and consists of 144 rows (samples) by 14 columns (chemical parameters). The clustering of cases (rows) is chosen to cluster the samples, or the clustering of variables (columns) is chosen to cluster the chemical parameters. Next is the choice of the Amalgamation (linkage) rule (Ward's method in this study), and the choice of the Distance measure (Euclidean distance in this study). The results of the cluster analysis include the tree diagram for the 144 cases or 14 variables for clustering of samples or chemical parameters, respectively. The tree diagram is called a dendrogram in this paper.

### **5.3.4 Principal components analysis (PCA)**

The PCA is a data transformation technique that attempts to reveal a simple underlying structure that is presumed to exist within a multivariate dataset (Davis, 1986). It transforms a set of interrelated variables into a new coordinate system in which the axes are linear combinations of the original variables and are mutually orthogonal and uncorrelated (Alley, 1993). Thus a high number of variables, 14 chemical parameters for this study, is reduced to some composite and independent variables that are the principal components. The first component explains the largest quantity of variance in the dataset, the second explains the largest of the remaining variance, and so forth. The first few principal components, that usually explain the majority of the variance in the dataset, are useful to identify mechanisms and geochemical processes responsible for the observed variations.

PCA extracts the eigenvalues and eigenvectors from a covariance or a correlation matrix (Davis, 1986). From the standardized geochemical data matrix of the present study, the extraction by principal components was done on the symmetrical correlation matrix computed for the 14 variables. This method, that is concerned with interrelations between variables, is referred to by Davis (1986) as the R-mode technique. The number of

components to keep was based on the Kaiser criterion. According to the Kaiser criterion, only the components with eigenvalues greater than 1 are retained (StatSoft Inc., 2004). This means that all components that contain a greater variance than the original standardized variables are kept (Davis, 1986). After taking off the components with eigenvalues lower than 1, the next step is the rotation of the remaining principal axes in order to maximize the variance on the new axes. The method used was the Varimax normalized rotation, which moves each axes to positions such that projections from each variable onto the axes are either near the extremities or near the origin (Davis, 1986). Other studies used the Varimax rotation in their analysis (Usunoff and Guzmán-Guzmán, 1989; Melloul and Collin, 1992; Schot and van der Wal, 1992; Jayakumar and Siraz, 1997; Adams et al., 2001; Aiuppa et al., 2003).

The Factor Analysis module in the Multivariate Exploratory Techniques of Statistica version 6.1 was used to carry out the PCA. The first step is to select the 14 variables of the geochemical standardized dataset. Thus, it is the same input file dataset as for the HCA. Second, the principal components is chosen as the extraction method. According to the Kaiser criterion, the minimum eigenvalue is set to 1. Finally, Varimax normalized is selected as factor rotation.

As mentioned by Davis (1986), there is some confusion in the terminology related to PCA. Published studies called "factor analyses" are actually PCA (Davis, 1986). Statistica version 6.1 also uses the term factor when performing analysis with the principal components extraction method. In this paper, it was chosen to keep the terminology of Davis (1986) when discussing the results of the PCA. These results include the eigenvalues that represent the variance extracted by the components (named factors in Statistica), the principal component loadings (named factor loadings in Statistica) that quantify the importance of each chemical parameter for the components thus representing the degree of correlation between the original chemical parameters and the components, and the principal component scores (named factor scores in Statistica) that represent the influence of the components on the groundwater samples.

## 5.4 MULTIVARIATE STATISTICAL ANALYSIS

### 5.4.1 Hierarchical cluster analysis (HCA)

The main result of the HCA performed on the 144 groundwater samples is the dendrogram of Figure 5.5. As mentioned previously, the classification of the samples into clusters is based on a visual observation of the dendrogram. The phenon line was drawn across the dendrogram at a linkage distance of about 19 (Fig. 5.5). Thus, samples with a linkage distance lower than 19 are grouped into the same cluster. This position of the phenon line allows a division of the dendrogram into seven clusters of groundwater samples, C1 to C7. The cluster number assigned to the sampling sites are presented in the Appendix. Observation of the dendrogram reveals some indications of the level of similarity between the 7 clusters (Fig. 5.5). Samples from C1 and C2 are linked to the other clusters at an elevated distance, indicating that these samples are geochemically distinct from the ones of the other five clusters. Among these five clusters, C3 is the less similar as it has a high linkage distance to clusters C4 to C7. C4 and C5 have the lower linkage distance between the defined clusters, and thus, have the largest similarity between all clusters. It can be expected that the geochemistry of the samples of C4 has similarities with the ones of C5. Similarities between the geochemistry of samples from C6 and C7 are also expected as both clusters are also linked at a low distance.

To evaluate the characteristics of each cluster of samples, Table 5.2 presents the median values of geochemical and physical data, including the 14 chemical parameters used in the HCA, the TDS, the total hardness, and the casing depth of the wells. For these sampling sites, the casing depth generally represents the thickness of surface sediments as boreholes are generally open to the rock aquifer. Thus, an elevated median value of casing depth generally indicates the presence of thick low permeability Champlain Sea clays, suggesting that a majority of the samples of the cluster are under confined conditions. On the other hand, low median values of casing depth indicate a majority of samples under unconfined recharge areas. The median values of the majors ions were used to determine a median groundwater type for each cluster using the classification

approach presented by Cloutier et al. (in prep c), and are represented on Stiff diagrams (Fig. 5.5). Minor and trace constituents with elevated median concentrations are also indicated on Figure 5.5, and these are important characteristics of the clusters.

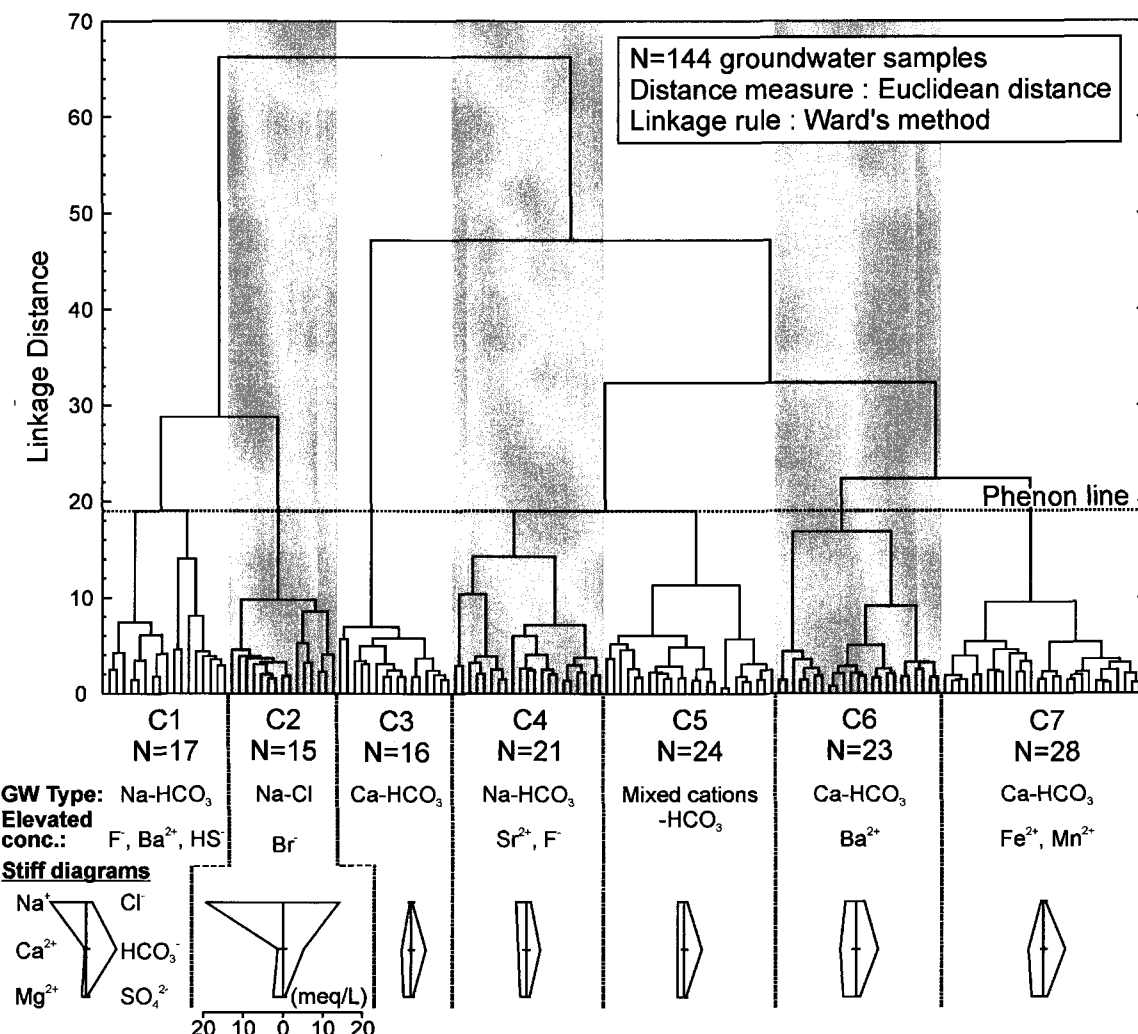


Figure 5.5. Dendrogram for the groundwater samples, showing the division into 7 clusters and the median Stiff diagram of each cluster (N: Number of samples, GW: Groundwater, conc.: concentrations).

Table 5.2. Geochemical and physical characteristics of each cluster (median concentrations in mg/L)

Parameters	C1	C2	C3	C4	C5	C6	C7
N	17	15	16	21	24	23	28
Ca <sup>2+</sup>	<u>7.9</u>	25.0	48.5	42.0	35.5	<b>78.0</b>	75.0
Mg <sup>2+</sup>	<u>14.0</u>	29.0	22.0	17.2	19.8	<b>39.0</b>	35.0
Na <sup>+</sup>	210.0	<b>450.0</b>	<u>6.5</u>	59.0	40.5	57.0	13.4
K <sup>+</sup>	14.10	<b>15.00</b>	<u>1.25</u>	4.50	4.80	10.00	4.15
HCO <sub>3</sub> <sup>-</sup>	<b>460.0</b>	321.3	226.9	<u>215.4</u>	274.6	346.4	332.8
Cl <sup>-</sup>	48.0	<b>510.0</b>	<u>8.1</u>	35.0	21.5	73.0	15.0
SO <sub>4</sub> <sup>2-</sup>	<u>9.0</u>	22.0	18.5	34.0	15.0	<b>58.0</b>	49.0
Fe <sup>2+</sup>	0.0190	0.2800	<u>0.0060</u>	0.0290	0.1550	0.1200	<b>0.5400</b>
Mn <sup>2+</sup>	0.0010	0.0580	<u>0.0003</u>	0.0110	0.0490	0.0150	<b>0.0885</b>
Br <sup>-</sup>	0.130	<b>2.300</b>	<u>0.010</u>	0.050	0.065	0.034	<u>0.010</u>
Sr <sup>2+</sup>	0.656	1.100	<u>0.095</u>	<b>2.000</b>	0.330	1.260	0.336
F <sup>-</sup>	0.99	0.48	<u>0.11</u>	<b>1.00</b>	0.31	0.34	0.16
Ba <sup>2+</sup>	<b>0.220</b>	0.120	<u>0.075</u>	0.100	0.140	0.210	0.140
HS <sup>-</sup>	<b>0.20</b>	0.04	<u>0.02</u>	<u>0.02</u>	<u>0.02</u>	<u>0.02</u>	<u>0.02</u>
TDS <sup>a</sup>	368	<b>1131</b>	276	310	<u>239</u>	509	383
Total hardness <sup>a</sup>	<u>72</u>	196	211	158	164	<b>355</b>	336
Casing depth (m)	21	<b>34</b>	10	14	27	15	<u>9</u>

N: Number of samples. Bold values: highest values. Underlined values: lowest values.

<sup>a</sup> Calculated (Total hardness as CaCO<sub>3</sub> ).

The descriptive statistics and the Stiff diagrams indicate that the seven clusters are geochemically distinct groups of samples (Fig. 5.5; Table 5.2). Samples from C1 have Na-HCO<sub>3</sub> groundwater, and are characterized by elevated concentrations in F<sup>-</sup>, Ba<sup>2+</sup> and HS<sup>-</sup> and by the lowest total hardness of all clusters. Samples from C2 have Na-Cl groundwater, and are characterized by elevated concentrations in Br<sup>-</sup>, and the highest TDS of all clusters. Samples from C3 have Ca-HCO<sub>3</sub> groundwater, and have the lowest concentrations for Na<sup>+</sup> and Cl<sup>-</sup>, as well as for all minor and trace constituents. Samples from C4 and C5 have Na-HCO<sub>3</sub> and mixed cations-HCO<sub>3</sub> groundwater respectively. The main differences between these two clusters are that C4 has higher Na<sup>+</sup> concentrations than C5, as well as elevated concentrations in Sr<sup>2+</sup> and F<sup>-</sup>. C5 has the particularity of having the lowest TDS of all clusters. Samples from C6 and C7, both Ca-HCO<sub>3</sub>

groundwater, have elevated total hardness and elevated  $\text{SO}_4^{2-}$  concentrations. C6 has elevated  $\text{Na}^+$  and  $\text{Cl}^-$  concentrations relative to C7, as well as elevated concentrations in  $\text{Ba}^{2+}$ . C7 is distinct from C6 by its elevated concentrations in  $\text{Fe}^{2+}$  and  $\text{Mn}^{2+}$ . The median values of casing depth is above 20 m for C1, C2 and C5, suggesting that a majority of the samples of these cluster are under confined conditions. The clusters C3, C4, C6 and C7 have median values of casing depth below 15 indicating a majority of samples under unconfined recharge areas.

The relation between chemical elements is studied by performing the HCA for the 14 chemical parameters. The lowest linkage distances in the dendrogram of Figure 5.6 are for  $\text{Na}^+$ ,  $\text{Br}^-$  and  $\text{Cl}^-$ . Other chemical elements linked at low distance include  $\text{Fe}^{2+}$  and  $\text{Mn}^{2+}$ ,  $\text{Ca}^{2+}$  and  $\text{Mg}^{2+}$ , as well as  $\text{Sr}^{2+}$  and  $\text{F}^-$ .

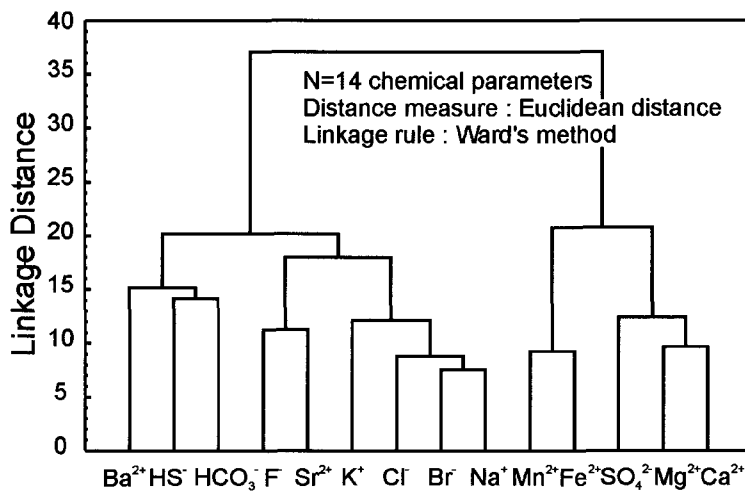


Figure 5.6. Dendrogram for the 14 chemical parameters.

#### 5.4.2 Principal components analysis (PCA)

Figure 5.7 is the scree plot of the PCA showing the eigenvalues for the fourteen components extracted. The first five components have eigenvalues greater than 1, and account for 78.3% of the total variance in the dataset. Varimax normalized rotation was applied to the first five principal axes in order to maximize their variance. Table 5.3 presents the principal component loadings for these five components, as well as their

respective explained variance. Loadings, that represent the importance of the variables for the components, are in bold for values greater than 0.7 (Table 5.3). Each component is characterized by a few high loadings, and many near-zero loadings, fulfilling the objectives of the rotation. As mentioned by Davis (1986), maximizing the variance implies maximizing the range of the loadings, which tends to produce either extreme, positive or negative, or near-zero loadings. The first two components explain 23% and 17.6% of the variance respectively, and thus, account for the majority of the variance in the original dataset. Components 3, 4 and 5 are not as important, and each of these three components explains about the same amount of variance, between 12% and 13.2%.

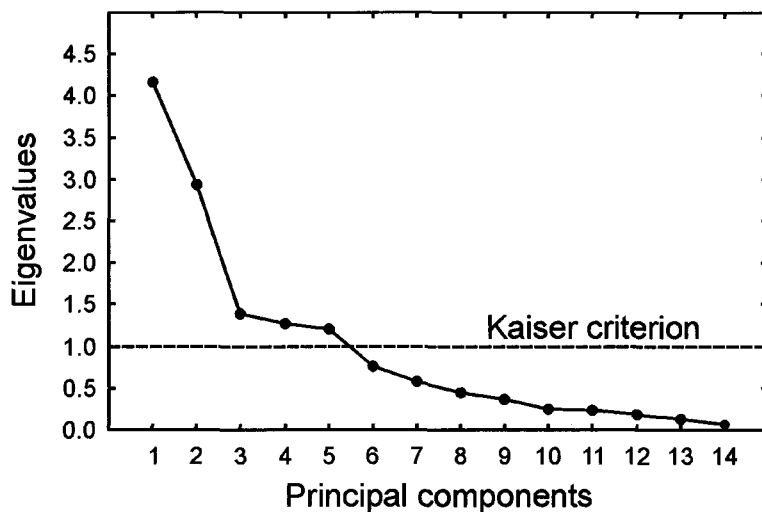


Figure 5.7. Scree plot (plot of eigenvalues) of the PCA.

To help visualize which chemical parameters are associated to each components, Figure 5.8 presents bar plots of principal component loadings for the five components. Component 1 explains the greatest amount of the variance, and is characterized by highly positive loadings in  $\text{Na}^+$ ,  $\text{Cl}^-$ , and  $\text{Br}^-$  (Fig. 5.8a). Because of the association of  $\text{Na}^+$ ,  $\text{Cl}^-$ , and  $\text{Br}^-$ , component 1 is defined as the "salinity" component. Component 2 is characterized by highly positive loadings in  $\text{Ca}^{2+}$  and  $\text{Mg}^{2+}$  (Fig. 5.8b). Thus, component 2 is defined as the "hardness" component. Loading is also high for  $\text{SO}_4^{2-}$  (Fig. 5.8b). Figure 5.9 summarizes this information by showing the position of the loadings of chemical parameters in the plane defined by the axes of components 1 and 2. The first

two components account for 40.6% of the variance in the hydrogeochemistry of the study area, indicating the regional importance of salinity and hardness in this aquifer system.

Table 5.3. Principal component loadings and explained variance for the five components with Varimax normalized rotation

Parameters	Component 1	Component 2	Component 3	Component 4	Component 5
Ca <sup>2+</sup>	-0.287	<b>0.839</b>	0.190	0.019	0.097
Mg <sup>2+</sup>	0.121	<b>0.851</b>	0.184	0.281	-0.151
Na <sup>+</sup>	<b>0.927</b>	-0.185	0.040	0.095	0.159
K <sup>+</sup>	0.600	0.058	0.203	0.425	0.373
HCO <sub>3</sub> <sup>-</sup>	0.371	0.013	-0.122	0.696	-0.256
Cl <sup>-</sup>	<b>0.886</b>	0.212	0.012	0.046	0.038
SO <sub>4</sub> <sup>2-</sup>	0.059	<b>0.778</b>	0.030	-0.334	0.116
Fe <sup>2+</sup>	0.097	0.116	<b>0.876</b>	0.077	0.064
Mn <sup>2+</sup>	0.046	0.176	<b>0.904</b>	-0.013	-0.083
Br <sup>-</sup>	<b>0.830</b>	-0.167	0.083	0.115	0.232
Sr <sup>2+</sup>	0.173	0.241	0.039	0.121	<b>0.850</b>
F <sup>-</sup>	0.463	-0.303	-0.104	-0.014	<b>0.701</b>
Ba <sup>2+</sup>	-0.034	0.028	0.226	<b>0.742</b>	0.267
HS <sup>-</sup>	0.184	-0.362	-0.241	0.473	0.356
Explained variance	3.222	2.471	1.842	1.676	1.754
Explained variance (%)	23.0	17.6	13.2	12.0	12.5
Cumulative % of variance	23.0	40.6	53.8	65.8	78.3

Bold values: loadings > 0.7.

Each of the last three components explains about 12.5% of variance, indicating that these components are related to more local effects than the first two components. Component 3 is clearly characterized by highly positive loadings in Fe<sup>2+</sup> and Mn<sup>2+</sup>, indicating a similar geochemical behavior for both elements (Fig. 5.8c). Component 4 is characterized by highly positive loadings in Ba<sup>2+</sup> (Fig. 5.8d). Loadings are also relatively high for HCO<sub>3</sub><sup>-</sup> and HS<sup>-</sup> as well. Finally, component 5 is characterized by highly positive loadings in Sr<sup>2+</sup> and F<sup>-</sup> (Fig. 5.8e).

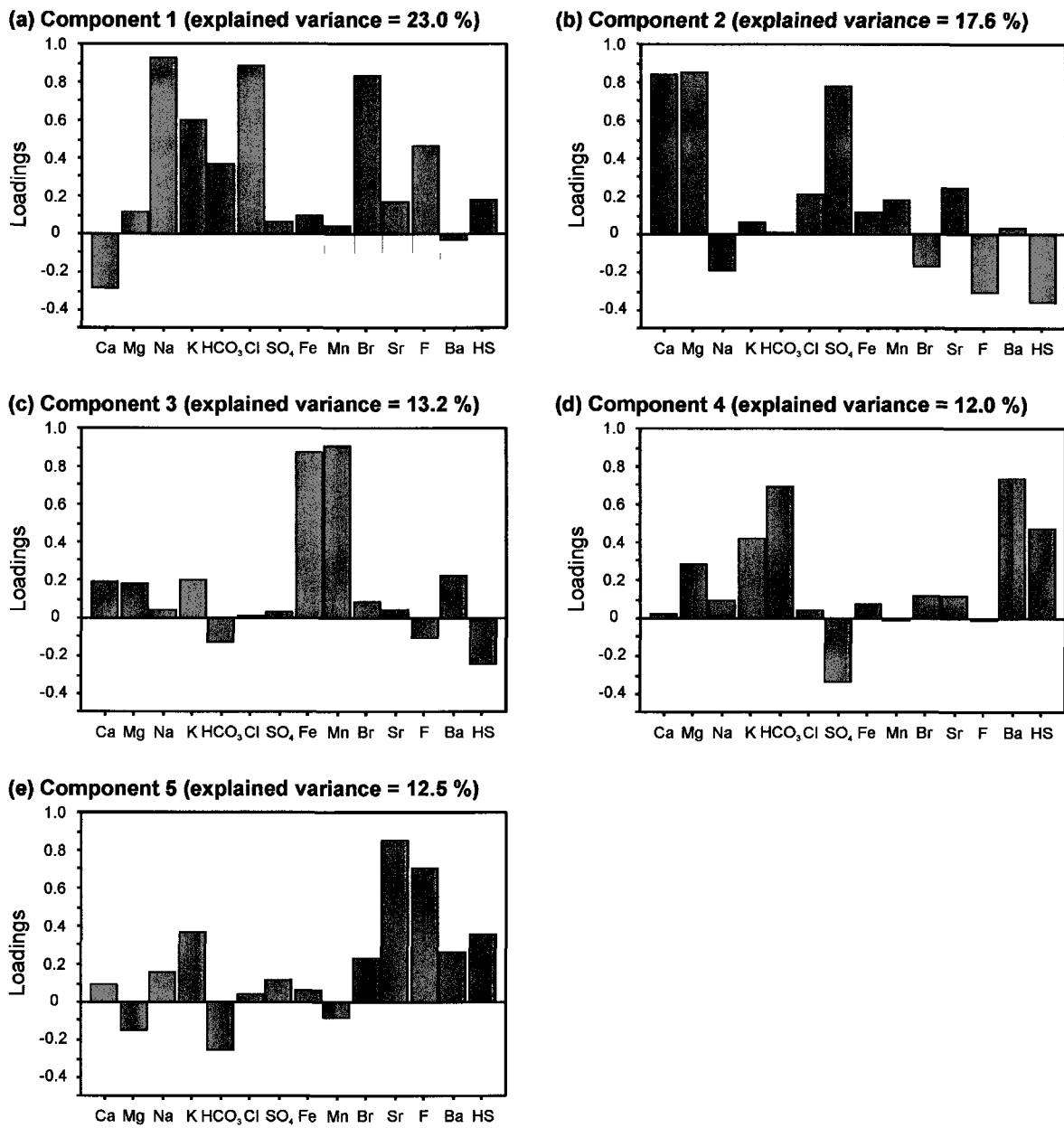


Figure 5.8. Bar plots of principal component loadings with Varimax normalized rotation for (a) component 1, (b) component 2, (c) component 3, (d) component 4, and (e) component 5.

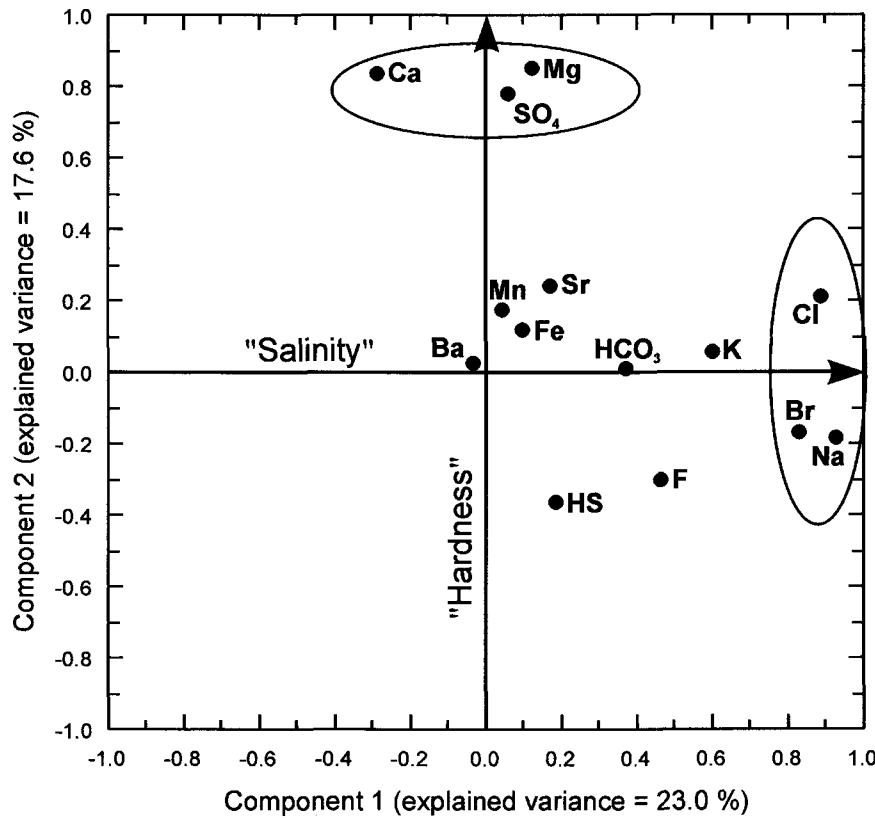


Figure 5.9. Plot of loadings for the first two components with Varimax normalized rotation.

## 5.5 GEOCHEMICAL INTERPRETATION

### 5.5.1 Groundwater groups and clusters

The Piper diagram of Figure 5.10 presents the groundwater samples labeled according to their respective cluster. Figure 5.11 provides for each of the seven groundwater clusters the distribution of samples into the four groundwater groups. Groundwater groups, as well as geological unit and hydrogeological condition, are presented in the Appendix. To allow a comparison with the groups defined by Cloutier et al. (in prep c), the groundwater group envelopes of Figure 5.3 are reported on the Piper diagram (Fig. 5.10). The majority of the samples from C1 belongs to G2 (Na-HCO<sub>3</sub>) and C2 to G3 (Na-Cl), and occupies the extreme lower and the right zones of the diamond-shaped field respectively. Samples from C1 have elevated Na<sup>+</sup> concentrations coupled to low Ca<sup>2+</sup> concentrations, suggesting

that  $\text{Ca}^{2+}$ - $\text{Na}^+$  ion exchange is an important geochemical process for samples of C1. Low  $\text{SO}_4^{2-}$  concentrations coupled to elevated  $\text{HS}^-$  concentrations suggest that sulfate reduction is also an important geochemical process for this cluster (Table 5.2). Samples from C2 have Na-Cl groundwater type, associated to elevated concentrations in  $\text{Br}^-$  (Fig. 5.5; Table 5.2). These characteristic samples were interpreted by Cloutier et al. (in prep a) to result from groundwater mixing with Pleistocene Champlain Sea water or from solutes diffusion from the marine clay aquitard.

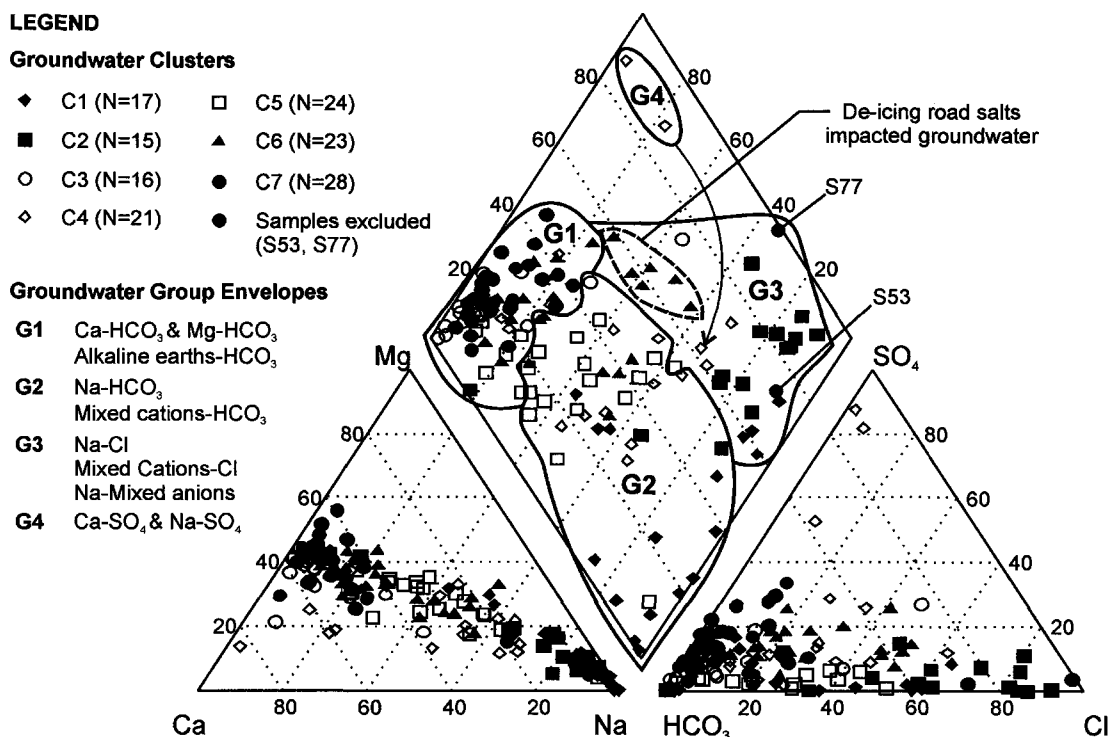


Figure 5.10. Piper diagram of the groundwater clusters with the groundwater group envelopes of Figure 5.3 (N: Number of samples).

The majority of the samples from C3 belongs to G1 (Ca-Mg-HCO<sub>3</sub>), and occupies the extreme left zone of the diamond-shaped field. Groundwater of G1 results from the dissolution of carbonates (Cloutier et al., in prep a). Samples from C4 and C5 are found in all groundwater groups, the majority of the samples being in G2 and G1, and thus are affected by  $\text{Ca}^{2+}$ - $\text{Na}^+$  ion exchange and carbonate dissolution. The samples occupy an intermediate zone between the extremes of C3, C1 and C2 (Fig. 5.10). All samples from C7 belong to G1, and C6 has samples in G1, G2 and G3 envelopes. Samples from C6 and C7, both Ca-HCO<sub>3</sub> groundwater, are thus affected by dissolution of carbonates (Fig. 5.5).

The samples defined by Cloutier et al. (in prep a) has being impacted by de-icing road salts all belong to C6, explaining the elevated  $\text{Na}^+$  and  $\text{Cl}^-$  concentrations of C6 relative to C7 (Table 5.2).

Clusters	Groups				N total
	G1	G2	G3	G4	
C1	0	<b>13</b>	4	0	17
C2	1	2	<b>12</b>	0	15
C3	<b>14</b>	1	1	0	16
C4	7	<b>9</b>	2	3	21
C5	8	<b>15</b>	1	0	24
C6	<b>10</b>	7	6	0	23
C7	<b>28</b>	0	0	0	28
N total :		68	47	26	3

Figure 5.11. Relationship between groundwater clusters and groups (N: Number of samples, Bold values : highest values).

### 5.5.2 Hydrogeological context

Figure 5.12 presents plots of the principal component scores for the first two components. As mentioned previously, the scores represent the influence of the component on the groundwater samples. In Figure 5.12a, the samples are labeled with the known hydrogeological conditions for the sampling sites. Grouping of samples is possible into this plane defined by the axes of components 1, the "salinity", and component 2, the "hardness". Samples from unconfined and semi-confined areas, as well as from surface sediments and springs, dominate in the upper-left quadrant of the diagram. Thus, these are characterized by elevated hardness and lower salinity. On the other hand, samples from confined areas dominate in the lower-right quadrant of the diagram, and thus are characterized by elevated salinity and lower hardness. The scores of the samples indicate that both first components, the "salinity" and the "hardness", are to some extent dependant, or related to, the hydrogeological context.

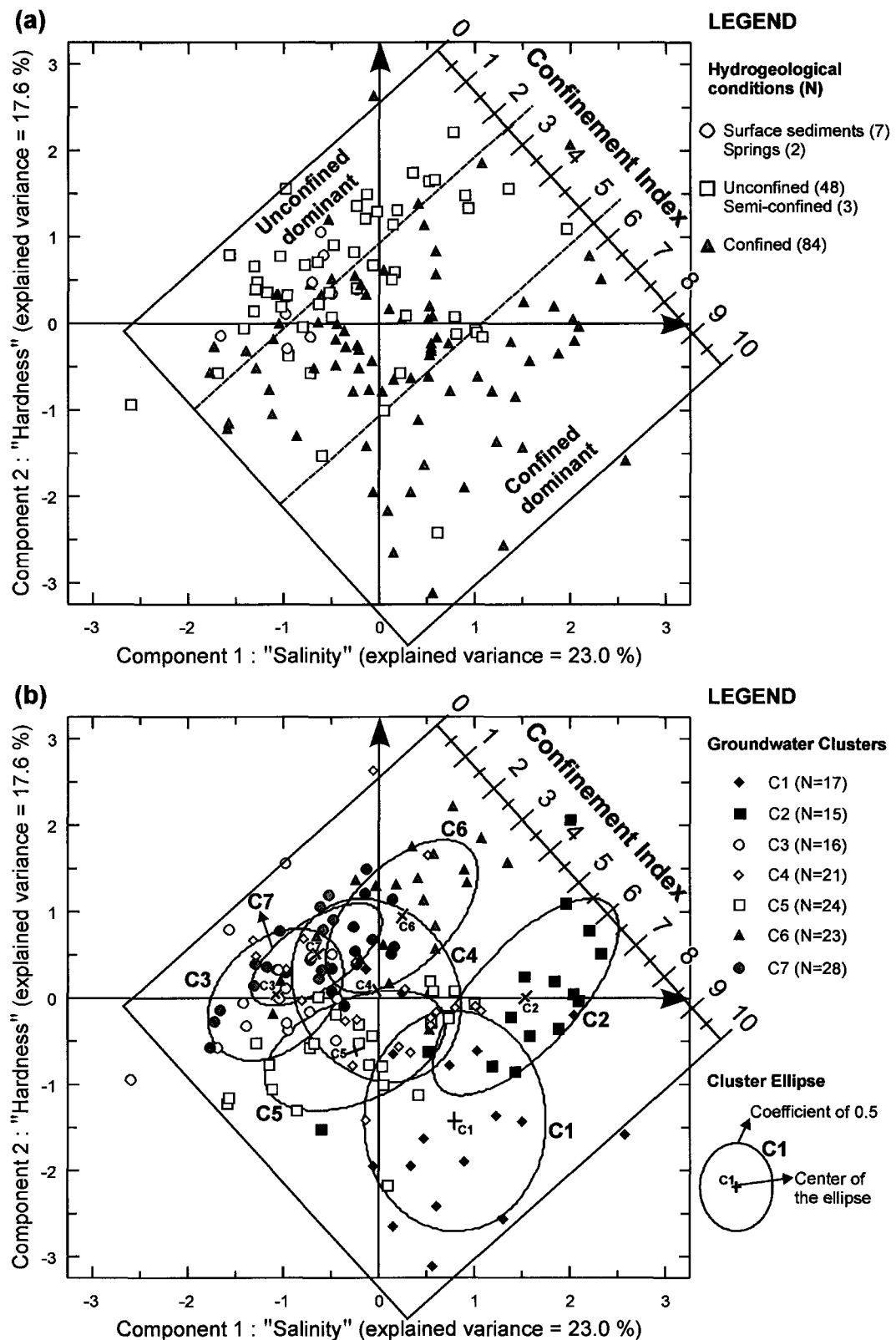


Figure 5.12. Plot of principal component scores for the first two components labeled with (a) the hydrogeological conditions, with the definition of the Confinement Index, and (b) the groundwater clusters, with ellipses at a coefficient of 0.5 for each cluster (N: Number of samples).

A Confinement Index (CI), based on the distribution of the scores of components 1 and 2, is defined to integrate both components into a unique parameter (Fig. 5.12a). CI ranges from unconfined conditions, at CI=0, to confined conditions, at CI=10. The index gives an "apparent" level of confinement for each sampling site. Confinement was chosen to relate components 1 and 2 as it is a parameter based on field knowledge of each sampling site. The "apparent" unconfined conditions dominate at a CI lower than 2.5, and the "apparent" confined conditions dominate at a CI above 5.5. From a CI of 2.5 to 5.5, the sampling sites are defined as "apparent" semi-confined.

Figure 5.12b presents the same data as Figure 5.12a, the groundwater samples being labeled this time with their respective cluster defined previously. Ellipses were drawn for each groundwater cluster at a coefficient of 0.5. The CI, defined in Figure 5.12a, is reported on Figure 5.12b to calculate the CI of each cluster ellipse. Table 5.4 presents the CI of the minimum, maximum, as well as center of the ellipses. Figure 5.12b is efficient at separating the various clusters in the plane defined by the axes of components 1 and 2, associated to "salinity" and "hardness" respectively. This diagram also provides a good visualization of the various groundwater types found in the Basses-Laurentides, as well as insight into the geochemical processes responsible of these variations.

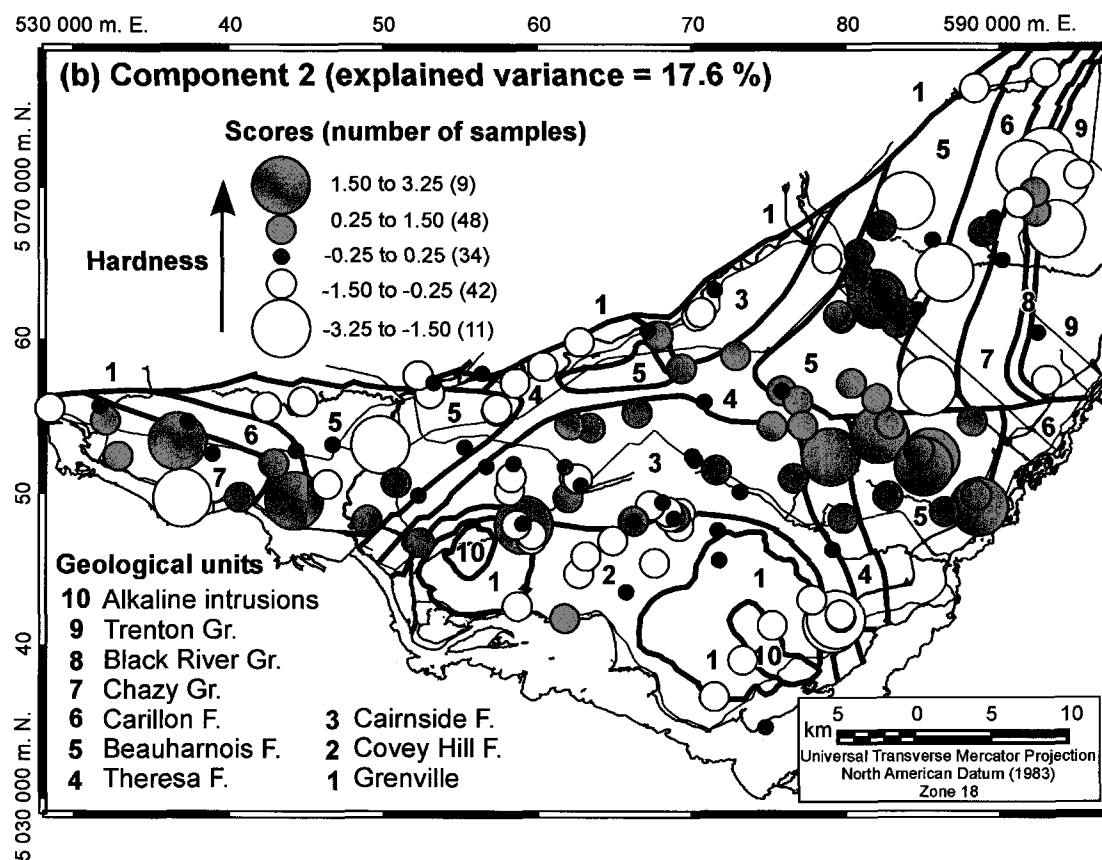
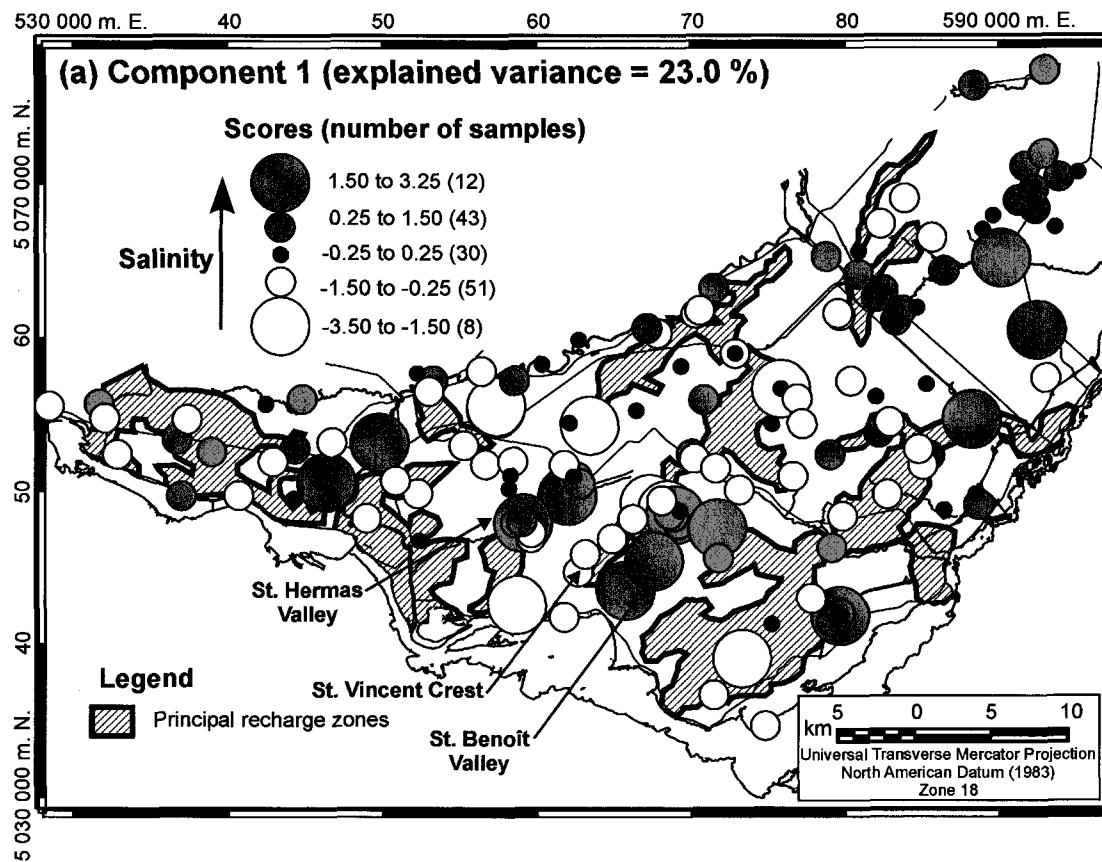
Table 5.4. Confinement Index for the cluster ellipses shown on Figure 5.12b

Cluster	Minimum	Center	Maximum
C1	5	7.25	9.5
C2	5	6.25	7.5
C3	1	2.25	3.5
C4	1.5	3.75	6
C5	3	4.5	6
C6	1.5	2.75	4
C7	1.5	2.25	3

Samples from C1 are in the lower-right quadrant of the diagram, and thus are associated to moderately elevated salinity coupled to low hardness (Fig. 5.12b). Samples from C2 are in upper-right and lower-right quadrant of the diagram, associated mainly to elevated salinity. Samples from C3 are all left of the component 1 zero line, on both side and relatively close to the component 2 zero line. These are associated mainly to low salinity. Samples from C4 are to the left and right of the component 1 zero line, on both side and relatively close to the component 2 zero line. Most of the samples from C5 are in the lower-left quadrant of the diagram, and are associated to low salinity as well as low hardness. Samples from C6 are above the component 1 zero line, on both side of the component 2 zero line. These samples are associated to elevated hardness, and some have moderately elevated salinity. Finally, samples from C7 are in the upper-left quadrant of the diagram, and thus are associated to elevated hardness coupled to low salinity.

### 5.5.3 Areal distribution and zoning

The relation between the components with the hydrogeological and geological contexts is better seen on the distribution maps of scores on Figure 5.13. Elevated scores for component 1 are associated to the aquifer system under confined conditions, as for St. Benoît Valley, St. Hermas Valley, St. Joseph, and the north-south segment of the du Nord River (Fig. 5.13a; see Fig. 5.2b for locations name). Numerous sites with moderately positive scores are found in the confined area of Ste. Anne-des-Plaines, and in the unconfined area of St. Janvier. Moderately to highly negative scores are found in the main recharge areas, from Lachute to St. Janvier, from the airport to St. Eustache, and the St. Vincent Crest (Fig. 5.13a). As it was seen, component 1 is defined by highly positive loadings in  $\text{Na}^+$ ,  $\text{Cl}^-$ , and  $\text{Br}^-$  (Fig. 5.8a). This association of chemical parameters is related to groundwater mixing with Champlain Sea water and solutes diffusion from the marine clay aquitard.  $\text{Ca}^{2+}$ - $\text{Na}^+$  ion exchange and local anthropogenic contamination are other processes that could be related to component 1. The negative loading of  $\text{Ca}^{2+}$ , in opposition to the positive loadings in  $\text{Na}^+$ , is consistent with the occurrence of ion exchange (Fig. 5.8a).



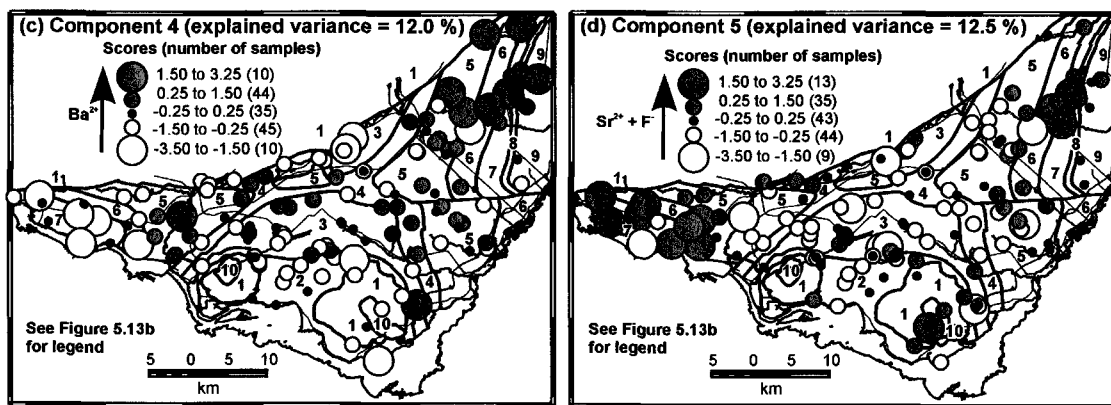


Figure 5.13. Regional distribution of principal component scores for (a) component 1 with the recharge zones (principal recharge zones to the rock aquifer modified from Paradis, in press c), (b) component 2, (c) component 4, and (d) component 5 with the geology (geological map modified from Rocher et al., in press) (see Fig. 5.2b for locations name).

The distribution map of the scores of component 2 illustrates the relation between the hardness and the geological units (Fig. 5.13b). Highly positive scores are associated with the dolostone of Theresa and Beauharnois formations, in the unconfined region around St. Janvier and from the airport to St. Eustache. Moderately to highly positive scores are also found in the dolostone and limestone formations of the Carillon Formation and Chazy Group in the western extremities of the study area. Moderately to highly negative scores are found in the confined area of Ste. Anne-des-Plaines, in the three buried valleys, and at St. Joseph. Component 2 is defined by highly positive loadings in  $\text{Ca}^{2+}$  and  $\text{Mg}^{2+}$ , as well as  $\text{SO}_4^{2-}$  (Fig. 5.8b). Geochemical processes important for component 2 could include dissolution of carbonate and sulfate minerals, and oxydation of pyrite. The negative scores in the limestone of Ste. Anne-des-Plaines are related to ion exchange.

The distribution map of the scores of component 3, related to concentrations in  $\text{Fe}^{2+}$  and  $\text{Mn}^{2+}$ , is highly variable and not presented here (presented in Fig. C2.1; *Appendice C2*). Highly positive scores are associated to both sandstone and dolostone, under confined and unconfined conditions. Highly positive loadings for both  $\text{Fe}^{2+}$  and  $\text{Mn}^{2+}$  indicate a similar geochemical behaviour for these parameters (Fig. 5.8c). The sources for these elements could be the dissolution of Fe-oxides, Mn-oxides, and the oxydation of sulfide minerals. The majority of the elevated scores for component 4 are associated to the dolostone and limestone formations in confined area of Ste. Anne-des-Plaines (Fig. 5.13c). Component

4 is related to concentrations in  $\text{Ba}^{2+}$ , indicating the interaction with Ba-bearing minerals. Loadings are also relatively high for  $\text{HCO}_3^-$  and  $\text{HS}^-$  as well (Fig. 5.8d). The positive loading for  $\text{HS}^-$  is associated to a negative loading for  $\text{SO}_4^{2-}$ , and could indicate the occurrence of sulfate reduction. The distribution map of the scores of component 5, associated to concentrations in  $\text{Sr}^{2+}$  and  $\text{F}^-$ , is clearly related to the geological units, and indicates the interaction with Sr-bearing and F-bearing minerals. Highly positive scores are associated to the dolostone and limestone formations at both West and East extremities of the study area, respectively the unconfined area from Grenville to St. Philippe, and the confined area of Ste. Anne-des-Plaines (Fig. 5.13d). Regarding the possible sources for components 4 and 5, Globensky (1987) mentioned that the presence of Ba and F was observed in the sedimentary formations of the St. Lawrence Platform.

Figure 5.14 shows the distribution map of the groundwater clusters for the 144 samples, and their relationships with the general hydrogeological conditions introduced previously. Geographical grouping is possible for the majority of the groundwater clusters. This geographical distribution of groundwater clusters was used by Cloutier et al. (in press) as a key information to divide the territory into seven groundwater quality zones, with the relative quality decreasing from zones *A* to *G*. In fact, the water quality zones were defined by combining the information from this multivariate statistical analysis, with the hydrogeological conditions map (Hamel et al., 2001), the surficial formations thickness map (Paradis, in press a), and by comparing geochemical parameters to guidelines for Canadian drinking water quality of Health Canada (2003) (Cloutier et al., in press).

Clusters C1, C2 and C5 characterize the aquifer system under confined conditions, coherent with their elevated median values of casing depth (Table 5.2). Samples from C1 dominate in the confined dolostone and limestone in the eastern area of Ste. Anne-des-Plaines (water quality zone *F*). Samples from C2 characterize the buried valleys of St. Benoît (water quality zone *G*). It is also found in other confined areas, as the middle of the buried valley of St. Hermas and at St. Joseph. Finally, samples from C5 are found mainly in the buried valley of St. Hermas, and in du Nord River Valley as well (water quality zones *A* and *B*).

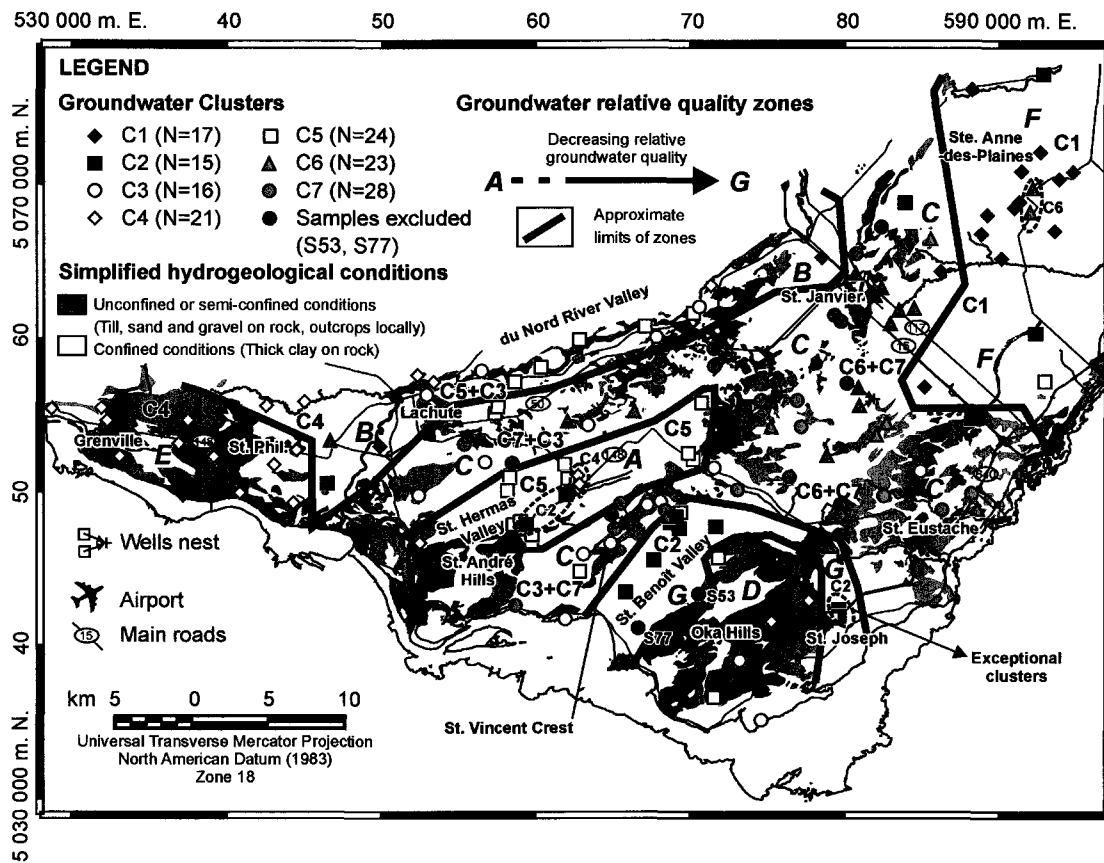


Figure 5.14. Zoning of groundwater quality: Regional distribution of groundwater clusters, and their relation to the groundwater relative quality zones and to the hydrogeological conditions (N: Number of samples; Areas with exceptional clusters are circled with dashed lines) (hydrogeological conditions map modified from Hamel et al., 2001; groundwater relative quality zones from Cloutier and Bourque, in press).

The preferential groundwater recharge areas are characterized by clusters C3, C4, C6 and C7 (Fig. 5.14). Samples from C4 are dominant in the limestone and dolostone of the area of Grenville to St. Philippe, in the western part of the territory (water quality zone E). The low linkage distance between C4 and C5 explains why two samples of C4 are found in the dominated C5 buried valley of St. Hermas (Fig. 5.5). Samples from C4 found in confined areas of the du Nord River Valley and in Oka Hills are related to geological factors as elevated concentrations in F<sup>-</sup> (Cloutier et al., in prep c). Samples from C3 and C7 characterize the main southwest-northeast recharge area between du Nord River and St. Hermas valleys, as well as the local recharge zone of St. Vincent Crest between St. Hermas and St. Benoît valleys (water quality zone C). The main distinction between these two clusters is the elevated concentrations in Fe<sup>2+</sup> and Mn<sup>2+</sup>, and elevated total hardness,

in C7 relative to C3 (Table 5.2). Samples from C3 are also found in the buried valley of du Nord River with samples of C5. The last area is the unconfined dolostone from the airport to St. Eustache and around St. Janvier that are dominated by clusters C6 and C7 (water quality zone C). The elevated median values for  $\text{Na}^+$  and  $\text{Cl}^-$  in C6 is due to samples contaminated by de-icing road salts along main roads in the area of St. Janvier. The other difference between both clusters is the elevated concentrations in  $\text{Fe}^{2+}$  and  $\text{Mn}^{2+}$  in C7 relative to C6 (Table 5.2).

From this areal distribution of principal component scores and groundwater clusters, it becomes apparent that the region can be divided into four main geochemical areas (see Fig. 5.15a): 1) the Western End, the area from Grenville to St. Philippe, 2) the Central Crests and Valleys, that include the three buried valleys and the crest from Lachute to the airport as well as St. Vincent Crest, 3) the Eastern Area, the area from the airport to St. Eustache and around St. Janvier, and 4) the Far Eastern End, the area of St. Anne-des-Plaines. This division will be used for the interpretation of the hydrogeochemical evolution of groundwater of the Basses-Laurentides aquifer system.

#### **5.5.4 Hydrogeochemical evolution**

Figure 5.15 presents relationships between the groundwater clusters, the main groundwater groups, and the Confinement Index (CI) obtained from components 1 and 2, and this, for the four main geochemical areas. The groundwater clusters are positioned according to their relative importance within each geochemical area. The CI of cluster ellipses calculated from Figure 5.12b (Table 5.4) and the "apparent" level of confinement defined in Figure 5.12a are integrated in Figure 5.15a. The figure also indicates the number of unconfined and confined sampling sites for each cluster according to field knowledge. In this case, the unconfined condition includes the semi-confined, as well as the surface sediments and spring samples. Figure 5.15b shows the relationship between the clusters and the main groundwater groups, and allows the classification of the clusters into levels of groundwater evolution. Median concentrations of selected elements from the clusters are also reported to facilitate the link between the groundwater evolution and

geochemical processes presented by Cloutier et al. (in prep a). As a complement to Figure 5.15, Table 5.5 presents the main geochemical areas, geological and hydrogeological contexts with their respective groundwater clusters as well as the main geochemical processes inferred responsible for the hydrogeochemical evolution of groundwater.

The Western End area, dominated by samples of cluster C4, is generally an unconfined region, with a strong hydraulic gradient, and consists of dolostone and limestone formations (Fig. 5.2). C4 is characterized mainly by groundwater groups G1 (Ca-Mg-HCO<sub>3</sub>) and G2 (Na-HCO<sub>3</sub>), thus modern recharge and evolved groundwater respectively (Fig. 15b). Its CI varies from 1.5 to 6, indicating "apparent" hydrogeological conditions from unconfined to confined (Fig. 5.15a). This "apparent" confined conditions is coherent with the presence of 9 sites under confined conditions in C4. On the other hand, most of these confined sites are in the Central Crests and Valleys area, in St. Hermas and the du Nord River valleys and in Oka Hills, and belong to G2. C4 has a strong geological signature on its water composition, as revealed by elevated concentrations in Sr<sup>2+</sup> and F<sup>-</sup>.

The Central Crests and Valleys area, dominated by samples of cluster C3, C5 and C2, has alternating confined buried valleys and unconfined crests, and consists of sandstone and dolostone formations. C3 is characterized by groundwater group G1, representing modern recharge groundwater (Fig. 5.15b). With a CI from 1 to 3.5, C3 is under "apparent" unconfined to semi-confined condition (Fig. 5.15a). Samples of C3 are generally located on unconfined crests, in preferential groundwater recharge areas. Thus these are affected by strong topographic gravity driven hydraulic gradient. With its low Cl<sup>-</sup> and Na<sup>+</sup> concentrations, C3 is clearly recharge groundwater. G1 groundwater is the result of dissolution of carbonates, calcite and dolomite, in the till and rock formations (Cloutier et al., in prep a).

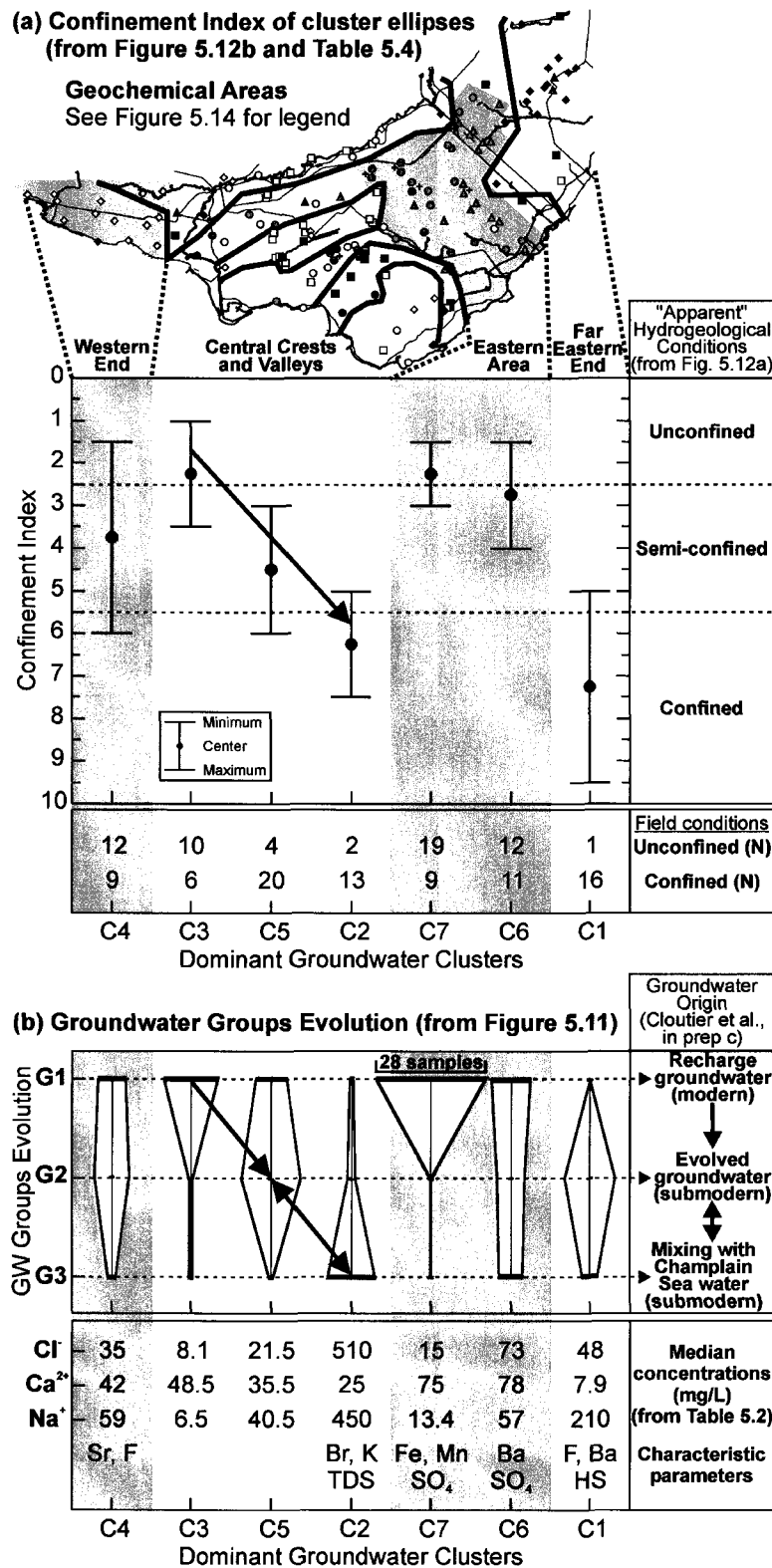


Figure 5.15. Evolution of groundwater geochemistry: (a) Range plot of the Confinement Index for the cluster ellipses related to the main geochemical areas (N: Number of samples), and (b) plot showing the relationship between the clusters and the groundwater groups evolution within the main geochemical areas (see Fig. 5.3 for definition of groundwater groups).

Table 5.5. Main geochemical areas, geological and hydrogeological contexts related to identified groundwater clusters. The main geochemical processes inferred responsible for the evolution of groundwater geochemistry are also indicated.

Geochemical Area (see Fig. 5.15a)	Western End	Central Crests and Valleys	Eastern Area	Far Eastern End
Main groundwater clusters	C4	C3, C5, C2	C7, C6	C1
Geological context	- Dolostone - Limestone	- Sandstone - Dolostone	- Dolostone	- Dolostone - Limestone
Hydrogeological conditions	Mainly unconfined	From unconfined to confined	Mainly unconfined	Confined
Relative hydraulic gradient	Strong	Strong to moderate	Small	Small
<b><u>GW Evolution : GW Group</u></b>				
Recharge GW	: G1	C4 (unconfined)	C3 (unconfined)	C7/C6 (unconfined)
Evolved GW	: G2	C4 (confined)	C5 (confined)	C6 (confined)
Ancient Champlain Sea water	: G3		C2 (confined)	C6 (contaminated)
Confinement Index (CI)	1.5 to 6	1 to 3.5 (C3) 3 to 6 (C5) 5 to 7.5 (C2)	1.5 to 3 (C7) 1.5 to 4 (C6)	5 to 9.5
High principal components scores	Component 5	Component 1 in buried valleys	Component 2	Components 4 and 5
Characteristic parameters	Sr, F	Br, K, TDS (C2)	SO <sub>4</sub> (C7/C6) Fe, Mn (C7) Ba (C6)	F, Ba, HS
Main geochemical processes	- Dissolution of carbonates  - Dissolution of Sr-bearing and F-bearing minerals	- Dissolution of carbonates (C3)  - Ion exchange (C5)  - Groundwater mixing (C2)  - Solute diffusion from marine clays (C2)	- Dissolution of carbonates and sulfates (C7/C6)  - Dissolution of Fe- oxides, Mn-oxides, and oxidation of sulfide minerals (C7)  - Anthropogenic NaCl (C6)	- Ion exchange  - Sulfate reduction  - Dissolution of F-bearing and Ba- bearing minerals

C5 is characterized by groundwater groups G1 and mostly G2, representing the evolution of modern recharge to evolved groundwater (Fig. 5.15b). With a CI from 3 to 6, C5 is under "apparent" semi-confined to confined condition (Fig. 5.15a). In fact, field conditions confirm that most of the sites are under confined conditions. Samples of C5

are located in the buried valleys, mainly St. Hermas Valley, and in intermediate locations between recharge zones and "stagnant" valley centers. The evolved groundwater of G2 is mostly affected by  $\text{Ca}^{2+}$ - $\text{Na}^+$  ion exchange (Cloutier et al., in prep a). This is consistent with the  $\text{Na}^+$  concentration of C5 larger than its  $\text{Ca}^{2+}$  and  $\text{Cl}^-$  concentrations.

C2 is dominated by the groundwater group G3 (Na-Cl), defined as evolved and ancient groundwater (Fig. 5.15b). C2 has a CI from 5 to 7.5, indicating "apparent" semi-confined to confined condition, and has most of its sites under field confined conditions. Samples of C2 are located in the buried valleys, mainly St. Benoît Valley, and in the central "stagnant" part of St. Hermas Valley and of St. Joseph. Groundwater mixing with Pleistocene Champlain Sea water as well as solutes diffusion from the marine clay aquitard are the main processes affecting the evolution of the evolved and ancient groundwater of G3 (Cloutier et al., in prep a). This is consistent with the elevated  $\text{Cl}^-$ ,  $\text{Na}^+$ ,  $\text{Br}^-$ , and  $\text{K}^+$  concentrations, as well as elevated TDS, of C2. The lowest linkage distances in the dendrogram are for  $\text{Na}^+$ ,  $\text{Br}^-$  and  $\text{Cl}^-$ , confirming the importance of the Pleistocene Champlain Sea water end-member in the Basses-Laurentides aquifer system (Fig. 5.6).

The Eastern Area, dominated by samples of clusters C7 and C6, is generally an unconfined plateau, with small hydraulic gradients, and consists mainly of dolostone of the Theresa and Beauharnois formations (Fig. 5.2). C7 is characterized exclusively by the recharge groundwater of G1 (Fig. 5.15b). Its CI varies from 1.5 to 3, indicating "apparent" hydrogeological conditions from unconfined to semi-confined (Fig. 5.15a). Actually, field data indicate that the majority of the sites are under unconfined conditions. The recharge groundwater of C7 is distinct from the one of C3 by its elevated concentrations in  $\text{Fe}^{2+}$  and  $\text{Mn}^{2+}$ , as well as its elevated concentrations in  $\text{Ca}^{2+}$ ,  $\text{Mg}^{2+}$ , and  $\text{SO}_4^{2-}$ , showing the influence of lithology on groundwater composition.

C6 is characterized by groundwater of the three main groups, particularly G1. Thus, this could indicate the evolution of recharge to evolved and ancient groundwater (Fig. 5.15b). With a CI from 1.5 to 4, C6 is in "apparent" unconfined to semi-confined condition (Fig.

5.15a). Actually, field conditions indicate that about half of the samples of C6 are under confined conditions. The presence of G3 groundwater is actually the result of a modern salinity source, and not of the mixing with ancient Champlain Sea water. As mentioned previously, the samples defined by Cloutier et al. (in prep a) as being impacted by de-icing road salts all belong to C6. This explains the presence of G3 groundwater of C6 in the area of St. Janvier, as well as its elevated  $\text{Na}^+$  and  $\text{Cl}^-$  concentrations relative to C7. As C7, C6 has elevated concentrations in  $\text{Ca}^{2+}$ ,  $\text{Mg}^{2+}$ , and  $\text{SO}_4^{2-}$  related to the geological context.

The Far Eastern End area, dominated by samples of cluster C1, is generally a confined region, with a relatively low hydraulic gradient, and consists of dolostone and limestone formations (Fig. 5.2). Pieces of evidences of preferential flow at the interface between the highly fractured rock and the marine clay were obtained from isotopic data profiles (Cloutier et al., in prep c). C1 is characterized mainly by the evolved groundwater groups G2, with some ancient G3 (Fig. 5.15b). Its CI varies from 5 to 9.5, indicating that "apparent" confined conditions dominate the Far Eastern End area, in agreement with the field knowledge (Fig. 5.15a). The evolved groundwater of G2 is the result of  $\text{Ca}^{2+}$ - $\text{Na}^+$  ion exchange (Cloutier et al., in prep a). For C1, elevated concentrations in  $\text{Na}^+$ , relative to  $\text{Ca}^{2+}$  and  $\text{Cl}^-$  concentrations, is coherent with ion exchange (Fig. 5.15b). C1 has also a strong geological signature on its water composition, as revealed by elevated concentrations in  $\text{F}^-$  and  $\text{Ba}^{2+}$ . Elevated  $\text{HS}^-$  concentrations, resulting of sulfate reduction, are also evidence of confined anoxic conditions.

Figure 5.15 and Table 5.5 indicate that the complete hydrogeochemical evolution of groundwater of this aquifer system, from modern recharge to evolved and ancient groundwater, is only found in the Central Crests and Valleys area. Figure 5.16 presents this complete hydrogeochemical evolution path using the cluster ellipses into the plane of principal components 1 and 2. The arrow from the center of the ellipse C3 to C5 is the ion exchange path from G1( $\text{Ca}-\text{Mg}-\text{HCO}_3$ ) modern recharge groundwater in "apparent" unconfined condition to G2 ( $\text{Na}-\text{HCO}_3$ ) evolved groundwater in "apparent" semi-confined condition. The double arrow between ellipses C5 and C2 represents the mixing of evolved

groundwater G2 with Champlain Sea water of G3 (Na-Cl) under "apparent" confined conditions. The fact that the hydrogeochemical evolution of groundwater can be represented in the plane of components 1 and 2 confirms the importance of these first two components, the "salinity" and the "hardness" in the hydrogeochemistry of the Basses-Laurentides aquifer system.

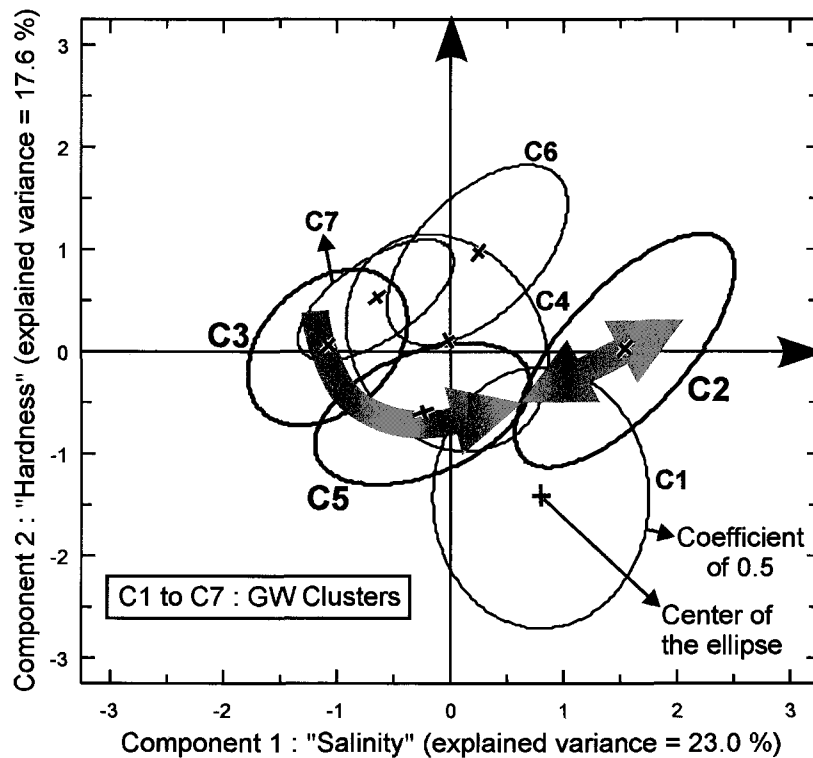


Figure 5.16. Hydrogeochemical evolution of groundwater of the Central Crests and Valleys area into the plane of principal components 1 and 2 (cluster ellipses from Fig. 5.12b).

## 5.6 CONCLUSION

The following conclusion first summarizes briefly the approaches used in the characterization and in the analysis of the geochemical data. The conclusion then focuses on the hydrogeochemical interpretation that allowed a global understanding of this aquifer system. The last part of the conclusion relates the findings of this study to the general problem of forecasting the long-term evolution of hydrogeological systems.

### 5.6.1 Approach and methodology

Regional groundwater samples were collected at 153 sites in the study area. This sampling density adequately characterized the aquifer system geochemistry under unconfined and confined conditions as well as for all geological formations. Moreover, all geochemical end-members were characterized, including precipitation and marine clay pore water. Based on available information, the hydrogeochemical data could be interpreted by considering both the geological and hydrogeological contexts. Numerous methods, including conventional approaches such as classification of groundwater types, descriptive statistics and graphical representations, where used, in combination to the hierarchical cluster analysis (HCA) and the principal components analysis (PCA) presented in this paper, to analyze and represent the geochemical data. This paper showed that combining these methods allowed a detailed interpretation of the geochemical evolution of groundwater in the area.

### 5.6.2 Interpretation of groundwater evolution

The interpretation of the groundwater evolution in the study area takes into account previous work which identified the origin of groundwater (Cloutier et al., in prep c), and recognizes the on-going geochemical processes as well as the Quaternary geological events that influenced groundwater geochemistry in this aquifer system (Cloutier et al., in prep a).

Based on major ion concentrations, the groundwater samples of the Basses-Laurentides were classified into six dominant and four mixed groundwater types that were associated into four main groundwater groups, G1 to G4 (Cloutier et al., in prep c). The interpretation of groundwater groups were done by considering sampling sites within their hydrogeological context instead of site by site. Thus, it was shown that the hydrogeological conditions exert a major control on the geochemistry of the groundwater. The preferential recharge areas are characterized by groundwater of G1 (Ca-Mg-HCO<sub>3</sub>) and G4 (Ca-SO<sub>4</sub>, Na-SO<sub>4</sub>), and have modern tritiated groundwater. Submodern groundwater from G2 (Na-HCO<sub>3</sub>) and G3 (Na-Cl) characterizes the aquifer under confined conditions. Samples obtained in the till belong to groundwater group G1, and were interpreted by Cloutier et al. (in prep c) to represent the major ions geochemistry of the recharge water and thus, it is a geochemical groundwater end-member of the aquifer system. Sample S77, located in the buried valley of St. Benoît, has a Na-Cl geochemistry very similar to the marine clay pore-water extracted in the middle of clay accumulations. Both of these were interpreted to represent Champlain Sea water, a second geochemical end-member to the aquifer system.

Numerous geochemical processes lead to the highly variable groundwater geochemistry observed today in the study area. Cloutier et al. (in prep a) identified that dissolution of carbonates, calcite and dolomite, dominates in the preferential recharge areas resulting in Ca-Mg-HCO<sub>3</sub> (G1) groundwater. In the aquifer system under confined conditions, Ca<sup>2+</sup>-Na<sup>+</sup> ion exchange is the cause of groundwater evolution to Na-HCO<sub>3</sub> type (G2). Groundwater mixing with Pleistocene Champlain Sea water and solutes diffusion from the marine clay aquitard are the causes of the occurrence of Na-Cl groundwater (G3) under confined conditions as well. The marine invasion that resulted in the Champlain Sea is the cause of the salinization of the aquifer system (Cloutier et al., in prep a). The conservative tracers Cl<sup>-</sup> and Br<sup>-</sup>, as well as δ<sup>18</sup>O, indicated that the original Champlain Sea water in the study area was a mixture of about 34% seawater and 66% freshwater (Pleistocene meteoric water and glacial meltwater). The current geochemistry of the groundwater indicates that the aquifer system is at different stages of desalinization, ranging from the original Champlain Sea water still present in hydraulically stagnant

areas of the aquifer to fully flushed conditions in the more active parts of the aquifer system, especially in recharge zones. A modern salinity source, de-icing road salts, was also identified in a recharge area in the unconfined area of St. Janvier, leading to the occurrence of Na-Cl (G3) groundwater. Thus, this interpretation of groundwater groups within the hydrogeological contexts defined the main geochemical processes, thus providing the meaning to these groups in terms of groundwater evolution.

To further refine geochemical interpretation, multivariate statistical methods, hierarchical cluster analysis (HCA) and principal components analysis (PCA), were applied to a subgroup of the dataset that consisted of 144 samples and 14 parameters ( $\text{Ca}^{2+}$ ,  $\text{Mg}^{2+}$ ,  $\text{Na}^+$ ,  $\text{K}^+$ ,  $\text{HCO}_3^-$ ,  $\text{Cl}^-$ ,  $\text{SO}_4^{2-}$ ,  $\text{Fe}^{2+}$ ,  $\text{Mn}^{2+}$ ,  $\text{Br}^-$ ,  $\text{Sr}^{2+}$ ,  $\text{F}^-$ ,  $\text{Ba}^{2+}$ , HS). The HCA classified the groundwater samples into seven geochemically distinct clusters, C1 to C7. Three clusters, C1, C2, and C5, characterize samples from the aquifer system under confined conditions. Samples that belong to the other four clusters, C3, C4, C6, and C7, are located mostly in preferential recharge areas. In addition to recognizing the importance of hydrogeological conditions on groundwater geochemistry, the distribution of clusters also identified the importance of the geological formations on minor and trace elements, such as  $\text{Fe}^{2+}$ ,  $\text{Mn}^{2+}$ ,  $\text{Sr}^{2+}$ ,  $\text{F}^-$  et  $\text{Ba}^{2+}$ . The first five components of the PCA account for 78.3% of the total variance in the dataset. A Confinement Index (CI), based on the distribution of the scores of the "salinity" component 1 and the "hardness" component 2, was defined to integrate both components into a unique parameter. Components 3 to 5 are related to more local and geological effects.

Relations were established between the seven groundwater clusters and the four groundwater groups. The majority of the samples from C3, C6, and C7 belong to G1 ( $\text{Ca}-\text{Mg}-\text{HCO}_3$ ), the majority of the samples from C1 belong to G2 ( $\text{Na}-\text{HCO}_3$ ), and the majority of the samples from C2 belong to G3 ( $\text{Na}-\text{Cl}$ ). Samples from C4 and C5 have a majority of samples from G2, with samples belonging to G1 as well. The scores of the samples calculated in the PCA indicated that both first components, the "salinity" and the "hardness", are to some extent dependant, or related to, the hydrogeological context. Scores of samples labeled with their clusters were represented in the plane defined by the

axes of components 1 and 2, and the Confinement Index (CI) was calculated for each cluster ellipse. Distribution maps of score were presented to establish the relations between the components with the hydrogeological and geological contexts. Elevated scores for component 1 are associated to the aquifer system under confined conditions. Highly positive scores for component 2 are associated with the dolostone of Theresa and Beauharnois formations, illustrating the relation between the hardness and the geological units. The distribution of components 3 to 5 are related to more local and geological effects. The distribution of groundwater clusters showed the geographical grouping was possible within the study area, and is related to the hydrogeological conditions as well as geological contexts.

The integration of all classification methods within the geological and hydrogeological contexts allowed the division of the region into four main geochemical areas, and these were used to refine the interpretation of the hydrogeochemical evolution of groundwater of the Basses-Laurentides aquifer system (Fig. 5.15; Table 5.5). Every geochemical area can be distinguished by the geological formations, hydrogeological contexts, hydraulic gradients, groundwater groups and clusters, CI, as well as main geochemical processes. Thus the following factors were recognized as influencing the evolution of groundwater identified in every geochemical areas: 1) geological characteristics including sedimentary rock type and till mineralogy; 2) hydrogeological characteristics represented by the level of confinement and the hydraulic gradient; and 3) geological history by the latest glaciation as well as Champlain Sea invasion. The main geochemical processes identified for this aquifer system are all apparent in the Central Crests and Valleys area. This hydrogeochemical evolution includes carbonate dissolution in recharge areas, to ion exchange in the confined areas, as well as groundwater mixing with Champlain Sea water, and solute diffusion from the marine clay aquitard in the deepest portions of the aquifer system. When interpreted within the hydrogeological and geological contexts, the division into main geochemical areas contributes significantly to the global understanding of the hydrogeochemical evolution of the Basses-Laurentides aquifer system while recognizing the significant impact of geological formations.

The presence of modern groundwater in the preferential recharge areas, identified by the distribution of Ca-Mg-HCO<sub>3</sub> water G1, tritium as well as the clusters, indicate that an important area of the aquifer system is vulnerable to contamination. The high NO<sub>3</sub><sup>-</sup> concentration at one site in a recharge area, and the detection of de-icing road salts, confirmed this vulnerability. Even though anthropogenic effects are limited so far, it is essential to protect the preferential recharge areas to prevent a potential degradation of groundwater quality.

### **5.6.3 Complementarity of interpretation methods**

Table 5.6 presents the relative advantages and disadvantages of the conventional and multivariate methods in their capacity to classify groundwater samples, define distinct geochemical zones, establish relationships between chemical elements, visualize geochemical data, and facilitate the interpretation of geochemical processes. The table shows that conventional and multivariate methods are complementary. There are undeniable advantages in combining the results of multivariate statistical analysis, to conventional methods such as groundwater types, descriptive statistics and graphical representations. Within these methods, the grouping into clusters is the link between the groundwater classification in groups and the Confinement Index defined from the first two components obtained from the PCA. It is this integration of methods that allowed the subdivision of the region into four main geochemical areas. Moreover, this integration allowed the recognition of the significant effects of geology and general context as well as the prevalent role of confinement on the highly variable geochemical signature of groundwater in the area.

Table 5.6. Relative advantages (+) and disadvantages (-) of conventional and multivariate methods for the classification, representation and interpretation of regional hydrogeochemical data

Objectives of the methods	Conventional GW Types and Groups	Hierarchical cluster Analysis (HCA)	Principal Components Analysis (PCA)
Classification of groundwater samples	+ Good method + Widely used + Comparison between aquifer systems possible - Limited to major ions - If numerous, GW types must be classified into GW groups	+ Good to form geochemically distinct groups (the clusters) + Unlimited parameters (chemical, isotopic, physical) - Descriptive statistics required to characterize the clusters - Clusters are specific to the studied aquifer system	- PCA is not a data classification method
Zoning of groundwater samples	+ Good and simple method + Integration of major ions	+ Good method + Finer than conventional as it integrates more parameters	+ Good - Zoning by component scores, less global than other methods
Relationships among chemical elements and groups of samples	+ Correlation, two parameters at the time + Descriptive statistics between GW groups	+ Correlations between all variables + Dendrogram of chemical parameters + Descriptive statistics between clusters	+ Loadings of components + x-y diagram of principal component scores labeled with groundwater clusters
Visualisation of data, by chemical elements, groups or geographical area	+ Simple and widely used (Piper, Stiff, Map of GW types) - Limited to major ions - Representation limited if numerous samples (needs grouping)	+ Good for distribution map of clusters + Conventional graphics to represent the clusters	+ Good map of scores + Conventional graphics to represent the principal component loadings and scores
Interpretation of geochemical processes	+ Direct link to potential geochemical processes + Comparison to previous studies (historical advantage) + Distribution of GW groups relative to hydrogeological and geological contexts	+ Dendrogram of chemical parameters provides information - Not easy for clusters alone (must use conventional graphics and methods)	+ Loadings of components + Distribution of scores relatives to hydrogeological and geological contexts

The possibility to compare results between aquifer systems is the main advantage of conventional groundwater types and groups (Table 5.6). For this reason, one can compare the groundwater types of an aquifer system to aquifer systems studied previously, giving a strong historical advantage to these methods. Moreover, the classification by groundwater types provides a direct link to potential geochemical processes. The HCA is efficient at forming geochemically distinct groups of samples (the clusters). The main advantage of HCA is that an unlimited number of parameters, including chemical, isotopic and physical parameters, can be included in the analysis. Because of this last possibility, HCA is finer than conventional methods regarding the geographical zoning of samples. The results of the PCA, including the loadings of components and the distribution of scores, offer advantages regarding the interpretation of geochemical processes. Finally, the x-y plot of component score, as Fig. 5.12b, provides a good visualization of the various groundwater types, as well as insights into the geochemical processes.

#### 5.6.4 Long-term system evolution

One of the future challenges of hydrogeology is the forecasting of the long-term evolution of hydrogeological systems. By studying the paleo-hydrogeology of an active groundwater system, and by showing that this system is still influenced by a major Quaternary geological event, this study presents an example of the long-term evolution of hydrogeological systems, and of the importance of groundwater as geological agent. Ingebretsen and Sanford (1998) presented numerous examples of the groundwater role in major geological processes, such as hydrocarbons migration, metamorphism and diagenesis. Tóth (1999) demonstrated the role of groundwater as geological agent in a regional, gravity-driven flow system. The present study identifies several processes discussed by Tóth (1999). The processes contribute to the evolution of groundwater, from the preferential recharge areas and along the flow system. A distinctive feature of the Basses-Laurentides aquifer system is that it was affected by a major geological event, rather than following a steady and continuous evolution. The Champlain Sea water invaded the aquifer system, thus imposing new hydrogeological and hydrogeochemical

conditions to the system about 10 000 years ago. These conditions are still present in some hydraulically stagnant parts of the system in the center of buried valleys, as well as in the marine clay pore water. These saline waters will continue to influence the geochemistry of the underlying aquifer system for a long time. This aquifer system thus shows how long it may take for systems to attain a geochemical "steady state" compared to a flow steady state. This hydrogeochemical study brings independent and new pieces of information on the aquifer system dynamic. Thus, a better understanding of the groundwater flow system and of the geochemical processes could emerge from the interaction between hydraulic and geochemical modeling.

## ACKNOWLEDGEMENTS

The project was carried out by the Geological Survey of Canada (GSC), in collaboration with INRS-Eau, Terre & Environnement (INRS-ETE), Université Laval and Environment Canada. Funding and logistical support for the study also came from the GSC, Economic Development Canada, Regional County Municipalities (RCM) of Argenteuil, Mirabel, Deux-Montagnes and Thérèse-de-Blainville, Department of the Environment of Québec, Conseil Régional de Développement-Laurentides, and Association des Professionnels de Développement Économique des Laurentides. Financial support for the first author was provided by the Natural Sciences and Engineering Research Council (NSERC) of Canada, Fonds québécois de la recherche sur la nature et les technologies, and INRS-ETE as postgraduate scholarships. We acknowledge the Department of the Environment of Québec for providing the analyses of inorganic constituents in groundwater. The drilling was partly supported by the Department of Transports of Québec. NSERC also supported R.L. and R.T. through operating grants. The work of all students involved in the project as field assistants, and the collaboration of the population of the RCM giving site access are greatly appreciated.

**APPENDIX**

Non standardized dataset of the multivariate statistical analysis (concentrations in mg/L; see note following the Table for details)

ID	GU	H	G	C	Ca <sup>2+</sup>	Mg <sup>2+</sup>	Na <sup>+</sup>	K <sup>+</sup>	HCO <sub>3</sub> <sup>-</sup>	Cl <sup>-</sup>	SO <sub>4</sub> <sup>2-</sup>	Fe <sup>2+</sup>	Mn <sup>2+</sup>	Br <sup>-</sup>	Sr <sup>2+</sup>	F <sup>-</sup>	Ba <sup>2+</sup>	HS <sup>-</sup>
S1	10	3	1	7	81	36	26	3.8	367.5	49	22	1.4	0.15	0.02	0.24	0.2	0.22	0.02
S2	6	0	1	7	76	39	21	6.5	320.3	72	34	0.52	0.069	0.04	0.34	0.24	0.22	<0.02
S3	10	3	1	7	53	23	3.7	0.76	214.3	0.6	49	0.34	0.3	<0.01	0.107	0.04	0.06	<0.02
S4	5	0	1	7	87	27	49	4.7	338.2	66	50	0.84	0.08	0.04	0.45	0.06	0.07	<0.02
S5	5	1	1	7	83	47	10.1	4.8	414.8	15	80	0.48	0.028	<0.01	0.32	0.2	0.17	0.02
S6	10	3	1	7	84	44	9.4	4.6	436.5	0.8	75	0.97	0.13	<0.01	0.42	0.34	0.01	0.02
S7	6	0	1	7	72	28	46	5	318.9	37	130	2.8	0.53	0.03	0.49	0.22	0.07	<0.02
S8	10	3	1	7	95	26	7.2	13	368.5	15	50	0.67	0.44	0.01	0.143	0.15	0.06	0.03
S9	10	3	1	3	48	24	3	1.2	238.3	6.1	15	0.007	<0.0003	0.0081	0.06	0.12	0.02	<0.02
S10	5	1	1	7	74	40	6.8	1.7	461.3	13	12	1.2	0.17	0.008	0.16	0.08	0.22	0.04
S11	8	1	1	5	27	14.3	13	3.7	179.8	1.3	10	0.7	0.037	0.01	0.177	0.24	0.05	<0.02
S12	8	1	1	5	35	17	7.5	3.2	179.3	2.4	21	0.026	0.18	<0.01	0.177	0.22	0.16	<0.02
S13	11	1	2	5	42	23	35	2.7	274.6	29	9	0.1	0.36	0.15	0.23	0.3	0.32	<0.02
S14	11	1	2	5	56	24	74	4.7	295.0	76	8.5	0.064	0.015	0.41	0.09	0.34	0.14	0.02
S15	7	1	1	3	56	24	6.1	1.3	239.1	5.1	15	0.004	0.015	0.02	0.09	0.12	0.1	0.02
S16	8	1	3	2	110	76	485	13	242.7	940	95	0.28	0.19	4.4	0.87	0.25	0.12	0.04
S17	7	0	1	4	52	29	24	2.9	295.4	18	34	0.005	0.029	0.04	0.56	0.45	0.1	0.02
S18	11	1	2	5	32	23	100	6.7	294.7	120	16	0.021	0.058	0.4	0.36	0.47	0.14	0.03
S19	2	1	2	6	61	30	110	13	427.9	73	85	0.49	0.096	0.38	2.5	0.48	0.3	0.06
S20	1	1	2	1	2.4	2.7	180	8.8	426.4	2	2	0.013	0.0008	0.07	0.17	1.3	0.04	0.58
S21	1	1	2	1	25	25	100	18	349.0	73	9	0.011	0.009	0.13	1.09	0.54	0.23	3.7
S22	3	1	2	1	3.1	3.8	220	16	509.7	15	20	0.043	0.002	0.11	0.72	1.5	0.4	0.2
S23	1	1	2	1	3.1	1.7	300	9.5	489.3	170	0.5	0.009	0.0008	1.31	0.656	1.7	0.06	0.51
S24	4	1	2	1	38	30	77	14	366.5	26	65	0.019	0.003	0.09	2	0.86	0.8	0.34
S25	4	1	2	2	37	29	180	12	454.6	140	<1	0.32	0.002	0.67	2.3	0.73	0.86	0.04
S26	3	1	3	1	15.9	14.3	560	16	449.3	620	110	0.003	0.0006	6.5	3.1	2.5	0.04	3.4
S27	4	1	2	1	25	28	96	14	362.3	48	33	0.099	<0.0003	0.29	1.6	0.72	0.67	0.17
S28	3	1	2	1	9.8	14.7	210	30	579.5	90	9	0.006	0.0007	0.48	9.2	1.4	0.38	0.96
S29	2	1	2	1	5.9	14	190	14.1	552.8	10	<0.5	0.15	0.003	0.07	1	0.93	0.12	0.04
S30	3	1	1	6	94	39	54	17	426.8	64	95	0.46	0.17	0.16	1.7	0.28	0.2	<0.02
S31	5	0	1	7	81	41	18.4	12	332.3	35	120	0.16	0.092	0.017	0.37	0.13	0.16	<0.02
S32	5	0	1	2	35	22	17.2	9.8	284.9	1.3	<1	0.096	0.004	14.2	0.4	0.47	0.48	0.24
S33	5	0	1	7	77	38	14.1	3.6	261.0	35	130	2.1	0.3	0.033	0.2	0.11	0.13	0.02
S34	5	1	3	6	110	55	140	7.4	405.5	260	80	0.016	0.017	0.06	0.29	0.14	0.07	<0.02
S35	7	1	1	7	64	34	15	4.3	333.1	8.3	47	0.72	0.049	0.009	0.346	0.25	0.17	<0.02
S36	6	0	1	6	140	56	57	34	494.9	85	170	0.034	0.007	0.017	0.154	0.1	0.08	<0.02
S37	5	0	1	6	130	45	57	1.9	473.0	90	110	0.006	0.01	0.023	0.195	0.1	0.11	<0.02
S38	5	0	1	3	92	47	4.5	0.13	390.9	10	75	0.013	<0.0003	0.04	1.037	0.18	0.09	<0.02

## Non standardized dataset of the multivariate statistical analysis (next)

ID	GU	H	G	C	Ca <sup>2+</sup>	Mg <sup>2+</sup>	Na <sup>+</sup>	K <sup>+</sup>	HCO <sub>3</sub> <sup>-</sup>	Cl <sup>-</sup>	SO <sub>4</sub> <sup>2-</sup>	Fe <sup>2+</sup>	Mn <sup>2+</sup>	Br <sup>-</sup>	Sr <sup>2+</sup>	F <sup>-</sup>	Ba <sup>2+</sup>	HS <sup>-</sup>
S39	5	0	1	6	56	33.4	25	8.7	309.5	10	55	0.097	0.013	0.02	2.072	(0.14)	0.24	0.04
S40	5	0	2	6	51	27	42	9.4	310.0	10	45	0.014	0.01	0.03	1.49	0.66	0.52	0.04
S41	8	1	3	2	21	17	240	12	311.8	330	50	1.5	0.15	1.1	0.46	0.39	0.04	0.04
S42	11	1	3	2	19.5	30	240	15	321.3	290	15	0.12	0.085	1.01	(0.734)	0.51	0.13	(0.025)
S43	7	1	2	6	16	26	82	8	295.8	63	15	0.12	0.017	0.24	1.272	0.62	0.13	(0.025)
S44	7	1	1	7	46	32	14.7	4.4	332.5	<0.1	22	0.5	0.12	0.008	0.48	0.29	0.27	(0.025)
S45	7	1	3	2	18	55	1260	16.8	276.8	1900	15	0.23	0.043	7	1.2	0.42	0.25	(0.025)
S46	8	1	2	2	13	12.6	240	7.8	348.7	200	24	0.11	0.13	1.2	0.28	0.49	0.08	0.03
S47	7	1	2	5	25	18.6	61	4.9	299.9	15	9.5	0.1	0.33	0.08	0.44	0.36	0.19	<0.02
S48	7	0	1	3	47	21	1.6	0.56	252.1	1	2	0.006	<0.0003	<0.01	0.06	0.06	0.02	0.02
S49	7	0	1	3	57	25	1.7	0.6	275.3	1.9	9.5	0.015	0.003	<0.01	0.051	0.05	0.02	0.02
S50	8	0	1	3	35	15.1	6.3	1.4	167.7	11	9	0.004	<0.0003	<0.01	0.08	0.1	0.04	0.03
S51	8	1	3	2	28	28	460	16	118.8	630	120	1	0.058	2.3	0.91	0.32	0.03	0.07
S52	7	0	1	7	63.2	27	19	2.3	286.0	15	55	1.4	0.56	0.05	0.22	0.13	0.17	0.03
S53	11	1	3	n.a.	11.4	7.2	240	2.8	179.1	280	12	n.a.	0.009	1.2	1.3	n.a.	0.25	0.09
S54	5	0	3	2	41	32	320	28	439.9	340	140	(0.039)	0.003	0.59	2.5	0.81	0.02	0.02
S55	1	1	3	2	100	24	690	11	364.3	1000	22	0.52	0.029	13	0.2	1.7	0.17	0.04
S56	6	1	3	5	24	15.2	93	15	227.6	150	3.5	0.15	0.029	0.56	0.37	0.39	0.47	0.07
S57	3	1	1	4	48	9.5	22	2.4	178.7	35	23	0.003	0.037	0.046	0.35	0.31	0.1	<0.02
S58	7	1	1	5	26	9.7	12.3	4.1	143.0	3.2	16	0.026	0.017	0.01	0.31	0.24	0.13	<0.02
S59	12	3	1	3	64	29	7.4	0.77	274.4	13	27	0.006	0.002	<0.01	0.05	0.06	0.03	0.03
S60	6	0	2	5	38	27	120	11	274.9	140	27	0.36	0.039	0.67	0.36	0.26	0.06	0.06
S61	7	0	3	4	31	16.6	150	8.3	154.0	210	55	0.091	0.034	0.66	1.1	0.61	0.07	<0.02
S62	7	1	3	3	20	6	27	0.89	40.0	44	34	0.01	0.0004	0.016	0.11	0.1	0.06	<0.02
S63	4	0	2	4	31	20	54	4.5	202.1	63	43	0.064	<0.0003	0.22	3.5	2.3	0.11	<0.02
S64	5	1	2	4	19	8.8	44	5.2	142.5	33	3	0.039	0.053	0.119	0.57	1.1	0.14	0.02
S65	5	1	2	4	35	13.1	77	7	178.3	57	88	0.12	0.008	0.21	0.57	1.6	0.04	0.1
S66	3	0	1	4	64	24	12.7	4.1	285.5	5	43	0.041	0.007	0.004	17	1	0.14	0.04
S67	5	1	3	2	12.7	26	450	22	492.7	510	17	0.61	0.012	1.9	1.8	0.91	0.12	0.04
S68	4	1	4	4	480	48	21	5.3	181.3	20	1200	0.46	0.005	<0.01	15	1.3	0.004	0.03
S69	4	0	1	4	61	31	27	1.6	243.0	75	45	0.5	0.018	<0.01	29	0.59	0.28	0.04
S70	6	0	2	5	18.6	14.5	41	12	198.8	28	10	0.59	0.039	0.1	0.21	0.32	0.13	0.02
S71	7	1	2	6	33	23	86	14	262.6	71	68	0.33	0.011	0.23	1.4	0.82	0.15	0.06
S72	5	0	3	6	87	46	180	8.6	344.4	250	210	0.47	0.027	0.62	1.99	0.35	0.06	<0.02
S73	5	0	1	7	120	44	22	6.6	426.8	15	130	0.074	0.033	0.02	0.9	0.32	0.08	<0.02
S74	5	0	1	7	85	42	5.6	1.2	354.7	38	68	0.56	0.64	<0.01	0.17	0.12	0.05	0.02
S75	6	0	1	7	81	35	5.3	2.3	356.6	5	65	0.13	0.013	0.02	0.29	0.16	0.22	<0.02
S76	5	0	1	7	82	37	34	5.5	354.9	47	90	0.12	0.01	0.06	1.2	0.25	0.1	<0.02
S77	8	1	3	n.a.	790	390	3100	26	116.2	6500	350	2.1	0.58	23	22.6	0.1	0.04	<0.02
S78	3	0	4	4	210	38	90	7.2	117.1	40	660	0.62	0.008	0.2	12	3.1	0.02	0.04
S79	3	0	1	4	62	26	7.4	1.3	286.7	12	30	0.016	0.0008	0.003	6.1	0.29	0.09	0.04
S80	4	0	1	4	64	16.1	16.9	3.5	268.4	24	20	0.29	0.012	0.05	19	0.56	0.14	0.07
S81	3	0	2	1	0.2	0.04	150	0.21	327.2	30	45	0.024	0.001	<0.01	0.02	0.39	0.05	0.02

## Non standardized dataset of the multivariate statistical analysis (next)

ID	GU	H	G	C	Ca <sup>2+</sup>	Mg <sup>2+</sup>	Na <sup>+</sup>	K <sup>+</sup>	HCO <sub>3</sub> <sup>-</sup>	Cl <sup>-</sup>	SO <sub>4</sub> <sup>2-</sup>	Fe <sup>2+</sup>	Mn <sup>2+</sup>	Br <sup>-</sup>	Sr <sup>2+</sup>	F <sup>-</sup>	Ba <sup>2+</sup>	HS <sup>-</sup>
S82	3	0	1	4	44	25	10.2	4.5	249.5	21	23	0.024	0.011	<0.01	9.5	0.52	0.18	0.03
S83	11	1	2	4	13.6	13.1	73	9	209.3	35	27	0.013	0.05	0.13	0.61	0.43	0.11	<0.02
S84	7	0	1	3	68	34	2.5	1.3	358.2	3.3	32	0.004	0.002	0.002	0.066	0.05	0.18	<0.02
S85	7	1	2	5	36	21	38	4.8	274.6	10	25	0.23	0.26	0.04	0.63	0.27	0.06	0.02
S86	11	1	2	5	28	22	43	4.8	269.3	10	30	0.094	0.009	<0.01	0.3	0.34	0.16	0.02
S87	7	1	1	7	48	27	26	4.5	307.2	17	27	0.39	0.1	0.02	0.21	0.3	0.14	0.03
S88	7	0	1	6	78	39	31	11	404.6	57	45	0.002	<0.0003	0.019	0.1	0.12	0.15	0.02
S89	7	1	3	2	21	33	290	17	219.4	440	63	0.068	0.26	1.4	1.23	0.38	0.12	0.04
S90	7	1	2	5	47	27	40	3.5	320.2	47	14	0.15	0.31	0.13	0.21	0.24	0.17	0.3
S91	4	1	2	1	1.3	0.1	130	0.29	267.0	17	27	0.013	0.0009	0.006	<0.005	0.12	0.001	<0.02
S92	5	1	3	6	69	38	110	11	283.7	180	65	0.37	0.028	0.21	1.2	0.61	0.49	<0.02
S93	11	1	3	1	10.3	15.6	400	16.5	460.0	430	3	0.16	0.011	1.5	0.28	0.83	0.22	0.2
S94	5	0	1	6	42	31	28	16	346.4	3.3	36	0.085	0.017	<0.01	1.45	0.6	1.1	0.05
S95	5	0	3	6	130	49	170	18	374.8	300	95	7	0.36	0.12	0.88	0.32	0.29	0.02
S96	5	1	1	6	110	49	68	7.2	365.6	150	120	1.6	0.1	0.06	0.37	0.22	0.43	<0.02
S97	9	1	2	4	13.9	8.7	63	4.75	200.3	25	26	0.029	0.014	0.03	1.3	1	0.3	0.02
S98	9	1	2	4	25	23	59	3.6	308.2	10	37	1.4	0.019	0.02	4.15	1.7	0.07	<0.02
S99	7	1	2	5	3.6	2.9	120	1.9	284.9	12	11	0.68	0.037	0.05	0.14	1.3	0.13	0.04
S100	7	1	3	2	25	66	1000	15	453.1	1400	<5	0.24	0.008	7.3	1.3	0.55	0.56	0.02
S101	7	1	3	2	49	27	690	7.6	268.4	1000	<1	0.89	0.096	3.9	1.7	0.27	0.67	0.04
S102	11	1	2	1	1.2	1.4	230	3	514.0	2.5	<0.5	0.045	0.002	0.06	0.1	0.48	0.008	0.1
S103	5	0	1	7	61	32	7.1	2.5	321.6	10	22	0.095	0.081	0.02	0.17	0.1	0.04	0.04
S104	9	0	2	4	45	9.6	67	3.1	247.2	40	9	0.018	0.002	0.15	2	1.5	0.03	0.04
S105	5	1	3	1	1.5	19.2	820	17	922.0	780	2	0.15	0.002	1.14	0.14	1.1	0.24	0.02
S106	5	1	1	5	28	17.3	14.7	8.3	237.8	0.5	(5)	0.44	0.065	0.01	0.188	(0.1)	0.26	0.08
S107	6	0	2	4	27	17.2	120	7.7	228.3	130	34	0.021	0.002	0.49	0.33	0.73	0.04	<0.02
S108	11	1	1	3	33	12	16.1	3.7	166.2	20	16	0.002	0.0003	0.057	1.7	0.13	0.04	0.02
S109	5	0	1	7	50	35	3.9	2.7	319.2	2.5	37	0.17	0.025	<0.01	0.45	0.12	0.11	0.04
S110	5	1	1	7	87	35	42	6.31	354.8	100	49	4.1	0.28	<0.01	0.51	0.25	0.52	0.04
S111	4	1	2	1	7.9	9.5	75	12	290.5	7	1	(0.013)	0.0008	0.12	0.34	0.99	0.1	0.09
S112	5	1	1	3	55	10.2	6.6	2	191.9	4	21	0.018	0.005	0.008	0.111	0.07	0.14	0.03
S113	5	1	1	5	29	17.5	14.2	6.9	223.8	0.6	(5)	0.16	0.062	0.01	0.177	(0.1)	0.23	0.08
S114	10	3	1	3	31	10.9	7	1.1	114.0	12	25	<0.0007	<0.0003	0.026	0.09	0.1	0.03	<0.02
S115	9	0	1	3	36	13.5	2.1	0.87	156.5	<0.1	5	0.003	<0.0003	0.005	0.544	1.4	0.25	<0.02
S116	9	0	2	5	29	18.2	37	3.2	238.6	3.8	19	0.15	0.029	<0.01	0.83	0.76	0.09	0.02
S117	3	1	3	4	21	8.5	93	3.2	142.7	76	75	0.025	0.006	0.24	13	3.2	0.03	<0.02
S118	8	1	2	3	51	23	42	2.1	215.4	92	22	0.001	<0.0003	<0.002	0.12	0.11	0.24	<0.02
S119	8	1	3	2	21	35	550	24	342.7	950	23	0.69	0.085	3.3	1.1	0.48	0.12	0.03
S120	8	1	1	5	40	15.6	20	1.2	200.7	29	4.5	15	0.45	<0.01	0.12	0.12	0.09	0.1
S121	12	3	1	3	43	18.7	7.5	3.4	179.7	13	8	0.026	0.0005	<0.01	0.1	0.12	0.11	0.02
S122	8	1	1	7	51	18.2	9.2	2	250.1	<0.2	21	0.39	0.053	<0.01	0.7	0.28	0.1	0.03
S123	5	1	2	6	31	26	86	13	309.5	86	39	0.12	0.003	0.034	1.26	0.68	0.52	0.05
S124	3	1	3	1	16.6	15.4	418	18	532.7	430	18	0.005	<0.0003	1.528	4.297	2.3	1.1	4.7

## Non standardized dataset of the multivariate statistical analysis (next)

ID	GU	H	G	C	Ca <sup>2+</sup>	Mg <sup>2+</sup>	Na <sup>+</sup>	K <sup>+</sup>	HCO <sub>3</sub> <sup>-</sup>	Cl <sup>-</sup>	SO <sub>4</sub> <sup>2-</sup>	Fe <sup>2+</sup>	Mn <sup>2+</sup>	Br <sup>-</sup>	Sr <sup>2+</sup>	F <sup>-</sup>	Ba <sup>2+</sup>	HS <sup>-</sup>
S125	5	0	3	6	98	41	250	3.4	390.8	350	130	0.02	0.099	0.022	0.23	0.1	0.13	<0.02
S126	9	0	2	5	55	22	130	3.9	379.7	110	25	0.13	0.059	0.22	0.94	0.51	0.06	<0.02
S127	5	1	1	6	43	26	15.8	4.1	286.0	6.3	23	0.28	0.015	0.02	0.73	0.34	0.54	0.08
S128	7	1	2	4	24	18.5	94	8.1	249.1	98	33	0.007	0.22	0.26	0.94	0.43	0.16	<0.02
S129	6	1	1	7	56	28	7.5	3.4	286.6	6.7	40	0.28	0.02	0.006	0.371	0.15	0.15	<0.02
S130	6	1	2	5	42	22	71	7.5	296.8	76	3	0.4	0.035	0.119	0.35	0.38	0.39	0.04
S131	5	1	2	6	58	32	40	11	309.4	42	48	0.16	0.012	0.06	1.395	0.48	0.2	<0.02
S132	5	1	2	6	50	31	35	10	298.6	37	44	0.37	0.02	0.027	1.3	0.45	0.27	<0.02
S133	6	1	2	5	42	28	53	11	284.8	57	42	0.29	0.04	0.2	0.49	0.37	0.08	<0.02
S134	11	1	1	5	55	30	12.6	5.7	285.7	6.7	21	0.22	0.48	0.04	0.52	0.27	0.13	<0.02
S135	11	1	2	5	49	31	68	7.1	297.1	110	26	0.27	0.93	0.38	0.6	0.31	0.16	0.03
S136	7	2	1	6	92	44	28	2.8	390.3	86	58	0.017	0.011	<0.01	0.15	0.13	0.14	0.03
S137	11	1	1	7	61	31	12.6	6	323.1	15	43	0.57	0.085	<0.01	0.17	0.14	0.14	0.03
S138	7	1	1	3	49	26	7.3	1.7	261.7	4	28	0.009	<0.0003	<0.01	0.15	0.15	0.09	0.02
S139	7	0	1	6	91	41	20	5.7	438.5	35	49	0.003	0.002	<0.01	0.12	0.1	0.24	0.02
S140	3	0	4	4	42	13	140	4.6	215.4	33	240	0.01	0.005	0.037	<0.007	2.6	0.05	<0.02
S141	5	1	2	1	7.9	12.6	280	19	468.1	230	7	0.045	0.004	1.106	0.28	1	0.4	0.33
S142	5	0	3	6	110	56	89	11	342.2	250	47	0.13	0.011	0.038	1.293	0.35	0.21	<0.02
S143	1	1	1	5	44	13.1	32	3.9	238.6	8.8	16	0.13	0.016	0.019	0.4	0.24	0.14	0.03
S144	7	2	1	7	40	35	5.6	4	285.7	2.5	30	0.65	0.12	0.005	0.595	0.22	0.16	<0.02
S145	7	2	1	7	62	39	6.2	3	342.2	5	46	1.6	0.06	(0.01)	0.331	0.14	0.18	0.14
S146	10	3	1	7	92	47	14.5	3.7	506.7	5	49	0.25	0.019	(0.01)	0.19	0.09	0.11	0.05

**Note :**

GU: Geological Units : 1	Trenton G.	7	Cairnside F.
2	Black River G.	8	Covey Hill F.
3	Chazy G.	9	Grenvillian basement
4	Carillon F.	10	Surface sediments
5	Beauharnois F.	11	Sediments under clay
6	Theresa F.	12	Spring
H: Hydrogeological Conditions : 0	Unconfined	2	Semi-confined
1	Confined	3	Surface sediments and springs
G: Groundwater Groups : 1	G1 (Ca-HCO <sub>3</sub> , Mg-HCO <sub>3</sub> , Alkaline earth-HCO <sub>3</sub> )		
2	G2 (Na-HCO <sub>3</sub> , Mixed cations-HCO <sub>3</sub> )		
3	G3 (Na-Cl, Mixed cations-Cl, Na-Mixed anions)		
4	G4 (Ca-SO <sub>4</sub> , Na-SO <sub>4</sub> )		

C: Groundwater Clusters (C1 to C7)

HCO<sub>3</sub><sup>-</sup> calculated from total alkalinity using PHREEQC 2.6 (Parkhurst and Appelo 1999).

n.a.: not analyzed

Values in brackets are estimated values of not analyzed elements.

Two samples excluded from the multivariate statistical analysis : S53 and S77.

## **Chapitre 6**

### **CONCLUSIONS**

#### **6.1 CONCLUSIONS GÉNÉRALES**

Cette thèse de doctorat a été réalisée dans le cadre d'un projet multidisciplinaire de caractérisation et d'inventaire des ressources en eau souterraine de la Commission géologique du Canada (CGC). Le projet intitulé «caractérisation hydrogéologique régionale du système aquifère fracturé du sud-ouest du Québec» fait aussi partie du programme national en hydrogéologie de la CGC. Ce projet a été réalisé en partenariat avec le Ministère de l'Environnement du Québec et les MRC de la région, et avec la participation de plusieurs universités. Un des objectifs de ce projet était d'acquérir une meilleure connaissance des eaux souterraines et du potentiel aquifère dans la région, afin de supporter la gestion et la protection de la ressource en eaux souterraines. Un second objectif de l'étude était de développer une méthodologie permettant de caractériser, à l'échelle régionale, un système aquifère en milieu fracturé (Savard et al., *in press*). Le projet de cartographie de la CGC était donc composé de plusieurs volets, dont la caractérisation géologique du roc et du Quaternaire, la caractérisation hydrogéologique et hydrogéochimique, ainsi que l'étude de la recharge des nappes. Ce doctorat faisait partie intégrante du volet sur la caractérisation hydrogéochimique des eaux souterraines.

Les principaux objectifs de ce projet de doctorat étaient de développer une méthodologie de caractérisation hydrogéochimique régionale pour un système aquifère de roc fracturé, d'évaluer la qualité régionale des eaux souterraines, d'évaluer différentes méthodes pour classifier et analyser les données hydrogéochimiques, de connaître l'origine des eaux souterraines, de déterminer l'influence des contextes hydrogéologiques et géologiques sur

la géochimie des eaux souterraines, d'identifier et comprendre les processus géochimiques principaux contrôlant la géochimie des eaux souterraines et son évolution dans l'espace et le temps, ainsi que de développer un modèle intégré de l'évolution hydrogéochimique des eaux souterraines du système aquifère des Basses-Laurentides. Ces objectifs ont été atteints et sont discutés ci-dessous par thème.

### ***Caractérisation régionale***

La caractérisation hydrogéochimique régionale d'un système aquifère implique la détermination de la nature géochimique et isotopique de l'eau souterraine dans différentes parties du système d'écoulement, ainsi que des différentes sources qui peuvent influencer la composition des eaux souterraines. Dans le cas du système aquifère des Basses-Laurentides, ces sources vont des précipitations dans les zones de recharge, à l'eau interstitielle des argiles marines dans les vallées enfouies. La méthodologie utilisée dans ce projet de doctorat était la suivante : échantillonnage de l'eau souterraine des zones de recharge aux zones d'émergence, caractérisation géochimique de l'eau souterraine contenue dans l'ensemble des lithologies et dans les différents contextes géologiques et hydrogéologiques, utilisation combinée de la géochimie inorganique et isotopique, ainsi que la caractérisation isotopique des précipitations locales. Un système d'échantillonnage multi-niveaux dans le roc fracturé, ainsi qu'un système de collecte de précipitations pour les isotopes stables de l'eau, ont été développés dans le cadre de ce projet de recherche afin d'acquérir les données scientifiques nécessaires pour appliquer la méthodologie de caractérisation.

Deux méthodes d'échantillonnage ont été utilisées lors de la caractérisation du système aquifère. La première était l'échantillonnage régional, une méthode conventionnelle qui a permis d'assurer la couverture régionale par l'échantillonnage de puits municipaux, de puits privés et de puits d'observations. La seconde méthode était l'échantillonnage avec le système multi-niveaux, une méthode qui a permis d'étudier les variations de qualité d'eau en fonction de la profondeur. Des échantillons d'eau souterraine ont ainsi été prélevés à 153 sites, ce qui a permis de caractériser l'ensemble des unités géologiques et des contextes hydrogéologiques jusqu'à une profondeur de 140 m. De ces 153 sites, 17 puits

au roc ont été échantillonnés avec le système multi-niveaux. L'eau souterraine a été analysée pour les constituants inorganiques majeurs, mineurs et traces, les isotopes stables  $\delta^2\text{H}$ ,  $\delta^{18}\text{O}$  et  $\delta^{13}\text{C}$  du carbone inorganique dissous (CID), et certains échantillons ont été analysés pour  $^{87}\text{Sr}/^{86}\text{Sr}$ ,  $^3\text{H}$  et  $^{14}\text{C}$  du CID. Les précipitations ont été échantillonnées pour les isotopes stables  $\delta^2\text{H}$  et  $\delta^{18}\text{O}$ . Cette caractérisation a permis d'établir la Droite des Eaux Météoriques des Basses-Laurentides, de caractériser la recharge et d'interpréter les résultats d'isotopes stables des eaux souterraines. Enfin, l'eau interstitielle a été extraite d'échantillons d'argiles marines et analysée pour les éléments majeurs,  $\text{Br}^-$ ,  $\text{Sr}^{2+}$ ,  $\delta^2\text{H}$  et  $\delta^{18}\text{O}$ . Les résultats de la caractérisation des argiles ont été très importants dans la compréhension de l'origine de la salinité de l'eau souterraine dans les vallées enfouies.

### ***Analyse des résultats***

Plusieurs méthodes ont été utilisées pour l'analyse et l'interprétation des données hydrogéochimiques, incluant :

- des représentations géochimiques qualitatives classiques, dont les cartes à points de paramètres chimiques, les diagrammes de paramètres chimiques en fonction de la profondeur et de la distance le long d'une ligne d'écoulement, le diagramme de Piper, le diagramme de Stiff, les diagrammes radiaux, le diagramme de Scholler, l'histogramme, les nuages de points, et les diagrammes en boîte (*box plot*);
- la classification des échantillons d'eau souterraine en types d'eau dominants et mixtes, ainsi que le regroupement de ces types d'eau en groupes d'eau souterraine sur la base des concentrations en ions majeurs;
- la modélisation géochimique qui a permis de déterminer l'indice de saturation de l'eau souterraine par rapport aux phases minérales;
- l'analyse statistique multivariable, une méthode quantitative moins couramment utilisée en hydrogéochimie, dont la méthode d'analyse par classification automatique hiérarchique (*hierarchical cluster analysis*), et l'analyse en composantes principales (*principal components analysis*);

- les statistiques descriptives de base (moyenne, médiane, minimum, maximum et écart type) pour les échantillons d'eau souterraine par unité géologique, condition hydrogéologique, groupes d'eau souterraine, et *cluster*.

### ***Classification, regroupement et zonation***

Ce projet de recherche a généré une quantité importante de données hydrogéochimiques. La compréhension globale du système aquifère a été possible, en grande partie, grâce à l'utilisation judicieuse de différentes méthodes de classification ayant permis le regroupement des échantillons, ainsi que la zonation de ceux-ci dans la région d'étude.

Une première méthode de classification a permis de diviser les 146 échantillons en six types d'eau dominants et quatre types d'eau mixtes. Ces dix types d'eau ont été regroupés en quatre groupes d'eau souterraine, G1 à G4 : G1 avec 68 échantillons (incluant les types Ca-HCO<sub>3</sub>, Mg-HCO<sub>3</sub> et Alcalino terreux-HCO<sub>3</sub>), G2 avec 47 échantillons (comprenant les types Na-HCO<sub>3</sub> et Cations mixtes-HCO<sub>3</sub>), G3 avec 28 échantillons (incluant les types Na-Cl, Cations mixtes-Cl et Na-Anions mixtes), et G4 avec 3 échantillons (avec les types Ca-SO<sub>4</sub> et Na-SO<sub>4</sub>). La distribution régionale des types d'eau a montré l'importance du contrôle des conditions hydrogéologiques sur la chimie des éléments majeurs des eaux souterraines (Fig. 3.10; Chapitre 3 et Fig. 4.4; Chapitre 4). En effet, les zones préférentielles de recharge sont caractérisées par une eau souterraine des groupes G1 et G4, principalement par le type d'eau dominant Ca-HCO<sub>3</sub>. Les groupes G2 et G3 caractérisent les zones confinées, dominées par les types d'eau dominants Na-HCO<sub>3</sub> pour G2 et Na-Cl pour G3.

La seconde méthode utilisée est la classification automatique hiérarchique qui a permis de diviser les échantillons en sept *clusters*, C1 à C7 : C1 avec 17 échantillons (eau souterraine de type Na-HCO<sub>3</sub> avec des concentrations élevées en F<sup>-</sup>, Ba<sup>2+</sup> et HS<sup>-</sup>, et la plus faible dureté totale), C2 avec 15 échantillons (eau souterraine de type Na-Cl avec des concentrations élevées en Br<sup>-</sup> et K<sup>+</sup>, et la concentration en matières dissoutes totales (MDT) la plus élevée), C3 avec 16 échantillons (eau souterraine de type Ca-HCO<sub>3</sub>), C4 avec 21 échantillons (eau souterraine de type Na-HCO<sub>3</sub> avec des concentrations élevées

en  $\text{Sr}^{2+}$  et  $\text{F}^-$ ), C5 avec 24 échantillons (eau souterraine de type Cations mixtes- $\text{HCO}_3^-$  et la plus faible MDT), C6 avec 23 échantillons (eau souterraine de type Ca- $\text{HCO}_3^-$  avec des concentrations élevées en  $\text{SO}_4^{2-}$  et  $\text{Ba}^{2+}$ , et la dureté totale la plus élevée), et C7 avec 28 échantillons (eau souterraine de type Ca- $\text{HCO}_3^-$  avec des concentrations élevées en  $\text{Fe}^{2+}$ ,  $\text{Mn}^{2+}$  et  $\text{SO}_4^{2-}$ ). Les *clusters* C1, C2 et C5 caractérisent le système aquifère en conditions confinées, alors que les *clusters* C3, C4, C6, et C7 sont majoritairement localisés dans les zones préférentielles de recharge (Fig. 5.14). Par rapport à la classification en groupes, la classification en *clusters* est plus distinctive car elle intègre un nombre supérieur de paramètres. Donc, en plus de reconnaître l'importance des conditions hydrogéologiques, la distribution régionale des *clusters* a permis de reconnaître l'importance des formations géologiques sur les concentrations en éléments mineurs et traces, comme  $\text{Fe}^{2+}$ ,  $\text{Mn}^{2+}$ ,  $\text{Sr}^{2+}$ ,  $\text{F}^-$  et  $\text{Ba}^{2+}$ .

En termes de qualité des eaux souterraines, le territoire d'étude a été subdivisé en 7 secteurs classés sur une échelle de qualité relative de 1 (meilleure qualité) à 7 (qualité inférieure). Cette division a tenu compte des propriétés hydrogéochimiques (cartes de distribution des paramètres chimiques, des types d'eau et des *clusters*), des dépassements des critères de qualité reliés à la santé et des critères esthétiques (Santé Canada, 2001; Health Canada, 2003), des conditions hydrogéologiques, de l'épaisseur des sédiments, ainsi que de la vulnérabilité à la contamination. La Carte 2.17 à l'échelle du 1/100 000 *Qualité de l'eau souterraine* (Appendice H) présente les secteurs et intègre l'ensemble des informations ayant servi à la classification en secteurs de qualité relative de l'eau souterraine. Pour cette carte, les échantillons ont été représentés par leur type d'eau simplifié (cation et anion dominant).

L'intégration de ces différentes méthodes de classification et de regroupement avec le contexte géologique et hydrogéologique a permis de diviser le territoire d'étude en quatre régions géochimiques (*geochemical areas*) (Fig. 5.15; Chapitre 5): 1) l'Extrémité Ouest (*Western End*), 2) les Crêtes et Vallées Centrales (*Central Crests and Valleys*), 3) la Région Est (*Eastern Area*), et l'Extrémité Est (*Far Eastern End*). Chacune de ces régions

géochimiques a des caractéristiques distinctes aux niveaux de l'évolution de l'eau souterraine ainsi que des processus géochimiques dominants.

### ***Origine des eaux souterraines***

L'interprétation qualitative des données de tritium a indiqué que les zones de recharge préférentielles, caractérisées par une eau souterraine des groupes G1 (Ca-Mg-HCO<sub>3</sub>) et G4 (Ca-SO<sub>4</sub>, Na-SO<sub>4</sub>), ont une eau souterraine d'âge moderne, enrichie en tritium. Le système aquifère en conditions confinées, caractérisé par les groupes G2 (Na-HCO<sub>3</sub>) et G3 (Na-Cl), a une eau souterraine d'âge submoderne. L'eau souterraine du groupe G2 résulte de l'évolution de l'eau souterraine moderne du groupe G1. L'eau souterraine du groupe G3 résulte du mélange d'eau du groupe G2 avec l'eau Pléistocène de la Mer de Champlain, ainsi que de la diffusion d'ions des argiles marines (Fig. 3.12; Chapitre 3). Deux sources d'eau souterraine (*groundwater end-member*) ont donc été identifiées dans le système aquifère des Basses-Laurentides : 1) l'eau météorique moderne présente dans les zones préférentielles de recharge et échantillonnée dans l'unité de till (sous-groupe G1<sub>Till</sub> de type Ca-HCO<sub>3</sub>), et 2) l'eau Pléistocène de la Mer de Champlain observée dans la vallée enfouie de Saint-Benoît (site S77) et dans les échantillons d'eau interstitielle extraite de l'argile marine.

### ***Processus et évolution géochimiques des eaux souterraines***

L'interprétation des données hydrogéochimiques a permis d'identifier les processus géochimiques principaux qui contribuent à l'évolution de l'eau souterraine. Ceux-ci ont été présentés selon leur position dans le système d'écoulement (Fig. 4.14; Chapitre 4). La dissolution de minéraux carbonatés, calcite et dolomie, domine dans les zones préférentielles de recharge produisant une eau souterraine du groupe G1 (Ca-Mg-HCO<sub>3</sub>). Dans le système aquifère en conditions confinées, l'échange ionique Ca<sup>2+</sup>-Na<sup>+</sup> est responsable pour l'évolution de l'eau au groupe G2 (Na-HCO<sub>3</sub>), alors que le mélange avec l'eau Pléistocène de la Mer de Champlain et la diffusion d'ions des argiles marines sont responsables pour la présence d'eau du groupe G3 (Na-Cl). L'invasion marine qui a produit la Mer de Champlain est la cause de la salinisation passée du système aquifère

caractérisé. Les traceurs conservateurs  $\text{Cl}^-$  et  $\text{Br}^-$ , ainsi que  $\delta^{18}\text{O}$ , ont permis de déterminer que l'eau originale de la Mer de Champlain, dans la région d'étude, était un mélange d'environ 34% d'eau de mer et de 66% d'eau douce (eau météorique et eau de fonte glaciaire Pléistocène). La géochimie actuelle de l'eau souterraine a permis de déterminer que le système aquifère se trouve à différentes étapes du processus de désalinisation, de l'eau ancienne de la Mer de Champlain encore présente dans les parties stagnantes, aux secteurs plus actifs où celle-ci a été complètement remplacée par une eau souterraine moderne, particulièrement dans les zones de recharge préférentielles. Enfin, une source moderne de salinité, le sel déglaçant, a été identifiée en zone de recharge dans la région de Saint-Janvier, expliquant la présence d'eau souterraine du groupe G3 dans ce secteur.

### ***Compréhension globale du système aquifère des Basses-Laurentides***

L'intégration de cette étude hydrogéochimique régionale aux autres volets du projet de cartographie de la CGC permet d'obtenir une compréhension globale du système aquifère des Basses-Laurentides. Plus spécifiquement, les données de datation de puits échantillonnés avec le système multi-niveaux ont permis de valider le modèle conceptuel de l'écoulement qui supposait un écoulement plus rapide dans la zone de roc très fracturé, à l'interface de la surface des formations sédimentaires et de l'argile marine. De plus, la distribution régionale des groupes d'eau, ainsi que les données en tritium, sont très cohérentes avec la carte des conditions hydrogéologiques. Ces données géochimiques permettent ainsi de valider l'évaluation de la distribution de la recharge et de la vulnérabilité du système aquifère obtenue par des études indépendantes.

L'intégration des interprétations hydrogéochimiques, incluant les connaissances sur l'origine, l'évolution de l'eau souterraine et les processus géochimiques, avec les contextes géologiques et hydrogéologiques a permis de diviser le territoire d'étude en quatre régions géochimiques (Fig. 5.15; Chapitre 5). Les facteurs suivants sont reconnus comme influençant l'évolution de l'eau souterraine observée dans chacune des régions géochimiques : 1) les caractéristiques géologiques, incluant le type de roche sédimentaire et la composition minéralogique du till ; 2) les caractéristiques hydrogéologiques, dont le niveau de confinement et le gradient hydraulique ; et 3) l'histoire géologique, marquée

par la dernière glaciation et l'invasion de la Mer de Champlain. Parmi ces régions géochimiques, celle des Crêtes et Vallées Centrales (*Central Crests and Valleys*) possède le cycle "complet" de l'évolution hydrogéochimique du système aquifère, de l'eau souterraine moderne en zones de recharge, aux eaux souterraines évoluées en zones confinées et aux eaux anciennes avec une forte proportion d'eau de la Mer de Champlain au cœur des vallées enfouies. La présence de ces eaux anciennes dans la région des Crêtes et Vallées Centrales semble être reliée à des points singuliers du système d'écoulement où l'écoulement est divergent et convergent, limitant ainsi la circulation de l'eau souterraine au centre des vallées enfouies. Avec leur intégration cohérente entre l'hydrogéochimie et l'hydraulique, ces régions géochimiques procurent un portrait global de la dynamique du système aquifère des Basses-Laurentides.

### ***Gestion de la ressource en eau souterraine***

À l'échelle régionale, l'eau souterraine du territoire est de qualité variable et très peu contaminée par les activités humaines. Le bilan des dépassements des critères de qualité reliés à la santé nous indique une eau souterraine de bonne qualité sur la majorité du territoire. En effet, un seul dépassement directement relié à l'activité humaine, soit un excès en nitrates, a été identifié dans une zone de recharge. De plus, deux dépassements des critères de qualité reliés à la santé sont notés pour le baryum, et dix pour les fluorures. Plusieurs dépassements des critères esthétiques sont observés à partir des échantillons d'eau, mais ils sont généralement reliés à des processus naturels. Seuls les quelques dépassements en chlorures et en sodium dans les secteurs à nappe libre à proximité d'autoroutes peuvent être attribués à l'activité humaine, soit l'utilisation de sel déglaçant. Enfin, bien que ne faisant pas l'objet de recommandations ou de normes, la dureté est relativement élevée sur l'ensemble de la région.

L'intégration de la distribution des secteurs de qualité relative de l'eau souterraine à une étude quantitative des ressources en eau souterraine a permis d'identifier trois zones plus favorables pour l'exploitation de l'eau souterraine (Nastev et al., in press). Ces zones coïncident bien avec les secteurs offrant le meilleur potentiel d'exploitabilité obtenus à

partir de l'intégration des propriétés hydrogéochimiques et hydrauliques (Savard et al., 2002).

La présence d'eau souterraine moderne dans les zones de recharge, identifiée par les types d'eau et les données de tritium, indique qu'une superficie importante du système aquifère est vulnérable à la contamination. Le dépassement pour les nitrates ainsi que la détection de sel déglaçant confirment la vulnérabilité du système aquifère. Bien que présentement le système aquifère soit très peu contaminé par les activités humaines, il est essentiel de protéger les zones préférentielles de recharge afin de prévenir une dégradation éventuelle de la qualité des ressources en eaux souterraines.

## **6.2 CONTRIBUTIONS SCIENTIFIQUES ET APPORTS À L'AVANCEMENT DES CONNAISSANCES**

Ces travaux de doctorat apportent plusieurs contributions scientifiques ayant des incidences à différents niveaux, dont : la gestion et la protection de la ressource en eau souterraine des Basses-Laurentides, l'approche et la méthodologie utilisées dans ce projet et ses applications possibles dans d'autres études hydrogéochimiques régionales, la compréhension du système aquifère des Basses-Laurentides et le transfert des connaissances acquises de ce système à d'autres systèmes complexes d'écoulement régional, et de façon plus globale, la contribution à l'avancement de la compréhension à long terme de systèmes hydrogéologiques. Ces contributions sont regroupées et présentées ci-dessous par thème.

### ***Choix de la région d'étude***

La région étudiée, le système aquifère des Basses-Laurentides, présente des intérêts indéniables du point de vue scientifique. En effet, la région est caractérisée par des variations significatives de la géochimie et de la qualité des eaux souterraines. Ces variations impliquent l'existence de processus géochimiques importants et actifs. Il y avait donc nécessité d'identifier ces processus afin de bien comprendre le système aquifère. Ce projet de doctorat a ainsi montré l'importance de la dernière glaciation, de

l'invasion de la Mer de Champlain, de la diversité des lithologies, et des systèmes d'écoulement locaux sur la grande variété de types d'eau et d'origine d'eau souterraine à l'intérieur d'une région relativement restreinte.

### ***Qualité de l'eau souterraine***

La division de la région d'étude en secteurs de qualité relative de l'eau souterraine est une contribution pratique puisqu'elle procure un portrait régional et intégré de la qualité de l'eau nécessaire à la gestion de la ressource et au suivi ultérieur de sa qualité (Carte 2.17; Appendice H)

### ***Étude multidisciplinaire***

Le caractère multidisciplinaire du projet de cartographie hydrogéologique de la CGC a permis que les connaissances acquises lors de ces travaux d'hydrogéochimie puissent contribuer à d'autres volets du projet de la CGC. Comme mentionné précédemment, les données de datation de puits échantillonnés avec le système multi-niveaux ont contribué à valider le modèle conceptuel de l'écoulement du système aquifère, et la distribution régionale des groupes d'eau et des données en tritium ont contribué à valider l'évaluation de la distribution de la recharge et de la vulnérabilité du système aquifère, ce qui représente une application pratique et originale de la géochimie pour la gestion des ressources. De plus, l'information obtenue de l'échantillonnage avec le système multi-niveaux a été utilisée pour les études locales, contribuant par exemple à la compréhension de la problématique de salinité du secteur de Saint-Benoît (Nastev et al., 2002).

### ***Approche de l'étude et caractérisation***

Les résultats et les interprétations de ce projet de recherche reposent sur une approche bien fondée, et une caractérisation rigoureuse. Celle-ci a contribué à produire une série de données hydrogéochimiques exhaustives, incluant la géochimie inorganique, les isotopes stables et la datation de l'eau souterraine, pour le système aquifère des Basses-Laurentides. Cette série de données est une contribution scientifique pour la région d'étude, mais aussi une contribution dans la compréhension des systèmes régionaux

d'écoulement et des milieux fracturés. De plus, la Droite des Eaux Météoriques des Basses-Laurentides est une contribution à l'étude des isotopes dans les précipitations. Ainsi, la Droite des Eaux Météoriques des Basses-Laurentides pourrait être utilisée dans le cadre d'autres projets situés à proximité de la région étudiée. Enfin, l'approche intégrée de cette étude pourrait être transférée, et appliquée, dans l'étude d'autres systèmes d'écoulement régional. La base de données géochimiques pour cette région est d'autant plus importante puisqu'elle est combinée à une caractérisation exaustive du système d'écoulement, permettant ainsi d'appuyer l'interprétation géochimique sur un cadre hydrogéologique bien défini.

#### ***Approche originale pour l'analyse des données***

La grande quantité de données géochimiques produites lors d'études régionales peut entraîner des difficultés d'interprétation. Dans ce doctorat, la combinaison de méthodes géochimiques classiques et statistiques, dont l'utilisation de diagrammes géochimiques, la classification en types d'eau, la modélisation géochimique, la classification automatique hiérarchique, et l'analyse en composantes principales, a permis de faire la lumière complète sur l'origine et l'évolution géochimique des eaux souterraines des Basses-Laurentides. De plus, les avantages relatifs de chacune des méthodes ont été identifiés (Table 5.6; Chapitre 5), ce qui représente une contribution scientifique pour l'analyse de données géochimiques.

#### ***Compréhension d'un système d'écoulement complexe***

Les connaissances sur l'origine et l'évolution géochimique des eaux souterraines provenant de l'étude hydrogéochimique sont nécessaires à la compréhension complète du système d'écoulement. La distribution des eaux modernes, évoluées et anciennes, ainsi que les données de datation de l'eau souterraine, apportent des informations capitales sur la dynamique du système aquifère, informations qui ne peuvent être obtenues sur la seule base d'une modélisation hydrogéologique. Carrillio-Rivera (2003) présente des exemples démontrant qu'une vision large du système eau souterraine (*system-wide groundwater view*) est essentielle à la compréhension d'un système d'écoulement de l'eau souterraine.

Ainsi, les interprétations relatives à un aquifère ne doivent pas tenir compte des réponses hydrauliques seules, mais aussi des évidences chimiques, biologiques et géologiques (Carrillio-Rivera, 2003). Spécifiquement, le modèle développé pour expliquer l'origine de la salinité est une contribution scientifique puisqu'il pourra être appliqué pour vérifier la possibilité de mélange avec une eau de mer ancienne dans des contextes similaires.

#### ***Paléo-hydrogéologie et compréhension à long terme de système hydrogéologique***

Une des contributions scientifiques majeures de ce projet de doctorat est d'avoir démontré, par des évidences géochimiques et isotopiques, l'origine de la salinité dans le système aquifère en secteur confiné. Ainsi, il a été démontré que la salinité est le résultat de l'invasion marine par la Mer de Champlain. Bien que le système soit, depuis le retrait de la Mer de Champlain, en processus de désalinisation, les traces de l'épisode de salinisation sont encore présentes dans des parties stagnantes ou d'écoulement moindre du système aquifère, ainsi que dans les dépôts d'argiles marines. L'événement géologique majeur qu'a été la Mer de Champlain a donc eu une influence qui se remarque encore sur le système aquifère des Basses-Laurentides après plus de 10 000 ans. En reconstituant les étapes de salinisation et de désalinisation dans le temps, et en appréciant l'importance de ces événements sur l'hydrogéologie passée et présente du système aquifère, cette étude apporte ainsi une contribution à un axe de recherche encore peu développé, soit la paléo-hydrogéologie.

Un des défis futurs de la recherche en hydrogéologie est la compréhension de l'évolution à long terme de systèmes hydrogéologiques. En étudiant la paléo-hydrogéologie d'un système aquifère actif, et en démontrant que ce système est encore influencé par un événement géologique Quaternaire majeur, ce projet de recherche contribue à l'avancement des connaissances en caractérisant un système aquifère qui peut être considéré comme un analogue hydrogéologique de l'évolution à long terme des systèmes d'écoulement. Ainsi, cette étude pourrait aider à comprendre, et éventuellement à quantifier, les conséquences possibles à long terme, par exemple, d'une intrusion marine majeure sur un aquifère côtier.

Ce projet de doctorat présente un cas de terrain montrant que l'eau souterraine est un agent géologique important. Ingebritsen et Sanford (1998) ont présenté plusieurs exemples du rôle des eaux souterraines dans des processus géologiques majeurs, incluant la migration des hydrocarbures, le métamorphisme et la diagénèse. Tóth (1999) a démontré le rôle des eaux souterraines comme agent géologique dans un système régional d'écoulement gravitaire. Ce projet de doctorat a reconnu plusieurs des processus discutés par Tóth (1999). Ces processus contribuent à l'évolution de l'eau souterraine, à partir de la recharge et le long du système d'écoulement. De plus, le cas des Basses-Laurentides démontre que l'eau souterraine est un agent géologique dans le temps. En effet, la Mer de Champlain, un événement géologique majeur, a envahi la partie supérieure du système aquifère, imposant de nouvelles conditions hydrogéologiques et hydrogéochimiques au système il y a environ 10 000 ans. Ces conditions sont encore présentes dans certaines parties du système, ainsi que dans l'eau interstitielle des argiles marines qui continueront d'influencer la géochimie du système aquifère sous-jacent pour encore longtemps.

### **6.3 QUESTIONS EN SUSPENS, TRAVAUX FUTURS ET PERSPECTIVES**

Ces travaux de recherche ont permis de répondre aux principaux objectifs de départ, et ont aussi apporté de nouvelles questions. La section suivante présente les incertitudes qui demeurent à certains niveaux des conclusions, ainsi que des travaux qui pourraient être complétés dans la région d'étude à partir, en grande partie, des données géochimiques présentées dans cette thèse.

#### ***Mécanismes de désalinisation***

Les travaux réalisés dans ce projet de doctorat ont permis de conclure, sur la base d'évidences géochimiques, isotopiques et la géologie du Quaternaire, que la salinité identifiée dans l'aquifère rocheux des Basses-Laurentides est le résultat de l'invasion marine par la Mer de Champlain et que le système aquifère se trouve à différentes étapes d'un processus de désalinisation. Ces conclusions soulèvent toutefois des questions sur les mécanismes physiques reliés à cette désalinisation, notamment les processus de

mélange et de transport de masse dans un milieu fracturé hétérogène. Des travaux sont donc nécessaires afin d'évaluer la faisabilité hydraulique, dans le temps et l'espace, du processus de désalinisation invoqué. La plausibilité du processus de désalinisation depuis le retrait de la Mer de Champlain, soit environ 10 000 ans, doit d'abord être évaluée par l'interprétation quantitative des données de datation de l'eau souterraine. Cette plausibilité doit aussi être évaluée selon les connaissances hydrogéologiques du système aquifère. Ces connaissances hydrogéologiques comprennent le contexte d'écoulement, notamment la présence de singularités hydrauliques et d'écoulement divergent dans les vallées enfouies où l'écoulement est très lent, un bilan du taux de renouvellement de l'eau souterraine dans l'aquifère, une évaluation des vitesses d'écoulement dans les différents secteurs de l'aquifère ainsi que l'influence de la couverture d'argiles marines sur la géochimie de l'aquifère. Cette évaluation doit aussi tenir compte du processus de mélange qui implique la diffusion entre l'eau salée présente dans les fractures et les pores ne participant pas ou peu à l'écoulement et l'eau souterraine moderne dans les zones d'écoulement préférentiel. La faisabilité du processus de désalinisation, considérant un milieu à double porosité conduisant à un lessivage non efficace de l'aquifère, du mélange par diffusion et de l'influence des argiles, devrait donc être évaluée par la modélisation du transport réactif le long de sections du système aquifère sur la base des données acquises dans le cadre de ce projet de doctorat.

### ***La modélisation hydrogéochimique***

Ces travaux de doctorat ont établi la base nécessaire pour une modélisation hydrogéochimique inverse. Cette base inclut la série de données et l'interprétation de l'évolution hydrogéochimique du système aquifère. La modélisation géochimique inverse utilise les données géochimiques et isotopiques le long d'une même ligne d'écoulement afin d'identifier et de quantifier les réactions responsables de l'évolution de l'eau selon cette ligne d'écoulement (Parkhurst et Plummer, 1993; Glynn et Brown, 1996). La région géochimique Crêtes et Vallées Centrales, qui possède le cycle complet de l'évolution hydrogéochimique du système aquifère, représente le meilleur endroit pour initier ces travaux de modélisation. Plus spécifiquement, ces travaux pourraient cibler la section localisée dans la Vallée de Saint-Hermas (voir la section A-A' de la Fig. 3.2; Chapitre 3).

Parmi les raisons qui favorisent ce secteur, mentionnons le bon contrôle sur la géologie, l'hydrogéologie, le nombre important de données géochimiques, ainsi que des données de datation (Fig. 3.7a; Chapitre 3). De plus, deux puits ayant été échantillonnés avec le système multi-niveaux sont localisés le long de cette section.

### ***Interprétation quantitative des données de datation***

L'interprétation quantitative des données de datation va permettre de préciser l'âge des eaux souterraines évoluées et anciennes. Cette interprétation pourrait se faire de paire avec les travaux de modélisation hydrogéochimique.

### ***La modélisation du transport des ions dans les argiles***

La modélisation des profils géochimiques de l'eau interstitielle des argiles marines pourrait permettre d'évaluer le dynamisme et la migration des ions dans ces dépôts argileux. Ces travaux pourraient quantifier la contribution des argiles à la salinité du système aquifère, et ainsi, contribuer à la modélisation hydrogéochimique. Dans l'optique de la compréhension à long terme du système aquifère, il pourrait être possible d'envisager des scénarios de modélisation pour évaluer le temps nécessaire pour remplacer l'eau interstitielle salée des argiles pour une eau fraîche.

### ***Analyse minéralogique et géochimique de la roche***

Dans les puits qui ont été échantillonnés avec le système multi-niveaux, cinq ont été carottés en continu. Bien que la géologie des formations sédimentaires soit bien caractérisée dans la région d'étude, l'analyse minéralogique et géochimique de la roche (matrice et fractures), aux profondeurs échantillonnées, pourrait procurer de l'information importante pour quantifier les processus géochimiques, et valider le nombre de réactions possibles. L'analyse d'échantillons de roche pour  $^{87}\text{Sr}/^{86}\text{Sr}$  pourrait aussi compléter l'étude de l'interaction eau/roche.

### ***Secteurs avec particularités géochimiques***

Des particularités géochimiques locales ont été identifiées, principalement dans la région confinée de Sainte-Anne-des-Plaines. Des données ciblées, incluant de nouvelles données de datation et la géochimie des roches, combinées aux données existantes d'échantillons multi-niveaux, pourraient permettre d'éclairer ces particularités géochimiques.

### ***Retour sur le modèle d'écoulement de façon interactive***

Tel que mentionné précédemment, la distribution des eaux modernes, évoluées et anciennes, ainsi que les données de datation de l'eau souterraine, ont apporté des informations indépendantes et nouvelles sur la dynamique du système aquifère. Un retour sur le modèle d'écoulement de l'eau souterraine pourrait permettre d'évaluer les cohérences et incohérences possibles entre les simulations hydrauliques et les connaissances géochimiques du système. Une meilleure compréhension de la dynamique d'écoulement et des processus géochimiques pourrait donc émerger de l'interaction entre les simulations hydrauliques et l'hydrogéochimie.

Ce projet de recherche est une étude hydrogéochimique régionale intégrée, qui a utilisé la géochimie inorganique, les isotopes stables, la datation de l'eau souterraine, la modélisation géochimique, et différentes méthodes d'analyse et d'interprétation dans le but de définir et de comprendre un système régional d'écoulement complexe. Ce doctorat a atteint les principaux objectifs fixés grâce, entre autre, aux importants travaux de terrain qui ont permis de caractériser l'hydrogéochimie de l'ensemble des sources et formations géologiques de la région d'étude. De plus, cette étude hydrogéochimique repose à la fois sur la caractérisation géologique et hydrogéologique du système aquifère, procurant ainsi le cadre physique qui a permis une interprétation cohérente et intégrée de l'origine et l'évolution géochimique des eaux souterraines du système aquifère des Basses-Laurentides.

## LISTE DES RÉFÉRENCES

- Abbott, M.D., Lini, A., Bierman, P.R., 2000.  $\delta^{18}\text{O}$ ,  $\delta\text{D}$  and  ${}^3\text{H}$  measurements constrain groundwater recharge patterns in an upland fractured bedrock aquifer, Vermont, USA. *Journal of Hydrology*, 228, 101-112.
- Adams, S., Titus, R., Pietersen, K., Tredoux, G., Harris, C., 2001. Hydrochemical characteristics of aquifers near Sutherland in the Western Karoo, South Africa. *Journal of Hydrology*, 241, 91-103.
- Adar, E.M., Rosenthal, E., Issar, A.S., Batelaan, O., 1992. Quantitative assessment of the flow pattern in the southern Arava Valley (Israel) by environmental tracers and a mixing cell model. *Journal of Hydrology*, 136, 333-352.
- Aeschbach-Hertig, W., Schlosser, P., Stute, M., Simpson, H.J., Ludin, A., Clark, J.F., 1998. A  ${}^3\text{H}/{}^3\text{He}$  study of ground water flow in a fractured bedrock aquifer. *Ground Water*, 36(4), 661-670.
- Aiuppa, A., Bellomo, S., Brusca, L., D'Alessandro, W., Federico, C., 2003. Natural and anthropogenic factors affecting groundwater quality of an active volcano (Mt. Etna, Italy). *Applied Geochemistry*, 18, 863-882.
- Alley, W.M., 1993. Establishing a conceptual framework. In: Alley, W.M. (Ed.), *Regional Ground-Water Quality*, New York, van Norstrand Reinhold, 23-60.
- Allison, J.D., Brown, D.S., Novo-Gradac, K.J., 1991. MINTEQA2/PRODEFA2, A geochemical assessment model for environmental systems: Version 3.0 User's Manual. Environmental research laboratory, U.S. Environmental Protection Agency, EPA/600/3-91/021.
- Andreasen, D.C., Fleck, W.B., 1997. Use of bromide: chloride ratios to differentiate potential sources of chloride in a shallow, unconfined aquifer affected by brackish-water intrusion. *Hydrogeology Journal*, 5(2), 17-26.
- Appelo, C.A.J., Postma, D., 1993. *Geochemistry, Groundwater and Pollution*. A.A. Balkema, Rotterdam.
- Appelo, C.A.J., 1994. Cation and proton exchange, pH variations, and carbonate reactions in a freshening aquifer. *Water Resources Research*, 30(10), 2793-2805.
- Appelo, C.A.J., Drijver, B., Hekkenberg, R., de Jonge, M., 1999. Modeling in situ iron removal from ground water. *Ground Water*, 37 (6), 811-817.

- Aravena, R., Evans, M.L., Cherry, J.A., 1993. Stable isotopes of oxygen and nitrogen in source identification of nitrate from septic systems. *Ground Water*, 31, 180-186.
- Aravena, R., Robertson, W.D., 1998. Use of multiple isotope tracers to evaluate denitrification in ground water: Study of nitrate from a large-flux septic system plume. *Ground Water*, 36(6), 975-982.
- Ayalon, A., Bar-Matthews, M., Sass, E., 1998. Rainfall-recharge relationships within a karstic terrain in the Eastern Mediterranean semi-arid region:  $\delta^{18}\text{O}$  and  $\delta\text{D}$  characteristics. *Journal of Hydrology*, 207, 18-31.
- Ayora, C., Taberner, C., Saaltink, M.W., Carrera, J., 1998. The genesis of dedolomites: a discussion based on reactive transport modeling. *Journal of Hydrology*, 209, 346-365.
- Back, W., 1961. Techniques for mapping of hydrochemical facies. U.S. Geological Survey Professional Paper 424-D, 380-382.
- Back, W., 1966. Hydrochemical facies and ground-water flow patterns in northern part of Atlantic Coastal Plain. U.S. Geological Survey Professional Paper 498-A.
- Back, W., Hanshaw, B.B., 1970. Comparison of chemical hydrogeology of the carbonate peninsulas of Florida and Yucatan. *Journal of Hydrology*, 10, 330-368.
- Back, W., Hanshaw, B.B., Plummer, L.N., Rahn, P.H., Rightmire, C.T., Rubin, M., 1983. Process and rate of dedolomitization: Mass transfer and  $^{14}\text{C}$  dating in a regional carbonate aquifer. *Geological Society of America Bulletin*, 94, 1415-1429.
- Back, W., Baedecker, M.J., Wood, W.W., 1993. Scales in chemical hydrogeology: A historical Perspective. In: Alley, W.M., (ed.). *Regional Ground-Water Quality*, New York, van Nostrand Reinhold, 111-129.
- Bain, J.G., Blowes, D.W., Robertson, W.D., Frind, E.O., 2000. Modelling of sulfide oxidation with reactive transport at a mine drainage site. *Journal of Contaminant Hydrology*, 41, 23-47.
- Ball, J.W., Nordstrom, D.K., 1991. User's Manual for WATEQ4F, with revised thermodynamic database and test cases for calculating speciation of major, trace and redox elements in natural waters. U.S. Geological Survey, Open-File Report 91-183, 189 p.
- Banner, J.L., Wasserburg, G.L., Dobson, P.F., Carpenter, A.B., Moore, C.H., 1989. Isotopic and trace element constraints on the origin and evolution of saline groundwaters from central Missouri. *Geochimica et Cosmochimica Acta*, 53, 383-398.
- Banner, J.L., Hanson, G.N., 1990. Calculation of simultaneous isotopic and trace element variations during water-rock interaction with applications to carbonate diagenesis. *Geochimica et Cosmochimica Acta*, 54, 3123-3137.

- Bäverman, C., Strömberg, Moreno, L., Neretnieks, 1999. CHEMFRONTS: a coupled geochemical and transport simulation tool. *Journal of Contaminant Hydrology*, 36, 333-351.
- Berkowitz, B., Bear, J., Braester, C., 1988. Continuum models for contaminants transport in fractured porous formations. *Water Resources Research*, 24, 1225-1236.
- Bernstein, L., 1992. A revised lithostratigraphy of the Lower-Middle Ordovician Beekmantown Group, St. Lawrence Lowlands, Quebec and Ontario. *Canadian Journal of Earth Science*, 29:2667-2694.
- Bodvarsson, G.S., Boyle, W., Patterson, R., Williams, D., 1999. Overview of scientific investigations at Yucca Mountain-the potentiel repository for high-level nuclear waste. *Journal of Contaminant Hydrology*, 38, 3-24.
- Bolduc, A.M., Ross, M., 2001. Géologie des formations superficielles, Lachute-Oka, Québec. Geological Survey of Canada, Open File 3520.
- Bourque, É., Cloutier, V., Lefebvre, R., Savard, M.M., Nastev, M., Martel, R., 2001. Résultats initiaux de la caractérisation hydrogéochemique des aquifères fracturés du sud-ouest du Québec. Commission géologique du Canada, Recherches en cours 2001-D8, 9 p., <http://www.nrcan.gc.ca/gsc/bookstore>.
- Cane, G., Clark, I.D., 1998. Tracing ground water recharge in an agricultural watershed with isotopes. *Ground Water*, 37(1), 133-139.
- Carrillo-Rivera, 2003. Lack of a conceptual system view of groundwater resources in Mexico (Editor's Message). *Hydrogeology Journal*, 11(5), 519-520.
- Castro, M.C., Goblet, P., Ledoux, E., Violette, S., Marsily, G. de, 1998. Noble gases as natural tracers of water circulation in the Paris Basin 2. Calibration of a groundwater flow model using noble gas isotope data. *Water Resources Research*, 34(10), 2467-2483.
- CCME - Conseil canadien des ministres de l'environnement, 1999. Recommandations canadiennes pour la qualité de l'environnement, Sommaire des recommandations canadiennes existantes pour la qualité de l'environnement, tableau sommaire, 13 p.
- Champ, D.R., Gulens, Jackson, R.E., 1979. Oxidation-reduction sequences in ground water flow systems. *Canadian Journal of Earth Science*, 16, 12-23.
- Chapelle, F.H., Knobel, L.L., 1983. Aqueous geochemistry and the exchangeable cation composition of glauconite in the Aquia Aquifer, Maryland. *Ground Water*, 21(3), 343-352.

Chapelle, F.H., Knobel, L.L., 1985. Stable carbon isotopes of  $\text{HCO}_3^-$  in the Aquia Aquifer, Maryland: Evidence for an isotopically heavy source of CO<sub>2</sub>. *Ground Water*, 23(5), 592-599.

Charlton, S.R., Parkhurst, D.L., 2002. PHREEQCI – A Graphical User Interface to the Geochemical Model PHREEQC. USGS Fact Sheet FS-031-02, April 2002.

Chebotarev, I.I., 1955. Metamorphism of natural waters in the crust of weathering-1, 2, 3. *Geochimica et Cosmochimica Acta*, 8, 22-48, 137-170, 198-212.

Cheng, H.-P., Yeh, G.-T., 1998. Development and demonstrative application of a 3-D numerical model of subsurface flow, heat transfer, and reactive chemical transport: 3DHYDROGEOCHEM. *Journal of Contaminant Hydrology*, 34, 47-83.

Chi, G., Lavoie, D., Salad Hersi, O., 2000. Dolostone units of the Beekmantown Group in the Montréal area, Québec: diagenesis and constraints on timing of hydrocarbon activities. Geological Survey of Canada, Current Research 2000-D1, <http://www.nrcan.gc.ca/gsc/bookstore>.

Clark, I., Fritz, P., 1997. Environmental Isotopes in Hydrogeology. Lewis Publishers, New York.

Clark, J.F., Davisson, M.L., Hudson, G.B., Macfarlane, P.A., 1998. Noble gases, stable isotopes, and radiocarbon as tracers of flow in the Dakota aquifer, Colorado and Kansas. *Journal of Hydrology*, 211, 151-167.

Clark, T.H., 1972. Montréal Area. Department of Natural Resources, General Direction of Mines, Geological Exploration Service, Québec, Geological report 152.

Cloutier, V., 1994. Stable isotopes of chlorine as indicators of the source and migration paths of solutes within glacial deposits and bedrock formations, Lambton County, southwestern Ontario. MSc Thesis, University of Waterloo, Ontario, Canada, 131 p.

Cloutier, V., Bourque, É., Lefebvre, R., Savard, M.M., Nastev, M., Martel, R., Therrien, R., 2001. Regional groundwater hydrogeochemistry of fractured rock aquifers in south-western Quebec. Proceedings, 2nd Joint IAH-CNC and CGS, Groundwater Specialty Conference, 54th Canadian Geotechnical Conference, Sept. 16-19, 2001, Calgary, Canada, 1068-1076.

Cloutier, V., Bourque, É., sous presse. Groundwater relative quality zones map. In: Regional hydrogeological characterization of the fractured aquifer system in south-western Quebec: Part III-Hydrogeologic atlas, CD-ROM, Fig. 41. Geological Survey of Canada, Bulletin.

Cloutier, V., Bourque, É., Lefebvre, R., Savard, M.M., Martel, R., sous presse. Hydrogeochemical characterization and groundwater quality: Part I-Regional hydrogeology of the aquifer system. Geological Survey of Canada, Bulletin.

Cloutier, V., Lefebvre, R., Savard, M.M., Therrien, R., en prep a. Geochemical processes in the Basses-Laurentides sedimentary rock aquifer system, St. Lawrence Lowlands, Québec, Canada.

Cloutier, V., Lefebvre, R., Therrien, R., Savard, M.M., en prep b. Multivariate statistical analysis of geochemical data as indicative of the hydrogeochemical evolution of groundwater of the Basses-Laurentides sedimentary rock aquifer system, St. Lawrence Lowlands, Québec, Canada.

Cloutier, V., Lefebvre, R., Savard, M.M., Bourque, É., Therrien, R., en prep c. Hydrogeochemistry and groundwater origin of the Basses-Laurentides sedimentary rock aquifer system, St. Lawrence Lowlands, Québec, Canada. *Hydrogeology Journal* (submitted).

Cohen, A.J.B., Karasaki, K., Benson, S., Bodvarsson, G., Freifeld, B., Benito, P., Cook, P., Clyde, J., Grossenbacher, K., Peterson, J., Solbau, R., Thapa, B., Vasco, D., Zawislanski, P., 1996. Hydrogeologic Characterization of Fractured Rock Formations : A Guide for Groundwater Remediations. U.S. Environmental Protection Agency, Project Summary, EPA/600/S-96/001, 11 p.

Coleman, M.L., Shepherd, T.J., Durham, J.J., Rousse, J.E., Moore, G.R., 1982. Reduction of water with zinc for hydrogen isotope analysis. *Analytical Chemistry*, 54(6), 993-995.

Cook, P.G., Solomon, D.K., Sanford, W.E., Busenberg, E., Plummer, L.N., Poreda, R.J., 1996. Inferring shallow groundwater flow in saprolite and fractured rock using environmental tracers. *Water Resources Research*, 32(6), 1501-1509.

Cook, P.G., Love, A.J., Dighton, J.C., 1999. Inferring ground water flow in fractured rock from dissolved radon. *Ground Water*, 37(4), 606-610.

Craig, H., 1961. Isotopic variations in meteoric waters. *Science*, 133, 1702-1703.

Dahan, O., Nativ, R., Adar, E.M., Berkowitz, B., Weisbrod, N., 2000. On fracture structure and preferential flow in unsaturated chalk. *Ground Water*, 38(3), 444-451.

Davis, J.C., 1986. *Statistics and Data Analysis in Geology*. John Wiley & Sons Inc., New York.

Davis, S.N., Cecil, L.D., Zreda, M., Moysey, S., 2001. Chlorine-36, bromide, and the origin of spring water. *Chemical Geology*, 179, 3-16.

Desaulniers, D.E., Cherry, J.A., Fritz, P., 1981. Origin, age and movement of pore waters in argillaceous Quaternary deposits at four sites in southwestern Ontario. *Journal of Hydrology*, 50, 231-257.

- Desaulniers, D.E., Cherry, J.A., 1989. Origin and movement of groundwater and major ions in a thick deposit of Champlain Sea clay near Montréal. Canadian Geotechnical Journal, 26, 80-89.
- Doughty, C., 1999. Investigation of conceptual and numerical approaches for evaluating moisture, gas, chemical, and heat transport in fractured unsaturated rock. Journal of Contaminant Hydrology, 38, 69-106.
- Drever, J.I., 1988. The Geochemistry of Natural Waters. Prentice-Hall, Inc., Englewood Cliffs, New Jersey.
- Drimmie, R.J., Aravena, R., Wassenaar, L.I., Fritz, P., Hendry, M.J., Hut, G., 1991. Radiocarbon and stable isotopes in water and dissolved constituents, Milk River aquifer, Alberta, Canada. Applied Geochemistry, 6, 381-392.
- Eberts, S.M., George, L.L., 2000. Regional ground-water flow and geochemistry in the Midwestern Basins and Arches Aquifer System in parts of Indiana, Ohio, Michigan, and Illinois. U.S. Geological Survey Professional Paper 1423-C.
- Edmunds, W.M., Bath, A.H., Miles, D.L., 1982. Hydrochemical evolution of the East Midlands Triassic Sandstone aquifer. Geochimica et Cosmochimica Acta, 46, 2069-2081.
- Eggenkamp, H.G.M., 1994. The geochemistry of chlorine isotopes. Ph.D. Thesis, University of Utrecht, 150 p.
- Environment Canada, 1998. CAPMoN precipitation sampling standard operation procedures, Canadian Network for Isotopes in Precipitation (CNIP), Version 1.1, June 1998, 4 p.
- Étienne, M., 2002. Caractérisation in situ des milieux fracturés à l'aide des diagraphies géophysiques. Mémoire de maîtrise, Université Laval, Québec, Canada, 246 p.
- Fagnan, N., Bourque, É., Michaud, Y., Lefebvre, R., Boivert, É., Parent, M., Martel, R., 1999. Hydrogéologie des complexes deltaïques sur la marge nord de la mer de Champlain, Québec. Hydrogéologie, 4, 9-22.
- Fagnan, N., Nastev, M., Lefebvre, R., Martel, R., Savard, M.M., 2001. Résultats initiaux d'une partie des travaux de caractérisation hydrogéologique des aquifères fracturés du sud-ouest du Québec. Commission géologique du Canada, Recherches en cours 2001-D7, 9 p., <http://www.nrcan.gc.ca/gsc/bookstore>.
- Feast, N.A., Hiscock, K.M., Dennis, P.F., Andrews, J.N., 1998. Nitrogen isotope hydrochemistry and denitrification within the Chalk aquifer system of north Norfolk, UK. Journal of Hydrology, 211, 233-252.

- Feenstra, S., Cherry, J.A., Sudicky, E.A., Haq, Z., 1984. Matrix diffusion effects on contaminant migration from an injection well in fractured sandstone. *Ground Water*, 22(3), 307-316.
- Frape, S.K., Fritz, P., McNutt, R.H., 1984. Water-rock interaction and chemistry of groundwaters from the Canadian Shield. *Geochimica et Cosmochimica Acta*, 48, 1617-1627.
- Freeze, R.A., Witherspoon, P.A., 1967. Theoretical analysis of regional ground water flow 2. The effect of water-table configuration and subsurface permeability variation. *Water Resources Research*, 3, 623-634.
- Freeze, R.A., Cherry, J.A., 1979. Groundwater. Prentice-Hall, Inc., Englewood Cliffs, New Jersey.
- Fritz, P., Drimmie, R.J., Frape, S.K., O'Shea, K.J., 1987. The isotopic composition of precipitation and groundwater in Canada. In: Isotope Techniques in Water Resources Development, IAEA Symposium 299, March 1987, Vienna, 539-550.
- Fritz, S.J., Drimmie, R.J., Fritz, P., 1991. Characterizing shallow aquifers using tritium and  $^{14}\text{C}$  periodic sampling based on tritium half-life. *Applied Geochemistry*, 6, 17-33.
- Garven, G., Appold, M.S., Toptygina, V.I., Hazlett, T.J., 1999. Hydrogeologic modeling of the genesis of carbonate-hosted lead-zinc ores. *Hydrogeology Journal*, 7(1), 108-126.
- Gerke, H.H., Molson, J.W., Frind, E.O., 1998. Modelling the effects of chemical heterogeneity on acidification and solute leaching in overburden mine spoils. *Journal of Hydrology*, 209, 166-185.
- Ghogomu, N.F., Therrien, R., 2000. Reactive mass transport modelling in discretely-fractured porous media. Invited paper, Computational Methods in Water Resources XIII, Bentley et al. (eds), Calgary, 25-29 June 2000, 285-292.
- Gibs, J., Szabo, Z., Ivahnenko, T., Wilde, F.D., 2000. Change in field turbidity and trace element concentrations during well purging. *Ground Water*, 38(4), 577-588.
- Gibson, J.J., Prowse, T.D., 1999. Isotopic characteristics of ice cover in a large northern river basin. *Hydrological processes*, 13, 2537-2548.
- Glynn, P., Brown, J., 1996. Reactive transport modeling of acidic metal-contaminated ground water at a site with sparse spatial information. In: Lichtner, P., Steefel, C.T., and Oelkers, E.H., (Eds.). *Reactive Transport in Porous Media*, Review in Mineralogy 34, Mineralogical Society of America, 377-438.

- Globensky, Y., 1972. Gas-Oil-Salt Water in wells drilled in Québec between 1860 and 1970. Department of Natural Resources, General Direction of Mines, Mineral Deposits Service, Québec, Report S-127AF.
- Globensky, Y., 1987. Géologie des Basses-Terres du St-Laurent. Department of Energy and Resources, General Direction of geological and mineral exploration, Québec, Report MM 85-02.
- GNIP, 1996. IAEA-WMO programme on isotopic composition of precipitation: Global Network for Isotopes in Precipitation (GNIP), Technical procedure for sampling, Vienna, September 1996, 2 p.
- Gold, D.P., 1972. The Monteregian Hills: ultra-alkaline rocks and the Oka carbonatite complex. International Geological Congress, 24<sup>th</sup>, Montréal, Canada, Guidebook B-11.
- Gosselin, D.C., Harvey, F.E., Frost, C.D., 2001. Geochemical evolution of ground water in the Great Plains aquifer of Nebraska: Implications for the management of a regional aquifer system. *Ground Water*, 39(1), 98-108.
- Gouvernement du Québec, 2001. Règlement sur la qualité de l'eau potable. Q-2, r.4.1, Éditeur officiel, 7 p.
- Güler, C., Thyne, G.D., McCray, J.E., Turner, A.K., 2002. Evaluation of graphical and multivariate statistical methods for classification of water chemistry data. *Hydrogeology Journal*, 10, 455-474.
- Guvenasen, V., Wade, S.C., Barcelo, M.D., 2000. Simulation of regional ground water flow and salt water intrusion in Hernando County, Florida. *Ground Water*, 38(5), 772-783.
- Hamel, A., Therrien, R., Gélinas, P., 2001. Groundwater recharge of fractured rock aquifers in south-western Québec. In: 2nd Joint IAH-CGS Groundwater Specialty Conf, Calgary, pp 1078-1084.
- Hamel, A., 2002. Détermination de la recharge des aquifères de roc fracturé du sud-ouest du Québec. Mémoire de maîtrise, Université Laval, Québec, Canada, 271 p.
- Hanshaw, B.B., Back, W., 1979. Major geochemical processes in the evolution of carbonate aquifer system. *Journal of Hydrology*, 43, 287-312.
- Harrison, B., Sudicky, E.A., Cherry, J.A., 1992. Numerical analysis of solute migration through fractured clayey deposits into underlying aquifers. *Water Resources Research*, 28(2), 515-526.

- Harvey, F.E., 2001. Use of NADP archive samples to determine the isotope composition of precipitation: Characterizing the meteoric input function for use in ground water studies. *Ground Water*, 39(3), 380-390.
- Health Canada, 2003. Summary of guidelines for Canadian drinking water quality. Prepared by the Federal-Provincial-Territorial Committee on Drinking Water of the Federal-Provincial-Territorial Committee on Environmental and Occupational Health, April 2003, <http://www.hc-sc.gc.ca/waterquality>.
- Hem, J.D., 1985. Study and interpretation of the chemical characteristics of natural water. U.S. Geological Survey Water-Supply Paper 2254, Third Edition.
- Henderson, T., 1985. Geochemistry of ground water in two sandstone aquifer systems in the Northern Great Plains in parts of Montana, Wyoming, North Dakota, and South Dakota. U.S. Geological Survey Professional Paper 1402-C.
- Hendry, M.J., Schwartz, F.W., 1988. An alternative view on the origin of chemical and isotopic patterns in groundwater from the Milk River Aquifer, Canada. *Water Resources Research*, 24(10), 1747-1763.
- Hendry, M.J., Schwartz, F.W., 1990. The chemical evolution of ground water in the Milk River Aquifer, Canada. *Ground Water*, 28(2), 253-261.
- Héroux, Y., Bertrand, R., 1991. Maturation thermique de la matière organique dans un bassin du Paléozoïque inférieur, basses-terres du Saint-Laurent, Québec, Canada. *Canadian Journal of Earth Sciences*, 28, 1019-1030.
- Hillaire-Marcel, C., 1988. Isotopic composition ( $^{18}\text{O}$ ,  $^{13}\text{C}$ ,  $^{14}\text{C}$ ) of biogenic carbonates in Champlain Sea Sediments. In: Gadd, N.R. (ed) *The late Quaternary Development of the Champlain Sea Basin: Geological Association of Canada, Special Paper 35*, 177-194.
- Himmelsbach, T., Hötzl, H., Maloszewski, P., 1998. Solute transport processes in a highly permeable fault zone of Lindau fractured rock test site (Germany). *Ground Water*, 36(5), 792-800.
- Hiscock, K.M., Dennis, P.F., Saynor, P.R., Thomas, M.O., 1996. Hydrochemical and stable isotope evidence for the extent and nature of the effective Chalk aquifer of north Norfolk, UK. *Journal of Hydrology*, 180, 79-107.
- Hitchon, B., Friedman, I., 1969. Geochemistry and origin of formation waters in the western Canada sedimentary basin-I. Stable isotopes of hydrogen and oxygen. *Geochimica et Cosmochimica Acta*, 33, 1321-1349.
- Hounslow, A.E., 1995. *Water Quality Data: Analysis and Interpretation*. Lewis Publishers.

- Husain, M.M., Cherry, J.A., Fidler, S., Frape, S.K., 1998. On the long-term hydraulic gradient in the thick clayey aquitard in the Sarnia region, Ontario. Canadian Geotechnical Journal, 35, 986-1003.
- IAEA, 2001. GNIP maps and animations. International Atomic Energy Agency, Vienna, <http://isohis.iaea.org>.
- IAEA/WMO, 2001. Global Network for Isotopes in Precipitation. The GNIP database, <http://isohis.iaea.org>.
- Ingebritsen, S.E., Sanford, W.E., 1998. Groundwater in Geologic Processes. Cambridge University Press, Cambridge, New York.
- Jayakumar, R., Siraz, L., 1997. Factor analysis in hydrogeochemistry of coastal aquifers – a preliminary study. Environmental Geology, 31(3/4), 174-177.
- Johnson, T.M., Roback, R.C., McLing, T.L., Bullen, T.D., DePaolo, D.J., Doughty, C., Hunt, R.J., Smith, R.W., Cecil, L.D., Murrell, M.T., 2000. Groundwater "fast paths" in the Snake River Plain aquifer: Radiogenic isotope ratios as natural groundwater tracers. Geology, 28(10), 871-874.
- Jones, I., Lerner, D.N., Baines, O.P., 1999. Multiport sock samplers: A low-cost technology for effective multilevel ground water sampling. Ground Water Monitoring Review, Winter 1999, 134-142.
- Jørgensen, N.O., Morthorst, J., Holm, P.M., 1999. Strontium-isotope studies of "brown water" (organic-rich groundwater) from Denmark. Hydrogeology Journal, 7(6), 533-539.
- Karanta, G., Martel, R., Nastev, M., Therrien, R., Paradis, D., Lefebvre, R., 2001. Comparative study of methods for wellhead protection area delineation in fractured rocks. In: 2nd Joint IAH-CGS Groundwater Specialty Conf, Calgary, pp 1350-1357.
- Karasaki, K., Freifeld, B., Cohen, A., Grossenbacher, K., Cook, P., Vasco, D., 2000. A multidisciplinary fractured rock characterization study at Raymond field site, Raymond, CA. Journal of Hydrology, 236, 17-34.
- Katz, B.G., Catches, J.S., Bullen, T.D., Michel, R.L., 1998. Changes in the isotopic and chemical composition of ground water resulting from a recharge pulse from a sinking stream. Journal of Hydrology, 211, 178-207.
- Kaufmann, R.S., Frape, S.K., McNutt, R., Eastoe, C., 1993. Chlorine stable isotope distribution of Michigan Basin formation waters. Applied Geochemistry, 8, 403-407.
- Kauffman, S.J., Herman, J.S., Jones, B.F., 1998. Lithological and hydrological influences on ground-water composition in a heterogeneous carbonate-clay aquifer system. Geological Society of America Bulletin, 110(9), 1163-1173.

- Keating, E.H., Bahr, J.M., 1998. Using reactive solutes to constrain groundwater flow models at a site in northern Wisconsin. *Water Resources Research*, 34(12), 3561-3571.
- Kendall, C., McDonnell, 1998. Isotope tracers in catchment hydrology. Elsevier Science B.V., Amsterdam.
- Knobel, L.L., Phillips, S.W., 1988. Aqueous geochemistry of the Magothy Aquifer, Maryland. U.S. Geological Survey, Water-Supply Paper 2323.
- Kueper, B.H., McWhorter, D.B., 1992. The behaviour of dense, nonaqueous phase liquids in fractured clay and rock. *Ground Water*, 29(5), 716-728.
- Landon, M.K., Delin, G.N., Komor, S.C., Regan, C.P., 2000. Relation of pathways and transit times of recharge water to nitrate concentrations using stable isotopes. *Ground Water*, 38(3), 381-395.
- Langmuir, D., 1971. The geochemistry of some carbonate ground waters in central Pennsylvania. *Geochimica et Cosmochimica Acta*, 35, 1023-1045.
- Lapcevic, P., Novakowski, K., Voralek, J., Bickerton, G., Talbot, C., Zanini, L., 2000. Results of investigations in the proximity of the source zone at the CWML site, Smithville, Ontario. National Water Research Institute, Environment Canada, NWRI Contribution Number 00-056, 60 p.
- Lee, K.-S., Wenner, D.B., Lee, I., 1999. Using H- and O-isotopic data for estimating the relative contributions of rainy and dry season precipitation to groundwater: example from Cheju Island, Korea. *Journal of Hydrology*, 222, 65-74.
- Le Gal La Salle, C., Marline, C., Savoye, S., Fontes, J.-C., 1996. Geochemistry and  $^{14}\text{C}$  dating of groundwaters from Jurassic aquifers of North Aquitaine Basin (France). *Applied Geochemistry*, 11, 433-445.
- Lemieux, J.-M., 2002. Caractérisation multiapproche à petite échelle de l'écoulement de l'eau souterraine dans un aquifère carbonaté fracturé et implications pour les changements d'échelle. Mémoire de maîtrise, Université Laval, Québec, Canada, 100 p.
- Lévesque, G., 1982. Géologie des dépôts Quaternaires de la région de Oka - St-Scholastique, Québec. Mémoire de maîtrise, Université du Québec à Montréal, Québec, Canada.
- Lewis, D.W., 1971. Qualitative petrographic interpretation of Potsdam Sandstone (Cambrian), Southwestern Québec. *Canadian Journal of Earth Sciences*, 8, 853-882.

- Lichtner, P.C., 1996. Continuum formulation of multicomponent-multiphase reactive transport. In: Lichtner, P., Steefel, C.T., and Oelkers, E.H., (Eds.). Reactive Transport in Porous Media, Review in Mineralogy 34, Mineralogical Society of America, 1-81.
- Lichtner, P.C., 1999. Multicomponent reactive transport in fractured porous media: Methods and applications. In: Proceedings of the International Symposium on Dynamics of Fluids in Fractured Rocks, Concepts and Recent Advances, Earth Science Division, Ernest Orlando Lawrence Berkeley National Laboratory, Berkeley, California, February 1999, 36-39.
- Long, D.T., Wilson, T.P., Takacs, M.J., Rezabek, D.H., 1988. Stable-isotope geochemistry of saline near-surface ground water: East-central Michigan basin. Geological Society of America Bulletin, 100, 1568-1577.
- Machel, H.G., 1999. Effects of groundwater flow on mineral diagenesis, with emphasis on carbonate aquifers. *Hydrogeology Journal*, 7(1), 94-107.
- Matray, J.M., Lambert, M., Fontes, J.-C., 1994. Stable isotope conservation and origin of saline waters from the Middle Jurassic aquifers of the Paris Basin, France. *Applied Geochemistry*, 9, 297-309.
- Mayo, A.L., Koontz, W., 2000. Fracture flow and groundwater compartmentalization in the Rollins Sandstone, Lower Mesaverde Group, Colorado, USA. *Hydrogeology Journal*, 8(4), 430-446.
- Mazor, E., 1991. Applied chemical and isotopic groundwater hydrology. Open University Press, Great Britain.
- McKay, L.D., Novakowski, K., McCarthy, J.F., 1994. Groundwater sampling in fractured clay and rock. In: EPA Ground Water Sampling – A Workshop Summary. Dallas, Texas, EPA/600/R-94/205, 37-38.
- McLaren, R.G., Forsyth, P.A., Sudicky, E.A., VanderKwaak, J.E., Schwartz, F.W., Kessler, J.H., 2000. Flow and transport in fractured tuff at Yucca Mountain: numerical experiments on fast preferential flow mechanisms. *Journal of Contaminant Hydrology*, 43, 211-238.
- McNutt, R.H., Frape, S.K., Dollar, P., 1987. A strontium, oxygen and hydrogen isotopic composition of brines, Michigan and Appalachian Basins, Ontario and Michigan. *Applied Geochemistry*, 2, 495-505.
- McNutt, R.H., Frape, S.K., Fritz, P., Jones, M.G., MacDonald, I.M., 1990. The  $^{87}\text{Sr}/^{86}\text{Sr}$  values of Canadian Shield brines and fracture minerals with applications to groundwater mixing, fracture history, and geochronology. *Geochimica et Cosmochimica Acta*, 54, 205-215.

- Melloul, A., and Collin, M., 1992. The ‘principal components’ statistical method as a complementary approach to geochemical methods in water quality factor identification; application to the Coastal Plain aquifer of Israel. *Journal of Hydrology*, 140, 49-73.
- MENV, 2000. Portrait régional de l'eau: Laurentides, région administrative 15. Department of the Environment, Québec, <http://www.menv.gouv.qc.ca/eau/regions/region15/index.htm>.
- Morin, R.H., Senior, L.A., Decker, E.R., 2000. Fractured-aquifer hydrogeology from geophysical logs: Brunswick Group and Lockatong Formation, Pennsylvania. *Ground Water*, 38(2), 182-192.
- Nastev, M., Savard, M.M., Lapcevic, P., Paradis, D., Lefebvre, R., Martel, R., 2001. Investigation of hydraulic properties of regional fractured rock aquifers. In: 2nd Joint IAH-CGS Groundwater Specialty Conf, Calgary, pp 1058-1066.
- Nastev, M., Bourque, É., Cloutier, V., Paradis, D., Ross, M., 2002. Étude détaillée d'un site sélectionné : Cas du secteur de St-Benoît, Mirabel. Dans : Partie IV, Études locales de secteurs choisis du système aquifère fracturé du sud-ouest du Québec, rapport final. Édité par Savard, M.M., Lefebvre, R., Nastev, M., p. 13-28, 79-88.
- Nastev, M., Savard, M.M., Paradis, D., Lefebvre, R., Ross, M., sous presse. Regional hydrogeological characterization of the fractured aquifer system in south-western Quebec: Part II-Quantitative study of groundwater resources. Geological Survey of Canada, Bulletin.
- Nastev, M., Rivera, A., Lefebvre, R., Savard, M.M., en prep a. Numerical simulation of regional groundwater flow in sedimentary rock aquifers. *Hydrogeology Journal* (submitted).
- Nastev, M., Savard, M.M., Lapcevic, P., Lefebvre, R., Martel, R., en prep b. Hydraulic properties and scale effects investigation in regional rock aquifers. *Hydrogeology Journal* (submitted).
- Neretnieks, I., 1993. Solute transport in fractured rock – Applications to radionuclide waste repositories. In: Bear, J., Tsang, C.-F., and de Marsily, G., (Eds.). *Flow and Contaminant Transport in Fractured Rock*. Academic Press, Inc., 39-127.
- Nordstrom, D.K., Wilde, F.D., 1998. Reduction-oxidation potential (electrode method). In: National field manual for the collection of water-quality data. U.S. Geological Survey Techniques of Water-Resources Investigations, book 9, chap. A6.5, [http://water.usgs.gov/owq/FieldManual/Chapter6/6.5\\_contents.html](http://water.usgs.gov/owq/FieldManual/Chapter6/6.5_contents.html).
- Novakowski, K.S., Lapcevic, P.A., 1994. Field measurement of radial solute transport in fractured rock. *Water Resources Research*, 30(1), 37-44.

- Ophori, D.U., Tóth, J., 1989. Patterns of ground-water chemistry, Ross Creek Basin, Alberta, Canada. *Ground Water*, 27(1):20-26.
- Osenbrück, K., Lippmann, J., Sonntag, C., 1998. Dating very old pore waters in impermeable rocks by noble gas isotopes. *Geochimica et Cosmochimica Acta*, 62(18), 3041-3045.
- Özler, H.M., 1999. Water balance and water quality in the Çürüksu basin, western Turkey. *Hydrogeology Journal*, 7(4), 405-418.
- Paillet, F.L., Reese, S., 2000. Integrating borehole logs and aquifer tests in aquifer characterization. *Ground Water*, 38(5), 713-725.
- Palmer, C.D., Cherry, J.A., 1984. Geochemical evolution of groundwater in sequences of sedimentary rocks. *Journal of Hydrology*, 75, 27-65.
- Pankow, J.F., Jonhson, R.L., Hewetson, J.P., Cherry, J.A., 1986. An evaluation of contaminant migration patterns at two waste disposal sites on fractured porous media in terms of the equivalent porous media (EPM) model. *Journal of Contaminant Hydrology*, 1, 65-76.
- Panno, S.V., Hackley, K.C., Cartwright, K., Liu, C.L., 1994. Hydrochemistry of the Mahomet bedrock valley aquifer, East-Central Illinois: Indicators of recharge and ground-water flow. *Ground Water*, 32(4), 591-604.
- Paradis, D., sous presse a. Surficial formations thickness map. In: Regional hydrogeological characterization of the fractured aquifer system in south-western Quebec: Part III-Hydrogeologic atlas, CD-ROM, Fig. 15. Geological Survey of Canada, Bulletin.
- Paradis, D., sous presse b. Potentiometric surface map. In: Regional hydrogeological characterization of the fractured aquifer system in south-western Quebec: Part III-Hydrogeologic atlas, CD-ROM, Fig. 23. Geological Survey of Canada, Bulletin.
- Paradis, D., sous presse c. Principal recharge areas of the bedrock aquifer. In: Regional hydrogeological characterization of the fractured aquifer system in south-western Quebec: Part III-Hydrogeologic atlas, CD-ROM, Fig. 45. Geological Survey of Canada, Bulletin.
- Parent, M., Occhietti, S. 1988. Late Wisconsinian deglaciation and Champlain Sea invasion in the St. Lawrence Valley, Québec. *Géographie physique et Quaternaire*, 42(3), 215-246.
- Parker, B.L., McWorter, D.B., Cherry, J.A., 1997. Diffusive loss of non-aqueous phase organic solvents from idealized fracture networks in geologic media. *Ground Water*, 35(6), 1077-1088.

- Parkhurst, D.L., Thorstenson, D.C., Plummer, L.N., 1980. PHREEQE - A computer program for geochemical calculations. U.S. Geological Survey Water-Resources Investigations Report 80-96.
- Parkhurst, D.L., Plummer, L.N., 1993. Geochemical models. In: Alley, W.M., (ed.). Regional Ground-Water Quality, New York, van Norstrand Reinhold, 199-225.
- Parkhurst, D.L., 1995. User's guide to PHREEQC - A computer program for speciation, reaction-path, advective transport, and inverse geochemical calculations. U.S. Geological Survey, Water-Resources Investigations Report 95-4227, 143 p.
- Parkhurst, D.L., Christenson, S., Breit, G.N., 1996. Ground-Water-Quality Assessment of the Central Oklahoma Aquifer, Oklahoma - Geochemical and Geohydrologic Investigations. U.S. Geological Survey, Special Paper 2357-C, 101 p.
- Parkhurst, D.L., 1997. Geochemical mole-balance modeling with uncertain data. *Water Resources Research*, 33(8), 1957-1970.
- Parkhurst, D.L., Appelo, C.A.J., 1999. User's guide to PHREEQC (version 2) - A computer program for speciation, batch-reaction, one-dimensional transport, and inverse geochemical calculations. U.S. Geological Survey, Water-Resources Investigations Report 99-4259.
- Phillips, F.M., Bentley, H.W., Davis, S.N., Elmore, D., Swanick, G., 1986. Chlorine-36 dating of very old groundwater. 2. Milk River aquifer, Alberta, Canada. *Water Resources Research*, 22, 2003-2016.
- Piper, A.M., 1944. A graphic procedure in the geochemical interpretation of water-analyses. *American Geophysical Union. Papers, Hydrology*, 914-923.
- Plummer, L.N., Vacher, H.L., Mackenzie, F.T., Bricker, O.P., Land, L.S., 1976a. Hydrogeochemistry of Bermuda: A case history of ground-water diagenesis of biocalcareous. *Geological Society of America Bulletin*, 87, 1301-1316.
- Plummer, L.N., Jones, B.F., Truesdell, A.H., 1976b. WATEQF - A Fortran IV Version of WATEQ, A computer program for calculating chemical equilibrium of natural waters. U.S. Geological Survey, Water-Resources Investigations 76-13.
- Plummer, L.N., Back, W., 1980. The mass balance approach: application to interpreting the chemical evolution of hydrologic systems. *American Journal of Science*, 280, 130-142.
- Plummer, L.N., Parkhurst, D.L., Thorstenson, D.C., 1983. Development of reaction models of ground-water systems. *Geochimica et Cosmochimica Acta*, 47, 665-686.

- Plummer, L.N., Parkhurst, D.L., Fleming, G.W., Dunkle, S.A., 1988. A computer program incorporating Pitzer's equations for calculation of geochemical reaction in brines. U.S. Geological Survey, Water-Resources Investigations 88-4153.
- Plummer, L.N., Busby, J.F., Lee, R.W., Hanshaw, B.B., 1990. Geochemical modeling of the Madison aquifer in part of Montana, Wyoming, and South Dakota. *Water Resources Research*, 26, 1981-2014.
- Plummer, L.N., Prestemon, E.C., Parkhurst, D.L., 1994. An interactive code (NETPATH) for modeling net chemical reactions along a flow path version 2.0. U.S. Geological Survey Water-Resources Investigations Report 94-4169.
- Plummer, L.N., Rupert, M.G., Busenberg, E., and Schlosser, P., 2000. Age of irrigation water in ground water from the Eastern Snake River Plain Aquifer, South-Central Idaho. *Ground Water*, 38(2), 264-283.
- Pohll, G., Hassan, A.E., Chapman, J.B., Papelis, C., Andricevic, R., 1999. Modeling groundwater flow and radioactive transport in a fractured aquifer. *Ground Water*, 37(5), 770-784.
- Postma, D., Appelo, C.A.J., 2000. Reduction of Mn-oxides by ferrous iron in a flow system: Column experiment and reactive transport modeling. *Geochimica et Cosmochimica Acta*, 64(7), 1237-1247.
- Powell, J.L., Hurley, P.M., Fairbairn, H.W., 1966. The strontium isotopic composition and origin of carbonatites. In: Tuttle, O.F., Gittins, J. (ed) Carbonatites. Interscience publishers, John Wiley & Sons, 365-378.
- Pruess, K., Oldenburg, C., Moridis, 1999. TOUGH2 User's Guide, Version 2.0. Earth Sciences Division, Lawrence Berkeley National Laboratory, California, LBNL-43134.
- Ribeiro, L., Macedo, M.E., 1995. Application of multivariate statistics, trend- and cluster analysis to groundwater quality in the Tejo and Sado aquifer. In: Groundwater Quality: Remediation and Protection. Proceedings of the Prague Conference , May 1995. IAHS Publ. No. 225, 39-47.
- Richter, B.C., Kreitler, B.E., 1993. Geochemical techniques for identifying sources of ground-water salinization. C.K. Smoley, Boca Raton, FL.
- Robertson, W.D., Cherry, J.A., 1989. Tritium as indicator of recharge and dispersion in a groundwater system in central Ontario. *Water Resources Research*, 25(6), 1097-1109.
- Rocher, M., Salad-Hersi, O., Castonguay, S., sous presse. Geologic map of St. Lawrence Lowlands – Sector west of Montreal (update). In: Regional hydrogeological characterization of the fractured aquifer system in south-western Quebec: Part III-Hydrogeologic atlas, CD-ROM, Fig. 4. Geological Survey of Canada, Bulletin.

- Rosen, M.R., Bright, J., Carran, P., Stewart, M.K., Reeves, R., 1999. Estimating rainfall recharge and soil water residence times in Pukekohe, New Zealand, by combining geophysical, chemical, and isotopic methods. *Ground Water*, 37(6), 836-844.
- Ross, M., Bolduc, A., 2001. Successions Quaternaires de la région des Basses Laurentides, Ouest de Montréal. In: Lavoie, D., Bolduc, A., Castonguay, S., Malo, M., Ross, M., Salad Hersi, O., Séjourné, S., Tremblay, A., Lauzière, K., McIntosh, A., The St. Lawrence Platform, Humber Zone, and Quaternary successions along Transect #1: Montreal-Appalachians. Geological Survey of Canada, Open File 2812.
- Ross, M., Parent, M., Bolduc, A.M., Hunter, J., Benjumea, B., 2001. Étude préliminaire des formations quaternaires comblant les vallées des basses Laurentides, nord-ouest de Montréal, Québec. Commission géologique du Canada, Recherches en cours 2001-D5, 15 p., <http://www.nrcan.gc.ca/gsc/bookstore>.
- Ross, M., Martel, R., Parent, M., Lefebvre, R., Savard, M.M., 2003. The use of a 3D geologic framework model of surficial sediments to define bedrock aquifer vulnerability in the St. Lawrence Lowlands, Quebec, Canada. In: Rodriguez, R., Civita, M., de Maio, M. (Eds.), proceedings of the First International Workshop on Aquifer Vulnerability and Risk, Salamanca, Mexico, vol. 1, pp. 157-168.
- Rozanski, K., Araguás-Araguás, L., Gonfiantini, R., 1993. Isotopic patterns in modern global precipitations. *Climate Change in Continental Isotopic Records*, Geophysical Monograph 78, American Geophysical Union, 1-36.
- Ruland, W.W., Cherry, J.A., Feenstra, S., 1991. The depth of fractures and active ground-water flow in a Clayey Till Plain in southwestern Ontario. *Ground Water*, 29(3), 405-417.
- Salad Hersi, O., Lavoie, D., 2001. The Potsdam and Beekmantown Groups, evolution of the shallow marine passive margin in southern Québec. In: Lavoie, D., Bolduc, A., Castonguay, S., Malo, M., Ross, M., Salad Hersi, O., Séjourné, S., Tremblay, A., Lauzière, K., McIntosh, A., The St. Lawrence Platform, Humber Zone, and Quaternary successions along Transect #1: Montreal-Appalachians. Geological Survey of Canada, Open File 2812.
- Salad Hersi, O., Lavoie, D., Nowlan, G.S., 2003. Reappraisal of the Beekmantown Group sedimentology and stratigraphy, Montréal area, southwestern Quebec: implication for understanding the depositional evolution of the Lower-Middle Ordovician Laurentian passive margin of eastern Canada. *Canadian Journal of Earth Sciences*, 40, 149-176.
- Salama, R.B., Otto, C.J., Fitzpatrick, R.W., 1999. Contributions of groundwater conditions to soil and water salinization. *Hydrogeology Journal*, 7(1), 46-64.
- Santé Canada, 2001. Résumé des recommandations pour la qualité de l'eau potable au Canada. Préparé par le Comité fédéral-provincial-territorial sur l'eau potable du Comité fédéral-provincial-territorial de l'hygiène du milieu et du travail, mars 2001.

Savard, M., Dessau, J.C., Pellerin, E. 1998. Le Radon à Oka – Rapport d'intervention de santé publique. Direction régionale de la santé publique des Laurentides. 134 p. ISBN 2-921581-83-3.

Savard, M.M., Nastev, M., Lefebvre, R., Martel, R., Fagnan, N., Bourque, É., Cloutier, V., Lauzière, K., Gélinas, P., Kirkwood, D., Lapcevic, P., Karanta, G., Hamel, A., Bolduc, A., Ross, M., Parent, M., Lemieux, J.-M., Boisvert, E., Salad Hersi, O., Lavoie, D., Girard, F., Novakowski, K., Therrien, R., Etienne, M., Fortier, R., 2000. Regional Hydrogeology of fractured rock aquifers of southwestern Quebec (St.Lawrence Lowlands). In: First Joint IAH-CNC and CGS Groundwater Specialty Conference, October 2000, Montréal, 247-254.

Savard, M.M., Lefebvre, R., Nastev, M., Paradis, D., Cloutier, V., Martel, R., 2002. 6. Conclusions générales et recommandations. Dans Savard et al., éd., Hydrogéologie régionale du système aquifère fracturé du sud-ouest du Québec. Rapport final, Commission Géologique du Canada, 15 mai 2002, 26-32.

Savard, M.M., Nastev, M., Paradis, D., Lefebvre, R., Martel, R., Cloutier, V., Murat, V., Bourque, É., Ross, M., Lauzière, K., Parent, M., Hamel, A., Lemieux, J.-M., Therrien, R., Kirkwood, D., Gélinas, P., sous presse. Regional hydrogeological characterization of the fractured aquifer system in south-western Quebec: Part I-Regional hydrogeology of the aquifer system. Geological Survey of Canada, Bulletin.

Schmelling, S.G., Ross, R.R., 1989. Contaminant Transport in Fractured Media: Models for Decision Makers. In: EPA Superfund Ground Water Issue. EPA/540/4-89/004, 8 p.

Schot, P.P., van der Wal, J., 1992. Human impact on regional groundwater composition through intervention in natural flow patterns and changes in land use. Journal of Hydrology, 134, 297-313.

Schreiber, M.E., Moline, G.R., Bahr, J.M., 1999. Using hydrochemical facies to delineate ground water flowpaths in fractured shale. Ground Water Monitoring Review, Winter 1999, 95-109.

Schulze-Makush, D., Carlson, D.A., Cherkauer, D.S., Malik, P., 1999. Scale dependency of hydraulic conductivity in heterogeneous media. Ground Water, 37(6), 904-919.

Schwartz, F.W., Muehlenbachs, K., Chorley, D.W., 1981. Flow-system controls of the chemical evolution of groundwater. Journal of Hydrology, 54, 225-243.

Shapiro, S.D., LeBlanc, D., Schlosser, P., Ludin, A., 1999. Characterizing a sewage plume using the  $^{3}\text{H}$ - $^{3}\text{He}$  dating technique. Ground Water, 37(6), 861-878.

Siegel, M.D., Anderholm, S., 1994. Geochemical evolution of groundwater in the Culebra dolomite near the waste isolation pilot plant, southeastern New Mexico, USA. Geochimica et Cosmochimica Acta, 58(10), 2299-2323.

- Simard, G., 1977. Carbon 14 and tritium measurements of groundwaters in the Eaton River Basin and in the Mirabel area, Québec. Canadian Journal of Earth Science, 14, 2325-2338.
- Simard, G., 1978. Hydrogéologie de la région de Mirabel. Department of Natural Resources, Groundwater Service, Québec, Report H.G.-11.
- Simonetti, A., Gariépy, C., Carignan, J. 2000. Pb and Sr evidence for sources of atmospheric heavy metals and their deposition budgets in northeastern North America. Geochimica et Cosmochimica Acta, 64(20), 3439-3452.
- Simpkins, W.W. 1995. Isotopic composition of precipitation in central Iowa. Journal of Hydrology, 172, 185-207.
- Singh, S.K., Trivedi, J.R., Pande, K., Ramesh, R., Krishnaswami, S., 1998. Chemical and strontium, oxygen, and carbon isotopic compositions of carbonates from the Lesser Himalaya, Implications to the strontium isotope composition of the source waters of the Ganga, Ghaghara, and the Indus rivers. Geochimica et Cosmochimica Acta, 62(5), 743-755.
- Solomon, D.K., Poreda, R.J., Schiff, S.L., Cherry, J.A., 1992. Tritium and helium 3 as groundwater age tracers in the Borden Aquifer. Water Resources Research, 28(3), 741-755.
- Soucy, D., 1998. Cartographie des indicateurs de qualité des eaux souterraines à l'échelle régionale. Mémoire de maîtrise, INRS-Eau, Québec, Canada.
- Starinsky, A., Bielski, M., Lazar, B., Steinitz, G., Raab, M., 1983. Strontium isotope evidence on the history of oilfield brines Mediterranean Coastal Plain, Israel. Geochimica et Cosmochimica Acta, 47, 687-695.
- StatSoft Inc., 2004. STATISTICA (data analysis software system), version 6. <http://www.statsoft.com>
- Steefel, C.I., MacQuarrie, K.T.B., 1996. Approaches to modeling reactive transport in porous media. In: Lichtner, P., Steefel, C.T., and Oelkers, E.H., (Eds.). Reactive Transport in Porous Media, Review in Mineralogy 34, Mineralogical Society of America, 83-129.
- Steefel, C.I., Lichtner, P.C., 1998. Multicomponent reactive transport in discrete fractures: I. Controls on reaction front geometry. Journal of Hydrology, 209, 186-199.
- Steefel, C.I., Lichtner, P.C., 1998. Multicomponent reactive transport in discrete fractures: II. Infiltration of hyperalkaline groundwater at Maqrin, Jordan, a natural analogue site. Journal of Hydrology, 209, 200-224.

- Steinhorst, R.K., Williams, R.E., 1985. Discrimination of groundwater sources using cluster analysis, MANOVA, canonical analysis and discriminant analysis. *Water Resources Research*, 21(8), 1149-1156.
- Stigter, T.Y., van Ooijen, S.P.J., Post, V.E.A., Appelo, C.A.J., Carvalho Dill, A.M.M., 1998. A hydrogeological and hydrochemical explanation of the groundwater composition under irrigated land in a Mediterranean environment, Algarve, Portugal. *Journal of Hydrology*, 208, 262-279.
- Stimson, J., Frape, S., Drimmie, R., Rodolph, D., 2001. Isotopic and geochemical evidence of regional-scale anisotropy and interconnectivity of an alluvial fan system, Cochabamba Valley, Bolivia. *Applied Geochemistry*, 16, 1097-1114.
- Stuyfzand, P.J., 1999. Patterns in groundwater chemistry resulting from groundwater flow. *Hydrogeology Journal*, 7 (1), 15-27.
- Sultan, M., Sturchio, N.C., Gheith, H., Abdel Hady, Y., El Anbeawy, M., 2000. Chemical and isotopic constraints on the origin of Wadi El-Tarfa ground water, Eastern desert, Egypt. *Ground Water*, 38(5), 743-751.
- Szabo, Z., Rice, D.E., Plummer, L.N., Buseberg, E., Drenkard, S., Schlosser, P., 1996. Age dating of shallow groundwater with chlorofluorocarbons, tritium/helium 3, and flow path analysis, southern New Jersey coastal plain. *Water Resources Research*, 32(4), 1023-1038.
- Tellam, J.H., 1996. Interpreting the borehole water chemistry of the Permo-Triassic sandstone aquifer of the Liverpool area, UK. *Geological Journal*, 31, 61-87.
- Therrien, R., Sudicky, E.A., 1996. Three-dimensional analysis of variably saturated flow and solute transport in discretely fractured porous media. *Journal of Contaminant Hydrology*, 23, 1-44.
- Thorstenson, D.C., Fisher, D.W., Croft, M.G., 1979. The geochemistry of the Fox Hills-Basal Hell Creek Aquifer in Southwestern North Dakota and Northwestern South Dakota. *Water Resources Research*, 15(6), 1479-1498.
- Toran, L.E., Saunders, J.A., 1999. Modeling alternative paths of chemical evolution of Na-HCO<sub>3</sub>-type groundwater near Oak Ridge, Tennessee, USA. *Hydrogeology Journal*, 7(4), 355-364.
- Tóth, J., 1963. A theoretical analysis of groundwater flow in small drainage basins. *Journal of Geophysical Research*, 68(16), 4795-4812.
- Tóth, J., 1999. Groundwater as a geologic agent: An overview of the causes, processes, and manifestations. *Hydrogeology Journal*, 7(1), 1-14.

- Unesco, 1975. Legends for geohydrochemical maps. Technical papers in hydrology, The Unesco Press, Switzerland.
- Usunoff, E.J., Guzmán-Guzmán, A., 1989. Multivariate analysis in hydrochemistry: An example of the use of factor and correspondence analyses. *Ground Water*, 27(1), 27-34.
- Valenza, A., Grillot, J.C., Dazy, J., 2000. Influence of groundwater on the degradation of irrigated soils in a semi-arid region, the inner delta of the Niger River, Mali. *Hydrogeology Journal*, 8, 417-429.
- Van Brekelenkamp, B.M., Appelo, C.A.J., Olsthoorn, T.N., 1998. Hydrogeochemical transport modeling of 24 years of Rhine water infiltration in the dunes of the Amsterdam Water Supply. *Journal of Hydrology*, 209, 281-296.
- Vengosh, A., Gill, J., Davisson, M.L., Hodson, G.B., 2002. A multi-isotope (B, Sr, O, H, and C) and age dating ( $^3\text{H}$ - $^3\text{He}$  and  $^{14}\text{C}$ ) study of groundwater from Salinas Valley, California: Hydrogeochemistry, dynamics, and contamination processes. *Water Resources Research*, 38(1), 10.1029/2001WR000517.
- Viswanathan, H.S., Robinson, B.A., Valocchi, A.J., Triay, I.R., 1998. A reactive transport model of neptunium migration from the potential repository at Yucca Mountain. *Journal of Hydrology*, 209, 251-280.
- Vuillemenot, P., Guerin, R., 1995. Hydrogéologie du bassin de Lodève (Hérault, France). Relations avec les minéralisations uranifères. *Hydrogéologie*, 3, 19-30.
- Waterloo Hydrogeologic Inc., 1999. AquaChem v.3.7, Aqueous geochemical data analysis, plotting and modeling. User's manual, 184 p.
- Weaver, T.R., Frape, S.K., Cherry, J.A., 1995. Recent cross-formational fluid flow and mixing in the shallow Michigan Basin. *Geological Society of America Bulletin*, 107(6), 697-707.
- White, S.P., Xu, T., Pruess, K., 1998. Reactive chemical transport. In: TOUGH Workshop 98, Lawrence Berkeley National Laboratory (LBNL), Berkeley, California, May 1998.
- Wigley, T.M.L., 1977. WATSPEC: A computer program for determining the equilibrium speciation of aqueous solutions. British Geomorphological Research Group, Technical Bulletin No. 20, 40 p.
- Wolery, T.J., 1992. EQ3/6, A software package for geochemical modeling of aqueous systems. Lawrence Livermore National Laboratory Report UCRL-MA-110662-PT-I.

- Woods, T.L., Fullagar, P.D., Spruill, R.K., Sutton, L.C., 2000. Strontium isotopes and major elements as tracers of ground water evolution: Example from the Upper Castle Hayne Aquifer of North Carolina. *Ground Water*, 38(5), 762-771.
- Xu, T., Pruess, K., Brimhall, G., 1998. Introducing reactive chemical transport to TOUGH2: Application to supergene copper enrichment. In: TOUGH Workshop 98, Lawrence Berkeley National Laboratory (LBNL), Berkeley, California, May 1998.
- Xue, Y., Wu, J., Ye, S., Zhang, Y., 2000. Hydrogeological and hydrogeochemical studies for salt water intrusion on the south coast of Laizhou Bay, China. *Ground Water*, 38(1), 38-45.
- Yeh, G.-T., Cheng, H.-P., 1999. 3DHYDROGEOCHEM: A 3-Dimensional Model of Density-Dependent Subsurface Flow and Thermal Multispecies-Multicomponent HYDROGEOCHEMical Transport. U.S. Environmental Protection Agency, EPA/600/R-98/159, 150 p.
- Zanini, L., Novakowski, K.S., Lapcevic, P., Bickerton, G.S., Voralek, J., Talbot, C., 2000. Ground water flow in a fractured carbonate aquifer inferred combined hydrogeological and geochemical measurements. *Ground Water*, 38(3), 350-360.
- Zubari, W.K., 1999. The Dammam aquifer in Bahrain – Hydrochemical characterization and alternatives for management of groundwater quality. *Hydrogeology Journal*, 7(2), 197-208.

## **TROISIÈME PARTIE**

### **APPENDICES**



## **Appendice A**

### **RÉSULTATS DES ANALYSES GÉOCHIMIQUES ET ISOTOPHIQUES DES EAUX SOUTERRAINES**

## A1 Échantillonnage régional

### Notes pour les tableaux des appendices A1 et A2 :

Unité = mg/L lorsque non spécifiée

d.n.d. : donnée non disponible

n.a. : non analysé

<sup>a</sup> Date d'échantillonnage

<sup>b</sup> Projection Transverse de Mercator, Système de référence géodésique nord-américain (1983),  
Zone 18

<sup>c</sup> Altitudes en mètres au-dessus du niveau moyen de la mer

<sup>d</sup> Unité géologique :	1	Groupe de Trenton
	2	Groupe de Black River
	3	Groupe de Chazy
	4	Formation de Carillon
	5	Formation de Beauharnois
	6	Formation de Theresa
	7	Formation de Cairnside
	8	Formation de Covey Hill
	9	Socle Grenvillien
	10	Sédiments de surface
	11	Sédiments sous l'argile
	12	Source captée

<sup>e</sup> Unité hydrostratigraphique:	1	Sédiments de surface
	2	Sédiments sous l'argile
	3	Mixtes (sédiments sous l'argile et roc)
	4	Roc
	5	Source captée

<sup>f</sup> Condition hydrogéologique:	0	Condition de nappe libre
	1	Condition de nappe captive
	2	Condition de nappe semi-captive
	3	Sédiments de surface et source captée

<sup>g</sup> Puits artésien (coulant)	0	Non
	1	Oui

<sup>h</sup> Point-milieu de l'intervalle ouvert

<sup>i</sup> Température

<sup>j</sup> Conductivité électrique spécifique à 25 °C

<sup>k</sup> Oxygène dissous

<sup>l</sup> Potentiel mesuré sur le terrain

<sup>m</sup> Potentiel de l'échantillon relatif à l'électrode standard d'hydrogène

<sup>n</sup> Électro-neutralité calculée avec PHREEQC 2.6 (Parkhurst et Appelo 1999)

<sup>o</sup> Tout les ions dont la concentration excède 10 milliéquivalents %

<sup>p</sup> Classification définie dans le Chapitre 3 (Table 3.5)

<sup>q</sup> Groupes d'eau souterraine (Types d'eau) (voir Fig. 4.4; Chapitre 4)	1	G1 (Ca-HCO <sub>3</sub> , Mg-HCO <sub>3</sub> , Alcalino terreux-HCO <sub>3</sub> )
	2	G2 (Na-HCO <sub>3</sub> , Cations mixtes -HCO <sub>3</sub> )
	3	G3 (Na-Cl, Cations mixtes-Cl, Na-Anions mixtes)
	4	G4 (Ca-SO <sub>4</sub> , Na-SO <sub>4</sub> )

<sup>r</sup> Cluster d'eau souterraine: C1 à C7 (voir Fig. 5.5 et 5.14 ; Chapitre 5)

<sup>s</sup> Secteur de qualité relative de l'eau souterraine (voir la Carte 2.17 à l'échelle du 1/100 000, *Qualité de l'eau souterraine, Aquifère fracturé du sud-ouest du Québec*; Appendice H, en pochette)

1	Saint-Hermas
2	Rivière-du-Nord
3	Lachute/Saint-Janvier, Sainte-Monique/Saint-Enstache, Saint-Vincent
4	Collines d'Oka
5	Grenville/Chatham
6	Sainte-Anne-des-Plaines, Sainte-Thérèse
7	Saint-Benoît

<sup>t</sup> Calculé

<sup>u</sup> Taux d'adsorption du sodium (voir la Carte 2.14 ; Appendice H)

<sup>v</sup> Valeur modélisée avec PHREEQC 2.6 (Parkhurst et Appelo 1999)

<sup>w</sup> Valeur mesurée

<sup>x</sup> Valeur corrigée pour le temps entre l'échantillonnage et l'analyse

<sup>y</sup> Valeur corrigée sur la base d'un  $\delta^{13}\text{C} = -25\text{\%}$ , en utilisant le ratio  $^{13}\text{C}/^{12}\text{C}$  mesuré

- Les duplicata ont été échantillonnés simultanément avec l'échantillon principal.

- Électro-neutralité calculée avec AquaChem 3.7 (Waterloo Hydrogeologic, 1999) pour les échantillons rejetés et les duplicata.

- La concentration en HCO<sub>3</sub><sup>-</sup> = 1.219 \* alcalinité totale en CaCO<sub>3</sub> composée par des HCO<sub>3</sub><sup>-</sup> pour les échantillons rejetés et les duplicata.

Tableau A1.1. Base de données géochimiques – Description des sites d'échantillonnage

ID Site	ID Projet CGC	Date <sup>a</sup>	Abscisse (m) <sup>b</sup>	Ordonnée (m) <sup>b</sup>	Élevation (m) <sup>c</sup>	Unité Géol. <sup>d</sup>	Unité Hydro. <sup>e</sup>	Cond. Hydro. <sup>f</sup>	Puits Coul. <sup>g</sup>	Profondeur de l'intervalle ouvert (m)		
										Haut	Bas	p.m. <sup>h</sup>
S1	AERO1	2000-10-30	569337	5058046	74.2	10	1	3	0	4.9	6.8	5.9
S2	AERO2	2000-10-30	569337	5058046	75.0	6	4	0	0	10.3	11.8	11.1
S3	AERO3	2000-10-30	575779	5056577	80.0	10	1	3	0	2.8	4.6	3.5
S4	AERO4	2000-10-30	575776	5056578	81.1	5	4	0	0	9.6	13.0	11.1
S5	AERO5	2000-10-31	579574	5061306	69.9	5	4	1	0	8.9	10.7	9.6
S6	AERO6	2000-10-31	579435	5061447	70.3	10	1	3	0	1.0	4.0	2.5
S7	AERO7	2000-10-31	572820	5058852	76.1	6	4	0	0	13.1	14.6	13.9
S8	AERO8	2000-10-31	572821	5058850	75.2	10	1	3	0	3.4	7.0	4.9
S9	ANDR1	2000-03-11	552287	5049813	75.0	10	1	3	0	7.0	7.6	7.3
S10	ANDR10	2000-07-05	550963	5050637	55.0	5	4	1	0	31.6	38.1	34.9
S11	ANDR11	2000-08-03	559673	5046961	46.0	8	4	1	0	26.5	69.2	47.9
S12	ANDR12	2000-08-04	559683	5047283	41.0	8	3	1	0	19.8	22.9	21.4
S13	ANDR13	2000-08-24	558247	5050129	50.0	11	2	1	1	25.0	25.0	25.0
S14	ANDR14	2000-08-25	558690	5047926	36.8	11	2	1	1	30.5	30.5	30.5
S15	ANDR15	2000-08-25	556742	5051698	57.0	7	4	1	0	39.7	82.6	61.2
S16	ANDR16	2000-08-25	559174	5047907	36.9	8	4	1	1	d.n.d.	36.5	–
S17	ANDR2	1999-09-14	552484	5046773	55.0	7	4	0	0	22.5	84.5	53.5
S18	ANDR3	1999-10-20	559086	5048001	38.0	11	2	1	1	32.0	32.0	32.0
S19	ANNE1	1999-03-09	592129	5068173	56.4	2	4	1	0	28.0	93.8	60.9
S20	ANNE10	1999-10-26	593430	5067017	64.9	1	4	1	0	d.n.d.	d.n.d.	–
S21	ANNE11	1999-10-26	594885	5070565	60.4	1	4	1	0	d.n.d.	34.0	–
S22	ANNE12	2000-10-26	591471	5070933	61.0	3	4	1	0	19.2	20.7	20.0
S23	ANNE15	2000-09-06	593663	5070253	62.0	1	4	1	0	22.0	68.3	45.1
S24	ANNE17	2000-06-27	588774	5066858	60.0	4	4	1	0	20.0	40.2	30.1
S25	ANNE18	2000-06-27	592739	5077165	61.0	4	4	1	0	33.2	33.5	33.4
S26	ANNE19	2000-08-15	589929	5065023	61.0	3	4	1	0	21.6	91.4	56.5
S27	ANNE3	2000-03-09	589430	5067770	60.4	4	4	1	0	22.5	25.3	23.9
S28	ANNE4	2000-08-24	591068	5068765	62.5	3	4	1	0	14.6	32.0	23.3
S29	ANNE8	2000-09-21	592645	5071729	61.0	2	4	1	0	17.7	19.1	18.4
S30	ANNE9	1999-09-23	592028	5069432	66.5	3	4	1	0	18.3	32.3	25.3
S31	ANTO1	1999-03-16	580746	5065453	65.0	5	4	0	0	4.3	41.5	22.9
S32	ANTO10	2000-06-28	583735	5068869	74.0	5	4	0	0	12.0	19.8	15.9
S33	ANTO2	2000-03-16	582193	5067234	74.0	5	4	0	0	11.0	82.0	46.5
S34	AUGU1	1999-09-09	582045	5053752	54.0	5	4	1	0	12.9	25.6	19.3
S35	AUGU10	2000-07-27	576529	5050922	52.0	7	4	1	0	9.1	12.5	10.8
S36	AUGU11	2000-07-28	578914	5052317	49.0	6	4	0	0	9.2	38.7	23.9
S37	AUGU12	2000-07-28	585326	5052255	62.0	5	4	0	0	3.4	30.5	16.9
S38	AUGU13	2000-08-08	584889	5051640	53.0	5	4	0	0	6.7	97.5	52.1
S39	AUGU14	2000-08-22	584605	5052669	54.5	5	4	0	0	22.0	25.0	23.5
S40	AUGU15	2000-08-24	582748	5054412	55.0	5	4	0	0	13.7	43.3	28.5
S41	BEN1	1999-08-18	567605	5045440	48.0	8	4	1	0	95.4	99.0	97.2
S42	BEN11	2000-06-15	568843	5048325	51.0	11	2	1	0	28.0	29.3	28.7
S43	BEN14	2000-06-22	568585	5048460	53.0	7	3	1	0	23.6	27.4	25.5
S44	BEN15	2000-06-22	568430	5048768	53.0	7	4	1	0	21.0	73.0	47.0
S45	BEN16	2000-07-07	568940	5048430	51.0	7	3	1	0	30.2	37.5	33.9
S46	BEN17	2000-08-02	569152	5047829	50.0	8	4	1	0	30.5	104.6	67.6
S47	BEN19	2000-08-16	569252	5048694	51.0	7	3	1	0	33.2	37.2	35.2
S48	BEN2	1999-08-19	567311	5049165	65.0	7	4	0	0	21.0	23.5	22.3
S49	BEN20	2000-08-18	568096	5049379	70.0	7	4	0	0	10.0	16.5	13.3
S50	BEN3	1999-08-26	564903	5046889	48.0	8	4	0	0	6.7	7.0	6.9
S51	BEN4	1999-08-26	571669	5047560	45.7	8	4	1	0	42.0	81.9	62.0
S52	BEN5	1999-09-02	573081	5050032	43.0	7	4	0	0	8.2	13.1	10.7
S53	BEN6	1999-09-28	570491	5043250	60.0	11	2	1	0	79.3	79.8	79.5
S54	BOIS1	1999-09-28	588046	5054599	48.0	5	4	0	0	5.5	73.2	39.3
S55	BOIS10	2000-07-21	592225	5060345	68.0	1	4	1	0	11.0	91.7	51.4

Tableau A1.1. (suite)

ID Site	ID Projet CGC	Date <sup>a</sup>	Abscisse (m) <sup>b</sup>	Ordonnée (m) <sup>b</sup>	Elévation (manm <sup>c</sup> )	Unité Géol. <sup>d</sup>	Unité Hydro. <sup>e</sup>	Cond. Hydro. <sup>f</sup>	Puits Coul. <sup>g</sup>	Profondeur de l'intervalle ouvert (m)		
										Haut	Bas	p.m. <sup>h</sup>
S56	BOURB1	1999-08-24	558622	5057107	68.0	6	4	1	0	d.n.d.	51.8	-
S57	CALU1	1999-03-08	528708	5055473	61.0	3	4	1	0	32.2	76.1	54.2
S58	CANU1	2000-03-16	570300	5061450	65.0	7	4	1	0	22.0	d.n.d.	-
S59	CANU10	2000-08-23	567812	5060174	73.0	12	5	3	1	d.n.d.	d.n.d.	-
S60	CANU11	2000-08-23	567147	5060504	68.0	6	4	0	0	15.6	37.7	26.7
S61	CANU2	2000-03-16	571450	5063100	72.0	7	4	0	0	7.0	88.4	47.7
S62	CANU3	1999-03-16	570550	5061650	75.0	7	4	1	0	d.n.d.	5.0	-
S63	CHAT1	1999-03-08	544508	5052722	79.3	4	4	0	0	15.2	91.5	53.4
S64	CHAT10	2000-07-04	542639	5055571	83.0	5	4	1	0	64.0	82.3	73.2
S65	CHAT11	2000-07-04	544995	5055921	77.0	5	4	1	0	82.0	92.1	87.0
S66	CHAT12	2000-07-05	540891	5049697	52.0	3	4	0	0	d.n.d.	d.n.d.	-
S67	CHAT2	1999-09-14	546521	5050544	58.0	5	4	1	0	45.7	50.3	48.0
S68	CHAT3	1999-09-16	544416	5049480	55.0	4	4	1	0	5.8	25.9	15.9
S69	CHAT4	1999-09-16	543088	5051888	54.9	4	4	0	0	13.1	15.9	14.5
S70	COLO1	1999-09-22	562749	5059746	68.0	6	4	0	0	39.0	57.3	48.2
S71	EUST1	1999-09-09	579043	5046300	53.0	7	4	1	0	30.8	37.2	34.0
S72	EUST10	2000-08-01	588478	5049064	35.5	5	4	0	0	65.0	82.1	73.6
S73	EUST11	2000-08-16	588304	5049789	41.0	5	4	0	0	3.4	94.3	48.9
S74	EUST2	1999-09-09	582601	5049758	45.0	5	4	0	0	2.7	30.5	16.6
S75	EUST3	1999-09-09	579725	5048330	53.3	6	4	0	0	2.4	38.4	20.4
S76	EUST4	1999-09-23	586253	5048745	36.0	5	4	0	0	8.2	38.1	23.2
S77	FROMA1	2000-07-11	566553	5040956	39.0	8	4	1	0	69.0	142.0	105.5
S78	GREN1	1999-09-16	536912	5053326	77.5	3	4	0	0	9.5	31.1	20.3
S79	GREN10	2000-07-05	532292	5054698	70.0	3	4	0	0	6.1	32.0	19.1
S80	GREN2	1999-09-16	537606	5054620	105.0	4	4	0	0	8.2	16.2	12.2
S81	GREN4	1999-09-20	537207	5049662	42.0	3	4	0	0	6.1	24.7	15.4
S82	GREN5	1999-09-20	533067	5052380	65.0	3	4	0	0	10.4	30.5	20.5
S83	HERM1	1999-03-16	562629	5050895	45.0	11	2	1	0	43.7	45.7	44.7
S84	HERM10	2000-07-18	563455	5054215	87.0	7	4	0	0	10.5	81.1	45.8
S85	HERM11	2000-08-29	562413	5050931	47.0	7	4	1	0	48.0	91.6	69.8
S86	HERM2	1999-09-02	561810	5051669	55.0	11	2	1	1	27.7	28.4	28.1
S87	HERM3	1999-09-08	558490	5051878	75.0	7	4	1	1	d.n.d.	30.5	-
S88	HERM4	1999-09-29	562153	5054379	76.0	7	4	0	0	8.1	27.4	17.8
S89	HERM5	1999-10-20	562010	5049667	48.0	7	3	1	0	35.1	35.1	35.1
S90	HERM6	1999-10-20	558355	5050986	74.0	7	4	1	0	55.2	56.4	55.8
S91	JANV10	2000-07-12	586242	5064198	57.0	4	4	1	0	18.3	19.8	19.1
S92	JANV1	1999-03-16	583145	5060985	70.0	5	4	1	0	11.0	82.3	46.7
S93	JANV2	1999-09-21	578664	5065135	69.0	11	2	1	0	36.5	36.6	36.6
S94	JANV3	1999-10-27	585489	5066343	61.0	5	4	0	0	6.7	36.6	21.7
S95	JANV4	1999-10-27	582316	5062964	72.0	5	4	0	0	7.0	44.2	25.6
S96	JANV5	1999-10-27	583528	5061651	69.0	5	4	1	0	d.n.d.	30.5	-
S97	JOSE1	1999-09-13	577721	5043033	85.0	9	4	1	0	80.8	109.8	95.3
S98	JOSE10	2000-07-27	575156	5041383	136.0	9	4	1	0	57.3	79.3	68.3
S99	JOSE11	2000-08-17	579253	5041761	50.0	7	4	1	0	70.1	70.1	70.1
S100	JOSE12	2000-08-24	579549	5041900	50.0	7	4	1	0	86.3	86.6	86.5
S101	JOSE13	2000-08-30	579516	5042057	50.0	7	4	1	0	102.4	103.6	103.0
S102	JOSE2	1999-10-26	578997	5041496	53.0	11	2	1	0	65.9	65.9	65.9
S103	LACH1	1999-09-14	555344	5052931	75.0	5	4	0	0	13.6	38.7	26.2
S104	LACH2	1999-09-22	552373	5057589	82.0	9	4	0	0	4.3	105.2	54.8
S105	LACH20	2000-07-04	549932	5053106	66.0	5	4	1	0	d.n.d.	d.n.d.	-
S106	LACH21	2000-07-19	557429	5055322	76.2	5	4	1	0	18.0	19.8	18.9
S107	LACH3	1999-09-22	553376	5057114	65.0	6	4	0	0	7.0	24.4	15.7
S108	LACH4	1999-10-20	556487	5057721	85.0	11	2	1	0	23.2	23.2	23.2
S109	LACH5	1999-10-21	549097	5048214	42.0	5	4	0	0	10.7	38.7	24.7
S110	MONI1	1999-09-13	580269	5057055	69.0	5	4	1	0	11.9	36.0	23.9

Tableau A1.1. (suite)

ID Site	ID Projet CGC	Date <sup>a</sup>	Abscisse (m) <sup>b</sup>	Ordonnée (m) <sup>b</sup>	Elévation (manm) <sup>c</sup>	Unité Géol. <sup>d</sup>	Unité Hydro. <sup>e</sup>	Cond. Hydro. <sup>f</sup>	Puits Coul. <sup>g</sup>	Profondeur de l'intervalle ouvert (m)		
										Haut	Bas	p.m. <sup>b</sup>
S111	MONI2	1999-09-28	585136	5056851	67.0	4	4	1	0	29.3	31.4	30.4
S112	MT1	2000-07-25	553129	5056422	79.3	5	4	1	0	19.0	19.7	19.4
S113	MT16	2000-07-19	557449	5055442	76.2	5	4	1	0	18.0	18.3	18.2
S114	OKA1	1999-03-10	574750	5034800	26.0	10	1	3	0	8.8	21.6	15.2
S115	OKA11	2000-06-20	573256	5039137	100.0	9	4	0	0	1.0	91.4	46.2
S116	OKA12	2000-08-24	571432	5036800	140.0	9	4	0	0	d.n.d.	d.n.d.	—
S117	PE2	2000-07-26	531925	5055621	76.0	3	4	1	0	30.3	85.6	58.0
S118	PLA1	1999-03-10	561789	5041833	30.5	8	3	1	0	10.4	12.1	11.3
S119	PLA2	1999-08-18	565773	5043548	59.0	8	4	1	0	68.6	76.3	72.5
S120	PLA3	1999-08-19	562712	5044748	66.0	8	4	1	0	18.0	27.5	22.8
S121	PLA4	1999-08-23	563173	5045888	49.0	12	5	3	1	d.n.d.	d.n.d.	—
S122	PLA5	1999-09-14	558760	5042630	33.0	8	4	1	0	40.9	61.6	51.3
S123	PUIT_STJA1	2000-07-06	584527	5061810	69.0	5	4	1	0	16.0	73.2	44.6
S124	PUITS_P9	2000-07-06	591048	5068721	61.4	3	4	1	0	17.4	57.0	37.2
S125	Puits_R14	2000-07-07	580729	5063973	68.6	5	4	0	0	5.2	48.7	27.0
S126	Puits_R15	2000-06-27	571749	5045622	68.6	9	4	0	0	6.7	91.5	49.1
S127	PUITSR3	2000-07-04	546878	5053122	76.2	5	4	1	0	21.9	91.4	56.7
S128	R16	2000-07-17	562829	5050472	45.7	7	4	1	0	44.5	61.0	52.8
S129	R270	2000-07-12	576829	5055922	73.2	6	4	1	0	9.0	45.5	27.3
S130	RIVNORD	2000-07-10	560393	5058165	56.0	6	4	1	1	47.8	117.1	82.5
S131	SABLPP1	2000-08-03	581881	5056057	70.9	5	4	1	0	20.4	106.7	63.6
S132	SABLPZ1	2000-07-31	581876	5056051	70.9	5	3	1	0	18.4	18.8	18.6
S133	SCHO1	2000-03-16	570807	5055872	70.0	6	3	1	1	11.9	39.0	25.5
S134	SCHO10	2000-08-24	570176	5052090	43.0	11	2	1	1	d.n.d.	33.5	—
S135	SCHO11	2000-08-24	569977	5052376	45.7	11	2	1	0	29.3	29.3	29.3
S136	SCHO2	1999-09-01	575173	5054305	73.0	7	4	2	0	18.0	20.1	19.1
S137	SCHO3	1999-09-01	577131	5054326	67.0	11	2	1	0	11.2	11.2	11.2
S138	SCHO4	1999-09-02	571549	5051452	43.0	7	4	1	0	15.5	16.7	16.1
S139	SCHOS5	1999-09-02	566481	5055178	75.0	7	4	0	0	7.6	30.5	19.1
S140	Sintra_F3	2000-07-28	539133	5052525	91.1	3	4	0	0	1.2	61.9	31.6
S141	SOPH1	2000-06-28	588165	5076178	70.1	5	4	1	0	39.0	70.6	54.8
S142	STJA5	2000-07-13	581885	5062504	68.5	5	4	0	0	6.1	42.7	24.4
S143	THER1	2000-06-29	592805	5057257	61.0	1	4	1	0	27.4	31.1	29.3
S144	VINCPP	2000-07-25	566227	5048158	58.0	7	4	2	0	21.0	110.7	65.9
S145	VINCPZ1	2000-07-24	566215	5048170	58.0	7	3	2	0	21.6	22.0	21.8
S146	VINCPZ2	2000-07-24	566237	5048160	58.0	10	1	3	0	8.8	9.1	9.0
<b>Échantillons rejetés</b>												
R1	AERO9	—	570529	5059453	77.6	7	4	0	0	10.4	12.2	11.3
R2	BEN10	2000-06-13	568949	5048097	50.0	8	3	1	0	21.6	25.3	23.5
R3	BEN12	2000-06-15	569273	5048677	51.0	7	3	1	0	34.7	36.3	35.5
R4	BLAI1	1999-10-21	592182	5060402	68.0	1	4	1	0	15.2	15.2	15.2
SAP	CGQSteAnne	2000-06-13	589831	5067517	64.0	4	4	1	0	23.0	99.7	61.4
R5	LACH6	1999-10-27	554570	5053522	77.0	5	4	0	0	6.9	94.7	50.8
R6	PLA6	1999-10-21	566000	5039854	40.0	8	4	—	0	d.n.d.	d.n.d.	—
<b>Duplicata</b>												
D1	ANNE20	S26	589929	5065023	61.0	3	4	1	0	21.6	91.4	56.5
D2	AUGU16	S40	582748	5054412	55.0	5	4	0	0	13.7	43.3	28.5
D3	BEN18	S46	569152	5047829	50.0	8	4	1	0	30.5	104.6	67.6
D4	CHAT13	S66	540891	5049697	52.0	3	4	0	0	d.n.d.	d.n.d.	—
D5	EUST12	S73	588304	5049789	41.0	5	4	0	0	3.4	94.3	48.9
D6	EUST13	S72	588478	5049064	35.5	5	4	0	0	65.0	82.1	73.6
D7	FROMA2	S77	566553	5040956	39.0	8	4	1	0	69.0	142.0	105.5
D8	HERM12	S85	562413	5050931	47.0	7	4	1	0	48.0	91.6	69.8
D9	JANV6	S96	583528	5061651	69.0	5	4	1	0	d.n.d.	30.5	—
D10	R16B	S128	562829	5050472	45.7	7	4	1	0	44.5	61.0	52.8

Tableau A1.2. Base de données géochimiques – Paramètres de terrain et classifications

ID Site	T <sup>i</sup> (°C)	pH	CE <sup>j</sup> (µS/cm)	OD <sup>k</sup> (mg/L)	Potentiel Redox E <sup>l</sup> (mV)	Eh <sup>m</sup>	EN <sup>n</sup> (%)	Types d'eau <sup>o</sup>	Types d'eau dominants et mixtes <sup>p</sup>	G <sup>q</sup>	C <sup>r</sup>	S <sup>s</sup>
S1	8.2	7.30	718	2.4	-30	187	1.6	Ca-Mg-HCO <sub>3</sub>	Ca-HCO <sub>3</sub>	1	7	3
S2	7.8	7.38	742	1.0	10	227	-0.2	Ca-Mg-HCO <sub>3</sub> -Cl	Ca-HCO <sub>3</sub>	1	7	3
S3	10.9	7.50	409	1.2	79	294	1.2	Ca-Mg-HCO <sub>3</sub> -SO <sub>4</sub>	Ca-HCO <sub>3</sub>	1	7	3
S4	8.5	7.25	634	1.6	31	248	1.6	Ca-Mg-Na-HCO <sub>3</sub> -Cl	Ca-HCO <sub>3</sub>	1	7	3
S5	8.1	7.30	741	0.5	30	247	-2.9	Ca-Mg-HCO <sub>3</sub>	Ca-HCO <sub>3</sub>	1	7	3
S6	10.5	7.51	717	0.3	46	261	-3.8	Ca-Mg-HCO <sub>3</sub>	Ca-HCO <sub>3</sub>	1	7	3
S7	9.1	7.43	692	0.6	-1	215	-6.1	Ca-Mg-Na-HCO <sub>3</sub> -SO <sub>4</sub>	Ca-HCO <sub>3</sub>	1	7	3
S8	9.7	7.14	650	2.0	94	310	-0.7	Ca-Mg-HCO <sub>3</sub>	Ca-HCO <sub>3</sub>	1	7	3
S9	n.a.	7.60	435	n.a.	n.a.	n.a.	-2.4	Ca-Mg-HCO <sub>3</sub>	Ca-HCO <sub>3</sub>	1	3	3
S10	9.0	7.50	654	1.0	-103	114	-6.8	Ca-Mg-HCO <sub>3</sub>	Ca-HCO <sub>3</sub>	1	7	3
S11	10.0	7.46	274	4.2	53	269	-0.7	Ca-Mg-HCO <sub>3</sub>	Ca-HCO <sub>3</sub>	1	5	1
S12	9.1	7.60	304	2.1	53	269	0.8	Ca-Mg-HCO <sub>3</sub>	Ca-HCO <sub>3</sub>	1	5	1
S13	8.1	7.53	504	2.7	-58	159	0.0	Ca-Mg-Na-HCO <sub>3</sub>	Mixed cations-HCO <sub>3</sub>	2	5	1
S14	8.6	7.90	678	1.8	159	376	5.2	Na-Ca-Mg-HCO <sub>3</sub> -Cl	Na-HCO <sub>3</sub>	2	5	1
S15	8.4	7.13	396	2.5	172	389	6.5	Ca-Mg-HCO <sub>3</sub>	Ca-HCO <sub>3</sub>	1	3	3
S16	16.9	7.53	3403	1.2	92	303	0.7	Na-Cl	Na-Cl	3	2	1
S17	9.5	7.87	560	2.2	31	247	-1.0	Ca-Mg-HCO <sub>3</sub>	Ca-HCO <sub>3</sub>	1	4	1
S18	8.6	8.10	824	1.8	-50	167	-4.2	Na-Mg-HCO <sub>3</sub> -Cl	Na-HCO <sub>3</sub>	2	5	1
S19	n.a.	7.40	1030	n.a.	n.a.	n.a.	-1.3	Na-Ca-Mg-HCO <sub>3</sub>	Na-HCO <sub>3</sub>	2	6	6
S20	8.9	8.85	675	1.2	-143	74	3.9	Na-HCO <sub>3</sub>	Na-HCO <sub>3</sub>	2	1	6
S21	8.8	7.97	791	1.4	-169	48	-0.2	Na-Mg-HCO <sub>3</sub> -Cl	Na-HCO <sub>3</sub>	2	1	6
S22	9.3	8.78	856	1.7	-130	86	2.8	Na-HCO <sub>3</sub>	Na-HCO <sub>3</sub>	2	1	6
S23	8.3	8.57	1250	4.8	-223	-6	1.3	Na-HCO <sub>3</sub> -Cl	Na-HCO <sub>3</sub>	2	1	6
S24	9.2	7.88	768	9.5	-180	36	-1.0	Na-Mg-Ca-HCO <sub>3</sub>	Na-HCO <sub>3</sub>	2	1	6
S25	8.2	8.20	1155	0.2	-167	50	2.8	Na-HCO <sub>3</sub> -Cl	Na-HCO <sub>3</sub>	2	2	6
S26	8.3	7.62	2710	0.4	-96	121	-1.3	Na-Cl-HCO <sub>3</sub>	Na-Cl	3	1	6
S27	n.a.	8.10	800	n.a.	n.a.	n.a.	-0.7	Na-Mg-HCO <sub>3</sub>	Na-HCO <sub>3</sub>	2	1	6
S28	8.1	7.98	1140	4.3	-209	8	-3.2	Na-HCO <sub>3</sub> -Cl	Na-HCO <sub>3</sub>	2	1	6
S29	10.7	8.57	853	0.9	-171	44	0.8	Na-HCO <sub>3</sub>	Na-HCO <sub>3</sub>	2	1	6
S30	8.5	7.27	1008	1.2	-28	189	-0.9	Ca-Mg-Na-HCO <sub>3</sub>	Ca-HCO <sub>3</sub>	1	6	6
S31	n.a.	7.30	810	n.a.	n.a.	n.a.	-3.3	Ca-Mg-HCO <sub>3</sub> -SO <sub>4</sub>	Ca-HCO <sub>3</sub>	1	7	3
S32	8.6	7.83	411	0.1	-190	27	-4.1	Mg-Ca-HCO <sub>3</sub>	Alkaline earths-HCO <sub>3</sub>	1	2	3
S33	n.a.	7.20	740	n.a.	n.a.	n.a.	-2.2	Ca-Mg-HCO <sub>3</sub> -SO <sub>4</sub>	Ca-HCO <sub>3</sub>	1	7	3
S34	13.5	7.84	768	1.8	-137	76	1.0	Na-Ca-Mg-Cl-HCO <sub>3</sub>	Mixed cations-Cl	3	6	3
S35	9.3	7.28	583	5.4	109	325	-0.3	Ca-Mg-HCO <sub>3</sub>	Ca-HCO <sub>3</sub>	1	7	3
S36	9.4	6.82	1259	4.3	75	291	0.0	Ca-Mg-HCO <sub>3</sub> -SO <sub>4</sub>	Ca-HCO <sub>3</sub>	1	6	3
S37	11.0	6.79	1146	2.2	71	286	-0.9	Ca-Mg-HCO <sub>3</sub>	Ca-HCO <sub>3</sub>	1	6	3
S38	10.4	7.03	680	3.3	n.a.	n.a.	1.0	Ca-Mg-HCO <sub>3</sub>	Ca-HCO <sub>3</sub>	1	3	3
S39	10.8	7.32	582	2.5	82	297	2.3	Ca-Mg-HCO <sub>3</sub>	Ca-HCO <sub>3</sub>	1	6	3
S40	9.9	7.45	557	0.6	27	243	3.4	Ca-Mg-Na-HCO <sub>3</sub>	Mixed cations-HCO <sub>3</sub>	2	6	3
S41	11.0	7.31	1595	2.9	-121	94	-8.1	Na-Cl-HCO <sub>3</sub>	Na-Cl	3	2	7
S42	8.1	7.74	1401	8.5	n.a.	n.a.	1.4	Na-Cl-HCO <sub>3</sub>	Na-Cl	3	2	7
S43	9.0	8.10	629	1.2	-122	94	-2.6	Na-Mg-HCO <sub>3</sub> -Cl	Na-HCO <sub>3</sub>	2	6	7
S44	n.a.	7.66	529	0.2	-55	161	-3.1	Mg-Ca-HCO <sub>3</sub>	Mg-HCO <sub>3</sub>	1	7	3
S45	10.6	8.00	6312	1.5	98	313	1.7	Na-Cl	Na-Cl	3	2	7
S46	8.6	7.36	1125	3.1	52	269	1.6	Na-HCO <sub>3</sub> -Cl	Na-HCO <sub>3</sub>	2	2	7
S47	8.4	7.45	498	5.1	98	315	-0.4	Na-Mg-Ca-HCO <sub>3</sub>	Na-HCO <sub>3</sub>	2	5	7
S48	8.2	6.97	375	11.4	160	377	-1.3	Ca-Mg-HCO <sub>3</sub>	Ca-HCO <sub>3</sub>	1	3	3
S49	8.0	6.89	399	11.5	75	292	1.0	Ca-Mg-HCO <sub>3</sub>	Ca-HCO <sub>3</sub>	1	3	3
S50	11.4	7.38	296	8.3	70	285	-0.2	Ca-Mg-HCO <sub>3</sub>	Ca-HCO <sub>3</sub>	1	3	3
S51	10.0	7.21	2682	2.6	-159	57	4.1	Na-Cl	Na-Cl	3	2	7
S52	9.7	7.18	565	0.8	-102	114	-0.2	Ca-Mg-HCO <sub>3</sub>	Ca-HCO <sub>3</sub>	1	7	3
S53	10.3	8.79	1194	0.9	-150	66	1.6	Na-Cl-HCO <sub>3</sub>	Na-Cl	3	—	7
S54	9.1	7.63	1886	1.0	26	242	-1.5	Na-Cl-HCO <sub>3</sub>	Na-Cl	3	2	3
S55	9.2	8.22	3980	1.8	50	266	2.8	Na-Cl	Na-Cl	3	2	6

Tableau A1.2. (suite)

ID Site	T <sup>i</sup> (°C)	pH	CE <sup>j</sup> (µS/cm)	OD <sup>k</sup> (mg/L)	Potentiel Redox E <sup>l</sup> (mV)	Eh <sup>m</sup>	EN <sup>n</sup> (%)	Types d'eau °	Types d'eau dominants et mixtes p	G <sup>q</sup>	C <sup>r</sup>	S <sup>s</sup>
S56	8.6	7.47	812	2.2	-192	25	-7.6	Na-Cl-HCO <sub>3</sub>	Na-Cl	3	5	2
S57	n.a.	7.80	438	n.a.	n.a.	n.a.	-3.4	Ca-Na-HCO <sub>3</sub> -Cl	Ca-HCO <sub>3</sub>	1	4	5
S58	n.a.	8.00	265	n.a.	n.a.	n.a.	-1.6	Ca-Mg-HCO <sub>3</sub>	Ca-HCO <sub>3</sub>	1	5	2
S59	12.2	6.99	500	7.9	-81	133	3.3	Ca-Mg-HCO <sub>3</sub>	Ca-HCO <sub>3</sub>	1	3	2
S60	9.3	7.34	870	2.4	-97	119	2.8	Na-Mg-Ca-HCO <sub>3</sub> -Cl	Na-HCO <sub>3</sub>	2	5	2
S61	n.a.	8.00	1020	n.a.	n.a.	n.a.	-0.1	Na-Cl-HCO <sub>3</sub>	Na-Cl	3	4	2
S62	n.a.	6.40	305	n.a.	n.a.	n.a.	0.4	Na-Ca-Cl-SO <sub>4</sub> -HCO <sub>3</sub>	Na-Cl	3	3	2
S63	n.a.	7.90	600	n.a.	n.a.	n.a.	-3.9	Na-Mg-Ca-HCO <sub>3</sub> -Cl	Mixed cations-HCO <sub>3</sub>	2	4	5
S64	8.6	8.13	326	1.9	89	306	4.2	Na-Ca-Mg-HCO <sub>3</sub> -Cl	Na-HCO <sub>3</sub>	2	4	2
S65	8.8	7.94	636	2.3	-75	142	-0.9	Na-Ca-HCO <sub>3</sub> -SO <sub>4</sub> -Cl	Na-HCO <sub>3</sub>	2	4	2
S66	9.4	7.45	526	0.9	51	267	2.9	Ca-Mg-HCO <sub>3</sub>	Ca-HCO <sub>3</sub>	1	4	5
S67	9.3	8.18	2352	0.9	-190	26	-0.3	Na-Cl-HCO <sub>3</sub>	Na-Cl	3	2	2
S68	8.8	7.21	2147	1.2	25	242	1.3	Ca-SO <sub>4</sub>	Ca-SO <sub>4</sub>	4	4	5
S69	8.5	7.64	715	0.7	-88	129	2.2	Ca-Mg-HCO <sub>3</sub> -Cl	Ca-HCO <sub>3</sub>	1	4	5
S70	8.5	8.37	417	2.0	-138	79	-1.9	Na-Mg-Ca-HCO <sub>3</sub>	Na-HCO <sub>3</sub>	2	5	2
S71	10.0	7.65	718	1.8	-61	155	-1.1	Na-Mg-Ca-HCO <sub>3</sub> -Cl	Na-HCO <sub>3</sub>	2	6	7
S72	8.9	6.99	1570	3.6	n.a.	n.a.	-3.2	Na-Ca-Mg-Cl-HCO <sub>3</sub> -SO <sub>4</sub>	Na-Cl	3	6	3
S73	9.2	6.74	882	5.1	111	327	2.2	Ca-Mg-HCO <sub>3</sub> -SO <sub>4</sub>	Ca-HCO <sub>3</sub>	1	7	3
S74	11.2	7.33	642	2.2	-4	211	-3.0	Ca-Mg-HCO <sub>3</sub>	Ca-HCO <sub>3</sub>	1	7	3
S75	9.0	7.26	1544	5.7	70	287	-1.9	Ca-Mg-HCO <sub>3</sub>	Ca-HCO <sub>3</sub>	1	7	3
S76	8.5	7.61	822	6.2	12	229	-2.4	Ca-Mg-HCO <sub>3</sub> -SO <sub>4</sub>	Ca-HCO <sub>3</sub>	1	7	3
S77	9.8	7.09	18530	n.a.	n.a.	n.a.	3.7	Na-Cl	Na-Cl	3	-	7
S78	8.9	7.44	1554	2.1	-56	161	3.4	Ca-Na-SO <sub>4</sub>	Ca-SO <sub>4</sub>	4	4	5
S79	8.2	7.16	527	5.6	54	271	-0.7	Ca-Mg-HCO <sub>3</sub>	Ca-HCO <sub>3</sub>	1	4	5
S80	9.5	7.87	529	2.0	-92	124	1.2	Ca-Mg-HCO <sub>3</sub>	Ca-HCO <sub>3</sub>	1	4	5
S81	9.9	7.52	653	0.8	78	294	-4.8	Na-HCO <sub>3</sub>	Na-HCO <sub>3</sub>	2	1	5
S82	9.8	7.75	482	4.0	62	278	-2.5	Ca-Mg-HCO <sub>3</sub>	Ca-HCO <sub>3</sub>	1	4	5
S83	n.a.	8.50	520	n.a.	n.a.	n.a.	0.1	Na-Mg-HCO <sub>3</sub>	Na-HCO <sub>3</sub>	2	4	1
S84	7.6	6.95	557	9.3	59	277	-3.9	Ca-Mg-HCO <sub>3</sub>	Ca-HCO <sub>3</sub>	1	3	3
S85	9.4	7.64	467	1.0	n.a.	n.a.	-0.8	Ca-Mg-Na-HCO <sub>3</sub>	Mixed cations-HCO <sub>3</sub>	2	5	1
S86	8.7	8.28	479	1.6	-102	115	-2.8	Na-Mg-Ca-HCO <sub>3</sub>	Mixed cations-HCO <sub>3</sub>	2	5	1
S87	9.9	7.88	548	1.8	-75	141	-3.0	Ca-Mg-HCO <sub>3</sub>	Alkaline earths-HCO <sub>3</sub>	1	7	3
S88	9.0	7.08	873	4.7	136	353	-7.9	Ca-Mg-HCO <sub>3</sub>	Ca-HCO <sub>3</sub>	1	6	3
S89	8.5	8.36	1865	2.2	-113	104	-2.1	Na-Cl-HCO <sub>3</sub>	Na-Cl	3	2	1
S90	8.8	7.72	641	1.5	-94	123	-4.5	Ca-Mg-Na-HCO <sub>3</sub>	Mixed cations-HCO <sub>3</sub>	2	5	1
S91	8.9	7.26	483	1.1	70	287	2.6	Na-HCO <sub>3</sub>	Na-HCO <sub>3</sub>	2	1	3
S92	n.a.	7.60	1220	n.a.	n.a.	n.a.	1.9	Na-Ca-Mg-Cl-HCO <sub>3</sub>	Na-Cl	3	6	3
S93	8.9	8.74	1952	1.4	-120	97	-1.9	Na-Cl-HCO <sub>3</sub>	Na-Cl	3	1	2
S94	8.4	7.40	583	1.2	-44	173	-2.5	Mg-Ca-HCO <sub>3</sub>	Alkaline earths-HCO <sub>3</sub>	1	6	3
S95	12.5	6.97	1883	2.4	-51	163	5.4	Na-Ca-Mg-Cl-HCO <sub>3</sub>	Na-Cl	3	6	3
S96	10.5	7.19	1154	1.7	-51	164	-0.8	Ca-Mg-Na-HCO <sub>3</sub> -Cl	Ca-HCO <sub>3</sub>	1	6	3
S97	10.9	8.33	440	1.9	-59	156	-4.3	Na-HCO <sub>3</sub>	Na-HCO <sub>3</sub>	2	4	4
S98	9.8	7.89	524	0.9	100	316	-3.5	Na-Mg-Ca-HCO <sub>3</sub>	Na-HCO <sub>3</sub>	2	4	4
S99	11.2	8.25	471	3.2	86	301	2.6	Na-HCO <sub>3</sub>	Na-HCO <sub>3</sub>	2	5	7
S100	11.0	7.89	4856	1.2	-220	-5	3.3	Na-Cl	Na-Cl	3	2	7
S101	16.3	7.79	3619	n.a.	n.a.	n.a.	3.2	Na-Cl	Na-Cl	3	2	7
S102	9.9	9.26	850	1.2	-50	166	0.9	Na-HCO <sub>3</sub>	Na-HCO <sub>3</sub>	2	1	7
S103	10.0	7.31	547	1.4	44	260	-1.4	Ca-Mg-HCO <sub>3</sub>	Ca-HCO <sub>3</sub>	1	7	3
S104	10.0	8.14	623	1.5	-51	165	4.2	Na-Ca-HCO <sub>3</sub>	Na-HCO <sub>3</sub>	2	4	2
S105	10.7	8.55	3627	0.7	85	300	-0.1	Na-Cl-HCO <sub>3</sub>	Na-Cl	3	1	2
S106	8.7	7.78	341	4.5	17	234	-3.3	Mg-Ca-HCO <sub>3</sub>	Alkaline earths-HCO <sub>3</sub>	1	5	3
S107	9.6	7.31	848	2.1	24	240	-0.1	Na-HCO <sub>3</sub> -Cl	Na-HCO <sub>3</sub>	2	4	2
S108	10.5	8.01	340	2.1	15	230	-3.9	Ca-Mg-HCO <sub>3</sub>	Ca-HCO <sub>3</sub>	1	3	2
S109	8.2	7.84	514	10.6	-50	167	-5.4	Mg-Ca-HCO <sub>3</sub>	Mg-HCO <sub>3</sub>	1	7	3
S110	9.4	7.22	915	0.4	-83	133	-2.4	Ca-Mg-HCO <sub>3</sub> -Cl	Ca-HCO <sub>3</sub>	1	7	3

Tableau A1.2. (suite)

ID Site	T <sup>i</sup> (°C)	pH	CE <sup>j</sup> (µS/cm)	OD <sup>k</sup> (mg/L)	Potentiel Redox E <sup>l</sup> (mV)	Eh <sup>m</sup>	EN <sup>n</sup> (%)	Types d'eau <sup>o</sup>	Types d'eau dominants et mixtes <sup>p</sup>	G <sup>q</sup>	C <sup>r</sup>	S <sup>s</sup>
S111	8.6	8.52	446	2.7	-127	90	-5.1	Na-HCO <sub>3</sub>	Na-HCO <sub>3</sub>	2	1	6
S112	8.4	7.16	333	7.8	130	347	1.6	Ca-Mg-HCO <sub>3</sub>	Ca-HCO <sub>3</sub>	1	3	2
S113	7.9	8.10	326	2.9	14	231	-1.0	Ca-Mg-HCO <sub>3</sub>	Alkaline earths-HCO <sub>3</sub>	1	5	3
S114	n.a.	8.00	279	n.a.	n.a.	n.a.	-0.3	Ca-Mg-HCO <sub>3</sub>	Ca-HCO <sub>3</sub>	1	3	4
S115	8.6	7.08	279	8.5	196	413	3.2	Ca-Mg-HCO <sub>3</sub>	Ca-HCO <sub>3</sub>	1	3	4
S116	13.0	7.70	403	10.8	-44	170	1.5	Na-Mg-Ca-HCO <sub>3</sub>	Mixed cations-HCO <sub>3</sub>	2	5	4
S117	8.7	8.08	585	3.8	76	293	-0.8	Na-HCO <sub>3</sub> -Cl-SO <sub>4</sub>	Na-Mixed anions	3	4	5
S118	n.a.	7.10	680	n.a.	n.a.	n.a.	-3.4	Ca-Mg-Na-HCO <sub>3</sub> -Cl	Mixed cations-HCO <sub>3</sub>	2	3	3
S119	10.6	7.79	3509	2.5	-114	101	-7.5	Na-Cl	Na-Cl	3	2	7
S120	10.1	6.98	464	2.8	-72	144	4.8	Ca-Mg-HCO <sub>3</sub>	Ca-HCO <sub>3</sub>	1	5	3
S121	8.7	7.15	381	6.6	120	337	0.7	Ca-Mg-HCO <sub>3</sub>	Ca-HCO <sub>3</sub>	1	3	3
S122	9.1	7.66	414	0.5	-108	108	-1.5	Ca-Mg-HCO <sub>3</sub>	Ca-HCO <sub>3</sub>	1	7	3
S123	8.5	7.73	794	2.0	-23	194	-3.9	Na-Mg-HCO <sub>3</sub> -Cl	Na-HCO <sub>3</sub>	2	6	3
S124	7.9	8.17	2022	1.1	-180	37	-2.3	Na-Cl-HCO <sub>3</sub>	Na-Cl	3	1	6
S125	9.4	7.22	1828	4.0	76	292	0.1	Na-Ca-Cl-HCO <sub>3</sub>	Na-Cl	3	6	3
S126	11.8	7.66	937	3.7	n.a.	n.a.	1.4	Na-Ca-HCO <sub>3</sub> -Cl	Na-HCO <sub>3</sub>	2	5	4
S127	8.1	7.57	469	3.8	145	362	-3.4	Ca-Mg-HCO <sub>3</sub>	Ca-HCO <sub>3</sub>	1	6	2
S128	8.1	8.06	710	2.6	36	253	-4.3	Na-Mg-HCO <sub>3</sub> -Cl	Na-HCO <sub>3</sub>	2	4	1
S129	8.1	7.28	487	3.8	96	313	-2.7	Ca-Mg-HCO <sub>3</sub>	Ca-HCO <sub>3</sub>	1	7	3
S130	8.4	7.76	659	2.3	-48	169	0.2	Na-Ca-Mg-HCO <sub>3</sub> -Cl	Na-HCO <sub>3</sub>	2	5	2
S131	8.0	7.29	642	3.3	64	281	1.4	Ca-Mg-Na-HCO <sub>3</sub>	Mixed cations-HCO <sub>3</sub>	2	6	3
S132	9.4	7.19	638	1.6	n.a.	n.a.	-0.8	Mg-Ca-Na-HCO <sub>3</sub>	Mixed cations-HCO <sub>3</sub>	2	6	3
S133	n.a.	7.80	690	n.a.	n.a.	n.a.	-5.1	Na-Mg-Ca-HCO <sub>3</sub> -Cl	Mixed cations-HCO <sub>3</sub>	2	5	1
S134	9.6	7.35	474	3.0	-32	184	4.7	Ca-Mg-HCO <sub>3</sub>	Ca-HCO <sub>3</sub>	1	5	1
S135	8.5	7.50	775	5.7	-23	194	-2.8	Na-Mg-Ca-HCO <sub>3</sub> -Cl	Mixed cations-HCO <sub>3</sub>	2	5	1
S136	9.7	7.37	879	5.5	25	241	-4.3	Ca-Mg-HCO <sub>3</sub> -Cl	Ca-HCO <sub>3</sub>	1	6	3
S137	8.9	6.30	555	3.3	-90	127	-3.1	Ca-Mg-HCO <sub>3</sub>	Ca-HCO <sub>3</sub>	1	7	3
S138	10.1	7.66	448	6.9	115	331	-1.7	Ca-Mg-HCO <sub>3</sub>	Ca-HCO <sub>3</sub>	1	3	3
S139	8.8	7.32	796	5.2	133	350	-2.8	Ca-Mg-HCO <sub>3</sub>	Ca-HCO <sub>3</sub>	1	6	3
S140	n.a.	7.68	918	7.1	-11	205	-1.5	Na-Ca-SO <sub>4</sub> -HCO <sub>3</sub>	Na-SO <sub>4</sub>	4	4	5
S141	8.5	8.29	1354	0.2	-200	17	-2.0	Na-HCO <sub>3</sub> -Cl	Na-HCO <sub>3</sub>	2	1	6
S142	8.2	7.07	1320	1.9	66	283	1.7	Ca-Mg-Na-Cl-HCO <sub>3</sub>	Mixed cations-Cl	3	6	3
S143	8.2	7.77	432	0.2	-139	78	2.3	Ca-Na-Mg-HCO <sub>3</sub>	Ca-HCO <sub>3</sub>	1	5	6
S144	10.9	7.36	460	1.7	90	305	-2.4	Mg-Ca-HCO <sub>3</sub>	Mg-HCO <sub>3</sub>	1	7	3
S145	16.8	7.44	592	1.7	27	238	-1.5	Mg-Ca-HCO <sub>3</sub>	Mg-HCO <sub>3</sub>	1	7	3
S146	16.3	7.33	803	9.0	45	256	-3.1	Ca-Mg-HCO <sub>3</sub>	Ca-HCO <sub>3</sub>	1	7	3
<b>Échantillons rejetés</b>												
R1	n.a.	n.a.	n.a.	n.a.	n.a.	—	—	—	—	—	—	—
R2	9.8	8.02	780	2.4	-40	—	-99.0	HCO <sub>3</sub> -Cl	—	—	—	—
R3	8.2	7.70	474	2.4	n.a.	—	-99.4	HCO <sub>3</sub>	—	—	—	—
R4	9.8	7.31	1779	1.2	-56	—	17.0	Ca-Na-Cl-HCO <sub>3</sub>	—	—	—	—
SAP	8.9	8.38	2001	1.7	-160	—	-99.2	Cl-HCO <sub>3</sub>	—	—	—	—
R5	10.2	7.00	5551	1.5	-15	—	-5.2	Na-Ca-Cl	—	—	—	—
R6	11.9	8.20	917	0.6	-153	—	22.4	Na-HCO <sub>3</sub> -Cl	—	—	—	—
<b>Duplicata</b>												
D1	8.3	7.62	2710	0.4	-96	—	-0.8	Na-Cl-HCO <sub>3</sub>	—	—	—	—
D2	9.9	7.45	557	0.6	27	—	2.3	Ca-Mg-Na-HCO <sub>3</sub>	—	—	—	—
D3	8.6	7.36	1125	3.1	52	—	0.8	Na-Cl-HCO <sub>3</sub>	—	—	—	—
D4	8.2	7.16	527	5.6	54	—	1.6	Ca-Mg-HCO <sub>3</sub>	—	—	—	—
D5	9.2	6.74	882	5.1	111	—	-9.8	Ca-Mg-HCO <sub>3</sub> -SO <sub>4</sub>	—	—	—	—
D6	n.a.	n.a.	n.a.	n.a.	n.a.	—	—	—	—	—	—	—
D7	9.8	7.09	18530	n.a.	n.a.	—	2.1	Na-Cl	—	—	—	—
D8	9.4	7.64	467	1.0	n.a.	—	-1.6	Ca-Na-Mg-HCO <sub>3</sub>	—	—	—	—
D9	10.5	7.19	1154	1.7	-51	—	-0.8	Ca-Mg-Na-HCO <sub>3</sub> -Cl	—	—	—	—
D10	8.1	8.06	710	2.6	36	—	-3.0	Na-Mg-HCO <sub>3</sub> -Cl	—	—	—	—

Tableau A1.3. Base de données géochimiques – Paramètres chimiques (# 1)

ID Site	Ca	Mg	Na	K	Cl	SO <sub>4</sub>	Alc. Tot. (en CaCO <sub>3</sub> )	CID	Fe	Mn	Br	Sr	F	Ba	HS (en S)	SiO <sub>2</sub>
S1	81	36	26	3.8	49	22	310	76	1.4	0.15	0.02	0.24	0.2	0.22	0.02	15.7
S2	76	39	21	6.5	72	34	270	68	0.52	0.069	0.04	0.34	0.24	0.22	<.02	14.3
S3	53	23	3.7	0.76	0.6	49	180	45	0.34	0.3	<.01	0.107	0.04	0.06	<.02	10.7
S4	87	27	49	4.7	66	50	290	69	0.84	0.08	0.04	0.45	0.06	0.07	<.02	11.2
S5	83	47	10.1	4.8	15	80	350	85	0.48	0.028	<.01	0.32	0.2	0.17	0.02	13.7
S6	84	44	9.4	4.6	0.8	75	370	93	0.97	0.13	<.01	0.42	0.34	0.01	0.02	11.5
S7	72	28	46	5	37	130	270	67	2.8	0.53	0.03	0.49	0.22	0.07	<.02	9.4
S8	95	26	7.2	13	15	50	310	78	0.67	0.44	0.01	0.143	0.15	0.06	0.03	9.3
S9	48	24	3	1.2	6.1	15	200	50	0.007	<.0003	0.0081	0.06	0.12	0.02	<.02	11.9
S10	74	40	6.8	1.7	13	12	390	81	1.2	0.17	0.008	0.16	0.08	0.22	0.04	17.8
S11	27	14.3	13	3.7	1.3	10	150	36	0.7	0.037	0.01	0.177	0.24	0.05	<.02	9.5
S12	35	17	7.5	3.2	2.4	21	150	n.a.	0.026	0.18	<.01	0.177	0.22	0.16	<.02	12.2
S13	42	23	35	2.7	29	9	230	56	0.1	0.36	0.15	0.23	0.3	0.32	<.02	11.1
S14	56	24	74	4.7	76	8.5	250	n.a.	0.064	0.015	0.41	0.09	0.34	0.14	0.02	18.1
S15	56	24	6.1	1.3	5.1	15	200	n.a.	0.004	0.015	0.02	0.09	0.12	0.1	0.02	7.9
S16	110	76	485	13	940	95	210	n.a.	0.28	0.19	4.4	0.87	0.25	0.12	0.04	14
S17	52	29	24	2.9	18	34	250	60	0.005	0.029	0.04	0.56	0.45	0.1	0.02	17.3
S18	32	23	100	6.7	120	16	250	60	0.021	0.058	0.4	0.36	0.47	0.14	0.03	16.1
S19	61	30	110	13	73	85	360	93	0.49	0.096	0.38	2.5	0.48	0.3	0.06	18.5
S20	2.4	2.7	180	8.8	2	2	380	89	0.013	0.0008	0.07	0.17	1.3	0.04	0.58	14.2
S21	25	25	100	18	73	9	300	74	0.011	0.009	0.13	1.09	0.54	0.23	3.7	21
S22	3.1	3.8	220	16	15	20	450	100	0.043	0.002	0.11	0.72	1.5	0.4	0.2	10.2
S23	3.1	1.7	300	9.5	170	0.5	420	99	0.009	0.0008	1.31	0.656	1.7	0.06	0.51	8.1
S24	38	30	77	14	26	65	310	76	0.019	0.003	0.09	2	0.86	0.8	0.34	22
S25	37	29	180	12	140	<1	390	99	0.32	0.002	0.67	2.3	0.73	0.86	0.04	13.1
S26	15.9	14.3	560	16	620	110	380	94	0.003	0.0006	6.5	3.1	2.5	0.04	3.4	13
S27	25	28	96	14	48	33	310	77	0.099	<.0003	0.29	1.6	0.72	0.67	0.17	14.5
S28	9.8	14.7	210	30	90	9	490	120	0.006	0.0007	0.48	9.2	1.4	0.38	0.96	10.8
S29	5.9	14	190	14.1	10	<.5	481	120	0.15	0.003	0.07	1	0.93	0.12	0.04	13.4
S30	94	39	54	17	64	95	360	88	0.46	0.17	0.16	1.7	0.28	0.2	<.02	21
S31	81	41	18.4	12	35	120	280	76	0.16	0.092	0.017	0.37	0.13	0.16	<.02	10.7
S32	35	22	17.2	9.8	1.3	<1	240	56	0.096	0.004	14.2	0.4	0.47	0.48	0.24	14.2
S33	77	38	14.1	3.6	35	130	220	62	2.1	0.3	0.033	0.2	0.11	0.13	0.02	16.5
S34	110	55	140	7.4	260	80	350	91	0.016	0.017	0.06	0.29	0.14	0.07	<.02	9
S35	64	34	15	4.3	8.3	47	280	68	0.72	0.049	0.009	0.346	0.25	0.17	<.02	15.6
S36	140	56	57	34	85	170	420	n.a.	0.034	0.007	0.017	0.154	0.1	0.08	<.02	10.8
S37	130	45	57	1.9	90	110	400	n.a.	0.006	0.01	0.023	0.195	0.1	0.11	<.02	7.6
S38	92	47	4.5	0.13	10	75	330	77	0.013	<.0003	0.04	1.037	0.18	0.09	<.02	11.6
S39	56	33.4	25	8.7	10	55	260	61	0.097	0.013	0.02	2.072	n.a.	0.24	0.04	13.9
S40	51	27	42	9.4	10	45	260	62	0.014	0.01	0.03	1.49	0.66	0.52	0.04	14
S41	21	17	240	12	330	50	260	67	1.5	0.15	1.1	0.46	0.39	0.04	0.04	10.8
S42	19.5	30	240	15	290	15	270	66	0.12	0.085	1.01	n.a.	0.51	0.13	n.a.	11.3
S43	16	26	82	8	63	15	250	n.a.	0.12	0.017	0.24	1.272	0.62	0.13	n.a.	15
S44	46	32	14.7	4.4	<.1	22	280	n.a.	0.5	0.12	0.008	0.48	0.29	0.27	n.a.	21
S45	18	55	1260	16.8	1900	15	240	n.a.	0.23	0.043	7	1.2	0.42	0.25	n.a.	6.9
S46	13	12.6	240	7.8	200	24	290	69	0.11	0.13	1.2	0.28	0.49	0.08	0.03	10.2
S47	25	18.6	61	4.9	15	9.5	250	61	0.1	0.33	0.08	0.44	0.36	0.19	<.02	12.2
S48	47	21	1.6	0.56	1	2	210	54	0.006	<.0003	<.01	0.06	0.06	0.02	0.02	10.6
S49	57	25	1.7	0.6	1.9	9.5	230	n.a.	0.015	0.003	<.01	0.051	0.05	0.02	0.02	10
S50	35	15.1	6.3	1.4	11	9	140	36	0.004	<.0003	<.01	0.08	0.1	0.04	0.03	12.7
S51	28	28	460	16	630	120	100	59	1	0.058	2.3	0.91	0.32	0.03	0.07	9.1
S52	63.2	27	19	2.3	15	55	240	65	1.4	0.56	0.05	0.22	0.13	0.17	0.03	12
S53	11.4	7.2	240	2.8	280	12	160	39	n.a.	0.009	1.2	1.3	n.a.	0.25	0.09	11.3
S54	41	32	320	28	340	140	370	88	n.a.	0.003	0.59	2.5	0.81	0.02	0.02	9.4
S55	100	24	690	11	1000	22	320	n.a.	0.52	0.029	13	0.2	1.7	0.17	0.04	7.8

Tableau A1.3. (suite)

ID Site	Ca	Mg	Na	K	Cl	SO <sub>4</sub>	Alc. Tot. (en CaCO <sub>3</sub> )	CID	Fe	Mn	Br	Sr	F	Ba	HS (en S)	SiO <sub>2</sub>
S56	24	15.2	93	15	150	3.5	190	46	0.15	0.029	0.56	0.37	0.39	0.47	0.07	12
S57	48	9.5	22	2.4	35	23	150	38	0.003	0.037	0.046	0.35	0.31	0.1	<.02	14.7
S58	26	9.7	12.3	4.1	3.2	16	120	30	0.026	0.017	0.01	0.31	0.24	0.13	<.02	12.6
S59	64	29	7.4	0.77	13	27	230	59	0.006	0.002	<.01	0.05	0.06	0.03	0.03	9.4
S60	38	27	120	11	140	27	230	58	0.36	0.039	0.67	0.36	0.26	0.06	0.06	9.1
S61	31	16.6	150	8.3	210	55	130	33	0.091	0.034	0.66	1.1	0.61	0.07	<.02	10.3
S62	20	6	27	0.89	44	34	33	14.4	0.01	0.0004	0.016	0.11	0.1	0.06	<.02	12.4
S63	31	20	54	4.5	63	43	170	44	0.064	<.0003	0.22	3.5	2.3	0.11	<.02	8.9
S64	19	8.8	44	5.2	33	3	120	27	0.039	0.053	0.119	0.57	1.1	0.14	0.02	9.4
S65	35	13.1	77	7	57	88	150	35	0.12	0.008	0.21	0.57	1.6	0.04	0.1	10.2
S66	64	24	12.7	4.1	5	43	240	58	0.041	0.007	0.004	17	1	0.14	0.04	12.3
S67	12.7	26	450	22	510	17	420	98	0.61	0.012	1.9	1.8	0.91	0.12	0.04	13.7
S68	480	48	21	5.3	20	1200	n.a.	43	0.46	0.005	<.01	15	1.3	0.004	0.03	11.6
S69	61	31	27	1.6	75	45	n.a.	52	0.5	0.018	<.01	29	0.59	0.28	0.04	11.6
S70	18.6	14.5	41	12	28	10	170	41	0.59	0.039	0.1	0.21	0.32	0.13	0.02	11.7
S71	33	23	86	14	71	68	220	56	0.33	0.011	0.23	1.4	0.82	0.15	0.06	14
S72	87	46	180	8.6	250	210	290	73	0.47	0.027	0.62	1.99	0.35	0.06	<.02	11.4
S73	120	44	22	6.6	15	130	360	92	0.074	0.033	0.02	0.9	0.32	0.08	<.02	10.1
S74	85	42	5.6	1.2	38	68	300	73	0.56	0.64	<.01	0.17	0.12	0.05	0.02	17
S75	81	35	5.3	2.3	5	65	300	76	0.13	0.013	0.02	0.29	0.16	0.22	<.02	12.4
S76	82	37	34	5.5	47	90	300	73	0.12	0.01	0.06	1.2	0.25	0.1	<.02	9.8
S77	790	390	3100	26	6500	350	110	30	2.1	0.58	23	22.6	0.1	0.04	<.02	15.6
S78	210	38	90	7.2	40	660	n.a.	26	0.62	0.008	0.2	12	3.1	0.02	0.04	9.7
S79	62	26	7.4	1.3	12	30	240	64	0.016	0.0008	0.003	6.1	0.29	0.09	0.04	11.8
S80	64	16.1	16.9	3.5	24	20	n.a.	56	0.29	0.012	0.05	19	0.56	0.14	0.07	22
S81	0.2	0.04	150	0.21	30	45	270	63	0.024	0.001	<.01	0.02	0.39	0.05	0.02	15.6
S82	44	25	10.2	4.5	21	23	210	51	0.024	0.011	<.01	9.5	0.52	0.18	0.03	15.7
S83	13.6	13.1	73	9	35	27	180	48	0.013	0.05	0.13	0.61	0.43	0.11	<.02	13.8
S84	68	34	2.5	1.3	3.3	32	300	73	0.004	0.002	0.002	0.066	0.05	0.18	<.02	11.1
S85	36	21	38	4.8	10	25	230	55	0.23	0.26	0.04	0.63	0.27	0.06	0.02	15.4
S86	28	22	43	4.8	10	30	230	56	0.094	0.009	<.01	0.3	0.34	0.16	0.02	13.5
S87	48	27	26	4.5	17	27	260	66	0.39	0.1	0.02	0.21	0.3	0.14	0.03	14.1
S88	78	39	31	11	57	45	340	81	0.002	<.0003	0.019	0.1	0.12	0.15	0.02	12
S89	21	33	290	17	440	63	190	49	0.068	0.26	1.4	1.23	0.38	0.12	0.04	14.5
S90	47	27	40	3.5	47	14	270	66	0.15	0.31	0.13	0.21	0.24	0.17	0.3	12
S91	1.3	0.1	130	0.29	17	27	220	54	0.013	0.0009	0.006	<.005	0.12	0.001	<.02	14.8
S92	69	38	110	11	180	65	240	73	0.37	0.028	0.21	1.2	0.61	0.49	<.02	12.8
S93	10.3	15.6	400	16.5	430	3	410	98	0.16	0.011	1.5	0.28	0.83	0.22	0.2	9.3
S94	42	31	28	16	3.3	36	290	76	0.085	0.017	<.01	1.45	0.6	1.1	0.05	18.6
S95	130	49	170	18	300	95	320	100	7	0.36	0.12	0.88	0.32	0.29	0.02	17.9
S96	110	49	68	7.2	150	120	310	80	1.6	0.1	0.06	0.37	0.22	0.43	<.02	15.8
S97	13.9	8.7	63	4.75	25	26	170	40	0.029	0.014	0.03	1.3	1	0.3	0.02	16.6
S98	25	23	59	3.6	10	37	260	59	1.4	0.019	0.02	4.15	1.7	0.07	<.02	16.8
S99	3.6	2.9	120	1.9	12	11	240	56	0.68	0.037	0.05	0.14	1.3	0.13	0.04	7.2
S100	25	66	1000	15	1400	<5	390	n.a.	0.24	0.008	7.3	1.3	0.55	0.56	0.02	14.2
S101	49	27	690	7.6	1000	<1	230	60	0.89	0.096	3.9	1.7	0.27	0.67	0.04	10
S102	1.2	1.4	230	3	2.5	<.5	500	110	0.045	0.002	0.06	0.1	0.48	0.008	0.1	9.9
S103	61	32	7.1	2.5	10	22	270	67	0.095	0.081	0.02	0.17	0.1	0.04	0.04	9.8
S104	45	9.6	67	3.1	40	9	210	51	0.018	0.002	0.15	2	1.5	0.03	0.04	10.8
S105	1.5	19.2	820	17	780	2	810	180	0.15	0.002	1.14	0.14	1.1	0.24	0.02	5.5
S106	28	17.3	14.7	8.3	0.5	n.a.	200	46	0.44	0.065	0.01	0.188	n.a.	0.26	0.08	18.2
S107	27	17.2	120	7.7	130	34	190	51	0.021	0.002	0.49	0.33	0.73	0.04	<.02	9.9
S108	33	12	16.1	3.7	20	16	140	33	0.002	0.0003	0.057	1.7	0.13	0.04	0.02	17.6
S109	50	35	3.9	2.7	2.5	37	270	64	0.17	0.025	<.01	0.45	0.12	0.11	0.04	14.1
S110	87	35	42	6.31	100	49	300	76	4.1	0.28	<.01	0.51	0.25	0.52	0.04	24

Tableau A1.3. (suite)

ID Site	Ca	Mg	Na	K	Cl	SO <sub>4</sub>	Alc. Tot. (en CaCO <sub>3</sub> )	CID	Fe	Mn	Br	Sr	F	Ba	HS (en S)	SiO <sub>2</sub>
S111	7.9	9.5	75	12	7	1	250	57	n.a.	0.0008	0.12	0.34	0.99	0.1	0.09	10.4
S112	55	10.2	6.6	2	4	21	160	39	0.018	0.005	0.008	0.111	0.07	0.14	0.03	13
S113	29	17.5	14.2	6.9	0.6	n.a.	190	43	0.16	0.062	0.01	0.177	n.a.	0.23	0.08	17.1
S114	31	10.9	7	1.1	12	25	96	23	<.0007	<.0003	0.026	0.09	0.1	0.03	<.02	13
S115	36	13.5	2.1	0.87	<.1	5	130	35	0.003	<.0003	0.005	0.544	1.4	0.25	<.02	9.1
S116	29	18.2	37	3.2	3.8	19	200	50	0.15	0.029	<.01	0.83	0.76	0.09	0.02	17.5
S117	21	8.5	93	3.2	76	75	120	29	0.025	0.006	0.24	13	3.2	0.03	<.02	10.6
S118	51	23	42	2.1	92	22	180	50	0.001	<.0003	<.002	0.12	0.11	0.24	<.02	13.3
S119	21	35	550	24	950	23	290	75	0.69	0.085	3.3	1.1	0.48	0.12	0.03	11.6
S120	40	15.6	20	1.2	29	4.5	170	53	15	0.45	<.01	0.12	0.12	0.09	0.1	14.6
S121	43	18.7	7.5	3.4	13	8	150	45	0.026	0.0005	<.01	0.1	0.12	0.11	0.02	12
S122	51	18.2	9.2	2	<.2	21	210	49	0.39	0.053	<.01	0.7	0.28	0.1	0.03	14.7
S123	31	26	86	13	86	39	260	63	0.12	0.003	0.034	1.26	0.68	0.52	0.05	11.7
S124	16.6	15.4	418	18	430	18	460	110	0.005	<.0003	1.528	4.297	2.3	1.1	4.7	10.5
S125	98	41	250	3.4	350	130	330	n.a.	0.02	0.099	0.022	0.23	0.1	0.13	<.02	9.8
S126	55	22	130	3.9	110	25	320	82	0.13	0.059	0.22	0.94	0.51	0.06	<.02	9.5
S127	43	26	15.8	4.1	6.3	23	240	58	0.28	0.015	0.02	0.73	0.34	0.54	0.08	14
S128	24	18.5	94	8.1	98	33	210	47	0.007	0.22	0.26	0.94	0.43	0.16	<.02	12.9
S129	56	28	7.5	3.4	6.7	40	240	58	0.28	0.02	0.006	0.371	0.15	0.15	<.02	10.8
S130	42	22	71	7.5	76	3	250	60	0.4	0.035	0.119	0.35	0.38	0.39	0.04	11.4
S131	58	32	40	11	42	48	260	60	0.16	0.012	0.06	1.395	0.48	0.2	<.02	17.6
S132	50	31	35	10	37	44	250	62	0.37	0.02	0.027	1.3	0.45	0.27	<.02	18.1
S133	42	28	53	11	57	42	240	63	0.29	0.04	0.2	0.49	0.37	0.08	<.02	10.3
S134	55	30	12.6	5.7	6.7	21	240	58	0.22	0.48	0.04	0.52	0.27	0.13	<.02	11.5
S135	49	31	68	7.1	110	26	250	58	0.27	0.93	0.38	0.6	0.31	0.16	0.03	10
S136	92	44	28	2.8	86	58	330	85	0.017	0.011	<.01	0.15	0.13	0.14	0.03	12.1
S137	61	31	12.6	6	15	43	270	68	0.57	0.085	<.01	0.17	0.14	0.14	0.03	15.3
S138	49	26	7.3	1.7	4	28	220	56	0.009	<.0003	<.01	0.15	0.15	0.09	0.02	10.8
S139	91	41	20	5.7	35	49	370	95	0.003	0.002	<.01	0.12	0.1	0.24	0.02	10
S140	42	13	140	4.6	33	240	180	n.a.	0.01	0.005	0.037	<.007	2.6	0.05	<.02	7.3
S141	7.9	12.6	280	19	230	7	400	88	0.045	0.004	1.106	0.28	1	0.4	0.33	8.2
S142	110	56	89	11	250	47	290	n.a.	0.13	0.011	0.038	1.293	0.35	0.21	<.02	10.4
S143	44	13.1	32	3.9	8.8	16	200	n.a.	0.13	0.016	0.019	0.4	0.24	0.14	0.03	14.6
S144	40	35	5.6	4	2.5	30	240	58	0.65	0.12	0.005	0.595	0.22	0.16	<.02	17.3
S145	62	39	6.2	3	5	46	290	73	1.6	0.06	n.a.	0.331	0.14	0.18	0.14	24
S146	92	47	14.5	3.7	5	49	430	110	0.25	0.019	n.a.	0.19	0.09	0.11	0.05	20
<b>Échantillons rejetés</b>																
R1	n.a.	n.a.	n.a.	n.a.	n.a.	n.a.	n.a.	n.a.	n.a.	n.a.	n.a.	n.a.	n.a.	n.a.	n.a.	n.a.
R2	n.a.	n.a.	n.a.	n.a.	85	13	190	66	n.a.	n.a.	0.31	n.a.	0.62	n.a.	n.a.	11.3
R3	n.a.	n.a.	n.a.	n.a.	8.2	15	240	61	n.a.	n.a.	0.02	n.a.	0.37	n.a.	n.a.	12.7
R4	360	9.1	150	4.4	420	48	260	69	1.8	0.16	<.01	0.76	0.1	0.43	0.04	9.6
SAP	n.a.	n.a.	n.a.	n.a.	500	35	360	88	n.a.	n.a.	2.5	n.a.	1.7	n.a.	2.7	11.1
R5	210	86	650	38	1500	220	250	97	0.098	0.39	0.35	1.64	0.17	0.39	0.03	16.9
R6	33	21	250	8.4	140	9.5	250	63	0.36	0.078	0.5	0.51	0.51	0.37	0.03	14.4
<b>Duplicata</b>																
D1	16.8	14.4	570	16	610	120	380	94	0.007	0.001	6.3	3.06	2.7	0.04	4.2	13
D2	46	26	43	9.2	10	47	250	62	0.031	0.007	0.03	1.5	0.68	0.52	0.04	10.9
D3	13.4	12.4	230	7.8	200	22	280	66	0.1	0.13	1.2	0.28	0.48	0.08	0.02	10.1
D4	62	23	12.6	4	5	41	240	58	0.039	0.007	0.004	17	1	0.14	0.04	12.4
D5	88	39	19.5	5.8	13	140	360	92	0.063	0.026	0.02	0.9	0.35	0.07	<.02	10.2
D6	n.a.	n.a.	n.a.	n.a.	n.a.	n.a.	n.a.	n.a.	n.a.	n.a.	n.a.	n.a.	n.a.	n.a.	n.a.	n.a.
D7	780	380	3000	26	6500	400	76	30	2.1	0.58	23	19.9	0.11	0.04	<.02	15.7
D8	34	20	38	4.8	8.8	22	230	55	0.22	0.26	<.01	0.63	0.24	0.06	0.02	15.3
D9	110	49	68	7.2	150	120	310	80	1.5	0.1	0.06	0.37	0.22	0.42	0.02	15.8
D10	25	18.6	96	8.1	98	32	210	47	0.013	0.22	0.31	0.96	0.35	0.16	<.02	13

Tableau A1.4. Base de données géochimiques – Paramètres chimiques (# 2)

ID Site	B	Al	Li	NO <sub>3</sub> (en N)	NH <sub>4</sub> (en N)	PO <sub>4</sub> (en P)	COD	Ag	As	Cd	CN	Cr	Cu	Hg	I
S1	<.002	<.007	0.005	<.02	0.11	0.04	1.5	<.0003	0.001	0.0018	<.003	0.003	<.001	n.a.	<.1
S2	0.03	<.007	0.004	<.02	0.03	0.01	1.5	<.0003	<.001	0.0017	<.033	0.001	<.001	n.a.	<.1
S3	<.002	<.007	0.001	<.02	<.02	<.01	4	<.0003	0.001	0.0013	<.003	0.002	<.001	n.a.	<.1
S4	<.002	0.7	<.001	0.04	0.02	<.01	1.9	<.0003	0.002	0.0016	0.011	0.004	<.001	n.a.	<.1
S5	0.02	<.007	0.006	<.02	0.11	0.025	0.9	n.a.	n.a.	n.a.	n.a.	0.006	<.001	n.a.	n.a.
S6	<.002	<.007	0.009	<.02	0.06	0.025	1.4	n.a.	n.a.	n.a.	n.a.	0.002	<.001	n.a.	n.a.
S7	<.002	0.18	0.003	<.02	0.09	<.01	1.6	n.a.	n.a.	n.a.	n.a.	0.002	<.001	n.a.	n.a.
S8	<.002	<.007	0.001	<.02	<.02	<.01	1.9	n.a.	n.a.	n.a.	n.a.	0.002	<.001	n.a.	n.a.
S9	0.009	0.02	n.a.	3.7	<.02	<.01	0.3	0.0003	<.001	0.0012	n.a.	<.0009	<.001	<.0001	<.1
S10	<.002	<.007	0.003	<.02	0.02	0.03	0.7	<.0001	0.002	0.0012	<.003	0.002	<.001	<.0001	<.1
S11	0.05	0.01	<.001	<.02	0.03	0.06	0.5	0.0001	<.001	0.0009	<.003	0.002	<.001	<.0001	<.1
S12	0.05	0.02	<.001	0.03	0.02	0.07	0.5	0.0003	<.001	0.001	<.003	0.002	<.001	0.0001	<.1
S13	0.08	<.007	0.002	<.02	0.22	0.055	0.3	0.0003	0.002	0.0013	<.003	0.002	<.001	<.0001	<.1
S14	0.1	<.007	<.001	<.02	0.33	0.13	0.8	0.0002	0.001	0.0009	<.003	0.001	<.001	<.0001	<.1
S15	0.02	0.03	0.002	0.25	<.02	<.01	0.6	0.0003	<.001	0.0009	<.003	0.001	<.001	<.0001	<.1
S16	0.11	0.04	0.001	<.02	0.23	0.07	1	0.0004	0.001	0.002	<.003	0.002	<.001	<.0001	<.1
S17	0.02	<.007	<.01	0.06	<.02	0.03	1	<.0003	<.001	0.0015	<.003	<.0009	0.032	<.0001	<.1
S18	0.11	0.01	0.018	0.04	0.31	0.125	0.6	<.0003	0.001	0.0005	<.003	<.0009	<.001	<.0001	<.1
S19	0.37	0.01	n.a.	<.02	1.13	0.51	3.7	<.0003	<.001	0.0017	n.a.	0.002	<.001	<.0001	<.1
S20	0.57	0.009	0.019	0.03	0.69	2.1	7.9	<.0003	<.001	<.0003	<.003	<.0009	<.001	<.0001	<.1
S21	0.34	<.007	0.024	0.02	1.62	0.56	5.9	<.0003	0.001	0.0006	<.003	<.0009	<.001	<.0001	<.1
S22	0.99	<.007	0.042	0.05	0.8	1.77	8.7	<.0003	<.001	0.0004	<.003	<.0009	<.001	<.0001	<.1
S23	0.76	<.007	0.082	<.02	0.48	0.125	6.1	<.0003	<.001	<.0003	<.003	<.0009	<.001	<.0001	<.1
S24	0.32	<.007	0.02	<.02	0.61	0.29	2.8	<.0001	<.001	0.0014	<.003	0.001	<.001	<.0001	<.1
S25	0.38	<.007	0.014	<.02	0.72	0.7	5.2	<.0001	<.001	0.0013	<.003	0.001	<.001	<.0001	<.1
S26	0.51	0.01	0.132	0.04	0.91	0.155	4.9	0.0001	0.001	0.0009	<.003	<.0009	<.001	<.0001	<.1
S27	0.43	0.02	n.a.	<.02	1.09	1.55	4.8	<.0003	<.001	0.0011	n.a.	<.0009	<.001	<.0001	<.1
S28	0.81	0.05	0.03	0.03	0.98	2.1	7.3	0.0003	<.001	0.0009	<.003	<.0009	<.001	<.0001	<.1
S29	0.74	0.009	0.02	<.02	1.02	1.7	13.8	<.0003	<.001	0.0004	<.003	<.0009	<.001	<.0001	<.1
S30	0.15	0.01	0.02	<.02	0.76	0.065	3.5	<.0003	<.001	0.0012	<.003	<.0009	<.001	<.0001	<.1
S31	0.04	0.02	n.a.	0.1	0.11	<.01	3.1	0.0003	<.001	0.0016	n.a.	<.0009	<.001	<.0001	<.1
S32	0.12	0.007	0.404	<.02	0.55	0.3	9.9	<.0001	<.001	0.0011	<.003	0.002	<.001	<.0001	<.1
S33	0.03	0.01	n.a.	<.02	0.24	0.045	4.8	<.0003	<.001	0.0015	n.a.	<.0009	<.001	<.0001	<.1
S34	0.02	<.007	<.01	<.02	<.02	<.01	0.5	<.0003	<.001	0.0021	0.004	<.0009	0.009	<.0001	<.1
S35	0.04	<.007	0.004	<.02	0.09	0.02	1.5	0.0001	<.001	0.0013	<.003	0.002	<.001	<.0001	<.1
S36	0.03	0.13	0.002	9	<.02	<.01	1.5	0.0004	<.001	0.0014	<.003	0.004	0.003	0.0001	<.1
S37	0.004	<.007	0.002	1.78	<.02	<.01	1.7	0.0005	<.001	0.0015	<.003	0.003	0.012	<.0001	<.1
S38	0.02	0.04	0.003	1.15	<.02	<.01	1.1	0.0004	0.001	0.0017	<.003	0.003	<.001	0.0001	<.1
S39	0.08	0.03	0.006	<.02	0.08	<.01	1.1	0.0003	<.001	0.0012	<.003	0.002	<.001	<.0001	<.1
S40	0.16	0.02	0.008	<.02	0.17	0.06	1.9	0.0002	<.001	0.0015	<.003	0.002	<.001	<.0001	<.1
S41	0.08	<.007	<.01	<.02	0.05	0.02	0.5	<.0003	<.001	0.0015	0.005	<.0009	<.001	<.0001	0.1
S42	0.2	<.007	n.a.	<.02	0.72	0.2	0.9	n.a.	n.a.	0.0006	n.a.	0.0009	<.001	n.a.	n.a.
S43	0.11	n.a.	0.004	0.09	0.35	0.09	n.a.	n.a.	n.a.	n.a.	n.a.	<.0009	<.001	n.a.	n.a.
S44	0.008	n.a.	0.005	0.02	0.1	0.1	n.a.	n.a.	n.a.	n.a.	n.a.	0.002	<.001	n.a.	n.a.
S45	0.42	0.13	<.01	<.02	1.98	0.01	5	n.a.	n.a.	n.a.	n.a.	0.003	<.001	n.a.	n.a.
S46	0.32	0.01	0.001	0.02	0.3	0.2	0.6	<.0001	<.001	0.0007	<.003	<.0009	<.001	<.0001	<.1
S47	0.11	<.007	0.002	<.02	0.22	0.12	1.4	n.a.	n.a.	n.a.	n.a.	<.0009	<.001	n.a.	n.a.
S48	0.004	<.007	<.01	n.a.	n.a.	n.a.	0.3	<.0003	<.001	0.0017	<.003	<.0009	<.001	<.0001	<.1
S49	0.02	0.03	<.001	0.7	0.05	<.01	0.7	0.0004	<.001	0.0012	<.003	0.002	<.001	<.0001	<.1
S50	0.005	0.04	<.01	0.28	0.02	<.01	0.6	<.0003	<.001	0.0005	<.003	<.0009	0.003	<.0001	<.1
S51	0.19	0.04	<.01	0.04	0.21	0.09	2.8	<.0003	<.001	0.0009	0.009	<.0009	<.001	<.0001	0.1
S52	0.04	0.01	<.01	<.02	0.05	0.025	6.2	<.0003	<.001	0.0013	<.003	<.0009	<.001	<.0001	<.1
S53	0.1	0.03	<.01	<.02	0.25	0.04	0.9	<.0003	<.001	0.0006	0.004	<.0009	<.001	<.0001	<.1
S54	0.39	0.03	0.03	<.02	0.16	<.01	0.7	<.0003	<.001	0.0013	0.005	<.0009	<.001	<.0001	<.1
S55	<.002	0.2	0.002	<.02	0.77	0.01	15.4	n.a.	n.a.	n.a.	n.a.	0.004	<.001	<.0001	0.3

Tableau A1.4. (suite)

ID Site	B	Al	Li	NO <sub>3</sub> (en N)	NH <sub>4</sub> (en N)	PO <sub>4</sub> (en P)	COD	Ag	As	Cd	CN	Cr	Cu	Hg	I
S56	0.18	0.06	<.01	0.03	1.15	0.15	4.6	0.0005	<.001	0.001	<.003	<.0009	<.001	<.0001	<.1
S57	0.04	0.02	n.a.	0.27	0.03	<.01	0.6	<.0003	<.001	0.0014	n.a.	<.0009	0.029	<.0001	<.1
S58	0.03	0.01	n.a.	<.02	<.02	<.01	0.2	<.0003	<.001	0.0006	n.a.	<.0009	0.003	<.0001	<.1
S59	0.04	0.01	<.001	0.47	<.02	<.01	0.6	0.0004	<.001	0.0011	<.003	0.003	<.001	<.0001	<.1
S60	0.12	<.007	0.011	<.02	0.05	0.015	0.9	<.0002	<.001	0.0016	<.003	0.003	<.001	<.0001	<.1
S61	0.15	0.01	n.a.	<.02	0.02	<.01	0.3	<.0003	<.001	0.001	n.a.	<.0009	0.002	<.0001	<.1
S62	0.007	0.02	n.a.	0.86	0.03	<.01	0.6	<.0003	<.001	0.0004	n.a.	<.0009	<.001	<.0001	<.1
S63	0.1	0.02	n.a.	<.02	0.04	<.01	0.4	<.0003	<.001	0.0011	n.a.	<.0009	<.001	<.0001	<.1
S64	0.09	0.02	0.005	<.02	0.17	0.01	0.5	<.0001	0.001	0.0006	<.003	0.001	<.001	<.0001	<.1
S65	0.15	0.01	0.004	<.02	0.55	0.025	0.3	<.0001	<.001	0.0011	<.003	0.008	<.001	0.0001	<.1
S66	0.12	0.03	0.012	<.02	0.03	<.01	0.9	<.0002	0.001	0.0016	<.003	0.027	<.001	<.0001	<.1
S67	0.45	<.007	0.01	<.02	1.24	0.14	4.3	<.0003	0.001	0.0013	<.003	<.0009	<.001	0.0001	0.2
S68	0.12	0.008	<.01	0.02	0.05	<.01	0.6	0.0009	<.001	0.0034	n.a.	<.0009	<.001	<.0001	<.1
S69	0.02	<.007	<.01	<.02	0.05	<.01	0.5	<.0003	<.001	0.0026	n.a.	<.0009	<.001	<.0001	<.1
S70	0.15	0.01	<.01	<.02	0.16	0.065	1.3	<.0003	<.001	0.0003	<.003	<.0009	<.001	<.0001	<.1
S71	0.17	<.007	0.01	<.02	0.07	0.015	2.5	<.0003	<.001	0.0014	<.003	<.0009	<.001	<.0001	<.1
S72	0.15	<.007	0.013	<.02	0.07	0.01	1.2	0.0002	<.001	0.0017	<.003	0.004	<.001	0.0001	<.1
S73	0.08	0.009	0.005	0.08	0.06	<.01	2.1	0.0005	<.001	0.0015	<.003	0.002	<.001	<.0001	<.1
S74	0.008	<.007	<.01	<.02	<.02	0.045	0.3	<.0003	<.001	0.0016	<.003	<.0009	<.001	<.0001	<.1
S75	0.01	<.007	<.01	<.02	<.02	<.01	0.9	<.0003	0.001	0.0013	<.003	<.0009	<.001	<.0001	<.1
S76	0.04	0.008	<.01	<.02	0.04	<.01	1.1	<.0003	0.001	0.0008	<.003	<.0009	<.001	<.0001	<.1
S77	0.21	<.007	0.07	<.02	0.34	<.01	4	0.0023	0.001	0.0049	<.003	0.008	<.001	0.0003	n.a.
S78	0.3	<.007	0.02	0.05	0.13	<.01	0.5	0.0005	<.001	0.0023	n.a.	<.0009	<.001	<.0001	<.1
S79	0.02	<.007	0.001	0.58	<.02	0.01	0.9	0.0002	<.001	0.0014	<.003	0.007	0.034	<.0001	<.1
S80	0.07	<.007	<.01	<.02	0.07	<.01	3.8	<.0003	<.001	0.0021	n.a.	<.0009	<.001	<.0001	<.1
S81	0.18	<.007	<.01	<.02	0.03	<.01	5.5	<.0003	<.001	0.0005	<.003	<.0009	0.002	<.0001	<.1
S82	0.29	<.007	0.01	0.1	0.24	<.01	0.6	<.0003	<.001	0.0014	<.003	<.0009	<.001	<.0001	<.1
S83	0.12	0.01	n.a.	0.08	0.13	<.01	0.4	<.0003	0.001	0.0003	n.a.	<.0009	<.001	<.0001	<.1
S84	<.002	<.007	<.001	1.13	<.02	<.01	4	<.0002	<.001	0.0012	<.003	0.002	<.001	<.0001	<.1
S85	0.06	<.007	0.004	<.02	0.04	0.01	0.3	<.0001	0.001	0.0011	<.003	0.001	<.001	<.0001	<.1
S86	0.11	0.01	<.01	<.02	0.22	0.03	1.3	<.0003	<.001	0.0012	<.003	<.0009	<.001	<.0001	<.1
S87	n.a.	<.007	<.01	<.02	0.25	0.125	2	<.0003	0.003	0.001	<.003	<.0009	<.001	<.0001	<.1
S88	0.01	0.01	<.01	11.7	0.02	<.01	0.6	<.0003	<.001	0.0007	<.003	<.0009	0.002	<.0001	<.1
S89	0.19	0.02	0.036	0.47	0.25	0.105	0.7	<.0003	0.001	0.0006	0.006	0.002	<.001	<.0001	<.1
S90	0.07	0.01	0.012	0.02	0.19	0.08	1.2	<.0003	<.001	0.0007	<.003	<.0009	<.001	0.0001	<.1
S91	0.02	0.01	<.001	0.02	<.02	0.04	2.1	<.0002	<.001	<.0003	0.003	<.0009	<.001	<.0001	<.1
S92	0.17	0.02	n.a.	0.05	0.18	0.02	2.2	<.0003	<.001	0.0015	n.a.	<.0009	<.001	<.0001	<.1
S93	0.45	0.007	<.01	<.02	1.25	0.4	4.3	<.0003	<.001	0.0005	0.008	<.0009	<.001	<.0001	0.3
S94	0.34	0.007	0.021	0.02	0.33	0.065	3.5	<.0003	<.001	0.0009	<.003	<.0009	<.001	<.0001	<.1
S95	0.14	0.01	0.011	<.02	0.69	0.01	8.2	<.0003	0.001	0.0014	0.004	<.0009	<.001	<.0001	<.1
S96	0.07	0.01	0.009	<.02	0.08	0.02	2.5	<.0003	<.001	0.0013	<.003	<.0009	<.001	<.0001	<.1
S97	0.08	<.007	<.01	0.02	0.07	0.025	0.8	<.0003	<.001	0.001	<.003	<.0009	<.001	<.0001	<.1
S98	<.002	<.007	0.004	<.02	0.03	0.01	0.3	0.0001	0.001	0.0009	<.003	0.001	<.001	<.0001	<.1
S99	0.18	<.007	0.001	<.02	0.3	0.25	1.4	<.0002	<.001	0.0009	<.003	0.002	<.001	<.0001	<.1
S100	0.32	<.007	0.005	<.02	2.3	0.23	3	<.0001	0.001	0.0016	<.003	0.001	<.001	<.0001	0.5
S101	0.04	0.05	0.002	0.02	0.97	0.11	0.9	0.0003	0.001	0.0015	<.003	0.001	<.001	0.0003	0.6
S102	0.57	0.009	0.02	<.02	0.26	0.32	7.4	<.0003	<.001	<.0003	<.003	<.0009	<.001	<.0001	<.1
S103	0.01	<.007	<.01	1.3	<.02	<.01	0.8	<.0003	<.001	0.0014	<.003	<.0009	<.001	<.0001	<.1
S104	0.27	0.02	0.01	<.02	0.02	<.01	0.6	<.0003	<.001	0.0007	<.003	<.0009	<.001	<.0001	<.1
S105	1.4	<.007	0.006	<.02	7	0.3	16.2	<.0002	0.001	0.0006	0.01	0.001	<.001	<.0001	0.1
S106	<.002	<.007	0.004	<.02	1.1	0.51	10	<.0002	<.001	0.0007	n.a.	0.0009	<.001	n.a.	<.1
S107	0.16	0.01	<.01	0.05	0.25	<.01	0.8	<.0003	<.001	0.0006	<.003	<.0009	<.001	<.0001	<.1
S108	0.02	0.01	<.01	0.6	0.02	<.01	0.5	<.0003	<.001	0.0004	<.003	<.0009	0.003	<.0001	<.1
S109	0.02	<.007	0.006	0.02	<.02	<.01	0.9	<.0003	0.001	0.001	<.003	<.0009	<.001	<.0001	<.1
S110	0.05	<.007	0.01	<.02	0.29	0.07	3.5	<.0003	<.001	0.0017	<.003	<.0009	<.001	<.0001	<.1

Tableau A1.4. (suite)

ID Site	B	Al	Li	NO <sub>3</sub> (en N)	NH <sub>4</sub> (en N)	PO <sub>4</sub> (en P)	COD	Ag	As	Cd	CN	Cr	Cu	Hg	I
S111	0.4	0.03	<.01	<.02	0.42	0.87	5.3	<.0003	<.001	0.0003	<.003	<.0009	<.001	<.0001	<.1
S112	0.02	0.04	0.001	0.86	<.02	<.01	0.5	<.0001	<.001	0.0013	<.003	0.002	<.001	0.0001	<.1
S113	<.002	<.007	0.004	<.02	0.84	0.48	6	<.0002	0.001	0.0009	<.003	0.001	<.001	<.0001	<.1
S114	0.02	0.02	n.a.	0.22	<.02	0.03	0.3	<.0003	0.001	0.0006	n.a.	<.0009	0.002	<.0001	<.1
S115	0.04	<.007	<.001	1.06	<.02	<.01	0.3	<.0003	<.001	0.0007	<.003	0.002	0.004	<.0001	<.1
S116	0.04	<.007	0.007	<.02	0.16	0.125	0.5	0.0001	<.001	0.0008	<.003	<.0009	<.001	<.0001	<.1
S117	0.16	0.01	0.008	<.02	0.06	<.01	0.6	0.0001	<.001	0.0009	<.003	0.002	<.001	<.0001	<.1
S118	0.008	0.02	n.a.	1.6	<.02	<.01	0.4	<.0003	<.001	0.0015	n.a.	<.0009	0.002	<.0001	<.1
S119	0.31	<.007	<.01	0.2	0.7	0.085	5.7	<.0003	<.001	0.002	0.01	<.0009	<.001	<.0001	0.2
S120	0.005	0.007	<.01	n.a.	n.a.	n.a.	3.7	<.0003	0.001	0.0021	<.003	<.0009	<.001	<.0001	<.1
S121	0.009	0.04	<.01	7.3	0.06	0.02	0.6	<.0003	<.001	0.0008	<.003	<.0009	<.001	<.0001	<.1
S122	0.02	0.009	<.01	0.08	<.02	0.065	0.4	<.0003	<.001	0.0015	<.003	<.0009	<.001	<.0001	<.1
S123	0.34	<.007	0.013	<.02	0.7	0.29	3	<.0001	<.001	0.0009	<.003	0.002	<.001	<.0001	<.1
S124	0.79	<.007	0.094	0.04	0.84	1.4	5.3	<.0002	<.001	0.0011	0.005	0.002	<.001	<.0001	<.1
S125	0.03	<.007	0.003	0.18	0.03	<.01	3.3	0.0004	0.001	0.0015	0.006	0.005	<.001	<.0001	<.1
S126	0.05	0.05	0.002	0.33	0.03	0.01	0.8	0.0002	<.001	0.0011	<.003	0.002	0.001	<.0001	<.1
S127	0.06	<.007	0.004	<.02	0.29	0.15	1.6	0.0001	0.002	0.001	<.003	0.002	<.001	<.0001	<.1
S128	0.04	<.007	0.005	<.02	0.14	0.04	0.4	<.0002	0.001	0.0008	<.003	0.003	<.001	0.0001	<.1
S129	<.002	<.007	0.003	<.02	<.02	<.01	1.3	<.0002	<.001	0.0011	<.003	0.003	<.001	<.0001	<.1
S130	0.11	0.02	0.006	<.02	0.38	0.06	1.8	0.0001	<.001	0.0011	<.003	0.005	<.001	n.a.	<.1
S131	0.16	0.08	0.009	<.02	0.11	0.01	3.6	0.0003	<.001	0.0014	<.003	0.002	<.001	0.0001	<.1
S132	0.16	<.007	0.009	<.02	0.1	0.03	3.8	n.a.	n.a.	n.a.	n.a.	0.002	<.001	n.a.	n.a.
S133	0.11	0.01	n.a.	6.1	0.05	<.01	0.8	<.0003	<.001	0.0013	n.a.	<.0009	<.001	<.0001	<.1
S134	0.04	0.02	0.006	<.02	0.06	0.025	<.2	0.0003	0.001	0.0011	<.003	0.002	<.001	<.0001	<.1
S135	0.08	0.03	0.009	<.02	0.07	0.025	0.4	0.0003	0.002	0.001	<.003	0.002	<.001	<.0001	<.1
S136	0.03	<.007	<.01	1.26	0.11	<.01	0.8	<.0003	<.001	0.0016	0.003	<.0009	<.001	<.0001	<.1
S137	0.03	<.007	<.01	<.02	0.07	0.01	2.6	<.0003	<.001	0.0014	<.003	<.0009	<.001	<.0001	<.1
S138	0.01	0.01	0.15	0.54	<.02	0.02	0.6	<.0003	<.001	0.0011	<.003	<.0009	0.005	<.0001	<.1
S139	0.02	0.009	<.01	0.36	0.02	<.01	1.2	<.0003	0.005	0.0018	<.003	<.0009	0.007	<.0001	<.1
S140	0.42	<.007	0.022	<.02	0.1	<.01	0.9	n.a.	n.a.	n.a.	n.a.	0.003	<.001	n.a.	n.a.
S141	0.35	0.009	0.009	<.02	1.13	2	6.7	<.0001	<.001	0.0006	0.003	0.001	<.001	<.0001	<.1
S142	0.01	<.007	0.009	<.02	0.15	<.01	1.3	0.0003	0.001	0.0016	<.003	0.003	<.001	<.0001	<.1
S143	0.07	<.007	0.004	<.02	0.35	0.055	n.a.	0.0001	<.001	0.0006	<.003	0.002	<.001	<.0001	<.1
S144	<.002	<.007	0.003	<.02	0.05	0.17	0.7	<.0001	0.002	0.0012	<.003	0.001	<.001	<.0001	<.1
S145	<.002	<.007	0.004	<.02	0.05	0.03	1.4	n.a.	n.a.	n.a.	n.a.	0.001	<.001	n.a.	n.a.
S146	<.002	<.007	0.004	<.02	0.02	<.01	1.7	n.a.	n.a.	n.a.	n.a.	0.001	<.001	n.a.	n.a.
<b>Échantillons rejetés</b>															
R1	n.a.	n.a.	n.a.	n.a.	n.a.	n.a.	n.a.	n.a.	n.a.	n.a.	n.a.	n.a.	n.a.	n.a.	n.a.
R2	n.a.	n.a.	n.a.	<.02	0.45	0.15	1.3	n.a.	n.a.	n.a.	n.a.	n.a.	n.a.	n.a.	n.a.
R3	n.a.	n.a.	n.a.	<.02	0.21	0.16	1.3	n.a.	n.a.	n.a.	n.a.	n.a.	n.a.	n.a.	n.a.
R4	0.03	0.008	0.014	0.02	0.1	0.01	1.4	<.0003	<.001	0.0012	0.004	<.0009	<.001	<.0001	<.1
SAP	n.a.	n.a.	n.a.	0.02	1.27	0.87	4.3	n.a.	<.001	n.a.	0.009	n.a.	n.a.	<.0001	<.1
R5	0.04	0.01	0.019	0.71	0.08	<.01	7	<.0003	<.001	0.0018	0.017	<.0009	0.001	<.0001	<.1
R6	0.15	<.007	0.017	0.02	n.a.	0.105	0.8	<.0003	<.001	0.0008	<.003	<.0009	<.001	<.0001	0.2
<b>Duplicata</b>															
D1	0.54	0.03	0.135	0.03	0.9	0.155	4.9	0.0002	<.001	0.0009	<.003	0.001	<.001	<.0001	<.1
D2	0.17	0.04	0.007	<.02	0.17	0.065	2.2	0.0001	<.001	0.001	0.003	0.002	<.001	<.0001	<.1
D3	0.33	0.02	0.002	0.02	0.3	0.2	0.7	0.0002	<.001	0.0007	<.003	0.0009	<.001	<.0001	<.1
D4	0.13	0.02	0.011	<.02	0.03	<.01	0.9	0.0001	0.001	0.0016	<.003	0.003	<.001	<.0001	<.1
D5	0.08	<.007	0.005	0.13	0.06	<.01	1.8	0.0004	<.001	0.0016	<.003	0.002	<.001	<.0001	<.1
D6	n.a.	n.a.	n.a.	n.a.	n.a.	n.a.	n.a.	n.a.	n.a.	n.a.	n.a.	n.a.	n.a.	n.a.	n.a.
D7	0.19	0.04	0.07	<.02	0.3	<.01	4	0.0024	0.001	0.0051	<.003	0.007	<.001	0.0001	n.a.
D8	0.06	<.007	0.005	<.02	0.04	0.02	0.4	0.0001	0.001	0.0012	<.003	0.001	<.001	<.0001	<.1
D9	0.06	0.009	0.008	<.02	0.07	0.015	2.5	<.0003	<.001	0.001	<.003	<.0009	<.001	<.0001	<.1
D10	<.002	0.02	0.005	<.02	0.13	0.04	1.3	<.0002	0.001	0.0007	<.003	0.002	<.001	0.0001	<.1

Tableau A1.5. Base de données géochimiques – Paramètres chimiques (#3), calculés et modélisés

ID Site	Ni	Pb	Se	Zn	U	MDT <sup>t</sup>	Dureté Tot. <sup>t</sup> (en CaCO <sub>3</sub> )	TAS <sup>u</sup>	Spéciation <sup>v</sup> HCO <sub>3</sub> <sup>-</sup> /CO <sub>3</sub> <sup>2-</sup>	Log pCO <sub>2</sub> <sup>v</sup>	Indice de Saturation <sup>v</sup> Cal. Dol. Gyp.
S1	0.002	<.004	<.001	0.078	<.005	603.9	350.2	0.60	367.5 / 0.303	-1.84	0.03 / -0.20 / -2.21
S2	0.002	<.004	<.001	<.005	<.005	585.0	350.0	0.49	320.3 / 0.313	-1.98	0.02 / -0.18 / -2.05
S3	0.003	<.004	<.001	<.005	<.005	247.3	226.8	0.11	214.3 / 0.286	-2.25	-0.11 / -0.44 / -1.97
S4	0.004	<.004	<.001	1.2	0.012	464.2	328.1	1.18	338.2 / 0.252	-1.83	-0.03 / -0.47 / -1.84
S5	0.004	n.a.	<.001	<.005	n.a.	445.3	400.4	0.22	414.8 / 0.345	-1.79	0.07 / -0.02 / -1.68
S6	0.005	n.a.	<.001	<.005	n.a.	418.8	390.6	0.21	436.5 / 0.631	-1.97	0.35 / 0.54 / -1.71
S7	0.008	n.a.	<.001	<.005	n.a.	427.6	294.8	1.17	318.9 / 0.366	-2.03	0.03 / -0.23 / -1.51
S8	0.007	n.a.	<.001	<.005	n.a.	392.2	344.0	0.17	368.5 / 0.218	-1.67	-0.04 / -0.52 / -1.79
S9	<.0008	<.004	n.a.	<.005	n.a.	352.0	218.5	0.09	238.3 / 0.383	-2.31	-0.01 / -0.21 / -2.51
S10	0.002	<.004	<.001	0.01	<.005	369.4	349.2	0.16	461.3 / 0.614	-1.94	0.31 / 0.45 / -2.52
S11	<.0008	<.004	<.001	0.019	<.005	149.8	126.2	0.50	179.8 / 0.204	-2.29	-0.48 / -1.12 / -2.87
S12	0.001	<.004	<.001	0.008	<.005	180.6	157.3	0.26	179.3 / 0.277	-2.44	-0.26 / -0.73 / -2.46
S13	<.0008	<.004	<.001	0.019	<.005	267.8	199.4	1.08	274.6 / 0.364	-2.19	-0.11 / -0.39 / -2.79
S14	<.0008	<.004	<.001	0.096	<.005	400.9	238.4	2.08	295.0 / 0.962	-2.53	0.40 / 0.53 / -2.74
S15	<.0008	<.004	<.001	0.096	<.005	355.5	238.4	0.17	239.1 / 0.127	-1.85	-0.43 / -1.15 / -2.45
S16	0.002	<.004	<.001	0.14	<.005	1983.1	587.1	8.71	242.7 / 0.525	-2.23	0.21 / 0.50 / -1.72
S17	<.0008	<.004	<.001	<.005	0.006	306.9	249.0	0.66	295.4 / 0.908	-2.49	0.36 / 0.57 / -2.17
S18	<.0008	<.004	<.001	<.005	0.01	410.7	174.5	3.29	294.7 / 1.526	-2.73	0.35 / 0.65 / -2.70
S19	<.0008	<.004	n.a.	<.005	n.a.	509.2	275.6	2.88	427.9 / 0.473	-1.87	0.06 / -0.08 / -1.78
S20	0.0008	<.004	<.001	<.005	<.005	226.8	17.1	18.94	426.4 / 12.270	-3.32	0.10 / 0.36 / -4.73
S21	<.0008	<.004	<.001	<.005	0.01	372.9	165.2	3.38	349.0 / 1.344	-2.53	0.19 / 0.48 / -3.06
S22	<.0008	<.004	<.001	<.005	<.005	296.4	23.4	19.80	509.7 / 13.014	-3.17	0.20 / 0.61 / -3.66
S23	<.0008	<.004	<.001	0.02	<.005	507.3	14.7	34.00	489.3 / 7.711	-2.99	-0.03 / -0.23 / -5.26
S24	<.0008	<.004	<.001	<.005	<.005	367.8	218.2	2.27	366.5 / 1.171	-2.42	0.29 / 0.58 / -2.05
S25	<.005	<.004	<.001	<.005	<.005	545.3	211.6	5.38	454.6 / 3.057	-2.65	0.66 / 1.30 / -3.91
S26	<.0008	<.004	0.001	0.04	<.005	1357.0	98.5	24.54	449.3 / 0.893	-2.09	-0.38 / -0.72 / -2.36
S27	<.0008	<.004	n.a.	<.005	n.a.	351.2	177.6	3.13	362.3 / 1.927	-2.64	0.33 / 0.83 / -2.51
S28	<.0008	<.004	<.001	<.005	0.006	436.2	84.9	9.91	579.5 / 2.321	-2.33	-0.04 / 0.18 / -3.50
S29	<.0008	<.004	<.001	<.005	<.005	296.9	72.3	9.72	552.8 / 9.062	-2.92	0.34 / 1.21 / -4.97
S30	<.0008	<.004	<.001	0.047	0.006	565.8	395.0	1.18	426.8 / 0.343	-1.75	0.09 / -0.10 / -1.57
S31	0.003	<.004	n.a.	<.005	n.a.	466.9	370.8	0.42	332.3 / 0.288	-1.88	-0.02 / -0.22 / -1.52
S32	0.0009	<.004	<.001	<.005	<.005	224.0	177.8	0.56	284.9 / 0.753	-2.47	0.15 / 0.19 / -3.81
S33	<.0008	<.004	n.a.	<.005	n.a.	445.4	348.4	0.33	261.0 / 0.178	-1.88	-0.24 / -0.67 / -1.49
S34	0.001	<.004	<.001	<.005	0.006	1069.2	500.7	2.72	405.5 / 1.471	-2.32	0.75 / 1.40 / -1.67
S35	0.003	<.004	<.001	0.016	<.005	340.4	299.5	0.38	333.1 / 0.265	-1.86	-0.11 / -0.38 / -1.96
S36	0.005	<.004	<.001	0.3	n.a.	804.4	579.7	1.03	494.9 / 0.152	-1.24	-0.15 / -0.59 / -1.24
S37	0.009	<.004	<.001	0.012	n.a.	917.0	509.5	1.10	473.0 / 0.139	-1.22	-0.18 / -0.68 / -1.43
S38	<.0008	<.004	<.001	0.081	0.007	634.1	422.9	0.10	390.9 / 0.187	-1.54	-0.14 / -0.45 / -1.67
S39	0.0009	<.004	<.001	0.059	<.005	336.8	277.1	0.65	309.5 / 0.282	-1.92	-0.13 / -0.35 / -1.95
S40	0.001	<.004	<.001	0.008	<.005	316.6	238.3	1.18	310.0 / 0.369	-2.05	-0.05 / -0.26 / -2.06
S41	<.0008	<.004	<.001	<.005	<.005	727.0	122.3	9.44	311.8 / 0.299	-1.91	-0.61 / -1.17 / -2.46
S42	0.001	n.a.	n.a.	<.005	n.a.	717.7	172.1	7.96	321.3 / 0.760	-2.35	-0.23 / -0.20 / -3.01
S43	<.0008	n.a.	n.a.	<.005	n.a.	306.8	146.9	2.94	295.8 / 1.516	-2.73	0.07 / 0.46 / -3.00
S44	0.001	n.a.	n.a.	<.005	n.a.	276.2	246.4	0.41	332.5 / 0.627	-2.23	0.15 / 0.26 / -2.40
S45	0.003	n.a.	<.001	<.005	n.a.	3561.8	271.2	33.28	276.8 / 1.637	-2.69	-0.20 / 0.23 / -3.35
S46	<.0008	<.004	<.001	0.16	0.006	546.6	84.3	11.37	348.7 / 0.340	-1.92	-0.73 / -1.38 / -2.94
S47	0.002	n.a.	n.a.	<.005	n.a.	225.6	138.9	2.25	299.9 / 0.331	-2.07	-0.37 / -0.77 / -2.97
S48	<.0008	<.004	<.001	<.005	<.005	205.0	203.6	0.05	252.1 / 0.090	-1.66	-0.64 / -1.54 / -3.37
S49	0.003	<.004	<.001	0.076	<.005	382.2	245.1	0.05	275.3 / 0.083	-1.55	-0.61 / -1.50 / -2.64
S50	<.0008	<.004	<.001	<.005	0.007	259.1	149.4	0.22	167.7 / 0.166	-2.23	-0.46 / -1.14 / -2.82
S51	<.0008	<.004	<.001	0.006	<.005	1332.6	185.0	14.71	118.8 / 0.095	-2.25	-1.07 / -2.02 / -2.06
S52	0.002	<.004	<.001	<.005	<.005	323.2	268.8	0.50	286.0 / 0.182	-1.82	-0.27 / -0.79 / -1.89
S53	<.0008	<.004	<.001	<.005	0.007	595.5	58.1	13.70	179.1 / 4.898	-3.63	0.38 / 0.69 / -3.29
S54	<.0008	<.004	<.001	<.005	<.005	968.0	233.9	9.10	439.9 / 0.879	-2.10	0.06 / 0.13 / -1.82
S55	0.002	n.a.	n.a.	0.024	n.a.	2239.2	348.2	16.08	364.3 / 3.132	-2.79	0.92 / 1.32 / -2.35

Tableau A1.5. (suite)

ID Site	Ni	Pb	Se	Zn	U	MDT <sup>t</sup>	Dureté Tot. <sup>t</sup> (en CaCO <sub>3</sub> )	TAS <sup>u</sup>	Spéciation <sup>v</sup>		Log pCO <sub>2</sub> <sup>v</sup>	Indice de Saturation <sup>v</sup>		
									HCO <sub>3</sub> <sup>-</sup>	CO <sub>3</sub> <sup>2-</sup>		Cal.	Dol.	Gyp.
S56	<.0008	<.004	<.001	<.005	<.005	387.7	122.4	3.66	227.6	0.271	-2.21	-0.49	-1.09	-3.44
S57	0.0009	<.004	n.a.	<.005	n.a.	236.9	158.8	0.76	178.7	0.449	-2.64	0.07	-0.45	-2.30
S58	0.0008	<.004	n.a.	0.013	n.a.	137.7	104.8	0.52	143.0	0.547	-2.93	-0.06	-0.44	-2.66
S59	0.002	<.004	<.001	0.022	<.005	425.9	279.0	0.19	274.4	0.120	-1.63	-0.42	-1.01	-2.19
S60	0.002	<.004	<.001	0.04	<.005	481.0	205.9	3.64	274.9	0.257	-2.00	-0.36	-0.77	-2.43
S61	0.0009	<.004	n.a.	0.035	n.a.	537.2	145.6	5.41	154.0	0.661	-2.91	-0.04	-0.25	-2.20
S62	0.002	<.004	n.a.	0.017	n.a.	185.7	74.6	1.36	40.0	0.004	-1.88	-2.32	-5.06	-2.43
S63	<.0008	<.004	n.a.	<.005	n.a.	299.8	159.6	1.86	202.1	0.657	-2.69	0.01	-0.06	-2.25
S64	<.0008	<.004	<.001	0.038	<.005	173.2	83.6	2.09	142.5	0.724	-3.07	-0.09	-0.41	-3.52
S65	0.005	<.004	<.001	0.015	<.005	320.6	141.2	2.82	178.3	0.629	-2.79	0.02	-0.30	-1.90
S66	0.003	<.004	<.001	0.09	<.005	312.0	258.4	0.34	285.5	0.333	-2.09	0.01	-0.30	-1.98
S67	<.0008	<.004	<.001	<.005	<.005	1131.4	138.6	16.62	492.7	3.561	-2.60	0.16	0.75	-3.23
S68	<.0008	<.004	<.001	<.005	0.007	1890.5	1395.1	0.24	181.3	0.151	-2.08	0.16	-0.57	-0.13
S69	<.0008	<.004	<.001	<.005	<.005	526.3	279.7	0.70	243.0	0.437	-2.36	0.08	-0.04	-2.01
S70	<.0008	<.004	<.001	0.007	<.005	195.1	106.1	1.73	198.8	1.782	-3.16	0.26	0.51	-3.04
S71	<.0008	<.004	<.001	<.005	<.005	376.1	176.9	2.81	262.6	0.501	-2.33	-0.12	-0.28	-2.07
S72	0.005	<.004	<.001	<.005	0.005	909.5	406.3	3.88	344.4	0.155	-1.57	-0.36	-0.89	-1.34
S73	0.001	<.004	<.001	0.05	<.005	556.6	480.4	0.44	426.8	0.104	-1.22	-0.33	-0.98	-1.36
S74	<.0008	<.004	<.001	<.005	<.005	613.6	384.8	0.12	354.7	0.344	-1.87	0.10	0.04	-1.74
S75	<.0008	<.004	<.001	0.032	<.005	374.1	346.1	0.12	356.6	0.272	-1.81	-0.01	-0.29	-1.75
S76	<.0008	<.004	<.001	<.005	0.008	465.2	356.8	0.78	354.9	0.610	-2.17	0.31	0.37	-1.63
S77	0.005	<.004	<.001	0.051	<.005	11337.1	3575.3	22.55	116.2	0.112	-2.21	-0.06	-0.28	-0.84
S78	<.0008	<.004	<.001	<.005	0.006	1067.4	680.3	1.50	117.1	0.153	-2.49	-0.07	-0.78	-0.57
S79	0.004	<.004	<.001	0.006	<.005	296.1	261.6	0.20	286.7	0.165	-1.80	-0.30	-0.90	-2.14
S80	<.0008	<.004	<.001	<.005	0.005	310.0	225.9	0.49	268.4	0.819	-2.54	0.42	0.34	-2.30
S81	n.a.	<.004	<.001	0.005	<.005	214.2	0.7	80.10	327.2	0.446	-2.10	-2.35	-5.28	-4.38
S82	n.a.	<.004	<.001	<.005	<.005	267.7	212.6	0.30	249.5	0.576	-2.44	0.11	0.10	-2.38
S83	<.0008	<.004	n.a.	<.005	n.a.	222.2	87.8	3.39	209.3	2.646	-3.27	0.28	0.65	-2.77
S84	0.002	<.004	<.001	0.011	<.006	319.6	309.5	0.06	358.2	0.126	-1.50	-0.40	-1.03	-2.09
S85	0.001	<.004	<.001	0.017	<.005	242.1	176.2	1.25	274.6	0.485	-2.29	-0.05	-0.22	-2.41
S86	<.0008	<.004	<.001	<.005	0.007	230.2	160.4	1.48	269.3	2.029	-2.95	0.46	0.91	-2.44
S87	<.0008	<.004	<.001	<.005	0.006	287.0	230.8	0.74	307.2	0.973	-2.48	0.36	0.59	-2.29
S88	<.0008	<.004	<.001	0.005	0.005	470.2	355.0	0.72	404.6	0.209	-1.58	-0.17	-0.53	-1.94
S89	<.0008	<.004	<.001	<.005	<.005	956.7	188.1	9.20	219.4	2.257	-3.13	0.23	0.75	-2.40
S90	<.0008	<.004	<.001	<.005	0.008	320.8	228.3	1.15	320.2	0.685	-2.31	0.19	0.24	-2.59
S91	<.0008	<.004	<.001	0.013	<.005	176.2	3.7	29.58	267.0	0.190	-1.93	-1.88	-4.76	-3.75
S92	<.0008	<.004	n.a.	<.005	n.a.	773.4	328.5	2.64	283.7	0.502	-2.25	0.14	0.13	-1.86
S93	<.0008	<.004	<.001	<.005	<.005	942.4	89.9	18.35	460.0	11.628	-3.19	0.59	1.48	-4.06
S94	<.0008	<.004	<.001	<.005	0.008	296.0	232.3	0.80	346.4	0.350	-1.96	-0.16	-0.36	-2.23
S95	0.001	<.004	<.001	<.005	<.005	1164.8	525.9	3.22	374.8	0.181	-1.50	-0.10	-0.45	-1.54
S96	0.001	<.004	<.001	<.005	0.012	889.0	476.0	1.36	365.6	0.266	-1.73	0.03	-0.16	-1.45
S97	<.0008	<.004	<.001	<.005	<.005	187.0	70.5	3.26	200.3	1.758	-3.11	0.13	0.20	-2.76
S98	0.002	<.004	<.001	<.005	<.005	253.1	157.0	2.05	308.2	0.989	-2.49	0.09	0.26	-2.42
S99	0.002	<.004	<.001	0.02	<.005	167.6	20.9	11.41	284.9	2.116	-2.88	-0.38	-0.72	-3.72
S100	<.0008	<.004	<.001	0.023	<.005	2735.8	333.9	23.81	453.1	2.028	-2.36	0.07	0.71	-3.66
S101	0.001	<.004	<.001	0.13	<.005	2063.5	233.3	19.65	268.4	1.028	-2.45	0.17	0.32	-3.98
S102	<.0008	<.004	<.001	<.005	<.005	255.6	8.8	33.82	514.0	40.353	-3.65	0.20	0.63	-5.75
S103	<.0008	<.004	<.001	<.005	<.005	303.0	283.8	0.18	321.6	0.277	-1.90	-0.09	-0.33	-2.30
S104	<.0008	<.004	<.001	<.005	0.011	274.2	151.8	2.37	247.2	1.409	-2.84	0.51	0.48	-2.76
S105	0.001	<.004	<.001	0.017	0.006	1705.3	82.7	39.22	922.0	17.669	-2.71	-0.20	0.86	-5.23
S106	<.0008	<.004	<.001	<.005	<.005	174.4	141.0	0.54	237.8	0.550	-2.49	-0.06	-0.23	-
S107	<.0008	<.004	<.001	<.005	<.005	409.7	138.1	4.44	228.3	0.197	-2.05	-0.60	-1.29	-2.44
S108	<.0008	<.004	<.001	<.005	0.007	190.2	131.7	0.61	166.2	0.685	-2.87	0.12	-0.07	-2.59
S109	<.0008	<.004	<.001	<.005	0.008	284.5	268.7	0.10	319.2	0.880	-2.44	0.32	0.58	-2.15
S110	<.0008	<.004	<.001	0.008	<.005	704.6	361.0	0.96	354.8	0.257	-1.77	-0.03	-0.35	-1.87

Tableau A1.5. (suite)

ID Site	Ni	Pb	Se	Zn	U	MDT <sup>t</sup>	Dureté Tot. <sup>t</sup> (en CaCO <sub>3</sub> )	TAS <sup>u</sup>	Spéciation <sup>v</sup> HCO <sub>3</sub> <sup>-</sup> CO <sub>3</sub> <sup>2-</sup>	Log pCO <sub>2</sub> <sup>v</sup>	Indice de Saturation <sup>v</sup> Cal. Dol. Gyp.
S111	<.0008	<.004	<.001	<.005	<.005	161.0	58.8	4.25	290.5 3.704	-3.15	0.19 0.56 -4.42
S112	<.0008	<.004	<.001	0.1	<.005	207.7	179.2	0.21	191.9 0.106	-1.97	-0.49 -1.62 -2.27
S113	<.0008	<.004	<.001	<.005	<.005	174.1	144.3	0.51	223.8 1.053	-2.84	0.24 0.34 -
S114	<.0008	<.004	n.a.	<.005	n.a.	215.1	122.2	0.28	114.0 0.438	-3.03	-0.09 -0.52 -2.40
S115	<.0008	<.004	<.001	<.005	<.005	226.7	145.4	0.08	156.5 0.071	-1.97	-0.81 -1.96 -3.04
S116	<.0008	<.004	<.001	0.011	<.005	206.5	147.2	1.33	238.6 0.527	-2.39	-0.07 -0.17 -2.61
S117	0.002	<.004	0.009	0.02	<.005	309.8	87.4	4.33	142.7 0.686	-3.02	-0.15 -0.60 -2.17
S118	0.022	<.004	n.a.	0.022	n.a.	463.2	221.9	1.23	215.4 0.113	-1.86	-0.55 -1.33 -2.35
S119	<.0008	<.004	<.001	<.005	<.005	1725.4	196.4	17.07	342.7 1.103	-2.37	-0.17 0.02 -2.94
S120	<.0008	<.004	<.001	<.005	<.005	236.5	164.0	0.68	200.7 0.078	-1.76	-0.76 -1.82 -3.09
S121	<.0008	<.004	<.001	<.005	<.005	293.3	184.2	0.24	179.7 0.099	-1.99	-0.63 -1.52 -2.80
S122	<.0008	<.004	<.001	<.005	<.005	226.3	202.1	0.28	250.1 0.455	-2.35	0.09 -0.17 -2.33
S123	<.0008	<.004	<.001	0.006	<.005	383.1	184.3	2.76	309.5 0.682	-2.34	-0.02 -0.02 -2.33
S124	0.021	<.004	0.001	<.005	<.005	995.4	104.8	17.76	532.7 3.556	-2.57	0.29 0.62 -3.07
S125	0.009	<.004	<.001	0.007	0.011	1049.9	413.2	5.35	390.8 0.308	-1.74	-0.01 -0.29 -1.50
S126	0.002	<.004	<.001	0.13	<.005	479.1	227.7	3.75	379.7 0.805	-2.17	0.28 0.32 -2.33
S127	0.001	<.004	<.001	<.005	<.005	249.0	214.2	0.47	286.0 0.415	-2.21	-0.04 -0.22 -2.38
S128	0.002	<.004	<.001	<.005	0.005	351.9	136.0	3.51	249.1 1.140	-2.77	0.11 0.20 -2.49
S129	0.0009	<.004	<.001	<.005	<.005	281.5	254.9	0.20	286.6 0.216	-1.92	-0.23 -0.68 -2.05
S130	0.003	<.004	<.001	0.35	<.005	351.0	195.3	2.21	296.8 0.689	-2.39	0.14 0.10 -3.30
S131	0.001	<.004	<.001	0.16	<.005	387.4	276.3	1.05	309.4 0.244	-1.90	-0.19 -0.57 -1.99
S132	0.002	n.a.	n.a.	<.005	n.a.	351.8	252.3	0.96	298.6 0.193	-1.81	-0.34 -0.79 -2.08
S133	0.0008	<.004	n.a.	<.005	n.a.	356.9	220.0	1.55	284.8 0.755	-2.44	0.17 0.27 -2.18
S134	0.002	<.004	<.001	0.064	<.005	430.5	260.6	0.34	285.7 0.264	-1.99	-0.14 -0.43 -2.34
S135	0.006	<.004	<.001	0.064	<.005	437.8	249.8	1.87	297.1 0.389	-2.13	-0.07 -0.24 -2.33
S136	<.0008	<.004	<.001	<.005	0.01	715.6	410.5	0.60	390.3 0.405	-1.88	0.18 0.16 -1.79
S137	<.0008	<.004	<.001	<.005	<.005	326.3	279.7	0.33	323.1 0.026	-0.89	-1.12 -2.43 -2.01
S138	<.0008	<.004	<.001	<.005	0.006	248.1	229.2	0.21	261.7 0.495	-2.33	0.10 0.04 -2.25
S139	0.0008	<.004	<.001	<.005	0.008	459.6	395.7	0.44	438.5 0.391	-1.78	0.17 0.09 -1.85
S140	0.005	n.a.	n.a.	0.026	n.a.	428.3	158.3	4.84	215.4 0.448	-2.45	-0.15 -0.68 -1.49
S141	0.005	<.004	<.001	<.005	<.005	610.1	71.5	14.40	468.1 3.953	-2.73	0.08 0.45 -3.73
S142	0.001	<.004	<.001	<.005	0.006	918.1	504.8	1.72	342.2 0.178	-1.65	-0.15 -0.50 -1.85
S143	0.001	<.004	<.001	<.005	<.005	222.2	163.7	1.09	238.6 0.541	-2.49	0.10 -0.23 -2.50
S144	0.001	<.004	<.001	<.005	0.005	264.1	243.8	0.16	285.7 0.279	-1.99	-0.25 -0.42 -2.32
S145	<.0008	n.a.	n.a.	<.005	n.a.	348.1	315.1	0.15	342.2 0.485	-1.96	0.16 0.36 -2.02
S146	0.002	n.a.	n.a.	<.005	n.a.	455.1	422.9	0.31	506.7 0.572	-1.69	0.35 0.64 -1.89
<b>Échantillons rejetés</b>											
R1	n.a.	n.a.	n.a.	n.a.	n.a.	--	--	--	--	--	--
R2	n.a.	n.a.	n.a.	n.a.	n.a.	103.4	--	--	231.6	--	--
R3	n.a.	n.a.	n.a.	n.a.	n.a.	27.7	--	--	292.6	--	--
R4	<.0008	<.004	<.001	0.043	0.007	1321.8	935.6	2.133	316.9	--	--
SAP	n.a.	n.a.	0.001	n.a.	<.005	535.6	--	--	438.8	--	--
R5	0.003	<.004	<.001	<.005	0.012	3030.1	877.7	9.543	304.8	--	--
R6	<.0008	<.004	<.001	<.005	0.012	575.0	168.7	8.372	304.8	--	--
<b>Duplicata</b>											
D1	<.0008	<.004	0.001	0.053	<.005	1365.3	101.2	24.65	463.2	--	--
D2	<.0008	<.004	<.001	0.01	<.005	299.6	221.7	1.256	304.8	--	--
D3	0.0009	<.004	<.001	0.18	0.007	536.7	84.4	10.89	341.3	--	--
D4	0.002	<.004	<.001	0.079	<.005	302.8	249.3	0.347	292.6	--	--
D5	0.002	<.004	<.001	0.013	<.005	458.1	380.0	0.435	438.8	--	--
D6	n.a.	n.a.	n.a.	n.a.	n.a.	--	--	--	--	--	--
D7	0.006	<.004	<.001	0.26	<.005	11241.3	3509.3	22.03	92.6	--	--
D8	0.001	<.004	<.001	<.005	<.005	231.2	167.1	1.279	280.4	--	--
D9	<.0008	<.004	<.001	<.005	0.011	901.0	476.0	1.356	377.9	--	--
D10	<.0008	<.004	<.001	0.042	<.005	356.7	138.9	3.543	256	--	--

Tableau A1.6. Base de données géochimiques – Paramètres isotopiques

ID Site	$\delta^2\text{H}$ (‰)	$\delta^{18}\text{O}$ (‰)	$\delta^{13}\text{C}_{\text{CDP}}$ (‰)	$^{87}\text{Sr}/^{86}\text{Sr}$	$^{3}\text{H}^{\text{w}}$ (TU)	$^{3}\text{H}^{\text{x}}$ (TU)	$^{14}\text{C}^{\text{y}}$ (pMC)
S1	-69	-10.6	n.a.	n.a.	n.a.	n.a.	n.a.
S2	-70	-10.7	n.a.	n.a.	n.a.	n.a.	n.a.
S3	-56	-8.5	n.a.	n.a.	n.a.	n.a.	n.a.
S4	-77	-11.6	n.a.	n.a.	n.a.	n.a.	n.a.
S5	-71	-10.9	n.a.	n.a.	n.a.	n.a.	n.a.
S6	-68	-10.4	n.a.	n.a.	n.a.	n.a.	n.a.
S7	-77	-11.3	n.a.	0.708941	n.a.	n.a.	n.a.
S8	-78	-11.6	n.a.	n.a.	n.a.	n.a.	n.a.
S9	-79	-11.7	n.a.	n.a.	n.a.	n.a.	n.a.
S10	-75	-11.0	-15.7	n.a.	n.a.	n.a.	n.a.
S11	-79	-11.5	-14.6	n.a.	n.a.	n.a.	n.a.
S12	-77	-11.5	-14.7	n.a.	n.a.	n.a.	n.a.
S13	-80	-11.8	-14.3	n.a.	n.a.	n.a.	n.a.
S14	-81	-11.7	-15.8	n.a.	n.a.	n.a.	n.a.
S15	-81	-11.7	-13.0	n.a.	n.a.	n.a.	n.a.
S16	-76	-11.2	-15.1	n.a.	n.a.	n.a.	n.a.
S17	-74	-11.2	n.a.	n.a.	n.a.	n.a.	n.a.
S18	-79	-11.6	-15.3	n.a.	n.a.	n.a.	n.a.
S19	-72	-10.9	n.a.	n.a.	n.a.	n.a.	n.a.
S20	-65	-10.0	-13.3	n.a.	n.a.	n.a.	n.a.
S21	-72	-11.2	-12.3	n.a.	n.a.	n.a.	n.a.
S22	-73	-10.9	-12.4	n.a.	n.a.	n.a.	n.a.
S23	-73	-10.9	-9.3	n.a.	n.a.	n.a.	n.a.
S24	-71	-10.7	-15.0	n.a.	n.a.	n.a.	n.a.
S25	-73	-11.0	-14.8	n.a.	n.a.	n.a.	n.a.
S26	-77	-11.3	-14.8	n.a.	n.a.	n.a.	n.a.
S27	-69	-10.8	n.a.	0.709332	n.a.	n.a.	n.a.
S28	-72	-11.0	n.a.	n.a.	n.a.	n.a.	n.a.
S29	-70	-10.4	-4.7	n.a.	n.a.	n.a.	n.a.
S30	-74	-10.8	-14.1	n.a.	n.a.	n.a.	n.a.
S31	-76	-11.6	n.a.	n.a.	n.a.	n.a.	n.a.
S32	-72	-10.5	-18.9	n.a.	n.a.	n.a.	n.a.
S33	-72	-11.2	n.a.	n.a.	n.a.	n.a.	n.a.
S34	-77	-11.1	-13.4	0.708604	9.1 ± 0.8	10.4	55.7 ± 0.4
S35	-74	-11.0	-14.3	n.a.	n.a.	n.a.	n.a.
S36	-83	-12.0	-14.4	0.709147	n.a.	n.a.	n.a.
S37	-77	-11.5	n.a.	n.a.	n.a.	n.a.	n.a.
S38	-81	-11.9	-12.6	0.708201	n.a.	n.a.	n.a.
S39	-76	-11.3	-12.7	n.a.	n.a.	n.a.	n.a.
S40	-74	-11.1	-14.4	n.a.	n.a.	n.a.	n.a.
S41	-74	-11.5	-14.5	0.710220	n.a.	n.a.	n.a.
S42	-72	-11.0	-16.3	n.a.	n.a.	n.a.	n.a.
S43	-73	-11.1	-15.2	n.a.	n.a.	n.a.	n.a.
S44	-72	-10.7	-19.3	n.a.	n.a.	n.a.	n.a.
S45	-75	-10.6	-18.2	n.a.	n.a.	n.a.	n.a.
S46	-73	-11.0	-16.1	0.709295	n.a.	n.a.	n.a.
S47	-80	-11.4	-17.0	n.a.	n.a.	n.a.	n.a.
S48	-78	-12.2	n.a.	n.a.	n.a.	n.a.	n.a.
S49	-79	-11.7	n.a.	n.a.	n.a.	n.a.	n.a.
S50	-75	-11.8	n.a.	n.a.	n.a.	n.a.	n.a.
S51	-73	-11.3	-13.2	0.708860	n.a.	n.a.	n.a.
S52	-75	-11.6	-15.8	n.a.	n.a.	n.a.	n.a.
S53	-97	-14.0	n.a.	n.a.	n.a.	n.a.	n.a.
S54	-76	-11.7	n.a.	n.a.	n.a.	n.a.	n.a.
S55	-76	-11.2	-10.3	0.710750	n.a.	n.a.	n.a.

Tableau A1.6. (suite)

ID Site	$\delta^{2\text{H}}$ (‰)	$\delta^{18\text{O}}$ (‰)	$\delta^{13\text{C}_{\text{CID}}}$ (‰)	$^{87}\text{Sr}/^{86}\text{Sr}$	$^{3\text{H}}^{\text{w}}$ (TU)	$^{3\text{H}}^{\text{x}}$ (TU)	$^{14}\text{C}^{\text{y}}$ (pMC)
S56	-72	-11.5	n.a.	n.a.	n.a.	n.a.	n.a.
S57	-73	-11.2	n.a.	n.a.	n.a.	n.a.	n.a.
S58	-79	-11.5	n.a.	n.a.	n.a.	n.a.	n.a.
S59	-82	-12.0	-14.5	n.a.	n.a.	n.a.	n.a.
S60	-81	-11.6	-13.7	n.a.	n.a.	n.a.	n.a.
S61	-77	-11.6	n.a.	n.a.	n.a.	n.a.	n.a.
S62	-77	-11.0	n.a.	n.a.	n.a.	n.a.	n.a.
S63	-77	-11.6	n.a.	n.a.	n.a.	n.a.	n.a.
S64	-75	-11.1	-15.6	n.a.	n.a.	n.a.	n.a.
S65	-79	-11.7	-14.2	n.a.	n.a.	n.a.	n.a.
S66	-76	-10.9	-13.7	n.a.	n.a.	n.a.	n.a.
S67	-80	-11.2	-20.2	n.a.	n.a.	n.a.	n.a.
S68	-76	-12.2	-12.2	0.708883	n.a.	n.a.	n.a.
S69	-72	-11.5	-15.4	0.708878	n.a.	n.a.	n.a.
S70	-75	-11.3	-14.4	n.a.	n.a.	n.a.	n.a.
S71	-76	-11.6	-13.5	n.a.	n.a.	n.a.	n.a.
S72	-77	-11.4	-11.7	0.709003	$15.4 \pm 1.2$	16.6	$68.8 \pm 0.5$
S73	-76	-11.1	-13.3	n.a.	n.a.	n.a.	n.a.
S74	-77	-11.1	-13.9	n.a.	n.a.	n.a.	n.a.
S75	-78	-11.7	-13.0	n.a.	n.a.	n.a.	n.a.
S76	-73	-11.1	-13.9	n.a.	n.a.	n.a.	n.a.
S77	-79	-11.0	-17.4	0.707350	n.a.	n.a.	n.a.
S78	-75	-11.4	-9.4	n.a.	n.a.	n.a.	n.a.
S79	-79	-11.2	-15.5	n.a.	n.a.	n.a.	n.a.
S80	-75	-11.0	-17.2	n.a.	n.a.	n.a.	n.a.
S81	-72	-10.5	-15.9	n.a.	n.a.	n.a.	n.a.
S82	-79	-11.3	-15.1	0.710493	n.a.	n.a.	n.a.
S83	-81	-11.8	n.a.	n.a.	n.a.	n.a.	n.a.
S84	-80	-11.9	-14.6	n.a.	n.a.	n.a.	n.a.
S85	-82	-11.9	-13.2	0.706580	n.a.	n.a.	n.a.
S86	-83	-11.5	-14.6	0.708368	$11.7 \pm 1.0$	13.4	$45.7 \pm 1.4$
S87	-77	-11.6	-14.1	n.a.	n.a.	n.a.	n.a.
S88	-75	-11.6	n.a.	n.a.	n.a.	n.a.	n.a.
S89	-79	-11.5	-15.7	0.706881	$< 0.8 \pm 0.5$	$< 0.9$	$36.6 \pm 0.3$
S90	-77	-11.6	-14.8	n.a.	n.a.	n.a.	n.a.
S91	-73	-10.9	n.a.	n.a.	n.a.	n.a.	n.a.
S92	-80	-11.1	n.a.	n.a.	n.a.	n.a.	n.a.
S93	-78	-11.4	-18.8	n.a.	n.a.	n.a.	n.a.
S94	-73	-10.8	-16.1	n.a.	n.a.	n.a.	n.a.
S95	-74	-10.7	-16.3	n.a.	n.a.	n.a.	n.a.
S96	-74	-11.1	-15.9	n.a.	n.a.	n.a.	n.a.
S97	-86	-12.4	-9.9	n.a.	n.a.	n.a.	n.a.
S98	-86	-12.6	-8.8	n.a.	n.a.	n.a.	n.a.
S99	-80	-11.9	n.a.	n.a.	n.a.	n.a.	n.a.
S100	-77	-11.3	-18.6	0.710516	n.a.	n.a.	n.a.
S101	-77	-11.4	-18.5	n.a.	n.a.	n.a.	n.a.
S102	-83	-11.9	-15.3	n.a.	n.a.	n.a.	n.a.
S103	-76	-11.5	-14.1	n.a.	n.a.	n.a.	n.a.
S104	-75	-11.4	-11.3	n.a.	n.a.	n.a.	n.a.
S105	-69	-10.2	-8.4	n.a.	n.a.	n.a.	n.a.
S106	-72	-10.3	-16.7	n.a.	n.a.	n.a.	n.a.
S107	-76	-12.3	-13.9	n.a.	n.a.	n.a.	n.a.
S108	-75	-11.2	n.a.	n.a.	n.a.	n.a.	n.a.
S109	-68	-10.9	n.a.	n.a.	n.a.	n.a.	n.a.
S110	-72	-11.1	-15.6	n.a.	n.a.	n.a.	n.a.

Tableau A1.6. (suite)

ID Site	$\delta^2\text{H}$ (‰)	$\delta^{18}\text{O}$ (‰)	$\delta^{13}\text{C}_{\text{CID}}$ (‰)	$^{87}\text{Sr}/^{86}\text{Sr}$	$^{3}\text{H}^{\text{w}}$ (TU)	$^{3}\text{H}^{\text{x}}$ (TU)	$^{14}\text{C}^{\text{y}}$ (pMC)
S111	-73	-10.8	n.a.	n.a.	n.a.	n.a.	n.a.
S112	-79	-11.5	-13.5	n.a.	n.a.	n.a.	n.a.
S113	-69	-10.4	n.a.	n.a.	n.a.	n.a.	n.a.
S114	-81	-12.1	n.a.	n.a.	n.a.	n.a.	n.a.
S115	-86	-12.6	-13.0	n.a.	n.a.	n.a.	n.a.
S116	-85	-12.5	-11.5	n.a.	n.a.	n.a.	n.a.
S117	-77	-11.6	-10.9	n.a.	n.a.	n.a.	n.a.
S118	-79	-11.7	n.a.	n.a.	n.a.	n.a.	n.a.
S119	-80	-11.4	-18.6	0.709888	n.a.	n.a.	n.a.
S120	-70	-10.7	n.a.	n.a.	n.a.	n.a.	n.a.
S121	-76	-11.8	n.a.	n.a.	n.a.	n.a.	n.a.
S122	-79	-12.2	-11.7	n.a.	n.a.	n.a.	n.a.
S123	-72	-10.8	-15.2	n.a.	n.a.	n.a.	n.a.
S124	-73	-11.0	-14.9	n.a.	n.a.	n.a.	n.a.
S125	-69	-10.3	-14.8	n.a.	n.a.	n.a.	n.a.
S126	-84	-12.0	-11.7	n.a.	n.a.	n.a.	n.a.
S127	-69	-10.8	-15.4	n.a.	n.a.	n.a.	n.a.
S128	-79	-11.8	-13.8	n.a.	n.a.	n.a.	n.a.
S129	-77	-11.8	-13.3	0.708819	n.a.	n.a.	n.a.
S130	-74	-11.1	-15.5	n.a.	n.a.	n.a.	n.a.
S131	-73	-11.1	-15.3	0.708812	n.a.	n.a.	n.a.
S132	-72	-11.1	-15.2	n.a.	13.2 ± 1.1	14.4	66.6 ± 0.5
S133	-76	-11.5	n.a.	n.a.	n.a.	n.a.	n.a.
S134	-81	-12.3	-12.8	n.a.	n.a.	n.a.	n.a.
S135	-82	-12.0	-13.1	n.a.	n.a.	n.a.	n.a.
S136	-82	-12.4	-14.6	n.a.	n.a.	n.a.	n.a.
S137	-79	-11.9	-15.4	n.a.	n.a.	n.a.	n.a.
S138	-83	-12.6	-12.3	n.a.	n.a.	n.a.	n.a.
S139	-76	-11.9	-14.3	n.a.	n.a.	n.a.	n.a.
S140	-75	-11.0	-11.2	n.a.	n.a.	n.a.	n.a.
S141	-69	-10.2	-19.6	n.a.	n.a.	n.a.	n.a.
S142	-76	-11.3	-14.9	n.a.	n.a.	n.a.	n.a.
S143	-79	-11.7	-12.7	n.a.	n.a.	n.a.	n.a.
S144	-72	-11.0	-13.9	n.a.	n.a.	n.a.	n.a.
S145	-72	-10.9	-14.9	n.a.	7.6 ± 0.8	8.2	n.a.
S146	-75	-10.7	-15.0	n.a.	15.8 ± 1.3	17.1	n.a.
<b>Échantillons rejétés</b>							
R1	-73	-11.0	n.a.	n.a.	n.a.	n.a.	n.a.
R2	-74	-11.1	-16.6	n.a.	n.a.	n.a.	n.a.
R3	-75	-11.3	-16.9	n.a.	n.a.	n.a.	n.a.
R4	-78	-12.0	-14.1	n.a.	n.a.	n.a.	n.a.
SAP	-75	-11.2	-15.8	n.a.	n.a.	n.a.	n.a.
R5	-71	-10.4	-15.7	n.a.	n.a.	n.a.	n.a.
R6	-81	-11.9	-16.1	n.a.	n.a.	n.a.	n.a.
<b>Duplicata</b>							
D1	-77	-11.3	-14.8	n.a.	n.a.	n.a.	n.a.
D2	-75	-11.1	-14.4	n.a.	n.a.	n.a.	n.a.
D3	-78	-11.0	-16.2	0.709285	n.a.	n.a.	n.a.
D4	-78	-10.9	-14.7	n.a.	n.a.	n.a.	n.a.
D5	-75	-11.1	-13.1	n.a.	n.a.	n.a.	n.a.
D6	-79	-11.6	n.a.	n.a.	n.a.	n.a.	n.a.
D7	-79	-11.0	-17.4	n.a.	n.a.	n.a.	n.a.
D8	-80	-11.9	-13.1	n.a.	n.a.	n.a.	n.a.
D9	-74	-11.0	-16.0	n.a.	n.a.	n.a.	n.a.
D10	-78	-11.8	n.a.	n.a.	n.a.	n.a.	n.a.

## A2 Échantillonnage avec le système multi-niveaux

Tableau A2.1. Base de données géochimiques – Description des sites d'échantillonnage

ID Site	ID Projet CGC	Date <sup>a</sup>	Abscisse (m) <sup>b</sup>	Ordonnée (m) <sup>b</sup>	Elévation (m) <sup>c</sup>	Unité Géol. <sup>d</sup>	Unité Hydro. <sup>e</sup>	Cond. Hydro. <sup>f</sup>	Puits Coul. <sup>g</sup>	Profondeur de l'intervalle ouvert (m)		
										Haut	Bas	p.m. <sup>h</sup>
S144-L1	99CGQ01N1	2000-08-09	566227	5048158	58.0	7	4	2	0	21.8	25.5	23.7
S144-L2	99CGQ01N2	2000-08-10	566227	5048158	58.0	7	4	2	0	33.7	37.5	35.6
S144-L3	99CGQ01N3	2000-08-10	566227	5048158	58.0	7	4	2	0	52.4	56.2	54.3
S144-L4	99CGQ01N4	2000-08-10	566227	5048158	58.0	7	4	2	0	73.0	76.7	74.9
S144-L5	99CGQ01N5	2000-08-10	566227	5048158	58.0	7	4	2	0	89.8	93.6	91.7
S144-L6	99CGQ01N6	2000-08-11	566227	5048158	58.0	7	4	2	0	103.1	106.8	104.9
S85-L1	99CGQ04N1	2000-08-30	562413	5050931	47.0	7	4	1	0	53.4	57.1	55.3
S85-L2	99CGQ04N2	2000-08-30	562413	5050931	47.0	7	4	1	0	68.4	72.2	70.3
S85-L3	99CGQ04N3	2000-08-30	562413	5050931	47.0	7	4	1	0	86.0	89.7	87.9
S130-L1	99CGQ05N1	2000-07-26	560393	5058165	56.0	6	4	1	1	47.7	51.5	49.6
S130-L2	99CGQ05N2	2000-07-26	560393	5058165	56.0	6	4	1	1	58.1	61.9	60.0
S130-L3	99CGQ05N3	2000-07-26	560393	5058165	56.0	6	4	1	1	71.2	75.0	73.1
S130-L4	99CGQ05N4	2000-07-26	560393	5058165	56.0	6	4	1	1	84.0	87.7	85.9
S130-L5	99CGQ05N5	2000-07-27	560393	5058165	56.0	6	4	1	1	98.1	101.9	100.0
S130-L6	99CGQ05N6	2000-07-27	560393	5058165	56.0	6	4	1	1	101.8	105.6	103.7
SAP-L1	99CGQ06N1	2000-06-15	589831	5067517	64.0	4	4	1	0	24.7	28.5	26.6
SAP-L2	99CGQ06N2	2000-06-16	589831	5067517	64.0	4	4	1	0	49.7	53.5	51.6
SAP-L3	99CGQ06N3	2000-06-20	589831	5067517	64.0	4	4	1	0	87.4	91.2	89.3
S140-L1	F3N1	2000-08-03	539133	5052525	91.1	3	4	0	0	17.5	21.4	19.5
S140-L2	F3N2	2000-08-03	539133	5052525	91.1	3	4	0	0	36.3	40.2	38.3
S46-L1	F4N1	2000-08-25	569152	5047829	50.0	8	4	1	0	31.0	34.8	32.9
S46-L2	F4N2	2000-08-28	569152	5047829	50.0	8	4	1	0	44.7	48.5	46.6
S46-L3	F4N3	2000-08-29	569152	5047829	50.0	8	4	1	0	62.1	65.9	64.0
S46-L4	F4N4	2000-08-29	569152	5047829	50.0	8	4	1	0	76.9	80.7	78.8
S46-L4	F4N5	2000-08-29	569152	5047829	50.0	8	4	1	0	91.9	95.8	93.9
S123-L1	HamelN1	2000-08-16	584527	5061810	69.0	5	4	1	0	17.7	21.5	19.6
S123-L2	HamelN2	2000-08-16	584527	5061810	69.0	5	4	1	0	26.9	30.7	28.8
S123-L3	HamelN3	2000-08-17	584527	5061810	69.0	5	4	1	0	41.8	45.5	43.7
S123-L4	HamelN4	2000-08-17	584527	5061810	69.0	5	4	1	0	52.9	56.7	54.8
S123-L5	HamelN5	2000-08-17	584527	5061810	69.0	5	4	1	0	64.1	67.8	66.0
S84-L1	LavigneN1	2000-08-14	563455	5054215	87.0	7	4	0	0	11.6	15.4	13.5
S84-L2	LavigneN2	2000-08-14	563455	5054215	87.0	7	4	0	0	29.0	32.8	30.9
S84-L3	LavigneN3	2000-08-15	563455	5054215	87.0	7	4	0	0	44.1	47.9	46.0
S84-L4	LavigneN4	2000-08-15	563455	5054215	87.0	7	4	0	0	59.2	63.0	61.1
S84-L5	LavigneN5	2000-08-15	563455	5054215	87.0	7	4	0	0	75.3	79.1	77.2
S117-L1	PE2N1	2000-08-08	531925	5055621	76.0	3	4	1	0	32.3	36.0	34.1
S117-L2	PE2N2	2000-08-08	531925	5055621	76.0	3	4	1	0	43.3	47.1	45.2
S117-L3	PE2N3	2000-08-08	531925	5055621	76.0	3	4	1	0	61.1	64.9	63.0
S117-L4	PE2N4	2000-08-08	531925	5055621	76.0	9	4	1	0	72.3	76.1	74.2
S77-L1	Puits_FromN1	2000-07-18	566553	5040956	39.0	8	4	1	0	69.1	73.0	71.1
S77-L2	Puits_FromN2	2000-07-18	566553	5040956	39.0	8	4	1	0	80.3	84.2	82.3
S77-L3	Puits_FromN3	2000-07-18	566553	5040956	39.0	8	4	1	0	86.0	89.9	87.9
S77-L4	Puits_FromN4	2000-07-19	566553	5040956	39.0	8	4	1	0	91.6	95.5	93.5
S77-L5	Puits_FromN5	2000-07-19	566553	5040956	39.0	8	4	1	0	99.0	102.9	101.0
S124-L1	Puits_P9N1	2000-07-13	591048	5068721	61.4	3	4	1	0	19.2	23.1	21.1
S124-L2	Puits_P9N2	2000-07-13	591048	5068721	61.4	3	4	1	0	30.1	34.0	32.0
S124-L3	Puits_P9N3	2000-07-14	591048	5068721	61.4	3	4	1	0	37.3	41.2	39.3
S124-L4	Puits_P9N4	2000-07-14	591048	5068721	61.4	3	4	1	0	51.4	55.3	53.4
S125-L1	Puits_R14N1	2000-07-20	580729	5063973	68.6	5	4	0	0	7.4	11.3	9.4
S125-L2	Puits_R14N2	2000-07-20	580729	5063973	68.6	5	4	0	0	17.2	21.1	19.2
S125-L3	Puits_R14N3	2000-07-20	580729	5063973	68.6	5	4	0	0	27.2	31.1	29.2
S125-L4	Puits_R14N4	2000-07-20	580729	5063973	68.6	5	4	0	0	37.2	41.1	39.1

Tableau A2.1. (suite)

ID Site	ID Projet CGC	Date <sup>a</sup>	Abscisse (m) <sup>b</sup>	Ordonnée (m) <sup>b</sup>	Elévation (m) <sup>c</sup>	Unité Géol. <sup>d</sup>	Unité Hydro. <sup>e</sup>	Cond. Hydro. <sup>f</sup>	Puits Coul. <sup>g</sup>	Profondeur de l'intervalle ouvert (m)		
			(m) <sup>b</sup>	(m) <sup>b</sup>	(mam) <sup>c</sup>	Géol. <sup>d</sup>	Hydro. <sup>e</sup>	Cond. Hydro. <sup>f</sup>	Puits Coul. <sup>g</sup>	Haut	Bas	p.m. <sup>h</sup>
S126-L1	Puits_R15N1	2000-06-29	571749	5045622	68.6	9	4	0	0	18.4	22.3	20.3
S126-L2	Puits_R15N2	2000-07-03	571749	5045622	68.6	9	4	0	0	29.6	33.5	31.6
S126-L3	Puits_R15N3	2000-07-03	571749	5045622	68.6	9	4	0	0	55.8	59.7	57.7
S126-L4	Puits_R15N4	2000-07-04	571749	5045622	68.6	9	4	0	0	82.0	85.9	83.9
S129-L1	Puits_R270N1	2000-07-24	576829	5055922	73.2	6	4	1	0	10.6	14.3	12.4
S129-L2	Puits_R270N2	2000-07-24	576829	5055922	73.2	6	4	1	0	24.9	28.7	26.8
S129-L3	Puits_R270N3	2000-07-25	576829	5055922	73.2	6	4	1	0	38.7	42.4	40.6
S127-L1	Puits_R3N1	2000-07-05	546878	5053122	76.2	5	4	1	0	25.4	29.3	27.4
S127-L2	Puits_R3N2	2000-07-05	546878	5053122	76.2	5	4	1	0	42.0	45.9	44.0
S127-L3	Puits_R3N3	2000-07-10	546878	5053122	76.2	5	4	1	0	68.0	71.9	70.0
S127-L4	Puits_R3N4	2000-07-11	546878	5053122	76.2	5	4	1	0	82.6	86.5	84.6
S55-L1	StLouisN1	2000-07-31	592225	5060345	68.0	1	4	1	0	17.3	21.1	19.2
S55-L2	StLouisN2	2000-08-01	592225	5060345	68.0	1	4	1	0	39.8	43.6	41.7
S55-L3	StLouisN3	2000-08-01	592225	5060345	68.0	1	4	1	0	62.4	66.2	64.3
S55-L4	StLouisN4	2000-08-02	592225	5060345	68.0	1	4	1	0	84.9	88.7	86.8
S26-L3	R13N3	2000-08-22	589929	5065023	61.0	3	4	1	0	46.0	49.8	47.9
S26-L4	R13N4	2000-08-22	589929	5065023	61.0	3	4	1	0	64.6	68.4	66.5
S26-L5	R13N5	2000-08-23	589929	5065023	61.0	3	4	1	0	83.3	87.1	85.2
<b>Échantillons rejetés</b>												
R7	LACH10	1999-11-02	554570	5053522	77.0	5	4	0	0	78.1	94.7	78.6
R8	LACH11	1999-11-02	554570	5053522	77.0	5	4	0	0	64.3	77.3	70.8
R9	LACH12	1999-11-02	554570	5053522	77.0	5	4	0	0	45.8	63.4	55.4
R10	LACH13	1999-11-02	554570	5053522	77.0	5	4	0	0	31.4	44.9	38.5
R11	LACH14	1999-11-02	554570	5053522	77.0	5	4	0	0	19.0	30.5	25.6
R12	LACH15	1999-11-02	554570	5053522	77.0	5	4	0	0	6.9	18.1	12.5
R13	R13N1	2000-08-21	589929	5065023	61.0	3	4	1	0	27.3	31.1	29.2
R14	R13N2	2000-08-21	589929	5065023	61.0	3	4	1	0	36.6	40.5	38.6
<b>Duplicata</b>												
D11	99CGQ01R2	S144-L2	566227	5048158	58.0	7	4	0	0	33.7	37.5	35.6
D12	F4R1	S140-L1	569152	5047829	50.0	8	4	1	0	31.0	34.8	32.9
D13	LavigneR5	S84-L5	563455	5054215	87.0	7	4	0	0	75.3	79.1	77.2
D14	Puits_FromR1	S77-L1	566553	5040956	39.0	8	4	1	0	69.1	73.0	71.1
D15	Puits_R270R1	S129-L1	576829	5055922	73.2	6	4	1	0	10.6	14.3	12.4
D16	Puits_R3R1	S127-L1	546878	5053122	76.2	5	4	1	0	25.4	29.3	27.4
D17	StLouisR2	S55-L2	592225	5060345	68.0	1	4	1	0	39.8	43.6	41.7
<b>Échantillons test de qualité</b>												
T1	HamelN3A	S123-L3	584526.5	5061810	69.0	5	4	1	0	41.8	45.5	43.7
T2	LavigneN3A	S84-L3	563455	5054215	87.0	7	4	0	0	44.1	47.9	46.0
T3	PuitsR14A	S125	580729	5063973	68.6	5	4	0	0	5.2	48.7	27.0
T4	PuitsR14N1A	S125-L1	580729	5063973	68.6	5	4	0	0	7.4	11.3	9.4
T5	PuitsR14N2A	S125-L2	580729	5063973	68.6	5	4	0	0	17.2	21.1	19.2
T6	PuitsR14N3A	S125-L3	580729	5063973	68.6	5	4	0	0	27.2	31.1	29.2
T7	PuitsR14N4A	S125-L4	580729	5063973	68.6	5	4	0	0	37.2	41.1	39.1
T8	R13N3A	S26-L3	589929	5065023	61.0	3	4	1	0	46.0	49.8	47.9

- ID Site : par exemple, pour S26-L4, la première partie est le ID Site du site qui a aussi été échantillonné par méthode conventionnelle (S26 ; voir Tableau A1.1). La deuxième partie est le niveau échantillonné, le quatrième dans cet exemple (L4).

- Les échantillons R7 à R12 ont été rejettés, tout comme l'échantillon conventionnel de ce puits (R5 ; Tableau A1.1), car le puits est localisé à proximité d'un dépôt de sel déglaçant ayant contaminé le site.

- Les échantillons test de qualité ont été collectés après le double de volume de puits de l'échantillon principal (voir section 1.3.1.3 ; Chapitre 1)

Tableau A2.2. Base de données géochimiques – Paramètres de terrain et classification

ID Site	T <sup>i</sup> (°C)	pH	CE <sup>j</sup> (µS/cm)	OD <sup>k</sup> (mg/L)	Potentiel Redox E <sup>l</sup> (mV)	Eh <sup>m</sup>	EN <sup>n</sup> (%)	Types d'eau <sup>o</sup>
S144-L1	9.5	7.75	555	1.3	n.a.	—	0.38	Mg-Ca-HCO <sub>3</sub>
S144-L2	10.8	7.75	459	1.3	n.a.	—	-0.84	Mg-Ca-HCO <sub>3</sub>
S144-L3	9.7	7.34	418	0.4	n.a.	—	-2.84	Mg-Ca-HCO <sub>3</sub>
S144-L4	9.6	7.62	471	2.7	n.a.	—	-0.88	Mg-Ca-HCO <sub>3</sub>
S144-L5	9.2	7.64	457	3.0	n.a.	—	-0.41	Mg-Ca-HCO <sub>3</sub>
S144-L6	10.8	7.76	489	2.1	n.a.	—	-3.67	Mg-Ca-HCO <sub>3</sub>
S85-L1	9.6	8.20	499	0.6	n.a.	—	-2.00	Na-Mg-Ca-HCO <sub>3</sub>
S85-L2	9.2	7.69	486	0.4	n.a.	—	-1.61	Ca-Mg-Na-HCO <sub>3</sub>
S85-L3	8.7	7.79	501	0.4	n.a.	—	-1.53	Na-Mg-Ca-HCO <sub>3</sub>
S130-L1	10.5	7.80	3421	0.7	-164	—	0.15	Na-Cl
S130-L2	9.2	7.71	4690	0.2	-152	—	-1.64	Na-Cl
S130-L3	9.5	7.68	5140	n.a.	-135	—	-1.62	Na-Cl
S130-L4	9.1	7.83	2588	n.a.	-136	—	-0.09	Na-Cl
S130-L5	10.3	7.91	1675	0.5	-175	—	1.47	Na-Cl-HCO <sub>3</sub>
S130-L6	10.9	7.86	2012	0.5	-226	—	1.19	Na-Cl-HCO <sub>3</sub>
SAP-L1	10.5	8.24	1376	0.7	-185	—	-0.02	Na-Cl-HCO <sub>3</sub>
SAP-L2	14.1	7.99	7270	0.8	-244	—	0.65	Na-Cl
SAP-L3	16.9	7.31	7660	0.8	-209	—	5.97	Na-Cl
S140-L1	n.a.	7.88	460	1.2	48	—	-1.30	Ca-Na-Mg-HCO <sub>3</sub>
S140-L2	10.3	7.74	866	n.a.	n.a.	—	-0.83	Na-Ca-SO <sub>4</sub> -HCO <sub>3</sub>
S46-L1	9.8	8.11	1296	2.2	n.a.	—	-2.21	Na-Cl-HCO <sub>3</sub>
S46-L2	8.7	8.14	1268	5.2	297	—	-2.34	Na-Cl-HCO <sub>3</sub>
S46-L3	9.2	7.64	1225	0.5	n.a.	—	0.45	Na-HCO <sub>3</sub> -Cl
S46-L4	9.2	7.52	1222	0.5	n.a.	—	-0.02	Na-Cl-HCO <sub>3</sub>
S46-L4	9.3	7.59	1242	0.4	n.a.	—	-3.19	Na-Cl-HCO <sub>3</sub>
S123-L1	8.7	7.66	1371	0.1	15	—	2.57	Na-Mg-Ca-HCO <sub>3</sub> -Cl
S123-L2	8.9	7.67	1372	0.3	3	—	0.92	Na-Mg-Ca-HCO <sub>3</sub> -Cl
S123-L3	9.2	7.67	903	0.6	17	—	-0.68	Na-Mg-HCO <sub>3</sub> -Cl
S123-L4	16.1	7.67	1170	n.a.	n.a.	—	-1.61	Na-Mg-HCO <sub>3</sub> -Cl
S123-L5	8.1	7.48	1392	1.3	30	—	-1.41	Na-Mg-Ca-Cl-HCO <sub>3</sub>
S84-L1	8.9	7.16	609	8.4	n.a.	—	-1.60	Ca-Mg-HCO <sub>3</sub>
S84-L2	8.2	7.22	599	8.2	n.a.	—	-1.46	Ca-Mg-HCO <sub>3</sub>
S84-L3	9.1	7.15	585	2.6	22	—	-0.83	Ca-Mg-HCO <sub>3</sub>
S84-L4	8.6	7.13	605	3.4	89	—	-3.34	Ca-Mg-HCO <sub>3</sub>
S84-L5	8.6	7.22	603	7.8	117	—	-2.44	Ca-Mg-HCO <sub>3</sub>
S117-L1	10.0	8.30	693	0.2	-129	—	3.18	Na-Cl-HCO <sub>3</sub>
S117-L2	9.7	8.26	768	0.1	-71	—	1.28	Na-Cl-HCO <sub>3</sub> -SO <sub>4</sub>
S117-L3	9.9	8.23	912	0.1	-85	—	2.86	Na-Cl-HCO <sub>3</sub>
S117-L4	n.a.	8.27	805	n.a.	n.a.	—	7.12	Na-Cl-HCO <sub>3</sub>
S77-L1	11.1	7.28	18440	0.1	-117	—	-0.82	Na-Cl
S77-L2	10.3	7.37	18520	0.2	-116	—	-3.70	Na-Cl
S77-L3	9.5	7.51	18460	0.7	-133	—	0.94	Na-Cl
S77-L4	10.7	7.35	18510	0.0	-115	—	0.05	Na-Cl
S77-L5	9.9	7.52	18720	0.1	-144	—	0.00	Na-Cl
S124-L1	10.2	8.30	1650	0.4	-203	—	-2.16	Na-HCO <sub>3</sub> -Cl
S124-L2	13.2	8.35	1937	0.5	-207	—	-2.97	Na-Cl-HCO <sub>3</sub>
S124-L3	9.3	8.42	1572	0.6	-216	—	-0.04	Na-HCO <sub>3</sub> -Cl
S124-L4	10.1	8.21	3089	0.9	-227	—	-0.73	Na-Cl-HCO <sub>3</sub>
S125-L1	9.7	6.86	1825	0.1	-11	—	0.56	Na-Ca-Cl-HCO <sub>3</sub>
S125-L2	10.3	7.03	1732	0.2	-50	—	2.23	Na-Ca-Mg-Cl-HCO <sub>3</sub>
S125-L3	8.9	6.92	1850	0.2	-2	—	-4.20	Na-Ca-Cl-HCO <sub>3</sub>
S125-L4	8.4	6.93	1835	0.2	n.a.	—	-0.07	Na-Ca-Cl-HCO <sub>3</sub>

Tableau A2.2. (suite)

ID Site	T <sup>i</sup> (°C)	pH	CE <sup>j</sup> (µS/cm)	OD <sup>k</sup> (mg/L)	Potentiel Redox E <sup>l</sup> (mV) Eh <sup>m</sup>	EN <sup>n</sup> (%)	Types d'eau <sup>o</sup>
S126-L1	12.4	7.52	911	n.a.	n.a.	-	0.18 Na-Ca-Mg-HCO <sub>3</sub> -Cl
S126-L2	10.5	7.71	982	3.5	97	-	-0.11 Na-Ca-Mg-HCO <sub>3</sub> -Cl
S126-L3	10.0	8.49	938	1.2	82	-	0.37 Na-HCO <sub>3</sub> -Cl
S126-L4	10.8	8.26	936	0.9	-40	-	1.04 Na-HCO <sub>3</sub> -Cl
S129-L1	10.0	7.49	535	0.4	-87	-	-1.43 Ca-Mg-HCO <sub>3</sub> -SO <sub>4</sub>
S129-L2	8.8	7.53	449	0.5	n.a.	-	-0.82 Ca-Mg-HCO <sub>3</sub>
S129-L3	9.9	7.48	513	0.3	-68	-	-4.76 Ca-Mg-HCO <sub>3</sub>
S127-L1	11.4	7.85	465	0.9	-102	-	-0.65 Mg-Ca-HCO <sub>3</sub>
S127-L2	10.3	7.86	471	0.5	-104	-	-4.27 Ca-Mg-HCO <sub>3</sub>
S127-L3	10.6	7.88	483	0.5	-80	-	-1.02 Ca-Mg-HCO <sub>3</sub>
S127-L4	12.3	7.95	473	0.9	-83	-	-1.90 Ca-Mg-HCO <sub>3</sub>
S55-L1	n.a.	7.12	2330	0.8	n.a.	-	-2.07 Na-Ca-Cl-HCO <sub>3</sub>
S55-L2	10.7	7.33	2326	0.8	n.a.	-	3.43 Na-Ca-Cl-HCO <sub>3</sub>
S55-L3	n.a.	7.22	2443	n.a.	n.a.	-	-0.19 Na-Ca-Cl-HCO <sub>3</sub>
S55-L4	11.6	7.13	2383	0.6	-44	-	4.41 Na-Ca-Cl-HCO <sub>3</sub>
S26-L3	8.5	7.98	2797	0.3	-120	-	0.33 Na-Cl-HCO <sub>3</sub>
S26-L4	11.2	8.11	2814	n.a.	-96	-	0.41 Na-Cl-HCO <sub>3</sub>
S26-L5	n.a.	8.06	2837	n.a.	-70	-	-0.16 Na-Cl-HCO <sub>3</sub>
<b>Échantillons rejetés</b>							
R7	10.8	7.43	629	2.1	-56	-	-1.5 Ca-Mg-HCO <sub>3</sub>
R8	n.a.	7.41	694	2.0	-71	-	-1.4 Ca-Mg-HCO <sub>3</sub>
R9	n.a.	7.19	4749	1.2	-54	-	-0.4 Na-Ca-Cl
R10	n.a.	7.34	5500	9.1	102	-	0.3 Na-Cl
R11	n.a.	7.18	5500	3.7	125	-	1.8 Na-Cl
R12	n.a.	7.27	5440	7.6	30	-	0.9 Na-Cl
R13	8.5	8.03	2808	0.2	-115	-	-100.0 Cl-HCO <sub>3</sub>
R14	8.1	8.26	2828	0.9	-101	-	-100.0 Cl-HCO <sub>3</sub>
<b>Duplicata</b>							
D11	10.8	7.75	459	1.3	n.a.	-	-0.4 Mg-Ca-HCO <sub>3</sub>
D12	9.8	8.11	1296	2.2	n.a.	-	-1.6 Na-Cl-HCO <sub>3</sub>
D13	8.6	7.22	603	7.8	117	-	-1.6 Ca-Mg-HCO <sub>3</sub>
D14	11.1	7.28	18440	0.1	-117	-	-0.8 Na-Cl
D15	10.0	7.49	535	0.4	-87	-	-3.8 Ca-Mg-HCO <sub>3</sub> -SO <sub>4</sub>
D16	11.4	7.85	465	0.9	-102	-	-2.8 Mg-Ca-HCO <sub>3</sub>
D17	10.7	7.33	2326	0.8	n.a.	-	1.6 Na-Ca-Cl-HCO <sub>3</sub>
<b>Échantillons test de qualité</b>							
T1	9.3	7.70	898	0.7	-15	-	0.2 Na-Mg-HCO <sub>3</sub> -Cl
T2	9.7	7.23	583	2.6	47	-	-2.2 Ca-Mg-HCO <sub>3</sub>
T3	9.4	7.22	1828	4.0	76	-	-4.2 Na-Ca-Cl-HCO <sub>3</sub>
T4	9.7	6.87	1820	0.1	-9	-	-0.2 Na-Ca-Cl-HCO <sub>3</sub>
T5	9.9	7.03	1741	0.1	-52	-	-0.8 Na-Ca-Mg-Cl-HCO <sub>3</sub>
T6	8.5	6.94	1860	0.2	n.a.	-	-2.9 Na-Ca-Cl-HCO <sub>3</sub>
T7	8.4	6.96	1839	0.2	n.a.	-	0.0 Na-Ca-Mg-Cl-HCO <sub>3</sub>
T8	n.a.	7.93	2806	n.a.	-143	-	-1.0 Na-Cl-HCO <sub>3</sub>

Tableau A2.3. Base de données géochimiques – Paramètres chimiques (# 1)

ID Site	Ca	Mg	Na	K	Cl	SO <sub>4</sub>	Alc. Tot. (en CaCO <sub>3</sub> )	CID	Fe	Mn	Br	Sr	F	Ba	HS (en S)	SiO <sub>2</sub>
S144-L1	51	40	6.3	3.4	3.3	43.5	260	64	1.1	0.042	0.02	0.51	0.12	0.26	0.04	24
S144-L2	36	36	6	3.8	1.3	28	230	55	0.39	0.14	<.01	0.6	0.21	0.12	<.02	17.6
S144-L3	38	29	4.2	5.3	2	21	220	n.a.	0.48	0.17	<.01	0.62	0.27	0.1	0.09	10.3
S144-L4	41	36	5.7	4.1	1.3	31	240	n.a.	0.42	0.16	0.01	0.59	0.2	0.16	0.05	16.6
S144-L5	39	35	5.5	4.1	0.6	30	230	n.a.	0.54	0.16	<.01	0.59	0.2	0.15	0.04	16.8
S144-L6	41	37	6.1	3.7	2.5	39	250	n.a.	0.48	0.11	0.01	0.57	0.19	0.16	0.08	18.9
S85-L1	23	17.2	56	6.1	17	24	220	51	0.16	0.12	0.08	0.54	0.35	0.11	0.1	13.7
S85-L2	38	21	31	3.9	8.9	21	230	55	0.41	0.39	0.04	0.52	0.23	0.06	<.02	14.4
S85-L3	33	21	41	6.1	14	24	230	55	0.17	0.13	0.05	0.87	0.3	0.05	<.02	15
S130-L1	55	48	540	18	880	95	190	52	1.2	0.07	2.68	0.974	0.39	0.16	<.02	13
S130-L2	67	63	800	25	1300	200	230	53	1	0.064	4.16	1.27	0.37	0.13	<.02	10.8
S130-L3	72	69	920	26	1540	200	200	52	1.1	0.067	4.6	1.39	0.37	0.13	<.02	10
S130-L4	50	42	400	15	640	75	210	55	0.71	0.048	1.97	0.77	0.4	0.27	<.02	11.1
S130-L5	43	33	250	11	370	37	220	n.a.	0.65	0.04	1.2	0.58	0.37	0.33	0.04	11.3
S130-L6	47	36	310	12	470	50	220	n.a.	0.62	0.041	1.66	0.654	0.38	0.31	0.03	11.2
SAP-L1	16.3	17.3	256	n.a.	270	47	240	56	0.015	0.002	2.05	n.a.	0.83	0.16	1.4	12.7
SAP-L2	35	21	1611	29	2300	32	400	n.a.	0.008	0.003	9.11	6.3	n.a.	2.3	12	7.8
SAP-L3	93	73	1600	44	2300	25	350	100	0.18	0.004	11.15	12.2	4	3	6.4	7.9
S140-L1	39	16.7	37	7	5	36	220	n.a.	0.008	0.034	0.05	2.18	0.73	0.14	0.04	9.9
S140-L2	41	13	140	4.9	13	260	200	n.a.	0.023	0.007	0.05	19	2.9	0.06	<.02	7.4
S46-L1	14.6	24	220	9.3	240	16	300	n.a.	0.31	0.15	1.2	0.53	0.53	0.11	0.03	8.3
S46-L2	10.4	14.8	250	9	240	24	310	71	0.07	0.2	0.89	0.32	0.45	0.09	0.05	8.8
S46-L3	10.8	15.2	230	8.6	200	23	290	70	0.22	0.17	0.79	0.136	0.47	0.09	0.04	9.2
S46-L4	10.5	12.2	240	7.8	210	22	290	70	0.14	0.13	0.78	0.29	0.43	0.08	0.08	10.1
S46-L4	11.6	13.7	240	7.3	230	22	310	70	0.096	0.18	0.79	0.3	0.46	0.09	<.02	10.1
S123-L1	58	52	140	22	190	100	290	74	0.15	0.004	0.2	3.706	0.71	0.27	<.02	10.4
S123-L2	55	52	140	22	200	100	290	74	0.17	0.003	0.2	3.75	0.74	0.45	<.02	10.1
S123-L3	35	28	110	18	140	23	250	n.a.	0.032	<.0003	0.32	2.802	1.8	0.2	0.03	6.7
S123-L4	43	36	120	20	170	50	270	n.a.	0.004	0.005	0.27	3.186	1.5	0.17	n.a.	7.6
S123-L5	58	53	140	22	220	95	310	n.a.	0.089	0.002	0.2	4.121	0.75	0.1	0.02	10.3
S84-L1	74	38	2.6	1.4	3	31	320	79	0.003	<.0003	0.02	0.059	0.06	0.2	0.03	11.3
S84-L2	73	37	2.5	1.3	3.3	33	310	79	0.004	<.0003	0.02	0.058	0.06	0.2	0.02	11.3
S84-L3	69	36	3.3	2.8	2.5	41	290	74	0.003	0.064	<.01	0.149	0.09	0.17	0.04	10.9
S84-L4	73	36	2.7	1.6	2.5	44	310	77	0.005	0.065	<.01	0.087	0.08	0.19	0.02	11.1
S84-L5	74	37	2.7	1.4	5	41	310	77	0.009	0.046	<.01	0.074	0.08	0.19	0.02	11.4
S117-L1	17.7	9.1	110	3.5	92	60	120	29	0.047	0.006	0.35	13	2.9	0.04	<.02	8.8
S117-L2	19	8.8	120	3.3	98	85	120	29	0.026	0.005	0.37	14	3.5	0.02	<.02	9.6
S117-L3	18.7	10.1	160	4.6	160	65	120	30	0.035	0.003	0.59	4.47	3.6	0.02	<.02	7.2
S117-L4	19	10.2	160	4.5	130	75	120	30	0.02	0.004	0.44	5.2	3.5	0.02	0.02	8.2
S77-L1	680	340	3000	25	6600	450	51	30	2.3	0.53	23	23	0.28	0.04	<.02	15.2
S77-L2	500	290	3000	26	6500	430	90	28	3.2	0.56	23	23	0.27	0.04	<.02	14.3
S77-L3	660	330	3100	26	6400	430	150	29	3.3	0.55	23	22	0.27	0.04	<.02	13.6
S77-L4	670	340	2900	26	6300	450	70	29	2.8	0.54	23	22	0.3	0.04	<.02	14.3
S77-L5	710	360	2900	26	6500	410	25	28	3.3	0.55	23	23	0.29	0.04	0.04	12.9
S124-L1	13	13.4	350	17	290	17	480	n.a.	0.009	0.005	2.16	4.333	2.9	0.81	4.5	10.3
S124-L2	13	13	380	17	360	10	470	n.a.	0.23	0.002	2.888	3.641	3	0.89	3.7	9.7
S124-L3	6	7.2	350	16	245	16	460	n.a.	0.005	<.0003	1.58	2.912	3.1	0.36	5.2	9.6
S124-L4	21	18.5	610	23	820	32	310	n.a.	0.005	<.0003	5.92	3.475	4.4	0.79	9.8	12.4
S125-L1	110	43	220	3.4	340	130	310	83	0.012	0.11	0.06	0.224	0.09	0.12	<.02	10.6
S125-L2	110	48	180	8.6	340	66	290	78	0.26	0.026	0.09	0.796	0.41	0.25	<.02	10.9
S125-L3	110	43	220	3.5	360	150	350	n.a.	0.071	0.1	0.07	0.245	0.08	0.13	<.02	10.5
S125-L4	110	43	210	3.5	340	120	310	n.a.	0.045	0.1	0.07	0.255	0.09	0.13	<.02	10.6

Tableau A2.3. (suite)

ID Site	Ca	Mg	Na	K	Cl	SO <sub>4</sub>	Alc. Tot. (en CaCO <sub>3</sub> )	CID	Fe	Mn	Br	Sr	F	Ba	HS (en S)	SiO <sub>2</sub>
S126-L1	58	27	110	4.4	110	25	320	n.a.	0.078	0.12	0.021	1.23	0.5	0.09	<.02	10.3
S126-L2	58	27	120	3.2	120	23	330	78	0.11	0.1	0.02	1.13	0.46	0.07	0.02	9.9
S126-L3	21	9.5	200	2.2	82	37	370	83	0.076	0.043	0.03	0.5	1	0.04	0.02	10.1
S126-L4	29	13	190	2.1	85	38	370	84	0.53	0.057	0.03	0.61	1.4	0.06	0.02	8.6
S129-L1	61	31	4.4	2.8	7.5	59	230	56	0.33	0.021	0.005	0.276	0.12	0.19	<.02	11.1
S129-L2	50	25	6.1	2.8	3.8	42	200	50	0.28	0.018	0.004	0.278	0.13	0.13	<.02	10.5
S129-L3	56	28	7.6	3.5	6.7	42	250	58	0.28	0.02	0.008	0.36	0.2	0.15	0.03	10.8
S127-L1	42	26	15.2	4.5	5	8	240	58	0.31	0.013	0.009	0.75	0.42	0.55	0.04	13.2
S127-L2	46	27	13.5	4	6.3	25	250	59	0.33	0.016	0.008	0.742	0.37	0.54	0.02	14.1
S127-L3	47	28	14.7	4.1	3.3	22	250	60	0.41	0.018	0.008	0.75	0.23	0.55	0.04	14.3
S127-L4	45	26	15.2	4.4	5	22	240	58	0.25	0.019	0.002	0.76	0.25	0.55	<.02	13.9
S55-L1	200	12.3	260	4.7	550	65	330	70	0.66	0.16	0.01	0.84	0.16	0.44	0.02	7.4
S55-L2	140	9.4	350	5.9	502	63	310	n.a.	0.26	0.072	0.46	0.808	0.43	0.29	0.02	8.1
S55-L3	160	9.9	320	5.5	550	63	310	n.a.	1.1	0.12	0.56	0.759	0.43	0.34	0.03	8.6
S55-L4	210	12.4	290	4.9	540	71	280	n.a.	0.82	0.12	0.14	0.79	0.1	0.45	0.02	9.3
S26-L3	19.8	20	560	23	630	95	380	95	0.012	<.0003	6.92	3.23	2.3	0.05	4.2	13
S26-L4	18.8	19.5	570	22	630	90	400	95	0.06	0.003	6.94	3.16	2.2	0.05	1.1	12.1
S26-L5	18.7	19.2	550	22	620	75	400	96	0.12	0.013	7.2	3.2	2.3	0.07	1.2	10.9
<b>Échantillons rejetés</b>																
R7	68	33	17.4	5.4	18	45	290	74	0.5	0.05	0.05	0.492	0.25	0.1	n.a.	9.2
R8	72	35	19.3	7.2	26	60	290	75	1.6	0.086	0.05	0.362	0.21	0.43	n.a.	10.8
R9	200	87	660	27	1300	180	330	100	0.87	0.23	0.3	1.445	0.17	0.24	n.a.	16.4
R10	210	88	790	32	1500	180	330	97	0.055	0.39	0.4	1.68	0.15	0.39	n.a.	16.7
R11	210	91	800	32	1500	200	260	100	0.18	0.32	0.35	1.68	0.14	0.35	n.a.	16.3
R12	210	84	810	35	1500	180	330	97	0.13	0.37	0.3	1.56	0.16	0.4	n.a.	16.8
R13	n.a.	n.a.	n.a.	n.a.	620	n.a.	390	94	n.a.	n.a.	n.a.	n.a.	n.a.	n.a.	3.2	n.a.
R14	n.a.	n.a.	n.a.	n.a.	640	n.a.	390	95	n.a.	n.a.	n.a.	n.a.	n.a.	n.a.	4.1	n.a.
<b>Duplicata</b>																
D11	36	37	6	3.9	1.3	29	230	55	0.34	0.14	0.1	0.6	0.19	0.12	<.02	17.5
D12	14.7	24	230	9	250	16	300	n.a.	0.33	0.16	1.1	0.54	0.54	0.11	0.03	8.3
D13	74	37	2.6	1.4	1.7	39	310	78	0.0009	0.046	<.01	0.073	0.08	0.19	0.02	11.4
D14	680	350	3000	26	6650	400	71	30	2.3	0.54	24	23	0.29	0.04	<.02	15.2
D15	60	30	4.3	2.8	6.3	68	230	56	0.31	0.021	0.005	0.269	0.12	0.19	0.03	11
D16	42	26	15.4	4.6	6.3	7.5	250	58	0.31	0.013	0.009	0.77	0.44	0.55	0.04	13.3
D17	130	9.3	360	6	520	63	320	n.a.	0.24	0.069	0.46	0.805	0.45	0.28	0.02	8.1
<b>Échantillons test de qualité</b>																
T1	36	29	100	19	130	25	240	n.a.	0.034	0.0003	0.32	2.785	1.9	0.2	0.02	6.7
T2	69	36	3.4	3	2.5	41	300	74	0.022	0.062	0.007	0.159	0.1	0.17	0.03	10.9
T3	97	41	240	3.4	350	140	380	n.a.	0.016	0.098	0.026	0.25	0.11	0.13	<.02	9.8
T4	110	44	210	3.4	330	120	330	84	0.011	0.11	0.07	0.217	0.09	0.12	<.02	10.5
T5	100	48	170	8.7	340	60	300	n.a.	0.26	0.026	0.09	0.821	0.4	0.24	<.02	10.7
T6	120	43	220	3.7	370	120	370	n.a.	0.071	0.1	0.07	0.269	0.09	0.13	<.02	10.5
T7	110	46	200	4.1	340	110	310	n.a.	0.051	0.098	0.07	0.348	0.43	0.13	<.02	11
T8	19.5	19.8	550	23	630	95	380	94	0.01	<.0003	6.99	3.26	2.3	0.05	4.5	13.1

Tableau A2.4. Base de données géochimiques – Paramètres chimiques (# 2)

ID Site	B	Al	Li	NO <sub>3</sub> (en N)	NH <sub>4</sub> (en N)	PO <sub>4</sub> (en P)	COD	Ag	As	Cd	CN	Cr	Cu	Hg	I
S144-L1	0.008	<.007	0.005	0.03	0.08	0.075	1.2	n.a.	n.a.	n.a.	n.a.	0.002	<.001	n.a.	n.a.
S144-L2	0.04	0.02	0.003	0.03	0.04	0.24	0.4	n.a.	n.a.	n.a.	n.a.	0.002	<.001	n.a.	n.a.
S144-L3	0.03	<.007	<.001	0.02	0.1	0.14	0.4	n.a.	n.a.	n.a.	n.a.	0.003	<.001	n.a.	n.a.
S144-L4	0.02	<.007	0.003	<.02	0.06	0.16	0.6	n.a.	n.a.	n.a.	n.a.	0.002	<.001	n.a.	n.a.
S144-L5	0.02	<.007	0.003	<.02	0.06	0.175	0.4	n.a.	n.a.	n.a.	n.a.	0.001	<.001	n.a.	n.a.
S144-L6	0.01	<.007	0.005	<.02	0.05	0.125	0.6	n.a.	n.a.	n.a.	n.a.	0.001	<.001	n.a.	n.a.
S85-L1	0.08	0.02	0.006	<.02	0.16	0.02	0.9	n.a.	n.a.	n.a.	n.a.	0.002	<.001	n.a.	n.a.
S85-L2	0.12	0.21	0.005	0.02	<.02	0.01	0.4	n.a.	n.a.	n.a.	n.a.	0.002	<.001	n.a.	n.a.
S85-L3	0.18	0.009	0.006	0.02	0.02	0.01	0.4	n.a.	n.a.	n.a.	n.a.	0.002	<.001	n.a.	n.a.
S130-L1	0.34	<.007	0.015	<.02	0.22	0.02	9.6	n.a.	n.a.	n.a.	n.a.	0.002	<.001	n.a.	n.a.
S130-L2	0.47	<.007	0.019	<.02	0.28	0.02	3	n.a.	n.a.	n.a.	n.a.	0.003	<.001	n.a.	n.a.
S130-L3	0.51	<.007	0.02	<.02	0.29	0.02	7	n.a.	n.a.	n.a.	n.a.	0.003	<.001	n.a.	n.a.
S130-L4	0.3	<.007	0.012	<.02	0.33	0.05	5.6	n.a.	n.a.	n.a.	n.a.	0.003	<.001	n.a.	n.a.
S130-L5	0.22	<.007	0.009	<.02	0.36	0.05	1.9	n.a.	n.a.	n.a.	n.a.	0.002	<.001	n.a.	n.a.
S130-L6	0.26	0.01	0.009	<.02	0.36	0.05	3.1	n.a.	n.a.	n.a.	n.a.	0.003	<.001	n.a.	n.a.
SAP-L1	0.56	<.007	n.a.	<.02	1.25	0.32	2.4	n.a.	n.a.	0.0006	n.a.	0.0009	<.001	n.a.	n.a.
SAP-L2	0.66	0.01	0.419	0.23	1.28	0.035	n.a.	n.a.	n.a.	0.0042	n.a.	0.002	<.001	n.a.	n.a.
SAP-L3	0.87	<.007	0.727	<.02	1.59	<.01	n.a.	n.a.	n.a.	0.0021	n.a.	0.003	<.001	n.a.	n.a.
S140-L1	0.34	0.24	0.012	0.18	0.11	<.01	2.6	n.a.	n.a.	n.a.	n.a.	0.002	0.001	n.a.	n.a.
S140-L2	0.38	<.007	0.021	0.02	0.1	<.01	0.6	n.a.	n.a.	n.a.	n.a.	0.003	<.001	n.a.	n.a.
S46-L1	0.24	0.03	<.001	<.02	0.64	0.2	1.1	n.a.	n.a.	n.a.	n.a.	<.0009	<.001	n.a.	n.a.
S46-L2	0.34	0.02	0.001	<.02	0.44	0.16	0.9	n.a.	n.a.	n.a.	n.a.	0.007	<.001	n.a.	n.a.
S46-L3	0.3	<.007	0.003	<.02	0.42	0.19	0.5	n.a.	n.a.	n.a.	n.a.	<.0009	<.001	n.a.	n.a.
S46-L4	0.3	<.007	0.001	0.02	0.35	0.2	0.5	n.a.	n.a.	n.a.	n.a.	<.0009	<.001	n.a.	n.a.
S46-L4	0.28	<.007	0.001	<.02	0.34	0.24	0.7	n.a.	n.a.	n.a.	n.a.	<.0009	<.001	n.a.	n.a.
S123-L1	0.42	<.007	0.02	<.02	0.42	0.025	2.4	n.a.	n.a.	n.a.	n.a.	0.002	<.001	n.a.	n.a.
S123-L2	0.41	<.007	0.02	<.02	0.39	0.04	2.2	n.a.	n.a.	n.a.	n.a.	0.003	<.001	n.a.	n.a.
S123-L3	0.39	<.007	0.024	<.02	0.42	<.01	0.6	n.a.	n.a.	n.a.	n.a.	0.002	<.001	n.a.	n.a.
S123-L4	0.36	0.11	0.022	0.04	0.46	n.a.	n.a.	n.a.	n.a.	n.a.	n.a.	0.002	<.001	n.a.	n.a.
S123-L5	0.37	<.007	0.02	<.02	0.35	<.01	2.4	n.a.	n.a.	n.a.	n.a.	0.003	<.001	n.a.	n.a.
S84-L1	0.01	<.007	0.001	1.05	0.15	<.01	0.6	n.a.	n.a.	n.a.	n.a.	0.002	<.001	n.a.	n.a.
S84-L2	0.01	<.007	0.001	0.79	0.09	0.035	0.4	n.a.	n.a.	n.a.	n.a.	0.002	<.001	n.a.	n.a.
S84-L3	0.04	<.007	0.002	0.33	0.05	<.01	1	n.a.	n.a.	n.a.	n.a.	0.003	<.001	n.a.	n.a.
S84-L4	0.01	<.007	0.002	0.6	0.02	<.01	1.2	n.a.	n.a.	n.a.	n.a.	0.003	<.001	n.a.	n.a.
S84-L5	0.02	<.007	0.002	0.61	<.02	<.01	1.4	n.a.	n.a.	n.a.	n.a.	0.004	0.002	n.a.	n.a.
S117-L1	0.13	<.007	0.008	<.02	0.06	<.01	0.5	n.a.	n.a.	n.a.	n.a.	0.002	<.001	n.a.	n.a.
S117-L2	0.13	<.007	0.009	<.02	0.05	<.01	0.3	n.a.	n.a.	n.a.	n.a.	0.002	<.001	n.a.	n.a.
S117-L3	0.13	<.007	0.011	<.02	0.07	<.01	0.4	n.a.	n.a.	n.a.	n.a.	0.002	<.001	n.a.	n.a.
S117-L4	0.13	0.03	0.01	0.03	0.06	<.01	0.7	n.a.	n.a.	n.a.	n.a.	0.003	<.001	n.a.	n.a.
S77-L1	<.002	<.007	0.069	<.02	0.38	<.01	<2	n.a.	n.a.	n.a.	n.a.	0.005	<.001	n.a.	n.a.
S77-L2	0.25	<.007	0.069	<.02	0.32	<.01	2	n.a.	n.a.	n.a.	n.a.	0.006	<.001	n.a.	n.a.
S77-L3	<.002	<.007	0.068	<.02	0.42	0.01	2	n.a.	n.a.	n.a.	n.a.	0.005	<.001	n.a.	n.a.
S77-L4	<.002	<.007	0.071	<.02	0.41	0.01	2	n.a.	n.a.	n.a.	n.a.	0.005	<.001	n.a.	n.a.
S77-L5	<.002	<.007	0.065	<.02	0.49	<.01	3.2	n.a.	n.a.	n.a.	n.a.	0.006	<.001	n.a.	n.a.
S124-L1	0.16	<.007	0.071	<.02	0.77	1.45	6.4	n.a.	n.a.	n.a.	n.a.	<.0009	<.001	n.a.	n.a.
S124-L2	0.07	<.007	0.08	<.02	0.78	1.4	5.5	n.a.	n.a.	n.a.	n.a.	0.001	<.001	n.a.	n.a.
S124-L3	0.19	<.007	0.061	<.02	0.7	1.55	6	n.a.	n.a.	n.a.	n.a.	<.0009	<.001	n.a.	n.a.
S124-L4	<.002	<.007	0.155	<.02	0.89	0.31	9	n.a.	n.a.	n.a.	n.a.	0.002	<.001	n.a.	n.a.
S125-L1	0.03	<.007	0.004	<.02	0.03	0.01	3.1	n.a.	n.a.	n.a.	n.a.	0.002	<.001	n.a.	n.a.
S125-L2	<.002	<.007	0.007	<.02	0.1	<.01	1.4	n.a.	n.a.	n.a.	n.a.	0.002	<.001	n.a.	n.a.
S125-L3	<.002	<.007	0.003	0.02	0.02	<.01	2.6	n.a.	n.a.	n.a.	n.a.	0.002	<.001	n.a.	<.1
S125-L4	<.007	<.007	0.004	0.04	0.02	<.01	2.9	n.a.	n.a.	n.a.	n.a.	0.002	<.001	n.a.	<.1

Tableau A2.4. (suite)

ID Site	B	Al	Li	NO <sub>3</sub> (en N)	NH <sub>4</sub> (en N)	PO <sub>4</sub> (en P)	COD	Ag	As	Cd	CN	Cr	Cu	Hg	I
S126-L1	0.04	0.02	0.002	0.11	0.5	<.01	n.a.	n.a.	n.a.	n.a.	n.a.	0.002	<.001	n.a.	n.a.
S126-L2	0.06	0.03	0.002	0.07	0.03	<.01	0.9	n.a.	n.a.	n.a.	n.a.	0.003	<.001	n.a.	n.a.
S126-L3	0.11	0.02	0.003	0.02	0.04	0.01	1	n.a.	n.a.	n.a.	n.a.	0.0009	<.001	n.a.	n.a.
S126-L4	0.11	0.02	0.003	0.06	0.04	0.01	1.2	n.a.	n.a.	n.a.	n.a.	0.011	<.001	n.a.	n.a.
S129-L1	<.002	0.01	0.002	<.02	0.02	<.01	0.4	n.a.	n.a.	n.a.	n.a.	0.001	<.001	n.a.	n.a.
S129-L2	<.002	<.007	0.003	<.02	0.02	<.01	0.7	n.a.	n.a.	n.a.	n.a.	0.001	<.001	n.a.	n.a.
S129-L3	<.002	<.007	0.004	<.02	0.02	<.01	0.6	n.a.	n.a.	n.a.	n.a.	0.002	<.001	n.a.	n.a.
S127-L1	0.07	<.007	0.004	<.02	0.23	0.095	1.3	n.a.	n.a.	n.a.	n.a.	0.002	<.001	n.a.	n.a.
S127-L2	0.06	<.007	0.004	<.02	0.3	0.13	1.5	n.a.	n.a.	n.a.	n.a.	0.002	<.001	n.a.	n.a.
S127-L3	0.05	0.008	0.004	<.02	0.3	0.14	1.4	n.a.	n.a.	n.a.	n.a.	0.002	<.001	n.a.	n.a.
S127-L4	0.06	<.007	0.004	<.02	0.33	0.125	2.5	n.a.	n.a.	n.a.	n.a.	0.002	<.001	n.a.	n.a.
S55-L1	0.04	0.04	0.008	<.02	0.07	<.01	5.6	n.a.	n.a.	n.a.	n.a.	0.004	<.001	n.a.	n.a.
S55-L2	0.29	0.01	0.039	<.02	0.29	<.01	4	n.a.	n.a.	n.a.	n.a.	0.003	<.001	n.a.	<.1
S55-L3	0.12	0.11	0.029	<.02	0.19	0.01	7.4	n.a.	n.a.	n.a.	n.a.	0.004	<.001	n.a.	<.1
S55-L4	0.04	0.009	0.006	<.02	0.08	<.01	4.8	n.a.	n.a.	n.a.	n.a.	0.003	<.001	n.a.	<.1
S26-L3	0.57	<.007	0.131	<.02	0.85	0.145	5.1	n.a.	n.a.	n.a.	n.a.	0.002	<.001	n.a.	n.a.
S26-L4	0.58	0.15	0.133	<.02	0.83	0.125	5.3	n.a.	n.a.	n.a.	n.a.	0.001	<.001	n.a.	n.a.
S26-L5	0.65	0.16	0.138	<.02	0.81	0.115	5.1	n.a.	n.a.	n.a.	n.a.	<.0009	<.001	n.a.	n.a.
<b>Échantillons rejetés</b>															
R7	0.04	n.a.	<.001	<.02	0.04	n.a.	2.7	n.a.	n.a.	0.0011	n.a.	<.0009	<.001	n.a.	n.a.
R8	0.02	n.a.	<.001	<.02	0.07	n.a.	2.8	n.a.	n.a.	0.0013	n.a.	<.0009	<.001	n.a.	n.a.
R9	0.01	n.a.	0.014	<.02	0.07	n.a.	3	n.a.	n.a.	0.0023	n.a.	<.0009	<.001	n.a.	n.a.
R10	0.02	n.a.	0.011	0.28	0.09	n.a.	3.5	n.a.	n.a.	0.0023	n.a.	<.0009	<.001	n.a.	n.a.
R11	0.02	n.a.	0.01	0.44	0.09	n.a.	3.3	n.a.	n.a.	0.0023	n.a.	<.0009	<.001	n.a.	n.a.
R12	0.01	n.a.	0.008	0.27	0.08	n.a.	2.7	n.a.	n.a.	0.0025	n.a.	<.0009	0.003	n.a.	n.a.
R13	n.a.	n.a.	n.a.	n.a.	n.a.	0.145	4.9	n.a.	n.a.	n.a.	n.a.	n.a.	n.a.	n.a.	n.a.
R14	n.a.	n.a.	n.a.	n.a.	n.a.	0.145	5.2	n.a.	n.a.	n.a.	n.a.	n.a.	n.a.	n.a.	n.a.
<b>Duplicata</b>															
D11	0.02	0.01	0.004	0.04	0.04	0.24	0.4	n.a.	n.a.	n.a.	n.a.	0.001	<.001	n.a.	n.a.
D12	0.23	0.03	0.001	<.02	0.64	0.2	1.2	n.a.	n.a.	n.a.	n.a.	<.0009	<.001	n.a.	n.a.
D13	0.02	<.007	0.002	0.9	<.02	<.01	1.2	n.a.	n.a.	n.a.	n.a.	0.002	0.002	n.a.	n.a.
D14	<.002	<.007	0.07	<.02	0.34	0.01	<2	n.a.	n.a.	n.a.	n.a.	0.005	<.001	n.a.	n.a.
D15	<.002	<.007	0.003	<.02	0.02	<.01	0.4	n.a.	n.a.	n.a.	n.a.	0.002	<.001	n.a.	n.a.
D16	0.08	<.007	0.003	<.02	0.24	0.095	1.3	n.a.	n.a.	n.a.	n.a.	0.002	<.001	n.a.	n.a.
D17	0.3	0.01	0.039	<.02	0.27	<.01	4.2	n.a.	n.a.	n.a.	n.a.	0.003	<.001	n.a.	<.1
<b>Échantillons test de qualité</b>															
T1	0.34	<.007	0.23	<.02	0.43	<.01	0.6	n.a.	n.a.	n.a.	n.a.	0.002	<.001	n.a.	n.a.
T2	0.03	<.007	0.002	0.33	0.04	<.01	1	n.a.	n.a.	n.a.	n.a.	0.006	<.001	n.a.	n.a.
T3	0.03	0.008	0.004	0.14	0.02	<.01	4.2	0.0005	0.001	0.0016	0.006	0.003	<.001	<.0001	<.1
T4	<.002	<.007	0.003	<.02	0.03	<.01	3	n.a.	n.a.	n.a.	n.a.	0.002	<.001	n.a.	n.a.
T5	<.002	<.007	0.006	<.02	0.1	<.01	1.6	n.a.	n.a.	n.a.	n.a.	0.002	<.001	n.a.	<.1
T6	<.002	<.007	0.004	0.02	0.02	<.01	2.6	n.a.	n.a.	n.a.	n.a.	0.002	<.001	n.a.	<.1
T7	<.002	<.007	0.005	0.02	0.04	<.01	2.8	n.a.	n.a.	n.a.	n.a.	0.002	<.001	n.a.	<.1
T8	0.56	<.007	0.134	<.02	0.85	0.145	5.2	n.a.	n.a.	n.a.	n.a.	0.001	<.001	n.a.	n.a.

Tableau A2.5. Base de données géochimiques – Paramètres chimiques (#3), calculés et modélisés

ID Site	Ni	Pb	Se	Zn	U	MDT <sup>t</sup>	Dureté Tot. <sup>t</sup> (en CaCO <sub>3</sub> )	TAS <sup>u</sup>	Spéciation <sup>v</sup>	Log pCO <sub>2</sub> <sup>v</sup>	Indice de Saturation <sup>v</sup>				
							HCO <sub>3</sub> <sup>-</sup>	CO <sub>3</sub> <sup>2-</sup>	Cal.	Dol.	Gyp.				
S144-L1	0.001	n.a.	n.a.	0.023	n.a.	321.7	291.8	0.16	306.5	0.719	-2.36	0.24	0.48	-2.09	
S144-L2	0.001	n.a.	n.a.	0.023	n.a.	255.8	237.9	0.17	271.9	0.648	-2.40	0.08	0.29	-2.39	
S144-L3	0.002	n.a.	n.a.	0.007	n.a.	227.2	214.1	0.12	262.7	0.234	-2.01	-0.33	-0.67	-2.47	
S144-L4	0.0008	n.a.	n.a.	0.088	n.a.	268.5	250.4	0.16	284.7	0.488	-2.26	0.00	0.05	-2.30	
S144-L5	0.0008	n.a.	n.a.	0.066	n.a.	259.1	241.3	0.15	272.8	0.482	-2.30	-0.02	0.01	-2.32	
S144-L6	0.0009	n.a.	n.a.	0.29	n.a.	278.6	254.5	0.17	295.1	0.727	-2.38	0.17	0.42	-2.21	
S85-L1	0.003	n.a.	n.a.	<.005	n.a.	220.7	128.1	2.15	259.1	1.658	-2.88	0.30	0.58	-2.61	
S85-L2	0.001	n.a.	n.a.	<.005	n.a.	235.9	181.2	1.00	272.3	0.535	-2.35	0.02	-0.11	-2.46	
S85-L3	<.0008	n.a.	n.a.	<.005	n.a.	242.2	168.7	1.37	274.1	0.669	-2.45	0.05	0.01	-2.47	
S130-L1	0.003	n.a.	n.a.	0.42	n.a.	1878.1	334.7	12.84	221.9	0.735	-2.57	0.06	0.19	-1.94	
S130-L2	0.004	n.a.	n.a.	0.11	n.a.	2604.6	426.3	16.85	268.4	0.745	-2.42	0.05	0.20	-1.63	
S130-L3	0.003	n.a.	n.a.	0.28	n.a.	3079.1	463.5	18.59	232.7	0.624	-2.45	-0.02	0.07	-1.63	
S130-L4	0.003	n.a.	n.a.	0.31	n.a.	1485.5	297.5	10.09	246.4	0.804	-2.56	0.10	0.23	-2.03	
S130-L5	0.003	n.a.	n.a.	<.001	0.43	n.a.	882.3	243.0	6.98	258.3	0.986	-2.60	0.20	0.42	-2.32
S130-L6	0.003	n.a.	n.a.	<.001	0.43	n.a.	1200.0	265.4	8.28	258.1	0.918	-2.55	0.18	0.38	-2.19
SAP-L1	<.0008	n.a.	n.a.	<.005	n.a.	663.7	111.8	10.53	279.0	2.221	-2.89	0.16	0.47	-2.59	
SAP-L2	0.002	n.a.	n.a.	<.005	n.a.	4152.4	173.7	53.17	443.7	2.951	-2.47	0.30	0.58	-2.80	
SAP-L3	0.0009	n.a.	n.a.	<.005	n.a.	4580.7	532.3	30.16	397.1	0.605	-1.82	0.03	0.20	-2.54	
S140-L1	0.002	n.a.	n.a.	0.28	n.a.	232.1	166.0	1.25	259.3	0.796	-2.56	0.20	0.15	-2.22	
S140-L2	0.004	n.a.	n.a.	0.05	n.a.	433.0	155.8	4.88	238.8	0.588	-2.46	-0.05	-0.46	-1.48	
S46-L1	<.008	n.a.	n.a.	0.028	n.a.	607.3	135.2	8.23	353.6	2.032	-2.66	0.08	0.50	-3.09	
S46-L2	<.0008	n.a.	n.a.	0.08	n.a.	597.2	86.8	11.67	367.1	2.186	-2.68	-0.04	0.17	-3.05	
S46-L3	<.0008	n.a.	n.a.	0.079	n.a.	539.1	89.5	10.58	347.6	0.657	-2.20	-0.52	-0.79	-3.04	
S46-L4	<.0008	n.a.	n.a.	0.051	n.a.	547.5	76.4	11.94	348.4	0.500	-2.08	-0.65	-1.14	-3.07	
S46-L4	<.0008	n.a.	n.a.	0.016	n.a.	575.0	85.3	11.30	372.0	0.633	-2.12	-0.52	-0.85	-3.03	
S123-L1	0.001	n.a.	n.a.	<.005	n.a.	731.1	358.6	3.22	342.2	0.695	-2.24	0.17	0.39	-1.78	
S123-L2	0.002	n.a.	n.a.	<.005	n.a.	733.5	351.1	3.25	342.2	0.715	-2.25	0.16	0.39	-1.80	
S123-L3	0.001	n.a.	n.a.	<.005	n.a.	473.9	202.5	3.36	297.9	0.593	-2.30	-0.04	-0.06	-2.53	
S123-L4	0.001	n.a.	n.a.	0.15	n.a.	574.9	255.4	3.27	318.5	0.787	-2.24	0.16	0.47	-2.17	
S123-L5	0.001	n.a.	n.a.	<.005	n.a.	762.7	362.7	3.20	367.1	0.486	-2.03	0.01	0.06	-1.80	
S84-L1	0.002	n.a.	n.a.	0.021	n.a.	348.1	340.9	0.06	380.7	0.229	-1.68	-0.11	-0.42	-2.09	
S84-L2	0.001	n.a.	n.a.	0.036	n.a.	342.7	334.3	0.06	368.8	0.249	-1.76	-0.08	-0.37	-2.07	
S84-L3	0.022	n.a.	n.a.	0.29	n.a.	333.3	320.2	0.08	345.2	0.203	-1.71	-0.19	-0.56	-1.99	
S84-L4	0.035	n.a.	n.a.	0.29	n.a.	343.0	330.2	0.06	369.1	0.205	-1.67	-0.17	-0.55	-1.94	
S84-L5	0.034	n.a.	n.a.	0.29	n.a.	350.4	336.8	0.06	368.6	0.252	-1.76	-0.07	-0.36	-1.97	
S117-L1	0.001	n.a.	n.a.	0.025	n.a.	329.2	81.6	5.30	141.2	1.175	-3.24	0.01	-0.15	-2.35	
S117-L2	0.0008	n.a.	n.a.	0.011	n.a.	359.0	83.6	5.71	141.5	1.077	-3.20	-0.02	-0.26	-2.18	
S117-L3	<.0008	n.a.	n.a.	0.022	n.a.	446.9	88.2	7.41	141.7	1.029	-3.17	-0.06	-0.26	-2.32	
S117-L4	0.002	n.a.	n.a.	0.072	n.a.	423.2	89.4	7.36	141.1	1.107	-3.22	-0.02	-0.20	-2.25	
S77-L1	0.004	n.a.	n.a.	0.25	n.a.	11214.4	3095.2	23.46	54.2	0.083	-2.72	-0.24	-0.62	-0.78	
S77-L2	0.004	n.a.	n.a.	2.1	n.a.	10910.4	2440.4	26.41	97.1	0.176	-2.56	-0.04	-0.16	-0.89	
S77-L3	0.005	n.a.	n.a.	2.8	n.a.	11170.9	3004.2	24.60	158.4	0.393	-2.49	0.42	0.67	-0.80	
S77-L4	0.003	n.a.	n.a.	2.2	n.a.	10826.0	3070.3	22.77	74.2	0.131	-2.65	-0.05	-0.22	-0.77	
S77-L5	0.004	n.a.	n.a.	3.8	n.a.	10999.6	3252.3	22.12	26.0	0.067	-3.29	-0.32	-0.79	-0.79	
S124-L1	<.0008	n.a.	n.a.	<.005	n.a.	769.8	87.6	16.27	553.5	5.197	-2.66	0.37	0.89	-3.18	
S124-L2	<.0008	n.a.	n.a.	<.005	n.a.	864.7	85.9	17.83	539.3	6.256	-2.71	0.45	1.08	-3.43	
S124-L3	<.0008	n.a.	n.a.	<.005	n.a.	682.3	44.6	22.80	527.8	6.275	-2.81	0.13	0.45	-3.52	
S124-L4	<.0008	n.a.	n.a.	<.005	n.a.	1619.8	128.5	23.41	345.5	2.861	-2.79	0.24	0.56	-2.79	
S125-L1	0.007	n.a.	n.a.	0.01	n.a.	1225.1	451.3	4.50	367.3	0.127	-1.41	-0.34	-0.97	-1.46	
S125-L2	0.001	n.a.	n.a.	0.033	n.a.	1108.2	471.9	3.60	342.5	0.177	-1.60	-0.17	-0.58	-1.73	
S125-L3	0.007	n.a.	n.a.	0.092	n.a.	1075.1	451.3	4.50	414.9	0.162	-1.42	-0.25	-0.80	-1.40	
S125-L4	0.008	n.a.	n.a.	0.05	n.a.	1205.4	451.3	4.30	367.3	0.144	-1.48	-0.29	-0.89	-1.48	

Tableau A2.5. (suite)

ID Site	Ni	Pb	Se	Zn	U	MDT <sup>t</sup>	Dureté Tot. <sup>t</sup> (en CaCO <sub>3</sub> )	TAS <sup>u</sup>	Spéciation <sup>v</sup> HCO <sub>3</sub> <sup>-</sup> CO <sub>3</sub> <sup>2-</sup>	Log pCO <sub>2</sub> <sup>v</sup>	Indice de Saturation <sup>v</sup> Cal. Dol. Gyp.
S126-L1	0.0009	n.a.	n.a.	0.043	<.005	485.3	255.8	2.99	380.2 0.595	-2.03	0.18 0.19 -2.31
S126-L2	0.002	n.a.	n.a.	0.25	<.005	502.6	255.8	3.26	390.6 0.900	-2.22	0.35 0.49 -2.35
S126-L3	0.001	n.a.	n.a.	0.061	<.005	395.6	91.5	9.10	429.4 5.796	-2.95	0.70 1.19 -2.55
S126-L4	0.001	n.a.	n.a.	0.13	<.005	420.6	125.8	7.37	433.6 3.546	-2.72	0.63 1.06 -2.41
S129-L1	0.0008	n.a.	n.a.	<.005	n.a.	308.8	279.7	0.11	273.5 0.356	-2.15	0.02 -0.14 -1.87
S129-L2	<.0008	n.a.	n.a.	<.005	n.a.	251.4	227.6	0.18	238.5 0.322	-2.25	-0.09 -0.38 -2.06
S129-L3	<.0008	n.a.	n.a.	<.005	n.a.	282.4	254.9	0.21	297.8 0.376	-2.10	0.01 -0.16 -2.04
S127-L1	0.001	n.a.	n.a.	0.007	n.a.	238.5	211.7	0.45	284.0 0.861	-2.48	0.28 0.50 -2.86
S127-L2	0.002	n.a.	n.a.	<.005	n.a.	258.3	225.8	0.39	295.7 0.897	-2.48	0.32 0.53 -2.34
S127-L3	0.002	n.a.	n.a.	<.005	n.a.	261.7	232.4	0.42	295.1 0.947	-2.50	0.35 0.61 -2.38
S127-L4	0.001	n.a.	n.a.	0.015	n.a.	251.7	219.2	0.45	282.7 1.113	-2.58	0.41 0.75 -2.40
S55-L1	0.007	n.a.	n.a.	1.8	n.a.	1491.3	549.6	4.82	387.4 0.251	-1.65	0.19 -0.72 -1.54
S55-L2	0.004	n.a.	n.a.	0.31	n.a.	1448.5	388.0	7.73	366.3 0.394	-1.88	0.25 -0.54 -1.67
S55-L3	0.004	n.a.	n.a.	0.4	n.a.	1486.8	439.9	6.64	365.2 0.296	-1.78	0.17 -0.75 -1.63
S55-L4	0.005	n.a.	n.a.	0.6	n.a.	1469.4	575.0	5.26	328.3 0.232	-1.72	0.18 -0.72 -1.49
S26-L3	<.0008	n.a.	n.a.	<.005	n.a.	1398.9	131.7	21.23	442.8 2.035	-2.46	0.07 0.24 -2.33
S26-L4	<.0008	n.a.	n.a.	<.005	n.a.	1397.8	127.1	21.99	467.2 3.141	-2.55	0.24 0.64 -2.39
S26-L5	<.0008	n.a.	n.a.	<.005	n.a.	1360.3	125.6	21.34	468.6 2.658	-2.51	0.17 0.46 -2.46
<b>Échantillons rejetés</b>											
R7	n.a.	n.a.	<.001	0.022	n.a.	352.8	305.4	0.433	353.5 --	--	--
R8	n.a.	n.a.	<.001	<.005	n.a.	390.0	323.6	0.467	353.5 --	--	--
R9	n.a.	n.a.	0.001	0.14	n.a.	2876.3	856.9	9.807	402.3 --	--	--
R10	n.a.	n.a.	<.001	0.37	n.a.	3223.9	885.9	11.54	402.3 --	--	--
R11	n.a.	n.a.	<.001	0.096	n.a.	3170.4	898.3	11.61	316.9 --	--	--
R12	n.a.	n.a.	<.001	0.12	n.a.	3242.6	869.5	11.95	402.3 --	--	--
R13	n.a.	n.a.	n.a.	n.a.	n.a.	623.3	--	--	475.4 --	--	--
R14	n.a.	n.a.	n.a.	n.a.	n.a.	644.2	--	--	475.4 --	--	--
<b>Duplicata</b>											
D11	0.001	n.a.	n.a.	0.017	n.a.	260.0	242.0	0.168	280.4 --	--	--
D12	<.008	n.a.	n.a.	0.032	n.a.	628.1	135.4	8.598	365.7 --	--	--
D13	0.032	n.a.	n.a.	0.28	n.a.	347.8	336.8	0.062	377.9 --	--	--
D14	0.003	n.a.	n.a.	<.005	n.a.	11258.7	3136.3	23.3	86.5 --	--	--
D15	<.0008	n.a.	n.a.	<.005	n.a.	304.9	273.1	0.113	280.4 --	--	--
D16	0.002	n.a.	n.a.	0.008	n.a.	240.5	211.7	0.46	304.8 --	--	--
D17	0.004	n.a.	n.a.	0.29	n.a.	1278.4	362.6	8.223	390.1 --	--	--
<b>Échantillons test de qualité</b>											
T1	0.0009	n.a.	n.a.	<.005	n.a.	462.2	209.1	3.008	292.6 --	--	--
T2	0.025	n.a.	n.a.	0.26	n.a.	334.3	320.2	0.083	365.7 --	--	--
T3	0.009	<.004	<.001	0.028	0.009	1041.6	410.7	5.151	463.2 --	--	--
T4	0.007	n.a.	n.a.	0.01	n.a.	1231.4	455.4	4.28	402.3 --	--	--
T5	0.0009	n.a.	n.a.	0.036	n.a.	1105.5	447.0	3.498	365.7 --	--	--
T6	0.007	n.a.	n.a.	0.096	n.a.	1099.4	476.3	4.385	451 --	--	--
T7	0.007	n.a.	n.a.	0.037	n.a.	1200.7	463.7	4.04	377.9 --	--	--
T8	0.0008	n.a.	n.a.	<.005	n.a.	1389.0	130.1	20.97	463.2 --	--	--

Tableau A2.6. Base de données géochimiques – Paramètres isotopiques

ID Site	$\delta^{2}\text{H}$ (‰)	$\delta^{18}\text{O}$ (‰)	$\delta^{13}\text{C}_{\text{CD}}$ (‰)	$^{87}\text{Sr}/^{86}\text{Sr}$	$^{3}\text{H}^{\text{w}}$ (TU)	$^{3}\text{H}^{\text{x}}$ (TU)	$^{14}\text{C}^{\text{y}}$ (pMC)
S144-L1	-77	-10.8	-14.3	n.a.	n.a.	n.a.	n.a.
S144-L2	-75	-10.6	-13.5	n.a.	n.a.	n.a.	n.a.
S144-L3	-78	-11.4	-13.6	n.a.	$<0.8 \pm 0.5$	$<0.9$	$55.9 \pm 0.5$
S144-L4	-75	-11.1	-13.8	n.a.	n.a.	n.a.	n.a.
S144-L5	-74	-10.8	-13.6	n.a.	n.a.	n.a.	n.a.
S144-L6	-73	-10.9	-13.7	n.a.	n.a.	n.a.	n.a.
S85-L1	-80	-11.7	-13.4	n.a.	n.a.	n.a.	n.a.
S85-L2	-80	-12.1	-13.3	n.a.	$0.9 \pm 0.5$	1.0	$53.3 \pm 0.5$
S85-L3	-80	-11.9	-13.2	n.a.	n.a.	n.a.	n.a.
S130-L1	-73	-11.1	-13.9	n.a.	n.a.	n.a.	n.a.
S130-L2	-74	-11.1	-13.1	n.a.	n.a.	n.a.	n.a.
S130-L3	-76	-11.1	-12.8	n.a.	n.a.	n.a.	n.a.
S130-L4	-75	-10.9	-14.6	n.a.	n.a.	n.a.	n.a.
S130-L5	-75	-11.2	-15.1	n.a.	n.a.	n.a.	n.a.
S130-L6	-74	-11.0	-14.9	n.a.	n.a.	n.a.	n.a.
SAP-L1	-71	-10.9	-15.5	n.a.	$8.5 \pm 0.8$	9.2	$46.5 \pm 0.5$
SAP-L2	-88	-12.9	-5.5	0.711037	n.a.	n.a.	n.a.
SAP-L3	-91	-13.0	-10.4	0.711231	$<0.8 \pm 0.5$	$<0.9$	$3.0 \pm 0.1$
S140-L1	-72	-10.6	-15.3	n.a.	n.a.	n.a.	n.a.
S140-L2	-76	-11.1	-11.4	0.709066	n.a.	n.a.	n.a.
S46-L1	-74	-10.9	-17.1	n.a.	n.a.	n.a.	n.a.
S46-L2	-76	-10.9	-16.6	n.a.	n.a.	n.a.	n.a.
S46-L3	-72	-10.9	-16.6	n.a.	$<0.8 \pm 0.5$	$<0.9$	$34.4 \pm 0.3$
S46-L4	-71	-10.8	-16.5	n.a.	n.a.	n.a.	n.a.
S46-L4	-71	-10.8	-16.7	n.a.	n.a.	n.a.	n.a.
S123-L1	-80	-10.8	-15.2	n.a.	n.a.	n.a.	n.a.
S123-L2	-74	-10.9	-15.4	n.a.	n.a.	n.a.	n.a.
S123-L3	-75	-10.9	-11.4	n.a.	n.a.	n.a.	n.a.
S123-L4	-75	-11.0	n.a.	n.a.	n.a.	n.a.	n.a.
S123-L5	-74	-10.9	n.a.	n.a.	n.a.	n.a.	n.a.
S84-L1	-80	-11.7	-14.7	n.a.	n.a.	n.a.	n.a.
S84-L2	-80	-11.9	-15.0	n.a.	n.a.	n.a.	n.a.
S84-L3	-81	-12.1	-14.2	n.a.	$15.0 \pm 1.2$	16.2	$83.5 \pm 0.5$
S84-L4	-80	-11.8	-14.3	n.a.	n.a.	n.a.	n.a.
S84-L5	-80	-11.9	-14.6	n.a.	n.a.	n.a.	n.a.
S117-L1	-77	-11.5	-11.0	n.a.	n.a.	n.a.	n.a.
S117-L2	-78	-11.5	-10.5	n.a.	n.a.	n.a.	n.a.
S117-L3	-77	-11.5	-11.1	n.a.	n.a.	n.a.	n.a.
S117-L4	-80	-11.5	-10.4	0.708987	n.a.	n.a.	n.a.
S77-L1	-77	-11.0	-17.6	n.a.	n.a.	n.a.	n.a.
S77-L2	-78	-11.0	-17.6	n.a.	n.a.	n.a.	n.a.
S77-L3	-79	-11.0	-17.8	n.a.	$<0.8 \pm 0.4$	$<0.9$	$10.9 \pm 0.2$
S77-L4	-77	-11.0	-18.0	n.a.	n.a.	n.a.	n.a.
S77-L5	-77	-11.0	-18.0	n.a.	n.a.	n.a.	n.a.
S124-L1	-72	-10.8	-14.8	n.a.	n.a.	n.a.	n.a.
S124-L2	-75	-10.9	-14.9	n.a.	n.a.	n.a.	n.a.
S124-L3	-73	-10.8	-14.5	n.a.	n.a.	n.a.	n.a.
S124-L4	-76	-11.1	-15.0	n.a.	n.a.	n.a.	n.a.
S125-L1	-72	-10.4	-14.9	n.a.	n.a.	n.a.	n.a.
S125-L2	-75	-11.1	-14.3	n.a.	n.a.	n.a.	n.a.
S125-L3	-70	-10.4	-15.0	n.a.	n.a.	n.a.	n.a.
S125-L4	-70	-10.5	-14.9	n.a.	n.a.	n.a.	n.a.

Tableau A2.6. (suite)

ID Site	$\delta^2\text{H}$ (‰)	$\delta^{18}\text{O}$ (‰)	$\delta^{13}\text{C}_{\text{CID}}$ (‰)	$^{87}\text{Sr}/^{86}\text{Sr}$	$^{3}\text{H}^w$ (TU)	$^{3}\text{H}^x$ (TU)	$^{14}\text{C}^y$ (pMC)
S126-L1	-83	-12.0	-11.9	n.a.	n.a.	n.a.	n.a.
S126-L2	-81	-12.1	-11.9	n.a.	n.a.	n.a.	n.a.
S126-L3	-82	-11.8	n.a.	n.a.	n.a.	n.a.	n.a.
S126-L4	-81	-12.0	-10.7	n.a.	n.a.	n.a.	n.a.
S129-L1	-80	-11.7	-13.3	n.a.	n.a.	n.a.	n.a.
S129-L2	-80	-11.9	-14.4	n.a.	n.a.	n.a.	n.a.
S129-L3	-77	-11.6	-13.2	n.a.	n.a.	n.a.	n.a.
S127-L1	-71	-10.8	-15.6	n.a.	n.a.	n.a.	n.a.
S127-L2	-73	-10.6	-15.6	n.a.	n.a.	n.a.	n.a.
S127-L3	-70	-10.6	-15.7	n.a.	n.a.	n.a.	n.a.
S127-L4	-69	-10.6	-15.5	n.a.	n.a.	n.a.	n.a.
S55-L1	-79	-11.6	-11.8	n.a.	n.a.	n.a.	n.a.
S55-L2	-79	-11.6	-13.8	n.a.	n.a.	n.a.	n.a.
S55-L3	-79	-11.6	-12.0	n.a.	n.a.	n.a.	n.a.
S55-L4	-80	-11.7	-13.6	n.a.	n.a.	n.a.	n.a.
S26-L3	-75	-11.4	-14.9	n.a.	n.a.	n.a.	n.a.
S26-L4	-77	-11.3	-14.7	n.a.	n.a.	n.a.	n.a.
S26-L5	-77	-11.3	-14.5	n.a.	n.a.	n.a.	n.a.
<b>Échantillons rejetés</b>							
R7	-78	-11.5	-13.2	n.a.	n.a.	n.a.	n.a.
R8	-76	-11.1	-13.8	n.a.	n.a.	n.a.	n.a.
R9	-69	-10.8	-15.7	n.a.	n.a.	n.a.	n.a.
R10	-71	-10.4	-15.4	n.a.	n.a.	n.a.	n.a.
R11	-70	-10.9	-15.4	n.a.	n.a.	n.a.	n.a.
R12	-74	-10.4	-15.5	n.a.	n.a.	n.a.	n.a.
R13	-79	-11.3	-14.8	n.a.	n.a.	n.a.	n.a.
R14	-76	-11.3	-14.9	n.a.	n.a.	n.a.	n.a.
<b>Duplicata</b>							
D11	-75	-10.8	-13.2	n.a.	n.a.	n.a.	n.a.
D12	-77	-11.0	-17.1	n.a.	n.a.	n.a.	n.a.
D13	-81	-11.8	-14.5	n.a.	n.a.	n.a.	n.a.
D14	-77	-10.9	-17.7	n.a.	n.a.	n.a.	n.a.
D15	-80	-11.7	-13.3	n.a.	n.a.	n.a.	n.a.
D16	-71	-10.7	-15.6	n.a.	n.a.	n.a.	n.a.
D17	-81	-11.5	-13.4	n.a.	n.a.	n.a.	n.a.
<b>Échantillons test de qualité</b>							
T1	-77	-11.0	-11.6	n.a.	n.a.	n.a.	n.a.
T2	-81	-11.9	-14.8	n.a.	n.a.	n.a.	n.a.
T3	-65	-9.8	n.a.	n.a.	n.a.	n.a.	n.a.
T4	-76	-10.5	-14.8	n.a.	n.a.	n.a.	n.a.
T5	-75	-11.1	n.a.	n.a.	n.a.	n.a.	n.a.
T6	-71	-10.5	n.a.	n.a.	n.a.	n.a.	n.a.
T7	-75	-10.7	n.a.	n.a.	n.a.	n.a.	n.a.
T8	-77	-11.3	-14.8	n.a.	n.a.	n.a.	n.a.



## **Appendice B**

### **LA CARACTÉRISATION ISOTOPIQUE DES PRÉCIPITATIONS**

## B1 Information sur les stations

Tableau B1.1. Stations d'échantillonnage de caractérisation isotopique des précipitations

ID Station (Fig. B1.1)	Nom de la Station	ID Site (Carte 2.1; Appendice H)	Localisation	Abscisse (m)	Ordonnée (m)
A	Calumet	S57	Puits municipal	528708	5055473
B	Saint-Philippe	S63	Puits municipal (Chatham)	544508	5052722
C	Lachute	—	Ministère des transports	554450	5053150
D	Thomas-Gore	—	Usine de filtration	556800	5059100
E	Saint-Hyacinthe	—	Terrain privé	562100	5054150
F	Saint-Vincent	S144	Terrain privé	566227	5048158
G	Oka	—	Terrain privé	572900	5039400
H	Sainte-Thérèse	—	Terrain privé	587400	5056650
I	Saint-Janvier	S92	Station de pompage	583145	5060985
J	Sainte-Anne	S27	Station de pompage	589430	5067770
1	Lachute	—	Centre de recyclage	554850	5053400
2	Saint-Vincent	S144	Terrain privé	566227	5048158
3	Montée-Guénette	S125	Terrain privé	580729	5063973

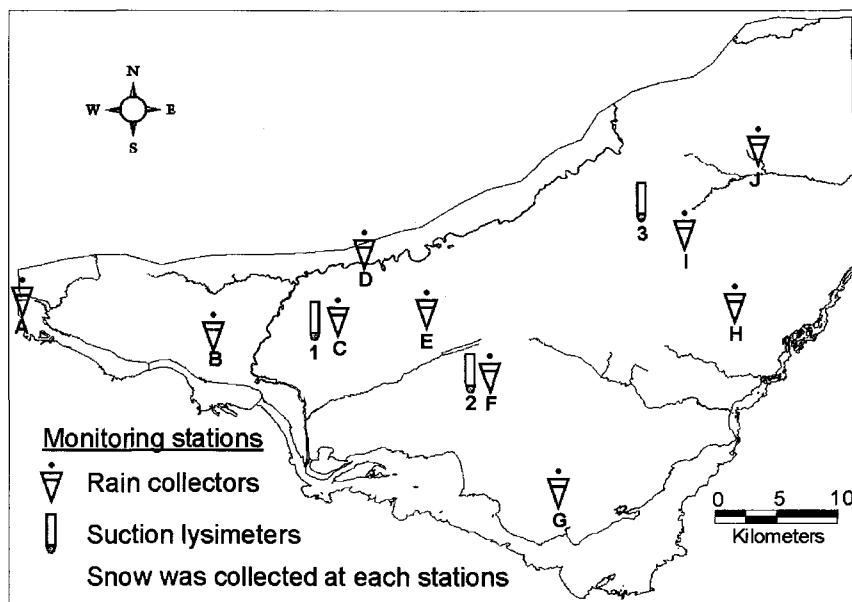


Figure B1.1. Localisation des stations d'échantillonnage de caractérisation isotopique des précipitations : collecteur de pluie, échantillonnage de la neige et lysimètres à succion.

## B2 Résultats des eaux de pluie

Tableau B2.1. Données isotopiques ( $\delta^{2\text{H}}$  et  $\delta^{18\text{O}}$ ) des échantillons de pluie ayant servi à établir la Droite des Eaux Météoriques des Basses-Laurentides (*Basses-Laurentides Meteoric Water Line*, Figure 3.4a; Chapitre 3)

Échantillons (Pluie/Station/mois/année)	Station ID (Fig. B1.1)	Date d'échantillonnage	$\delta^{18\text{O}} (\text{\textperthousand})$	$\delta^{2\text{H}} (\text{\textperthousand})$
P/Calumet/05/00	A	2000-05-31	-7.8	-46
P/Calumet/06/00	A	2000-06-29	-5.2	-37
P/Calumet/07/00	A	2000-08-01	-8.3	-54
P/Calumet/08/00	A	2000-08-31	-7.2	-41
P/Calumet/09/99	A	1999-10-05	-9.4	-61
P/Calumet/10/00	A	2000-10-30	-10.0	-62
P/Calumet/10/99	A	1999-11-01	-12.4	-82
P/Lachute/05/00	C	2000-05-31	-7.0	-39
P/Lachute/06/00	C	2000-06-29	-6.4	-36
P/Lachute/07/00	C	2000-08-01	-8.4	-55
P/Lachute/08/00	C	2000-08-31	-7.0	-40
P/Lachute/09/00	C	2000-09-28	-7.3	-43
P/Lachute/09/99	C	1999-10-05	-10.6	-71
P/Lachute/10/99	C	1999-11-01	-14.2	-96
P/Oka/05/00	G	2000-05-31	-7.1	-43
P/Oka/06/00	G	2000-06-29	-5.7	-33
P/Oka/07/00	G	2000-08-01	-8.3	-58
P/Oka/08/00	G	2000-08-31	-7.5	-48
P/Oka/09/00	G	2000-09-28	-6.5	-45
P/Oka/09/99	G	1999-10-05	-12.5	-88
P/Oka/10/00	G	2000-10-31	-10.5	-65
P/Oka/10/99	G	1999-11-01	-14.5	-98
P/Ste-Anne/05/00	J	2000-05-31	-7.5	-50
P/Ste-Anne/06/00	J	2000-06-29	-6.2	-35
P/Ste-Anne/07/00	J	2000-08-01	-7.8	-50
P/Ste-Anne/08/00	J	2000-09-01	-7.0	-40
P/Ste-Anne/09/99	J	1999-10-05	-11.7	-81
P/Ste-Anne/10/00	J	2000-10-30	-10.8	-64
P/Ste-Anne/10/99	J	1999-11-01	-13.7	-91
P/Ste-Therese/05/00	H	2000-05-31	-7.1	-39
P/Ste-Therese/06/00	H	2000-06-29	-5.9	-31
P/Ste-Therese/07/00	H	2000-08-01	-8.8	-57
P/Ste-Therese/08/00	H	2000-09-01	-6.7	-40
P/Ste-Thérèse/08/99	H	1999-08-31	-8.2	-52
P/Ste-Thérèse/09/99	H	1999-10-05	-12.4	-85
P/Ste-Therese/10/00	H	2000-10-30	-10.6	-64
P/Ste-Thérèse/10/99	H	1999-11-01	-14.4	-96

Tableau B2.1. (Suite)

Échantillons (Pluie/Station/mois/année)	Station ID (Fig. B1.1)	Date d'échantillonnage	$\delta^{18}\text{O}$ (‰)	$\delta^2\text{H}$ (‰)
P/St-Hyacinthe/06/00	E	2000-06-29	-6.7	-35
P/St-Hyacinthe/07/00	E	2000-08-01	-10.6	-75
P/St-Hyacinthe/08/00	E	2000-08-31	-7.2	-42
P/St-Hyacinthe/09/00	E	2000-09-28	-7.0	-40
P/St-Hyacinthe/09/99	E	1999-10-05	-11.3	-74
P/St-Hyacinthe/10/00	E	2000-10-31	-10.3	-66
P/St-Hyacinthe/10/99	E	1999-11-01	-12.9	-87
P/St-Janvier/05/00	I	2000-05-31	-7.6	-42
P/St-Janvier/06/00	I	2000-06-29	-6.3	-35
P/St-Janvier/07/00	I	2000-08-01	-9.0	-60
P/St-Janvier/08/00	I	2000-09-01	-7.2	-49
P/St-Janvier/09/99	I	1999-10-05	-11.7	-82
P/St-Janvier/10/00	I	2000-10-30	-10.7	-70
P/St-Philippe/05/00	B	2000-05-31	-9.6	-65
P/St-Philippe/06/00	B	2000-06-29	-6.7	-41
P/St-Philippe/07/00	B	2000-08-01	-7.9	-53
P/St-Philippe/08/00	B	2000-09-01	-6.9	-37
P/St-Philippe/09/00	B	2000-09-28	-7.6	-45
P/St-Philippe/09/99	B	1999-10-05	-9.7	-63
P/St-Philippe/10/00	B	2000-10-31	-9.7	-62
P/St-Vincent/05/00	F	2000-05-31	-7.2	-42
P/St-Vincent/08/00	F	2000-08-31	-7.2	-43
P/St-Vincent/09/00	F	2000-09-28	-7.0	-40
P/St-Vincent/09/99	F	1999-10-05	-11.9	-76
P/St-Vincent/10/00	F	2000-10-30	-10.9	-72
P/St-Vincent/10/99	F	1999-11-01	-12.7	-88
P/Thomas/05/00	D	2000-05-31	-7.0	-39
P/Thomas/06/00	D	2000-06-29	-5.8	-38
P/Thomas/07/00	D	2000-08-01	-8.1	-54
P/Thomas/08/00	D	2000-09-01	-6.9	-37
P/Thomas/09/00	D	2000-09-28	-7.2	-40
P/Thomas/09/99	D	1999-10-05	-11.4	-76
P/Thomas/10/00	D	2000-10-31	-10.3	-66
P/Thomas/10/99	D	1999-11-01	-12.2	-79

### B3 Résultats de la neige

Tableau B3.1. Données isotopiques ( $\delta^2\text{H}$  et  $\delta^{18}\text{O}$ ) des échantillons de neige présentés sur la figure de la Droite des Eaux Météoriques des Basses-Laurentides (*Basses-Laurentides Meteoric Water Line*, Figure 3.4a; Chapitre 3)

Échantillons (Neige/Station/année)	Station ID (Fig. B1.1)	Date	Épaisseur totale du dépôt	$\delta^{18}\text{O}$ (‰)	$\delta^2\text{H}$ (‰)
N/Anne/00	J	2000-03-02	24 cm	-18.8	-137
N/Anne/00#2	J	2000-03-10	—	-19.0	-139
N/Calu/00	A	2000-03-02	13 cm	-18.0	-129
N/Guen/00	3	2000-03-02	24 cm	-16.7	-121
N/Guen/00#2	3	2000-03-10	—	-17.8	-133
N/Henr/00	—	2000-03-02	39 cm	-18.4	-135
N/Henr/00#2	—	2000-03-10	—	-17.2	-126
N/Hyac/00	E	2000-03-02	20cm	-17.9	-133
N/Hyac/00#2	E	2000-03-10	—	-16.6	-121
N/Lach/00	1	2000-03-02	15 cm	-16.8	-128
N/Oka/00	G	2000-03-02	—	-20.2	-150
N/Oka/00#3	G	2000-03-16	—	-16.3	-112
N/Phil/00	B	2000-03-02	23 cm	-15.5	-108
N/Thom/00	D	2000-03-02	33cm	-17.9	-133
N/Vince/00	F	2000-03-02	27cm	-18.6	-136
N/Vince/00#2	F	2000-03-10	—	-16.9	-127
N/Vince/00#3	F	2000-03-16	—	-16.5	-121
N/Hyac/01	E	2001-03-09	50 cm	-16.4	-107
N/Lach/01	1	2001-03-09	35 cm	-14.7	-104
N/Phil/01	B	2001-03-09	25 cm	-15.9	-105
N/Vinc/01	F	2001-03-09	60 cm	-17.9	-113
N/Thom/01	D	2001-03-09	50 cm	-15.5	-96
N/Guen/01	3	2001-03-09	50 cm	-14.4	-101
N/Anne/01	J	2001-03-09	25 cm	-15.8	-107
N/Oka/01	G	2001-03-09	30 cm	-15.0	-94

Un carottier a été utilisé pour échantillonner l'épaisseur complète de la neige.

La station Henr (Henriette) est localisée au site S131(voir Carte 2.1; Appendice H)

Tableau B3.2. Données isotopiques ( $\delta^2\text{H}$  et  $\delta^{18}\text{O}$ ) des échantillons de neige prélevés à différentes profondeur dans le dépôt de neige

Échantillons (Neige/Station/niveau/année) (Fig. B1.1)	Station ID	Date	Niveau échantillonné	$\delta^{18}\text{O}$ (‰)	$\delta^2\text{H}$ (‰)
N/Guen-HB/00	3	2000-03-02	Horizon de base	-15.5	-111
N/Guen-N1/00	3	2000-03-02	Surface à 10 cm	-16.4	-116
N/Guen-N2/00	3	2000-03-02	10 cm à la base (24 cm)	-16.8	-123
N/Henr-HB/00	-	2000-03-02	Horizon de base	-17.6	-127
N/Henr-N1/00	-	2000-03-02	Surface à 20 cm	-18.5	-136
N/Henr-N2/00	-	2000-03-02	20 cm à la base (39 cm)	-18.3	-135
N/Lach-HB/00	1	2000-03-02	Horizon de base	-17.7	-132
N/Lach-HS/00	1	2000-03-02	Horizon de surface	-17.1	-128
N/Vinc-HB/00	F	2000-03-02	Horizon de base (15 cm)	-17.3	-126
N/Vinc-N1/00	F	2000-03-02	Surface à 13 cm	-18.1	-135
N/Vinc-N2/00	F	2000-03-02	13 cm à la base (27 cm)	-17.9	-133

La station Henr (Henriette) est localisée au site S131(voir Carte 2.1; Appendice H)

Tableau B3.3. Données isotopiques ( $\delta^2\text{H}$  et  $\delta^{18}\text{O}$ ) des échantillons d'eau de fonte

Échantillons (Eau de fonte/Station/année) (Fig. B1.1)	Station ID	Date	Provenance	$\delta^{18}\text{O}$ (‰)	$\delta^2\text{H}$ (‰)
F/Calu/00	A	2000-03-02	Sous la neige	-15.2	-104
F/Henr/00	-	2000-03-02	Sous la neige	-16.6	-117
F/Lach/00	1	2000-03-02	Dans un fossé	-18.1	-131
F/Phil/00	B	2000-03-02	Sous la neige	-16.7	-120

La station Henr (Henriette) est localisée au site S131(voir Carte 2.1; Appendice H)

#### B4 Résultats des eaux d'infiltration

Tableau B4.1. Données isotopiques ( $\delta^2\text{H}$  et  $\delta^{18}\text{O}$ ) des eaux d'infiltration échantillonnés dans les lysimètres à succion.

Échantillons (Lysinètre/Station/mois/année)	Station ID (Fig. B1.1)	Date d'échantillonnage	$\delta^{18}\text{O}$ (‰)	$\delta^2\text{H}$ (‰)
L/Guenette#1	3	2000-05-24	-11.1	-74
L/Guenette/05/00	3	2000-06-02	-11.2	-74
L/Guenette/06/00	3	2000-06-29	-10.1	-67
L/Guenette/07/00	3	2000-08-02	-9.2	-63
L/Lachute#1	1	2000-05-24	-11.2	-74
L/Lachute/05/00	1	2000-06-02	-11.3	-75
L/Lachute/06/00	1	2000-06-29	-11.2	-72
L/Lachute/07/00	1	2000-08-02	-11.2	-73
L/Lachute/08/00	1	2000-09-01	-11.3	-73
L/Lachute/09/00	1	2000-09-29	-11.4	-78
L/Lachute/10/00	1	2000-10-31	-11.4	-76
L/St-Vincent#1	2	2000-05-24	-10.8	-73
L/St-Vincent/07/00	2	2000-08-02	-10.9	-75
L/St-Vincent/09/00	2	2000-09-29	-11.0	-76
L/St-Vincent/10/00	2	2000-10-31	-10.8	-77

Tableau B4.2. Données isotopiques ( $\delta^2\text{H}$  et  $\delta^{18}\text{O}$ ) des eaux d'infiltration échantillonnés dans les cases lysimétriques

Échantillons	Site	Date	$\delta^{18}\text{O}$ (‰)	$\delta^2\text{H}$ (‰)
LAV-01	LAV-01	2001-02-03	-10.3	-63
LAV-02	LAV-01	2001-04-13	-9.0	-
LAV-03	LAV-01	2001-04-19	-9.7	-48
LAV-04	LAV-01	2001-06-01	-10.9	-61
LAV-05	LAV-01	2001-09-07	-10.9	-62
LAV-06	LAV-01	2001-11-02	-10.8	-99
JANV-01	JANV-01	2001-02-03	-9.5	-58
JANV-02	JANV-01	2001-03-17	-9.6	-54
JANV-03	JANV-01	2001-04-13	-15.7	-101
JANV-04	JANV-01	2001-04-27	-11.3	-83
JANV-05	JANV-01	2001-09-07	-10.7	-62
JANV-06	JANV-01	2001-09-28	-8.2	-54

Les échantillons ont été prélevés par Andréanne Hamel. Les détails sur les sites peuvent être trouvés dans Hamel (2002).

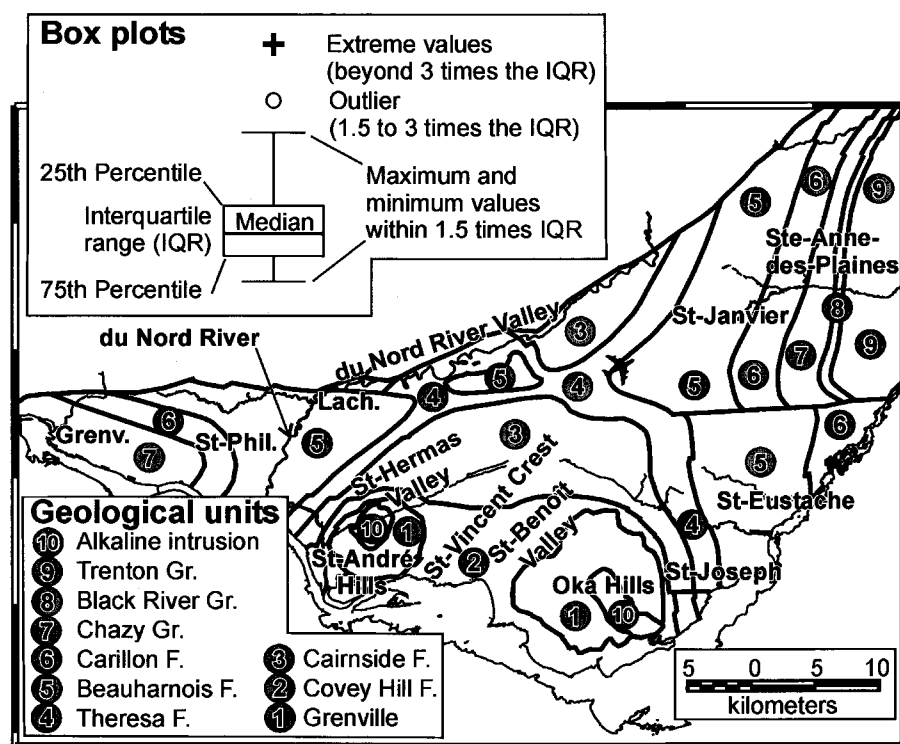


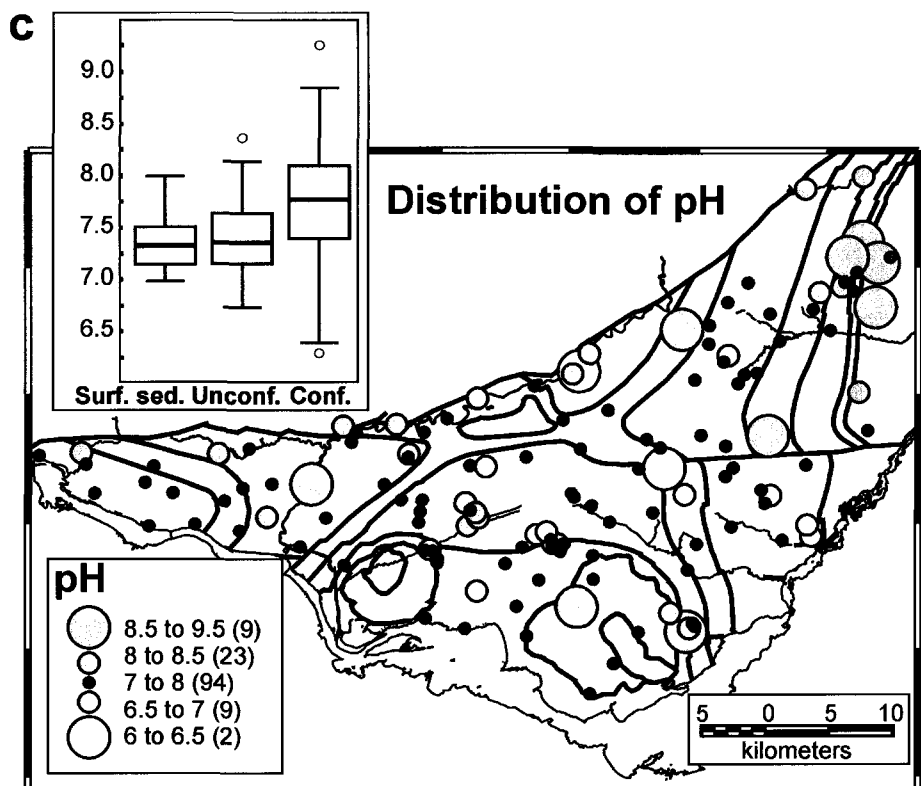
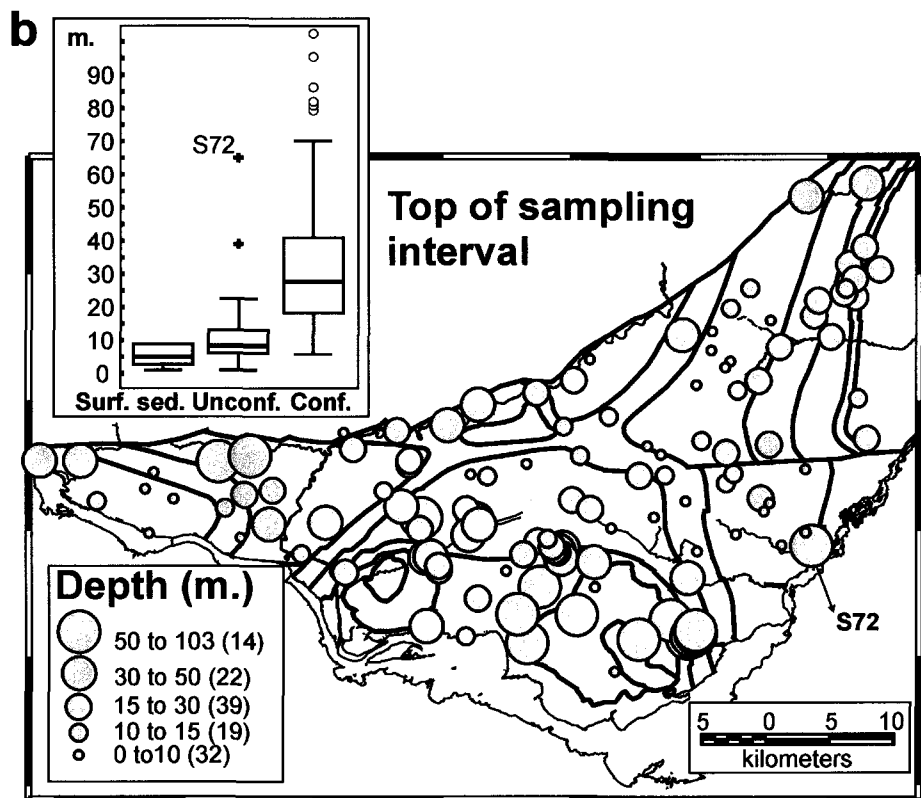
## **Appendice C**

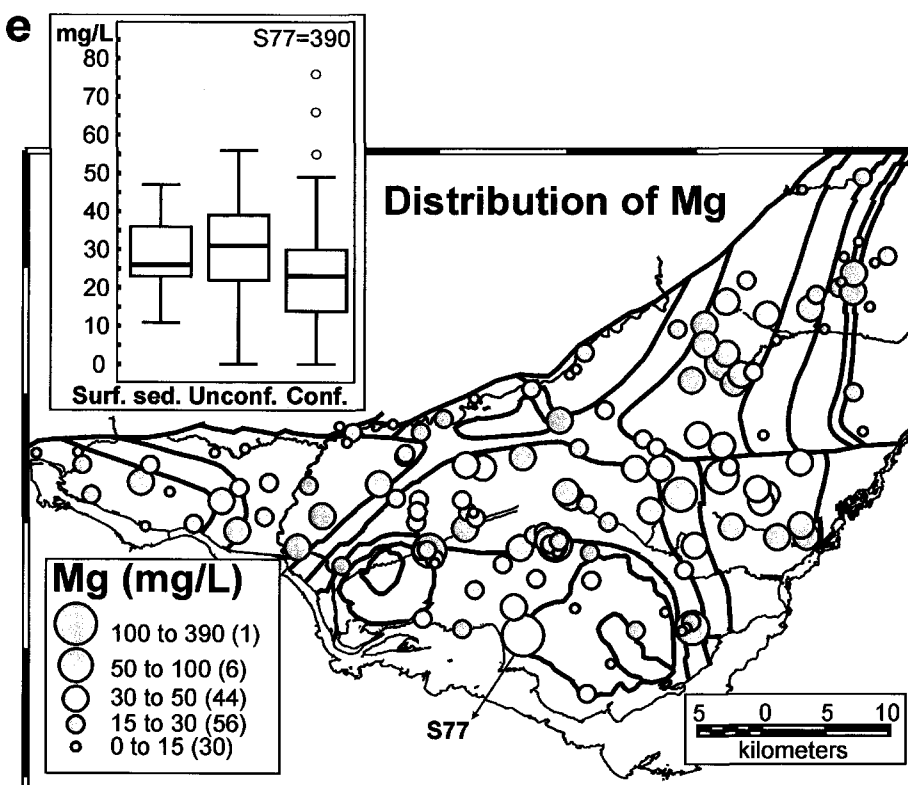
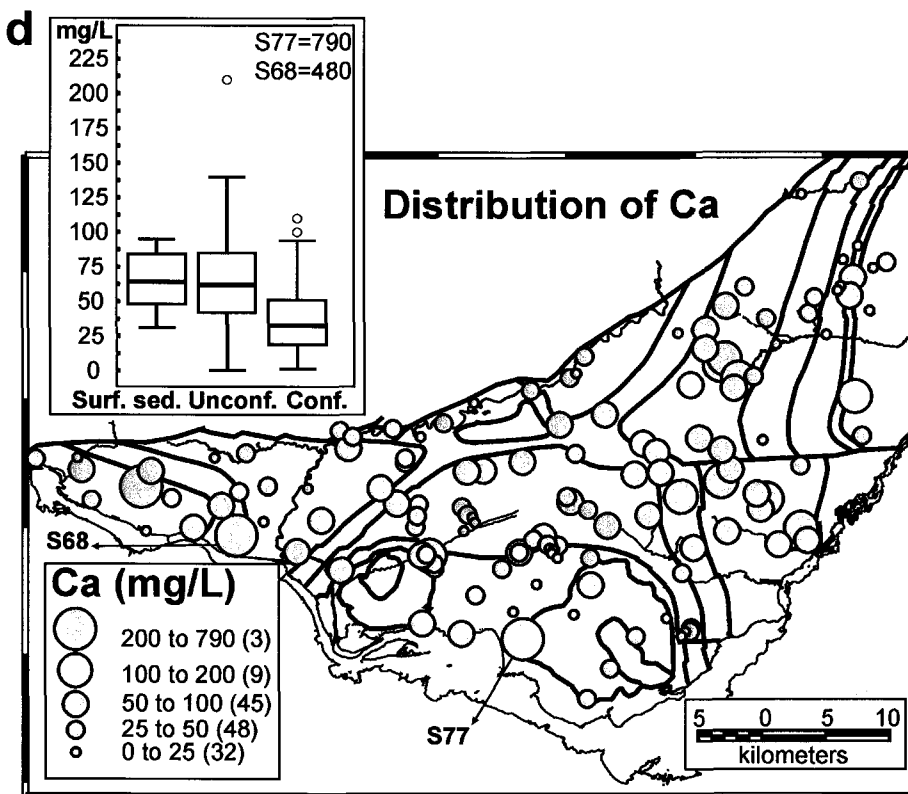
### **CARTES SUPPLÉMENTAIRES**

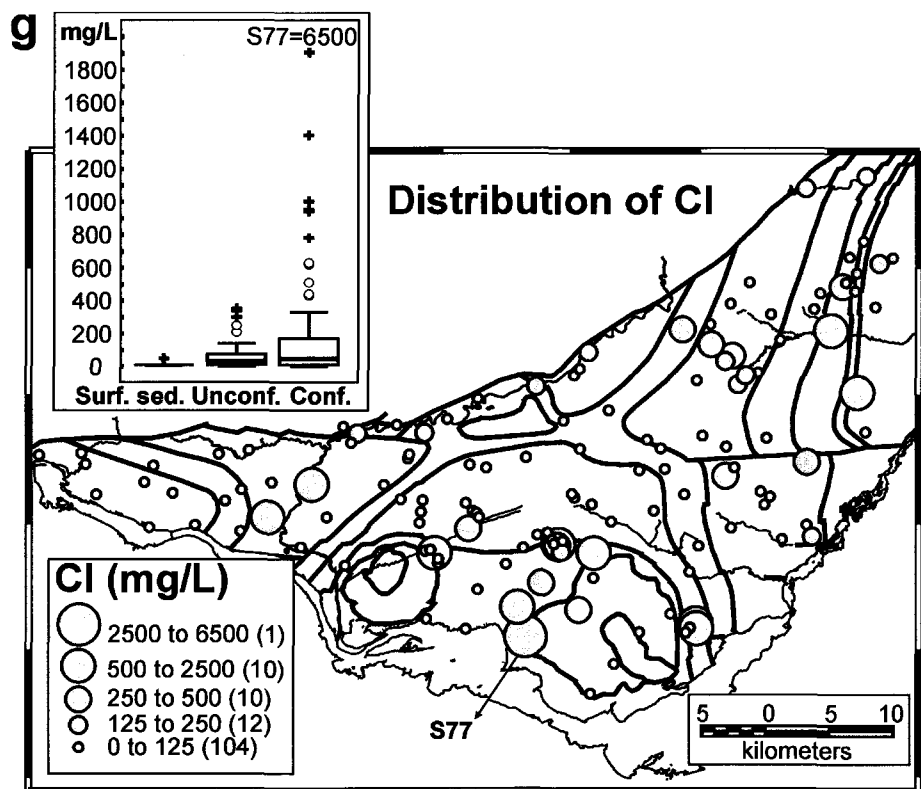
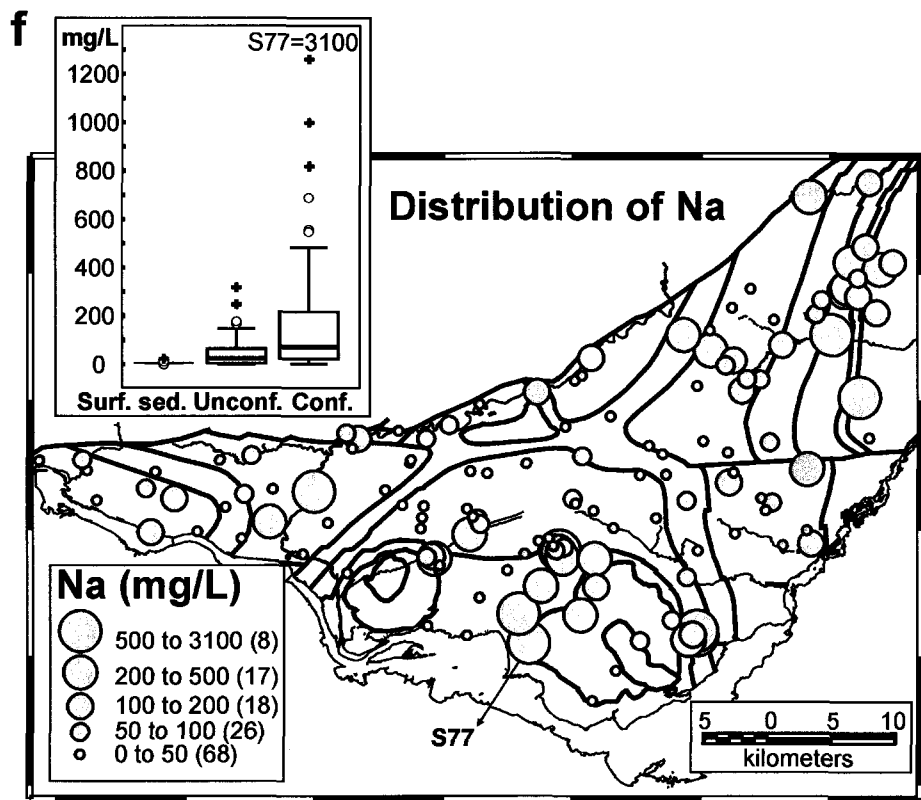
## C1 Chapitre 3

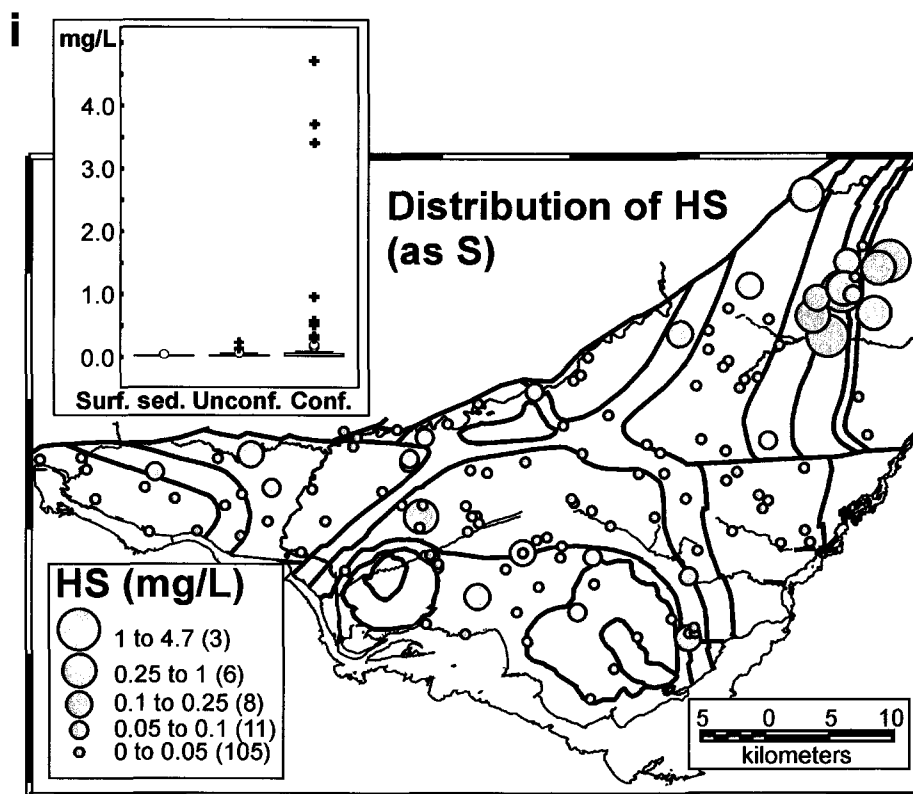
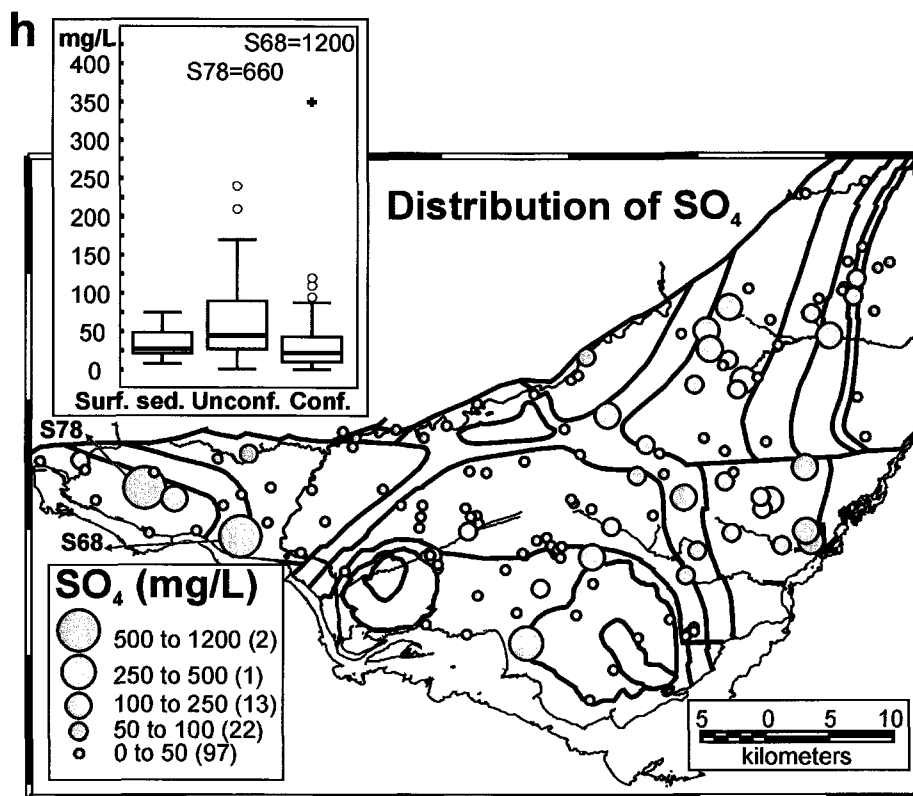
Figure C1.1. a Légende pour les Fig. C1.1b à C1.1t (Grenv. : Grenville, St. Phil. : St-Philippe, Lach. : Lachute; carte géologique modifiée de Rocher et al., in press). Diagrammes en boîte (*Box plots*) du système aquifère des Basses-Laurentides pour les conditions hydrogéologiques, et les cartes de distribution régionale pour les échantillons provenant des unités de roc, mixtes, et de sédiments sous l'argile pour b profondeur du haut de l'intervalle ouvert, c pH, d Ca, e Mg, f Na, g Cl, h SO<sub>4</sub>, i HS, j Br, k NO<sub>3</sub>, l Fe, m Mn, n F, o Sr, p Ba, q B, r PO<sub>4</sub>, s NH<sub>4</sub>, et t DOC (Surf. Sed. : Surface sediments and springs, Unconf.: Unconfined and semi-confined, Conf.: Confined)

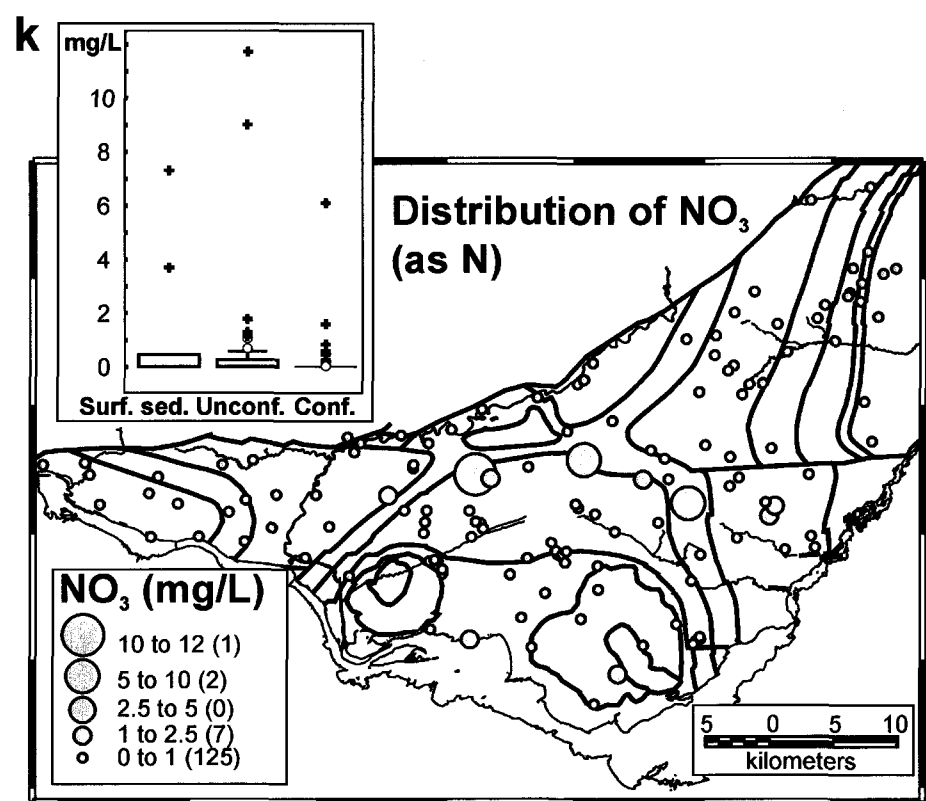
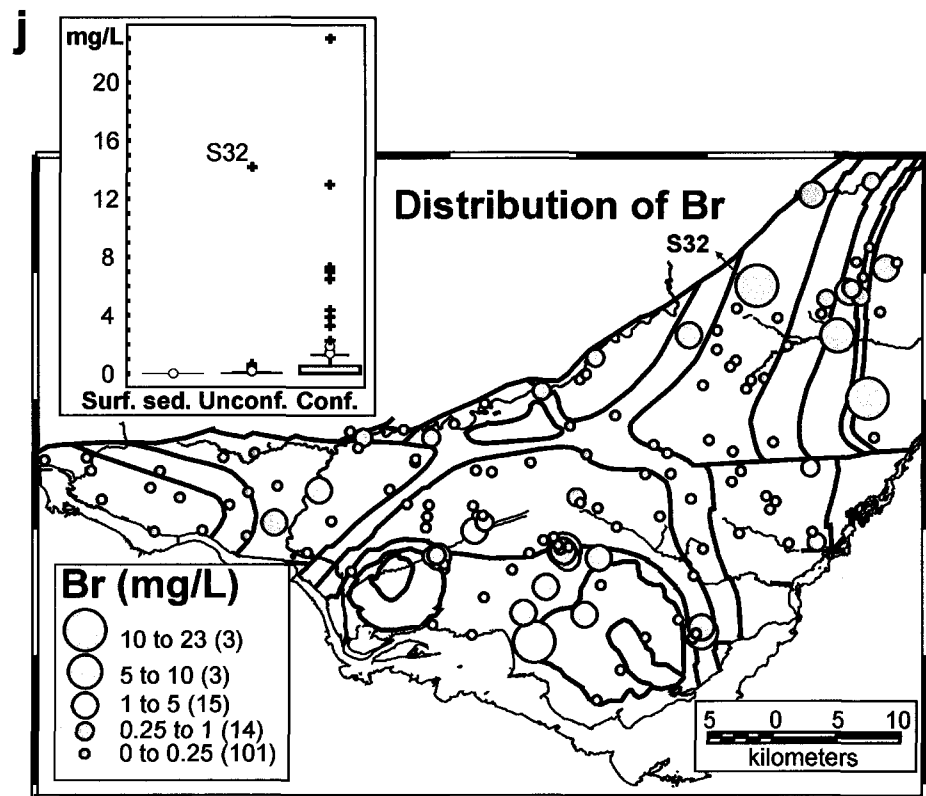
**a LEGEND**

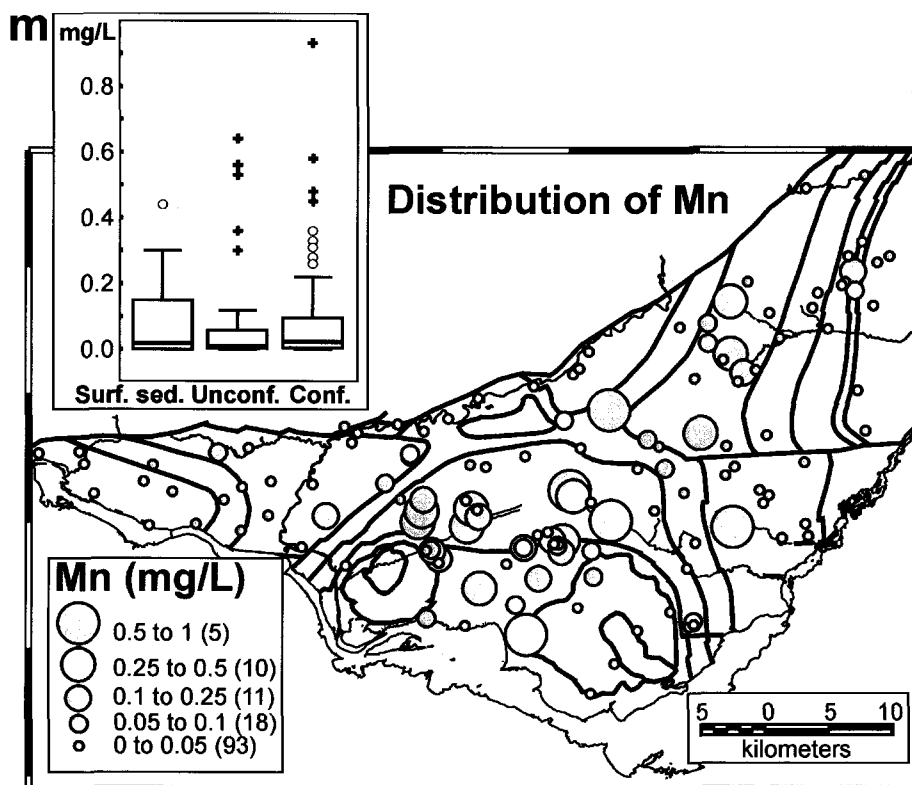
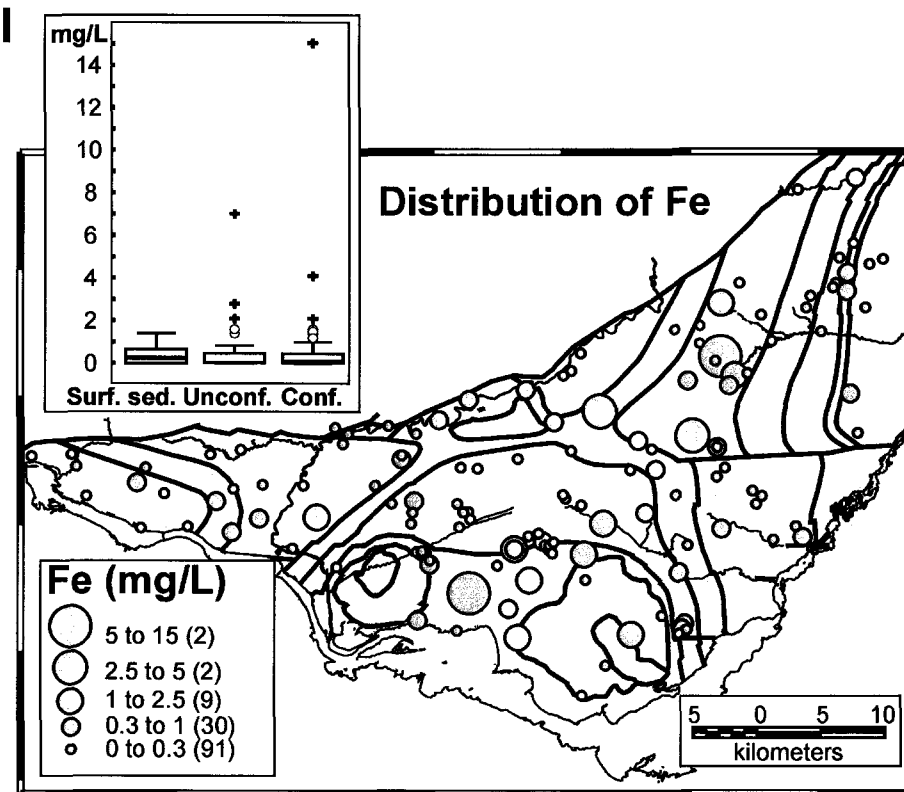


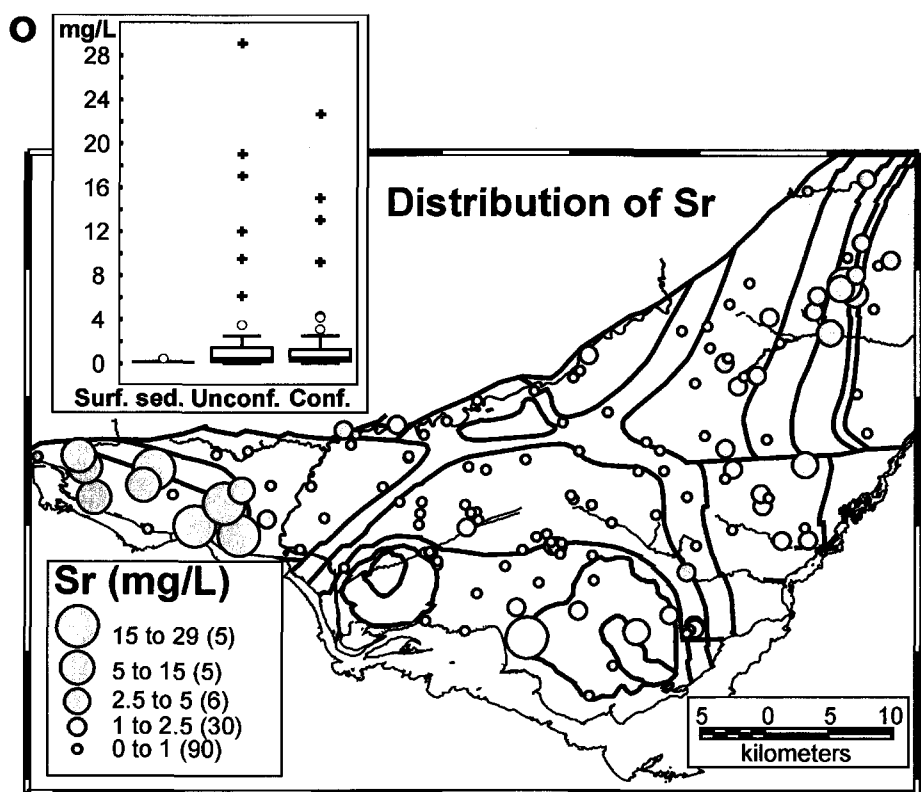
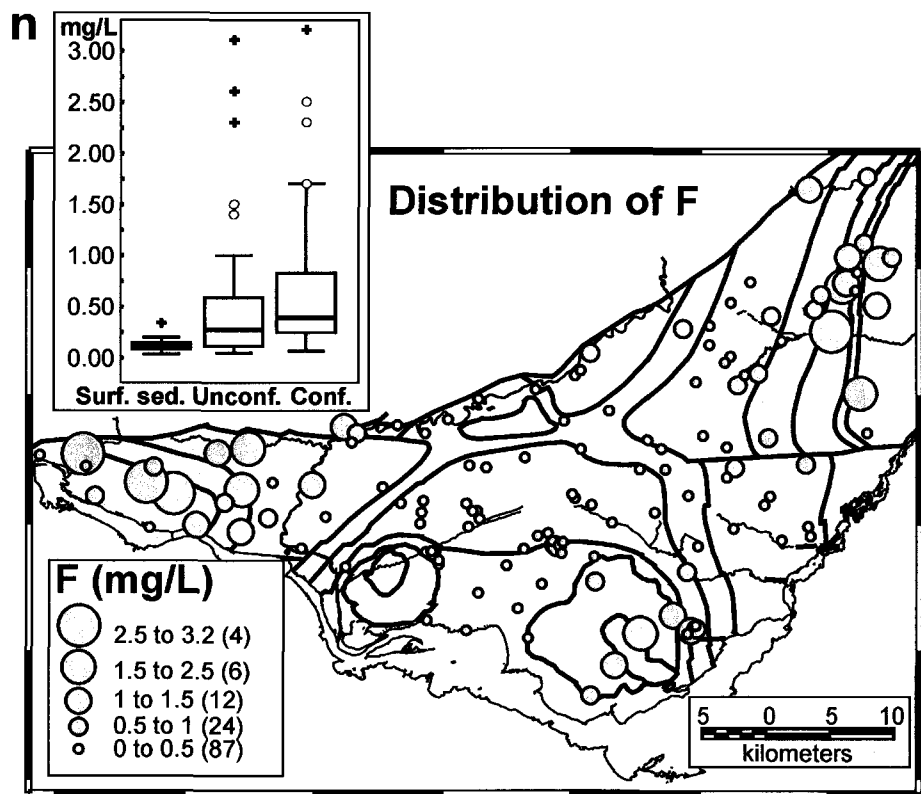


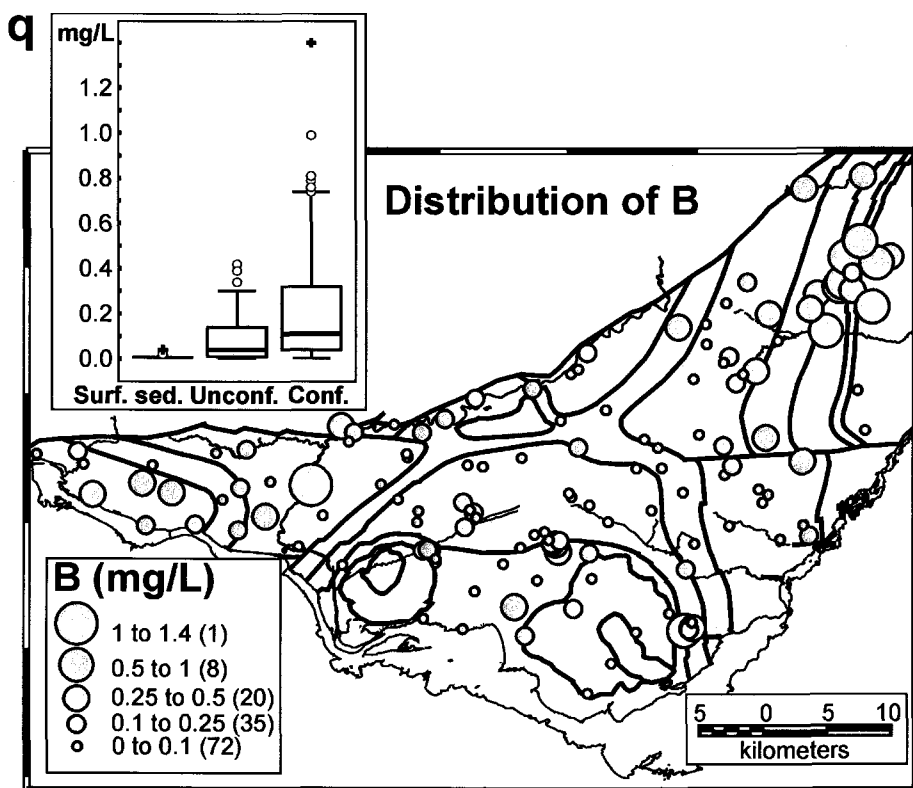
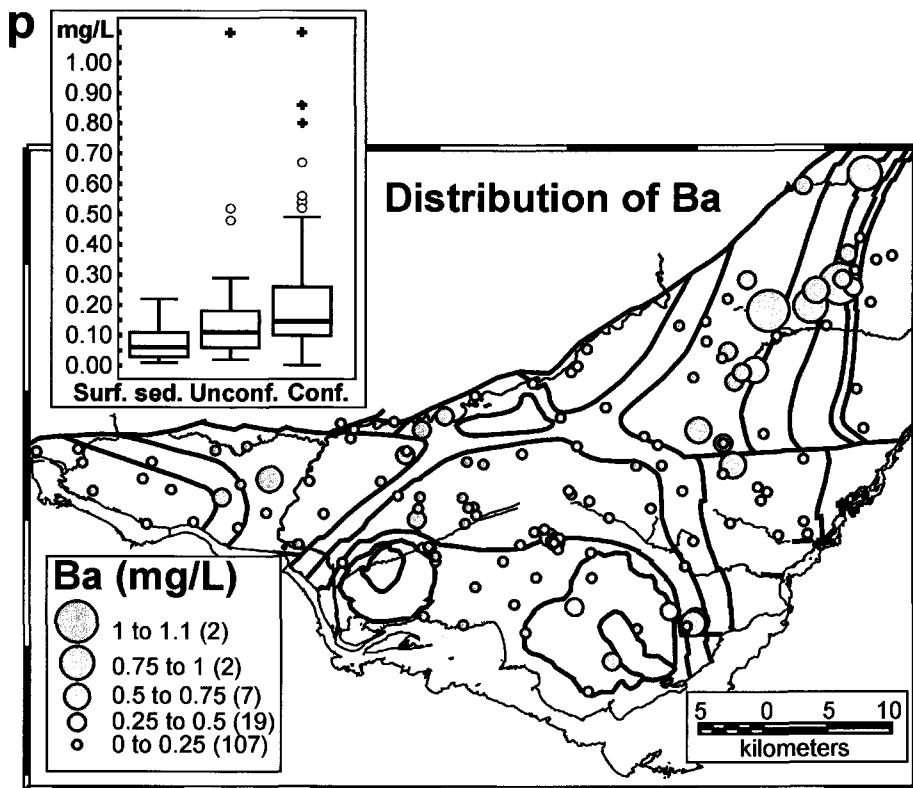


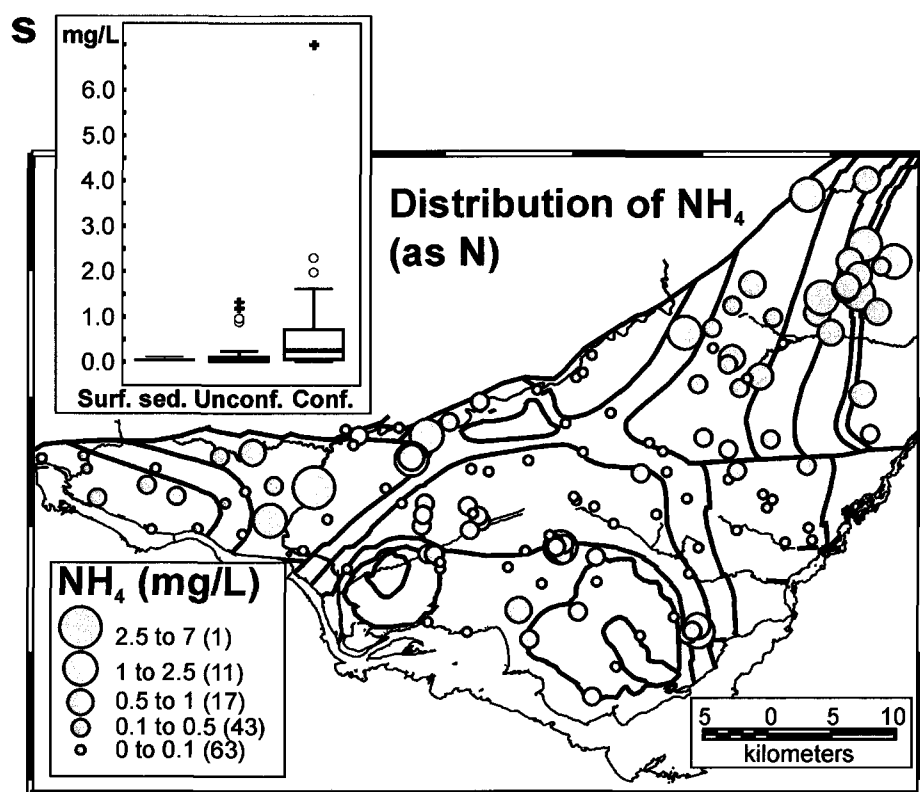
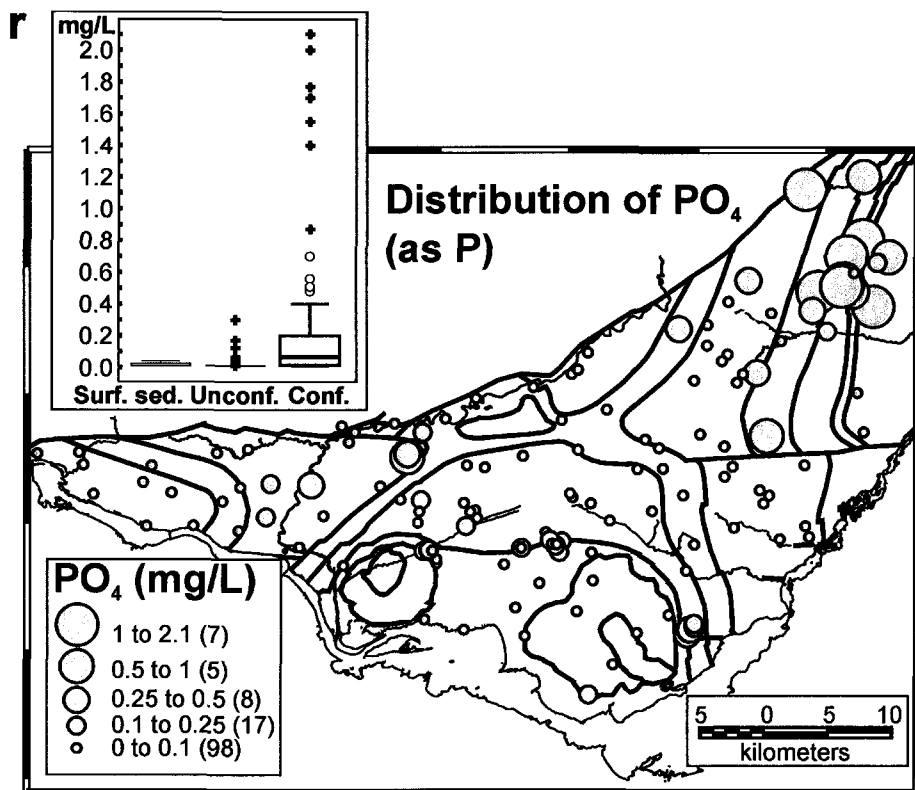


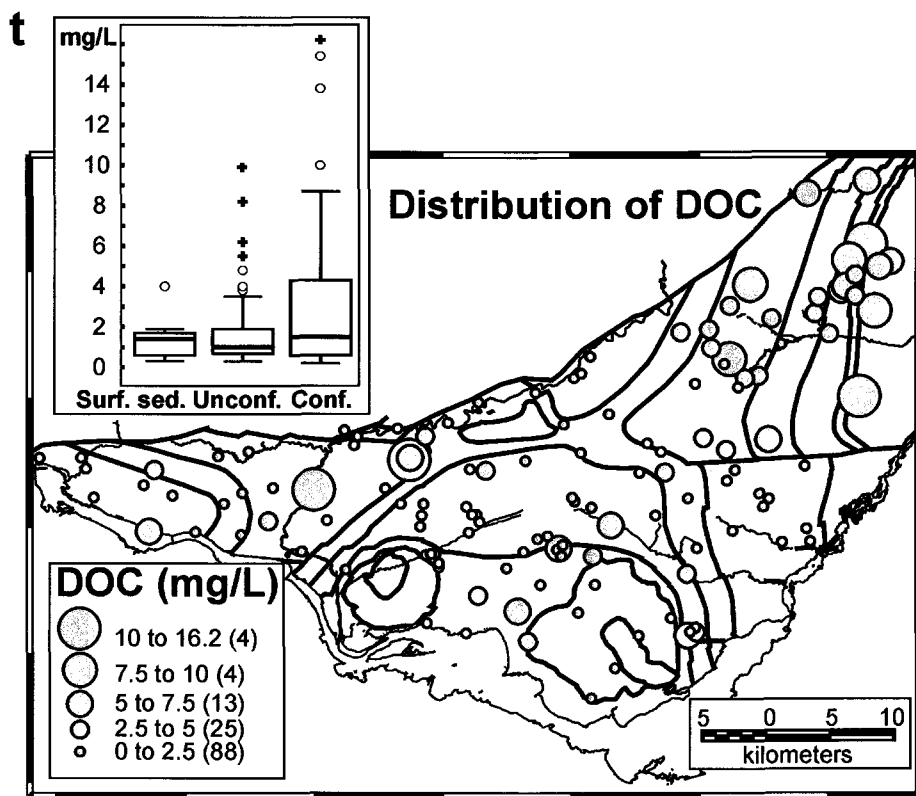












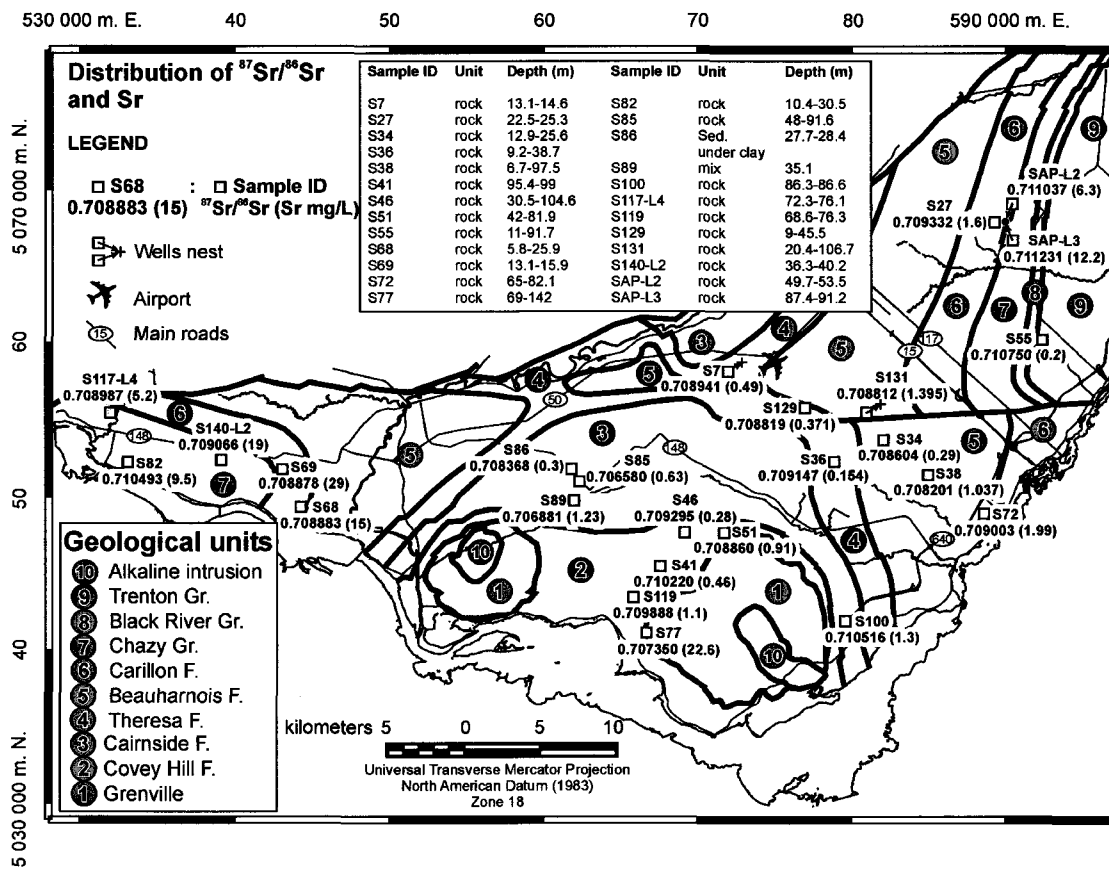


Figure C1.2. Distribution régionale de  $^{87}\text{Sr}/^{86}\text{Sr}$  et des concentrations en Sr (carte géologique modifiée de Rocher et al., sous presse).

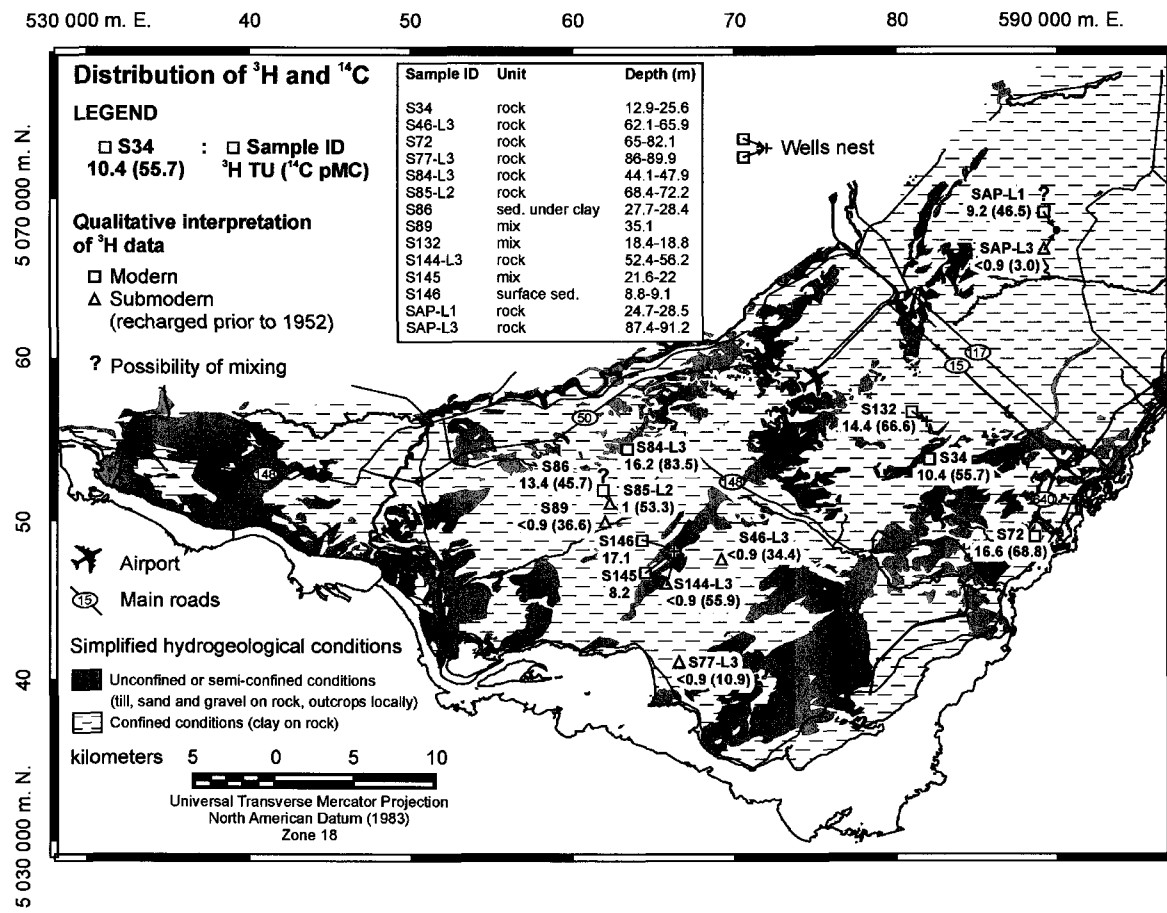


Figure C1.3. Distribution régionale du  $^3\text{H}$  et de  $^{14}\text{C}$  du CID (carte des conditions hydrogéologiques modifiée de Hamel et al., 2001).

## C2 Chapitre 5

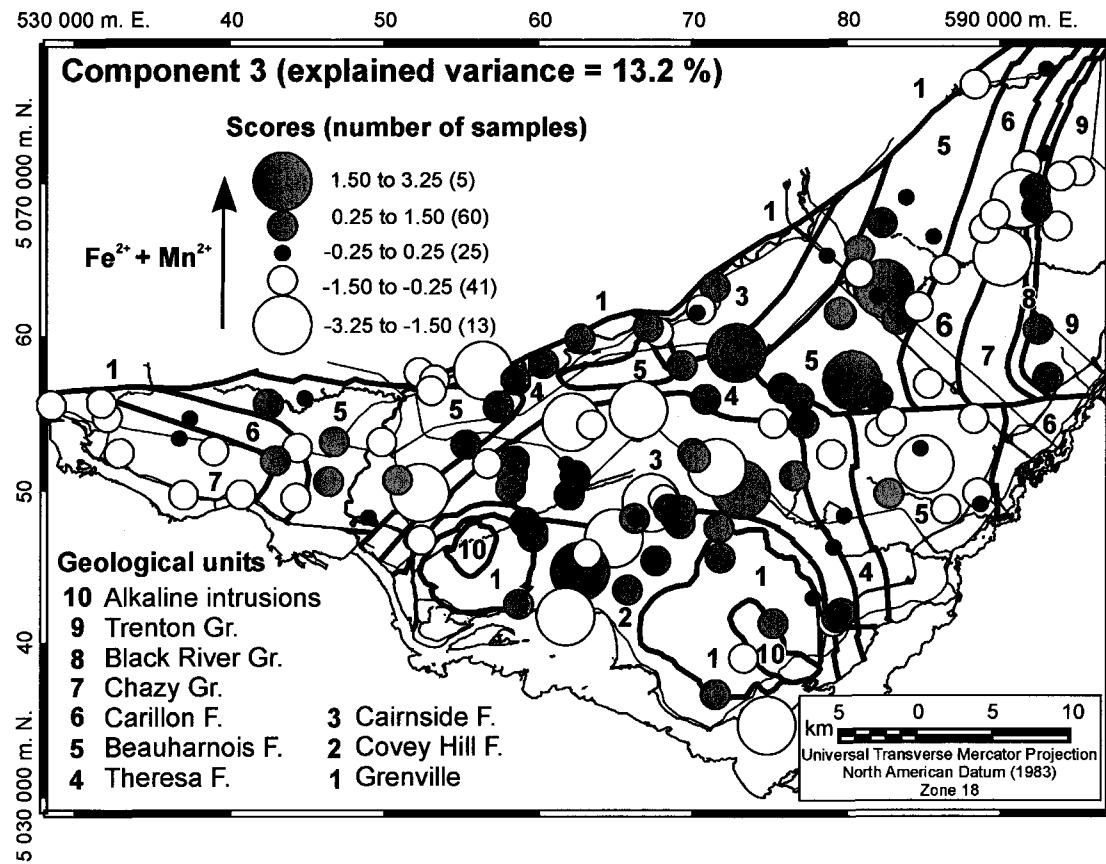
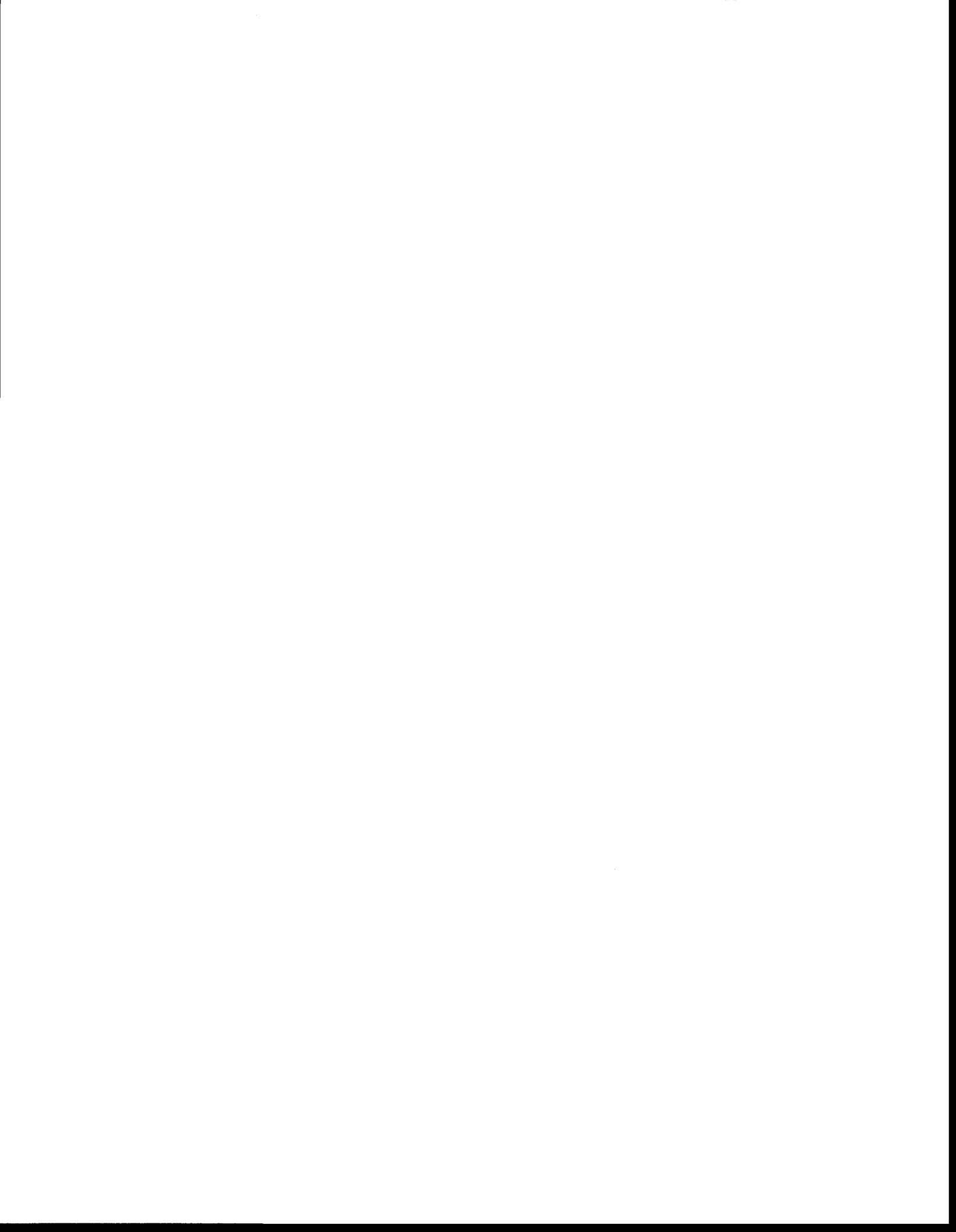


Figure C2.1. Distribution régionale des coordonnées pour la composante 3 avec la géologie (carte géologique modifiée de Rocher et al., sous presse).



## **Appendice D**

### **GÉOCHIMIE DE L'EAU INTERSTITIELLE DES ARGILES MARINES**

## D1 Introduction

Dans le cadre du projet de la Commission géologique du Canada (CGC) intitulé «caractérisation hydrogéologique régionale du système aquifère fracturé du sud-ouest du Québec», des échantillons d'argiles marines ont été prélevés en 1999 et 2000 lors de travaux de forage lors de l'installation de puits au roc et pour l'étude Quaternaire (voir la Fig. 3.3; Chapitre 3). L'eau interstitielle des argiles a été extraite à cinq sites dans le but d'améliorer la compréhension de l'origine de la salinité de l'eau souterraine dans les vallées enfouies. Les échantillons d'eau interstitielle ont été analysés pour les éléments majeurs, Br<sup>-</sup>, Sr<sup>2+</sup>, δ<sup>2</sup>H et δ<sup>18</sup>O. Les travaux d'extraction ont été réalisés par Constance Beaubien au département de géologie et génie géologique de l'Université Laval à l'été 2000, alors qu'elle effectuait un stage à l'INRS-ETE sous la responsabilité de René Lefebvre et de l'auteur. La méthodologie d'extraction de l'eau interstitielle des argiles, présentée dans l'Appendice D2, est extraite de son rapport de stage.

Le Tableau D1.1 présente les caractéristiques des cinq sites étudiés. Les sites Saint-Hermas et Sainte-Anne ont été échantillonnés lors de travaux de forage lors de l'installation de puits au roc (Site S85 et SAP), alors que ceux de Saint-Benoît, Saint-Joseph et Chemin des Sources ont été échantillonnés dans le cadre du projet de Martin Ross pour l'étude Quaternaire. Les échantillons d'argile ont été prélevés avec des tubes *Shelby* ou à l'aide de pistons. Les extrémités des tubes ont été scellées sur le site avec de la paraffine afin de préserver les échantillons. Les échantillons des sites Saint-Hermas et Sainte-Anne ont été conservés dans une chambre froide jusqu'au détubage pour l'extraction. Les échantillons des sites Saint-Benoît, Saint-Joseph et Chemin des Sources ont été conservés à la température de la pièce jusqu'au détubage pour l'extraction. La Figure D1.1 présente la localisation des sites dans la région d'étude.

Tableau D1.1. Caractéristiques générales des sites étudiés

Site	ID Site	Année Forée	Abscisse (m)	Ordonnée (m)	Épaisseur d'argile (m)	Géologie du roc	$\text{Cl}^-$ (mg/L) <sup>1</sup>	$\delta^{18}\text{O}$ (‰) <sup>2</sup>
00_STB_F5 (St-Benoît)	—	2000	569152	5047829	15	Covey Hill	240	-10.94
00_CHS_F1 (Ch. des Sources)	—	2000	558400	5049005	38	Covey Hill	—	—
00_STJPH (St-Joseph)	—	2000	579773	5042208	?	Cairnside	—	—
99_148 (St-Hermas)	S85	1999	562413	5050931	46	Cairnside	17	-11.73
99_BAR (Ste-Anne)	SAP	1999	589831	5067517	21	Carillon	270	-10.87

Le site 00\_STB\_F5 est localisé à côté du site S46.

<sup>1</sup>: Concentration en  $\text{Cl}^-$  dans l'aquifère de roc sous l'argile

<sup>2</sup>: Valeur en  $\delta^{18}\text{O}$  dans l'aquifère de roc sous l'argile

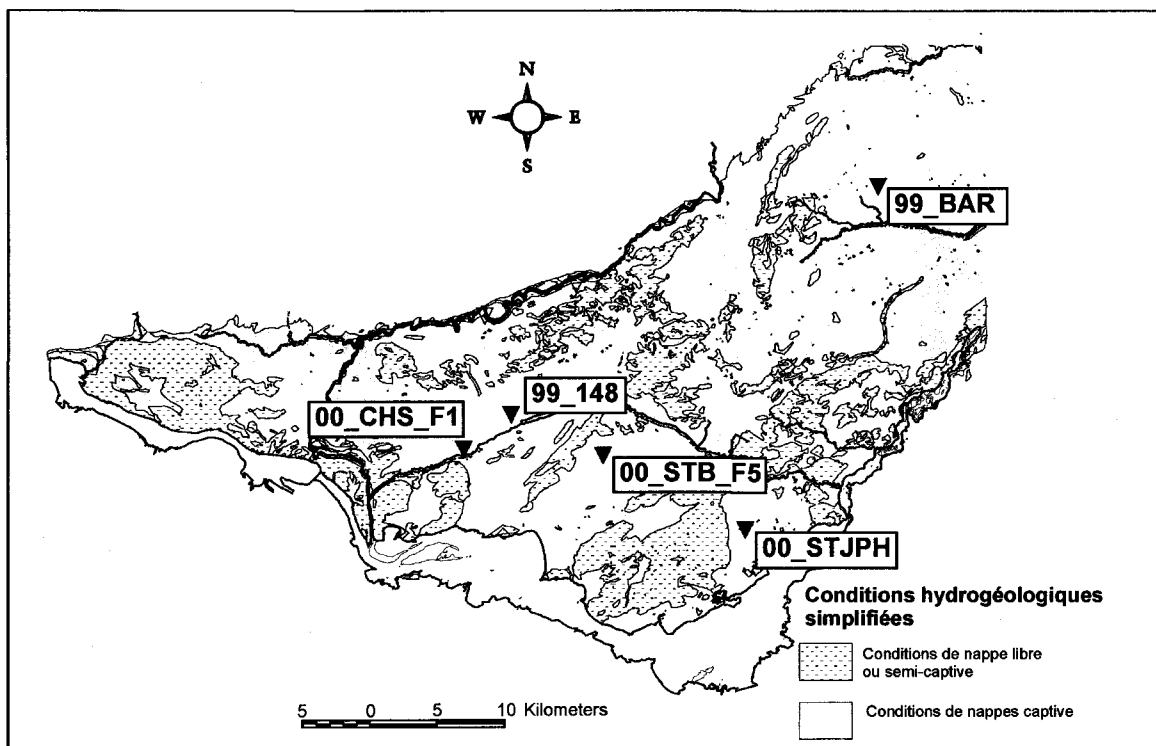


Figure D1.1. Localisation des sites étudiés (carte des conditions hydrogéologiques modifiée de Hamel et al., 2001).

## D2 Méthodologie d'extraction de l'eau interstitielle des argiles

Le montage d'extraction à air comprimé qui a été utilisé lors de l'extraction appartient à Monsieur Jacques Locat, professeur du département de géologie et génie géologique de l'Université Laval. Voici le matériel et la méthodologie ayant servi à l'extraction de l'eau interstitielle des argiles.

### Matériel nécessaire

- montage (cadre en bois, 4 compartiments en plexiglass, anneaux d'étanchéité en caoutchouc, 4 couvercles métalliques avec embranchement pour air comprimé, 4 petits tubes de plastique, 4 bagues métalliques d'étanchéité, 4 bouchons de caoutchouc perforés, 16 boulons et écrous)
- air comprimé
- eau distillée
- éprouvettes (4)
- échantillons d'argile (20 cm de longueur et 7cm de diamètre)
- spatules
- bols en porcelaine
- filtres Whatman 40
- gants de plastique
- seringues 60cc
- filtres pour seringue
- bouteilles pour les échantillons d'eau
- acide nitrique et compte-gouttes
- crayon feutre
- carnet de notes
- pellicule moulante
- contenants métalliques pour les teneurs en eau

## Étapes de l'extraction

- Laver le montage et les instruments à l'eau distillée pour éviter toute contamination entre chaque extraction (lavage avec du savon lorsque nécessaire).
- Dans le carnet, noter le numéro d'échantillon, la date d'extraction, la personne faisant les manipulations, la température de la pièce, la durée de l'extraction, les bouteilles remplies ainsi que les caractéristiques spéciales du sol, s'il y a lieu.
- Installer les tubes sur les compartiments.
- Découper 4 filtres Whatman 40 et les placer dans le fond des compartiments en plexiglass.
- Sortir l'échantillon du réfrigérateur.
- Déballer l'échantillon avec des gants de plastique.
- Enlever la couche extérieure avec une spatule, car elle a été altérée et remaniée avec la tige lors du détubage.
- Remanier l'échantillon dans le bol et en placer dans les quatre compartiments de plexiglass. Prendre le restant de l'échantillon pour une teneur en eau avant extraction.
- Placer par dessus les échantillons de la pellicule moulante, les anneaux de caoutchouc et les couvercles métalliques.
- Percer préalablement la pellicule moulante aux endroits où les boulons passeront.
- Visser le montage (16 boulons et écrous).
- Partir tranquillement l'air comprimé en vérifiant qu'il n'y a aucune fuite.
- Placer les tubes dans un bécher au début afin d'éliminer les 3 premières gouttes pour éviter le plus de contamination possible. Par la suite, placer les tubes dans les quatre éprouvettes.
- Laisser l'essai se dérouler sur une période d'environ 2-3 heures. Au-delà de ce temps, la quantité d'eau extraite est minime; donc, il devient inutile de continuer et il est préférable de recommencer avec un autre échantillon s'il manque d'eau.
- Une fois l'extraction faite, arrêter l'air comprimé et verser le contenu des quatre éprouvettes dans la seringue de 60cc et noter la quantité d'eau récoltée.
- Quatre bouteilles doivent être remplies selon les spécificités du Tableau D2.1.

Tableau D2.1. Différentes analyses effectuées sur l'eau extraite

ANALYSE	QUANTITÉ	PARTICULARITÉ
Na, Ca, Mg, K, Sr	14 ml	Filtrer, acidifier et réfrigérer <sup>a</sup>
Conductivité, pH, Alcalinité, Cl, SO <sub>4</sub>	15 ml	Remplir la bouteille au maximum et réfrigérer
Br	10 ml	Réfrigérer
Isotopes ( $\delta^{18}\text{O}$ et $\delta^2\text{H}$ )	10 ml	Remplir la bouteille au maximum, sceller le goulot avec du ruban électrique et réfrigérer

\* La filtration s'effectue par l'ajout d'un filtre au bout de la seringue. L'acidification, quant à elle, consiste à verser 3 gouttes d'acide nitrique dans la bouteille pour l'analyse en Na, Ca, Mg, K, Sr.

- Réfrigérer les bouteilles entre l'extraction et l'analyse.
- Prendre une teneur en eau après extraction à partir d'un échantillon comprimé d'un des compartiments.
- Placer les échantillons au four pour connaître la quantité d'eau extraite en pourcentage (différence entre les teneurs en eau avant et après).
- Nettoyer le montage avec de l'eau distillée pour éviter la contamination.
- Porter les bouteilles d'eau au laboratoire pour les analyses chimiques.

Note 1 : Un essai a été réalisé avec des disques de plastique placés sur le dessus des échantillons. Cela avait pour but d'augmenter la quantité d'eau extraite, mais l'expérience s'est avérée non concluante. Par conséquent, les disques ont été mis de côté.

Note 2 : Pour cette série d'extraction, une et demi à deux extractions étaient effectuées pour un même échantillon afin d'obtenir les ml nécessaires aux analyses. Cela prend une journée par échantillon.

### D3 Tableau des données géochimiques et isotopiques

Tableau D3.1. Liste des échantillons

Site	Altitude (manm)	N° Échantillon	Profondeur du tube p/r sol (m)	Profondeur point milieu p/r sol (m)	
00_STJPH	45 manm	2000_PIA_R064	2.44	à 3.20	
		2000_PIA_R070	7.01	à 7.77	
		2000_PIA_R073	11.58	à 12.34	
		2000_PIA_R075	17.68	à 18.44	
		2000_PIA_R077	24.38	à 25.15	
		2000_PIA_R078-B	31.09	à 31.85	
00_CHS_F1	46.5 manm	2000_PIA_R021	3.05	à 3.81	
		2000_PIA_R022	6.10	à 7.01	
		2000_PIA_R025	10.67	à 11.58	
		2000_PIA_R028	15.24	à 16.15	
		2000_PIA_R032	21.34	à 22.25	
		2000_PIA_R036	27.43	à 28.34	
		2000_PIA_R039	32.00	à 32.77	
		2000_PIA_R042	36.58	à 37.34	
00_STB_F5	48 manm	2000_PIA_R009	1.98	à 2.74	
		2000_PIA_R010	4.27	à 5.03	
		2000_PIA_R011	7.32	à 8.08	
		2000_PIA_R012	10.36	à 11.13	
		2000_PIA_R014	14.17	à 14.94	
99_148	47 manm	99_PIA_R040	7.62	à 8.38	
		99_PIA_R041	13.72	à 14.48	
		99_PIA_R043	20.42	à 21.18	
		99_PIA_R044	27.43	à 28.19	
		99_PIA_R045	33.53	à 34.29	
99_BAR	64 manm	99_PIA_R059	5.97	à 6.74	
		99_PIA_R060	12.04	à 12.80	
		99_PIA_R061	18.14	à 18.90	
				18.52	

Tableau D3.2. Base de données géochimiques de l'eau interstitielle des argiles

Échantillons	Alc. Tot.	Br	Ca	Cl	Cond.	K	Mg	Na	pH	SO <sub>4</sub>	Sr
UNITÉS	mg/L	mg/L	mg/L	mg/L	uS/cm	mg/L	mg/L	mg/L	-	mg/L	mg/L
99-PIA-R040	<b>0.1</b>	18	320	6400	14700	79	390	2600	<b>4.5</b>	180	4.4
99-PIA-R041	<b>0.1</b>	18	280	6900	15660	97	460	3200	<b>4.6</b>	280	4
99-PIA-R043	49	15	180	5600	14650	85	350	3000	7.1	270	3.2
99-PIA-R044	320	11	100	3900	11110	65	210	2300	7.9	160	2
99-PIA-R045	350	7	70	2700	7680	48	12.9	1700	7.9	48	1.3
99-PIA-R059	680	0.65	25	220	1670	31	50	300	8.3	4	0.43
99-PIA-R060	980	2	9.4	460	2900	32	28	630	8.1	6.5	0.22
99-PIA-R061	970	1	16.6	350	2530	36	35	600	8.5	21	1.3
2000-PIA-R009	290	0.47	31	160	510	4.8	22	170	8.2	2.5	0.17
2000-PIA-R010	300	2	48	560	2120	21	59	360	8	9.5	0.48
2000-PIA-R011	320	2	23	720	2630	24	39	570	8.2	21	0.35
2000-PIA-R012	480	3	17.4	630	2630	23	27	720	8.4	19	0.27
2000-PIA-R014	560	3	16.6	790	3230	25.7	33	720	8.3	DIF	0.4
2000-PIA-R021	250	4	81	1500	4670	23	99	890	7.9	DIF	0.83
2000-PIA-R022	550	6	60	2500	7580	40	120	1700	8.2	130	1.2
2000-PIA-R025	270	12	220	4800	12320	73	330	2500	7.3	230	3.4
2000-PIA-R028	<b>0.1</b>	22	1300	7800	17170	110	620	2300	<b>4.7</b>	35	7.7
2000-PIA-R032	300	14	160	4900	13530	79	290	2800	7.6	47	2.9
2000-PIA-R036	95	11	240	4500	12020	72	280	2200	6.7	22	2.9
2000-PIA-R039	280	6	44	1800	5100	45	76	1100	8.1	19	0.77
2000-PIA-R042	260	1	47	480	1920	23	47	350	8.2	78	0.58
2000-PIA-R064	220	0.44	36	3.1	410	8.2	19.9	41	8.3	12	0.27
2000-PIA-R070	300	0.66	10.3	3.3	560	10.8	8.6	14.3	8.5	19	0.09
2000-PIA-R073	500	0.68	2.9	23	970	8.3	1.6	280	8.7	12	0.03
2000-PIA-R075	720	0.28	7.6	120	1540	13.1	8.3	300	8.3	6.5	0.11
2000-PIA-R077	1000	2	7	330	2630	18.6	13.7	690	8.5	12	0.13
2000-PIA-R078B	1100	3	9.3	850	4140	25	23	1000	8.5	16	0.2

DIF : Difficultés techniques

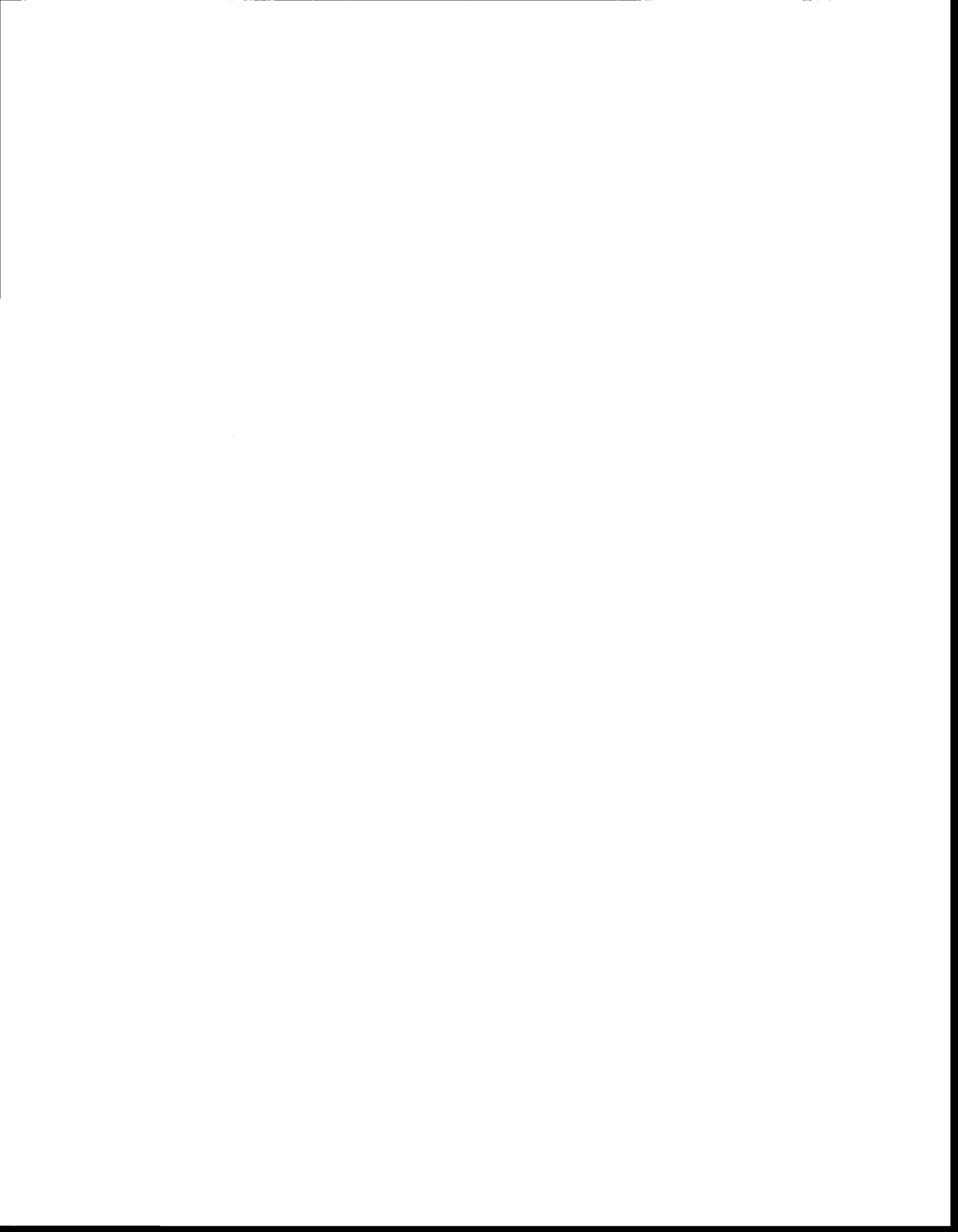
Alc. Tot. : Alcalinité Totale en CaCO<sub>3</sub>

Conductivité et pH mesurés en laboratoire

Valeurs en caractère gras = Problèmes de conservation

Tableau D3.3. Base de données isotopiques de l'eau interstitielle des argiles

Échantillons	$\delta^{18}\text{O}$ (‰)	$\delta^2\text{H}$ (‰)
99_PIA_R040	-	-71
99_PIA_R041	-10.9	-73
99_PIA_R043	-10.9	-81
99_PIA_R044	-10.9	-84
99_PIA_R045	-11.1	-80
99_PIA_R059	-9.9	-70
99_PIA_R060	-9.6	-68
99_PIA_R061	-10.2	-66
2000_PIA_R009	-9.8	-68
2000_PIA_R010	-9.6	-65
2000_PIA_R011	-9.9	-59
2000_PIA_R012	-10.1	-58
2000_PIA_R014	-10.3	-63
2000_PIA_R021	-10.0	-71
2000_PIA_R022	-10.2	-77
2000_PIA_R025	-10.5	-72
2000_PIA_R028	-10.4	-78
2000_PIA_R032	-11.5	-70
2000_PIA_R036	-11.0	-75
2000_PIA_R039	-11.3	-74
2000_PIA_R042	-11.6	-71
2000_PIA_R064	-12.0	-82
2000_PIA_R070	-12.4	-87
2000_PIA_R073	-12.3	-
2000_PIA_R075	-12.1	-60
2000_PIA_R077	-12.1	-81
2000_PIA_R078-B	-11.6	-81



## **Appendice E**

### **LA MODÉLISATION GÉOCHIMIQUE DE L'EAU SOUTERRAINE**

## Modélisation géochimique de l'eau souterraine

L'Appendice E présente un exemple de spéciation pour l'échantillon S86. Les fichiers de modélisation géochimique pour l'ensemble des échantillons sont inclus dans le disque compact (Appendice G). La modélisation géochimique a été réalisée avec PHREEQCI 2.8 (Charlton et Parkhurst, 2002). PHREEQCI est disponible gratuitement sur le site internet du USGS (<http://water.usgs.gov/software>)

### Fichier d'entrée :

```

TITLE Spéciation de l'échantillon S86
SOLUTION 1 S86
temp      8.7
pH        8.28
pe        2.0509
redox     pe
units     mg/l
density   1
O(0)     1.64
Ca        28
Mg        22
Na        43
K          4.8
Fe        0.094
Mn        0.009
Li        0.01
Sr        0.3
Ba        0.16
Si        13.5
Cl        10
Alkalinity 230
S(6)      30
S(-2)    0.02
F          0.34
Br        0.01
P          0.03
Al        0.01
B          0.11
Cu        0.001
Zn        0.005
N(5)      0.02
N(-3)    0.22
Cd        0.00012
-water    1 # kg
END

```

Fichier de résultats :

Input file: D:\phreeqc\S86.pqi  
 Output file: D:\phreeqc\S86.pqo  
 Database file: C:\Program Files\USGS\Phreeqc Interactive 2.6\phreeqc.dat

-----  
 Reading data base.  
 -----

SOLUTION\_MASTER\_SPECIES  
 SOLUTION\_SPECIES  
 PHASES  
 EXCHANGE\_MASTER\_SPECIES  
 EXCHANGE\_SPECIES  
 SURFACE\_MASTER\_SPECIES  
 SURFACE\_SPECIES  
 RATES  
 END

-----  
 Reading input data for simulation 1.  
 -----

DATABASE C:\Program Files\USGS\Phreeqc Interactive 2.6\phreeqc.dat  
 TITLE Spéciation de l'échantillon S86  
 SOLUTION 1 S86  
 temp 8.7  
 pH 8.28  
 pe 2.0509  
 redox pe  
 units mg/l  
 density 1  
 O(0) 1.64  
 Ca 28  
 Mg 22  
 Na 43  
 K 4.8  
 Fe 0.094  
 Mn 0.009  
 Li 0.01  
 Sr 0.3  
 Ba 0.16  
 Si 13.5  
 Cl 10  
 Alkalinity 230  
 S(6) 30  
 S(-2) 0.02  
 F 0.34  
 Br 0.01  
 P 0.03  
 Al 0.01  
 B 0.11  
 Cu 0.001  
 Zn 0.005  
 N(5) 0.02  
 N(-3) 0.22  
 Cd 0.0012  
 water 1 # kg  
 END

-----  
TITLE  
-----

Spéciation de l'échantillon S86

-----  
Beginning of initial solution calculations.  
-----

Initial solution 1. S86

-----  
Solution composition-----

Elements	Molality	Moles
Al	3.708e-007	3.708e-007
Alkalinity	4.598e-003	4.598e-003
B	1.018e-005	1.018e-005
Ba	1.165e-006	1.165e-006
Br	1.252e-007	1.252e-007
Ca	6.989e-004	6.989e-004
Cd	1.068e-008	1.068e-008
Cl	2.822e-004	2.822e-004
Cu	1.574e-008	1.574e-008
F	1.790e-005	1.790e-005
Fe	1.684e-006	1.684e-006
K	1.228e-004	1.228e-004
Li	1.442e-006	1.442e-006
Mg	9.053e-004	9.053e-004
Mn	1.639e-007	1.639e-007
N(-3)	1.571e-005	1.571e-005
N(5)	1.428e-006	1.428e-006
Na	1.871e-003	1.871e-003
O(0)	1.025e-004	1.025e-004
P	9.689e-007	9.689e-007
S(-2)	6.240e-007	6.240e-007
S(6)	3.124e-004	3.124e-004
Si	2.248e-004	2.248e-004
Sr	3.425e-006	3.425e-006
Zn	7.652e-008	7.652e-008

-----  
Description of solution-----

pH	=	8.280
pe	=	2.051
Activity of water	=	1.000
Ionic strength	=	7.011e-003
Mass of water (kg)	=	1.0000e+000
Total carbon (mol/kg)	=	4.591e-003
Total CO2 (mol/kg)	=	4.591e-003
Temperature (deg C)	=	8.700
Electrical balance (eq)	=	-2.919e-004
Percent error, 100*(Cat- An )/(Cat+ An )	=	-2.81
Iterations	=	9
Total H	=	1.110179e+002
Total O	=	5.552222e+001

-----  
Redox couples-----

Redox couple	pe	Eh (volts)
N(-3)/N(5)	5.3974	0.3018
O(-2)/O(0)	13.5961	0.7603
S(-2)/S(6)	-4.4688	-0.2499

## -----Distribution of species-----

	Species	Molality	Activity	Log Molality	Log Activity	Log Gamma
Al	OH-	5.414e-007	4.961e-007	-6.266	-6.304	-0.038
	H+	5.667e-009	5.248e-009	-8.247	-8.280	-0.033
	H2O	5.551e+001	9.998e-001	1.744	-0.000	0.000
Al		3.708e-007				
	Al(OH)4-	3.695e-007	3.391e-007	-6.432	-6.470	-0.037
	Al(OH)3	1.085e-009	1.087e-009	-8.965	-8.964	0.001
	Al(OH)2+	1.615e-010	1.482e-010	-9.792	-9.829	-0.037
	AlF2+	8.597e-013	7.889e-013	-12.066	-12.103	-0.037
	AlOH+2	6.736e-013	4.776e-013	-12.172	-12.321	-0.149
	AlF3	1.547e-013	1.550e-013	-12.810	-12.810	0.001
	AlF+2	1.529e-013	1.084e-013	-12.816	-12.965	-0.149
	Al+3	1.512e-015	7.572e-016	-14.820	-15.121	-0.300
	AlF4-	1.064e-015	9.761e-016	-14.973	-15.011	-0.037
	AlSO4+	4.121e-016	3.782e-016	-15.385	-15.422	-0.037
	Al(SO4)2-	2.376e-018	2.180e-018	-17.624	-17.661	-0.037
	AlF5-2	3.589e-019	2.545e-019	-18.445	-18.594	-0.149
	AlF6-3	1.234e-023	5.692e-024	-22.909	-23.245	-0.336
	AlHSO4+2	2.231e-025	1.582e-025	-24.652	-24.801	-0.149
B		1.018e-005				
	H3BO3	9.362e-006	9.377e-006	-5.029	-5.028	0.001
	H2BO3-	8.179e-007	7.506e-007	-6.087	-6.125	-0.037
	BF(OH)3-	5.393e-011	4.949e-011	-10.268	-10.305	-0.037
	BF2(OH)2-	4.928e-016	4.522e-016	-15.307	-15.345	-0.037
	BF3OH-	6.174e-023	5.666e-023	-22.209	-22.247	-0.037
	BF4-	2.145e-029	1.968e-029	-28.669	-28.706	-0.037
Ba		1.165e-006				
	Ba+2	1.064e-006	7.597e-007	-5.973	-6.119	-0.146
	BaSO4	7.508e-008	7.520e-008	-7.124	-7.124	0.001
	BaHCO3+	1.929e-008	1.770e-008	-7.715	-7.752	-0.037
	BaCO3	6.841e-009	6.852e-009	-8.165	-8.164	0.001
	BaOH+	5.345e-012	4.904e-012	-11.272	-11.309	-0.037
Br		1.252e-007				
	Br-	1.252e-007	1.146e-007	-6.902	-6.941	-0.038
C(4)		4.591e-003				
	HCO3-	4.414e-003	4.061e-003	-2.355	-2.391	-0.036
	CO2	6.371e-005	6.382e-005	-4.196	-4.195	0.001
	CO3-2	3.381e-005	2.422e-005	-4.471	-4.616	-0.145
	MgHCO3+	3.015e-005	2.767e-005	-4.521	-4.558	-0.037
	CaHCO3+	1.837e-005	1.690e-005	-4.736	-4.772	-0.036
	CaCO3	1.525e-005	1.527e-005	-4.817	-4.816	0.001
	MgCO3	1.092e-005	1.094e-005	-4.962	-4.961	0.001
	NaHCO3	3.905e-006	3.912e-006	-5.408	-5.408	0.001
	NaCO3-	3.528e-007	3.237e-007	-6.452	-6.490	-0.037
	FeCO3	2.962e-007	2.967e-007	-6.528	-6.528	0.001
	FeHCO3+	2.260e-007	2.074e-007	-6.646	-6.683	-0.037
	SrHCO3+	8.976e-008	8.257e-008	-7.047	-7.083	-0.036
	MnCO3	8.433e-008	8.446e-008	-7.074	-7.073	0.001
	ZnCO3	3.396e-008	3.402e-008	-7.469	-7.468	0.001
	Zn(CO3)2-2	2.484e-008	1.761e-008	-7.605	-7.754	-0.149
	SrCO3	2.215e-008	2.219e-008	-7.655	-7.654	0.001
	BaHCO3+	1.929e-008	1.770e-008	-7.715	-7.752	-0.037
	MnHCO3+	1.732e-008	1.589e-008	-7.762	-7.799	-0.037
	BaCO3	6.841e-009	6.852e-009	-8.165	-8.164	0.001
	ZnHCO3+	3.922e-009	3.599e-009	-8.407	-8.444	-0.037
	CdHCO3+	9.040e-010	8.295e-010	-9.044	-9.081	-0.037
	CdCO3	1.241e-010	1.243e-010	-9.906	-9.906	0.001
	Cd(CO3)2-2	1.342e-011	9.517e-012	-10.872	-11.022	-0.149
Ca		6.989e-004				
	Ca+2	6.495e-004	4.649e-004	-3.187	-3.333	-0.145
	CaHCO3+	1.837e-005	1.690e-005	-4.736	-4.772	-0.036
	CaSO4	1.557e-005	1.560e-005	-4.808	-4.807	0.001
	CaCO3	1.525e-005	1.527e-005	-4.817	-4.816	0.001
	CaHPO4	8.071e-008	8.084e-008	-7.093	-7.092	0.001
	CaF+	4.687e-008	4.301e-008	-7.329	-7.366	-0.037
	CaPO4-	2.869e-008	2.633e-008	-7.542	-7.580	-0.037
	CaOH+	1.602e-008	1.470e-008	-7.795	-7.833	-0.037

	CaH2PO4+	3.790e-010	3.478e-010	-9.421	-9.459	-0.037
	CaHSO4+	4.412e-013	4.049e-013	-12.355	-12.393	-0.037
Cd		1.068e-008				
	Cd+2	9.111e-009	6.460e-009	-8.040	-8.190	-0.149
	CdHCO3+	9.040e-010	8.295e-010	-9.044	-9.081	-0.037
	CdSO4	3.306e-010	3.312e-010	-9.481	-9.480	0.001
	CdCl+	1.641e-010	1.506e-010	-9.785	-9.822	-0.037
	CdCO3	1.241e-010	1.243e-010	-9.906	-9.906	0.001
	CdOH+	3.106e-011	2.850e-011	-10.508	-10.545	-0.037
	Cd(CO3)2-2	1.342e-011	9.517e-012	-10.872	-11.022	-0.149
	Cd(SO4)2-2	1.124e-012	7.969e-013	-11.949	-12.099	-0.149
	Cd(OH)2	1.046e-012	1.047e-012	-11.981	-11.980	0.001
	CdCl2	1.522e-013	1.524e-013	-12.818	-12.817	0.001
	Cd(OH)3-	2.440e-017	2.239e-017	-16.613	-16.650	-0.037
	CdCl3-	2.090e-017	1.918e-017	-16.680	-16.717	-0.037
	Cd(OH)4-2	5.361e-023	3.802e-023	-22.271	-22.420	-0.149
Cl		2.822e-004				
	Cl-	2.822e-004	2.586e-004	-3.549	-3.587	-0.038
	FeCl+	1.987e-010	1.823e-010	-9.702	-9.739	-0.037
	CdCl+	1.641e-010	1.506e-010	-9.785	-9.822	-0.037
	MnCl+	5.041e-011	4.626e-011	-10.297	-10.335	-0.037
	ZnCl+	2.496e-012	2.291e-012	-11.603	-11.640	-0.037
	CdCl2	1.522e-013	1.524e-013	-12.818	-12.817	0.001
	MnCl2	5.214e-015	5.222e-015	-14.283	-14.282	0.001
	ZnCl2	5.779e-016	5.788e-016	-15.238	-15.237	0.001
	CdCl3-	2.090e-017	1.918e-017	-16.680	-16.717	-0.037
	MnCl3-	4.054e-019	3.720e-019	-18.392	-18.429	-0.037
	ZnCl3-	1.650e-019	1.515e-019	-18.782	-18.820	-0.037
	FeCl2+	1.359e-020	9.638e-021	-19.867	-20.016	-0.149
	ZnCl4-2	2.415e-023	1.712e-023	-22.617	-22.766	-0.149
	FeCl2+	2.096e-023	1.923e-023	-22.679	-22.716	-0.037
	FeCl3	4.966e-028	4.974e-028	-27.304	-27.303	0.001
Cu(1)		8.944e-011				
	Cu+	8.944e-011	8.177e-011	-10.048	-10.087	-0.039
Cu(2)		1.565e-008				
	Cu(OH)2	1.558e-008	1.561e-008	-7.807	-7.807	0.001
	CuOH+	4.274e-011	3.921e-011	-10.369	-10.407	-0.037
	Cu+2	2.860e-011	2.058e-011	-10.544	-10.687	-0.143
	CuSO4	7.355e-013	7.367e-013	-12.133	-12.133	0.001
	Cu(OH)3-	1.952e-013	1.792e-013	-12.709	-12.747	-0.037
	Cu(OH)4-2	9.604e-018	6.810e-018	-17.018	-17.167	-0.149
F		1.790e-005				
	F-	1.733e-005	1.588e-005	-4.761	-4.799	-0.038
	MgF+	5.086e-007	4.667e-007	-6.294	-6.331	-0.037
	CaF+	4.687e-008	4.301e-008	-7.329	-7.366	-0.037
	NaF	1.563e-008	1.565e-008	-7.806	-7.805	0.001
	HF	9.404e-011	9.419e-011	-10.027	-10.026	0.001
	FeF+	8.838e-011	8.110e-011	-10.054	-10.091	-0.037
	BF(OH)3-	5.393e-011	4.949e-011	-10.268	-10.305	-0.037
	MnF+	5.257e-012	4.824e-012	-11.279	-11.317	-0.037
	AlF2+	8.597e-013	7.889e-013	-12.066	-12.103	-0.037
	AlF3	1.547e-013	1.550e-013	-12.810	-12.810	0.001
	AlF2+	1.529e-013	1.084e-013	-12.816	-12.965	-0.149
	HF2-	5.324e-015	4.885e-015	-14.274	-14.311	-0.037
	AlF4-	1.064e-015	9.761e-016	-14.973	-15.011	-0.037
	BF2(OH)2-	4.928e-016	4.522e-016	-15.307	-15.345	-0.037
	FeF2+	5.814e-017	4.122e-017	-16.236	-16.385	-0.149
	FeF2+	2.314e-017	2.123e-017	-16.636	-16.673	-0.037
	FeF3	5.032e-019	5.040e-019	-18.298	-18.298	0.001
	AlF5-2	3.589e-019	2.545e-019	-18.445	-18.594	-0.149
	BF3OH-	6.174e-023	5.666e-023	-22.209	-22.247	-0.037
	AlF6-3	1.234e-023	5.692e-024	-22.909	-23.245	-0.336
	BF4-	2.145e-029	1.968e-029	-28.669	-28.706	-0.037
	SiF6-2	2.816e-035	1.996e-035	-34.550	-34.700	-0.149
Fe(2)		1.255e-006				
	Fe+2	7.097e-007	5.107e-007	-6.149	-6.292	-0.143
	FeCO3	2.962e-007	2.967e-007	-6.528	-6.528	0.001
	FeHCO3+	2.260e-007	2.074e-007	-6.646	-6.683	-0.037
	FeSO4	1.306e-008	1.309e-008	-7.884	-7.883	0.001
	FeOH+	9.244e-009	8.483e-009	-8.034	-8.071	-0.037
	FeHPO4	8.884e-010	8.898e-010	-9.051	-9.051	0.001

FeCl+	1.987e-010	1.823e-010	-9.702	-9.739	-0.037
Fe(HS) 2	1.286e-010	1.288e-010	-9.891	-9.890	0.001
FeF+	8.838e-011	8.110e-011	-10.054	-10.091	-0.037
FeH2PO4+	1.137e-011	1.043e-011	-10.944	-10.982	-0.037
Fe(HS) 3-	8.135e-015	7.465e-015	-14.090	-14.127	-0.037
FeHSO4+	4.846e-016	4.447e-016	-15.315	-15.352	-0.037
Fe (3)	4.283e-007				
Fe(OH) 3	3.602e-007	3.608e-007	-6.443	-6.443	0.001
Fe(OH) 4-	3.416e-008	3.135e-008	-7.466	-7.504	-0.037
Fe(OH) 2+	3.396e-008	3.117e-008	-7.469	-7.506	-0.037
FeOH+2	1.340e-012	9.501e-013	-11.873	-12.022	-0.149
FeF+2	5.814e-017	4.122e-017	-16.236	-16.385	-0.149
FeF2+	2.314e-017	2.123e-017	-16.636	-16.673	-0.037
Fe+3	4.258e-018	2.132e-018	-17.371	-17.671	-0.300
FeSO4+	3.434e-018	3.152e-018	-17.464	-17.501	-0.037
FeF3	5.032e-019	5.040e-019	-18.298	-18.298	0.001
FeHPO4+	1.560e-019	1.431e-019	-18.807	-18.844	-0.037
FeH2PO4+2	3.297e-020	2.338e-020	-19.482	-19.631	-0.149
Fe(SO4) 2-	1.387e-020	1.273e-020	-19.858	-19.895	-0.037
FeCl+2	1.359e-020	9.638e-021	-19.867	-20.016	-0.149
Fe2(OH) 2+4	1.960e-022	4.955e-023	-21.708	-22.305	-0.597
FeCl2+	2.096e-023	1.923e-023	-22.679	-22.716	-0.037
FeHSO4+2	6.576e-026	4.663e-026	-25.182	-25.331	-0.149
Fe3(OH) 4+5	1.358e-026	1.584e-027	-25.867	-26.800	-0.933
FeCl3	4.966e-028	4.974e-028	-27.304	-27.303	0.001
H(0)	3.657e-024				
H2	1.828e-024	1.831e-024	-23.738	-23.737	0.001
K	1.228e-004				
K+	1.227e-004	1.124e-004	-3.911	-3.949	-0.038
KSO4-	1.259e-007	1.155e-007	-6.900	-6.937	-0.037
KHPO4-	1.046e-010	9.595e-011	-9.981	-10.018	-0.037
KOH	7.416e-011	7.427e-011	-10.130	-10.129	0.001
Li	1.442e-006				
Li+	1.440e-006	1.327e-006	-5.842	-5.877	-0.036
LiSO4-	1.246e-009	1.144e-009	-8.904	-8.942	-0.037
LiOH	5.781e-012	5.790e-012	-11.238	-11.237	0.001
Mg	9.053e-004				
Mg+2	8.454e-004	6.079e-004	-3.073	-3.216	-0.143
MgHCO3+	3.015e-005	2.767e-005	-4.521	-4.558	-0.037
MgSO4	1.802e-005	1.805e-005	-4.744	-4.743	0.001
MgCO3	1.092e-005	1.094e-005	-4.962	-4.961	0.001
MgF+	5.086e-007	4.667e-007	-6.294	-6.331	-0.037
MgHPO4	1.427e-007	1.429e-007	-6.846	-6.845	0.001
MgOH+	9.658e-008	8.862e-008	-7.015	-7.052	-0.037
MgPO4-	5.061e-008	4.644e-008	-7.296	-7.333	-0.037
MgH2PO4+	6.311e-010	5.792e-010	-9.200	-9.237	-0.037
Mn (2)	1.639e-007				
MnCO3	8.433e-008	8.446e-008	-7.074	-7.073	0.001
Mn+2	6.102e-008	4.391e-008	-7.215	-7.357	-0.143
MnHCO3+	1.732e-008	1.589e-008	-7.762	-7.799	-0.037
MnSO4	1.108e-009	1.110e-009	-8.955	-8.955	0.001
MnOH+	5.746e-011	5.273e-011	-10.241	-10.278	-0.037
MnCl+	5.041e-011	4.626e-011	-10.297	-10.335	-0.037
MnF+	5.257e-012	4.824e-012	-11.279	-11.317	-0.037
MnCl2	5.214e-015	5.222e-015	-14.283	-14.282	0.001
MnCl3-	4.054e-019	3.720e-019	-18.392	-18.429	-0.037
Mn(NO3) 2	3.101e-019	3.106e-019	-18.509	-18.508	0.001
Mn (3)	2.665e-032				
Mn+3	2.665e-032	1.230e-032	-31.574	-31.910	-0.336
N (-3)	1.571e-005				
NH4+	1.523e-005	1.392e-005	-4.817	-4.856	-0.039
NH3	4.454e-007	4.461e-007	-6.351	-6.351	0.001
NH4SO4-	3.860e-008	3.542e-008	-7.413	-7.451	-0.037
N (5)	1.428e-006				
NO3-	1.428e-006	1.307e-006	-5.845	-5.884	-0.038
Mn(NO3) 2	3.101e-019	3.106e-019	-18.509	-18.508	0.001
Na	1.871e-003				
Na+	1.865e-003	1.713e-003	-2.729	-2.766	-0.037
NaHCO3	3.905e-006	3.912e-006	-5.408	-5.408	0.001
NaSO4-	1.656e-006	1.520e-006	-5.781	-5.818	-0.037
NaCO3-	3.528e-007	3.237e-007	-6.452	-6.490	-0.037

	NaF	1.563e-008	1.565e-008	-7.806	-7.805	0.001
	NaOH	2.153e-009	2.156e-009	-8.667	-8.666	0.001
	NaHPO4-	1.593e-009	1.462e-009	-8.798	-8.835	-0.037
O (0)		1.025e-004				
	O2	5.127e-005	5.135e-005	-4.290	-4.289	0.001
P		9.689e-007				
	HPO4-2	6.182e-007	4.377e-007	-6.209	-6.359	-0.150
	MgHPO4	1.427e-007	1.429e-007	-6.846	-6.845	0.001
	CaHPO4	8.071e-008	8.084e-008	-7.093	-7.092	0.001
	MgPO4-	5.061e-008	4.644e-008	-7.296	-7.333	-0.037
	H2PO4-	4.438e-008	4.075e-008	-7.353	-7.390	-0.037
	CaPO4-	2.869e-008	2.633e-008	-7.542	-7.580	-0.037
	NaHPO4-	1.593e-009	1.462e-009	-8.798	-8.835	-0.037
	FeHPO4	8.884e-010	8.898e-010	-9.051	-9.051	0.001
	MgH2PO4+	6.311e-010	5.792e-010	-9.200	-9.237	-0.037
	CaH2PO4+	3.790e-010	3.478e-010	-9.421	-9.459	-0.037
	KHPO4-	1.046e-010	9.595e-011	-9.981	-10.018	-0.037
	PO4-3	5.794e-011	2.664e-011	-10.237	-10.574	-0.337
	FeH2PO4+	1.137e-011	1.043e-011	-10.944	-10.982	-0.037
	FeHPO4+	1.560e-019	1.431e-019	-18.807	-18.844	-0.037
	FeH2PO4+2	3.297e-020	2.338e-020	-19.482	-19.631	-0.149
S (-2)		6.240e-007				
	HS-	5.807e-007	5.321e-007	-6.236	-6.274	-0.038
	H2S	4.306e-008	4.313e-008	-7.366	-7.365	0.001
	Fe (HS) 2	1.286e-010	1.288e-010	-9.891	-9.890	0.001
	S -2	5.265e-012	3.759e-012	-11.279	-11.425	-0.146
	Fe (HS) 3 -	8.135e-015	7.465e-015	-14.090	-14.127	-0.037
S (6)		3.124e-004				
	SO4-2	2.768e-004	1.975e-004	-3.558	-3.704	-0.147
	MgSO4	1.802e-005	1.805e-005	-4.744	-4.743	0.001
	CaSO4	1.557e-005	1.560e-005	-4.808	-4.807	0.001
	NaSO4-	1.656e-006	1.520e-006	-5.781	-5.818	-0.037
	KSO4-	1.259e-007	1.155e-007	-6.900	-6.937	-0.037
	BaSO4	7.508e-008	7.520e-008	-7.124	-7.124	0.001
	SrSO4	7.289e-008	7.301e-008	-7.137	-7.137	0.001
	NH4SO4-	3.860e-008	3.542e-008	-7.413	-7.451	-0.037
	FeSO4	1.306e-008	1.309e-008	-7.884	-7.883	0.001
	LiSO4-	1.246e-009	1.144e-009	-8.904	-8.942	-0.037
	MnSO4	1.108e-009	1.110e-009	-8.955	-8.955	0.001
	CdSO4	3.306e-010	3.312e-010	-9.481	-9.480	0.001
	ZnSO4	2.850e-010	2.854e-010	-9.545	-9.545	0.001
	HSO4-	7.894e-011	7.244e-011	-10.103	-10.140	-0.037
	Cd (SO4) 2-2	1.124e-012	7.969e-013	-11.949	-12.099	-0.149
	Zn (SO4) 2-2	7.379e-013	5.232e-013	-12.132	-12.281	-0.149
	CuSO4	7.355e-013	7.367e-013	-12.133	-12.133	0.001
	CaHSO4+	4.412e-013	4.049e-013	-12.355	-12.393	-0.037
	FeH2SO4+	4.846e-016	4.447e-016	-15.315	-15.352	-0.037
	AlSO4+	4.121e-016	3.782e-016	-15.385	-15.422	-0.037
	FeSO4+	3.434e-018	3.152e-018	-17.464	-17.501	-0.037
	Al (SO4) 2-	2.376e-018	2.180e-018	-17.624	-17.661	-0.037
	Fe (SO4) 2 -	1.387e-020	1.273e-020	-19.858	-19.895	-0.037
	AlHSO4+2	2.231e-025	1.582e-025	-24.652	-24.801	-0.149
	FeHSO4+2	6.576e-026	4.663e-026	-25.182	-25.331	-0.149
Si		2.248e-004				
	H4SiO4	2.212e-004	2.215e-004	-3.655	-3.655	0.001
	H3SiO4-	3.603e-006	3.307e-006	-5.443	-5.481	-0.037
	H2SiO4-2	1.875e-011	1.330e-011	-10.727	-10.876	-0.149
	SiF6-2	2.816e-035	1.996e-035	-34.550	-34.700	-0.149
Sr		3.425e-006				
	Sr+2	3.240e-006	2.323e-006	-5.489	-5.634	-0.145
	SrHCO3+	8.976e-008	8.257e-008	-7.047	-7.083	-0.036
	SrSO4	7.289e-008	7.301e-008	-7.137	-7.137	0.001
	SrCO3	2.215e-008	2.219e-008	-7.655	-7.654	0.001
	SrOH+	2.469e-011	2.269e-011	-10.607	-10.644	-0.037
Zn		7.652e-008				
	ZnCO3	3.396e-008	3.402e-008	-7.469	-7.468	0.001
	Zn (CO3) 2-2	2.484e-008	1.761e-008	-7.605	-7.754	-0.149
	Zn+2	9.861e-009	7.040e-009	-8.006	-8.152	-0.146
	ZnHCO3+	3.922e-009	3.599e-009	-8.407	-8.444	-0.037
	Zn (OH) 2	3.212e-009	3.217e-009	-8.493	-8.493	0.001
	ZnOH+	4.333e-010	3.976e-010	-9.363	-9.401	-0.037

ZnSO4	2.850e-010	2.854e-010	-9.545	-9.545	0.001
ZnCl+	2.496e-012	2.291e-012	-11.603	-11.640	-0.037
Zn(OH)3-	2.112e-012	1.938e-012	-11.675	-11.713	-0.037
Zn(SO4)2-2	7.379e-013	5.232e-013	-12.132	-12.281	-0.149
ZnCl2	5.779e-016	5.788e-016	-15.238	-15.237	0.001
Zn(OH)4-2	8.253e-017	5.852e-017	-16.083	-16.233	-0.149
ZnCl3-	1.650e-019	1.515e-019	-18.782	-18.820	-0.037
ZnCl4-2	2.415e-023	1.712e-023	-22.617	-22.766	-0.149

## -----Saturation indices-----

Phase	SI	log IAP	log KT	
Al(OH)3(a)	-2.20	9.72	11.92	Al(OH)3
Albite	-1.10	4.27	5.37	NaAlSi3O8
Alunite	-7.77	-7.04	0.73	KAl3(SO4)2(OH)6
Anhydrite	-2.70	-7.04	-4.34	CaSO4
Anorthite	-3.38	25.36	28.73	CaAl2Si2O8
Aragonite	0.30	-7.95	-8.25	CaCO3
Barite	0.45	-9.82	-10.27	BaSO4
Ca-Montmorillonite	1.91	11.42	9.51	Ca0.165Al2.33Si3.67O10(OH)2
Calcite	0.46	-7.95	-8.41	CaCO3
Cd(OH)2	-5.28	8.37	13.65	Cd(OH)2
CdSiO3	-5.05	4.72	9.76	CdSiO3
CdSO4	-12.42	-11.89	0.52	CdSO4
Celestite	-2.70	-9.34	-6.64	SrSO4
Chalcedony	0.10	-3.65	-3.75	SiO2
Chlorite(14A)	0.39	75.19	74.80	Mg5Al2Si3O10(OH)8
Chrysotile	-1.61	32.72	34.33	Mg3Si2O5(OH)4
CO2(g)	-2.95	-21.18	-18.23	CO2
Dolomite	0.91	-15.78	-16.69	CaMg(CO3)2
Fe(OH)3(a)	2.28	20.60	18.32	Fe(OH)3
FeS(ppt)	-0.37	-4.29	-3.92	FeS
Fluorite	-2.11	-12.93	-10.82	CaF2
Gibbsite	0.64	9.72	9.08	Al(OH)3
Goethite	7.55	20.60	13.04	FeOOH
Gypsum	-2.44	-7.04	-4.59	CaSO4:2H2O
H2(g)	-20.66	-20.66	0.00	H2
H2O(g)	-1.96	-0.00	1.96	H2O
H2S(g)	-6.56	-14.55	-7.99	H2S
Halite	-7.90	-6.35	1.54	NaCl
Hausmannite	-17.03	48.27	65.30	Mn3O4
Hematite	17.04	41.20	24.16	Fe2O3
Hydroxyapatite	-0.73	-40.11	-39.38	Ca5(PO4)3OH
Illite	1.80	15.50	13.69	K0.6Mg0.25Al2.3Si3.5O10(OH)2
Jarosite-K	-6.81	25.60	32.41	KFe3(SO4)2(OH)6
K-feldspar	0.50	3.09	2.59	KAlSi3O8
K-mica	7.30	22.52	15.22	KAl3Si3O10(OH)2
Kaolinite	3.20	12.13	8.93	Al2Si2O5(OH)4
Mackinawite	0.36	-4.29	-4.65	FeS
Manganite	-5.81	19.53	25.34	MnOOH
Melanterite	-7.57	-10.00	-2.43	FeSO4:7H2O
NH3(g)	-8.47	3.42	11.89	NH3
O2(g)	-1.41	-4.29	-2.88	O2
Otavite	-0.71	-12.81	-12.10	CdCO3
Pyrite	20.78	1.82	-18.96	FeS2
Pyrochroite	-6.00	9.20	15.20	Mn(OH)2
Pyrolusite	-14.28	29.86	44.14	MnO2
Quartz	0.58	-3.65	-4.23	SiO2
Rhodochrosite	-0.90	-11.97	-11.07	MnCO3
Sepiolite	-0.49	15.72	16.21	Mg2Si3O7.5OH:3H2O
Sepiolite(d)	-2.94	15.72	18.66	Mg2Si3O7.5OH:3H2O
Siderite	-0.12	-10.91	-10.78	FeCO3
SiO2(a)	-0.80	-3.65	-2.85	SiO2
Smithsonite	-2.95	-12.77	-9.82	ZnCO3
Sphalerite	5.82	-6.15	-11.97	ZnS
Strontianite	-0.96	-10.25	-9.29	SrCO3
Sulfur	8.01	6.11	-1.90	S
Talc	2.05	25.41	23.36	Mg3Si4O10(OH)2
Vivianite	-4.03	-40.03	-36.00	Fe3(PO4)2:8H2O
Willemite	-3.58	13.16	16.74	Zn2SiO4

Witherite	-2.09	-10.74	-8.64	BaCO <sub>3</sub>
Zn(OH) <sub>2</sub> (e)	-3.09	8.41	11.50	Zn(OH) <sub>2</sub>

-----  
End of simulation.  
-----

-----  
Reading input data for simulation 2.  
-----

-----  
End of run.  
-----

## **Appendice F**

### **COMPTES RENDUS DE CONFÉRENCES**

**Comptes rendus de conférences**

L'Appendice F présente les deux comptes rendus de conférences suivants :

Cloutier, V., Bourque, É., Lefebvre, R., Savard, M.M., Nastev, M., Martel, R., Therrien, R., 2001. Regional groundwater hydrogeochemistry of fractured rock aquifers in south-western Quebec. Proceedings, 2nd Joint IAH-CNC and CGS, Groundwater Specialty Conference, 54th Canadian Geotechnical Conference, Sept. 16-19, 2001, Calgary, Canada, 1068-1076.

Cloutier, V., Bourque, É., Lefebvre, R., Savard, M.M., Nastev, M., Martel, R., 2000. Regional hydrogeochemical characterization of groundwater in fractured aquifers of the St-Lawrence Lowlands. Proceedings, First Joint IAH-CNC and CGS, Groundwater Specialty Conference, October 2000, Montréal, Canada, 3-10.

## REGIONAL GROUNDWATER HYDROGEOCHEMISTRY OF FRACTURED ROCK AQUIFERS IN SOUTH-WESTERN QUÉBEC

Vincent Cloutier, INRS-Géoressources, Centre géoscientifique de Québec, Québec, QC  
 Édith Bourque, Commission géologique du Canada, Centre géoscientifique de Québec, Québec, QC  
 René Lefebvre, INRS-Géoressources, Centre géoscientifique de Québec, Québec, QC  
 Martine M. Savard, Commission géologique du Canada, Centre géoscientifique de Québec, Québec, QC  
 Miroslav Nastev, Commission géologique du Canada, Centre géoscientifique de Québec, Québec, QC  
 Richard Martel, INRS-Géoressources, Centre géoscientifique de Québec, Québec, QC  
 René Thrherrien, Département de géologie et génie géologique, Université Laval, Québec, QC

### ABSTRACT

Groundwater hydrogeochemistry of fractured Lower Paleozoic rock aquifers in south-western Québec was studied as part of a regional hydrogeological mapping project. The goal of the study is to evaluate regional groundwater quality, identify geochemical processes controlling groundwater chemistry and its evolution in space and time. Precipitations were sampled for  $\delta^2\text{H}$  and  $\delta^{18}\text{O}$  to establish the local meteoric water line. Bulk and discrete samples of groundwater were collected in 154 and 18 wells respectively. Samples were analyzed for inorganic components and stable isotopes ( $\delta^2\text{H}$ ,  $\delta^{18}\text{O}$  and  $\delta^{13}\text{C}_{\text{DIC}}$ ). Three main groundwater types are found in confined aquifer: mixed-cations-HCO<sub>3</sub>, Na-HCO<sub>3</sub> and Na-Cl. Recharge areas are characterized by Ca-Mg-HCO<sub>3</sub> type groundwater. Two water sources were identified in the aquifer: modern meteoric water and Pleistocene water. The Pleistocene water source would be the result of mixing of Champlain Seawater with glacial meltwater and Pleistocene meteoric water.

### RÉSUMÉ

L'hydrogéochimie des eaux souterraines des aquifères de roc fracturé du Paléozoïque Inférieur est étudiée dans le cadre d'un projet de cartographie hydrogéologique. Le but est d'évaluer la qualité régionale des eaux souterraines, d'identifier les processus géochimiques contrôlant la géochimie des eaux souterraines et son évolution dans l'espace et le temps. Les précipitations ont été échantillonnées pour  $\delta^2\text{H}$  et  $\delta^{18}\text{O}$  afin d'établir la droite locale des eaux météoriques. Un échantillonnage composite et à niveaux multiples a été effectué dans 154 et 18 puits respectivement. Les échantillons ont été analysés pour les composantes inorganiques et les isotopes stables ( $\delta^2\text{H}$ ,  $\delta^{18}\text{O}$  et  $\delta^{13}\text{C}_{\text{DIC}}$ ). Trois types principaux d'eau souterraine se retrouvent dans l'aquifère confiné : mixte-cations-HCO<sub>3</sub>, Na-HCO<sub>3</sub> et Na-Cl. Les zones de recharge sont caractérisées par le type Ca-Mg-HCO<sub>3</sub>. Deux sources d'eau ont été identifiées dans l'aquifère : de l'eau météorique moderne et de l'eau Pléistocène. L'eau Pléistocène serait le résultat du mélange de l'eau de la Mer Champlain avec l'eau de fonte glaciaire et l'eau météorique Pléistocène.

### 1. INTRODUCTION

This study is part of a regional hydrogeological mapping project led by the Geological Survey of Canada, in collaboration with INRS-Géoressources, Laval University and Environment Canada. The general objective of this project is to get a better knowledge of the groundwater resources of the area, as a mean to develop a management and protection strategy for the resources (Savard *et al.* 2000). A second objective of this study is to develop a methodology to characterize, at the regional scale, fractured rock aquifers (Nastev *et al.* 2001).

The hydrogeochemical characterization aims to regionally assess groundwater quality, identify the processes controlling groundwater geochemistry and understand the geochemical evolution of groundwater in space and time. The following approach was developed for the hydrogeochemical characterization: (1) the combined use of inorganic and isotopic geochemistry, (2) an isotopic characterization of local precipitation, (3) a regional and three-dimensional geochemical characterization, from the groundwater recharge areas and along flow paths, and

(4) the geochemical characterization of all hydrogeological units.

This paper presents results of the regional groundwater geochemistry. Groundwater types in the aquifer and descriptive statistics showed the importance of the hydrogeological and geological contexts on the geochemistry of the groundwater. Two sites of interest are presented to discuss some specific aspects of the geochemical processes and groundwater evolution in this aquifer system.

### 2. GEOLOGY AND HYDROGEOLOGY

The study area covers approximately 1500 km<sup>2</sup> and is located in the physiographic region of the St. Lawrence Lowlands, north-west of Montréal (Figure 1). The area is bordered to the North by the Laurentians, to the West by the Rivière des Outaouais, to the South by the Lac des Deux-Montagnes and the Rivière des Mille-Îles, and to the East by the watershed of Rivière Mascouche.

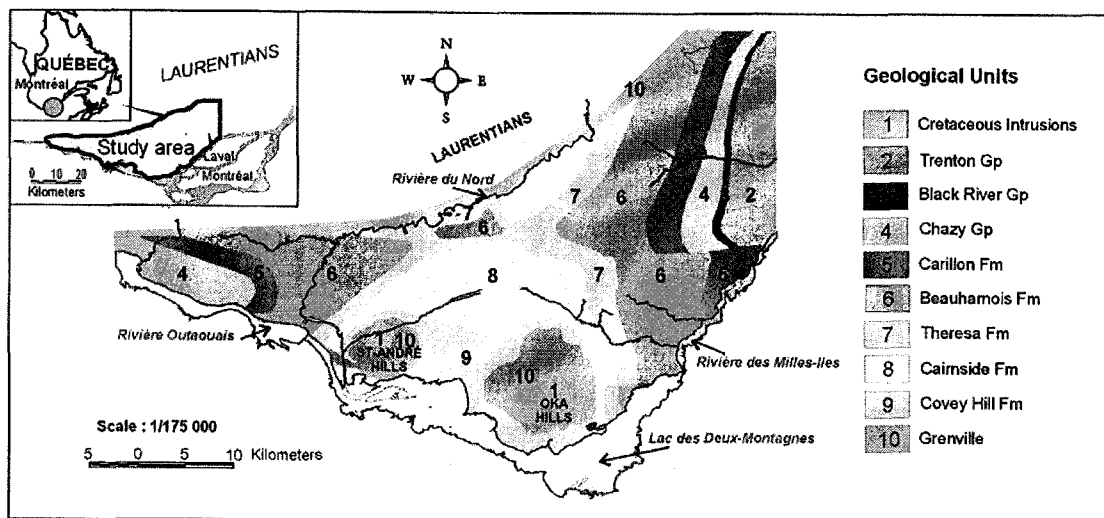


Figure 1. Location and geology of the study area (Geological map adapted from Rocher et al. 2001)

The regional aquifers are fractured sedimentary rocks belonging to Lower to Middle Paleozoic Formations. The geological map (Figure 1) shows the distribution of the main geological units (from the base): the Cambrian siliciclastic rocks of the Potsdam Group (Covey Hill and Cairnside formations), the Lower to Middle Ordovician dolostone rock of the Beekmantown Group (Theresa, Beauharnois and Carillon formations), and the limestone of the Chazy, Black River and Trenton Groups. The flat-lying Paleozoic formations sit in unconformity on Grenvillian Precambrian rocks. Precambrian rocks outcrop north of the study area (Laurentians), and around the Cretaceous intrusions (Oka and St-André Hills).

The rock formations are covered by marine and continental quaternary sediments (Bolduc and Ross 2000). Quaternary deposits are mainly Champlain Sea Clay. These deposits can reach a thickness of more than 40 meters in the buried valleys. Till deposits, with a thickness less than 5 meters, are found in the elevated topography areas. The aquifer is confined in areas where thick low permeability Quaternary deposits are found, such as in the buried valleys. Unconfined conditions exist in areas of elevated topography, where rock outcrops or sub-crops rock under thin sediments (generally till deposits).

### 3. METHODS OF INVESTIGATION

The approach used to study this fractured rock aquifer system was to determine the hydrogeochemistry of groundwater for all hydrogeological units, starting from the groundwater recharge areas, following the regional flow paths, down to discharge zones. The study also involves the hydrogeochemical recognition of all sources that could influence the composition of groundwater, from rain and snow in recharge zones, to sedimentary rocks interacting with water along the flow paths. The piezometric map (Figure 2) also shows the location of

stable isotopes monitoring stations and groundwater sampling sites. The program is described in more details by Bourque et al. (2001) and Cloutier et al. (2000).

#### 3.1 Precipitation and Groundwater Sampling

A network of 10 monitoring stations was established to evaluate the spatial and seasonal variability of the isotopic composition of rain and snow. Rain collectors were installed at each station with silicone oil to prevent evaporation. Rain sampling was done at the end of each month, and samples were analyzed for  $\delta^2\text{H}$  and  $\delta^{18}\text{O}$  values. Composite snow samples were collected at each of the 10 stations in March 1999 and 2000. Three suction lysimeters were also installed for the evaluation of infiltrated water in the vadose zone. The lysimeters and the rain collectors were sampled simultaneously. This characterization program allowed the establishment of a local meteoric water line for south-western Québec, and provided a good knowledge of the isotopic signature of recharge water.

Two methods were used for groundwater sampling. The first method is the bulk groundwater sampling of private, municipal and observation wells. Most of the wells in the area are open boreholes across all bedrock intervals under sediments without screens. A total of 154 wells were sampled using this method in 1999 and 2000, allowing the geochemical characterization of the main geological units. The second method uses discrete groundwater sampling of permeable zones isolated by packers in boreholes open to bedrock. A double packer system was used to isolate the intervals. This method allowed the characterization of vertical trends in groundwater geochemistry. Discrete groundwater sampling was performed in 18 wells, and a total of 78 intervals were sampled (3 to 6 intervals per well). The location of the intervals was based on the results of prior constant-head injection tests (Nastev et al. 2001).

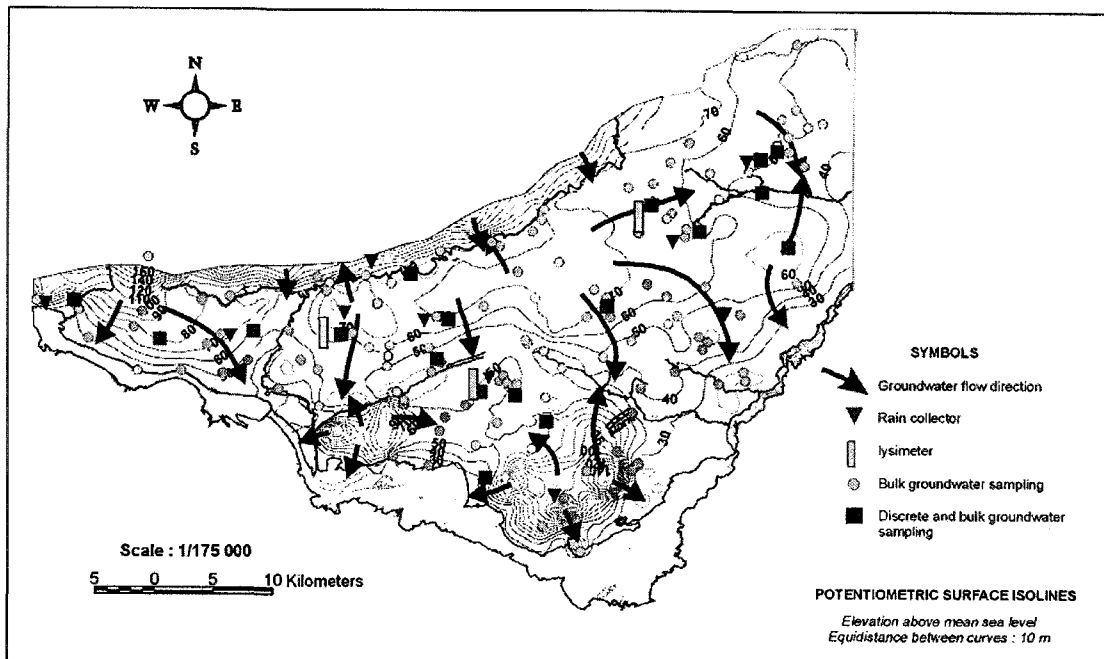


Figure 2. Piezometric map with the location of bulk and discrete groundwater samples, and stable isotopes monitoring stations (rain collectors, snow sampling, suction lysimeters) (Piezometric map simplified from Nastev et al. 2001)

Figure 2 shows the relation between the bulk and discrete groundwater sampling sites with groundwater flow. Wells were sampled along sections of groundwater flow paths, starting at preferential groundwater recharge areas. Regionally, the main groundwater flow paths are from North to South. Local groundwater flow systems are controlled by bedrock or surface topography.

### 3.2 Geochemical Characterization

Rain, snow and infiltration water were analyzed for  $\delta^2\text{H}$  and  $\delta^{18}\text{O}$ . All groundwater samples were analyzed for inorganic components, and  $\delta^2\text{H}$ ,  $\delta^{18}\text{O}$  and  $\delta^{13}\text{C}_{\text{DIC}}$ .  $\delta^{13}\text{C}_{\text{DIC}}$  results will not be discussed in this paper.

*In situ* field measurements were made on water samples for the following parameters: temperature with a glass thermometer, pH and electrical conductivity (E.C.) with a YSI 63 meter, dissolved oxygen (D.O.) with a YSI 95 meter and redox potential (Eh) with a Hanna ORP meter. Wells or sampling zones were purged until stabilization of measurements. Inorganic analyses were performed at the laboratory of the Ministère de l'Environnement du Québec using standard methods (Bourque et al. 2001).

Stable isotope analyses were performed at the Delta-Lab of GSC-Québec and at the G.G. Hatch Isotope Laboratories of the University of Ottawa.  $\text{H}_2$  gas was extracted from water samples using the zinc reduction method (Coleman et al. 1982). An IRM spectrometer (Micromass Prism III) (Delta-Lab) and an automated double collector VG 602E mass spectrometer (G.G.

Hatch) was used to analyze the  $\delta^2\text{H}$  ratios. Oxygen of 1 ml water samples was equilibrated with commercial  $\text{CO}_2$  at a controlled temperature using an automated system.  $\delta^{18}\text{O}_{\text{water}}$  was subsequently analyzed on the equilibrated  $\text{CO}_2$  with a VG-SIRA 12 IRMS. Isotopic results are reported with the standard  $\delta$  notation as per mil ( $\text{\textperthousand}$ ) deviations relative to V-SMOW. Analytical precision is  $\pm 0.1\text{\textperthousand}$  for  $\delta^{18}\text{O}$  and  $\pm 1.5\text{\textperthousand}$  for  $\delta^2\text{H}$ .

Duplicate samples (10% of the total) were submitted to verify data quality and accuracy. Charge balance was calculated to verify the analyses reliability. A charge balance of  $\pm 5\%$  is acceptable (Freeze and Cherry 1979). For the bulk groundwater samples, 135 samples have a charge balance below 5%, 12 between 5 and 8%, and 7 above 10%. Groundwater analysis with charge balance below 8% (147 samples) are retained for the interpretation of the inorganic data.

## 4. REGIONAL GROUNDWATER GEOCHEMISTRY

### 4.1 Groundwater Types and Hydrogeological Contexts

A groundwater sample is characterized by an assemblage of major ions. The dominants cations ( $\text{Ca}$ ,  $\text{Mg}$ ,  $\text{Na}$ ) and anions ( $\text{HCO}_3^-$ ,  $\text{Cl}^-$ ,  $\text{SO}_4^{2-}$ ) determine the groundwater type of the sample. Types are determined by converting ion concentrations in milli-equivalents per litre to percentages. All ions with concentrations exceeding 20% of the molar concentrations in solution define the groundwater type. The cations and anions

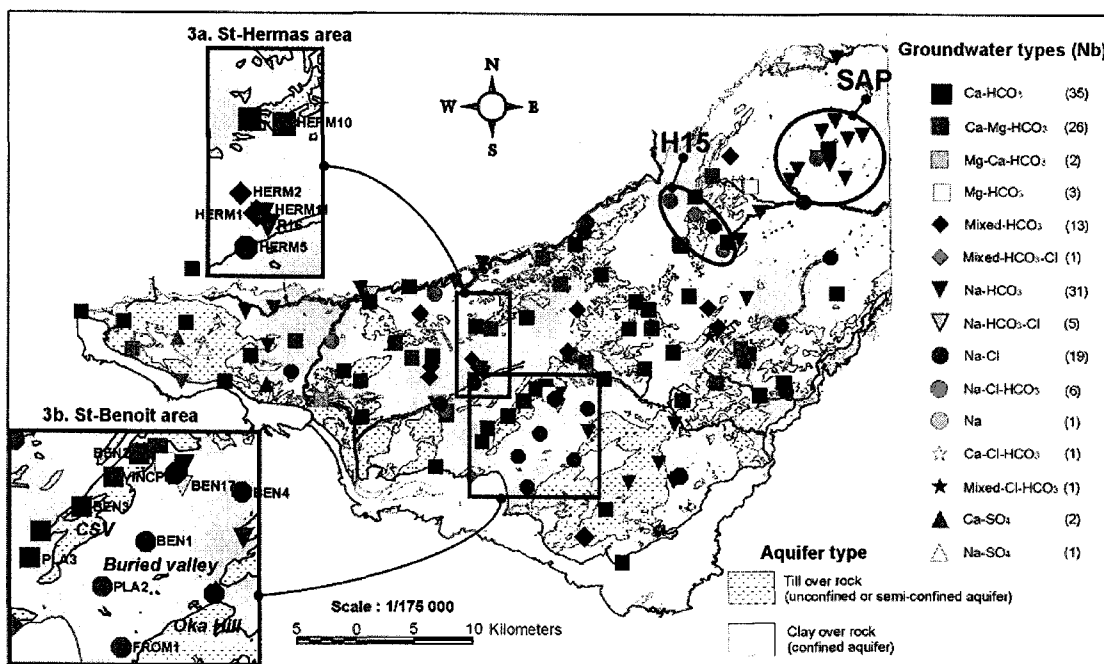


Figure 3. Regional distribution of groundwater types, and their relation to the hydrogeological contexts  
(Hydrogeological systems map adapted from Hamel et al. 2001, this volume)

exceeding 20% are listed in order of importance. Figure 3 shows the distribution of the groundwater types for the bulk samples, and its relation to the map of hydrogeological systems (Hamel et al. 2001, this volume). Figure 3 shows significant variations of groundwater types.

Figure 3 shows the five main groups of water types that are present in the study area. The first group (45 % of the samples) are bicarbonated groundwater, dominated by calcium and/or magnesium ( $\text{Ca}-\text{HCO}_3$ ,  $\text{Ca}-\text{Mg}-\text{HCO}_3$ ,  $\text{Mg}-\text{Ca}-\text{HCO}_3$ ,  $\text{Mg}-\text{HCO}_3$ ). These groundwaters are prevalent in the preferential groundwater recharge areas, and characterize modern meteoric water. The local groundwater flow systems play an important role in the distribution of  $\text{Ca}-\text{Mg}-\text{HCO}_3$  type groundwater, and on the geochemistry of this regional aquifer.

The next three groups mostly occur in the confined aquifers: (1) mixed-cations- $\text{HCO}_3$  (10% of the samples), (2)  $\text{Na}-\text{HCO}_3$  and  $\text{Na}-(\text{HCO}_3-\text{Cl})$  (24% of the samples), and (3)  $\text{Na}-\text{Cl}$  and  $\text{Na}-(\text{Cl}-\text{HCO}_3)$  (18% of the samples). The  $\text{Na}-\text{HCO}_3$  type groundwater is concentrated in the area of Ste-Anne-des-Plaines (SAP in Figure 3). The  $\text{Na}-\text{Cl}$  type groundwater is characteristic of groundwater found in the buried valley of St-Benoit, between Côte St-Vincent (CSV on Figure 3b) and Oka Hill. The  $\text{Na}-\text{Cl}$  type groundwater is also present in other confined areas, as in St-Hermas and Ste-Anne-des-Plaines. The interpretation for the presence of  $\text{Na}-\text{Cl}$  type groundwater will be discussed in the next section. The presence of  $\text{Na}-\text{Cl}$  or  $\text{Na}-\text{Cl}-\text{HCO}_3$  type groundwater in preferential groundwater

recharge areas may be the result of anthropogenic contamination. This could be the case for the sampling sites along Highway 15 (H15 on Figure 3). The last group are minors, and were only found in 3% of the samples. The interesting feature of this last group of groundwaters is the sulfate content ( $\text{Ca}-\text{SO}_4$  and  $\text{Na}-\text{SO}_4$ ) found in the western part of the region.

#### 4.2 Statistical Relationships Between Groundwater Types, Hydrogeological Contexts and Geology

Descriptive statistics are used in Figure 4 and 5 to define relationships between the groundwater geochemistry and the hydrogeological and geological contexts. Box plot diagrams are used to present the statistical results. They allow the display of the median, the 25<sup>th</sup> and 75<sup>th</sup> percentiles, and the outliers and extreme values.

Figure 4 shows the relations between E.C., Eh,  $\delta^{18}\text{O}$  and major ions (Ca, Na, Cl, SO<sub>4</sub>) with the hydrogeological contexts. The bulk groundwater samples for unconfined and confined conditions are represented for each parameters. The box plots show a decrease in Eh, Ca, SO<sub>4</sub> from unconfined to confined conditions. The decrease in Eh and SO<sub>4</sub>, indicating reducing conditions, correlates with field observations of H<sub>2</sub>S smells and higher H<sub>2</sub>S concentrations in confined areas. Higher Ca in unconfined areas are in agreement with the  $\text{Ca}-\text{Mg}-\text{HCO}_3$  type groundwater that dominates in recharge areas. The increase in E.C. is mainly due to the increase in Na and Cl observed for confined conditions. No significant variations are found in  $\delta^{18}\text{O}$  between unconfined and

confined conditions. This uniformity in  $\delta^{18}\text{O}$  could indicate a unique origin for the groundwater or well mixed groundwater sources in the aquifers. As it will be discussed further, inorganic chemistry will help discriminate between these possibilities.

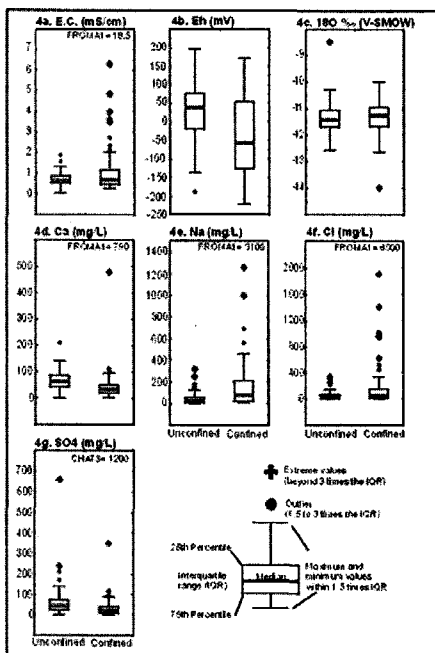


Figure 4. Box plots for unconfined and confined conditions

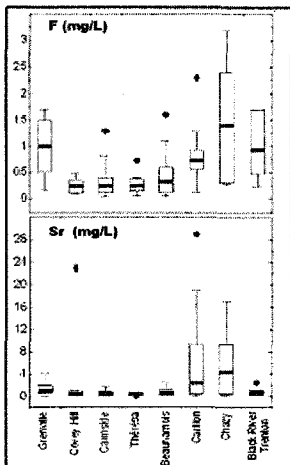


Figure 5. Box plots for the different geological units

Figure 5 shows the relation between minor ions (Sr, F) and the geological formations. Significant variations between geological units are seen for both ions. Sr dominates in the Carillon Formation and Chazy Group. F dominates in the Carillon Formation, the Chazy, Black River and Trenton Groups and the Precambrian rocks. The distribution of minor ions, as Sr and F, is thus influenced by the geological units.

#### 4.3 Precipitation and Groundwater Isotopic Signatures

The  $\delta^2\text{H}$  and  $\delta^{18}\text{O}$  results of rain water sampling are used to establish the local meteoric water line for the study area. Linear regression on the data results in the following relation,  $\delta^2\text{H} = 7.68\delta^{18}\text{O} + 11$  ( $r^2=0.97$ ), for the South-western Québec Meteoric Water Line (SWQMWL). The SWQMWL falls above the Global Meteoric Water Line (GMWL) (Craig 1961). Snow samples were not used to calculate the SWQMWL, since the samples were collected by coring the snowpack in March, and not at the time of precipitation. Results of our multiple snow sampling show a isotopic variation of the snow due to sublimation and vapour exchange, and isotope exchange between snow and meltwater during snow melt (Clark and Fritz 1997).

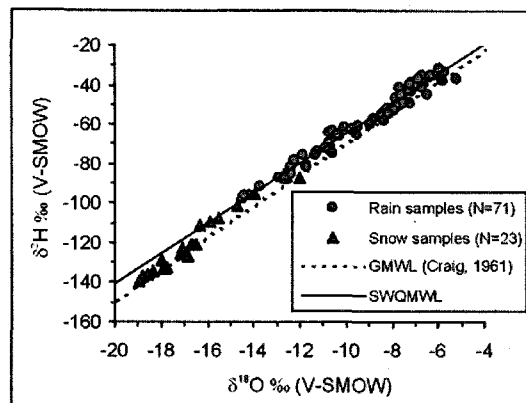
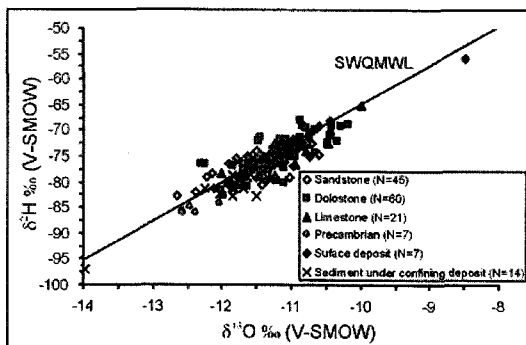


Figure 6. Local meteoric water line of the study area

Comparison of the isotopic results of the bulk groundwater samples to the SWQMWL is shown in Figure 7. The samples are distributed around the SWQMWL, indicating no significant modifications by water rock interaction. Figure 7 does not show preferential grouping of samples in relation to geology. The mean  $\delta^{18}\text{O}$  for all bulk groundwater samples is  $-11.3\text{‰}$ , with a standard deviation of 0.6. The  $\delta^{18}\text{O}$  of the modern meteoric water in the aquifer can be characterized by the mean  $\delta^{18}\text{O}$  of unconfined samples ( $-11.3\text{‰}$ , with a standard deviation of 0.6). This value is within the range obtained for infiltration water, and can be used as the average modern meteoric water for south-western Québec.

Figure 7. Diagram of  $\delta^2\text{H}$  and  $\delta^{18}\text{O}$  for groundwater

## 5. GROUNDWATER EVOLUTION IN THE AQUIFER

The previous section described the regional groundwater geochemistry of the aquifer, and its relation to the hydrogeological and geological contexts. The next step is to identify geochemical processes controlling groundwater chemistry and all water sources, and understand the geochemical evolution of groundwater. The approach taken is to follow geochemical changes along sections of groundwater flow paths, starting at preferential groundwater recharge areas. As local flow systems may play an important role in geochemical attributes of the aquifer, numerous sections have to be studied. This part of the article presents initial results obtained for a section, and proposes a conceptual model for the origin of salinity in the confined aquifers.

### 5.1 St-Hermas Section

The location of St-Hermas section is shown on Figure 3a. There are six sampling sites on this 5000 m long section, and groundwater flows from HERM10 in the recharge area, to HERM5 in a buried valley. Figure 8 shows the position of the groundwater samples on a Piper diagram (Piper 1944). The cation and anion triangles show an alignment of the samples from the recharge site HERM10 (Ca-Mg-HCO<sub>3</sub> type) to the southern site HERM5 (Na-Cl type).

A schematic cross-section shows the evolution of major ions and pH along the flow path (Figure 9). The diagrams show a decrease in Ca, Mg and HCO<sub>3</sub> along the flow path. This decrease is associated to an increase in Na, Cl, SO<sub>4</sub> and pH. Geochemical modeling will be performed to evaluate if geochemical processes, such as precipitation/dissolution or ion exchanges, could be responsible for part of this evolution. The other processes that will be investigated are the possible mixing of meteoric modern water with another water source, and the influence of the pore water chemistry of the upper marine clay deposit above the aquifer. The presence of a second water source is a possibility, as the conservative ion Br follows the Cl increase. Other information will be added to this study, such as the discrete groundwater samples for HERM10 and HERM11 and a <sup>14</sup>C date for well R16 (Simard 1977).

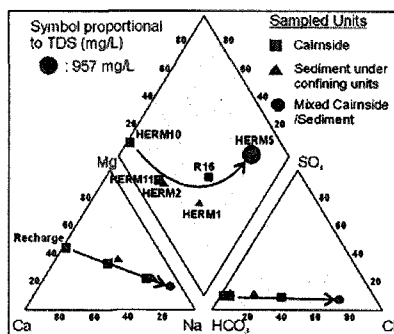


Figure 8. Piper diagram for the St-Hermas Section

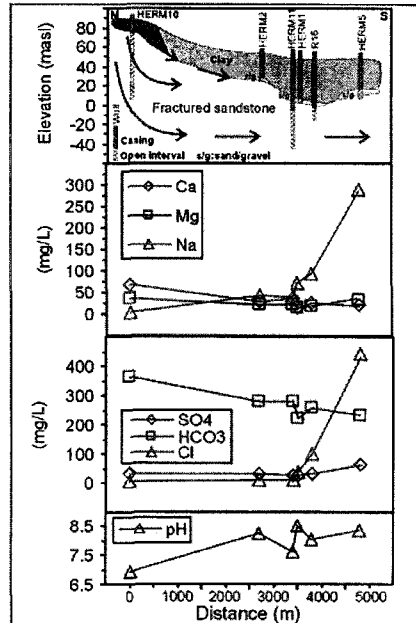


Figure 9. Schematic cross-section and evolution of major ions and pH along a flow path in the St-Hermas area

### 5.2 Origin of Groundwater Salinity: St-Benoit Area

The regional groundwater geochemistry shows that Na-Cl type groundwater includes 18% of the sites. Increasing salinity in groundwater may result from different processes, such as: (1) geochemical processes and water-rock interaction along the flow path, (2) presence of evaporite rocks, (3) anthropogenic contamination (de-icing salts), (4) mixing of meteoric water with formation water or seawater, and (5) diffusion from aquitard containing saline pore water (clay or shale units).

In the studied aquifer, the increase in salinity is associated with an increase in Cl and Na. In the geological context of the region, it is unlikely that geochemical processes and water-rock interactions could produce the Na-Cl type groundwater. As there are no evaporite formations in the aquifer, other sources must be

examined to explain the origin of salinity. Contamination by de-icing salts could explain the salinity along Highway 15, but not in the valleys as the aquifers are protected by clay deposits. Finally, mixing between meteoric water with a second water source and diffusion from aquitard, are processes that should be investigated in more details.

The St-Benoit area (Figure 3b) was chosen to propose an explanation for the origin of salinity, as samples with the highest salinity (FROM1, TDS expressed as salinity=11.4 g/L) and the largest concentration of Na-Cl type groundwater are found in this valley. The Piper diagram (Figure 10) shows the attributes of groundwater samples. The samples are located in two chemical sectors, the recharge area of Côte St-Vincent (CSV on Figure 3b) is on the Ca-Mg-HCO<sub>3</sub> pole, and the valley on the Na-Cl side of the diagram. An alignment is observed between the valley samples, from the lowest (BEN17) to highest (FROM1) TDS. Sample FROM1 falls near the composition of seawater. As the Champlain Sea occupied the study area during late Pleistocene, a seawater component could be the source of salinity in the area.

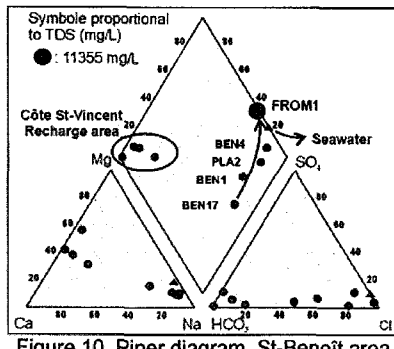


Figure 10. Piper diagram, St-Benoit area

The conservative ions Cl and Br are used as tracers to identify the seawater component. Table 1 compares molar ratios between seawater and samples from the valley. A good agreement is observed for both FROM1 and PLA2, indicating that seawater is a component of the valley samples. The agreement diminishes as TDS decreases.

Table 1. Molar ratios, seawater and valley samples

	Sea water	FROM 1	PLA2	BEN1	BEN4	BEN 17
Salinity	35	11.4	1.7	0.72	1.3	0.55
Na/Cl	0.858	0.735	0.893	1.122	1.126	1.851
Cl/Br	648.1	636.9	648.8	676.1	617.3	375.6

Table 2 compares ionic concentrations of FROM1 (in mmol) and seawater. If we assume that FROM1 is the original saline end-member of the area, conservative tracers can be used to determine the percentage of seawater present in the original formation water. By averaging the ratios of both ions, the calculated original formation water would have been a mixture of about 35%

of seawater and 65% of freshwater. In a study of Champlain Sea clay near Varennes, Desaulniers and Cherry (1989) calculated a very similar mixture of 33% of seawater and 67% of freshwater at a depth of 27 m in the clay deposit.

Table 2. Comparison between seawater and FROM1

Ion	Seawater (mmol) <sup>1</sup>	FROM1 (mmol)	FROM1/seawater
Cl	546	183	0.34
Br	0.84	0.29	0.35

<sup>1</sup>: Drever, 1997

Figure 11 uses Br and Cl diagrams to explain the mixing model proposed for the origin of salinity in the area. Step1 (Figure 11a) presents Champlain Seawater dilution with glacial meltwater and Pleistocene meteoric water. This dilution is responsible for the salinity of the original formation water observed in FROM1. FROM1 is a Pleistocene water source for the area. Step 2 (Figure 11b) illustrates the mixing of Pleistocene water source with modern meteoric water. FROM1 and Côte St-Vincent (CSV) samples form both end-members of the mixing model, and samples from the St-Benoit valley are located on the mixing line.

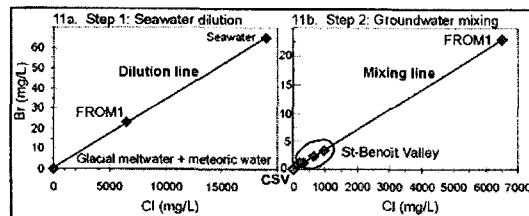


Figure 11. Diagram of Br versus Cl in the St-Benoit area

Figure 12 shows a diagram of  $\delta^{18}\text{O}$  and salinity based on the work of Hillaire-Marcel (1988). By mixing both end-members in a proportion of 35% seawater with 65% glacial meltwater and meteoric water, an original formation water with a  $\delta^{18}\text{O}$  of -10.4‰ and a salinity of 12.25 g/L is obtained. This is within the range of sample FROM1 ( $\delta^{18}\text{O} = -11.0\text{\textperthousand}$ , salinity=11.4 g/L). As it can be seen, the  $\delta^{18}\text{O}$  value of the Pleistocene water is similar to the average modern meteoric water, thus preventing the discrimination of Pleistocene water on the basis of  $\delta^{18}\text{O}$ .

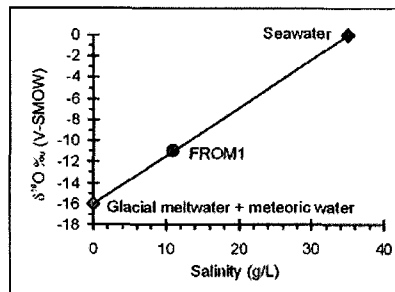


Figure 12. Diagram of  $\delta^{18}\text{O}$  versus salinity

## 6. SUMMARY AND CONCLUSION

This paper presented the results obtained from a regional hydrogeochemical groundwater characterization. These data are integrated in maps and graphs allowing first a qualitative understanding of the main geochemical processes controlling groundwater geochemistry and its spatial evolution. The hydrogeological contexts and the groundwater type map shows that the aquifer system is characterized by a number of groundwater recharge areas, introducing meteoric water ( $\text{Ca}-\text{Mg}-\text{HCO}_3$  type) into the aquifer. The distribution of groundwater types and the descriptive statistics show that the hydrogeological contexts exert an important control on the geochemistry of the groundwater. Minor ions, such as Sr and F, could be controlled instead by the geological formations.

Initial results of a section was presented to illustrate the approach used to characterize groundwater evolution along flow paths. A conceptual model for the origin of salinity in the confined aquifers was also proposed. The presence of local flow systems and the mixing of modern meteoric water with the Pleistocene water are important processes influencing groundwater geochemistry of this aquifer. Future work will include groundwater age dating along sections, determination of the clay pore water geochemistry and the integration of bulk and discrete groundwater analyses. Coupled flow and geochemical modeling will then be used to obtain a quantitative understanding of the controlling factors on the regional groundwater geochemistry.

## 7. ACKNOWLEDGEMENTS

Funding for this project was provided by the Geological Survey of Canada, Economic Development Canada, Conseil Régional de Développement-Laurentides, Ministère de l'Environnement du Québec, Regional County Municipalities of Argenteuil, Mirabel, Deux-Montagnes and Thérèse-de-Blainville, and Association des Professionnels de Développement Économique des Laurentides. Financial support for the first author was provided by NSERC as a postgraduate scholarship. The authors thank Normand Tassé (INRS-Géoressources) for his review. We thank all the students involved in the project for field assistance. We also thank M. Luzincourt (GSC-Québec), and W. Abdi (University of Ottawa) for isotope analyses. The collaboration of the population of the RCM giving site access is greatly appreciated.

## 8. REFERENCES

- Bolduc, A.M., and M. Ross, 2001. *Géologie des Formations superficielles, Lachute-Oka*; Commission géologique du Canada, Dossier public 3520, 1/50 000.
- Bourque, É., et al., 2001. *Résultats initiaux de la caractérisation hydrogéochemique des aquifères fracturés du sud-ouest du Québec*; Commission géologique du Canada, Recherche en cours 2001-D8, 9 p.
- Clark, I., and P. Fritz, 1997. *Environmental Isotopes in Hydrogeology*. Lewis Publishers, New York, 328 p.
- Cloutier, V., et al., 2000. Regional hydrogeochemical characterization of groundwater in fractured aquifers of the St-Lawrence Lowlands. In: *First Joint IAH-CNC and CGS Groundwater Specialty Conference, Montréal*, 3-10.
- Coleman, M.L., T.J. Shepherd, J.J. Durham, J.E. Rousse, and G.R. Moore, 1982. Reduction of water with zinc for hydrogen isotope analysis. *Analytical Chemistry*, 54 (6): 993-995.
- Craig, H., 1961. Isotopic variations in meteoric waters. *Science*, 133: 1702-1703.
- Desaulniers, D.E., and J.C., Cherry, 1989. Origin and movement of groundwater and major ions in a thick deposit of Champlain Sea clay near Montréal. *Canadian Geotechnical Journal*, 26: 80-89.
- Drever, J.I., 1997. *The Geochemistry of Natural Waters*. Prentice-Hall, 437 p.
- Freeze, R.A., and J.A. Cherry, 1979. *Groundwater*. Prentice-Hall, 604 p.
- Hamel, A. et al., 2001. Groundwater recharge for fractured rock aquifer in Southwestern Québec. In: *2<sup>nd</sup> Joint CGS-IAH Groundwater Specialty Conference, Calgary*.
- Hillaire-Marcel, C., 1988. Isotopic composition ( $^{18}\text{O}$ ,  $^{13}\text{C}$ ,  $^{14}\text{C}$ ) of biogenic carbonates in Champlain Sea Sediments. In: Gadd, N.R., ed., *The late Quaternary Development of the Champlain Sea Basin*: Geological Association of Canada, Special Paper 35, p. 177-194.
- Nastev, M. et al., 2001. *Regional hydrogeologic mapping project of the St-Lawrence Lowlands of southwestern Québec*; GSC, Current Research 2001-D9, 10 p.
- Nastev, M. et al., 2001. Investigation of hydraulic properties of regional fractured rock aquifers. In: *2<sup>nd</sup> Joint CGS-IAH Groundwater Specialty Conference, Calgary*.
- Piper, A.M., 1944. A graphic procedure in the geochemical interpretation of water-analyses. *American Geophysical Union. Papers, Hydrology*, 914-923.
- Rocher, M., et al., 2001. *Carte géologique des Basses-Terres du Saint-Laurent – Sud-Ouest du Québec*. En révision interne, CGC-Québec.
- Savard, M.M. et al., 2000. Regional Hydrogeology of fractured rock aquifers of southwestern Quebec. In: *First Joint IAH-CNC and CGS Groundwater Specialty Conference, Montréal*, p. 247-254.
- Simard, G., 1977. Carbon 14 and tritium measurements of groundwaters in the Eaton River Basin and in the Mirabel area, Québec. *Canadian Journal of Earth Science*, 14: 2325-2338.

## REGIONAL HYDROGEOCHEMICAL CHARACTERIZATION OF GROUNDWATER IN FRACTURED AQUIFERS OF THE ST. LAWRENCE LOWLANDS

Vincent Cloutier<sup>1</sup>, Édith Bourque<sup>2</sup>, René Lefebvre<sup>1</sup>, Martine M. Savard<sup>2</sup>, Miroslav Nastev<sup>2</sup> and Richard Martel<sup>1</sup>  
 1: INRS-Géoressources, Centre géoscientifique de Québec, 880 Chemin Sainte-Foy, C.P. 7500, Sainte-Foy,  
 Québec, Canada, G1V 4C7

2: Commission géologique du Canada, Centre géoscientifique de Québec, 880 Chemin Sainte-Foy, C.P. 7500,  
 Sainte-Foy, Québec, Canada, G1V 4C7

**ABSTRACT** This paper describes the initial results of a study aiming to characterize groundwater hydrogeochemistry at a regional scale ( $1500 \text{ km}^2$ ) in a fractured rock aquifer system. These data will allow the assessment of the quality of the groundwater resource of this area. The characterization will also be used to understand the geochemical processes controlling groundwater geochemistry. The first phase of groundwater sampling took place in 1999, and it will be completed in 2000. In 1999, inorganic and bacteriological parameters were analyzed in 69 groundwater samples. They were also analyzed for the stable isotopes  $\delta^{18}\text{O}$  and  $\delta^{13}\text{C}_{\text{PDB}}$ . In addition, precipitations were sampled for stable isotopes ( $\delta^{18}\text{O}$  and  $\delta^2\text{H}$ ) to establish the Local Meteoric Water Line of the study area. This paper presents the preliminary results of chemical and isotopic analyses in groundwater samples and precipitations (Local Meteoric Water Line). We noticed significant spatial variations of groundwater composition and quality in the area, and to date, aesthetical objectives of Health Canada (1996) are often exceeded.

**RÉSUMÉ** Cet article présente les résultats initiaux d'une étude dont le but est de caractériser l'hydrogéo chimie des eaux souterraines à l'échelle régionale ( $1500 \text{ km}^2$ ) dans un système aquifère de roc fracturé. Ces données vont permettre l'évaluation de la qualité de la ressource en eaux souterraines de ce secteur. Cette caractérisation sera aussi utilisée pour comprendre les processus géochimiques contrôlant la géochimie des eaux souterraines. La première phase de l'échantillonnage des eaux souterraines a commencé en 1999, et celui-ci sera complété en 2000. En 1999, les paramètres inorganiques et microbiologiques ont été analysés dans 69 échantillons d'eau souterraine. Ils ont aussi été analysés pour les isotopes stables  $\delta^{18}\text{O}$ , et  $\delta^{13}\text{C}_{\text{PDB}}$ . De plus, les précipitations ont été échantillonnées pour les isotopes stables ( $\delta^{18}\text{O}$  et  $\delta^2\text{H}$ ) afin d'établir la Droite Locale des Eaux Météoriques pour la région à l'étude. Dans cet article, nous présentons les résultats préliminaires des analyses chimiques et isotopiques dans les eaux souterraines et les précipitations (Droite Locale des Eaux Météoriques). Ces analyses révèlent des variations significatives de la composition et de la qualité des eaux souterraines dans la région, et les dépassages d'objectifs esthétiques de Santé Canada (1996) sont fréquents.

### 1. INTRODUCTION

A hydrogeochemical characterization of groundwater is underway in four southwestern Québec Regional County Municipalities (RCM): Argenteuil, Mirabel, Deux-Montagnes and Thérèse-de-Blainville (Figure 1). This study is part of a regional hydrogeological mapping project of southwestern Québec fractured rock aquifers conducted by the Geological Survey of Canada, in collaboration with INRS-Géoressources, Laval University and Environment Canada. This project aims to understand both the hydrodynamics and hydrogeochemistry of the aquifer system (Savard et al. 2000, this volume; Nastev et al. 2000, this volume). The overall characterization program thus covers both physical and hydrogeochemical parameters.

The hydrogeochemical study aims to assess the regional quality of groundwater and to understand the processes that control groundwater geochemistry. Within the larger project, the geochemical and isotopic data will be used to better constrain the conceptual hydrogeological and applied numerical models. In addition, the hydraulic characterization will be used to help identify geochemical processes affecting groundwater composition along its flow paths.

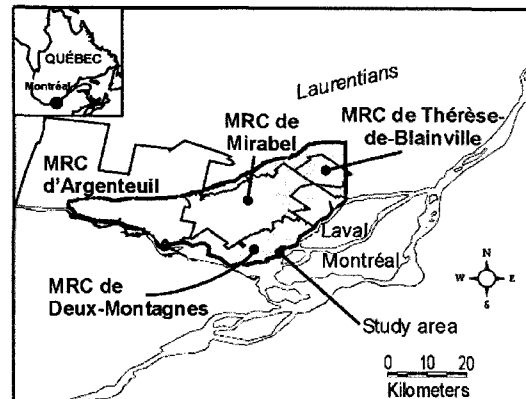


Figure 1. Location of the study area and the four RCM covered by this study.

## 2. GEOLOGY AND HYDROGEOLOGY

The study area is located in the physiographic region of the St. Lawrence Lowlands, northwest of Montréal. It is bordered to the North by the Canadian Shield (Laurentians), to the West by the Rivière des Outaouais, to the South by the Lac des Deux-Montagnes and the Rivière des Milles-îles, and to the East by the watershed of Rivière Mascouche.

The stratigraphy of the study area is presented by Savard et al. (2000, this volume). The regional aquifers are fractured sedimentary rocks of the Lower to Middle Paleozoic formations. The geological map (base map on Figure 5, adapted from Salad Hersi et al. 2000) shows the distribution of the main geological units: the Potsdam (Covey Hill and Cairnside formations), Beekmantown (Thérèsa and Beauharnois formations), Chazy, Black River and Trenton groups consisting of sandstone, dolostone and limestone rocks.

The hydrogeological contexts of the study area are presented in Figure 2. This schematic map is based on field observations and several maps such as: topography, surficial sediments thickness, piezometry (Savard et al. 2000, this volume), and the preliminary Quaternary geology

(Bolduc and Ross, in preparation). Groundwater flow directions, established from the piezometric map (Savard et al. 2000, this volume), are also presented on Figure 2.

The study area is divided into areas of preferential groundwater recharge and confined conditions. The recharge areas are outlined based on elevated topography, elevated piezometric conditions, and the presence of outcrops or sub-cropping conditions. The confined aquifer conditions are in areas where thick low permeability Quaternary deposits are present. They are often found in valleys filled with Champlain Sea clays. Associated to these valleys, we found an area of elevated salinity in the region of St-Benoît (BN on Figure 2). Saline conditions were also identified in previous studies (Simard 1978; Agéos and INRS-Eau 1998). There is saline water in other locations within the study area but they are not shown on Figure 2. Also, below a certain depth, saline water is found underlying fresh groundwater in many other locations. Regionally, the main groundwater flow paths are from North to South. Local groundwater flow systems are controlled by bedrock or surface topography.

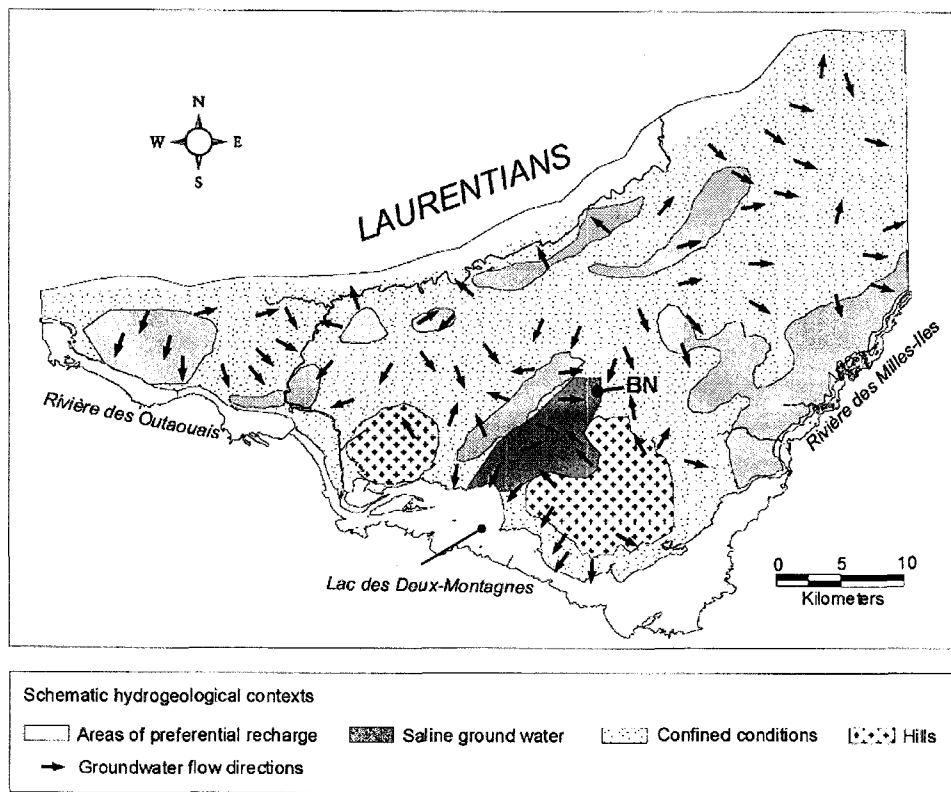


Figure 2. Schematic hydrogeological contexts and groundwater flow directions.

### 3. METHODS OF INVESTIGATION

The hydrogeochemical characterization of the fractured rock aquifer system involves the determination of geochemical and isotopic characteristics of groundwater for all hydrogeological units, from the recharge zones, along regional flow paths down to discharge zones. The study also involves the determination of the hydrogeochemistry of all the sources that can influence the composition of groundwater, from rain and snow in recharge zones, to the sedimentary rocks interacting with water along the flow paths.

The regional groundwater sampling, initiated in 1999, was performed in the following units: (1) the sedimentary rocks of Paleozoic formations (sandstones, dolostones and limestones), (2) the Precambrian rocks and the Cretaceous intrusions (Monteregian Hills), and (3) Quaternary deposits. Groundwater was sampled at 16 municipal wells and 53 domestic wells. Samples were analyzed for inorganic and bacteriological parameters,  $\delta^{18}\text{O}$ ,  $\delta^2\text{H}$  and  $\delta^{13}\text{C}_{\text{DIC}}$ . Results for bacteriological parameters and  $\delta^{13}\text{C}_{\text{DIC}}$  are not presented in this paper.

As part of the characterization program, a network of 10 monitoring stations was established to evaluate the spatial and seasonal variability of the isotopic composition of rain and snow (Figure 3). Rain collectors were installed at each station with silicone oil to prevent evaporation. Rain sampling is done at the end of each month, and the rainwater samples are analyzed for  $\delta^{18}\text{O}$  and  $\delta^2\text{H}$ . In March 2000, composite snow samples were also sampled at each of the 10 stations. Three suction lysimeters were also installed for the evaluation of infiltrated water in the vadose zone (Figure 3). The lysimeters and the rain collectors are sampled simultaneously.

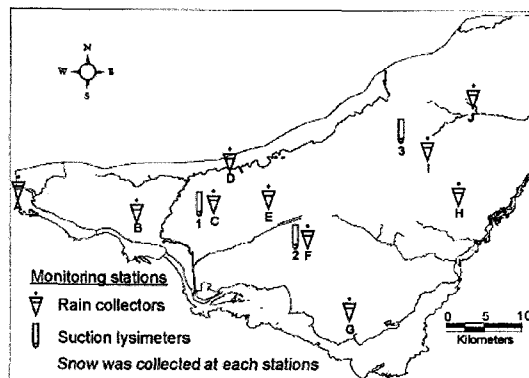


Figure 3. Location of stable isotope monitoring stations: rain collectors, snow sampling and suction lysimeters.

Field measurements were made *in situ* on collected water samples for the following parameters: temperature with a glass thermometer, pH and electrical conductivity (E.C.) with a YSI model 63 meter, dissolved oxygen (D.O.) with a YSI

model 95 meter and redox potential (Eh) with a Hanna ORP redox meter.

Both inorganic and bacteriological analyses were performed at the laboratory of the Ministère de l'Environnement du Québec using standard methods (MEF 1994).

Stable isotope analysis was performed at the Delta-Lab of GSC-Québec.  $\text{H}_2$  gas was extracted from rain samples using the zinc reduction method (Coleman et al. 1982), and an IRM spectrometer (Micromass Prism III) was used to analyze the  $\delta^2\text{H}$  ratios. Oxygen of 1 ml water samples was equilibrated with commercial  $\text{CO}_2$  at a controlled temperature using an autowater system.  $\delta^{18}\text{O}_{\text{water}}$  was subsequently analyzed on the equilibrated  $\text{CO}_2$  with a VG-SIRA 12 IRMS. Isotopic results are reported with the standard  $\delta$  notation as per mil (‰) deviations from V-SMOW. Analytical precision is  $\pm 0.2\text{‰}$  for  $\delta^{18}\text{O}$  and  $\pm 2\text{‰}$  for  $\delta^2\text{H}$ .

The hydrogeochemical program for year 2000 includes multilevel samples collected in boreholes within intervals isolated using packers. This will allow the characterization of vertical as well as areal trends in groundwater geochemistry.

### 4. RESULTS AND DISCUSSION

#### 4.1 Regional Groundwater Geochemistry

Table 1 summarizes the results of inorganic parameters of the 69 samples. Criteria for health (Health Canada 1996) are exceeded only for 3 parameters on very few samples (number in parenthesis): F (4),  $\text{NO}_3$  (1) and Ba (1). However, values above aesthetical parameters (Health Canada 1996) are frequent: Fe (14),  $\text{H}_2\text{S}$  (12), Mn (11), Na (8), Cl (7), pH (5) and  $\text{SO}_4$  (2).

Figures 4 and 5 present the regional distribution of selected geochemical parameters. Depending on the parameters, schematic hydrogeological contexts (Figure 4) or the bedrock geology (Figure 5) were chosen as base maps.

The regional distribution of water types (Figure 4a), electrical conductivity (E.C.) (Figure 4b), dissolved oxygen (Figure 4c) and nitrate concentrations (Figure 4d) are illustrated within the hydrogeological contexts. The objective is to evaluate their relationships with preferential groundwater recharge zones and confined conditions.

Water types (Figure 4a) are calculated by converting the milli-equivalents per liter of the major cations ( $\text{Na}$ ,  $\text{Ca}$ ,  $\text{Mg}$ ) and anions ( $\text{Cl}$ ,  $\text{SO}_4$ ,  $\text{HCO}_3$ ) to percentages (Waterloo Hydrogeologic Inc. 1999). To simplify the number of water types, we took as major ions all ions with concentrations exceeding 20% of the molar concentrations in solution. The map shows significant variations of water types.  $\text{Ca}-\text{HCO}_3$  and  $\text{Ca}-\text{Mg}-\text{HCO}_3$  water types generally characterize the areas of preferential groundwater recharge. On the other hand, groundwater from geological units below marine clay deposits, as in the St-Benoît area (BN on Figure 4a),

Table 1. Results of inorganic parameters.

Parameters	Units	M.A. <sup>1</sup>	Avg. <sup>2</sup>	St. Dev. <sup>3</sup>	N <sup>4</sup>
<b>Field</b>					
Temperature	°C	a	9.5	0.9	53
pH		a	7.7	0.3	69
E.C. <sup>5</sup>	µS/cm	a	865.6	605.7	69
D.O. <sup>6</sup>	mg/L	a	2.9	2.5	53
Eh	mV	a	-40	94	53
<b>Laboratory</b>					
Color	TCU	c	8.8	17.5	44
Total alkalinity	mg/L				
CaCO <sub>3</sub>	g	252.7	97.5	60	
DIC <sup>7</sup>	mg/L	c	62.6	23.2	69
DOC <sup>8</sup>	mg/L	c	2.3	2.7	69
Na	mg/L	b	91.2	115.0	69
K	mg/L	b	7.7	6.5	66
Mg	mg/L	b	24.4	13.1	69
Ca	mg/L	b	52.9	63.0	69
Sr	mg/L	b	2.0	4.7	69
Mn	mg/L	b	0.062	0.118	69
Fe	mg/L	b	0.64	2.07	66
NH <sub>4</sub>	mg/L	c	0.267	0.373	66
Li	mg/L	b	0.016	0.02	53
Ba	mg/L	b	0.166	0.177	69
F	mg/L	c	0.505	0.535	68
Cl	mg/L	g	97.4	163.0	69
Br	mg/L	f	0.263	0.568	69
I	mg/L	f	0.103	0.017	69
SO <sub>4</sub>	mg/L	c	65.5	161.1	69
NO <sub>3</sub>	mg/L	c	0.583	1.867	66
P total	mg/L	c	0.178	0.453	65
SiO <sub>2</sub>	mg/L	b	13.33	3.335	69
B	mg/L	b	0.163	0.205	68
H <sub>2</sub> S	mg/L	c	0.129	0.491	69
Zn	mg/L	b	0.007	0.007	69
Cu	mg/L	b	0.003	0.008	69
Ni	mg/L	b	0.001	0.003	67
Al	mg/L	b	0.013	0.01	69
As	mg/L	d	0.001	0.001	69
Cd	mg/L	b	0.001	0.001	69
Ag	mg/L	b	0.0	0.0	69
Cr	mg/L	b	0.001	0.0	69
Hg	mg/L	e	0.0	0.0	69
Pb	mg/L	b	0.004	0.0	69
Se	mg/L	d	0.001	0.0	53
CN	mg/L	c	0.003	0.001	48
U	mg/L	b	0.006	0.002	53
<b>Calculated</b>					
HCO <sub>3</sub>	mg/L		298.6	119.9	69
Total hardness	mg/L		232.2	194.5	69
TDS <sup>9</sup>	mg/L		480.3	362.4	69

<sup>1</sup>: Method of analysis:

a : Field meters

c : Colorimetry

e : Cold vapor

g : Conductivity

b : ICP-OES

d : Hydride generation

f : Ionic chromatography

<sup>2</sup> : Average<sup>3</sup> : Standard deviation<sup>4</sup> : Number of samples<sup>5</sup> : Corrected to 25 °C<sup>6</sup> : Dissolved oxygen<sup>7</sup> : Dissolved inorganic carbon<sup>8</sup> : Dissolved organic carbon<sup>9</sup> : Total dissolved solids

has a Na-Cl water type. This water type could result from rock-water interaction, or from mixing of recharge water with former Champlain Sea water. An interesting feature is the presence of Na-HCO<sub>3</sub> water type in the area of Sainte-Anne-des-Plaines (SAP on Figure 4a). The processes that generated this type of water are still being investigated.

The electrical conductivity, corrected to 25 °C, generally increases from the recharge zones to the confined areas (Figure 4b). As expected, the dissolved oxygen is higher in the preferential recharge zones compared to the confined areas (Figure 4c). Finally, nitrates are found in the preferential recharge areas or in their vicinity (Figure 4d), indicating an anthropogenic origin. Figure 4 thus shows that the hydrogeological context exerts an important control on groundwater geochemistry.

The regional distribution of selected parameters with respect to geology is presented on Figure 5. The iron distribution (Figure 5a) shows that many wells have iron concentrations exceeding the aesthetic criteria of Health Canada (1996) of 0.3 mg/L. Fluorides (Figure 5b), strontium (Figure 5c) and phosphorous (Figure 5d) are presented to illustrate the higher concentrations in the areas of St-Philippe and Sainte-Anne-des-Plaines (respectively SP and SAP on Figure 5) for fluorides and strontium, and in the area of Sainte-Anne-des-Plaines for phosphorous. The processes that generated these higher concentrations are still being investigated.

#### 4.2 Stable Isotopes

The isotopic characterization of precipitations constitutes a prerequisite to help discriminate between the potential sources of groundwaters in the study area, namely the Champlain Sea water, glacial meltwater, formation and precipitation waters. Figure 6 shows the local Southwestern Québec Meteoric Water Line (SWQMWL) established from the precipitations of September and October 1999, and 3 composite snow samples (stations D, J, F on figure 3) collected in March 2000. The SWQMWL falls above the Ottawa Meteoric Water Line (Fritz et al. 1987a) and the Global Meteoric Water Line (Craig 1961b). This relative position of the SWQMWL results from climatic conditions such as humidity at the site of ocean evaporation (tropical Atlantic ocean) which controls the deuterium excess, and mixing of air masses in Eastern Canada (Vitali et al. 1999). The isotopic results of 2000 should better constrain the SWQMWL and help understand the observed variations in the study area.

The oxygen isotope ratios of regional groundwater from wells range from -12.64‰ to -10.46‰, with 81% of the samples between -11.8‰ and -10.6‰ (Figure 7). The values of the 58 groundwater samples clearly fall in the range of δ<sup>18</sup>O ratios obtained for the regional precipitations (Figure 6), indicating the expected linkage between local precipitations and groundwaters. However, the integration of these results with the groundwater δ<sup>2</sup>H and <sup>87</sup>Sr/<sup>86</sup>Sr ratios that are now being analyzed is required to evaluate the influence of water-rock interaction and of mixing with other water sources on the geochemical attributes of Southwestern Québec groundwaters.

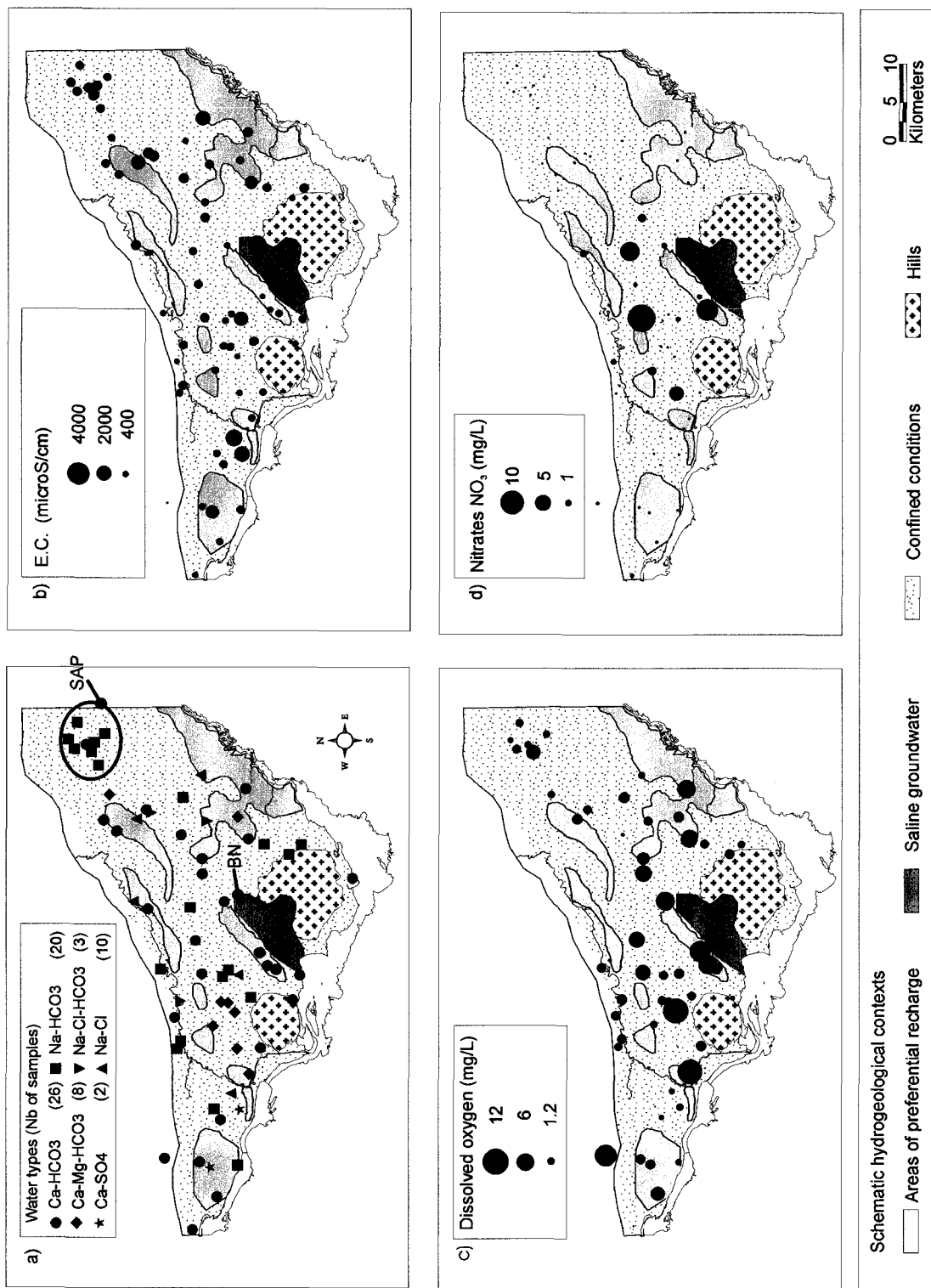


Figure 4: a) Water types and regional distribution of different parameters in groundwater b) E.C. c) dissolved oxygen d) nitrates

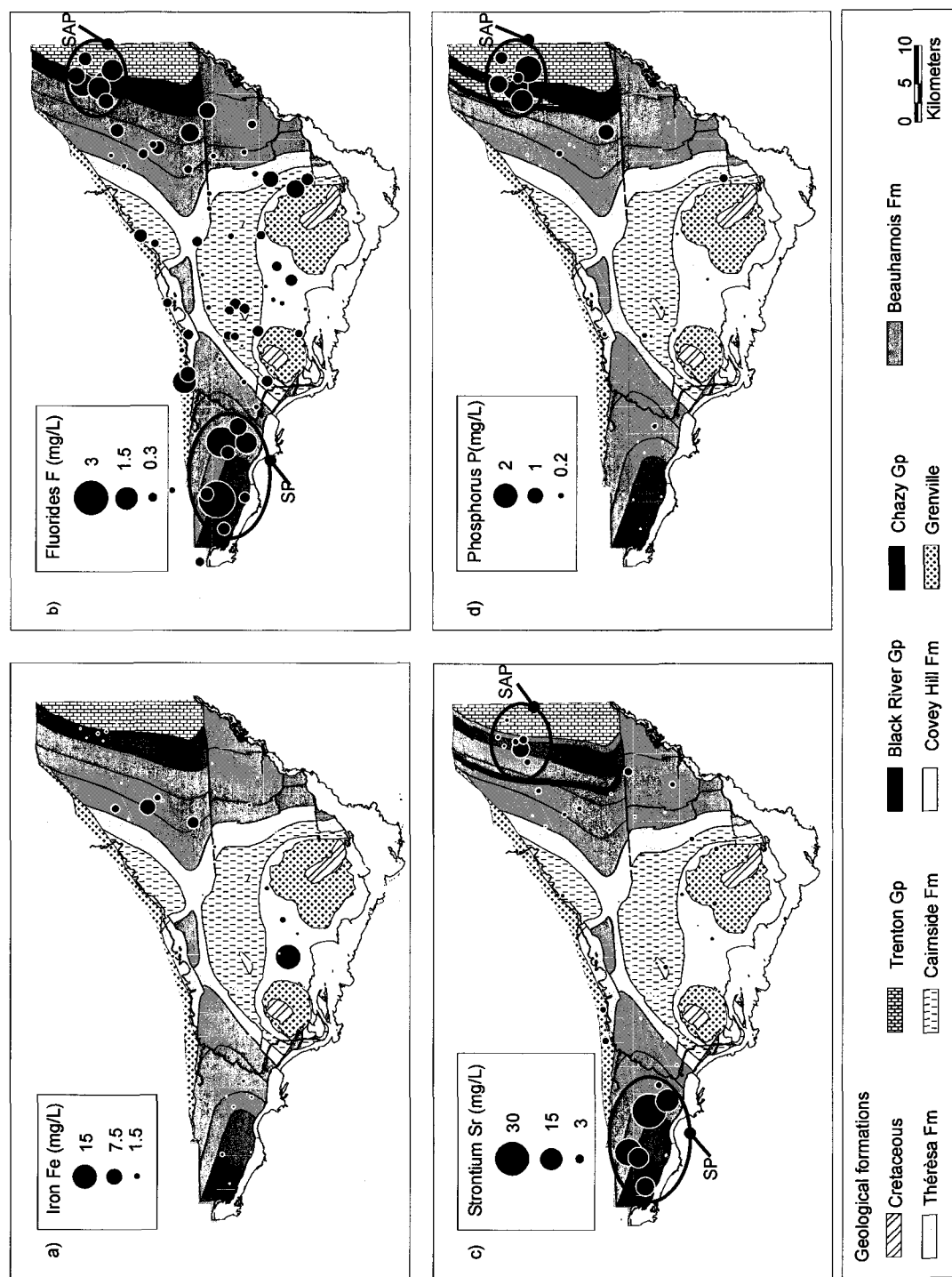


Figure 5. Regional distribution of selected chemical elements in groundwater: a) iron, b) fluoride, c) strontium, d) phosphorus.

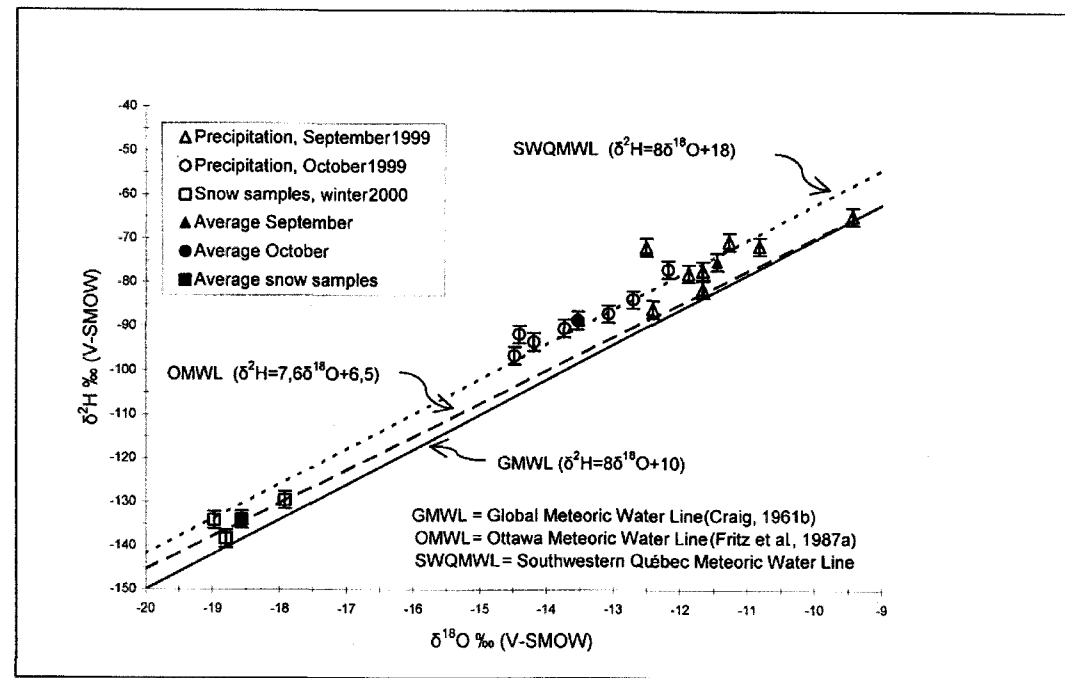


Figure 6. Local Meteoric Water Line of the study area.

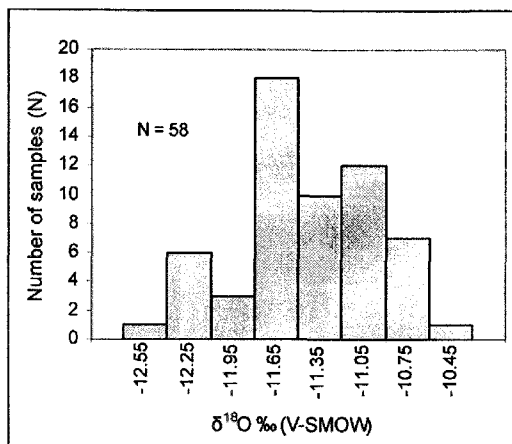


Figure 7. Frequency distribution of δ¹⁸O in groundwater.

## 5. CONCLUSION

The regional inorganic geochemistry for 69 groundwater samples were presented within the hydrogeological and geological contexts of the study area. It was shown that the context exerts an important control on the geochemistry of

the groundwater. The details of the geochemical processes affecting groundwater are still being investigated.

The paper also presented initials results for isotopes of oxygen and hydrogen. Precipitation and snow sampling allowed a first determination of the local Southwestern Québec Meteoric Water Line. Preliminary results for δ¹⁸O in groundwater show that samples fall in the range of δ¹⁸O ratios obtained for the regional precipitations.

These results form the basis for the next phase of hydrogeochemical characterization in the study area. The next phase is focusing on multi-level groundwater sampling in boreholes using packers to characterize groundwater hydrogeochemistry vertically in the aquifer formations. The composite and multi-level data will be integrated to understand the geochemical processes controlling the groundwater geochemistry and its evolution. Coupled flow and geochemical modeling will be used to obtain a quantitative understanding of the controlling factors on the regional groundwater geochemistry.

## ACKNOWLEDGEMENTS

Funding for this project was provided by the Geological Survey of Canada (GSC contribution No. 2000073), Economic Development Canada, Conseil Régional de Développement-Laurentides, Ministère de l'Environnement du Québec, Regional County Municipalities of Argenteuil, Mirabel, Deux-Montagnes and Thérèse-de-Blainville, and Association des Professionnels de Développement Économique des Laurentides. Financial support for the first author was provided by NSERC as a postgraduate scholarship. The authors thank Yves Michaud for his review. We thank Caroline Meilhac, Marjolaine Bessette, Nathalie Fagnan and John Voralec for field assistance. We also thank Marc Luzincourt (Delta-lab, GSC-Québec) for technical assistance with isotope analyses. The collaboration of the population of the RCM giving site access is greatly appreciated. Finally, we sincerely acknowledge the constant support from Jean-Luc Riopel, Marc Carrière, Carole Hart and Guy Raynault.

## REFERENCES

- AGÉOS et INRS-Eau, 31 mars 1998, Développement d'outils pour la gestion intégrée des usages de la ressource - eau souterraine et application à la région hydrogéologique Nord de Montréal, Rapport final d'activités, janvier 1995-mars 1998, 171 pp.
- Bolduc, A.M. and Ross, M., in preparation, Géologie des formations superficielles, région de Lachute, Québec, Geological Survey of Canada, Open File, 1:50,000.
- Coleman, M.L., Shepherd, T.J., Durham, J.J., Rousse, J.E. and Moore, G.R., 1982, Reduction of water with zinc for hydrogen isotope analysis, Analytical Chemistry, v. 54, no. 6, p. 993-995.
- Craig, H., 1961b, Isotopic variations in meteoric waters, Science, 133, p. 1702-1703.
- Fritz, P., Drimmie, R.J., Frapé, S.K. and O'Shea, K.J., 1987a, The isotopic composition of precipitation and groundwater in Canada, In: Isotope Techniques in Water Resources Development, IAEA Symposium 299, March 1987, Vienna, p. 539-550.
- Health Canada, 1996, Guidelines for Canadian drinking water quality, Sixth edition, 102 pp.
- MEF, 1994, Guide d'échantillonnage à des fins d'analyses environnementales, Cahier 3, Échantillonnage des eaux souterraines, Ministère de l'Environnement et de la Faune, Les éditions le Griffon d'argile, Sainte-Foy, Québec, Canada, 101 p.
- Nastev, M., Lapcevic, P., Voralek, J., Girard, F., Etienne, M., Savard, M.M., 2000, Hydraulic characterization of fractured aquifers of St.Lawrence lowlands in southwestern Quebec, In : First Joint IAH-CNC and CGS Groundwater Specialty Conference, Montréal.
- Salad Hersi O., and Lavoie, D., 2000. Stratigraphie et plaoenvironnements des unités de la marge passive (groupes de Potsdam et de Beekmantown), région de Montréal. Document du Ministère des Ressources Naturelles du Québec, en préparation.
- Savard, M.M., Nastev, M., Lefebvre, R., Martel, R., Fagnan, N., Bourque, É., Cloutier, V., Lauzière, K., Gélinas, P., Kirkwood, D., Lapcevic, P., Karanta, G., Hamel, A., Bolduc, A., Ross, M., Parent, M., Lemieux, J.-M., Boisvert, E., Salad Hersi, O., Lavoie, D., Girard, F., Novakowski, K., Therrien, R., Etienne, M., Fortier, R., 2000, Regional Hydrogeology of fractured rock aquifers of southwestern Quebec (St.Lawrence Lowlands), In : First Joint IAH-CNC and CGS Groundwater Specialty Conference, Montréal.
- Simard, G., 1978, Hydrogéologie de la région de Mirabel, Ministère des Richesses Naturelles du Québec, Service des eaux souterraines, 69 pp.
- Vitali, F., Savard, M.M., Bourque, É., and Michaud, Y., 1999, Environment isotope geochemistry of Laurentian piedmont groundwater, Québec, in Current Research 1999-E, Geological Survey of Canada, p. 139-148.
- Waterloo Hydrogeologic Inc., 1999, AquaChem v.3.7, Aqueous geochemical data analysis, plotting and modeling, User's Manual, 184 pp.

## **Appendice G**

### **DISQUE COMPACT DES DONNÉES HYDROGÉOCHIMIQUES**

**Disque compact des données hydrogéochimiques**

L'Appendice G présente les données hydrogéochimiques sous forme de fichiers numériques dans un disque compact (en pochette de la thèse). Le Tableau G.1 présente la liste des dossiers et des fichiers du disque compact, ainsi que le contenu des fichiers.

Le disque compact inclut la base de données géochimiques (échantillonnage régional, multi-niveaux, des précipitations et des argiles), les tableaux de données qui accompagnent les chapitres 3 et 5, la base de données géochimiques en format AquaChem (Waterloo Hydrogeologic, 1999), les fichiers de modélisation géochimique PHREEQCI 2.8 (Charlton et Parkhurst, 2002) de l'Appendice E et les fichiers d'entrée pour l'ensemble des échantillons, et les fichiers Statistica version 6.1 (StatSoft Inc., 2004) du Chapitre 5.

Tableau G.1. Liste des dossiers et des fichiers du disque compact (en pochette de la thèse), ainsi que le contenu des fichiers

Dossier (3 niveaux)	Fichier	Type	Contenu
<b>BD_Basses_Laurentides</b>			
Eaux_Souterraines	BD_Basses_Laurentides_ES_note.doc	Word	Information pour le fichier Excel
	BD_Basses_Laurentides_ES.xls	Excel	Données des eaux souterraines
Précipitations	BD_Basses_Laurentides_Precipitations.xls	Excel	Données des précipitations
Argiles	BD_Basses_Laurentides_Argile.xls	Excel	Données des argiles
Chapitre_3	vcloutier_ESM_1.xls	Excel	Table ESM-1 (voir p. 123)
	vcloutier_ESM_2.doc	Word	Table ESM-2 (p. 124)
	vcloutier_ESM_3doc	Word	Table ESM-3 (p. 125)
Chapitre_5	Chap5_appendix_note.doc	Word	Information pour le fichier Excel
	Chap5_appendix.xls	Excel	Appendice du Chap. 5 ( p. 221-224)
AquaChem	Basses_Laurentides_AquaChem_note.doc	Word	Information pour la base de données
Fichier_original_in	Basses_Laurentides.txt	Texte	Fichier de données importé dans
	Basses_Laurentides.xls	Excel	AquaChem
<b>BD_AquaChem</b>			
version_3_7	Basses_Laurentides.HC3	AquaChem 3.7	Base de données AquaChem
	Basses_Laurentides.CFG	AquaChem 3.7	
	Basses_Laurentides.MSK	AquaChem 3.7	
version_4	Basses_Laurentides.AQC	AquaChem 4	Base de données AquaChem
	Basses_Laurentides.sav	AquaChem 4	
	Basses_Laurentides.CFG	AquaChem 4	
<b>PHREEQCI</b>			
S86	S86.pqi	PHREEQCI	Exemple de spéciation pour
	S86.pqo	PHREEQCI	l'échantillon S86 (Appendice E)
Regional			
in	regional.pqi	PHREEQCI	Fichier d'entrée
out	regional.pqo	PHREEQCI	Fichier de résultats
	regional.sel	PHREEQCI	Fichier de résultats
	regional.xls	Excel	Fichier de résultats en Excel
Multi-Niveaux			
in	multiniveau.pqi	PHREEQCI	Fichier d'entrée
out	multiniveau.pqo	PHREEQCI	Fichier de résultats
	multiniveau.sel	PHREEQCI	Fichier de résultats
	multiniveau.xls	Excel	Fichier de résultats en Excel
<b>Statistica</b>			
Descriptive	Descriptive_note.doc	Word	Information sur les fichiers
	Descriptive.xls	Excel	Statistiques descriptives en Excel
	Descriptive.sta	Statistica 6.1	Statistiques descriptives
Multivariable	Multivariable_note.doc	Word	Information sur les fichiers
	HCA_PCA.xls	Excel	Analyse multivariable en Excel
	HCA_PCA.sta	Statistica 6.1	Analyse multivariable (Chapitre 5)
	PCA_scores_rotated.xls	Excel	Analyse multivariable en Excel
	PCA_scores_rotated.sta	Statistica 6.1	Analyse multivariable (Chapitre 5)



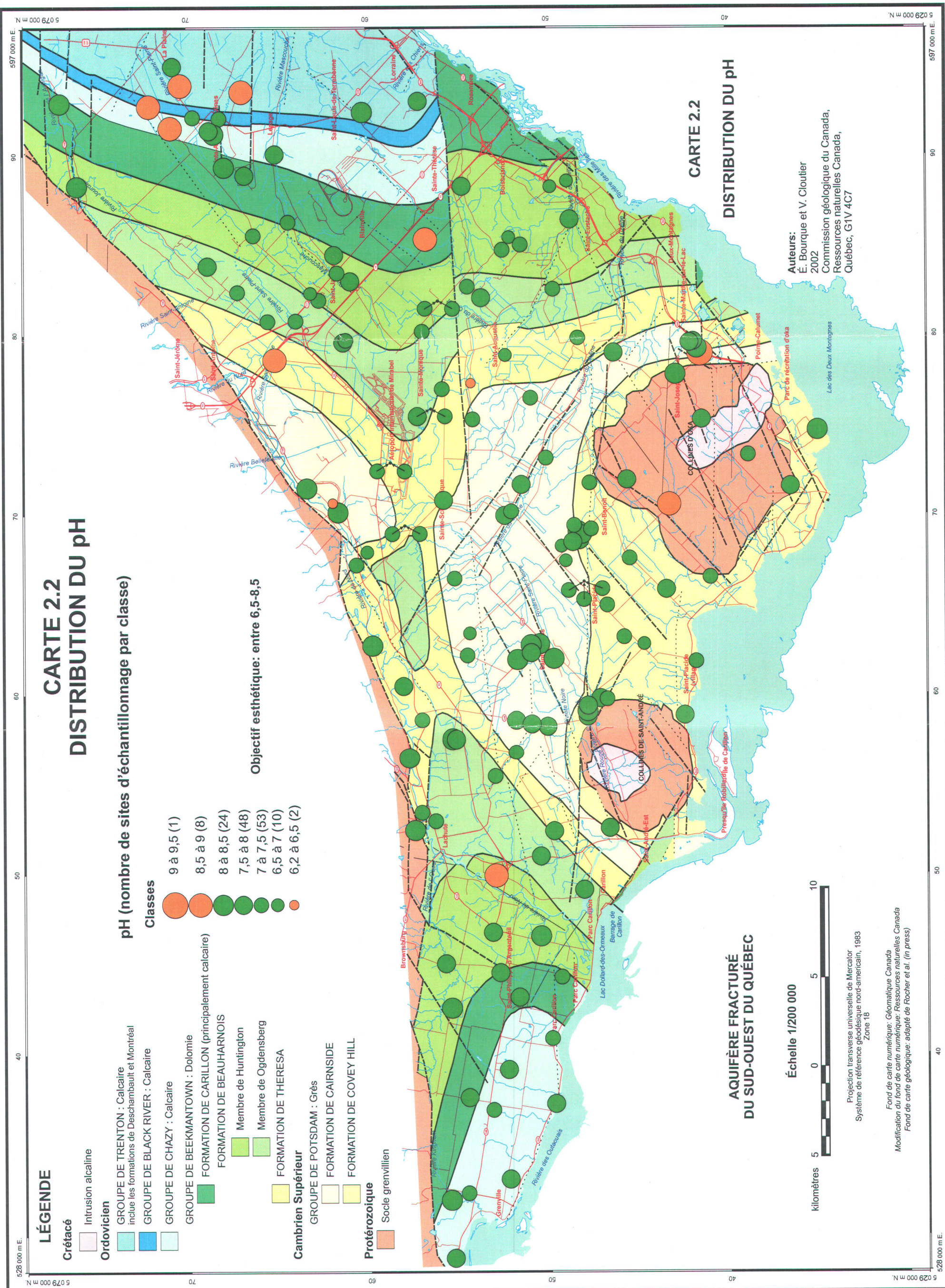
## **Appendice H**

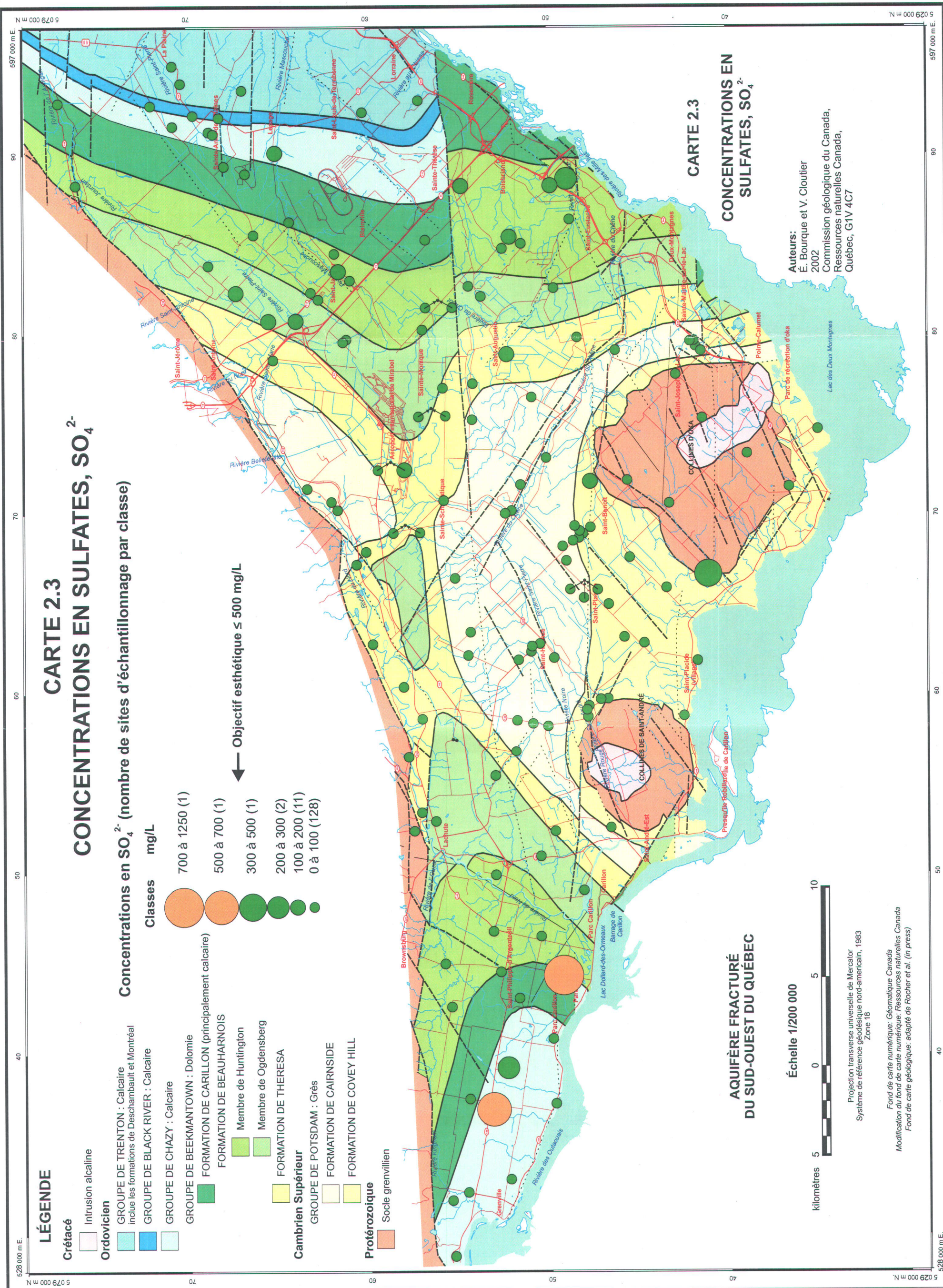
### **CARTES DU CHAPITRE 2**

**Cartes du Chapitre 2**Liste des cartes :

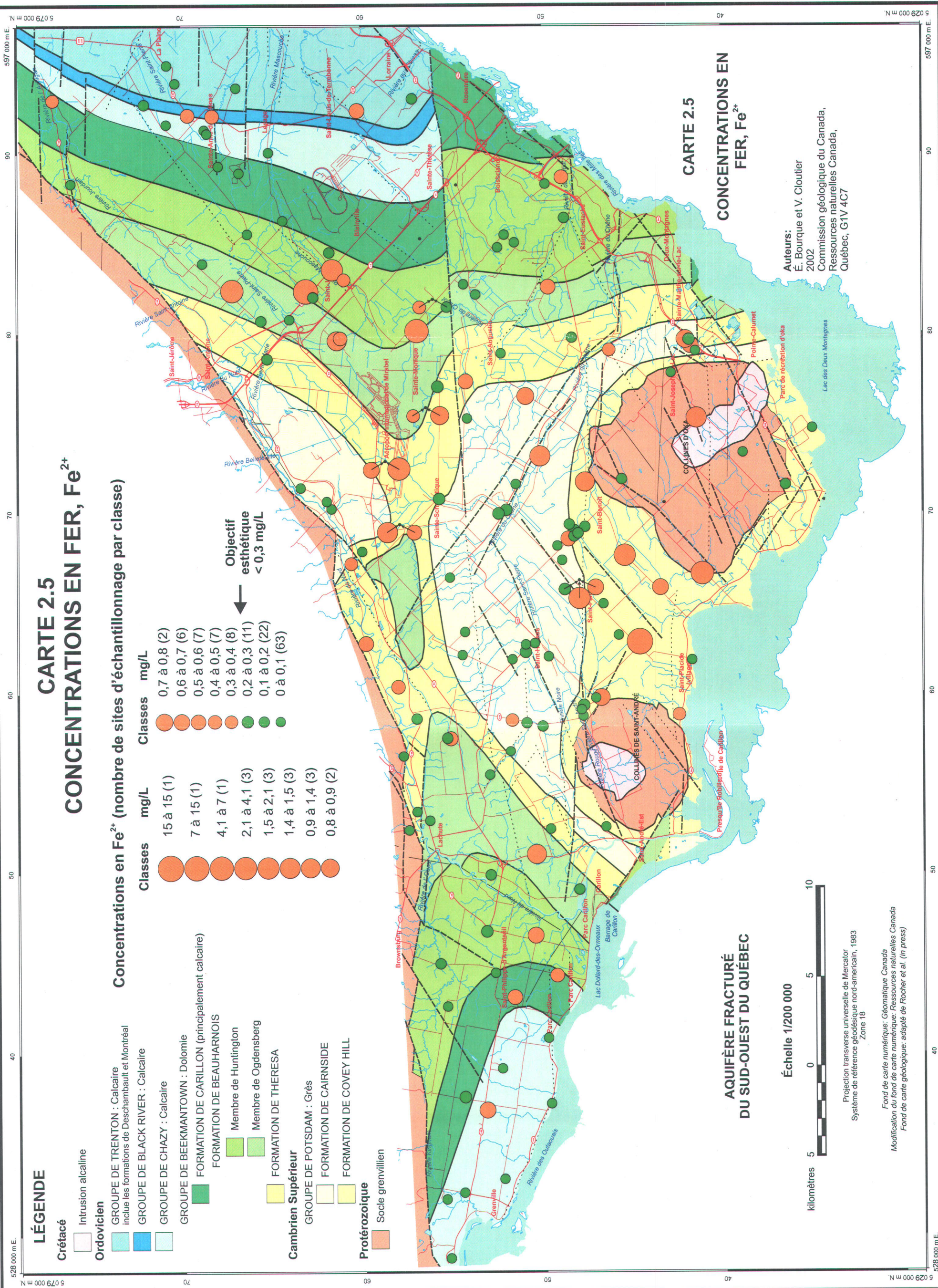
- Carte 2.1 Distribution des sites d'échantillonnage
- Carte 2.2 Distribution du pH
- Carte 2.3 Concentrations en sulfates,  $\text{SO}_4^{2-}$
- Carte 2.4 Concentrations en manganèse,  $\text{Mn}^{2+}$
- Carte 2.5 Concentrations en fer,  $\text{Fe}^{2+}$
- Carte 2.6 Concentrations en baryum,  $\text{Ba}^{2+}$
- Carte 2.7 Concentrations en sulfures,  $\text{HS}^-$
- Carte 2.8 Distribution de la dureté totale
- Carte 2.9 Concentrations en fluorures,  $\text{F}^-$
- Carte 2.10 Concentrations en sodium,  $\text{Na}^+$
- Carte 2.11 Concentrations en chlorures,  $\text{Cl}^-$
- Carte 2.12 Concentrations en matières dissoutes totales, MDT
- Carte 2.13 Concentrations en nitrates,  $\text{NO}_3^-$
- Carte 2.14 Distribution du taux d'adsorption du sodium, TAS
- Carte 2.15 Diagrammes radiaux et types d'eau
- Carte 2.16 Secteurs de qualité relative de l'eau souterraine
- Carte 2.17 Qualité de l'eau souterraine (carte à l'échelle du 1/100 000 en pochette)

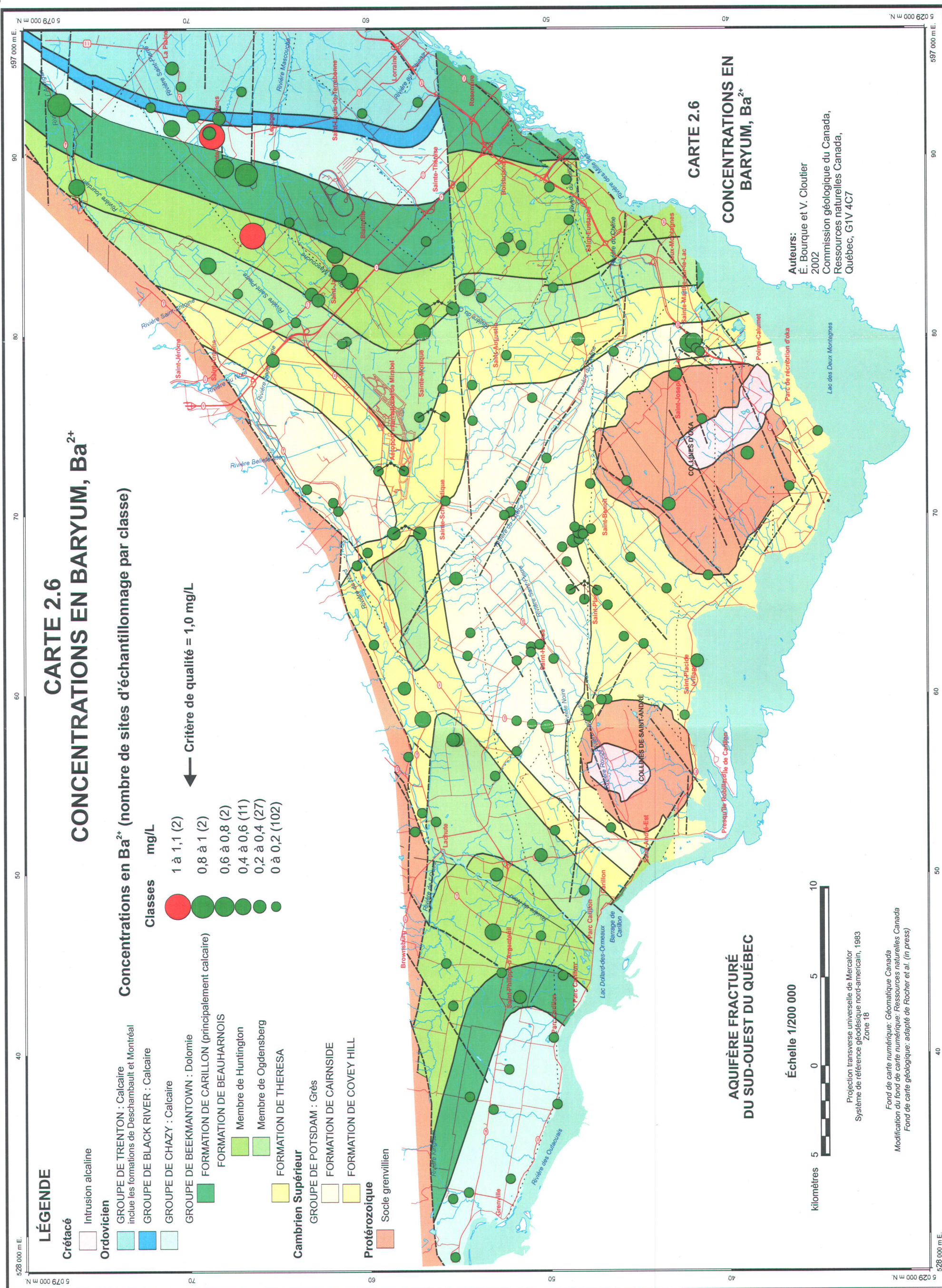


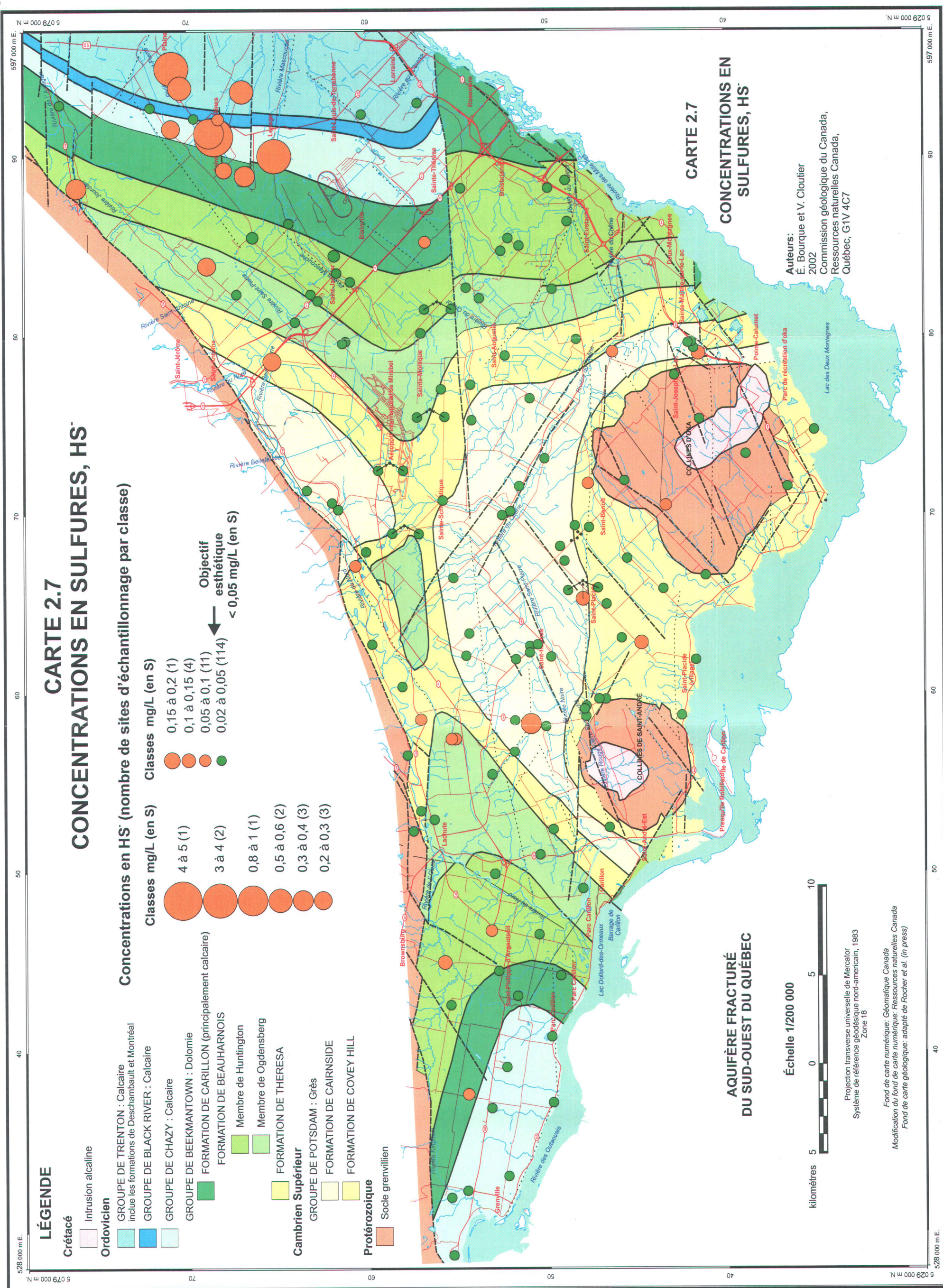




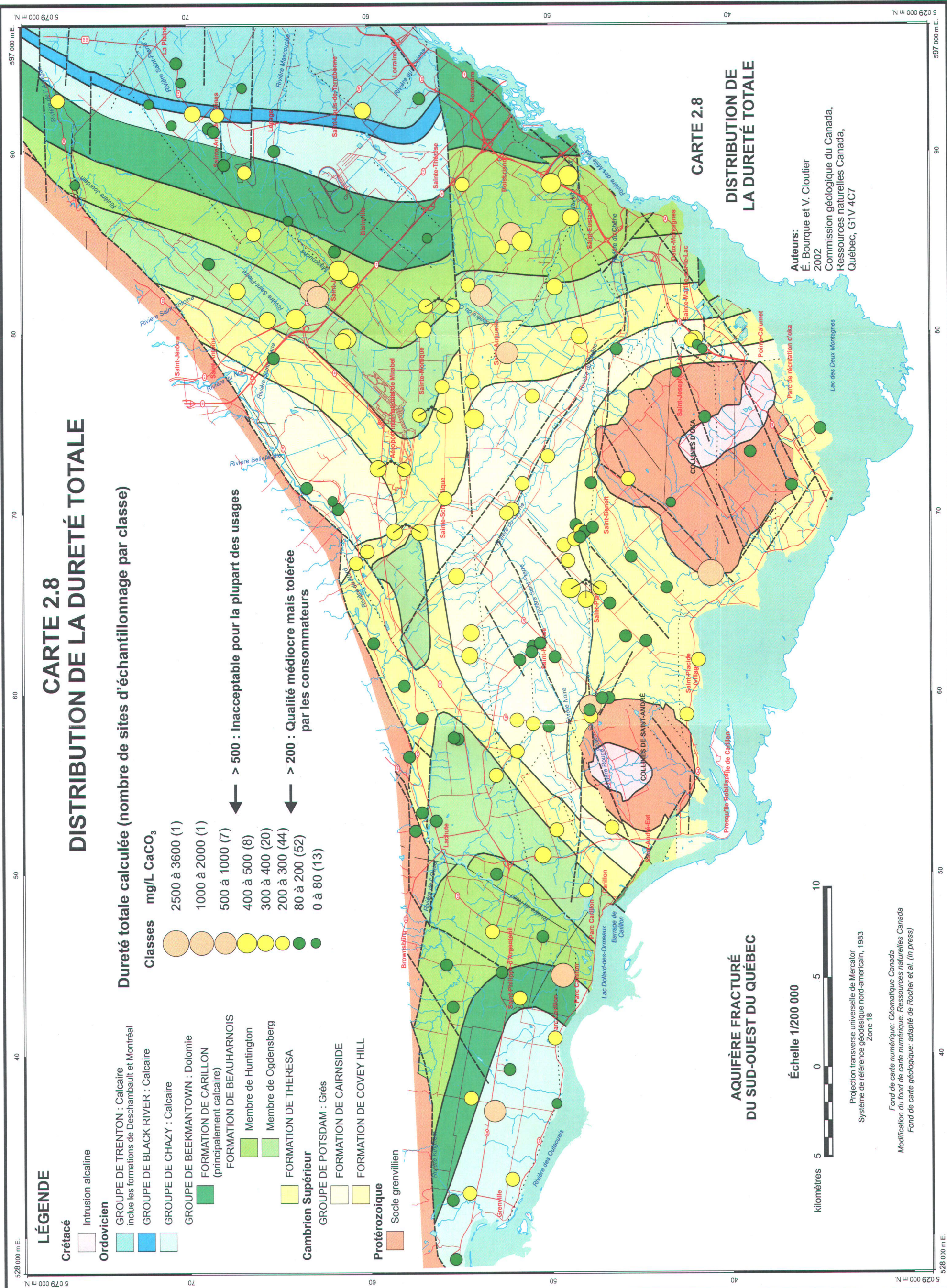




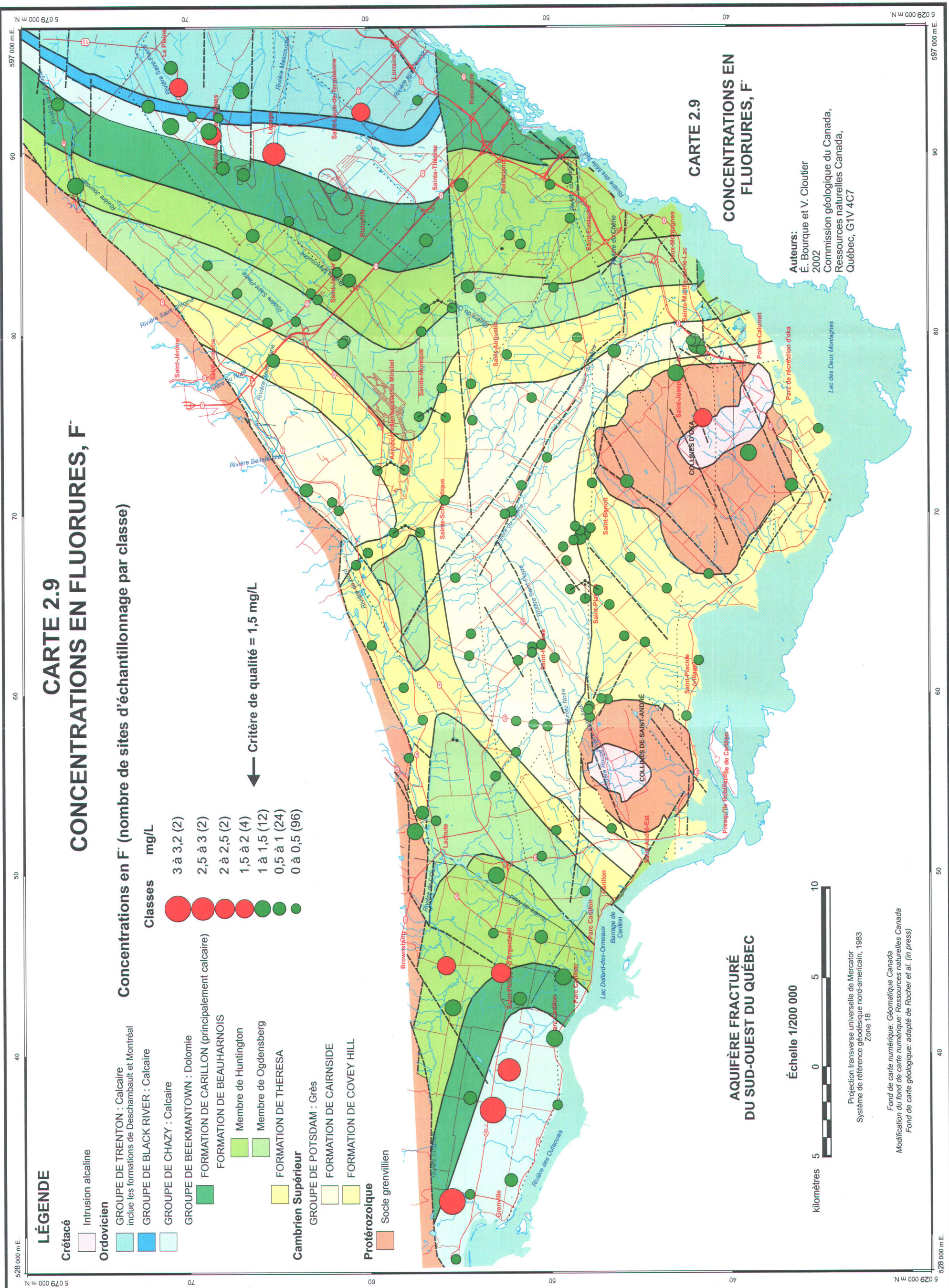




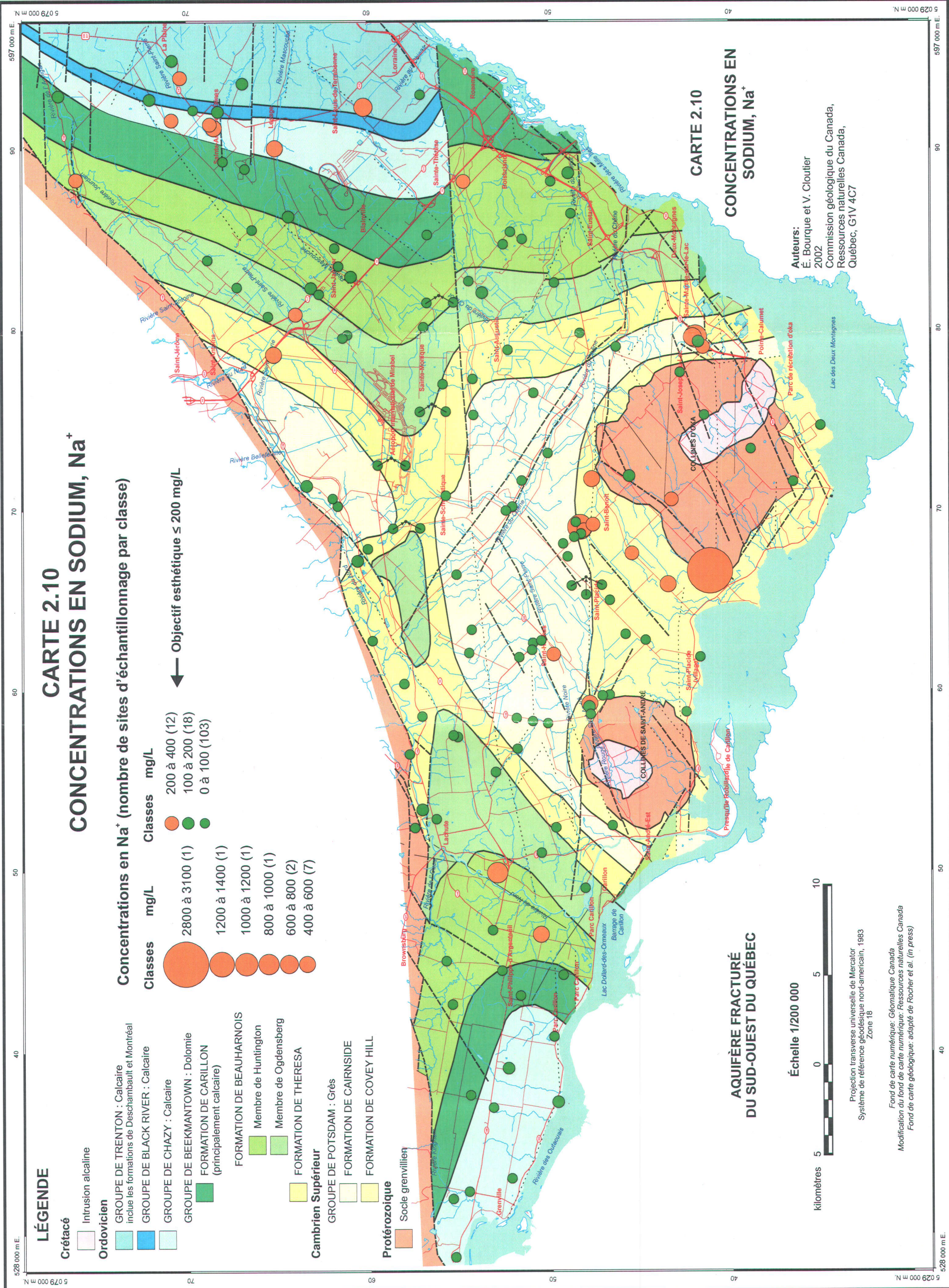
## CARTE 2.8 DISTRIBUTION DE LA DURETÉ TOTALE



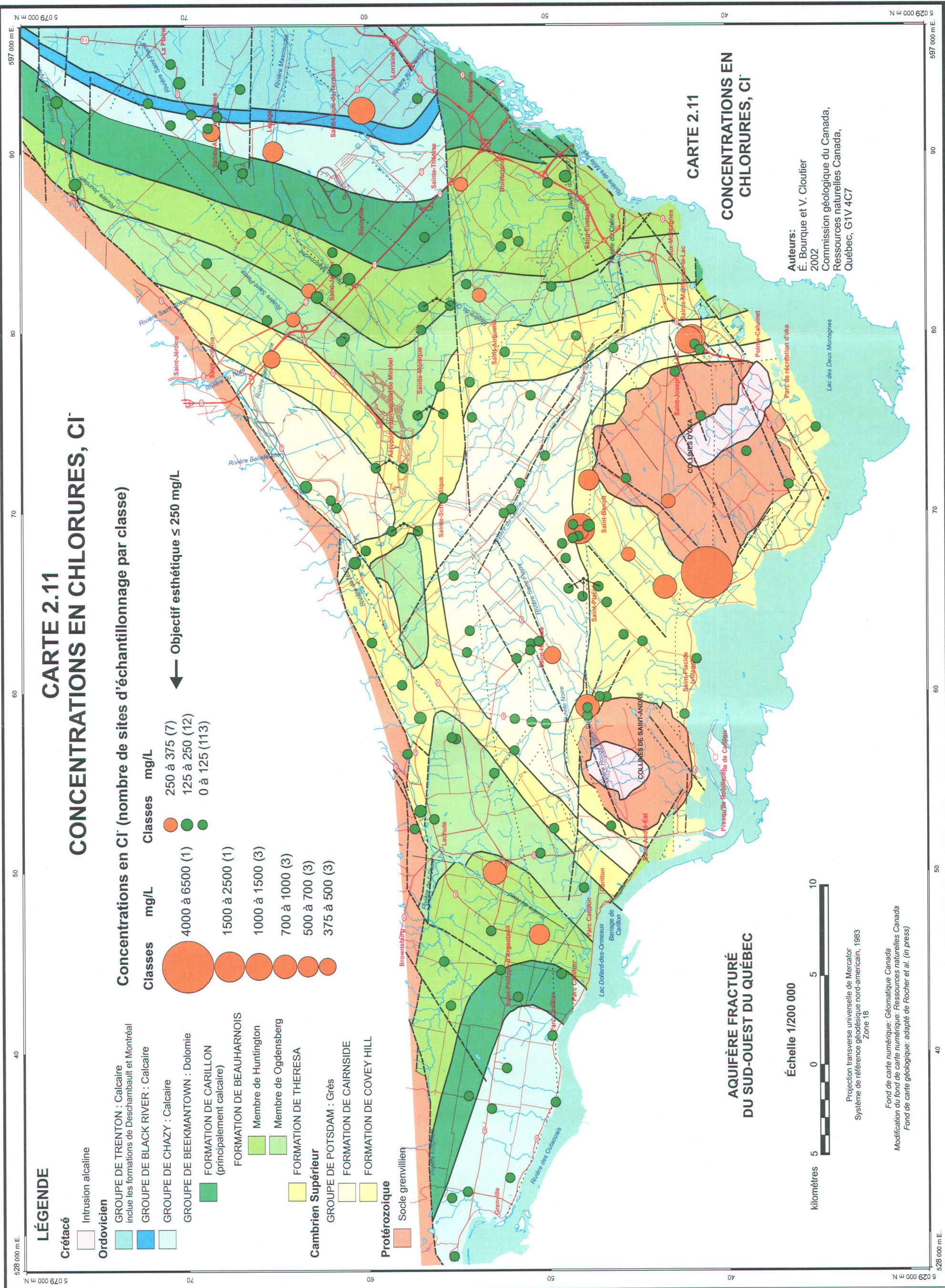
## CARTE 2.9 CONCENTRATIONS EN FLUORURES, F<sup>-</sup>



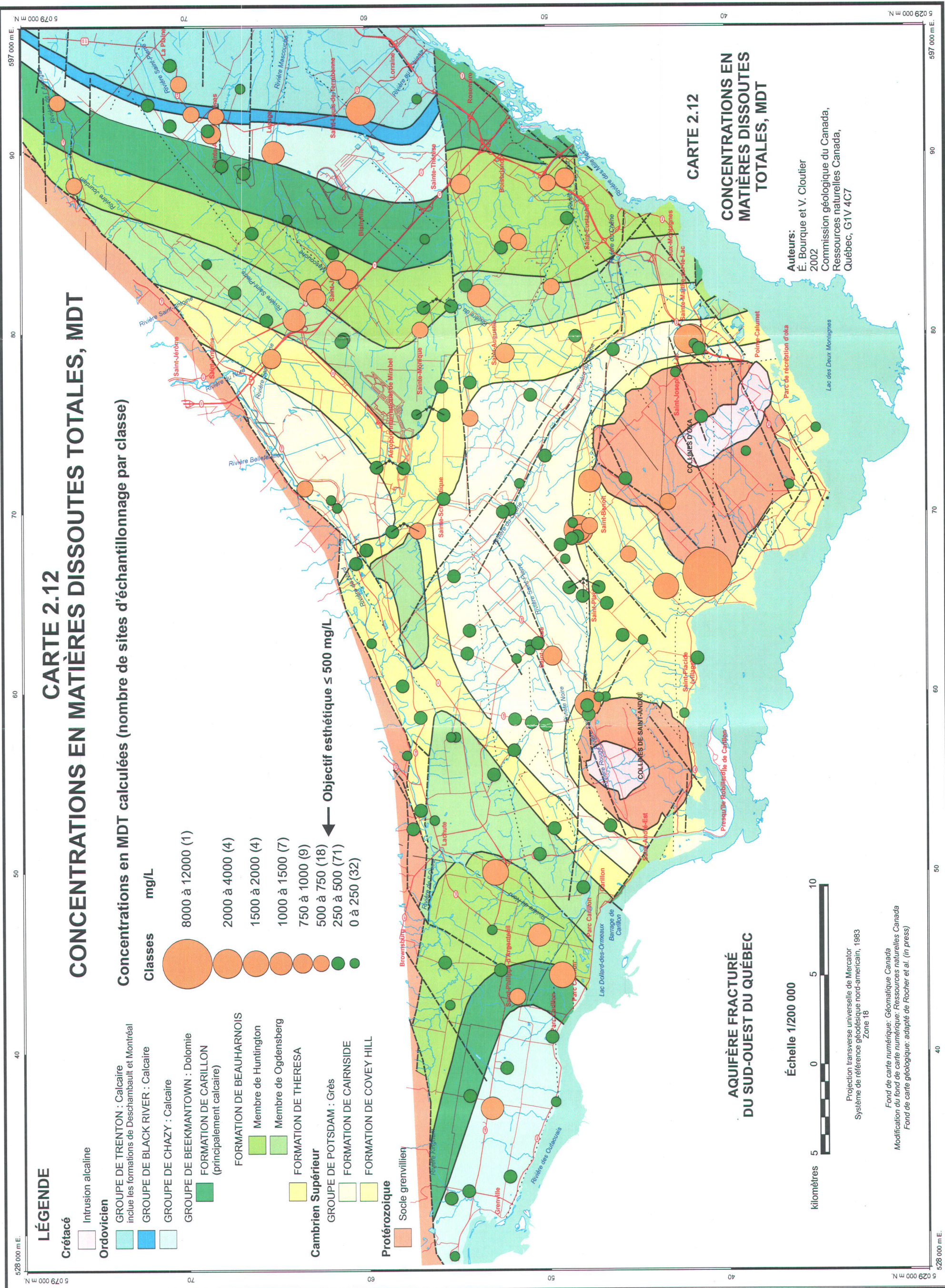
## CARTE 2.10 CONCENTRATIONS EN SODIUM, $\text{Na}^+$

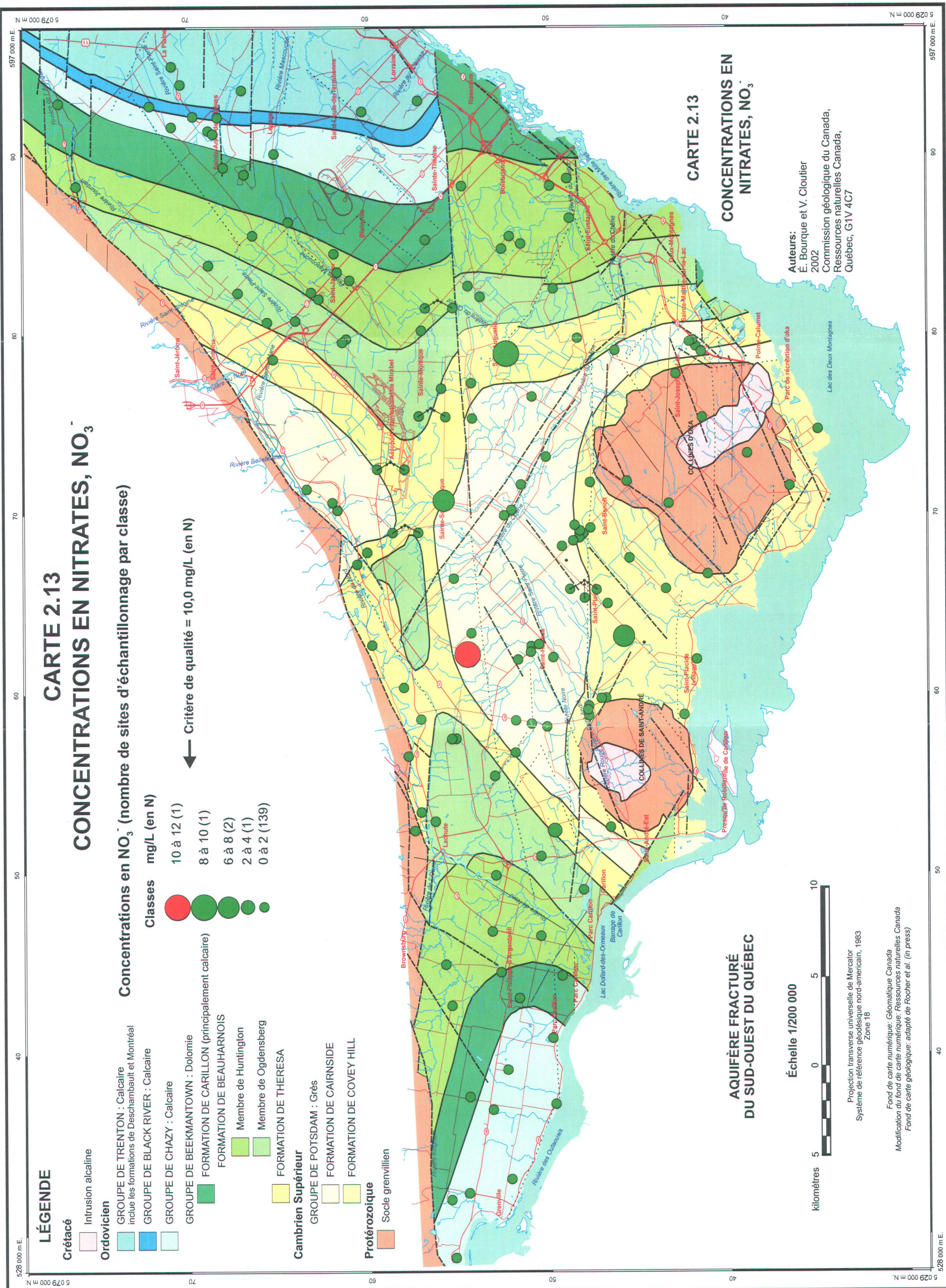


## CARTE 2.11 CONCENTRATIONS EN CHLORURES. CI-



## CARTE 2.12 CONCENTRATIONS EN MATIÈRES DISSOUTES TOTALES. MPT





## CARTE 2.14 DISTRIBUTION DU TAUX D'ADSORPTION DU SODIUM, TAS

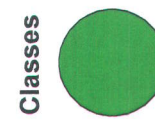
### LÉGENDE

#### Conditions hydrogéologiques simplifiées

Conditions de nappe libre ou semi-captive  
(Till, sable ou gravier sur roc)

Conditions de nappe captive  
(Argile sur roc)

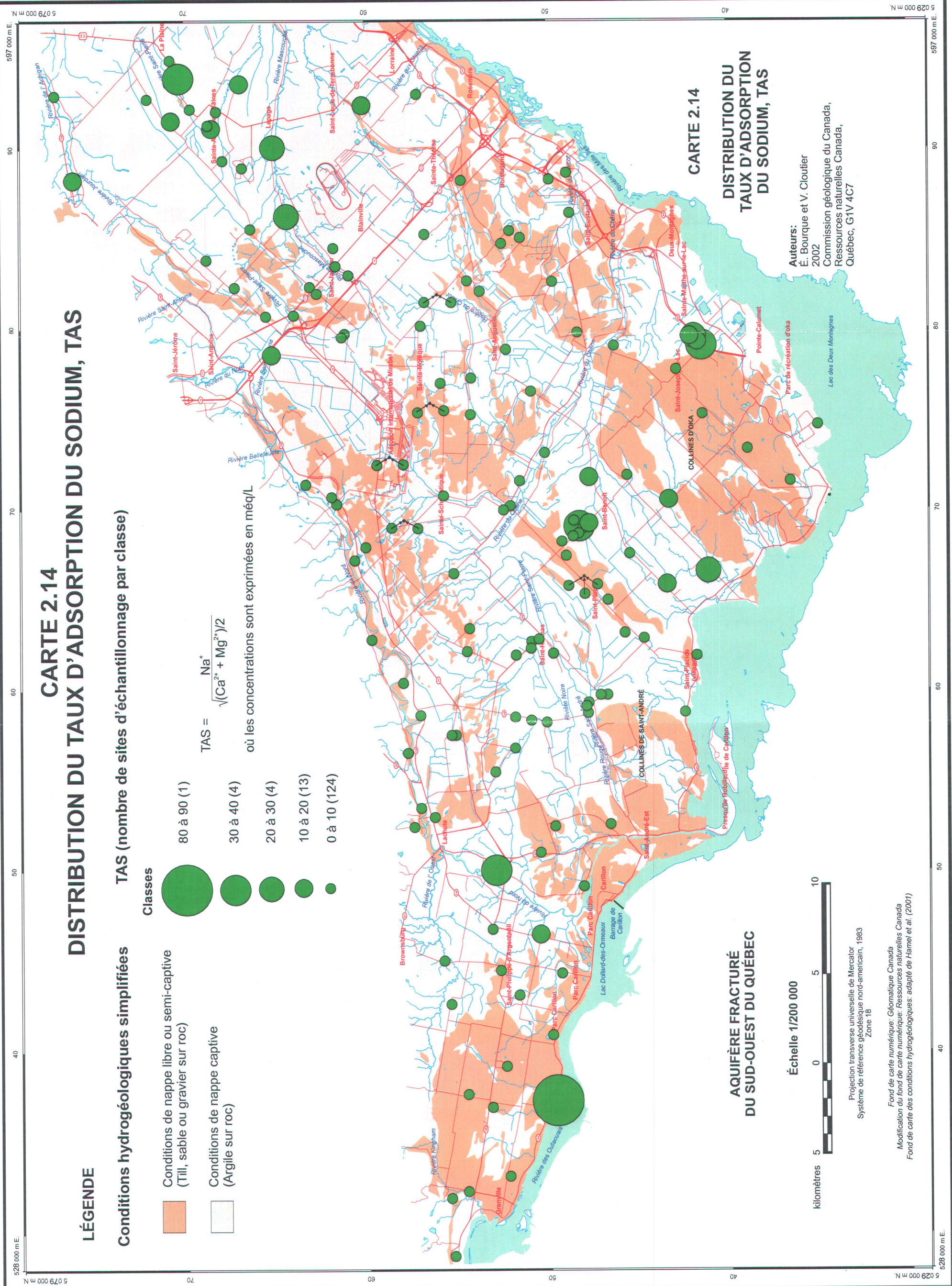
#### TAS (nombre de sites d'échantillonage par classe)



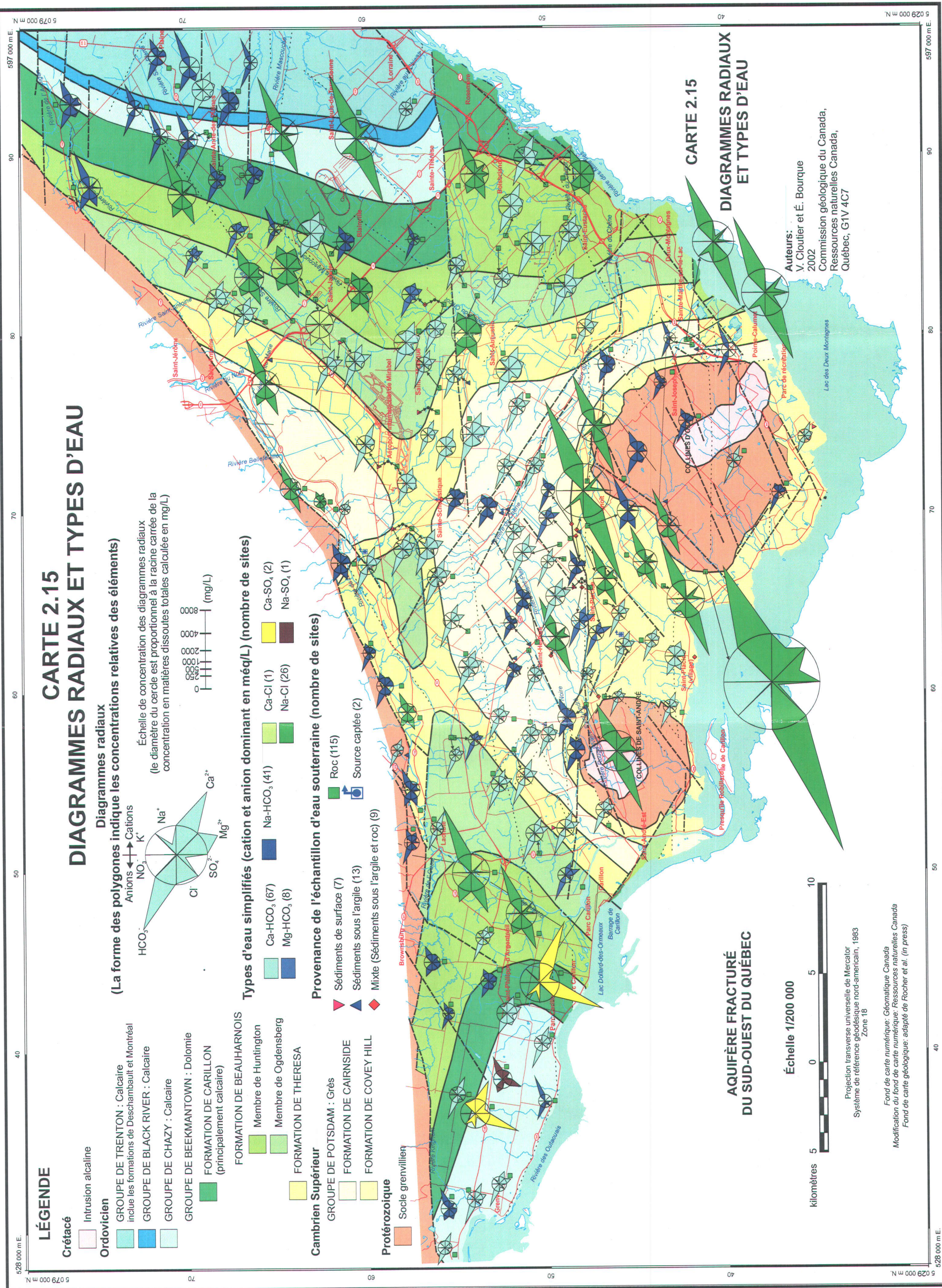
$$\text{TAS} = \frac{\text{Na}^+}{\sqrt{(\text{Ca}^{2+} + \text{Mg}^{2+})/2}}$$

où les concentrations sont exprimées en meq/L

80 à 90 (1)
30 à 40 (4)
20 à 30 (4)
10 à 20 (13)
0 à 10 (124)



## CARTE 2.15 DIAGRAMMES RADIAUX ET TYPES D'EAU



## CARTE 2.16 SÉCTEURS DE QUALITÉ RELATIVE DE L'EAU SOUTERRAINE

### LÉGENDE

#### Conditions hydrogéologiques simplifiées

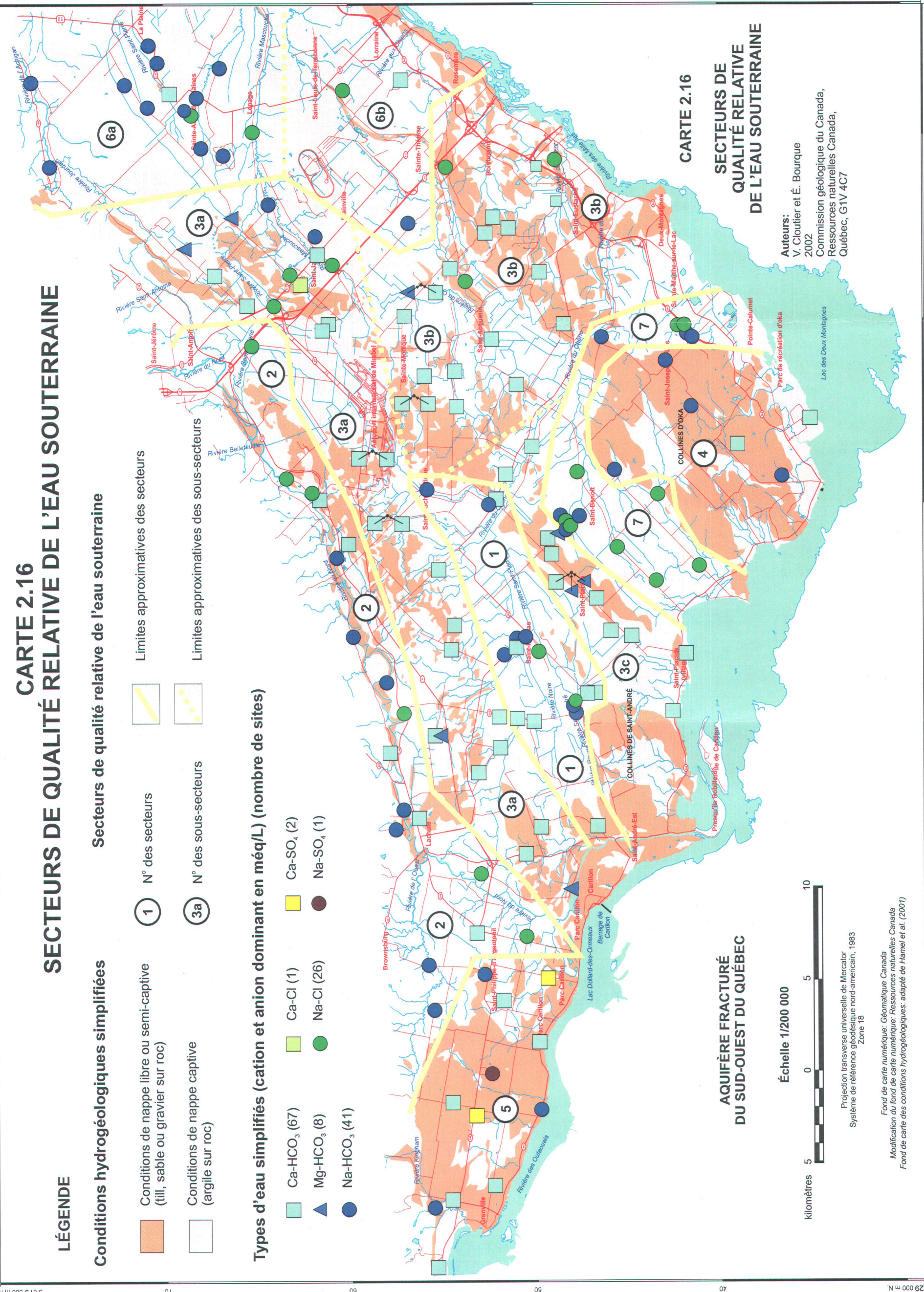
- Conditions de nappe libre ou semi-captive (till, sable ou gravier sur roc)
- Conditions de nappe captive (argile sur roc)

#### Secteurs de qualité relative de l'eau souterraine

- ① N° des secteurs
- ③a N° des sous-secteurs
- Limites approximatives des secteurs
- Limites approximatives des sous-secteurs

#### Types d'eau simplifiés (cation et anion dominant en mEq/L) (nombre de sites)

- |                          |            |                        |
|--------------------------|------------|------------------------|
| Ca-HCO <sub>3</sub> (67) | Ca-Cl (1)  | Ca-SO <sub>4</sub> (2) |
| Mg-HCO <sub>3</sub> (8)  | Na-Cl (26) | Na-SO <sub>4</sub> (1) |
| Na-HCO <sub>3</sub> (41) |            |                        |



**CARTE 2.16**  
**SÉCTEURS DE**  
**QUALITÉ RELATIVE**  
**DE L'EAU SOUTERRAINE**

Auteurs:  
V. Cloutier et É. Bourque  
2002  
Commission géologique du Canada,  
Ressources naturelles Canada,  
Québec, G1V 4C7

Projection transverse universelle de Mercator  
Système de référence géodésique nord-américain, 1983  
Zone 18

Fond de carte numérique: Géomatique Canada  
Modification du fond de carte numérique: Ressources naturelles Canada  
Fond de carte des conditions hydrogéologiques: adapté de Hamel et al. (2001)